Processus adaptatifs des végétaux marins face au changement climatique à différentes échelles de temps et d'espace : dynamique de populations, métabolomique, écophysiologie et potentiels de valorisation

Gwladys Surget

THÈSE / UNIVERSITÉ DE BRETAGNE OCCIDENTALE
sous le sceau de l'Université Bretagne Loire

pour obtenir le titre de
DOCTEUR DE L'UNIVERSITÉ DE BRETAGNE OCCIDENTALE
Mention : Biologie marine
École Doctorale des Sciences de la Mer

présentée par

Gwladys SURGET

Préparée à l'Institut Universitaire Européen de la Mer
Laboratoire des Sciences de l'Environnement Marin
UMR 6539 UBO/CNRS/IRD LEMAR

Processus adaptatifs des végétaux marins face au changement climatique à différentes échelles de temps et d'espace : dynamique de populations, métabolomique, écophysiologie et potentiels de valorisation

Thèse soutenue le 10 Juillet 2017
devant le jury composé de :

Joel FLEURENCE
Pr, MMS - Université de Nantes / *rapporteur*

Philippe POTIN
DR CNRS, Station biologique de Roscoff - UPMC / *rapporteur*

Jean-Paul CADORET
Dr, GREENSEA / *examinateur*

Dominique DAVOULT
Pr, Station biologique de Roscoff - UPMC / *examinateur*

Fabienne GUERARD
Pr, UBO / *examinateur*

Valérie STIGER-POUVREAU
Dr, UBO / *Directrice de thèse*

Nathalie POUPART
Dr, UBO / *Co-encadrante de thèse, invitée*

Eric DESLANDES
Pr, UBO / *invité*

Nelly KERVAREC
Ingénieur d'étude, UBO / *invitée*

Remerciements

Je souhaite tout d'abord remercier le Ministère de l'Enseignement Supérieur et de la Recherche pour m'avoir permis de réaliser cette thèse. Je remercie également les directeurs du LEMAR qui se sont succédés : Olivier Ragueneau et Luis Tito de Morais, pour m'avoir accueillie dans leur laboratoire. Mes remerciements s'addressent également à l'EDSM pour son investissement. J'exprime ensuite toute ma gratitude à l'ensemble des membres du jury pour l'intérêt qu'ils ont porté à ce travail et pour avoir accepté d'appartenir à ce jury.

Ma pensée va ensuite vers mes directrices de thèse, Valérie Stiger-Pouvreau et Nathalie Poupart sans qui ce travail n'aurait pas été possible. Merci de m'avoir fait dépasser mes limites et progresser.

Je remercie également vivement Vivian Husa pour cette superbe semaine d'échantillonnage en Norvège. Je suis contiente de la chance d'avoir eu l'opportunité de plonger et d'observer ces forêts de *Codium*.

Je souhaite remercier également Nelly Kervarec. C'est un réel plaisir de travailler avec toi et de se décortiquer les méninges à tes côtés pour trouver une molécule ou la quantifier à partir des spectres.

Un grand merci à Marie Aude pour m'avoir aidé à nettoyer ces kilos de vase, et à trier patiemment à la pince à épiler chaque fragment de cette charmante gracilaire dont nous rêvions… Et j'ai calculé, on en a compté et mesuré plus de 90 000! Je n'aurais jamais pu le faire sans toi. Egalement un grand merci à Isabelle pour m'avoir accompagnée à toutes ces sorties thalasso grandeur nature dans les rias de la Rade!

Je remercie également Gaspard pour m'avoir fait découvert le monde obscur de la photo-physiologie des algues…

Merci à Klervi pour tous ces moments et il y en a beaucoup… Merci à Leslie, à Geneu… ainsi qu'à tous les membres du labo du couloir du garage… Merci de m'avoir écoutée quand j'avais besoin de parler, merci de m'avoir fait partager votre joie de vivre tout au long de ces années.

Klervi, le club des mémés est toujours là avec toujours autant de sachets de thé dans le bureau…

Par ailleurs, cette thèse représente aussi à mes yeux trois vies, tellement elle fût riche d'émotions, pleine de tristesse et pleine de joie.

A travers cette thèse, je souhaite rendre hommage à Dominique Surget. Ton nom restera éternel comme tu le souhaitais… quatre papiers maintenant. Ce travail est un clin d'œil à ton paradis de daurades.

Je remercie tout particulièrement ma famille, des millions de merci pour avoir toujours été là au bon moment.

Enfin, je joins mon cœur au rayon de soleil qui illumine chacune de mes journées. Merci d'être tel que tu es.

Table des matières

Avant propos

Contexte du projet de thèse

Financée par la région Bretagne (Dispositif ARED) et par le LabexMer, cette thèse a été réalisée au sein du LEMAR (UMR 6539, IUEM-UBO) à Plouzané. Ce projet de thèse s'inscrit dans la concordance de deux projets européens, le projet MARMED (Dispositif INTERREG IVB) visant à développer de nouveaux biomatériaux et à augmenter leur fonctionnalité en utilisant des extraits algaux, et le projet INVASIVES (Dispositif ERA-NET, Seas-era) visant à mieux comprendre l'acclimatation de macroalgues invasives face au réchauffement climatique sur la façade atlantique. De ces projets sont issues deux collaborations internationales, l'une avec le CCMAR de l'Université d'Algarve, Département des sciences biomédicales et médecine à Faro (projet MARMED ; Portugal), l'autre avec l'université de Bergen, Département de Biologie à Bergen (projet INVASIVES, Norvège). Ce projet a bénéficié d'un financement du LabexMer pour la mobilité des doctorants, qui a permis la réalisation d'une campagne d'échantillonnage des espèces étudiées sur les côtes du Portugal et dans les fjords de Norvège (campagne côtière d'une semaine sur le bateau océanographique de l'université de Bergen). Les résultats issus de ces collaborations ont fait l'objet de plusieurs communications sous forme de posters et de communications orales listées ci-dessous. Ces travaux de thèse ont donné lieu à la parution d'articles scientifiques et à la rédaction de manuscrits pour publication qui sont présentés dans ce manuscrit et dont la liste des articles publiés est présentée ci-dessous.

Par ailleurs, les formations auxquelles j'ai participé m'ont permises, entre autres activités, de m'initier à la médiation scientifique au travers du concours Ma thèse en 180 secondes (finaliste de la finale Bretagne - Loire du concours 2016, *cf*. l'enregistrement suivant à 17 min 30 : https://www.youtube.com/watch?v=kpD84iDLUos&feature=player_embedded).

Durant ce doctorat, j'ai eu l'opportunité d'enseigner en biologie et physiologie végétale de la première année de Licence au Master 2 durant trois années de monitorat ainsi qu'une année en tant qu'attaché temporaire d'enseignement et de recherche, majoritairement sous forme de travaux pratiques (en salle et sur le terrain).

Communications scientifiques

Gwladys Le Diouron, Vânia Roberto, Sara Mira, Klervi Le Lann, Valérie Stiger-Pouvreau, Nathalie Poupart, Vincent Laizé, M Leonor Cancela and Fabienne Guérard (2013). Original bioactivities of *Codium fragile* and *Cladophora rupestris*: proliferative, mineralogenic and antioxidant activities. Journées de la SPF (Roscoff, France).

Vânia Roberto, Sara Mira, **Gwladys Le Diouron**, Vincent Laizé, Parameswaran V, Klervi Le Lann, Valerie Stiger-Pouvreau, Nathalie Poupart, Fabienne Guérard, M Leonor Cancela (2013). Proliferative and mineralogenic activities of seaweeds and marine plants extracts in a fish *in vitro* cell system. Colloque Microbiotec'13, (Aveiro, Portugal).

Gwladys Le Diouron, Klervi Le Lann, Valerie Stiger-Pouvreau, Couteau C., Coiffard L., Fabienne Guérard and Nathalie Poupart (2014). *Spartina alterniflora*: a source of bioactive compounds. Colloque ICI Spartina. (Rennes, France).

Jérémy Querné, **Gwladys Le Diouron**, Pablo Rault, Joy Versterren, Marie-Aude Poullaouec, Agathe Larzillière, Julie Le Noac'h, Maxime Hourdé, Valérie Stiger-Pouvreau, Emma Michaud, Christian Hily, Olivier Ragueneau and Nathalie Poupart (2014). Variation of growth and primary production of the invasive *Spartina alterniflora* and its effect on the macrofauna in tidal marshes of an European site: the Bay of Brest, France. Colloque ICI Spartina. (Rennes, France).

Gwladys Surget, Klervi Le Lann, Gaspard Delebecq, Nelly Kervarec, Fabienne Le Grand, Anne Donval, Vivian Husa, Nathalie Poupart et Valérie Stiger-Pouvreau (2015). Biochemical adaptation of the invasive macroalgae *Sargassum muticum* and *Codium fragile* along a gradient of seawater temperature. European Phycological Congress VI (Londres, Royaume-Uni).

Gwladys Surget, Klervi Le Lann, Gaspard Delebecq, Nelly Kervarec, Anne Donval, Nathalie Poupart et Valérie Stiger-Pouvreau (2016). Seasonal chemical ecology of introduced *Sargassum muticum* and *Codium fragile* in Brittany. International Seaweed Symposium (Copenhague, Danemark).

Gwladys Surget, Klervi Le Lann, Gaspard Delebecq, Nelly Kervarec, Anne Donval, Nathalie Poupart et Valérie Stiger-Pouvreau (2016). Seasonal phenology and metabolomic of *Gracilaria vermiculophylla* (Bay of Brest, France). International Seaweed Symposium (Copenhague, Danemark).

Articles publiés

Surget G, Stiger-Pouvreau V, Le Lann K, Couteau C, Coiffard L, Guérard F, Poupart N (2015) Sunscreen and antioxidant photoprotective capacities of polyphenolic compounds originated from a salt-marsh plant extract from Brittany (France). Journal of Photochemistry and Photobiology B: Biology 143, 52–60

Le Lann K, **Surget G**, Couteau C, Coiffard L, Cérantola S, Gaillard F, Larnicol M, Zubia M, Guérard F, Poupart N, Stiger-Pouvreau V (2016) Sunscreen, antioxidant, and bactericide capacities of phlorotannins from the brown macroalga *Halidrys siliquosa*. Journal of Applied Phycology 28:3547–3559

Surget G, Roberto V, Le Lann K, Mira S, Laizé V, Guérard F, Poupart N, Cancela ML, Stiger-Pouvreau V (2017) Green algae: a source of natural compounds with proliferative, mineralogenic and antioxidant activities. J Appl Phycol 29:575–584

Surget G, Le Lann K, Delebecq G, Kervarec N, Donval A, Poullouaec MA, Bihannic I, Poupart N, Stiger-Pouvreau V (2017) Seasonal phenology and metabolomic of the introduced red macroalga *Gracilaria vermiculophylla*, monitored in the Bay of Brest (France). J Appl Phycol doi:10.1007/s10811-017-1060-3

INTRODUCTION GENERALE

Parmi les végétaux marins, les macrophytes marins sont représentés majoritairement par les macroalgues, groupe de végétaux d'une grande biodiversité (Norton et al., 1996) mais également par les phanérogames marines, des angiospermes formant les herbiers des milieux vaseux. Ils représentent un groupe diversifié de végétaux pluricellulaires et photosynthétiques ayant la nécessité d'être immergés dans l'eau de mer, que ce soit de manière continue ou périodique, pour se développer (Dring, 1992 ; Sumich and Morrissey, 2004). Les macroalgues sont des organismes eucaryotes ne possédant pas de racines vraies, ni de tissus vascularisés, de tiges ou encore de feuilles contrairement aux phanérogames marines. Elles sont caractérisées par des structures reproductrices cryptiques et se développent dans la zone littorale benthique qui regroupe la majorité des peuplements des végétaux marins, *i.e.* de la zone tidale jusqu'à plus de 200 m de profondeur (De Reviers, 2002). Ces végétaux marins se distribuent dans toutes les zones biogéographiques (polaire, tempérée et tropicale) et sont adaptés aux contraintes environnementales des zones intertidale et subtidale, ces habitats côtiers soumis à la marée et aux embruns et imposant une variation constante des conditions abiotiques (Hurd et al., 2014; Wiencke and Bischof, 2012).

Les écosystèmes aquatiques, où se développent ces végétaux sont des composants clés de la biosphère de la Terre. Ils produisent plus de 50% de la biomasse de notre planète et ont la capacité d'incorporer au moins la même quantité de dioxyde de carbone atmosphérique que les écosystèmes terrestres (Häder et al., 2007; Zepp et al., 2007). Les macroalgues et phanérogames benthiques jouent un rôle prépondérant dans les écosystèmes littoraux marins, (*e.g.* Klöser et al., 1994) où elles constituent la base du réseau trophique (Häder et al., 2007). Ces producteurs primaires forment un habitat pour les espèces d'invertébrés (mobiles et sessiles) tels que les gastéropodes ou les bryozoaires, constituent une source de nourriture pour les herbivores et détritivores, ainsi qu'une zone de refuge pour les stades juvéniles de poissons et crustacés. Or ces écosystèmes présentant une forte biodiversité sont actuellement fragilisés par un ensemble de facteurs anthropiques résultant en la diminution de leurs fonctions et des services qu'ils rendent à la société, en raison de l'érosion de leur biodiversité (Costanza et al., 1997; Duarte, 2000).

En effet, dans un contexte général de changement climatique dont les conséquences sont de plus en plus visibles sur le domaine côtier, les activités anthropiques continuent de s'intensifier et le nombre des espèces exotiques continue d'augmenter. L'introduction d'espèces représente une menace pour la biodiversité des écosystèmes européens (Katsanevakis et al., 2014). Un des effets écologiques négatifs de ces espèces invasives consiste en la substitution à grande échelle de la flore autochtone (Boudouresque and Verlaque, 2002; Galil, 2007; Occhipinti-Ambrogi and Savini, 2003). Les algues représentent entre 20 et 29% des espèces marines introduites, ce qui en fait le compartiment du monde du vivant le plus introduit en Europe (Schaffelke et al., 2006). Cependant, peu d'études ont analysé l'acclimatation d'espèces végétales marines et leurs interactions avec les espèces natives dans un contexte de changement climatique. Ces espèces invasives, de par leur capacité à coloniser de nouveaux habitats présentent un potentiel élevé d'acclimatation à des variations des facteurs environnementaux (Nyberg and Wallentinus, 2005). Pour cette étude ont été choisies un échantillon de 4 espèces modèles de végétaux marins à large répartition en Europe, qui ont été suivies le long d'un gradient latitudinal s'étendant de la Norvège jusqu'au Portugal. Un gradient latitudinal se traduit par un gradient de divers paramètres environnementaux, comme la température (Gohin et al., 2010) par exemple (gradient thermique) qui structure la répartition latitudinale des espèces (Hu and Fraser, 2016). Une variation thermique est également l'une des conséquences principales du changement climatique (Harley et al., 2006). Comme les conséquences induites par le changement climatique sur les espèces en milieu naturel ne sont appréciables qu'à l'échelle de décennies, l'étude des processus d'acclimatation d'espèces invasives dans des zones géographiques plus chaudes (gradient sud) pourrait permettre de présager de leur acclimatation future dans des régions plus froides (gradient nord).

Les individus, les populations et les communautés des êtres vivants ne subissent pas de façon passive l'influence des facteurs écologiques. Chaque espèce présente à des degrés variés une plasticité écologique lui permettant, pour survivre, de s'adapter aux fluctuations des facteurs limitants dans les milieux auxquels elle est inféodée. La variabilité des facteurs écologiques implique ainsi l'aptitude pour chaque organisme de s'adapter. On distingue alors trois types d'adaptations aux facteurs écologiques : la régulation, l'acclimatation et l'adaptation (Hurd et al., 2014; Raven and Geider, 2003).

La régulation ou l'adaptation physiologique permet aux êtres vivants de maintenir constantes et à une valeur optimale leurs fonctions physiologiques face à un changement du

milieu ambiant. Les processus de régulations révèlent le potentiel physiologique d'un organisme à répondre à un changement immédiat des conditions environnementales. Ces variations se produisent à l'échelle de minutes ou de secondes.

L'acclimatation se produit à une échelle de temps plus longue, à l'échelle d'heures ou de jours. Elle implique des processus tels que l'expression génique et la synthèse de nouvelles protéines comme les enzymes. En effet, pour se mettre en harmonie avec leur environnement, certains êtres vivants, les plantes en particulier, développent des caractères non héréditaires appelées modifications. Cette acclimatation a lieu dans la limite des contraintes génétiques de l'espèce imposée par l'adaptation. Les individus qui subissent ces modifications sont appelés accommodats.

Et enfin, l'adaptation qui implique le développement de caractères héréditaires (fixation génétique) sous l'effet de la sélection des traits phénotypiques est le résultat de l'évolution qui peut se dérouler à l'échelle de millénaires. Elle correspond à la correspondance d'un organisme vivant avec les conditions environnementales à travers des changements stables induisant une adaptation génotypique. C'est la forme d'adaptation la plus parfaite d'une espèce aux conditions environnementales. Les individus d'une espèce ayant subi une adaptation génotypique ou héréditaire sont appelés des écotypes.

Dans ce travail de thèse sera traité l'adaptation physiologique des végétaux marins ou acclimatation. Cet événement implique un changement graduel et réversible de la physiologie, de la biochimie et de l'anatomie, chez un individu, suite à l'exposition de l'organisme à un environnement nouveau.

Le potentiel d'acclimatation face aux stress environnementaux des macrophytes marins, qu'elles soient invasives ou natives, leur confère une forte diversité chimique ou chimiodiversité (Stengel et al., 2011) :

- les espèces natives synthétisant des molécules de défense spécifiques aux habitats où elles se développent ;

- les espèces invasives développant une forte acclimatation phénotypique afin de coloniser de vastes habitats présentant des caractéristiques environnementales variables, acclimatation qui diffère de l'aire native d'où elles sont issues.

Les molécules impliquées dans l'acclimatation des espèces face aux facteurs abiotiques peuvent présenter deux types d'activités biologiques : 1) en lien avec le facteur

de stress étudié, *e.g.* production de molécules à propriétés photoprotectrices peuvent être synthétisées *de novo* ou en plus grande quantité en cas de stress lumineux ou d'irradiation aux ultraviolets, ou 2) sans lien direct avec un stress environnemental et ces molécules vont alors présenter des activités biologiques originales, telles que des molécules favorisant la minéralisation osseuse des animaux, leur conférant des propriétés ostéogéniques (chez une espèce algale non-calcifiée).

Dans ce contexte, cette thèse porte sur l'étude de l'écophysiologie et de l'adaptation chimique d'espèces de macrophytes invasifs face à une variation de facteurs environnementaux générée par le changement climatique global ainsi qu'aux voies de valorisation possibles des métabolites de stress étudiés chez des espèces natives et invasives. Cette thèse s'articule ainsi autour des trois problématiques suivantes :

- Quel est l'état des populations de ces espèces invasives à une échelle locale, *i.e.* en Bretagne ? Impactent-elles les écosystèmes qu'elles colonisent ? (Partie 1)

- Quelle est la variabilité écophysiologique de ces espèces à grande échelle ? Existe-il une acclimatation du métabolome de ces espèces invasives pour les populations situées au Sud et au Nord de leur aire de répartition le long de la façade Atlantique ? (Partie 2)

- La plupart des études montrent une incapacité de l'homme à éradiquer les espèces invasives. La valorisation de ce type d'espèce pourrait être envisagée étant donné les fortes biomasses qu'elles représentent. Ainsi, la problématique suivante a été abordée : en s'inspirant du vivant (concept de bio-inspiration), quelles sont les voies de valorisations possibles d'espèces de macrophytes natives et invasives ? (Partie 3)

La réponse à chacune de ces problématiques est développée au travers des trois parties qui structurent ce manuscrit. Par ailleurs, cette étude se place dans des thématiques pluridisciplinaires allant des invasions biologiques, au réchauffement climatique à la bio-inspiration. Les notions d'échelles quelles soient spatiales, temporelles ou biologiques sont déterminantes. Ces différents points sont définis et développés dans les paragraphes suivants (au terme de cette introduction) afin d'avoir une bonne compréhension du contexte bibliographique de cette thèse. Il s'ensuit une présentation des différents sites, des modèles biologiques, étudiés tout au long de ce travail de thèse ainsi que la description des objectifs et de la structure de la thèse.

1. Les espèces invasives

L'Homme, par son mode de vie et ses activités (maritimes, aquaculture, portuaires,…), a entraîné l'introduction de nouvelles espèces de manière volontaire ou accidentelle et ce, depuis le Néolithique avec le développement de l'agriculture et de l'élevage, puis au travers des grandes explorations au XV^{ème} siècle et du développement du commerce maritime notamment (Goudard, 2007; Mooney and Cleland, 2001). Ces dernières décennies, la globalisation et l'intensification des échanges commerciaux qui en découlent (échanges multipliés par 17 entre 1965 et 1990) ont conduit à une augmentation rapide du nombre d'espèces introduites quel que soit la région du monde considérée (Goudard, 2007; Perrings et al., 2005; Stiger-Pouvreau and Thouzeau, 2015). En effet, le long des côtes européennes, 50% des introductions de macrophytes marins se sont produites après les années 1960 (Viard and Comtet, 2009). En Europe, au sein de l'ensemble des organismes marins, les algues constituent l'un des plus grands groupes d'espèces allochtones (Schaffelke et al., 2006; Stiger-Pouvreau and Thouzeau, 2015). Or, les macrophytes marins représentent les principaux producteurs primaires des écosystèmes côtiers se répartissant sur l'estran, de l'étage infralittoral jusqu'à l'étage supralittoral. Ils incluent ainsi de nombreuses espèces ingénieures qui présentent une importance écologique vitale pour ces écosystèmes (Olafsson, 2016).

Les macrophytes marins : de l'introduction à l'invasion

Dans ce contexte et face à un intérêt grandissant de la communauté scientifique et de la société civile pour les espèces introduites et invasives, la terminologie utilisée a donné lieu à de nombreux débats. Actuellement, les termes adoptés relatifs aux invasions biologiques peuvent se définir comme indiqué ci-dessous :

Une espèce est définie comme étant **introduite** si elle répond aux 4 critères suivants (Boudouresque and Verlaque, 2002, 2005; Thévenot, 2013) : 1) l'espèce n'est pas native de l'aire géographique considérée ; 2) l'extension de son aire géographique est directement ou indirectement liée à des activités anthropogéniques ; 3) il existe une discontinuité géographique entre son aire de répartition naturelle et son aire d'introduction, c'est à dire qu'il ne s'agit pas de dispersion marginale (par émission de cellules de la reproduction) pouvant être liées à des facteurs climatiques ; 4) la population a la capacité de générer une nouvelle génération *in situ* indépendamment de toute intervention humaine mais la

reproduction sexuée est insuffisante pour permettre le maintien de la population.

De manière ultime, les populations introduites deviennent des **populations naturalisées**, c'est-à-dire des populations autonomes, se reproduisant régulièrement, assurant ainsi la pérennité de l'espèce allochtone et son implantation durable dans sa nouvelle aire géographique (Thévenot, 2013).

Une espèce introduite devient **invasive,** lorsque une fois établie dans sa nouvelle zone géographique (zone extérieure à son aire de distribution native), elle se disperse et génère un impact négatif sur l'écosystème et les espèces locales et/ou sur l'économie (définition de l'IUCN) (Stiger-Pouvreau and Thouzeau, 2015; Thévenot, 2013).

Ces différentes définitions correspondent plus précisément aux phases de développement d'une espèce exotique dans un nouvel environnement, de son introduction jusqu'à son invasion (présentées dans la Figure 1). Le passage d'une phase à une autre est possible grâce au franchissement d'un certain nombre de **filtres** ou barrières qui se succèdent. Ces filtres sont conditionnés par les facteurs physico-chimiques et les facteurs biotiques du milieu. Ils peuvent favoriser ou non l'implantation puis le développement de l'espèce exotique. **La pression des propagules est un déterminant important pour l'introduction d'une espèce** (Stiger-Pouvreau and Thouzeau, 2015). Il existe une relation positive entre la caractéristique des rejets de propagules c'est-à-dire leur fréquence et l'abondance des propagules rejetées à chaque fois et le succès d'une espèce exotique à traverser chaque filtre (Kolar and Lodge, 2001). Cette pression en propagules est dépendante du **vecteur d'introduction**. Les vecteurs d'introduction sont multiples : le transport maritime via les eaux de ballast ou les salissures de bateaux, l'aquaculture, l'aquariophilie, la navigation de plaisance (Cabioc'h et al., 2006)… Selon la « tens rules » de Williamson, environ 10% des espèces exotiques franchissent chacun des filtres majeurs, soient la barrière géographique, la barrière de la reproduction et les barrières écologiques et de la dispersion (Williamson and Fitter, 1996).

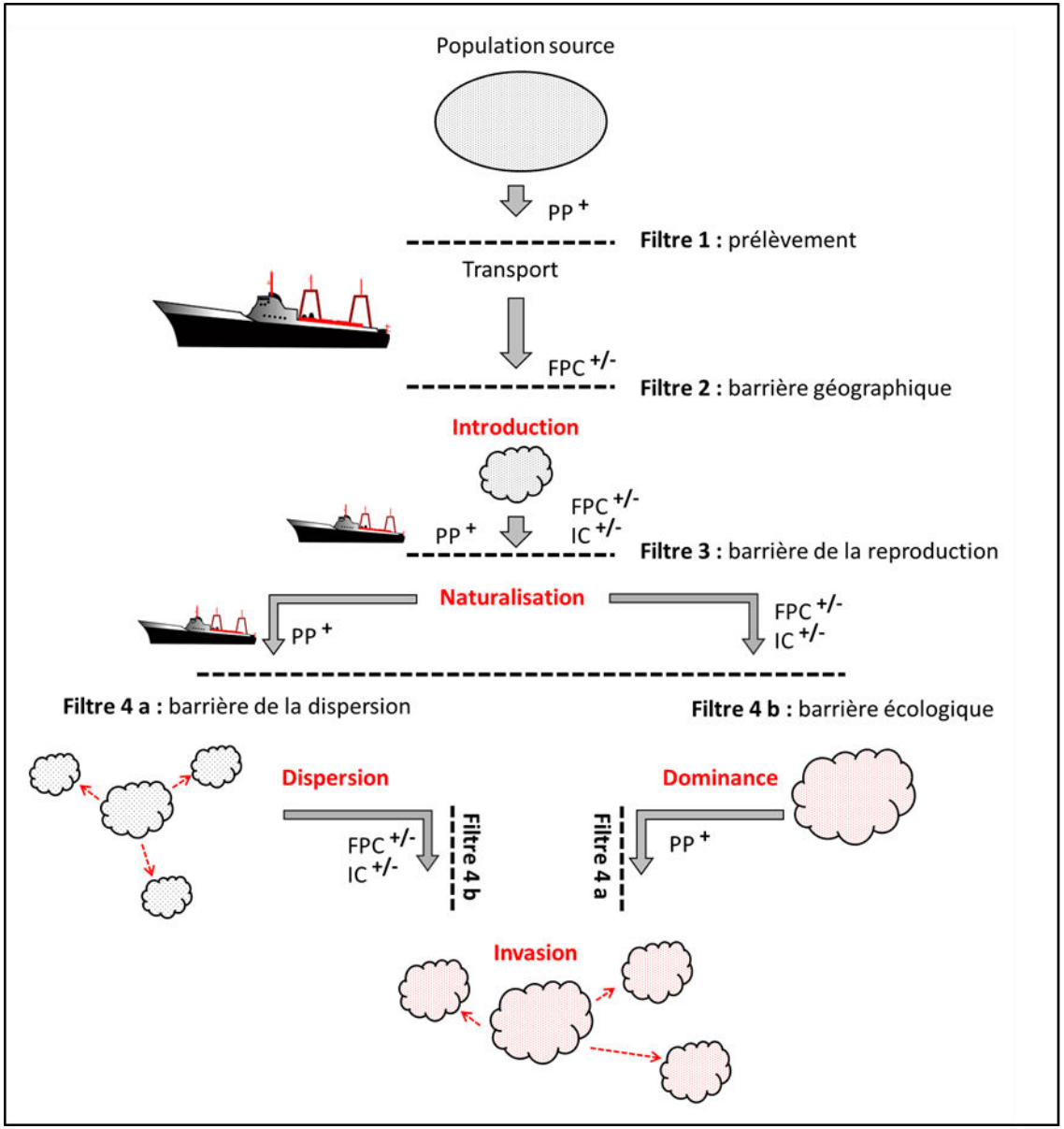

Fig. 1 Conceptualisation des phases de développement d'une espèce invasive issu d'Occhipinti et Ambrogi (2007) et modifié d'après Stiger-Pouvreau et Thouzeau (2015). Le passage à travers les différents filtres implique la survie des propagules.

Filtre 1 : La présence suffisante de propagules dans l'aire native est nécessaire afin que celles-ci soient prélevées en suffisamment grandes quantités pour être transportées sur de grandes distances et survivre.
Filtre 2 : Les propagules doivent survivre aux conditions physico-chimiques du transport afin de pouvoir être rejetées et se disséminer dans un nouvel environnement.
Filtre 3 : L'acclimatation à son nouvel environnement de l'espèce allochtone, tant en terme de facteurs abiotiques que biotiques, est déterminante afin d'améliorer la survie des individus et leur capacité de reproduction dans le but de former une nouvelle génération autonome.
Filtre 4 a : Les propagules ne sont pas seulement générées par un apport lié au transport mais également *in situ* par la population naturalisée.
Filtre 4 b : Des facteurs biotiques et abiotiques sont impliqués car ils peuvent affecter la croissance et le développement de la population introduite.
PP : Pression des Propagules ; *i.e.* il s'agit du nombre de propagules arrivant sur un site, dans un habitat, un écosystème ou une région (Viard and Comtet, 2009). Les propagules correspondent à toute partie de l'espèce exotique pouvant se disperser et générer un individu (Pyšek et al., 2009) ; FCP : Facteurs Physico-Chimiques ; IC : Interaction des Communautés (correspondant aux facteurs biotiques de l'écosystème considéré) ; +/- : effet positif ou négatif du déterminant.

La traversée d'un filtre n'est pas irréversible (Richardson et al., 2000). Une fluctuation des facteurs environnementaux (facteurs abiotiques et/ou biotiques) peut entraîner une baisse de la fitness d'une population jusqu'à son déclin.

La Figure 2 illustre deux types de dynamiques d'expansion observées chez les espèces invasives, l'expansion pouvant être définie en termes d'abondance ou d'élargissement de leur aire de distribution. Suite au rejet de propagules dans un nouvel environnement, il existe **une période de latence** durant laquelle les populations se naturalisent sans augmentation de l'abondance ou d'extension de l'espèce exotique. L'introduction de l'espèce peut ainsi passer inaperçue. Après être naturalisée, la population introduite connaît **une phase d'expansion** importante.

Au cours de la phase d'expansion, la taille de la population peut fluctuer jusqu'à atteindre un maximum (Figure 2). Par l'augmentation de ses fonctions physiologiques (croissance, reproduction, …) l'espèce colonise le milieu et peut occuper toutes les niches écologiques possibles jusqu'à ses limites physiologiques en interaction avec les nouveaux environnements colonisés. Ensuite, les populations entrent dans **une phase de persistance** plus ou moins longue suivant les espèces ou déclinent rapidement. Prévoir la dynamique future d'une espèce invasive est particulièrement complexe. Ceci va dépendre de sa capacité à s'acclimater et à s'adapter aux multiples facteurs caractérisant les nouveaux environnements dans lesquels elle se développe.

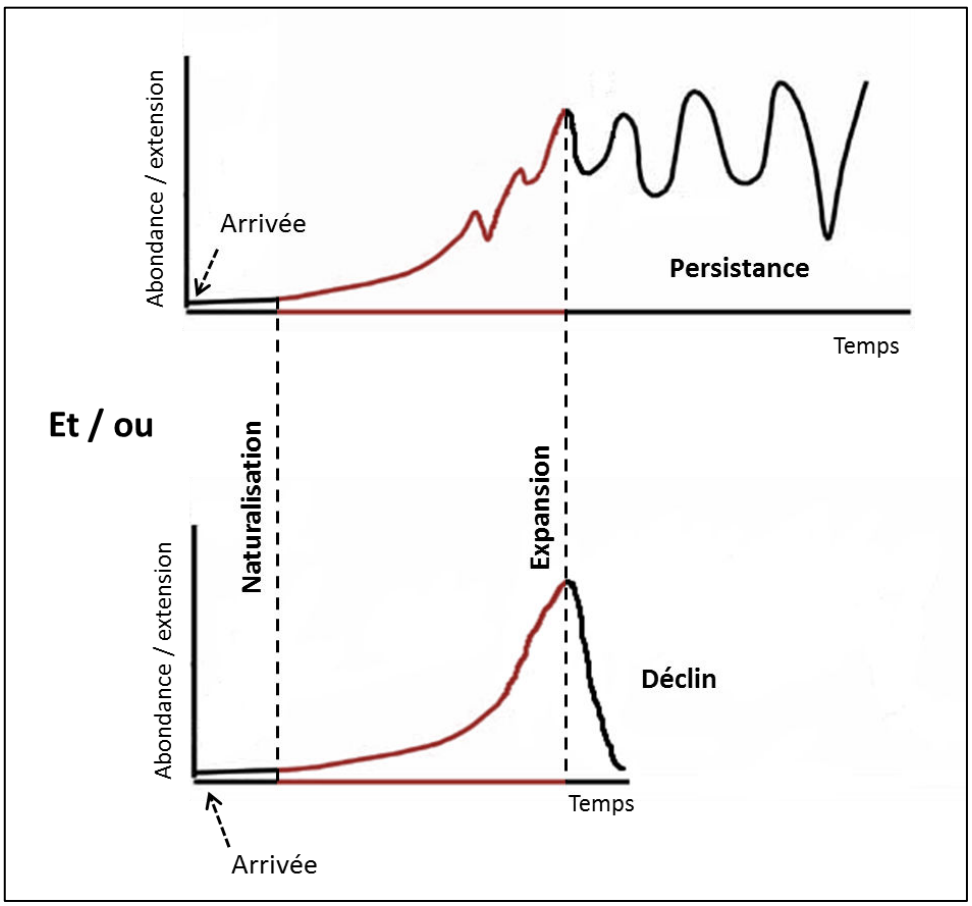

Fig. 2 Cinétique de l'abondance et/ou de l'extension de l'aire de répartition d'une espèce invasive initialement allochtone (issu de Boudouresque, 2003; Klein, 2011).

- **Les notions d'adaptation et d'acclimatation chez les espèces invasives**

L'acclimatation et l'adaptation (notions définies en introduction) des espèces exotiques à un nouvel environnement peut impliquer un certain nombre de processus liés à leur potentiel invasif incluant l'adaptation génétique par sélection sur la variation génétique permanente, les variations épigénétiques et phénotypiques notamment (Prentis et al., 2008). La plasticité phénotypique correspond à la capacité d'un génotype à exprimer des phénotypes diversifiés dans divers environnements. De manière générale, la sélection naturelle induit une augmentation de la fitness à travers les environnements. Des caractères morphologiques, physiologiques, comportementaux ou de croissance sont des traits qui influencent la fitness des populations. Or, la plasticité de ces traits peut permettre d'atteindre une fitness plus élevée dans des environnements variés (Huang et al., 2015). Plusieurs études se contredisent sur l'évidence d'une plasticité phénotypique significativement plus élevée chez les espèces invasives en comparaison des natives : les

deux cas ont été démontrés de manière empirique chez les végétaux (Davidson et al., 2011; Godoy et al., 2011; Huang et al., 2015).

Mais la vraie question que l'on est en droit de se poser est la suivante telle qu'énumérée par Huang et al. (2015) : quelles peuvent être les conséquences d'une plasticité plus élevée sur l'évolution de la fitness pour les espèces exotiques?

Le bénéfice adaptatif de cette plasticité vis-à-vis de la fitness n'est pas toujours avéré. Davidson et al. (2011) ont montré que les espèces invasives peuvent présenter parfois un gain de fitness en comparaison des espèces natives lorsque de nombreuses ressources sont disponibles. Au contraire, en conditions de stress ou de ressources limitées, les espèces natives montrent une réponse adaptative de la fitness plus probablement que les espèces invasives. Une plus forte plasticité phénotypique n'est pas synonyme de gain de fitness, caractère prédisposant pour devenir invasive (Davidson et al., 2011).

D'autre part, le succès d'une espèce introduite durant sa phase d'expansion (Figure 2) peut être expliqué en partie par le fait que dans ce nouvel environnement, l'espèce introduite est libérée de ces « ennemis natifs » (herbivores, parasites, maladies ou encore prédateurs) qui régulent la taille des populations de l'espèce dans son aire d'origine (Blossey, 2011). Cette idée est appelée **« enemy release hypothesis » ou ERH**. Grâce à une méta-analyse, Liu et Stiling (2006) ont mis en évidence, que la richesse en insectes herbivores est significativement plus élevée dans la zone native que la zone envahie et ce, de manière claire pour les herbivores spécialistes et les insectes se nourrissant des parties reproductives des plantes présentes sur zone. De plus, la diminution d'herbivores spécialistes au sein des populations invasives autorise l'allocation de moins d'énergie dans la protection contre ces herbivores spécialistes et ainsi l'allocation de plus d'énergie dans la croissance et la reproduction. D'un autre côté, cette énergie peut être allouée à une plus forte protection vis-à-vis des herbivores généralistes, comme montré chez la plante herbacée, *Senecio jacobaea* (Joshi and Vrieling, 2005). L'hypothèse de l'ERH a été largement débattue et pondérée (Heger and Jeschke, 2014) afin d'expliquer le succès des espèces invasives.

Ainsi si l'on intègre la théorie de l'ERH, les espèces invasives peuvent rencontrer des conditions plus favorables de croissance que dans leur zone native lorsqu'elles colonisent un nouvel environnement. Huang et al. (2015) supposent alors que tous les facteurs (tels que

l'absence des ennemis natifs, *i.e.* théorie de l'ERH), qui atténuent les stress rencontrés dans la région d'introduction diminueraient les coûts de la plasticité et augmenteraient les bénéfices qu'elle peut engendrer. Dans un environnement favorable, les organismes présenteraient ainsi une plasticité plus élevée (favorisée vers l'évolution d'une plasticité adaptative) que ceux se trouvant dans des conditions stressantes ce qui expliqueraient pourquoi certaines études ont observé des différences de plasticité entre espèce non-native et native, cette plasticité étant intimement reliée aux conditions environnementales dans l'aire d'introduction (Huang et al., 2015). Lande (2015) complète également cette hypothèse en avançant une augmentation transitoire de la plasticité lors de la colonisation d'un nouvel environnement : une augmentation initiale rapide de la plasticité entraînant une accélération de l'évolution vers un nouveau phénotype optimal suivi d'une faible assimilation génétique du nouveau phénotype et d'une réduction de la plasticité. Cette évolution vers un nouveau phénotype (présentant une variation des traits morphologiques par exemple), induite par l'environnement biotique et abiotique, et rapide sur une échelle écologique, a déjà été mise en évidence (Buswell et al., 2011). Cette hypothèse expliquerait les différentes phases d'expansion observées de l'introduction à l'invasion d'une espèce exotique et complète celle émise par Huang et al. (2015). Ainsi, une augmentation de la plasticité suite à une colonisation dépendrait de la différence entre le phénotype optimal dans le nouvel environnement avec le phénotype ancestral de la région native, mais aussi de l'environnement lui-même, du coût de la plasticité qui est fonction des conditions environnementales pour l'espèce exotique et du temps écoulé depuis l'établissement (Lande, 2015). Ceci expliquerait également l'invasion rapide d'une espèce exotique sachant qu'il est maintenant connu que les espèces invasives s'adaptent rapidement et que cette adaptation ne semble pas limitée par la variation génétique (Bock et al., 2015). Ces hypothèses sont à confirmer empiriquement mais de telles études demandent une connaissance approfondie des modèles biologiques étudiés, de leur histoire de colonisation ainsi que des paramètres environnementaux. Ces hypothèses seront discutées vis-à-vis des résultats apportés dans les autres parties de ce manuscrit.

- **Quels sont impacts des espèces invasives sur les espèces natives ?**

Depuis une dizaine d'années, de nombreuses travaux ont cherché à comprendre quel étaient les implications des espèces invasives sur les communautés autochtones de

l'environnement colonisé, sur les facteurs physico-chimiques caractéristiques de cet environnement et également à plus large échelle sur les fonctions de l'écosystème (Davidson et al., 2015; Schaffelke et al., 2006; Williams and Smith, 2007). Les écosystèmes présentant une faible diversité spécifique sont plus sensibles aux pressions induites par les activités humaines telles que l'introduction d'espèces exotiques (Cabioc'h et al., 2006). Or, l'introduction d'espèces exotiques représente une menace pour la biodiversité des écosystèmes marins en exerçant une pression sur ces environnements (Davidson et al., 2015). L'étude des impacts des espèces introduites est maintenant reconnue comme une priorité en recherche (Schaffelke and Hewitt, 2007). Malgré cet intérêt grandissant de la communauté scientifique pour les invasions biologiques, les impacts de moins de 30% des espèces allochtones ont été étudiés (Davidson et al., 2015). Ces impacts seraient aussi sous-estimés du fait de la nature des études menées, souvent de par la taille de l'échantillonnage ou des variations biologiques inhérentes à toute expérience (Davidson and Hewitt, 2014).

Les macrophytes marins invasifs perturbent l'environnement envahi, dont les impacts sont classifiés de la manière suivante, en distinguant les impacts écologiques et évolutifs d'une part et les impacts économiques et sociétaux d'autre part (Davidson et al., 2015; Ojaveer et al., 2015; Schaffelke and Hewitt, 2007). Les impacts écologiques et évolutifs sont multiples et décomposés en différentes catégories (Schaffelke and Hewitt, 2007) :

- **La compétition directe ou indirecte avec la biocénose native par monopolisation de l'espace et par des variations de la composition des communautés** : Il s'agit de l'impact majeur des macrophytes marins qui présentent dans la plupart des études une abondance élevée, souvent corrélée à une baisse de l'abondance ou de la diversité des espèces végétales autochtones (Davidson et al., 2015).
- **Les effets à des niveaux trophiques supérieurs** (par exemple sur les herbivores, la faune associée ou encore en induisant une toxicité)
- **Une modification du biotope** en entraînant un changement de sa structure ou une accumulation de la sédimentation
- **Une modification des processus régissant l'écosystème natif** entre autre par l'altération des relations trophiques

- **Des effets génétiques** au sein des espèces (introgression) ou entre les espèces (hybridation)

D'autre part, les effets économiques et sociétaux peuvent être directs ou indirects (Schaffelke and Hewitt, 2007) :

- Impacts directs :
    - le coût de la perte des fonctions ou de la valeur de l'écosystème
    - Impact sur l'aménité environnementale
    - Impact sur la santé humaine
- Impacts indirects :
    - Frais de gestions de ces invasions biologiques d'origine gouvernementale ou non
    - Coût de la recherche sur les espèces introduites
    - Coûts de la limitation de la colonisation, des suivis et mesures de contrôle
    - Coût des campagnes de sensibilisation

Ces impacts risquent d'être évolutifs sachant que l'on se situe dans une période de changement climatique, dans laquelle d'autres facteurs induits directement par les activités humaines (tels l'altération des usages des territoires) impactent les environnements et n'épargnent pas les environnements marins. Leur caractère dynamique va engendrer une complexification de ces impacts sur les écosystèmes où plusieurs facteurs interagissent potentiellement. Le changement climatique avec les invasions biologiques sont reconnus comme les deux facteurs prépondérants qui menacent l'équilibre des écosystèmes actuels (Bellard et al., 2013; Diez et al., 2012; Hellmann et al., 2008; Mooney and Cleland, 2001).

2. Les invasions biologiques dans un contexte de changement climatique

Qu'est-ce que le changement climatique ?

Le climat varie naturellement de manière cyclique à travers différentes échelles de temps, que ce soit suivant des cycles saisonniers, des cycles interannuels comme l'ENSO (El Niño Southern Oscillation), des cycles inter-décennaux, ou encore suivant des variations sur des milliers d'années telles que les transitions entre les aires glaciaires et interglaciaires (Harley et al., 2006). Il est dépendant du bilan thermique de la Terre. En effet, le soleil émet de l'énergie sous forme de radiations de courtes longueurs d'onde en direction de la Terre appelé « flux incident ». Pour moitié, ce flux incident va être absorbé par l'atmosphère et réfléchi par les nuages, ainsi que par certains constituants de l'atmosphère tels que les aérosols (Figure 3).

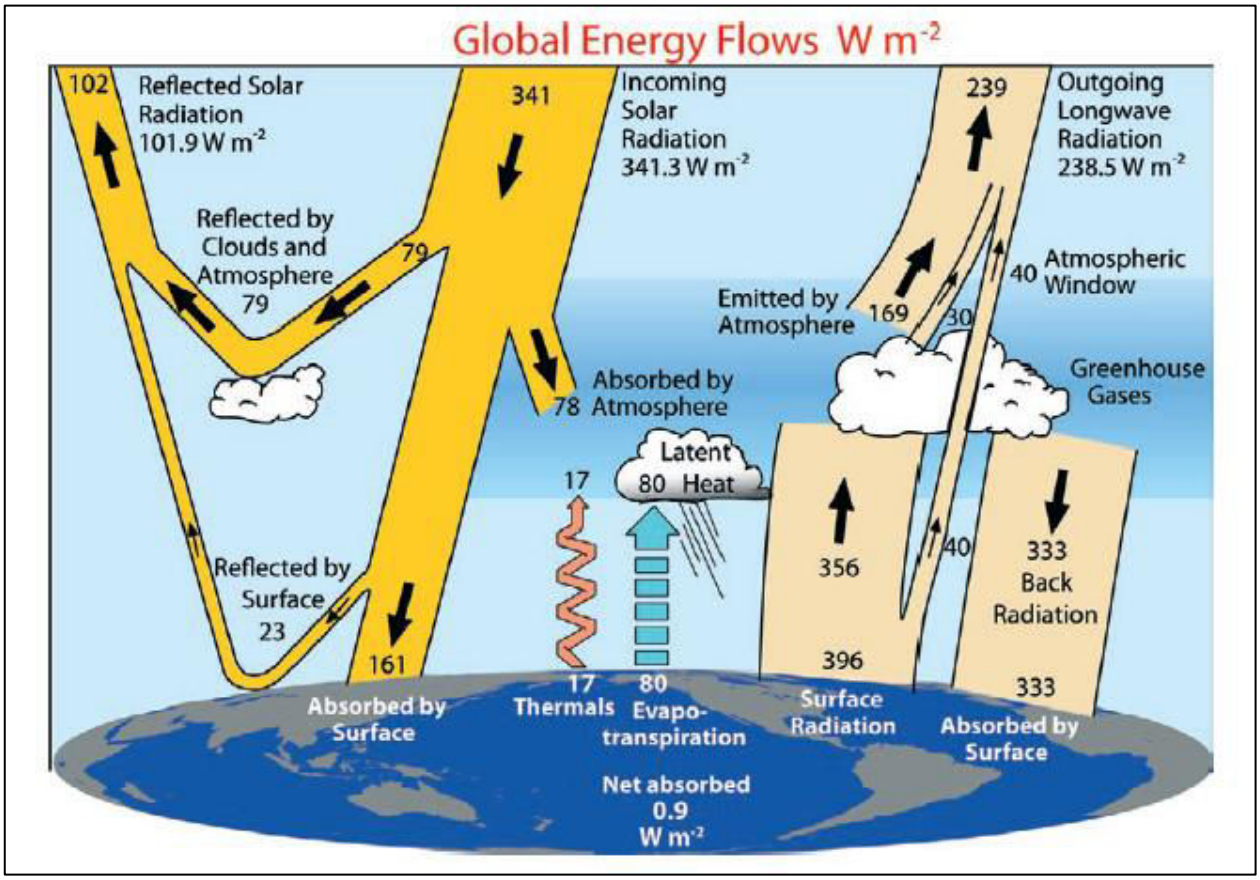

Fig. 3 Bilan énergétique global de la Terre moyenné sur la période de Mars 2000 à Mai 2004 ($W.m^{-2}$) (issu de Trenberth et al., 2009). La largeur des flèches représente schématiquement l'importance des flux énergétiques.

L'autre moitié de ce flux atteint la surface terrestre et est absorbée pour sa grande majorité par celle-ci. L'énergie ainsi absorbée est réémise par la surface terrestre sous forme de rayonnements infra-rouges thermiques correspondant à des radiations de grande longueur d'onde. Des gaz présents dans l'atmosphère ont la capacité d'absorber ces radiations infra-rouges thermiques et de les réémettre vers la surface de la Terre : ce sont les gaz à effet de serre (Guérin, 2006; Kiehl and Trenberth, 1997). Les principaux gaz à effet de serre sont la vapeur d'eau, le dioxyde de carbone (CO_2), l'oxyde nitreux (N_2O), le méthane (CH_4) et l'ozone (O_3) (Bernstein et al., 2007). Ce phénomène entraîne un effet de serre naturel permettant le maintien de la chaleur générée par les radiations infra-rouge dans le système troposphère / surface. Ainsi, la température moyenne de la surface terrestre atteint 14°C contre -19°C dans la troposphère (Bernstein et al., 2007). Une augmentation de la concentration en gaz à effet de serre engendre une opacification de l'atmosphère, qui résulte en un forçage radiatif dû à un déséquilibre du système global de balance énergétique Terre/Atmosphère (Haywood and Schulz, 2007). *In fine*, une augmentation de la concentration des gaz à effet de serre induit un effet de serre renforcé (Bernstein et al., 2007).

Précisément, le forçage radiatif est défini par le rapport du GIEC de 2007, comme la variation de l'éclairement énergétique net (différence entre l'éclairement descendant et l'éclairement ascendant, exprimée en $W.m^{-2}$) à la tropopause, qui est due à une modification d'un agent externe du changement climatique. Ainsi, un forçage radiatif peut être induit par des facteurs naturels tels que le volcanisme ou la variation du rayonnement solaire. Mais les variations naturelles enregistrées ne peuvent expliquer à elles seules le dérèglement climatique observé dès à présent (Bernstein et al., 2007).

Depuis l'ère préindustrielle, l'Homme est devenu une composante importante du climat. En effet, les activités humaines engendrent l'émission importante de gaz à effet de serre, principalement par la combustion de combustibles fossiles et de biomasse pour produire de l'énergie, mais aussi à cause de la déforestation, qui diminue le stockage du CO_2, et des activités agricoles et industrielles (Bernstein et al., 2007). Par exemple, les concentrations en CO_2 atmosphérique ont évolué de 280 ppm à l'ère préindustrielle (en 1800) à 367 ppm en 1999 et pourraient atteindre 540 à 970 ppm en 2100 selon le scénario

climatique considéré (Guérin, 2006; Harley et al., 2006). Ces dernières concentrations dépassent les variations naturelles observées durant les dernières 650 000 années (Bernstein et al., 2007). Ces émissions de source anthropogénique s'additionnent aux émissions naturelles et induisent une intensification de l'effet de serre expliquant le réchauffement climatique (Bernstein et al., 2007; Harley et al., 2006). Seuls les modèles intégrant les forçages anthropogéniques c'est-à-dire en tenant compte des émissions de gaz à effet de serre, permettent de simuler les variations climatiques observées actuellement (Bernstein et al., 2007). Le forçage radiatif est calculé comme la différence par rapport à l'année 1750 et se rapporte à une valeur moyenne annuelle à l'échelle du globe (Bernstein et al., 2007). Ce forçage radiatif anthropogénique permet de quantifier le changement climatique (Haywood and Schulz, 2007). En fonction des projections d'émissions de gaz à effet de serre d'ici à 2100, et ainsi du forçage radiatif exercé, plusieurs scénarios climatiques ont été modélisés. Ces différents scénarios sont présentés en Figure 4.

Les différents scénarios climatiques dépendent des différentes voies de développement du monde de demain suivant de multiples facteurs démographiques, économiques et technologiques et estiment les émissions de gaz à effet de serre qui en résultent. Ces prévisions tiennent compte uniquement des politiques actuelles sur le climat (Bernstein et al., 2007; IPCC, 2001, 2013). De la même façon, en fonction des scénarios et à partir des forçages radiatifs projetés, l'augmentation de la température moyenne de surface pourrait varier de 1,4 à 5,8 °C entre 1990 et 2100 (IPCC, 2001).

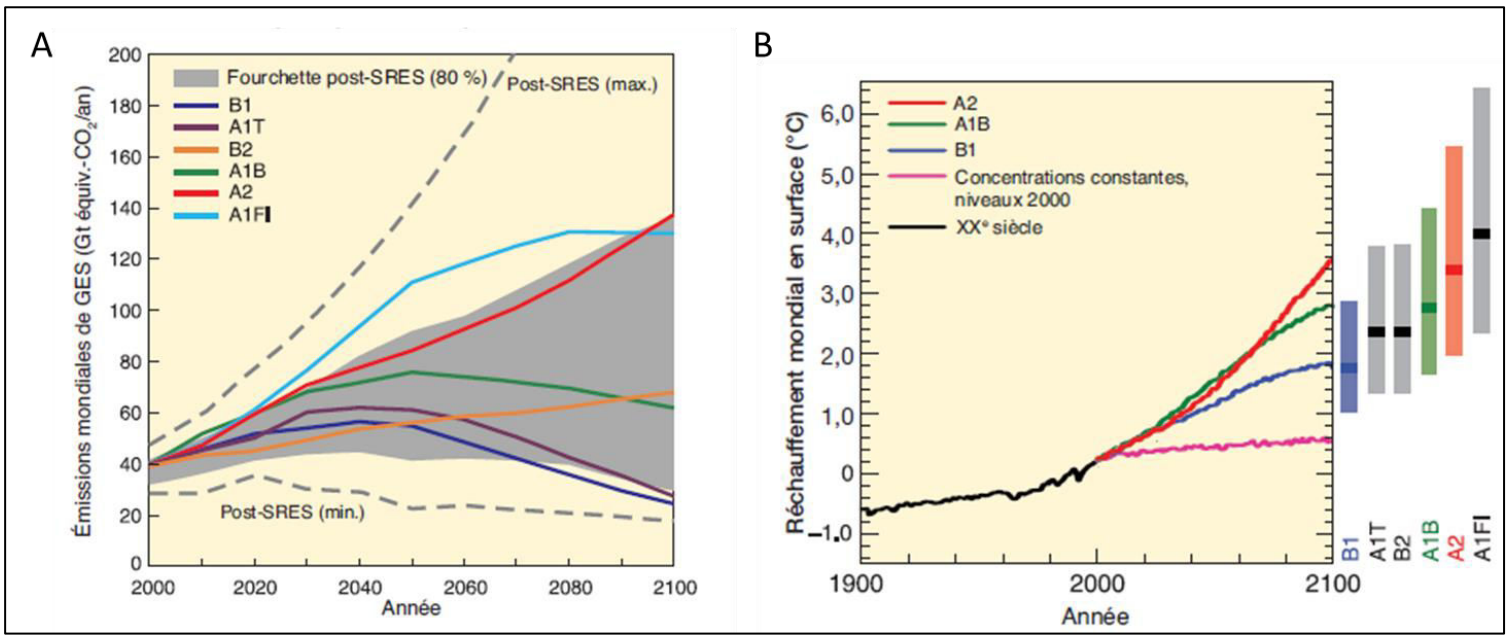

Fig. 4 **A**- Emissions mondiales de gaz à effet de serre (en Gt éq.CO_2. an^{-1}) selon six scénarios de référence expliqués ci-dessous et l'intervalle au 80è percentile des scénarios publiés après le rapport du SRES (Special Report on Emissions scenarios). Les courbes en pointillés délimitent des variations de l'ensemble des scénarios post-SERS. **B**- Moyennes mondiales multimodèles du réchauffement de la surface de la Terre en comparaison de la période de 1980 à 1999. Les barres à droite représentent en foncé les valeurs les plus probables et en clair l'intervalle de probabilité selon les six scénarios pour la période de 2090 à 2099 en comparaison de 1980 à 1999. Ces graphiques sont issus du rapport du GIEC (Bernstein et al., 2007).

Description des six scénarios de référence du SERS :

- **Scénario A1** : un monde caractérisé par une croissance économique très rapide et un pic de la population mondiale au milieu du siècle, ainsi que la mise au point rapide de nouvelles technologies efficaces.
  Ce scénario est décomposé en trois sous-groupes selon les sources d'énergie utilisées par ces nouvelles technologies : **A1FI** (principalement d'origine fossile), **A1T** (non fossile) et **A1B** (en équilibrant les sources fossiles et non fossiles).
- **Scénario B1** : un monde présentant une démographie similaire à A1, mais avec une évolution plus rapide des structures économiques et vers une économie de services et d'information.
- **Scénario B2** : monde caractérisé par des croissances démographique et économique intermédiaires, qui privilégie les actions locales pour une durabilité économique, sociale et environnementale.
- **Scénario A2** : monde présentant une forte croissance démographique couplée à un faible développement économique et des progrès technologiques ralentis

Quels effets du changement climatique sur les espaces côtiers ?

Cette augmentation de la concentration des gaz à effet de serre va engendrer une cascade de conséquences physiques et chimiques très variées (Harley et al., 2006). Les impacts abiotiques du changement climatique sur les estrans (synthétisés sur la Figure 5) vont façonner les habitats des écosystèmes côtiers. Dans cette partie seront abordées les conséquences les plus pertinentes, vis-à-vis des travaux effectués durant cette thèse, c'est-à-dire les conséquences qui vont impacter les milieux aquatiques et les estrans c'est-à-dire la zone littorale située dans la zone de balancement des marées, en particulier.

L'augmentation de la température de surface du globe est la première conséquence du changement climatique comme expliqué précédemment. Cette augmentation de la température de surface couplée à celle du CO_2 atmosphérique induit la variation d'un certain nombre de facteurs abiotiques décrits ci-dessous. L'augmentation du CO_2 atmosphérique va générer une acidification des océans. En effet, les océans absorbent environ un tiers des émissions de CO_2 liées aux activités humaines (Hoegh-Guldberg and Bruno, 2010). Cette absorption a entraîné une acidification de la surface des océans de l'ordre de 0,02 unité de pH par décennie ces trente dernières années (Doney et al., 2009; Hoegh-Guldberg and Bruno, 2010). Les prédictions annoncent une diminution du pH plus importante que toutes les variations de pH observées depuis 300 millions d'années à partir d'enregistrements géologiques (Caldeira and Wickett, 2003). Cette diminution du pH induit également la baisse des niveaux de saturation de minéraux tels que le carbonate de calcium. Si cette diminution du pH se poursuit, les coraux, et autres organismes calcaires (algues, mollusques, etc) ainsi que certaines espèces planctoniques pourront difficilement maintenir leur squelette externe composé de carbonate de calcium (Orr et al., 2005). D'autre part, le réchauffement climatique étant hétérogène à la surface du globe (Figure 6), il entraîne la formation de gradients atmosphériques plus importants le long des côtes résultant en une intensification des phénomènes de tempête. Ce gradient atmosphérique pourrait engendrer une intensification des upwellings mais les processus mis en jeu sont encore mal connus. Cette augmentation de la température atmosphérique induit également, par voie de conséquence, une augmentation de la température des océans.

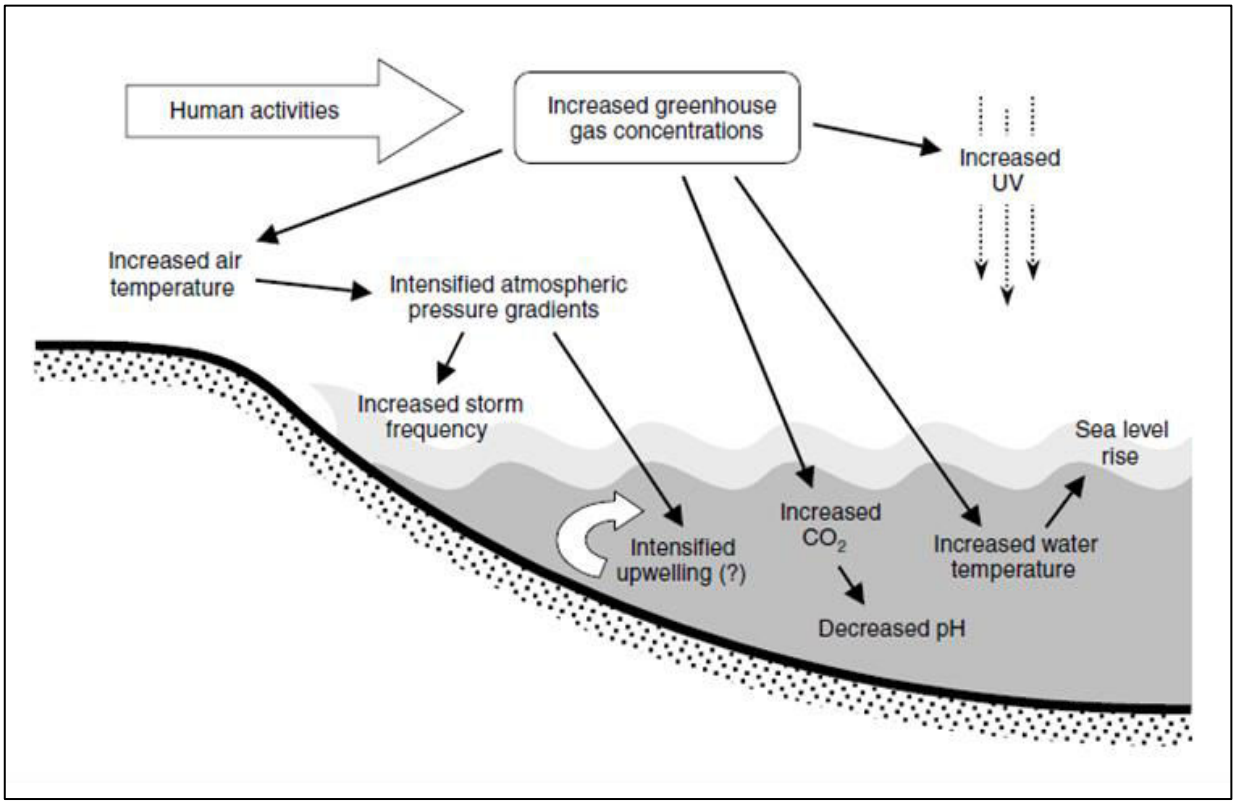

Fig. 5 Changements abiotiques (physique et chimique) impactant les milieux côtiers liés au changement climatique. Le point d'interrogation indique que la relation entre le changement climatique et une intensification des upwellings reste incertaine, issu de Harley et al. (2006).

Ce phénomène génère une expansion thermique des océans. S'ajoutant à la fonte des glaciers et des calottes glaciaires, le niveau des océans s'élèvera de 0,09m à 0,88m d'ici à 2100 en comparaison de 1990 (IPCC, 2001).

Cette augmentation du niveau de la mer va entraîner une modification du trait de côte et ainsi impacter tout l'environnement biotique des estrans côtiers et des zones intertidales en particulier (Ross et al., 2000). En effet, dans la zone de balancement des marées, le biota et notamment les végétaux marins sont stratifiés en fonction de la hauteur d'eau et de leurs capacités de tolérance à l'émersion (Cabioc'h et al., 2006).L'augmentation des gaz à effet de serre atmosphérique induit également une réduction de la couche d'ozone. L'absorption des radiations ultraviolettes (UV) est plus faible et une augmentation des taux de radiations UV a été observée notamment aux pôles, la couche d'ozone étant naturellement plus mince aux hautes latitudes.

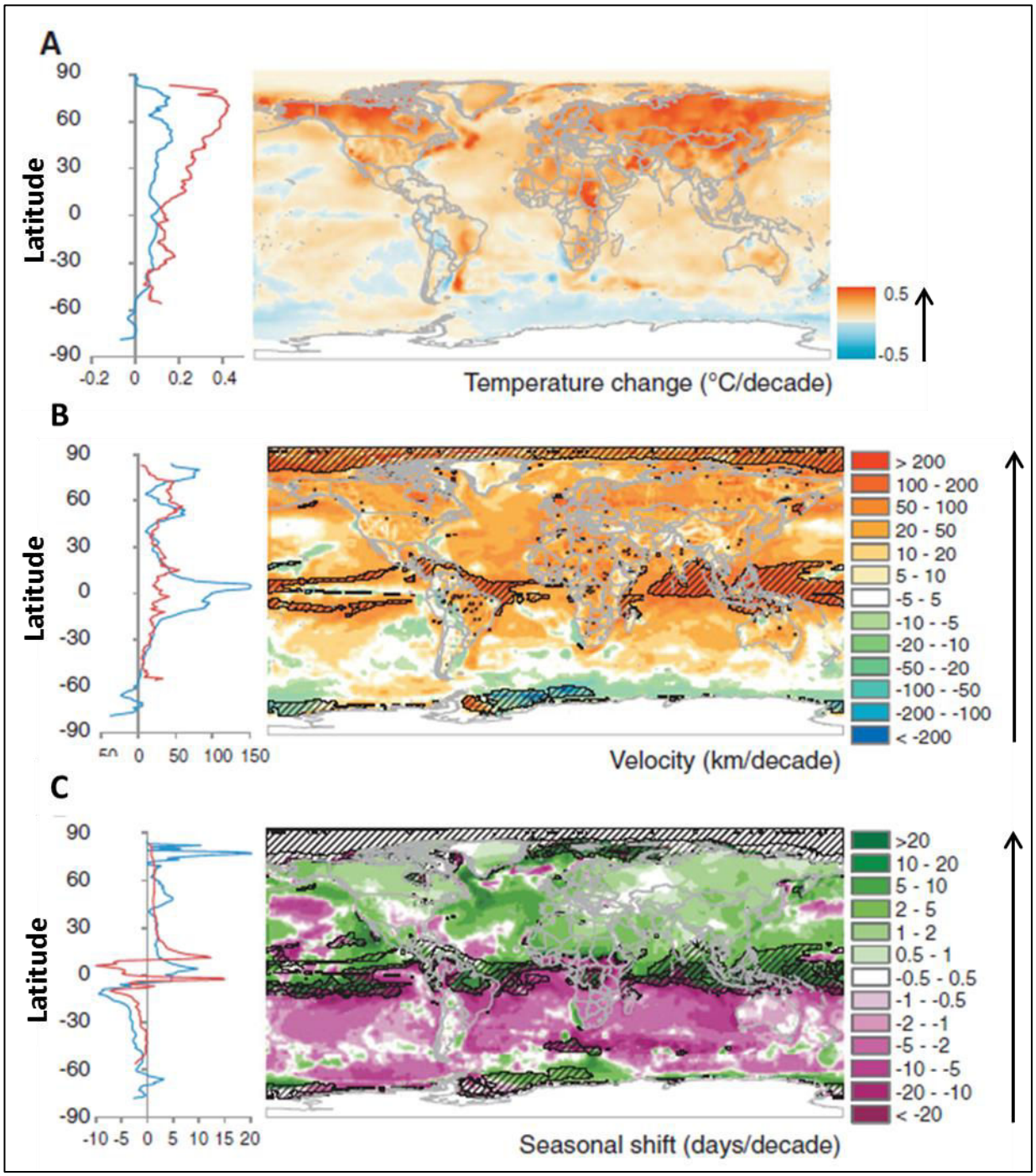

Fig. 6 **A** - Tendances thermiques des continents et des océans de 1960 à 2009 et courbes médianes des latitudes (bleu : océan ; rouge : continent). **B** - Vitesse du changement climatique (en km/décennie), vitesse à laquelle les isothermes se déplacent : vitesse positive dans les zones se réchauffant et vitesse négative dans les zones se refroidissant. **C** - Décalage saisonnier (en jours/décennie) : changement dans le temps des températures mensuelles en Avril (positif quand le décalage avance et négatif quand le décalage recule) ; Zones hachurées : zones où la variation de température est faible (<0,2°C/mois) mais où le décalage saisonnier peut être important, issu de Burrows et al. (2011).

Mais les politiques climatiques actuelles fonctionnent et ainsi, aux moyennes latitudes, des taux de radiations UV similaires à ceux enregistrés en 1980 devraient être retrouvés d'ici à 2050. Néanmoins, il est prédit que ce processus (de retour aux taux de radiations enregistrés en 1980) sera plus lent aux latitudes polaires. Cependant, la couche d'ozone affectant le changement climatique et vice-versa, les modèles prédisent une diminution du taux de radiations UV de 5% pour les moyennes latitudes, jusqu'à 20% pour les hautes latitudes, ainsi qu'une augmentation de 2 à 3% aux tropiques (McKenzie et al., 2011). Ces prédictions illustrent la complexité des processus mis en jeu. Le milieu océanique et en particulier les espèces du milieu intertidal sont sensibles aux radiations UV. Les espèces aquatiques utilisent de nombreuses stratégies de photoprotection vis-à-vis des radiations UV. Ce stress additionnel engendre un conflit de pression de sélection pour les espèces impactées par les radiations UV (Häder et al., 2007).

L'élévation moyenne des températures étant la conséquence majeure induite par le changement climatique, les variations thermiques observées et leur incidence sur les biotas des écosystèmes marins sont développées dans le paragraphe suivant.

- **Variations thermiques et incidences biotiques** :

Des études ont déjà mis en évidence un réchauffement global de 0,8°C (de la température de l'air) au cours du siècle dernier. Le XX^{ème} siècle est caractérisé par un réchauffement global lent avec de fortes fluctuations de 1900 à 1975 suivi d'un réchauffement plus intense de l'ordre de 0,2°C tous les 10 ans ces trois dernières décennies. De plus, ce réchauffement n'est pas homogène sur toute la surface du globe (Hansen et al., 2006; Hansen and Sato, 2016). L'effet est plus marqué en particulier au niveau des continents en comparaison des océans (Figure 6) et plus important aux hautes latitudes de l'hémisphère Nord (Levitus et al., 2000). Cependant, malgré un réchauffement plus lent des océans, la vitesse de décalage des isothermes ainsi que la variation saisonnières des températures est plus importante au niveau des océans pour certaines latitudes (Burrows et al., 2011).

Or, la distribution biogéographique des espèces océaniques est contrôlée par le climat (Bartsch et al., 2012). En effet, la température est le principal facteur abiotique qui contrôle les limites géographiques des algues marines (Figure 7) (Briggs, 1995). Plus précisément, l'interaction de la température et de la longueur du jour permet la

synchronisation des différentes étapes du cycle de vie des végétaux marins et régente leur distribution. La présence d'une algue dans une aire biogéographique donnée est donc principalement déterminée par la tolérance physiologique de son cycle de vie. Il existe trois types de températures limites définissant l'aire de distribution d'une espèce : la **température létale** définie par la capacité de l'espèce à survivre pendant la saison défavorable, la **température limite de reproduction** déterminée par la capacité de l'espèce à se reproduire durant la saison favorable puis la **température limite de croissance** déterminée par la capacité de l'espèce à se reproduire durant la saison favorable (Bartsch et al., 2012). Le forçage climatique s'exerce de manière plus forte au niveau des limites d'aire de répartition des espèces (IPCC, 2001, 2013) du fait que celles-ci se développent aux limites de leur tolérance thermique.

Le réchauffement climatique induit ainsi, à l'échelle du globe, un déplacement vers les hautes latitudes des différentes limites des aires biogéographiques (Figure 7) entraînant un décalage des biotas des écosystèmes côtiers vers les latitudes Nord (Bartsch et al., 2012). Une progression moyenne de 19 km par an vers le Nord est observée pour les espèces marines contre 0,6 km par an pour les espèces terrestres (Jueterbock et al., 2013; Sorte et al., 2010a). En effet, les espèces intertidales, et notamment les algues, constituent des modèles biologiques privilégiés pour l'étude du réchauffement climatique. Ce sont des espèces sentinelles du changement climatique, notamment du fait que leur distribution soit intimement corrélée à leur tolérance thermique. Les espèces intertidales présentent généralement une espérance de vie plus courte que les espèces terrestres, étant principalement des organismes ectothermes avec des stades vagiles et sessiles, qui sont périodiquement exposés à des extrêmes de température (Helmuth et al., 2002; Lima et al., 2007). Ainsi le changement climatique est variable en fonction de la latitude en terme d'amplitude et de vitesse (Figure 6) mais également en fonction des saisons (Bartsch et al., 2012).

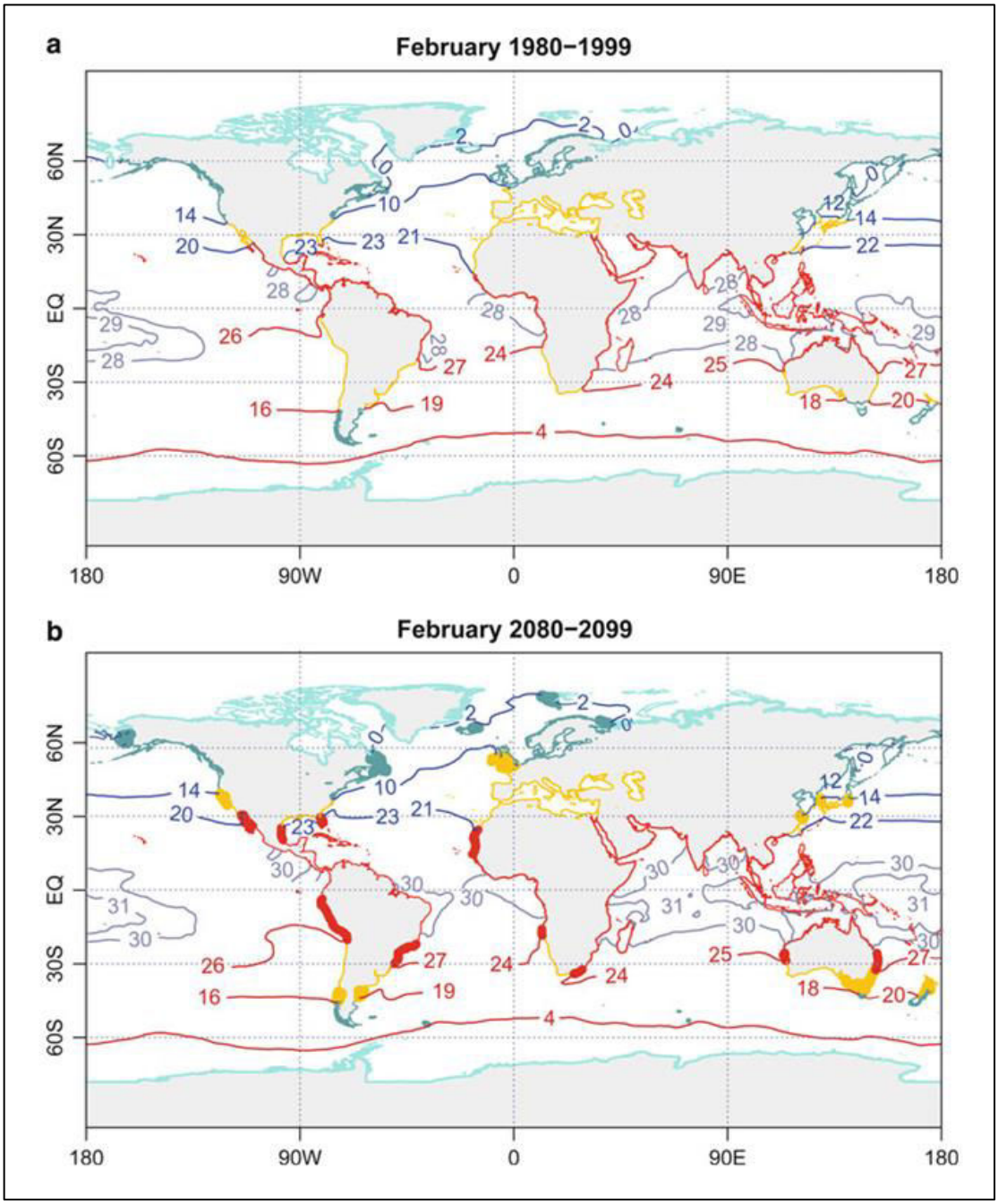

Fig. 7 Modifications et déplacements prévisionnels des régions biogéographiques actuelles définies par Briggs (1995) en raison du changement climatique d'après les moyennes actuelles des isothermes de la surface des océans au mois de Février entre la période de 1980 à 1999 et celle projetées pour la période de 2080 à 2099. (a) Moyennes actuelles des isothermes de la surface des océans qui délimitent les différentes aires biogéographiques. (b) Moyennes prévisionnelles des isothermes de la surface des océans entraînant une nouvelle délimitation des aires biogéographiques. Les variations attendues sont indiquées par une ligne de côte en gras. Les différentes aires biogéographiques sont : les régions polaires (en turquoise), les régions tempérées froides (en bleu-vert), les régions tempérées chaudes (en jaune), puis les régions tropicales (en rouge), issu de Bartsch et al. (2012).

Ainsi, Helthmuth et al. (2002) ont mis en évidence l'effet couplé du temps d'émersion et du climat terrestre sur les espèces intertidales. L'exposition à des extrêmes de température est ainsi variable dans le temps, entraînant non seulement un mouvement des espèces vers le Nord mais également une série d'extinctions locales (Helmuth et al., 2002). De plus, les espèces intertidales ne répondent pas de la même façon à ce réchauffement climatique. Lima et al. (2007) ont mis en évidence une différence marquée entre les espèces d'algues d'eaux froides et celles d'eaux chaudes le long des côtes portugaises depuis les années 1950. Ils ont observé une migration des espèces d'algues d'eaux chaudes vers le Nord alors que les algues d'eaux froides ne montrent pas de tendance marquée (Lima et al., 2007). Les espèces sont plus ou moins résilientes face à un stress. Les algues d'eaux chaudes présentent un cycle de vie aux caractéristiques plus opportunistes que les algues d'eaux froides (croissance plus rapide, reproduction plus précoce et espérance de vie plus courte) ce qui pourrait expliquer les différences de réponses observées (Lima et al., 2007).

Hoegh-Guldberg and Bruno (2010) expliquent que le changement climatique induit une baisse de la productivité océanique, une modification de la dynamique des réseaux trophiques, une réduction de l'abondance d'espèces ingénieures, un décalage des populations (comme expliqué ci-dessus) et une augmentation de l'incidence des maladies. Tout ceci entraîne le risque d'une transformation profonde et irréversible des écosystèmes marins en particuliers. On en déduit que la réponse des biotas intertidaux face à une augmentation des températures aériennes et océaniques est particulièrement complexe et difficilement prévisible à petites échelles (Helmuth et al., 2002; Hoegh-Guldberg and Bruno, 2010) car de nombreux facteurs biotiques et abiotiques façonnent localement les populations (Bartsch et al., 2012; Santelices et al., 2009). Les effets les plus prononcés sont attendus dans les zones de transition de régions biogéographiques comme par exemple le long des côtes européennes entre la région tempérée chaude et froide (Bartsch et al., 2012), où se situe la Bretagne. Or cette région correspond à un « hotspot » majeur de diversité biologique pour les organismes marins et particulièrement pour les végétaux marins.

Les invasions biologiques dans un contexte de réchauffement climatique ?

Au vu de l'ensemble de ces données, on en conclut que les invasions biologiques et le réchauffement climatique sont des forçages anthropiques clés impactant les écosystèmes et en particulier les écosystèmes marins. Mais est-ce que ces deux forçages anthropiques sont-ils indépendants ou non ? Il est difficile de différencier les effets du changement climatique des processus d'invasion tels que l'apport en propagules par exemple, s'agissant d'un facteur qui ne peut être contrôlé dans la plupart des études sur le terrain (Sorte et al., 2010b). Quelques études ont illustré l'interaction du changement climatique et des espèces invasives (Bellard et al., 2013; Diez et al., 2012; Rahel and Olden, 2008; Sorte et al., 2010b) et inversement (Qiu, 2015). Ainsi, le changement climatique affecte, à de multiples niveaux, les processus d'invasions en influant sur l'efficacité de l'ensemble des filtres déterminant une invasion biologique, tels que l'introduction, la naturalisation et le potentiel invasif des espèces exotiques (Rahel and Olden, 2008) et comme cela a été montré en Figure 1.

Le changement climatique offre aussi de nouvelles possibilités d'introduction. Walther (2010) suppose que le changement climatique permettrait aux espèces invasives de se développer dans des zones où elles ne pouvaient survivre ni se reproduire auparavant. Comme la température est un facteur clé de la distribution des espèces (comme expliqué dans les paragraphes précédents), la survie d'espèces exotiques provenant de régions plus chaudes et installées dans de nouvelles zones plus froides dépend localement de l'impact du réchauffement climatique, créant des zones de refuge ou « hotspot » pour ces espèces (Rahel and Olden, 2008; Walther, 2010). De plus, le changement climatique par l'intensification de phénomènes climatiques extrêmes tels que la sècheresse ou les tempêtes, améliore le transport des propagules d'espèces exotiques dans de nouvelles zones (Diez et al., 2012; Walther, 2010). En effet, ces phénomènes en stressant localement les écosystèmes diminuent la résistance biotique des espèces natives face à l'établissement de nouvelles espèces exotiques et parfois même mettent les espèces invasives déjà établies en situation de désavantage compétitif (Diez et al., 2012). Dans ce contexte, le rapport de la FAO soulève une question pertinente (Cochrane et al., 2009) : Comment les populations et les sociétés économiques vont-elles réagir aux conséquences du changement climatique ? Ainsi, si on intègre l'adaptation des activités humaines au changement climatique, les effets attendus seront amplifiés. Le changement climatique peut entraîner une modification du

commerce dans certaines régions du monde (Hellmann et al., 2008). Par exemple, en raison de l'adoucissement des températures, les aires géographiques présentant des températures propices pour l'aquaculture d'espèces d'eaux chaudes ainsi que la culture de poissons tropicaux vont s'étendre. La construction de réservoirs ou de bassins d'extérieurs pourront s'intensifier ; or ce sont des sources importantes d'espèces invasives (Rahel and Olden, 2008). Le changement climatique peut modifier les modes de transport de l'Homme (Hellmann et al., 2008). Ainsi, par exemple, la fonte des calottes glaciaires en été offre de nouvelles voies de navigation saisonnière (Walther, 2010). Toutes ces conséquences (liste non exhaustive) sont propices à l'introduction de nouvelles espèces.

Le changement climatique facilite la vitesse de colonisation et le succès reproducteur des espèces invasives. Il modifie les interactions compétitives entre espèces invasives et natives. Les espèces introduites provenant de régions plus chaudes peuvent être actuellement limitées physiologiquement par leur température limite de reproduction, empêchant ainsi leur naturalisation. Des températures plus élevées leur permettraient d'avoir une phase de croissance plus longue notamment (Walther, 2010) et de devenir mature plus facilement. De plus, le changement climatique, en générant localement des stress, altère les dominances de compétitivité entre espèces natives et invasives (Rahel and Olden, 2008), ces dernières étant plus résilientes et résistantes à un stress thermique comme illustré chez des invertébrés marins (Sorte et al., 2010b). Ces auteurs ont démontré que le taux de survie et la croissance étaient plus élevés chez les espèces introduites en comparaison des espèces natives, et en particulier aux stades précoces. Cette hypothèse est également vérifiée dans le milieu naturel. Ces caractéristiques induisent la nécessité d'un suivi de la phénologie de ces espèces. Les espèces invasives ont de manière générale des aires de répartition plus importantes que les espèces natives indiquant leur capacité à tolérer une gamme plus large de conditions environnementales et notamment en terme de température (Dukes et al., 1999). Le changement climatique peut amplifier les facteurs biotiques comme une augmentation de la prédation ou une augmentation de la virulence de certaines maladies sur les espèces natives (Burge et al., 2014; Hellmann et al., 2008; Rahel and Olden, 2008).

Le changement climatique va altérer la distribution des espèces invasives déjà existantes (Hellmann et al., 2008). En regardant l'agrégation spatiale de 100 espèces

invasives selon les scenarios A1B et B2 du SRES (*cf.* Figure 4), Bellard et al. (2013) ont défini trois zones particulièrement sensibles aux invasions biologiques : l'Europe, le Nord-Est des Etats-Unis et l'Océanie (Bellard et al., 2013). Les chercheurs ont modélisé la variation de l'aire de distribution des 100 espèces invasives majeures autour du globe ("100 of the world worst invasive species"). Les espèces marines présentent les plus forts taux d'expansion ; les invertébrés aquatiques présenteraient une expansion de leur aire de distribution de près de 59% et les plantes aquatiques de 12% d'ici à 2100 (Figure 8).

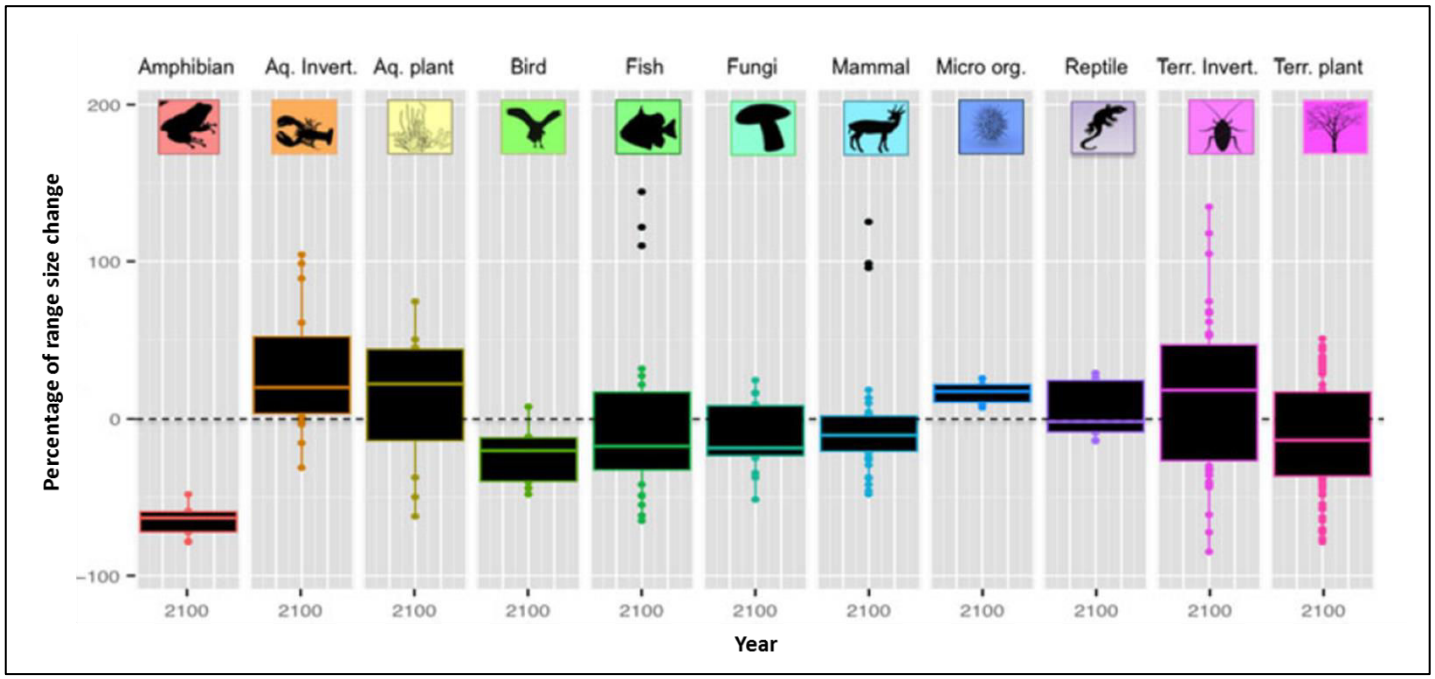

Fig. 8 Effet du changement climatique et des usages des territoires sur l'aire de distribution des espèces invasives d'après le scénario A1B du SERS pour chaque groupe taxonomique. Un total de 100 espèces invasives a été considéré dans cette étude (issu de Sorte et al. 2013).

Seuls les facteurs abiotiques ont été intégrés au modèle et ils ont supposé que le changement climatique et les changements d'utilisation des territoires étaient les seules sources responsables de la variation de l'aire de répartition des espèces invasives. Ils n'ont ainsi pas tenu compte des capacités de dispersion, des facteurs biotiques et des nouvelles opportunités d'introduction. Malgré ces limites, cette étude donne un aperçu des groupes taxonomiques favorisés par le changement climatique et des régions du monde les plus sensibles, en illustrant l'interaction entre le changement climatique et les invasions biologiques. Une autre équipe, Sorte et al. (2013) confirment l'hétérogénéité de l'effet du

changement climatique entre les écosystèmes terrestres et aquatiques en effectuant une méta-analyse. Ils ont montré que les espèces invasives et natives terrestres répondaient de manière similaire, tandis que les espèces invasives en milieu aquatique étaient largement favorisées lors d'une augmentation de la température ou de la concentration en CO_2 (Sorte et al., 2013).

Ainsi, un lien entre le changement climatique et l'augmentation de l'abondance d'espèces exotiques a été mis en évidence par plusieurs études (Rahel and Olden, 2008; Sorte et al., 2010b). D'autre part, des analyses de variabilités suggèrent que les variations thermiques à court-terme associées aux variations interannuelles masqueront les variations des isothermes à plus long terme et ce, pendant plusieurs décennies dans de nombreuses régions du monde (Isaak and Rieman, 2013). Des efforts importants de suivis biologiques sont nécessaires afin de documenter la variation des aires de distribution des espèces, dont les suivis s'inscriront à des échelles adaptées pour étudier le changement climatique.

3. Notions d'échelles

Les travaux menés au cours de cette thèse ont été réalisés à différentes échelles. Il est important de définir une expérience selon une échelle de temps et une échelle d'espace données et de voir à quelle échelle écologique elle s'inscrit. Durant les expérimentations menées, le but a été de coupler différentes échelles afin de tenter d'obtenir une vue intégrative des processus se déroulant chez les macrophytes marins étudiés. Les différentes échelles étudiées sont décrites ci-dessous.

- **Echelle spatiale :**

Les différents modèles biologiques se répartissent dans la zone littorale benthique, c'est-à-dire en zone côtière. Dans cette zone se concentre la majorité des peuplements végétaux. Tous les macrophytes marins étudiés sont des espèces intertidales qui se situent sur les estrans, entre le niveau moyen des pleines mers de vive-eau et celui des basses mers de vive-eau (coefficient 95), ou plus communément appelée zone de balancement des marées (Cabioc'h et al., 2006; Hupel et al., 2011). Les modèles biologiques suivis, qu'ils se répartissent en estran rocheux ou en estran vaseux, ont été étudiés à la fois à l'échelle locale et à l'échelle d'un gradient latitudinal s'étendant de la Norvège au Portugal, le long des côtes

européennes de l'Atlantique Nord. Les sites ont été choisis en fonction de la présence des modèles biologiques et de leur homogénéité en termes de topographie et de biotope.

Le gradient latitudinal permet d'avoir un proxy du réchauffement climatique. Comme expliqué dans le paragraphe précédent, les variations thermiques induites par le changement climatique peuvent être masquées par des variations à plus court terme. Ainsi, les impacts du réchauffement climatique sur les écosystèmes marins et les macrophytes marines en particulier ne sont pas appréciables à l'échelle de mois ni de quelques années sur les milieux naturels. L'étude de ces impacts nécessite des suivis biologiques à long terme (pluridécennaux). Ainsi, l'un des postulats majeurs de cette thèse a été d'utiliser un gradient latitudinal principalement régit par un gradient thermique afin de mimer les effets potentiels du réchauffement climatique sur les modèles biologiques d'algues étudiées. Ceci est d'autant plus déterminant que la température est le majeur facteur abiotique déterminant la biogéographie des algues, sachant que la température de surface des océans varie en fonction de la latitude et des courants marins (Hurd et al., 2014).

Les trois pays composant ce gradient latitudinal le long des côtes européennes de l'Atlantique Nord sont la Norvège, la France et le Portugal. Ce choix est déterminé par plusieurs critères :

1) La France, et la Pointe bretonne en particulier, ont été sélectionnées car elles représentent le point d'introduction majeur pour plusieurs des macrophytes invasifs étudiés (*cf.* présentation des modèles biologiques) et occupent une position intermédiaire entre le Portugal et la Norvège. La Norvège et le Portugal constituent les limites d'aire de répartition Nord et Sud respectivement des modèles biologiques en Europe.

2) L'effet du réchauffement climatique est plus prononcé aux limites d'aire de répartition des espèces étudiées, d'où le choix de ces deux pays, la Norvège et le Portugal.

3) De manière intéressante, ce gradient se traduit également par la succession de deux régions phytogéographiques, comme illustré en Figure 9. Les sites norvégiens sont soumis au climat tempéré froid, caractéristique de la région boréo-atlantique et les sites portugais au climat tempéré chaud, caractéristique de la région méditerranéo-

atlantique. La Bretagne se situe dans une zone de transition entre ces deux régions ; sa localisation lui conférant une importante richesse en végétaux marins. Plus de 800 espèces sont recensées sur le littoral breton (Cabioc'h et al., 2006).

Ce gradient thermique de la température de surface de la mer est très marqué et ce, quel que soit le mois de l'année considéré (Figure 10). Au cours d'une année, les températures moyennes mensuelles oscillent de 5 à 16°C dans le Sud de la Norvège, de 9 à 16°C à la pointe bretonne et de 14 à 18°C dans le Nord du Portugal (Figure 10).

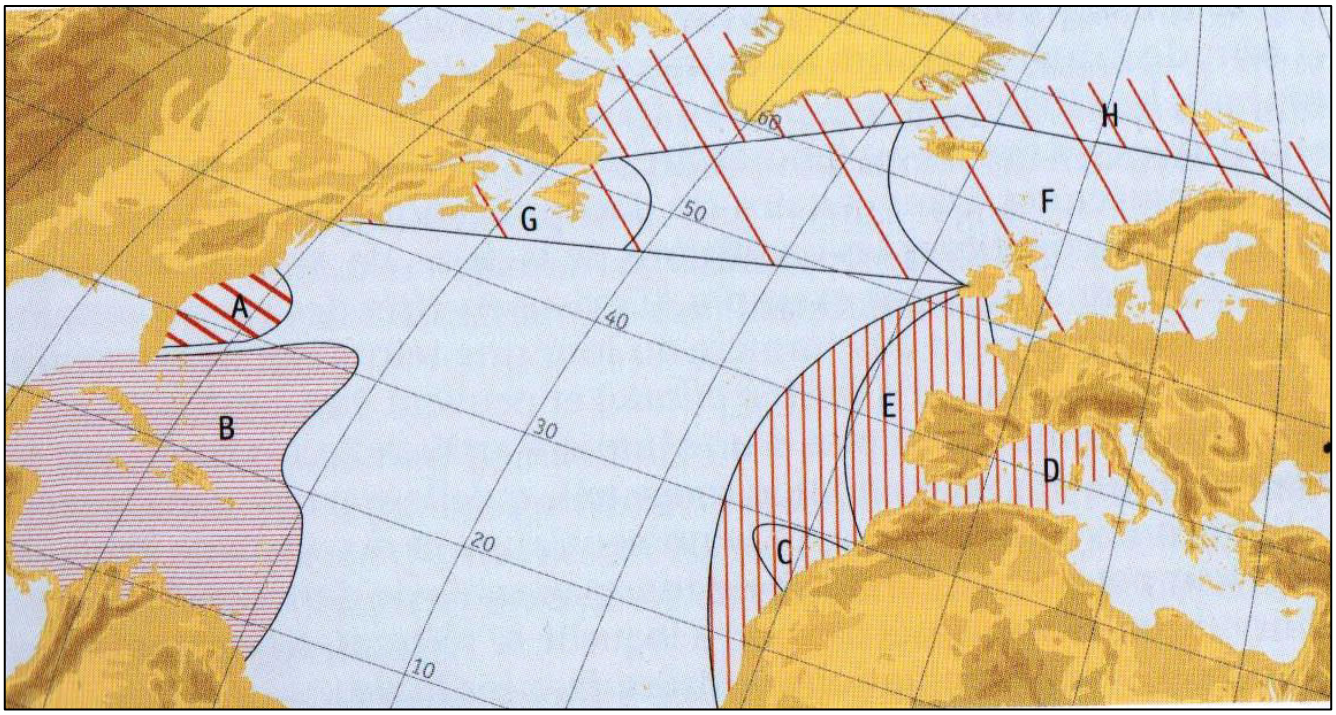

Fig. 9 Régions et provinces phytogéographiques de l'Atlantique Nord issu de (Cabioc'h et al., 2006). A : région tempérée chaude de Caroline ; B : Région tropicale d'Atlantique de l'Ouest ; C-D-E : région méditerranéo-atlantique tempérée chaude (C : province canarienne, D : province méditérannéenne, E : province lusitanienne) ; F-G : région atlantique tempérée froide (F : province de l'Est, G : province de l'Ouest) ; H : région arctique

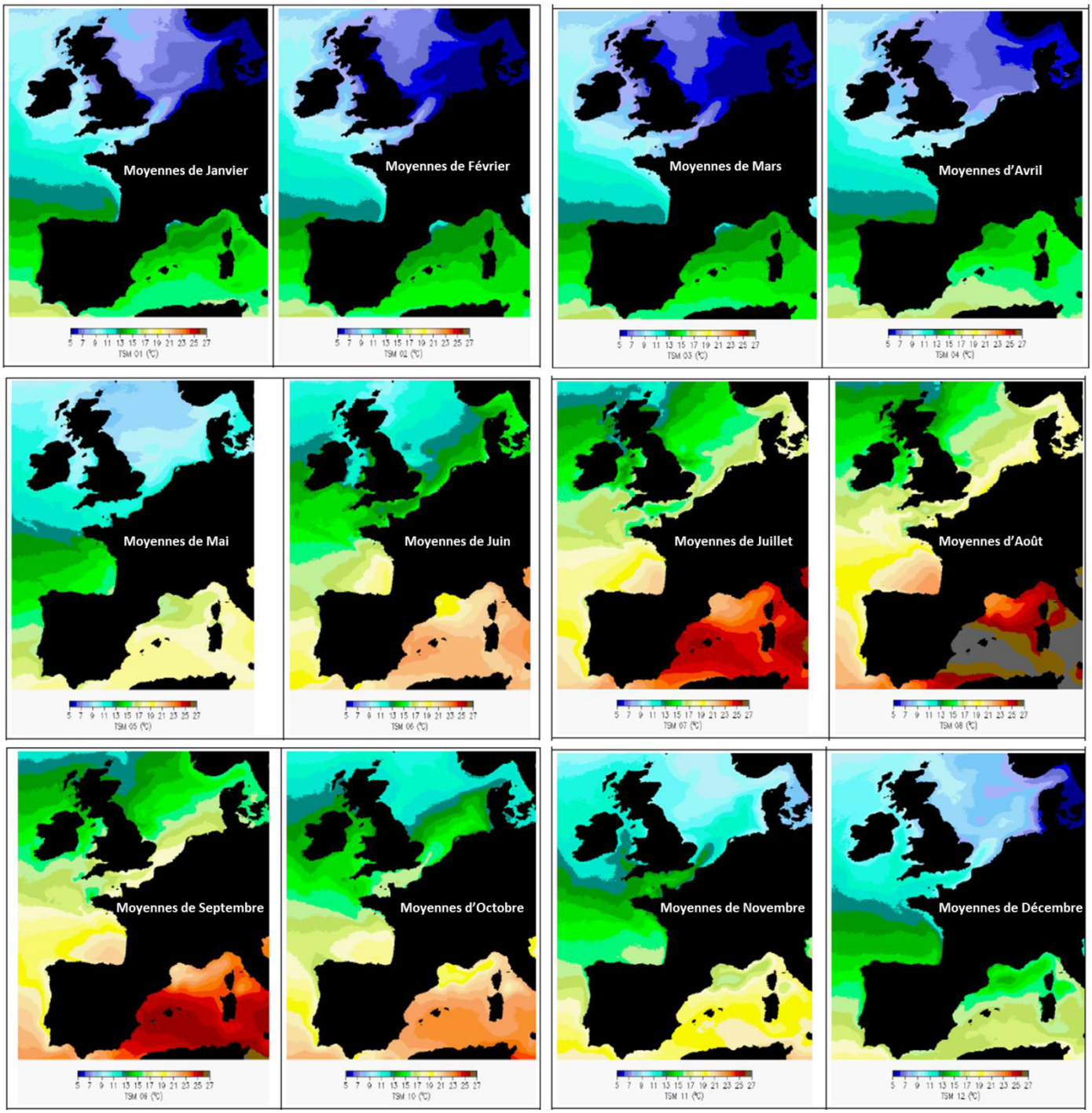

Fig. 10 Climatologie mensuelle de la température de surface de la mer (TSM) le long des côtes européennes sur la période de 1986 à 2009 (adaptée de Gohin et al., 2010).

- Les différents sites suivis :

  - Caractéristiques des estrans rocheux :

Les estrans rocheux se définissent selon différents modes : battu, moyennement battu ou abrités, en fonction de l'hydrodynamisme et donc de leur exposition par rapport à la houle dominante. Selon le mode d'exposition, ces estrans sont caractérisés par différents biotopes. Les sites choisis sont des sites exposés présentant des zones de moulières. Les populations végétales s'y développent principalement au niveau de mares intertidales formées lors des basses mers par des anfractuosités rocheuses (Figure 11).

Fig. 11 Illustration d'une mare intertidale découverte à marée basse en Février 2014 d'un estran rocheux en situation exposée (photo prise à la pointe du Minou, le 12-09-14)

Ces mares les abritent des effets d'arrachements et d'abrasion induits par l'hydrodynamisme ce qui permet leur implantation et leur développement. Les parties exposées des rochers sont dominées quant à elles par des communautés de balanes et de patelles (Cabioc'h et al., 2006). Un coefficient de marnage minimal de 90 est nécessaire afin que les mares restent découvertes suffisamment longtemps pour effectuer le suivi écologique des populations de macroalgues s'y développant (comptages et observations). Deux espèces invasives ont été suivies sur l'estran rocheux : l'algue brune *Sargassum muticum* et l'algue verte *Codium fragile*.

- En France :

Le littoral breton a été choisi pour les raisons énoncées précédemment. Il est caractérisé par un marnage important de l'ordre de 6 m aux abords de Brest, ainsi qu'un

hydrodynamisme élevé, généré par la houle Atlantique en fonction de la direction des vents et de la morphologie du littoral. Les sites choisis se situent à l'embouchure de la Rade de Brest, ainsi qu'à la limite de la Mer d'Iroise. Trois sites ont été sélectionnés : la pointe du Diable (48°21'15,36''N ; 4°33'31,26''O), la pointe du Minou (48°20'19,29''N ; 4°37'6,77''O) et la pointe de Kermorvan (48°21'53,24''N ; 4°46'27,14''O) (Figure 12).

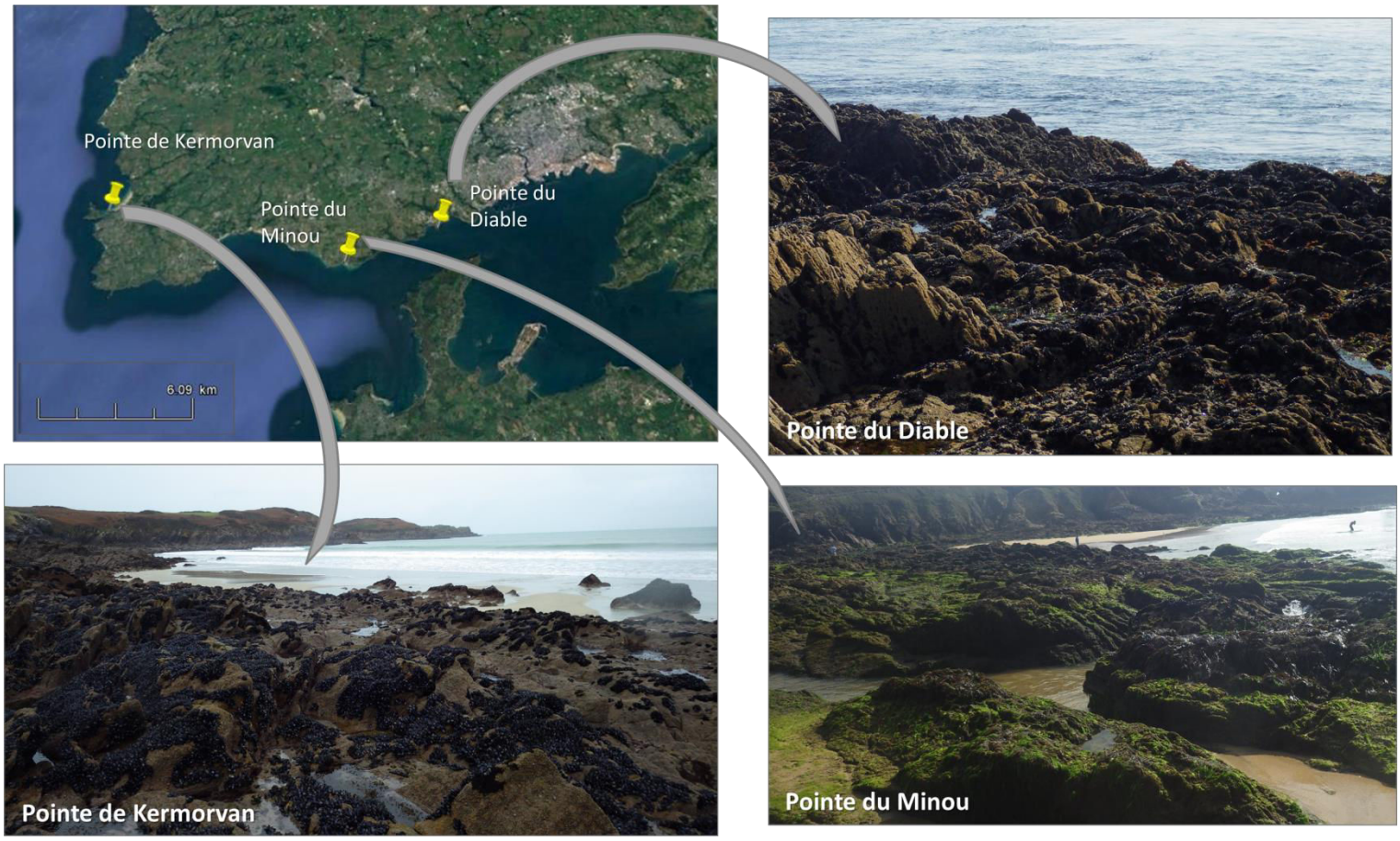

Fig. 12 Cartographie et illustration des trois sites rocheux sélectionnés à la pointe bretonne : sites de la Pointe du Diable (Plouzané, le 11-09-2014), de la Pointe du Minou (Plouzané, le 12-09-2014) et de la Pointe de Kermorvan (Le Conquet, le 04-03-2014)

- Au Portugal :

Le Portugal présente un climat et un littoral contrasté entre le Nord et le Sud du pays. Les sites d'études se répartissent du Nord de Porto jusqu'à proximité de la frontière avec l'Espagne. Ce sont trois sites rocheux exposés présentant des biotopes comparables aux sites bretons, se situant à Moledo (41°50'39.06"N ; 8°52'20.52"O), à la Praia de Âncora (41°49'3.42"N ; 8°52'20.52"O) et à Viano do Castelo (41°41'47.82"N ; 8°51'26.64"O) (Figure 13).

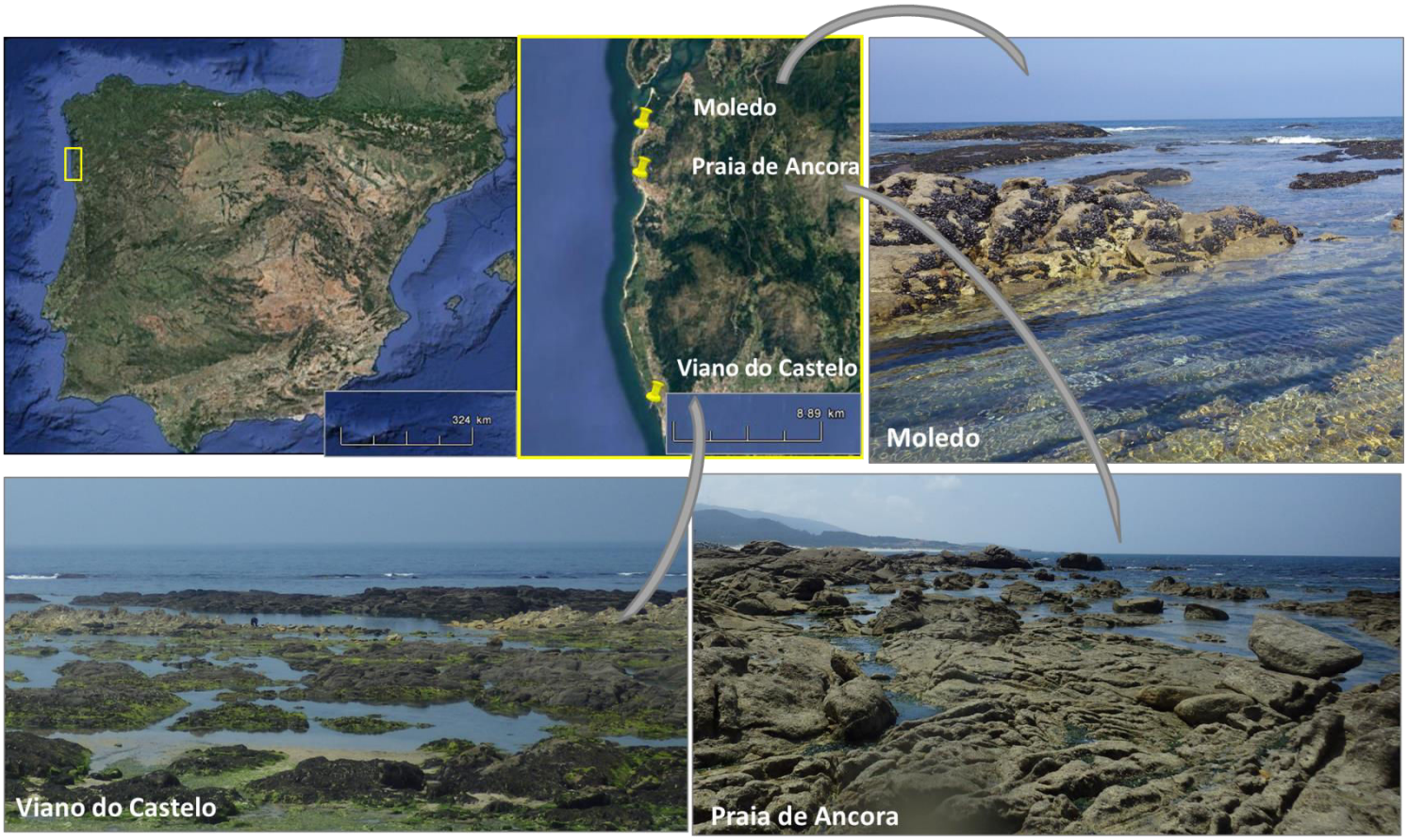

Fig. 13 : Localisation et illustration des trois sites rocheux de la côte Nord du Portugal, au nord de Porto (estrans rocheux des communes de Moledo, Âncora et Viano do Castelo, photos prises le 18-06-14).

- En Norvège :

Les côtes norvégiennes se caractérisent par la présence de fjords ainsi que d'une multitude de petites îles. Les caractéristiques des sites norvégiens divergent pour plusieurs raisons, des autres sites bretons et portugais. En raison de l'absence de marnage, les algues sont immergées en permanence. Ainsi, les espèces étudiées sont soumises uniquement aux variations thermiques de la température de surface de l'eau de mer et ne sont pas soumises aux stress inhérents à la marée en zone intertidale, comme dans les deux autres pays. En raison de sa position septentrionale, la Norvège présente une forte variation des cycles jour/nuit avec des jours très longs en été et très courts en hiver, ce qui n'est pas le cas des deux autres pays le long du gradient latitudinal. Les différents sites se répartissent au Sud de Bergen entre la Mer du Nord et la mer de Norvège (Figure 14) : Site 1 (59°46'13.60"N ; 5°30'19.51"E), site 2 (59°46'39.66"N ; 5°30'45.00"E), site 3 (59°46'57.48"N ; 5°39'53.64"E), site 4 (59°46'59.16"N ; 5°40'32.22"E). L'hydrodynamisme y est limité car les sites se situent enclavés dans les fjords (Figure 14).

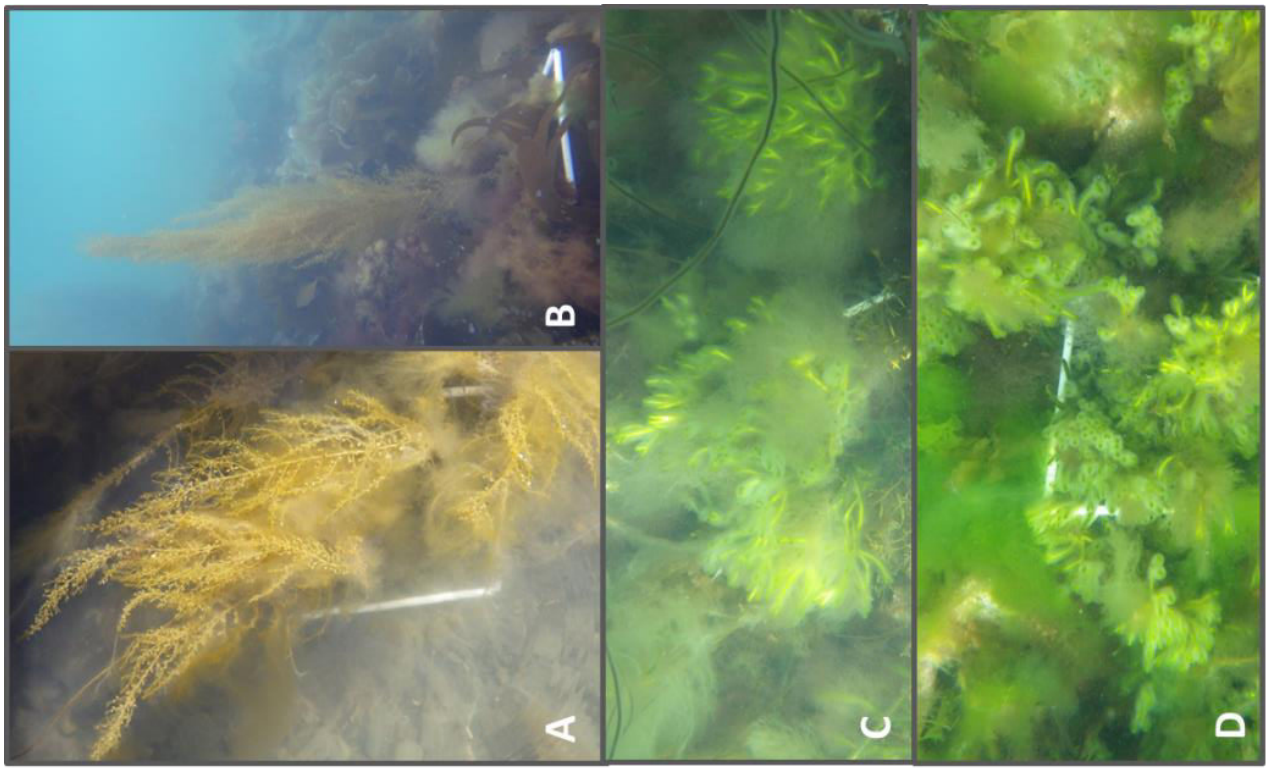

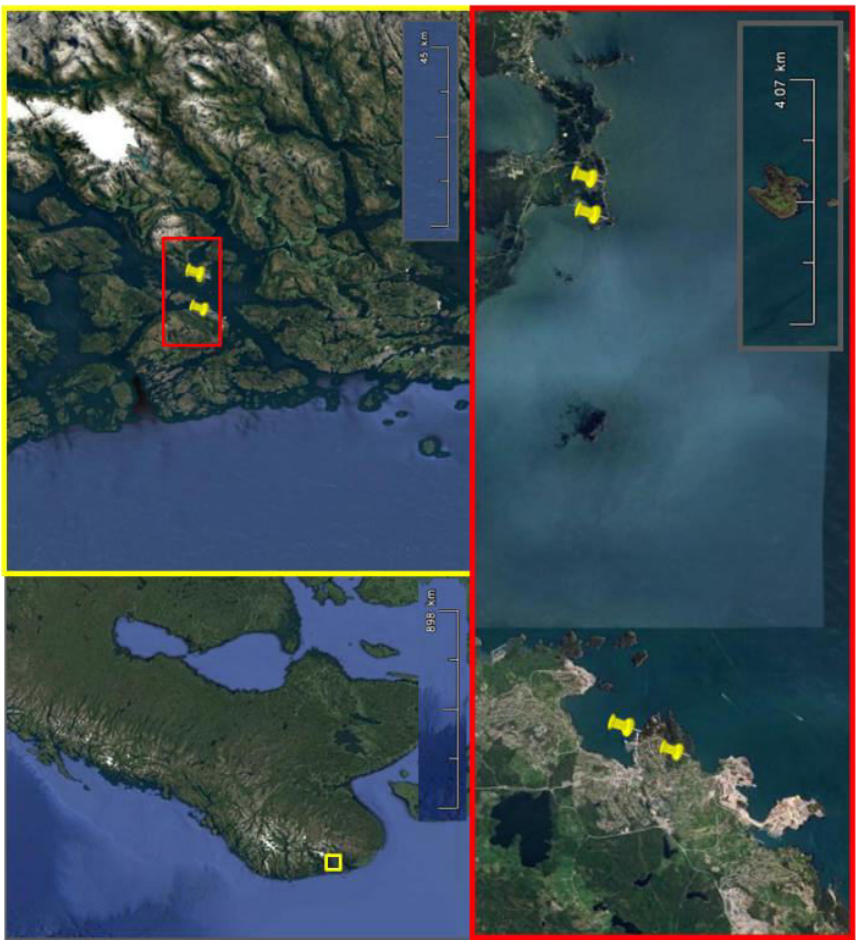

Fig. 14 : Localisation des 4 sites rocheux dans les fjords du Sud de la Norvège, à proximité de Bergen (à gauche) et illustration des fonds rocheux norvégiens (A : Site 1 ; B : Site 2 ; C : Site 3 ; D : Site 4 ; à droite) ; photos prises le 26-06-14.

- Caractéristiques des estrans vaseux

Les estrans vaseux ou marais maritimes constituent des zones de sédimentation des particules fines situées en fond de baie ou dans les estuaires par exemple. Les marais maritimes se distinguent en deux zones très contrastées (Figure 15). Le long d'un transect de la vasière, celle-ci présente en aval une zone recouverte à chaque marée, constituée généralement de vases molles et sans végétation apparente, que l'on appelle la slikke. En amont de ce transect, la vasière est composée d'une zone colonisée par une végétation halophile et recouverte seulement lors des marées de vives eaux (Lahondère, 2004). Ces zones constituent des zones de nourricerie pour de nombreuses espèces.

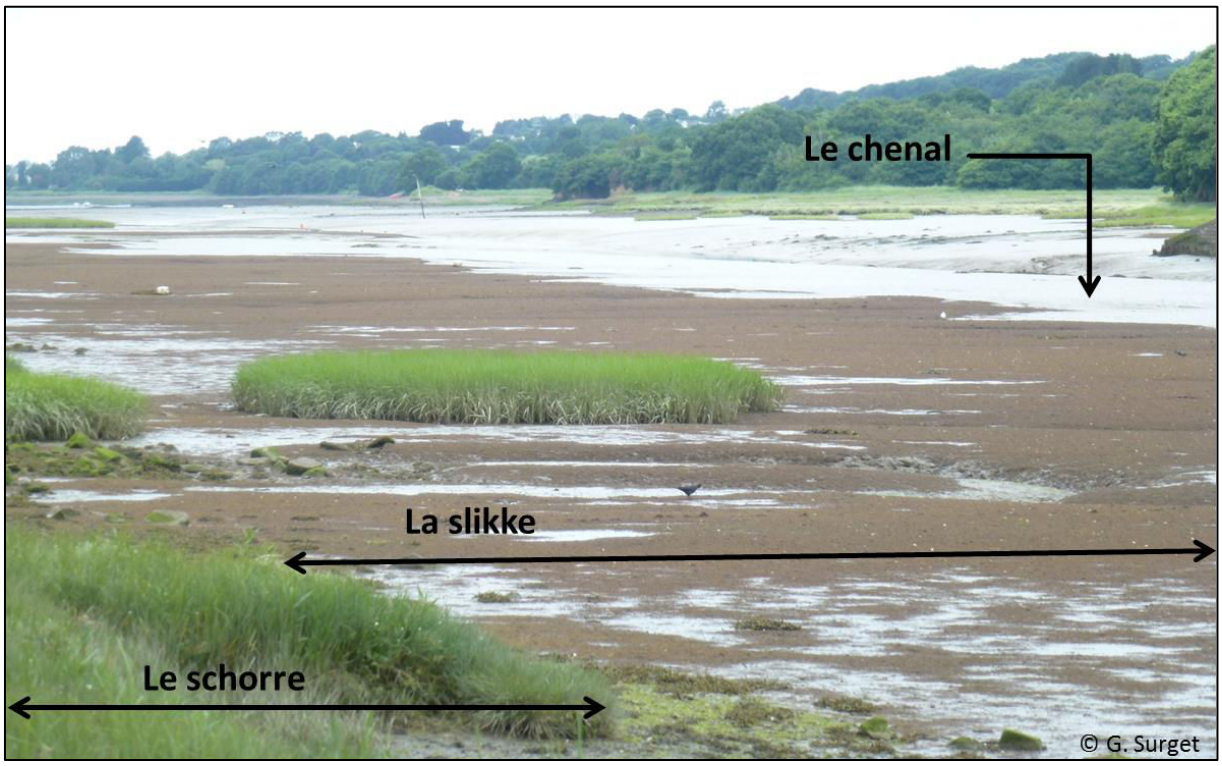

Fig. 15 Illustration de la structuration d'un estran vaseux en prenant l'exemple de la ria du Faou, en Bretagne (photo prise le 04/07/2013).

- En Rade de Brest (France) :

La Rade de Brest est une grande baie abritée d'environ 180 km^2 d'une profondeur moyenne de 8 m. Elle communique à l'Ouest avec la Mer d'Iroise par l'intermédiaire d'un goulet et présente un volume d'environ 2 milliards de m^3 (Larzilliere, 2014). La Rade reçoit des apports d'eau douce et de sels nutritifs de deux bassins versants de fleuves côtiers :

l'Aulne et l'Elorn. Elle est caractérisée par un trait de côte très découpé avec plusieurs presqu'îles et une succession de rias où se trouvent des vasières littorales. La partie Sud de la Rade de Brest présente deux sites Natura 2000. Bien que les apports anthropiques en nutriments ont fortement augmenté au cours de ces trente dernières années (concentration en azote atteignant une concentration de près de 800 µM en 1991), l'écosystème de la rade de Brest résiste à l'eutrophisation (Chauvaud et al., 2000).

Trois anses de la Rade de Brest ont été suivies (*cf.* Chapitre 1 pour l'illustration des sites suivis) : l'anse de Moulin Neuf (48°21,490'N-4°20,447'W), l'anse de Penfoul (48°21,619'N-4°19,186'W) et la ria du Faou (48°21,497'N-4°20,444'W), celles-ci présentant la co-existence au niveau de la haute slikke des deux modèles biologiques invasifs suivis en estran vaseux : *Gracilaria vermiculophylla* et *Spartina alterniflora*.

- Dans la Ria de Aveiro (Portugal) :

La Ria de Aveiro est située sur la Côte Nord du Portugal, à environ 80 km au Sud de Porto. La Ria de Aveiro est un milieu anthropisé et présente de nombreuses similitudes avec la Rade de Brest. Certaines zones ont subi des aménagements portuaires : c'est aussi le lieu de différentes activités industrielles mais aussi d'autres activités humaines telles que la pêche ou l'aquaculture. L'estuaire est peu profond et relié en permanence à l'océan Atlantique par un chenal unique. La profondeur moyenne de la ria est d'1 m hormis dans les zones de navigation qui ont été draguées jusqu'à une profondeur de 7 m. Le marnage y est plus faible qu'en Bretagne (d' 1 à 3 m). La ria est constituée principalement d'un chenal longiligne qui présente des ramifications successives. La circulation hydrologique de la ria est dominée par les échanges avec l'océan Atlantique car les apports d'eau douce issus des affluents sont faibles en comparaison des apports d'eaux de mer à chaque marée. Les valeurs moyennes mensuelles de température au sein de la ria oscillent entre 12 et 23°C et avec une salinité variant entre 15 et 36 ppm (Abreu et al., 2011; Lopes et al., 2007). Les trois sites étudiés sont répartis dans la Ria de Aveiro (Figure 16) et ont été notées de la manière suivante : site 1 (40°36'16.62"N ; 8°44'8.88"O), site 2 (40°33'54.90"N ; 8°45'25.62"O), site 3 (40°35'41.34"N ; 8°45'5.88"O).

- **Echelle temporelle**

Différentes échelles temporelles ont été suivies lors des expérimentations. Les différentes échelles temporelles ont une signification biologique donnée. Deux échelles temporelles différentes ont été suivies. Les expérimentations ont été menées à l'échelle d'une marée, c'est-à-dire à l'échelle de quelques heures, et les populations de végétaux marins ont été suivies en fonction des saisons, à l'échelle d'une année. Le but est de comparer les variations de ces deux échelles temporelles courtes avec des échelles de temps caractérisant le changement climatique mimé par le gradient latitudinal. Les résultats observés le long du gradient seront relativisés en comparaison de ceux obtenus à l'échelle des marées et d'une année permettant de les discuter quant à leur signification biologique pour les modèles biologiques étudiés.

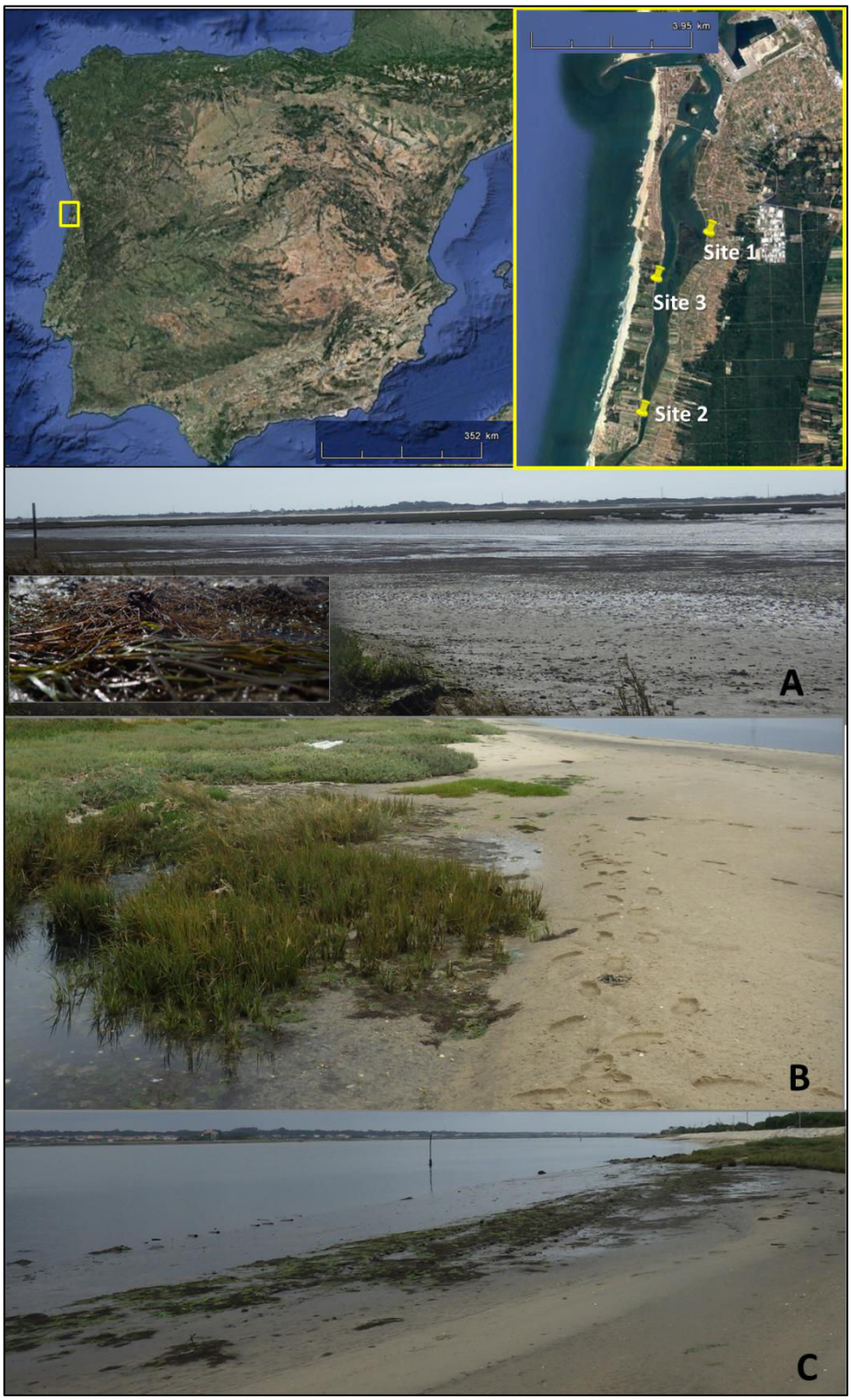

Fig. 16 Cartographie et illustration des trois sites vaseux de la Ria de Aveiro au Portugal (A : Site 1 ; B : Site 2 ; C : Site 3 ; photos prises le 19-06-14)

- **Echelle biologique**

Les différents niveaux hiérarchiques en biologie, en les listant du niveau d'organisation le moins complexe au plus complexe sont : la molécule, l'organite, l'organe, l'organisme, la population, l'écosystème, le biome puis enfin la biosphère (Figure 17).

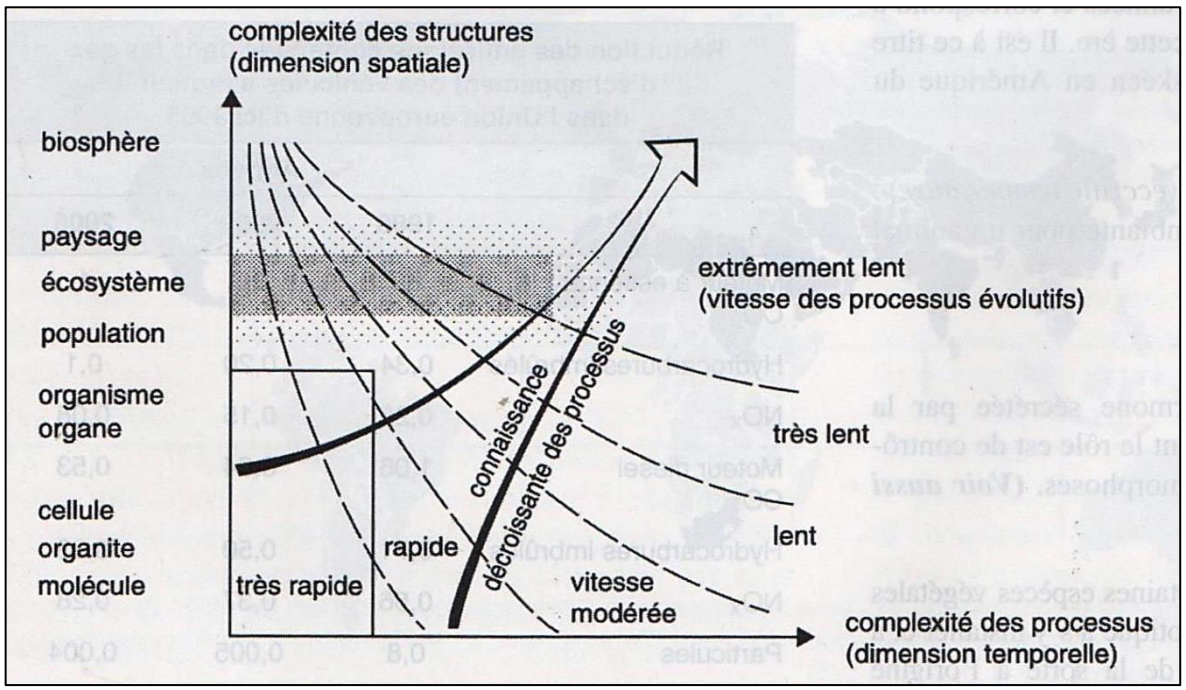

Fig. 17 Echelle spatio-temporelle des différents niveaux hiérarchiques de la biologie. En grisé : processus s'effectuant à l'échelle des populations et des écosystèmes étant des échelles pertinentes pour la compréhension de l'action de l'homme sur les écosystèmes.

A l'échelle biologique la plus réduite se trouve les atomes qui s'organisent en molécules biologiques plus ou moins complexes telles que la molécule d'ADN (Institute, 2015). Ces molécules sont organisées en entités fonctionnelles telles les organites. Différents organites aux fonctions complémentaires interagissent afin de former l'unité fondamentale de la vie : la cellule. Les organismes pluricellulaires présentent jusqu'à trois niveaux hiérarchiques supplémentaires : les cellules s'organisant en tissus, eux-mêmes se coordonnant pour donner lieu à un organe. Des groupes d'organes peuvent fonctionner ensemble et former un système d'organes, tel que le système digestif par exemple (Cain et al., 2006). Le niveau hiérarchique suivant est l'organisme qui correspond à tout être vivant individualisé et autonome. Plusieurs individus appartenant à la même espèce, occupant un biotope défini et pouvant se reproduire entre eux vont définir une population. Diverses populations localisées appartenant à différentes espèces qui vivent en interaction forment une communauté. Cette communauté interagit avec l'environnement abiotique qui l'entoure définissant un écosystème. Les écosystèmes constituent des entités en équilibre dynamique pouvant évoluer en fonction de variations spontanées ou induites par des facteurs externes, tels que le changement climatique comme illustré dans les paragraphes précédents. Plus haut, les biomes sont composés de communautés vivantes, présentes sur de grandes surfaces en milieu continental, soient des biocénoses propres à des macro-écosystèmes tels que les

récifs coralliens par exemple. L'ensemble des biomes constitue la biosphère (Ramade, 2002). La biosphère peut se définir simplement comme « la région de la planète dans laquelle la vie est possible en permanence et qui renferme l'ensemble des êtres vivants » (Ramade, 2002).

Ces différentes échelles biologiques font appel à une dimension spatiale en fonction de la complexité des structures et une dimension temporelle en fonction du niveau de complexité des processus biologiques observés.

Les différentes expériences menées durant cette thèse s'inscrivent sur trois échelles :

- à l'échelle des molécules grâce à un suivi métabolomique et des implications engendrées à l'échelle de l'organisme
- à l'échelle des populations par l'intermédiaire d'un suivi écologique sur le terrain
- à l'échelle de l'écosystème

Ces deux dernières échelles sont particulièrement pertinentes pour la compréhension de l'effet des facteurs anthropogéniques sur les écosystèmes (Ramade, 2002).

4. Notion de bio-inspiration

La bio-inspiration s'inspire des 3 préceptes suivants (Benyus, 2016) :

- **La nature comme modèle** : il s'agit d'une science en pleine expansion qui étudie les modèles présents dans la nature pour ensuite s'en inspirer ou la mimer afin de résoudre un problème de la société humaine
- **La nature comme étalon** : cette notion fait appel à une dimension écologique et d'innovation durable en accord avec notre environnement
- **La nature comme guide** : l'idée de ce concept est non pas d'extraire de la matière de la nature mais d'apprendre de celle-ci

Ainsi la bio-inspiration consiste à s'inspirer du génie du vivant comme une source d'innovation durable. Il consiste à observer et reproduire les propriétés caractérisant un ou plusieurs systèmes biologiques pour mettre au point des formes, des biomatériaux ou encore des procédés. Dans la nature, il existe trois principales sources d'inspiration : les formes présentes dans la nature, les procédés utilisés par le vivant pour répondre aux contraintes imposées par l'environnement, et les écosystèmes étant donné leur performance au vue de leur durabilité, de leur productivité et de leur adaptabilité (Ricard, 2015 ; Bœuf, 2015). De nombreux exemples de bio-inspiration existent d'ores et déjà tels que la forme des pales d'éoliennes inspirée de celle des nageoires de baleines (Ricard, 2015) ou encore la recherche sur la formulation de sang artificiel issue de l'étude de l'hémoglobine extracellulaire d'un annélide marin, *Arenicola marina* (Zal and Rousselot, 2014). En l'état actuel de nos connaissances, l'humain n'est encore pas capable de reproduire un écosystème mais tente de s'en inspirer avec un intérêt émergent pour la permaculture par exemple (Ricard, 2015).

Dans ce contexte, les végétaux marins constituent des modèles particulièrement intéressants à étudier dans une perspective de bio-inspiration. En raison du balancement des marées, les macrophytes de l'étage médiolittoral ont une tolérance accrue pour les fluctuations environnementales (Pessoa, 2012; Sampath-Wiley et al., 2008). Comme exposé précédemment, les végétaux marins présentent une grande richesse d'espèces en particulier en Bretagne (Cabioc'h et al., 2006). Ces macrophytes marins étant exondés périodiquement sont alors exposés à de nombreux stress abiotiques tels que les radiations

UV, une forte luminosité, des variations de température et de salinité ainsi que la dessication (Amsler et al., 2012). D'autre part, les végétaux marins sont en parallèle soumis à une gamme de stress biotiques tels que le broutage ou l'épiphytisme (Potin et al., 2002). Les mécanismes de défense ou les stratégies développées par ces organismes, afin de pouvoir tolérer les stress et se développer dans cet environnement qu'est la zone intertidale, sont autant de sources d'inspiration différentes pour des applications en biotechnologie marine, comme en santé ou en cosmétologie par exemple (Stiger-Pouvreau and Guérard, 2017).

Il est particulièrement intéressant d'intégrer les spécificités des espèces natives et invasives dans ce contexte. D'après les modes d'acclimatation et d'adaptation divergents entre les espèces natives et invasives (e.g. Wikström and Pavia, 2004), on peut ainsi supposer que :

- les espèces natives synthétiseraient des molécules de défense spécifiques présentant une adaptation spécifique aux biotopes où elles se développent.
- les espèces invasives, se développant sur des aires géographiques plus étendues et présentant de manière générale une faible variabilité génétique, utiliseraient des mécanismes de défense plus généralistes mais efficaces afin de coloniser de vastes habitats présentant des caractéristiques environnementales variables.

Ainsi les macrophytes marins, qu'ils soient autochtones ou allochtones, constituent du fait de leurs stratégies de défense, des sources d'inspirations indéniables, conduisant à leur utilisation dans divers domaines. Ce travail de thèse utilise la notion de bio-inspiration au sens large et comporte un but de bio-prospection de métabolites actifs issus de macrophytes marins natifs et invasifs en lien avec les conditions environnementales du milieu.

5. Les modèles biologiques

Parmi les végétaux marins étudiés durant cette thèse, quatre modèles de végétaux invasifs et trois autres espèces de macrophytes marins ont été choisis. Les espèces natives sélectionnées pour cette étude des estrans vaseux et rocheux permettent la comparaison entre espèce native et invasive et/ou présentent un intérêt en terme de bio-inspiration. Les quatre modèles invasifs étudiés font partie des principales espèces invasives de la zone intertidale le long des côtes européennes de l'Atlantique Nord-Est et notamment des côtes bretonnes (Stiger-Pouvreau and Thouzeau, 2015). Il s'agit de deux espèces invasives des estrans rocheux : une macroalgue brune, *Sargassum muticum* et une macroalgue verte, *Codium fragile* et de deux espèces invasives des estrans vaseux : une macroalgue rouge, *Gracilaria vermiculophylla* et une phanérogamme halophile, *Spartina alterniflora*. L'origine, l'historique d'introduction, la répartition, ainsi que les caractéristiques biologiques de ces quatre espèces sont détaillées ci-dessous.

- **espèces d'estran rocheux** :

  - *Sargassum muticum* (Yendo) Fensholt

S. muticum est une Phéophycée, *i.e.* une macroalgue brune, pseudo-pérenne et appartenant à l'ordre des Fucales et à la famille des Sargassaceae (Figure 18). Elle est considérée comme la macroalgue invasive la plus efficace dans le monde, étant donné l'étendue de sa distribution géographique en dehors de son aire native, et sa présence de l'Alaska à la Californie dans l'Est Pacifique, de la Norvège au Maroc dans l'Est Altlantique ainsi qu'en Méditérranée. Cette large zone d'introduction dépasse l'étendue de son aire native allant du Sud de la Russie au Sud de la Chine dans le Pacifique Ouest (Engelen et al., 2015).

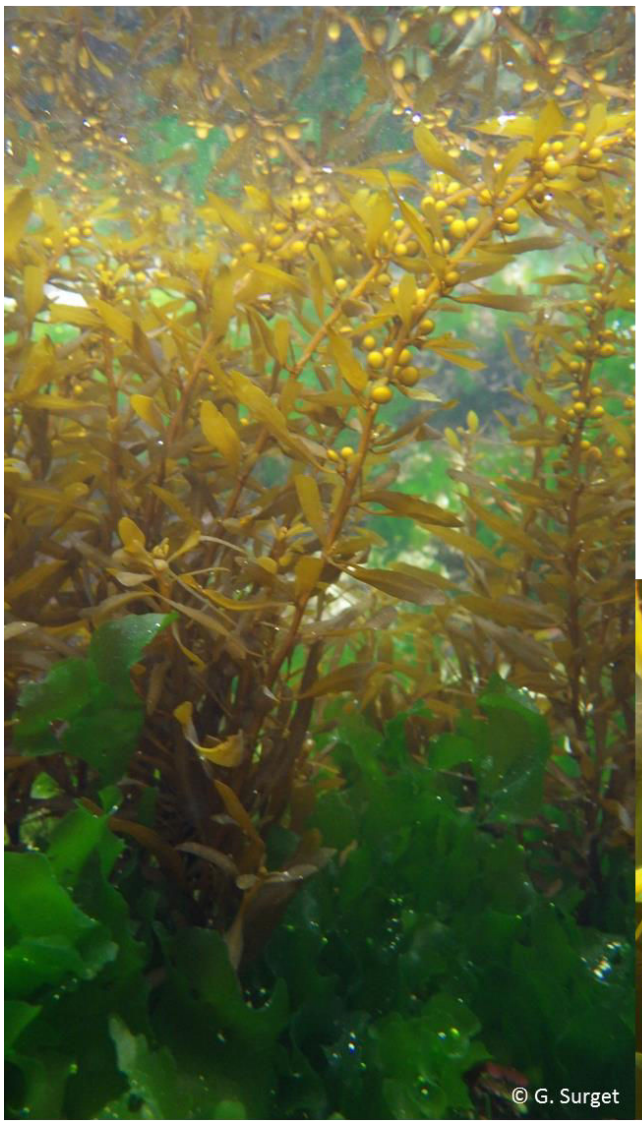

Taxonomie

Règne: Chromista
Phylum : Ochrophyta
Classe : Phaeophyceae
Sous-classe : Fucophycidae
Ordre : Fucales
Famille : Sargassaceae
Espèce : *Sargassum muticum*

(source : algaebase, **consulté le 09/01/2016**)
http://www.algaebase.org/search/species/detail/?species_id=4417

Fig. 18 Illustration de *Sargassum muticum*. A gauche : thalles observés dans une mare intertidale d'un estran breton (photo prise le 25/11/2014, site du Minou, Plouzané). En haut à droite : taxonomie de *Sargassum muticum*. En bas à droite : Détails des aérocystes d'une latérale.

Cette espèce, originaire du Japon, a été découverte pour la 1ère fois le long des côtes européennes en 1973, au Sud de l'Angleterre, probablement suite à l'importation de naissains de l'huître creuse *Crassostrea gigas* (Farnham et al., 1973). Elle a été répertoriée le long des côtes normandes seulement quatre années plus tard, en 1975 (Critchley, 1983; Critchley et al., 1990). Puis, elle a été introduite une seconde fois en France au niveau de l'étang de Thau dans les années 80 (Figure 19). A partir de ces différents points d'introduction en Europe, l'espèce s'est considérablement développée en l'espace de 30 ans le long des côtes Nord atlantiques européennes, étant maintenant installée de la Norvège au

Portugal (Stiger-Pouvreau and Thouzeau, 2015). L'expansion de cette espèce est toujours active, principalement en Angleterre ainsi que dans le Sud de la péninsule ibérique. De plus, elle a été récemment répertoriée sur les côtes marocaines (Sabour et al., 2013). *S. muticum* a la particularité de présenter une diversité génétique faible en comparaison d'autre macroalgues brunes invasives et homogène entre sa région native et les régions colonisées à travers le monde, non seulement en Europe mais aussi sur le continent américain (Cheang et al., 2010).

Cette algue de couleur marron pâle à jaune verdâtre (Figure 18) peut atteindre 12 m de long et jusqu'à 6-7 m en France. Son thalle de forme pyramidale est composé d'une partie pérenne à la base, constituée d'un crampon surmonté d'un ou plusieurs axes pérennes eux-mêmes pourvus de latérales saisonnières (Goulletquer, 2016). Après une période de dormance hivernale, ces latérales se développent jusqu'à ce que le thalle atteigne sa maturité à la fin du Printemps (Plouguerné, 2006). A maturité apparaissent sur ces latérales des réceptacles (vésicules cylindriques). Après la période de maturité estivale, les latérales se dégradent puis se détachent. Les latérales sont redressées dans la colonne d'eau grâce à la présence d'aérocystes, structures ayant le rôle de flotteur (Figure 18). Lorsque les latérales se détachent du reste du thalle, les aérocystes leur permettent de flotter à la surface de l'eau et de se disperser. Ces aérocystes sont de petite taille chez cette espèce (de 2 à 3 mm de diamètre), de formes ovoïdes et pédicellés (Goulletquer, 2016). La présence de cette espèce est discrète sur les estrans de Novembre à Février car seuls les crampons et les courts axes primaires subsistent mais l'espèce présente d'importantes biomasses à la période estivale, avec le développement des latérales.

S. muticum est définit comme un méiosporophyte diploïde produisant des gamètes (Stiger-Pouvreau and Thouzeau, 2015). Cette espèce est monoïque mais bien que les gamètes mâles et femelles soient situés sur le même réceptacle, ils se développent dans des conceptacles différents. Après une fécondation externe à la surface du réceptacle, l'embryon se développe en restant fixé sur le thalle parent puis est libéré dans la colonne d'eau afin qu'il puisse se fixer sur un substrat dur (Plouguerné, 2006; Tanniou, 2014).

S. muticum est capable de tolérer des conditions environnementales très variables notamment en terme de température (de -1°C à 30°C) et de salinité (supportant jusqu'à des valeurs inférieures à 10 ppm). Il s'agit également d'une espèce très compétitive vis-à-vis des

biocénoses natives, du fait des grandes tailles que peuvent atteindre ses latérales, formant ainsi une canopée dense dans les mares rocheuses intertidales ou peu profondément en zone subtidale, induisant ainsi à la fois une forte compétition pour l'espace et la lumière avec les autres espèces benthiques (Engelen et al., 2015).

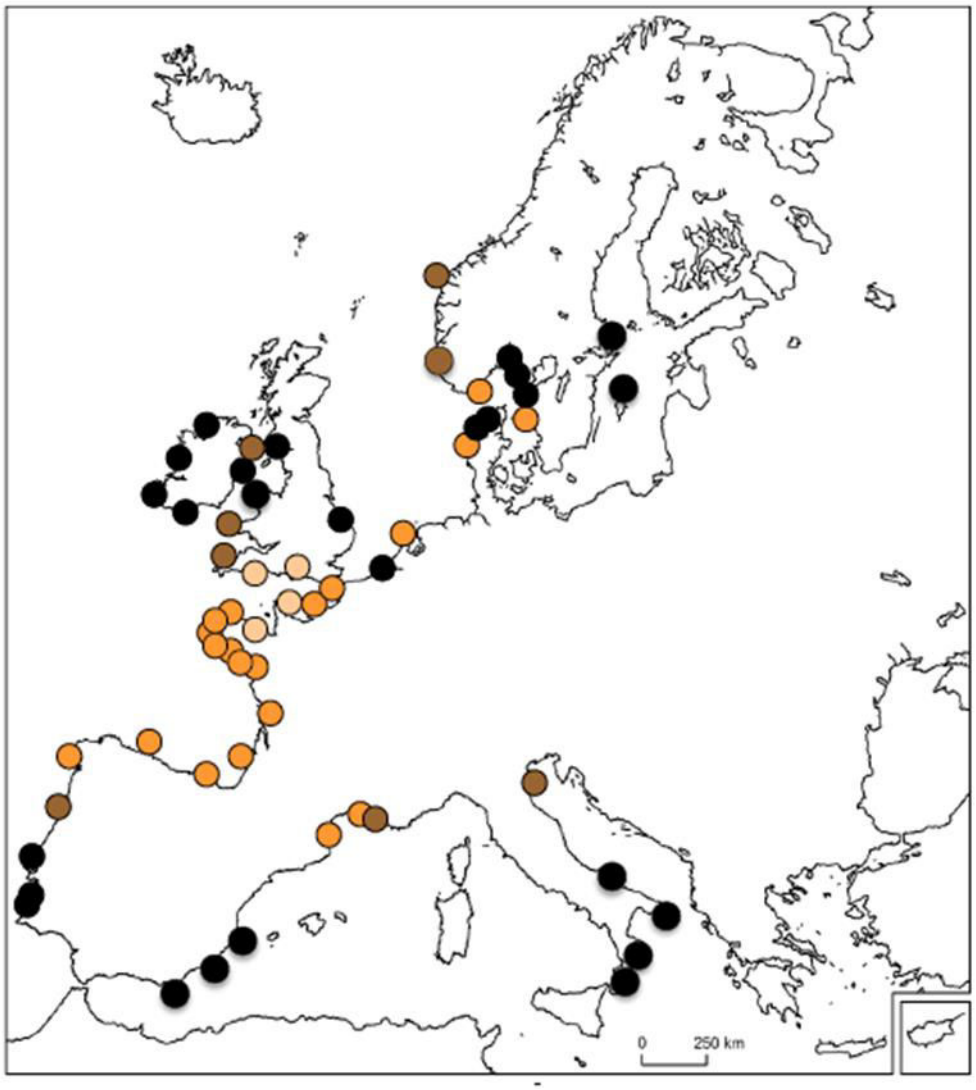

Fig. 19 Cartographie des principaux sites d'introduction et de prolifération de *Sargassum muticum* en Europe (beige : 1973-1980 ; orange : 1981-1990 ; marron : 1991-2000 ; noir : 2001-2015), issu de Stiger-Pouvreau and Thouzeau (2015).

- *Codium fragile* (Suringar) Hariot

Codium fragile est une macroalgue verte spongieuse et comestible appartenant au phylum des Chlorophyta, à la classe des Ulvophyceae, à l'ordre des Bryopsidales et à la famille des Codiaceae (Figure 20 ; Guiry and Guiry 2016).

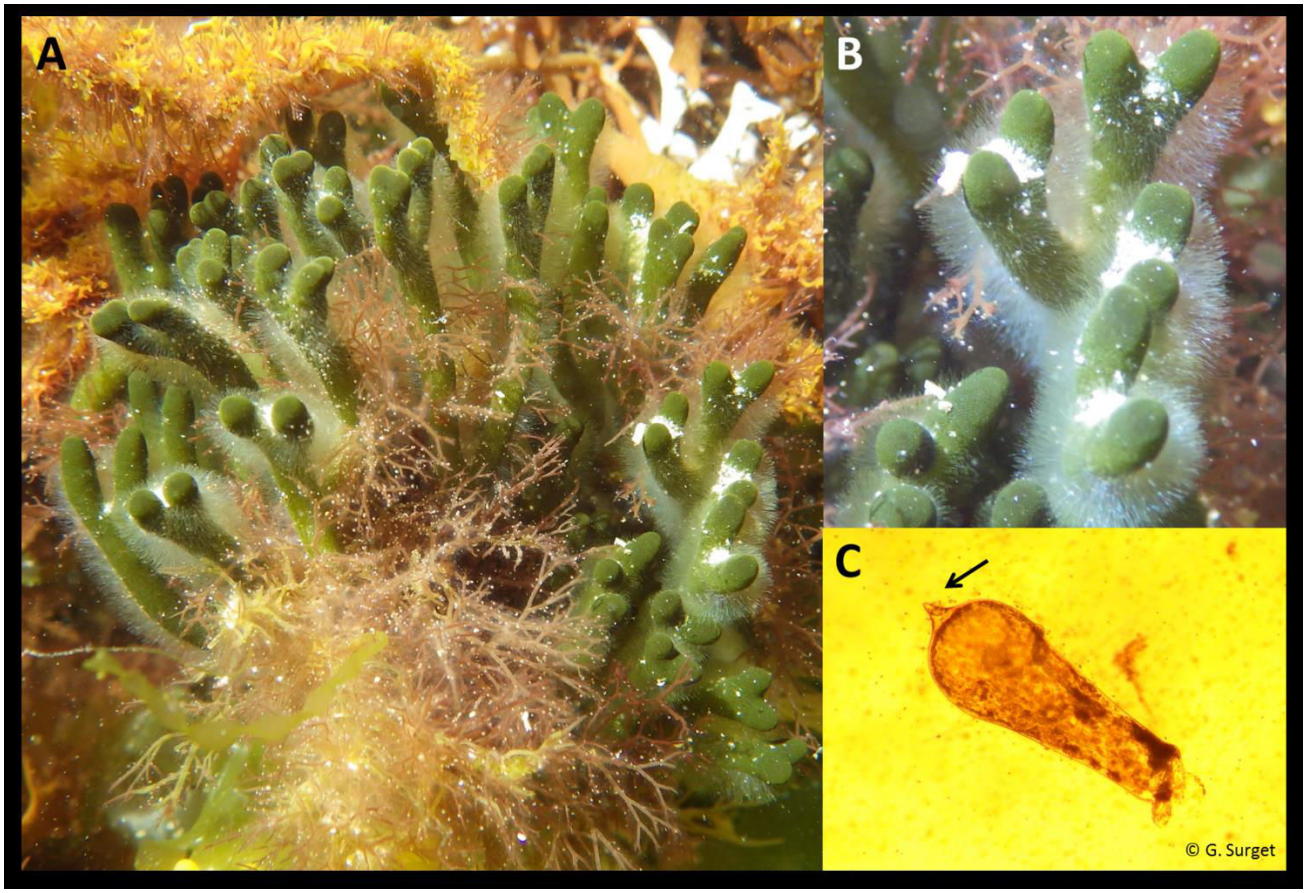

Fig. 20 **A** : Illustration d'un thalle de *Codium fragile* dans une mare intertidale de la pointe de Kermorvan (Conquet, France ; photo prise le 13/06/2014). **B** : Détails des poils abondants présents à la surface des thalles de *Codium fragile*. **C** : Détail d'un utricule présentant un mucron (flèche) en vue microscopique.

Cette espèce invasive est originaire du Japon et du Nord Pacifique. Elle a été introduite à travers le globe à la fois dans les mers chaudes et froides. Cette espèce a été répertoriée aux Pays-Bas en 1900 mais l'analyse génétique d'échantillons issus d'herbariums ont montré que cette espèce était présente dès 1839 dans les îles britanniques (Provan et al., 2008). Son introduction a été reportée en France vers 1940 (à Arcachon, en Bretagne Sud et en Méditérranée ; *cf.* Figure 21), sur les côtes Est Nord-américaines vers les années 1950, en Australie en 1975, en Afrique du Sud en 1999 et en Amérique du Sud en 2001 (Goulletquer, 2016; Provan et al., 2008). Cette espèce présente une diversité génétique très

faible en Europe avec l'haplotype 1 présent le long de la côte Atlantique et l'haplotype 2 en Méditérrannée indiquant deux phénomènes d'introduction différenciés (Figure 22).

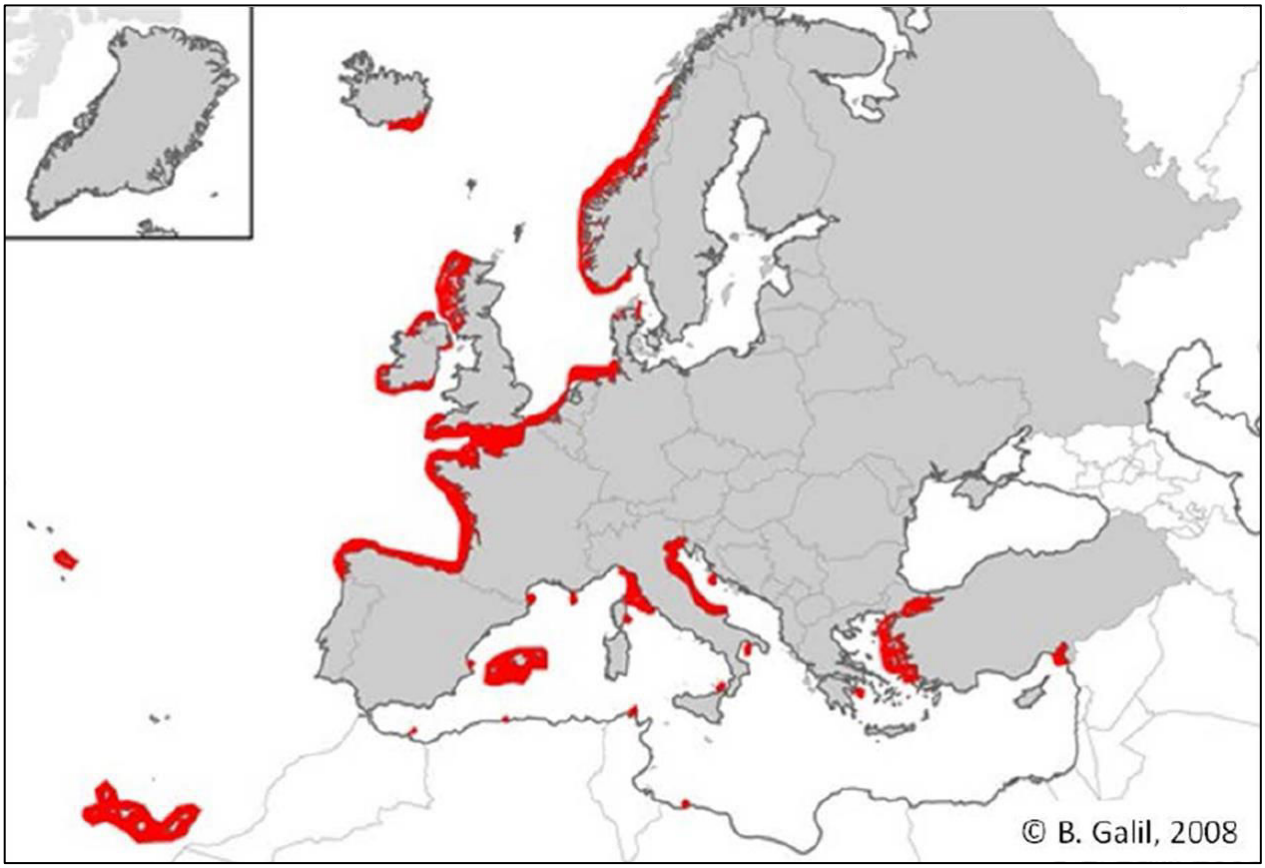

Fig. 21 Aire de répartition de l'espèce *Codium fragile* le long des côtes européennes en 2008 (issu de Stiger-Pouvreau and Thouzeau, 2015).

Il existe de nombreuses espèces et sous-espèces de *Codium*. Sur les estrans bretons échantillonnés, une seule sous-espèce semble exister *C. fragile ssp. fragile* anciennement prénommée *C. fragile ssp. tomentosoïdes,* distinguable par la forme des utricules et surtout la présence d'un mucron prononcé (Provan et al., 2008). Dans cette étude, un mucron a toujours été visible sur les utricules (Figure 20) confirmant la détermination de cette sous espèce comme modèle d'étude.

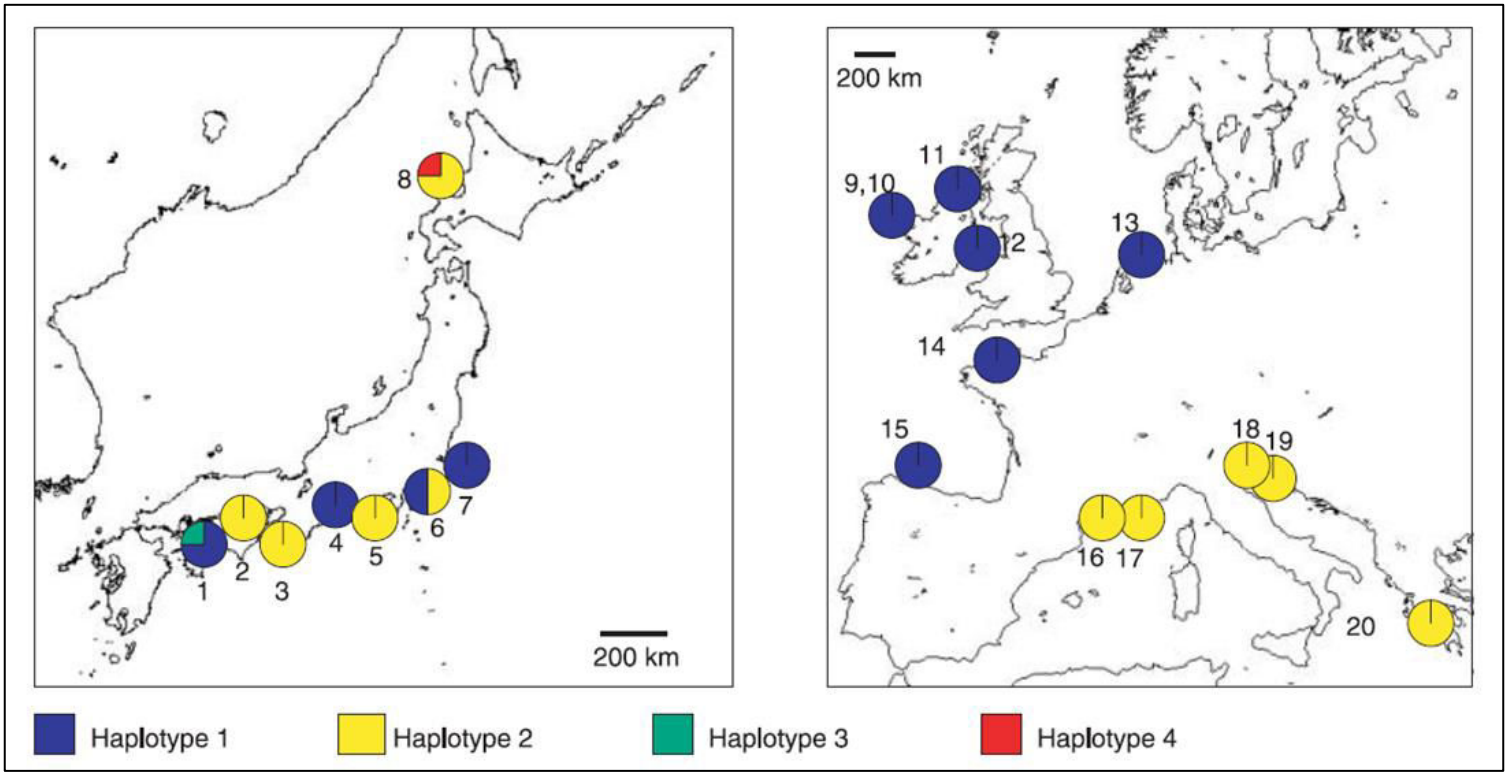

Fig. 22 Cartographie de la distribution des haplotypes (*i.e.* groupe d'allèles de différents loci situés sur un même chromosome et habituellement transmis ensemble) de *Codium fragile* dans son aire native au Japon (à gauche) et dans son aire invasive en Europe (à droite). Les chiffres désignent les sites d'échantillonnage (Provan et al., 2005).

Cette algue est caractérisée par un thalle dressé et siphonné de section cylindrique, à ramifications régulièrement dichotomes (Figure 20). Le thalle est fixé au substrat par un large disque basal également de consistance spongieuse et peut atteindre jusqu'à 30 cm. Cette espèce présente des utricules particuliers se terminant par une pointe appelée mucron observable en microscopie optique comme évoqué ci-dessus. Il existe de nombreuses espèces et sous-espèces de *Codium* mais l'espèce *Codium fragile ssp. fragile* se distingue notamment par la présence de ce mucron prononcé. Le thalle présente des poils bien visibles, caractéristiques du genre *Codium* (Cabioc'h et al., 2006; Goulletquer, 2016). Cette espèce se reproduit par reproduction sexuée, par émission de gamètes, mais également par reproduction asexuée sous différentes formes : soit par parthénogénèse (développement d'un gamète femelle sans fécondation), soit par fragmentation du thalle, soit par la libération d'excroissances formées durant la période estivale (Prince and Trowbridge, 2005; Trowbridge, 1998). Les cellules reproductrices sont libérées dans le milieu puis vont se fixer à un substrat dur et germer rapidement pour former des filaments indifférenciés appelé stade

vauchéroïde. La croissance des thalles est positivement corrélée à l'augmentation des températures durant la période estivale (Bégin and Scheibling, 2005).

Sa colonisation de l'estran est facilitée par sa capacité à se propager de manière végétative par fragmentation du thalle et par sa tolérance physiologique (Andreakis et Schaffelke, 2012). En effet, cette espèce photophile tout comme la sargasse est capable de tolérer des conditions environnementales très variables notamment en termes de salinité et de température (jusqu'à -2°C). De plus, les basses températures rencontrées en hiver induisent un rétrécissement du thalle qui favorise sa fragmentation et ainsi la dispersion de l'espèce (Goulletquer, 2016). Cette espèce à forte croissance se développe dans les mares intertidales mais également dans des milieux subtidaux peu profonds ainsi que dans des milieux abrités tels que les baies (Goulletquer, 2016), formant ainsi des peuplements denses de la surface jusqu'à une dizaine de mètres de profondeur (Bégin et Scheibling, 2003).

Ces deux espèces invasives, *Sargassum muticum* et *Codium fragile*, ont la particularité de pouvoir être observées en association au niveau des mares rocheuses intertidales d'estrans très battus caractérisés par la présence de moulière ce qui en justifie l'étude conjointe.

- **espèces d'estran vaseux**

  - *Gracilaria vermiculophylla* (Ohmi) Papenfuss

Gracilaria vermiculophylla est une espèce de macroalgue rouge agarophyte appartenant au phylum des Rhodophyta, ordre des Gracilariales et famille des Gracilariaceae (Figure 23). C'est une espèce exotique en Bretagne, et native du Nord Est de l'Asie. Actuellement, *G. vermiculophylla* est largement répandue à travers le monde étant présente dans l'Est Pacifique, dans l'Ouest et l'Est Atlantique et dans le Nord de la mer Baltique (Freshwater et al., 2006; Rueness, 2005; Thomsen et al., 2009, 2007, 2006; Weinberger et al., 2008).

Dans l'Est Atlantique, son aire de distribution s'étend du Maroc à la Norvège (Guillemin et al., 2008; Kim et al., 2010). Cette espèce a été décrite pour la première fois en Europe dans l'estuaire du Belon (en Bretagne) en 1996 (Rueness, 2005), puis s'est répandue rapidement le long des côtes européennes (Figure 24). Son introduction serait accidentelle et liée à l'aquaculture et plus probablement à l'importation de naissains de l'huître

japonaise, *Crassostrea gigas*. Par ailleurs, il a été montré que les diversités génétiques observées sur les populations des côtes américaines et européennes concordaient avec ces hypothèses (Kim et al., 2010; Rueness, 2005). Des phénomènes d'introductions multiples sont même supposés le long des côtes virginiennes (Gulbransen et al., 2012).

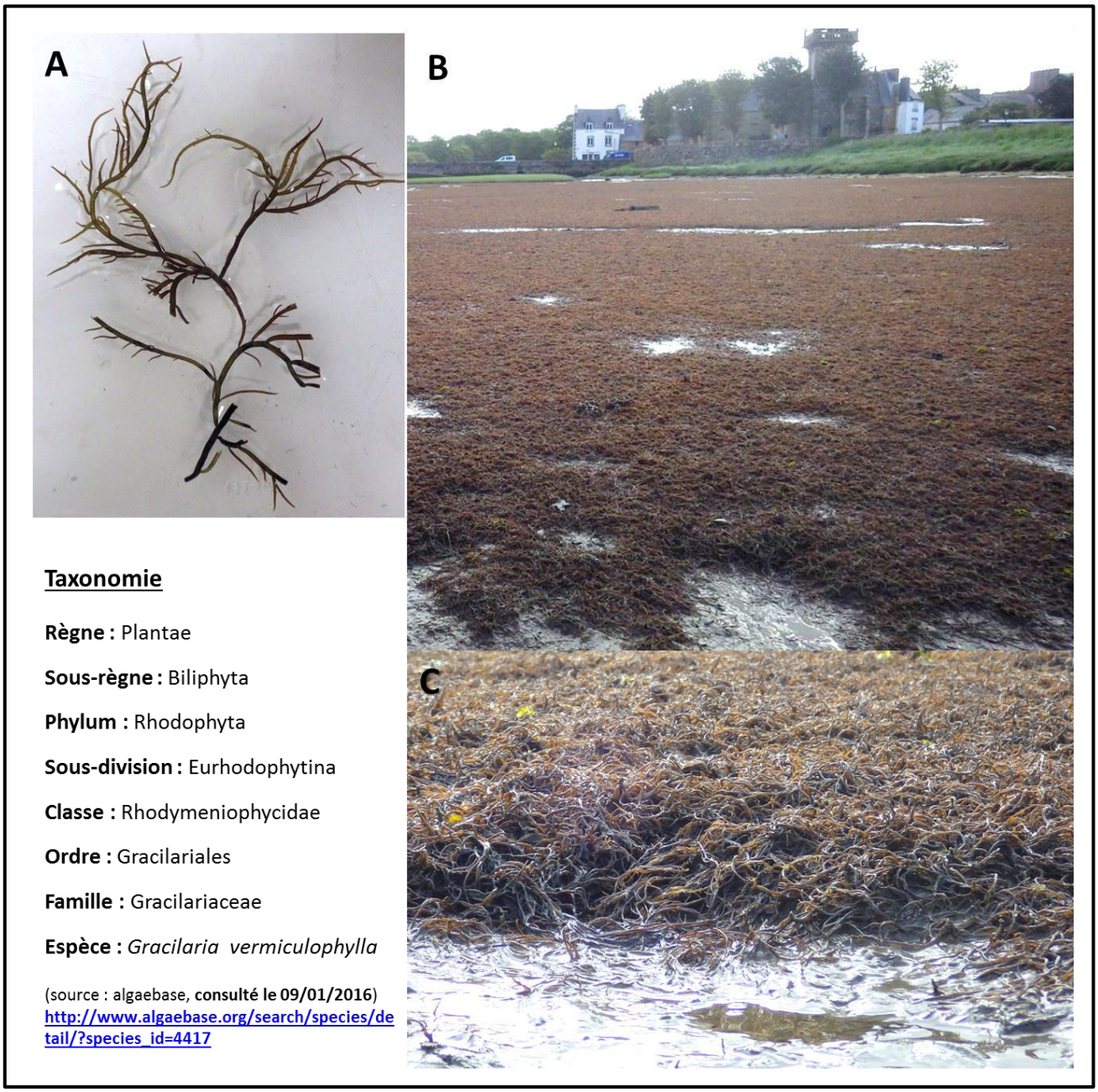

Fig. 23 (A) Illustration d'un thalle de *Gracilaria vermiculophylla*. (B) Photographie d'un tapis de *Gracilaria vermiculophylla* à marée basse d'une vasière intertidale et (C) zoom de l'épaisseur du tapis (photo prise sur le site du Faou, le 14/05/2014).

Selon ces études, *Gracilaria vermiculophylla* présente de manière intéressante, une diversité génétique très contrastée entre ses régions invasives et native, avec une diversité

plus faible en Europe en comparaison de sa région native, l'Asie du Nord Est. En effet, Kim et al. (2010) ont détecté 19 haplotypes mitochondriaux dont seulement 3 en Europe et en Amérique du Nord (Figure 25) et 17 en Asie du Nord-Est. Un seul haplotype est partagé entre les populations natives et invasives, l'haplotype 6. Cette étude démontre une diversité génétique faible de l'espèce dans les zones d'invasion avec la présence de l'haplotype 6 chez plus de 99% des échantillons prélevés dans les zones invasives.

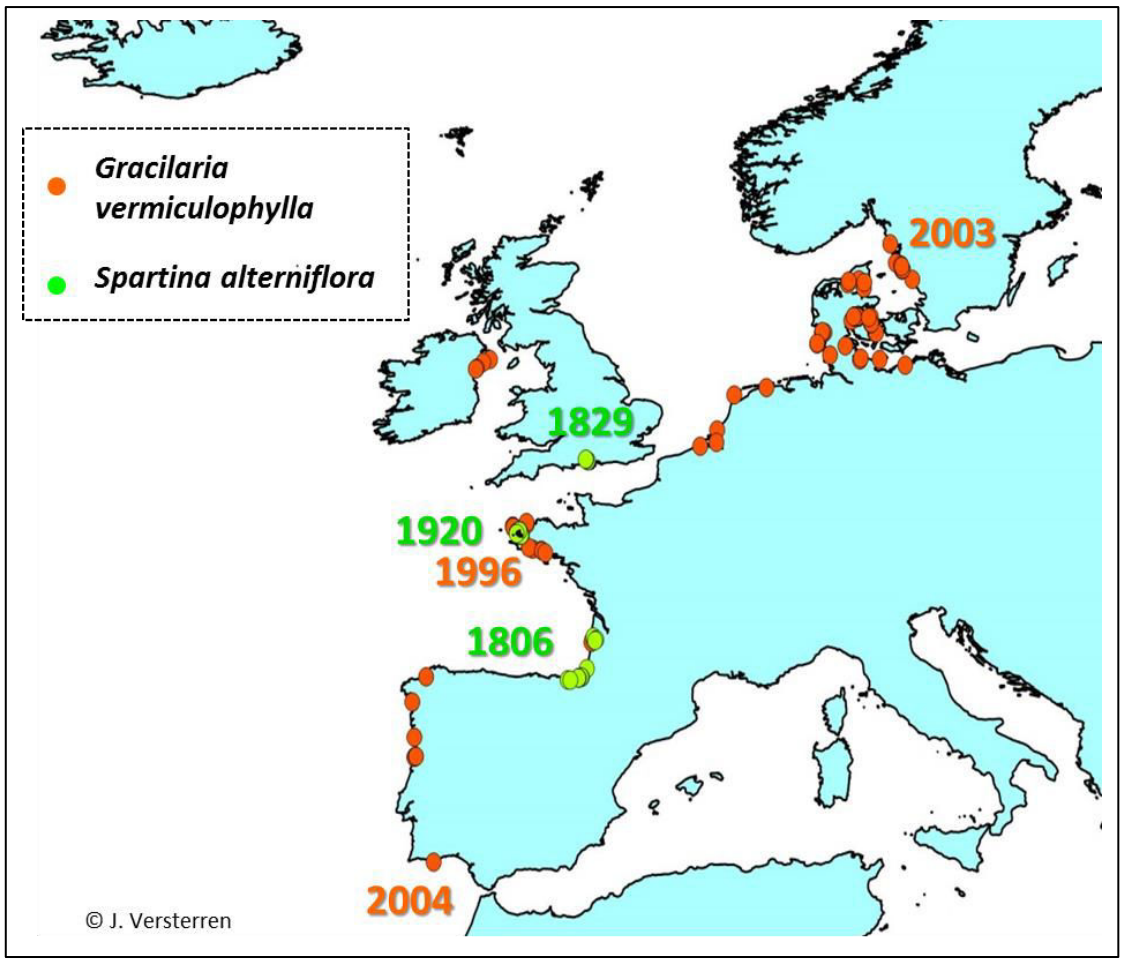

Fig. 24 Répartition et chronologie d'introduction et de prolifération de *Gracilaria vermiculophylla* et *Spartina alterniflora* le long des côtes Atlantiques européennes, modifié à partir de Stiger-Pouvreau et Thouzeau (2015). Les années en orange indiquent les dates de 1ère observation de *G. vermiculophylla* : à Gothenburg (Suède) en 2003, dans l'estuaire du Belon (France) en 1996, dans la Ria Formosa (Portugal) en 2004 (Rueness, 2005). Les années en vert indiquent les dates de 1ère observation de *S. alterniflora* : dans l'estuaire de la Bidassoa (pays Basque, France) en 1806, Southampton (Angleterre) en 1829, en Rade de Brest (France) en 1920 (Querné, 2011).

Gulbransen et al. (2012) ont modéré ce constat en démontrant une diversité génétique plus importante le long des côtes virginiennes, liée à un effort d'échantillonnage

conséquent. De nouvelles approches sont mises en place afin d'aller plus loin dans l'étude de l'histoire de l'introduction de *Gracilaria vermiculophylla* à travers le monde, comme l'utilisation de microsatellites (Kollars et al., 2015).Cet agarophyte se présente sous la forme de thalles filamenteux de couleur rouge sombre à brun foncé (Figure 23 A). Elle présente un disque basal et son axe principal peut mesurer de 4 à 50 cm de long. Le thalle est souple, à section cylindrique et présente des ramifications alternes le long de l'axe principal, ramifications elles-mêmes ramifiées. Les thalles de *Gracilaria vermiculophylla* se développent sur des zones de vases nues caractéristiques de la slikke, soit en étant simplement déposés à la surface du substrat ou enchevêtrés dans les premiers cm de la vase (Rueness, 2005), soit en se fixant aux tubes du polychète du genre *Diopatra* ou à des coquilles de bivalves (Abreu et al., 2011; Thomsen and McGlathery, 2005).

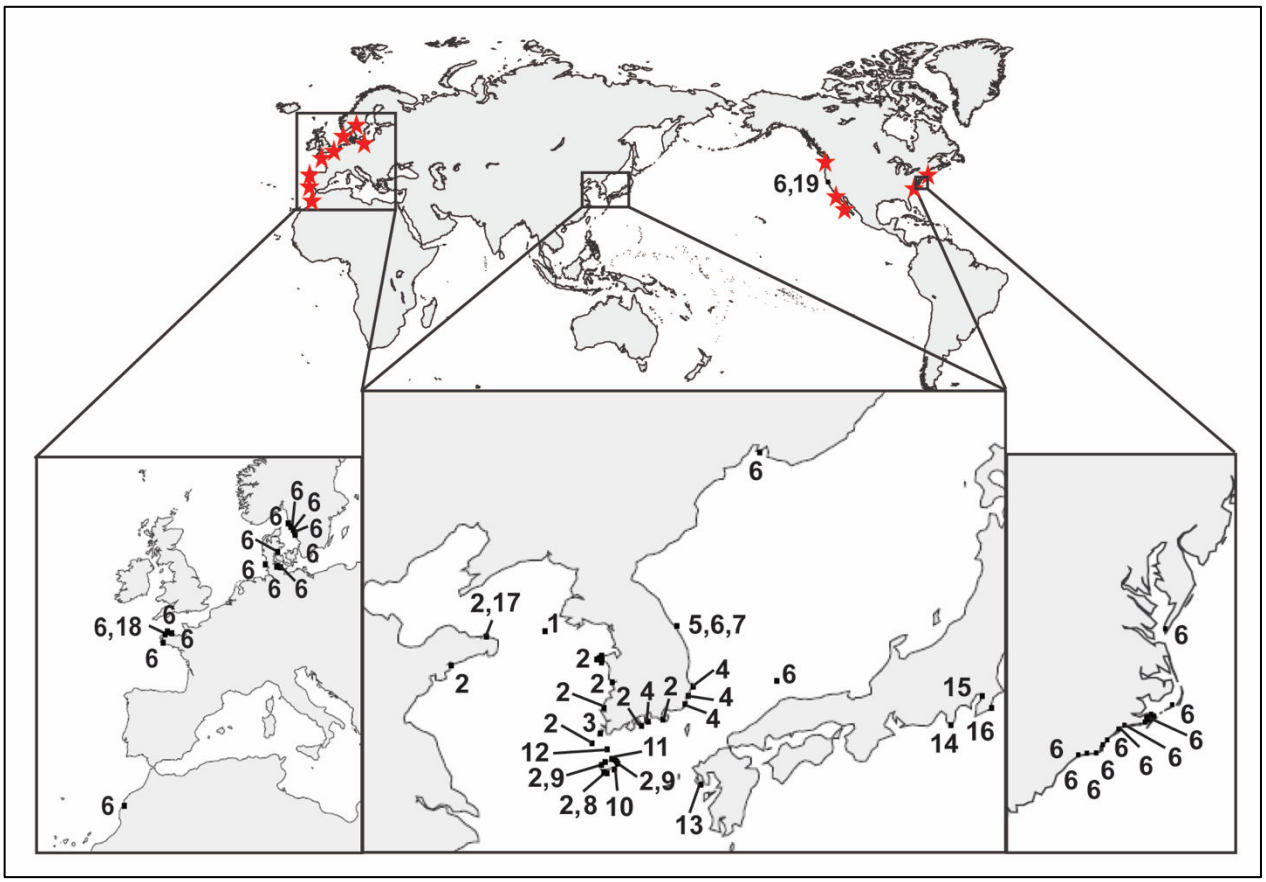

Fig. 25 Cartographie des haplotypes illustrant la diversité génétique de *Gracilaria vermiculophylla* par l'analyse de la séquence génétique mitochondriale de la sous unité 1 de la cytochrome c oxydase ou Cox1. Les numéros indiquent les haplotypes. Les haplotypes présentant un astérisque indiquent les zones connues où l'espèce est introduite (Kim et al., 2010).

Cette espèce peut devenir très abondante comme c'est le cas dans certaines rias bretonnes (Figure 23 B) et forme des tapis denses de quelques cm d'épaisseur. Selon les zones envahies, cette espèce invasive peut ainsi occuper une nouvelle niche écologique sans compétition avec d'autres espèces natives de macrophytes comme cela a été observé dans certaines rias de la Rade de Brest. *G. vermiculophylla* peut également entrer en compétition avec certaines populations natives, comme à titre d'exemple avec *Fucus vesiculosus* en Mer Baltique (Hammann et al., 2013). Elle présente un cycle de vie trigénétique et haplo-diplophasique, aux générations isomorphes avec plusieurs formes microscopiques de dispersion : les tétraspores et les carpospores (Figure 26).

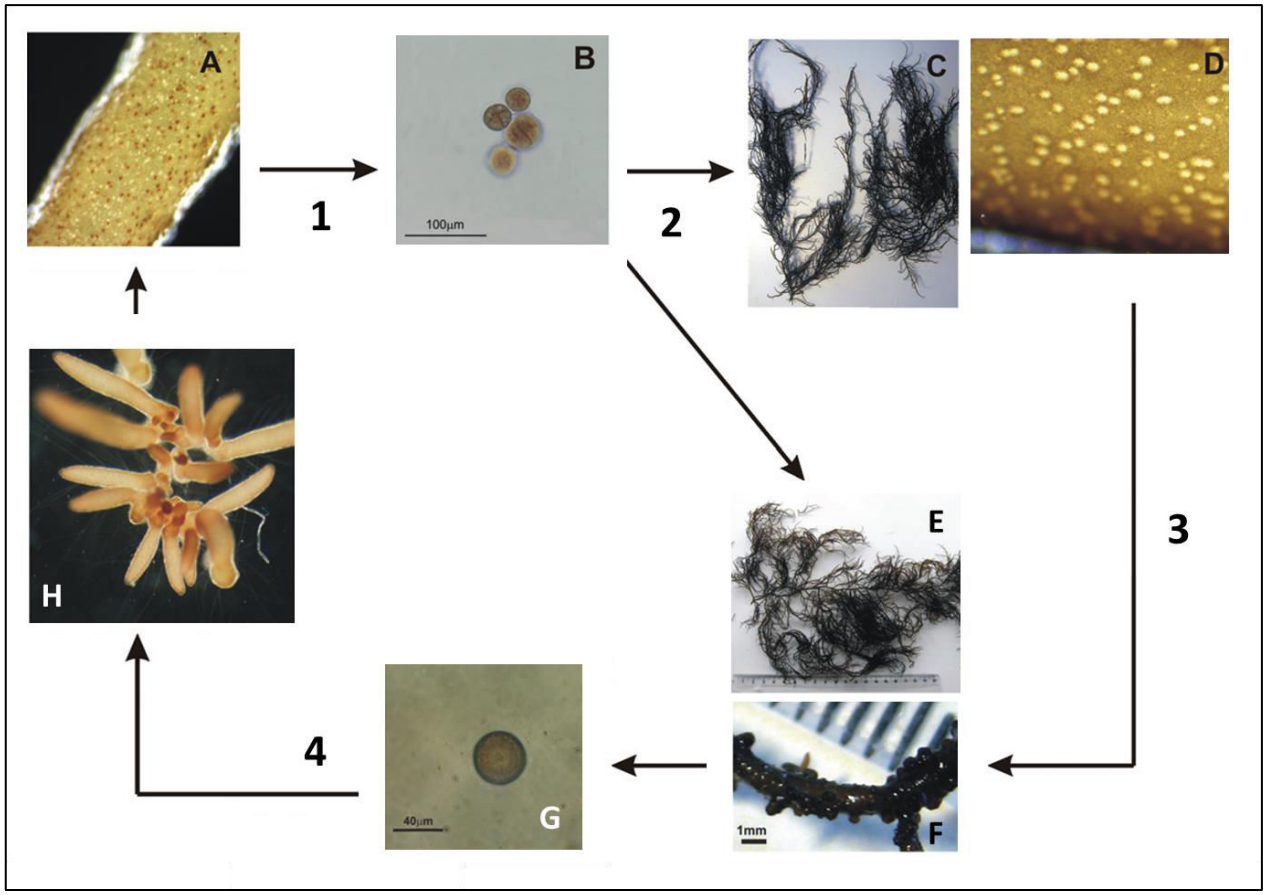

Fig. 26 Cycle de vie trigénétique de type haplo-diplophasique chez *Gracilaria vermiculophylla*, issu d'Abreu et al. (2011). **A** : tétrasporophyte (2n) présentant des tétrasporocystes ; **B** : tétraspores (n) ; **C** : gamétophyte mâle (n) ; **D** : vue macroscopique des loges des spermatocystes ; **E** : gamétophyte femelle (n) ; **F** : carposporophyte (2n) ou « thalle à verrues » présentant des carposporocystes ; **G** : carpospores (2n) ; **H** : jeunes tétrasporophytes (2n)
1 : méïose au sein des tétrasporocystes entraînant la formation de tétraspores (n)
2 : germination des tétraspores en gamétophytes mâle ou femelle par mitose
3 : fécondation et formation de carposporocystes (2n) sur le gamétophyte femelle
4 : germination des carpospores et développement du tétrasporophyte (2n)

- *Spartina alterniflora*

Spartina alterniflora est une plante herbacée invasive (Figure 27), originaire de la côte Atlantique du continent Nord-américain. Elle a été introduite dans de nombreuses régions du monde : sur la côte Ouest américaine, en Amérique du Sud, en Chine mais aussi en Australie, en Nouvelle-Zélande et également en Europe (Goulletquer, 2016). Cette espèce a été introduite accidentellement le long des côtes européennes atlantiques (Figure 24) : dans le Sud de l'Angleterre, ainsi qu'à la frontière espagnole au début du XIXème siècle. En Rade de Brest, elle serait introduite à la fin de première guerre mondiale, suite à la construction des bases militaires américaines (Sparfel et al., 2005). Des analyses génétiques montrent une très faible variabilité génétique entre les populations européennes, résultat attendu pour une espèce à dispersion majoritairement clonale (Baumel et al., 2003). Cependant, une variabilité mineure entre les populations basques et les populations anglaises et bretonnes indiqueraient au minimum une double introduction de l'espèce le long des côtes européennes. L'introduction initiale de *S. alterniflora* serait liée aux ballasts solides des bateaux du XIX^{ème} siècle (Goulletquer, 2016). Cette espèce a également été introduite intentionnellement et intensivement en qualité d'espèce ingénieure afin d'assécher des marais ou de créer des polders, favorisant ainsi son expansion à travers le monde comme l'a indiqué Querné (2011).

S. alterniflora colonise les schorres où elles supplantent les populations natives et homogénéise la végétation des estrans vaseux. Elle représente une menace par exemple pour la lavande de mer, *Limmonium humile*, une espèce présente en France uniquement dans les anses de la Rade de Brest (Quéré et al., 2010). Elle entre également en compétition avec les communautés autochtones à salicornes annuelles (Querné et al., 2012). Elle peut aussi se développer au niveau de la haute slikke nue avec une forte dynamique, se propageant par fragmentation du rhizome (Figure 28). Elle va former ainsi des prairies denses monospécifiques, appelées spartinaies, caractérisées par des populations à dominante clonale (Sparfel et al., 2005). Elle entraîne une réduction de la surface de vase nue et par voie de conséquence l'étendue des zones de nourrissage des oiseaux limicoles (Daehler, 1996). De plus, cette espèce ingénieure entraîne de multiples modifications des estrans notamment en terme de géomorphologie. Elle restreint le flux tidal en diminuant jusqu'à 76% la vitesse du courant (Neira et al., 2006). La présence de spartinaie engendre

ainsi une modification de la sédimentologie en augmentant le taux d'accrétion des sédiments (Neira et al., 2006). En réduisant les flux tidaux, une élévation des zones envahies par accumulation de sédiments fins est observée en comparaison des zones de vase nues entrainant un asséchement des marais maritimes (Grosholz et al., 2009).

Figure 27 : **A**- Illustration d'une spartinaie en Rade de Brest (photo prise le 12/06/2014, dans la ria du Faou). **B**- Photographie de *Spartina alterniflora* (photo prise le 04/06/2014, dans la ria de Penfoul).

Cette graminée vivace appartient à l'ordre des Poales et à la famille des Poacées. Elle présente des feuilles de couleur verte, alternes, lisses et dressées. Les pieds au stade feuillu mesurent de 40 à 60 cm et peuvent atteindre 3 m lorsque les épis floraux se forment. Le rhizome blanc est souterrain et enchevêtré de quelques cm dans la vase (Goulletquer, 2016). Dans ces zones d'invasion, la spartine ne fleurit pas et se reproduit uniquement de manière végétative pour maintenir ses populations. Par exemple, dans la baie de Willipa aux Etat-Unis, la floraison de *S. alterniflora* a été observée seulement 50 ans après son introduction (Goulletquer, 2016). Elle présente une tolérance importante vis-à-vis de nombreux facteurs écologiques, notamment la durée d'immersion et à sa particularité d'accumuler le silicium (Querné et al., 2012).

Les deux espèces suivies lors de cette étude, *Gracilaria vermiculophylla* et *Spartina alterniflora*, se développent au niveau de la haute slikke (Figure 15), au pied du schorre et également au niveau du bas schorre pour *S. alterniflora*. Ces deux espèces

présentent un intérêt tout particulier car elles peuvent se développer en association sur de larges zones de la haute slikke comme observé dans les trois rias de la Rade de Brest étudiées dans cette présente thèse. Un travail de cartographie a été entrepris par le Parc National Régional d'Armorique en collaboration avec ce projet de thèse (Figure 28).

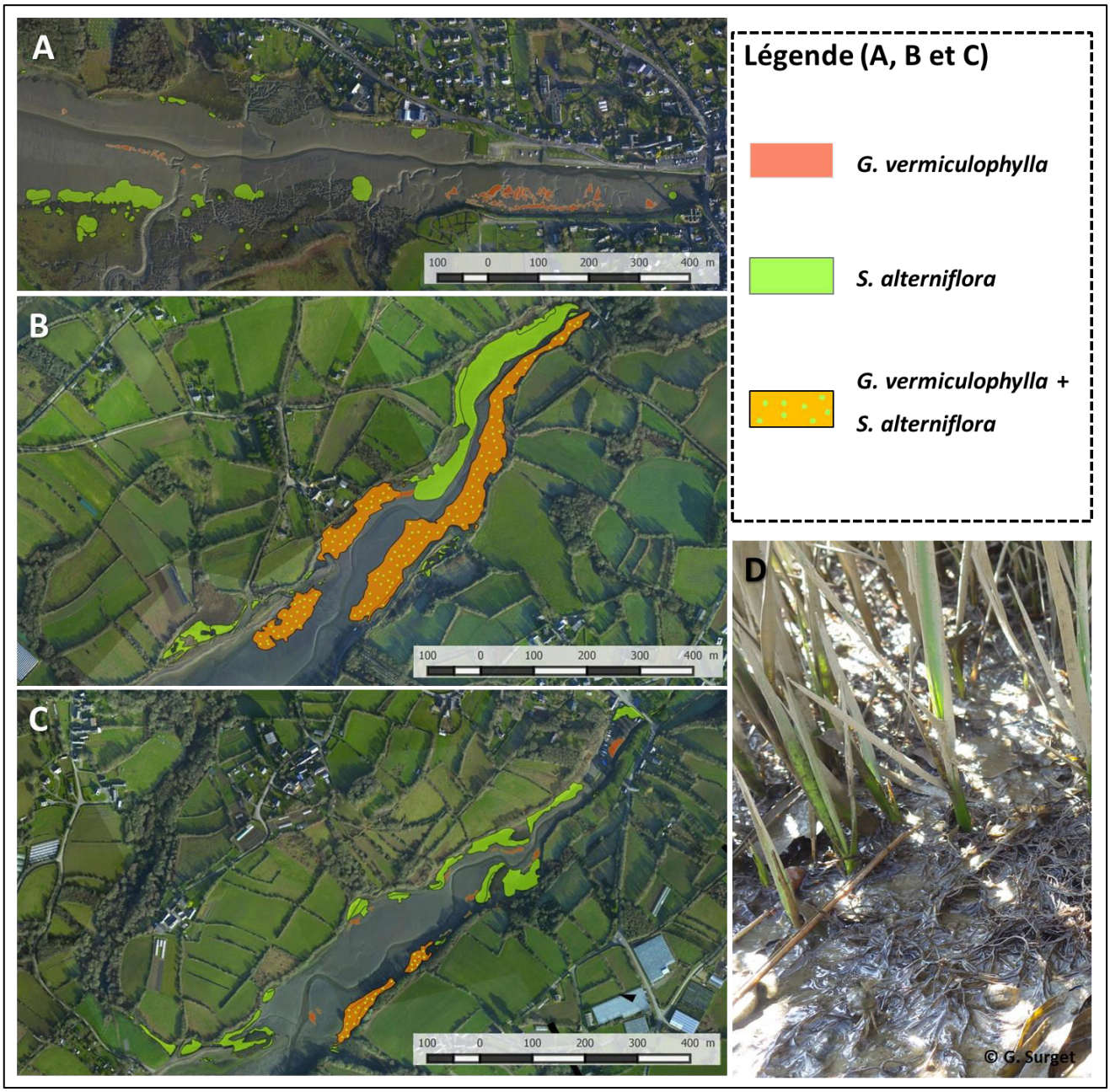

Fig. 29 Vues aériennes de la distribution de *Spartina alterniflora* et *Gracilaria vermiculophylla* dans trois rias de la Rade de Brest : dans la ria du Faou (A), dans l'anse de Penfoul (B) et dans la ria de Moulin Neuf (C) (issues d'orthophotographies 2012 et du stage de Joy Versterren intégré à cette thèse – Données provenant du PNRA/LEMAR). D-Illustration de l'association de *S.alterniflora* et *G. vermiculophylla* dans la Ria de Moulin Neuf (photo prise le 01/09/2014).

Ce travail a été réalisé en effectuant des relevés GPS *in situ* des contours des zones où se distribuent ces 2 espèces. Ce travail illustre la répartition de *G. vermiculophylla* dans ces trois rias de la Rade de Brest (première cartographie de cette espèce en Rade de Brest).

- **Autres végétaux marins d'intérêt : espèces natives**

Afin d'être en mesure de comparer les espèces invasives avec des espèces natives et de dans une optique de valorisation des macrophytes marins, quatre espèces ont été rajoutées à certaines expérimentations.

Bifurcaria bifurcata . R. Ross est une macroalgue brune de l'ordre des Fucales et de la famille des Sargasseceae (Cabioc'h et al., 2006). Cette phéophycée est une espèce indigène commune sur le littoral français qui se distribue uniquement le long des côtes atlantiques. Cette espèce possède une morphologie particulière : elle se développe sous la forme d'un faux rhizome rampant, duquel partent des axes cylindriques et dichotomes. Cette espèce native est une espèce de choix, appartenant à la même famille que son homologue invasive *Sargassum muticum* afin de réaliser des études comparatives entre espèces natives et invasives. *Bifurcaria bifurcata* se développe dans les mêmes mares intertidales que *S. muticum*.

Cladophora rupestris est une macroalgue verte native de la côte Est Atlantique et appartenant à la classe des Ulvophyceae, à l'ordre des Cladophorales et à la famille des Cladophoraceae. Elle est caractérisée par un thalle filamenteux touffu à ramifications régulières et de consistance rêche. Elle se distribue au niveau de l'étage médiolittoral et infralittoral (Cabioc'h et al., 2006). On peut l'observer à proximité de thalles de *C. fragile*.

Salicornia ramossissima et *S. fragilis* sont des plantes halophiles qui appartiennent à l'ordre des Caryophyllales et à la famille des Chenopodiaceae. Le genre *Salicornia* regroupe des espèces annuelles. Elles sont caractérisées par des organes végétatifs aériens succulents, constitués de tiges à rameaux opposés et articulés, décomposés en articles. Elles se développent en haut de l'étage médiolittoral au niveau des schorres d'estran vaseux. Cette phanérogame se développe ainsi dans le même type d'environnement que *G.vermiculophylla* et *S. alterniflora*. Ce sont des espèces halophiles comestibles et obligatoires adaptées notamment aux fortes salinités et à la dessiccation (Lahondère, 2004).

6. Objectifs et structure du projet de thèse

Comme présenté au début de cette introduction générale, cette thèse s'articule autour de trois problématiques qui en déterminent les différents objectifs.

Le premier objectif consiste à acquérir une connaissance importante de l'effet des principaux facteurs environnementaux sur la phénologie, l'écophysiologie et le métabolome des macrophytes marins invasifs étudiés et ce, *in situ* et à une échelle locale (au niveau de la Pointe bretonne). Les différentes études menées sont développées dans la partie 1, elle-même décomposée en quatre chapitres. En fonction des données pré-existantes dans la littérature, le choix s'est porté sur des espèces différentes pour les études effectuées. Cette partie (développée ci-après) va ainsi mettre en évidence les processus qui se déroulent lors de l'acclimatation de ces macrophytes invasives à leur environnement à l'échelle d'une population.

La seconde partie de ce manuscrit a pour objectif d'analyser les effets du gradient latitudinal sur les mêmes caractéristiques des macrophytes marins développées dans la partie précédente (*i.e.* la phénologie, l'écophysiologie et le métabolome) en intégrant les résultats de la partie 1 afin d'émettre des hypothèses quant à l'évolution des espèces étudiées dans un contexte de réchauffement climatique. Cette partie est décomposée en deux chapitres, l'un portant sur les espèces d'estran rocheux et l'autre sur *G. vermiculophylla* qui se développe en estran vaseux.

La dernière partie de ce manuscrit a pour but de démontrer l'émergence de voies de valorisation originales de ces macrophytes marins (par bio-inspiration) en intégrant le potentiel d'acclimatation de ces macrophytes (développé dans les deux parties précédentes) qui leur confère une forte chimiodiversité associée à des propriétés multifonctionnelles des métabolites (induits en réponse aux stress environnementaux). Cette partie 3 se compose d'une étude préliminaire qui a permis d'effectuer un criblage chez cinq macrophytes marins suivie de deux chapitres portant sur deux voies de valorisation différentes, en cosmétique en tant que filtre solaire et dans le domaine de la santé pour des applications potentielles dans la fonctionnalisation des biomatériaux par exemple.

Références

Abreu, M.H., Pereira, R., Sousa-Pinto, I., Yarish, C., 2011. Ecophysiological studies of the non-indigenous species *Gracilaria vermiculophylla* (Rhodophyta) and its abundance patterns in Ria de Aveiro lagoon, Portugal. Eur. J. Phycol. 46, 453–464.

Amsler, C.D. (2012) Chapter 9. Chemical ecology of seaweeds. In: *Seaweed Biology, novel insights into ecophysiology, ecology and utilization* (eds C. Wiencke and K. Bischof), Springer. Volume 219 of the series Ecological Studies. Springer-Verlag Berlin Heidelberg, pp 177-188

Bartsch, I., Wiencke, C., Laepple, T., 2012. Global seaweed biogeography under a changing climate: The prospected effects of temperature, in: Wiencke, C., Bischof, K. (Eds.), Seaweed Biology, Ecological Studies. Springer Berlin Heidelberg, pp. 383–406.

Baumel, A., Ainouche, M.L., Misset, M.T., Gourret, J.-P., Bayer, R.J., 2003. Genetic evidence for hybridization between the native *Spartina maritima* and the introduced *Spartina alterniflora* (Poaceae) in South-West France: *Spartina × neyrautii* re-examined. Plant Syst. Evol. 237, 87–97.

Bégin, C., Scheibling, R.E., 2005. Growth and survival of the invasive green alga *Codium* fragile ssp. tomentosoides in tide pools on a rocky shore in Nova Scotia. Bot. Mar. 46, 404–412.

Bellard, C., Thuiller, W., Leroy, B., Genovesi, P., Bakkenes, M., Courchamp, F., 2013. Will climate change promote future invasions? Glob. Change Biol. 19, 3740–3748.

Benyus, J.M., 2016. Biomimétisme: Quand la nature inspire des innovations durables. Rue de l'échiquier.

Bernstein, L., Bosch, P., Canziani, O., 2007. Changements Climatiques 2007: Rapport de synthèse. GIEC, Genève (Suisse).

Blossey, B., 2011. Enemy release hypothesis. Encycl. Biol. Invasions 193–196.

Bock, D.G., Caseys, C., Cousens, R.D., Hahn, M.A., Heredia, S.M., Hübner, S., Turner, K.G., Whitney, K.D., Rieseberg, L.H., 2015. What we still don't know about invasion genetics. Mol. Ecol. 24, 2277–2297.

Bœuf, G., 2015. Biomimétisme et bio-inspiration. Vraiment Durable 43–55.

Boudouresque, C.F., 2003. Les espèces introduites en milieu marin: faut-il s' en inquiéter?. GIS Posidonie.

Boudouresque, C.F., Verlaque, M., 2005. Nature conservation, marine protected areas, sustainable development and the flow of invasive species to the Mediterranean Sea. Trav. Sci. Parc Natl. Port-Cros 21, 29–54.

Boudouresque, C.F., Verlaque, M., 2002. Biological pollution in the Mediterranean Sea: invasive versus introduced macrophytes. Mar. Pollut. Bull. 44, 32–38.

Briggs, J.C., 1995. Global Biogeography. Elsevier.

Burge, C.A., Mark Eakin, C., Friedman, C.S., Froelich, B., Hershberger, P.K., Hofmann, E.E., Petes, L.E., Prager, K.C., Weil, E., Willis, B.L., 2014. Climate change influences on

marine infectious diseases: implications for management and society. Annu. Rev. Mar. Sci. 6, 249–277.

Burrows, M.T., Schoeman, D.S., Buckley, L.B., Moore, P., Poloczanska, E.S., Brander, K.M., Brown, C., Bruno, J.F., Duarte, C.M., Halpern, B.S., Holding, J., Kappel, C.V., Kiessling, W., O'Connor, M.I., Pandolfi, J.M., Parmesan, C., Schwing, F.B., Sydeman, W.J., Richardson, A.J., 2011. The pace of shifting climate in marine and terrestrial ecosystems. Science 334, 652–655.

Buswell, J.M., Moles, A.T., Hartley, S., 2011. Is rapid evolution common in introduced plant species? J. Ecol. 99, 214–224.

Cabioc'h, J., Floc'h, J.-Y., Le Toquin, A., Boudouresque, C.F., Meinesz, A., Verlaque, M., 2006. Guide des algues des mers d'Europe. Delachaux et Niestlé.

Cain, M.L., Damman, H., Lue, R.A., Yoon, C.K., 2006. Découvrir la biologie. De Boeck Supérieur.

Caldeira, K., Wickett, M.E., 2003. Oceanography: Anthropogenic carbon and ocean pH. Nature 425, 365–365.

Chauvaud, L., Jean, F., Ragueneau, O., Thouzeau, G., 2000. Long-term variation of the Bay of Brest ecosystem: benthic-pelagic coupling revisited. Mar. Ecol. Prog. Ser. 200, 35–48.

Cheang, C.C., Chu, K.H., Fujita, D., Yoshida, G., Hiraoka, M., Critchley, A., Choi, H.G., Duan, D., Serisawa, Y., Ang, P.O., 2010. Low Genetic variability of *Sargassum muticum* (phaeophyceae) revealed by a global analysis of native and introduced populations1. J. Phycol. 46, 1063–1074.

Cochrane, K., De Young, C., Soto, D., Bahri, T., 2009. Climate change implications for fisheries and aquaculture. FAO Fish. Aquac. Tech. Pap. 530, 212.

Costanza, R., d'Arge, R., Groot, R. de, Farber, S., Grasso, M., Hannon, B., Limburg, K., Naeem, S., O'Neill, R.V., Paruelo, J., Raskin, R.G., Sutton, P., Belt, M. van den, 1997. The value of the world's ecosystem services and natural capital. Nature 387, 253–260.

Critchley, A.T., 1983. *Sargassum muticum*: a taxonomic history including world-wide and western Pacific distributions. J. Mar. Biol. Assoc. U. K. 63, 617–625.

Critchley, A.T., Farnham, W.F., Yoshida, T., Norton, T.A., 1990. A bibliography of the invasive alga *Sargassum muticum* (Yendo) fensholt (Fucales; Sargassaceae). Bot. Mar. 33, 551–562.

Daehler, C.C., 1996. *Spartina* invasions in Pacific estuaries: biology, impact, and management, in: Proceedings of the Symposium on Non-Indigenous Species in Western Aquatic Ecosystems. Portland State University Lakes and Reservoirs Program, Publication (USA). pp. 96–98.

Davidson, A.D., Campbell, M.L., Hewitt, C.L., Schaffelke, B., 2015. Assessing the impacts of nonindigenous marine macroalgae: an update of current knowledge. Bot. Mar. 58, 55–79.

Davidson, A.D., Hewitt, C.L., 2014. How often are invasion-induced ecological impacts missed? Biol. Invasions 16, 1165–1173.

Davidson, A.M., Jennions, M., Nicotra, A.B., 2011. Do invasive species show higher phenotypic plasticity than native species and, if so, is it adaptive? A meta-analysis. Ecol. Lett. 14, 419–431.

De Reviers, B., 2002. *Biologie et Phylogénie des Algues*. Tome 1. Paris, Belin.

Diez, J.M., D'Antonio, C.M., Dukes, J.S., Grosholz, E.D., Olden, J.D., Sorte, C.J., Blumenthal, D.M., Bradley, B.A., Early, R., Ibáñez, I., Jones, S.J., Lawler, J.J., Miller, L.P., 2012. Will extreme climatic events facilitate biological invasions? Front. Ecol. Environ. 10, 249–257.

Doney, S.C., Fabry, V.J., Feely, R.A., Kleypas, J.A., 2009. Ocean acidification: the other CO2 problem. Annu. Rev. Mar. Sci. 1, 169–192.

Dring, M.J., 1992. The biology of marine plants. Cambridge University Press, Cambridge.

Duarte, C.M., 2000. Marine biodiversity and ecosystem services: an elusive link. J. Exp. Mar. Biol. Ecol. 250, 117–131.

Dukes, J.S., Mooney, H.A., Dukes, J.S., Mooney, H.A., Dukes, J.S., Mooney, H.A., 1999. Does global change increase the success of biological invaders? Trends Ecol. Evol. 14, 135–139.

Engelen, A.H., Serebryakova, A., Ang, P., Britton-Simmons, K., Mineur, F., Pedersen, M.F., Arenas, F., Fernandez, C., Steen, H., Svenson, R., 2015. Circumglobal invasion by the brown seaweed *Sargassum muticum*. Oceanogr. Mar. Biol. Annu. Rev. 53, 81–126.

Farnham, W.F., Fletcher, R.L., Irvine, L.M., 1973. Attached *Sargassum* Found in Britain. Nature 243, 231–232.

Freshwater, D.W., Montgomery, F., Greene, J.K., Hamner, R.M., Williams, M., Whitfield, P.E., 2006. Distribution and identification of an invasive *Gracilaria* species that is hampering commercial fishing operations in Southeastern North Carolina, USA. Biol. Invasions 8, 631–637.

Galil, B.S., 2007. Loss or gain? Invasive aliens and biodiversity in the Mediterranean Sea. Mar. Pollut. Bull., Marine Bioinvasions: A collection of reviews 55, 314–322.

Godoy, O., Valladares, F., Castro-Díez, P., 2011. Multispecies comparison reveals that invasive and native plants differ in their traits but not in their plasticity. Funct. Ecol. 25, 1248–1259.

Gohin, F., Saulquin, B., Bryere, P., 2010. Atlas de la Température, de la concentration en Chlorophylle et de la Turbidité de surface du plateau continental français et de ses abords de l'Ouest européen. Ifremer. http://archimer.ifremer.fr/doc/00057/16840/

Goudard, A., 2007. Fonctionnement des écosystèmes et invasions biologiques: importance de la biodiversité et des interactions interspécifiques. Université Paris VI.

Goulletquer, P., 2016. Guide des organismes exotiques marins. Belin.

Grosholz, E.D., Levin, L.A., Tyler, A.C., Neira, C., 2009. Changes in community structure and ecosystem function following *Spartina alterniflora* invasion of Pacific estuaries. Hum. Impacts Salt Marshes Glob. Perspect. Univ. Calif. Press Berkeley Los Angel. 23–40.

Guérin, F., 2006. Emission de gaz à effet de serre (CO_2, CH_4) par une retenue de barrage hydroélectrique en zone tropicale (Petit-Saut, Guyane Française): expérimentation et modélisation. Université Paul Sabatier-Toulouse III.

Guillemin, M.-L., Akki, S.A., Givernaud, T., Mouradi, A., Valero, M., Destombe, C., 2008. Molecular characterisation and development of rapid molecular methods to identify species of Gracilariaceae from the Atlantic coast of Morocco. Aquat. Bot. 89, 324–330.

Guiry in Guiry, M.D. & Guiry, G.M. 2016. *AlgaeBase*. World-wide electronic publication, National University of Ireland, Galway. http://www.algaebase.org; searched on 15 Janvier 2016.

Gulbransen, D.J., McGlathery, K.J., Marklund, M., Norris, J.N., Gurgel, C.F.D., 2012. *Gracilaria vermiculophylla* (rhodophyta, Gracilariales) in the Virginia Coastal Bays, Usa: Cox1 Analysis Reveals High Genetic Richness of an Introduced Macroalga. J. Phycol. 48, 1278–1283.

Häder, D.-P., Kumar, H.D., Smith, R.C., Worrest, R.C., 2007. Effects of solar UV radiation on aquatic ecosystems and interactions with climate change. Photochem. Photobiol. Sci. 6, 267–285.

Hammann, M., Buchholz, B., Karez, R., Weinberger, F., 2013. Direct and indirect effects of *Gracilaria vermiculophylla* on native *Fucus vesiculosus*. Aquat. Invasions 8, 121–132.

Hansen, J., Sato, M., 2016. Regional climate change and national responsibilities. Environ. Res. Lett. 11, 034009.

Hansen, J., Sato, M., Ruedy, R., Lo, K., Lea, D.W., Medina-Elizade, M., 2006. Global temperature change. Proc. Natl. Acad. Sci. 103, 14288–14293.

Harley, C.D.G., Randall Hughes, A., Hultgren, K.M., Miner, B.G., Sorte, C.J.B., Thornber, C.S., Rodriguez, L.F., Tomanek, L., Williams, S.L., 2006. The impacts of climate change in coastal marine systems. Ecol. Lett. 9, 228–241.

Haywood, J., Schulz, M., 2007. Causes of the reduction in uncertainty in the anthropogenic radiative forcing of climate between IPCC (2001) and IPCC (2007). Geophys. Res. Lett. 34, L20701.

Heger, T., Jeschke, J.M., 2014. The enemy release hypothesis as a hierarchy of hypotheses. Oikos 123, 741–750.

Hellmann, J.J., Byers, J.E., Bierwagen, B.G., Dukes, J.S., 2008. Five potential consequences of climate change for invasive species. Conserv. Biol. 22, 534–543.

Helmuth, B., Harley, C.D.G., Halpin, P.M., O'Donnell, M., Hofmann, G.E., Blanchette, C.A., 2002. Climate change and latitudinal patterns of intertidal thermal stress. Science 298, 1015–1017.

Hoegh-Guldberg, O., Bruno, J.F., 2010. The impact of climate change on the World's marine ecosystems. Science 328, 1523–1528.

Hu, Z.-M., Fraser, C., 2016. Seaweed phylogeography. Springer.

Huang, Q.Q., Pan, X.Y., Fan, Z.W., Peng, S.L., 2015. Stress relief may promote the evolution of greater phenotypic plasticity in exotic invasive species: a hypothesis. Ecol. Evol. 5, 1169–1177.

Hupel, M., Lecointre, C., Meudec, A., Poupart, N., Gall, E.A., 2011. Comparison of photoprotective responses to UV radiation in the brown seaweed *Pelvetia canaliculata* and the marine angiosperm *Salicornia ramosissima*. J. Exp. Mar. Biol. Ecol. 401, 36–47.

Hurd, C.L., Harrison, P.J., Bischof, K., Lobban, C.S., 2014. Seaweed ecology and physiology. Cambridge University Press.

Institute, N.A., 2015. Introduction to biology. Lulu.com.

IPCC, 2001. IPCC, 2001: climate change 2001: the scientific basis. Contribution of Working Group 1 to the Third Assessment Report of the Intergovernmental Panel on Climate Change, edited by J. T. Houghton, Y. Ding, D. J. Griggs, M. Noguer, P. J. van der Linden, X. Dai, K. Maskell and C. A. Johnson (eds). Cambridge University Press, Cambridge, UK, and New York, USA, 2001.

IPCC, I.P. on C.C., 2013. The physical science basis. Contribution of working group I to the fifth assessment report of the intergovernmental panel on climate change, Climate Change 2013 ed T Stocker et al. ed. USA: Cambridge University Press.

Isaak, D.J., Rieman, B.E., 2013. Stream isotherm shifts from climate change and implications for distributions of ectothermic organisms. Glob. Change Biol. 19, 742–751.

Joshi, J., Vrieling, K., 2005. The enemy release and EICA hypothesis revisited: incorporating the fundamental difference between specialist and generalist herbivores. Ecol. Lett. 8, 704–714.

Jueterbock, A., Tyberghein, L., Verbruggen, H., Coyer, J.A., Olsen, J.L., Hoarau, G., 2013. Climate change impact on seaweed meadow distribution in the North Atlantic rocky intertidal. Ecol. Evol. 3, 1356–1373.

Katsanevakis, S., Wallentinus, I., Zenetos, A., Leppäkoski, E., Çinar, M.E., Oztürk, B., Grabowski, M., Golani, D., Cardoso, A.C., 2014. Impacts of invasive alien marine species on ecosystem services and biodiversity: a pan-European review. Aquat. Invasions 9, 391–423.

Kiehl, J.T., Trenberth, K.E., 1997. Earth's annual global mean energy budget. Bull. Am. Meteorol. Soc. 78, 197–208.

Kim, S.Y., Weinberger, F., Boo, S.M., 2010. Genetic data hint at a common donor region for invasive Atlantic and Pacific populations of *Gracilaria vermiculophylla* (gracilariales, Rhodophyta)1. J. Phycol. 46, 1346–1349.

Klein, J.C., 2011. Les proliférations et invasions des macrophytes marins; Etat de l'art, rapport du projet OCEANS 25 p.

Klöser, H., Mercuri, G., Laturnus, F., Quartino, M.L., Wiencke, C., 1994. On the competitive balance of macroalgae at Potter Cove (King George Island, South Shetlands). Polar Biol. 14, 11–16.

Kolar, C.S., Lodge, D.M., 2001. Progress in invasion biology: predicting invaders. Trends Ecol. Evol. 16, 199–204.

Kollars, N.M., Krueger-Hadfield, S.A., Byers, J.E., Greig, T.W., Strand, A.E., Weinberger, F., Sotka, E.E., 2015. Development and characterization of microsatellite loci for the haploid–diploid red seaweed *Gracilaria vermiculophylla*. PeerJ 3, e1159. doi:10.7717/peerj.1159

Lahondère, C., 2004. Les salicornes s.l. (*Salicornia* L., *Sarcocornia* A. J. Scott et *Arthrocnemum* Moq.): sur les côtes françaises. Bulletin de la Société Botanique du Centre-Ouest 24.

Lande, R., 2015. Evolution of phenotypic plasticity in colonizing species. Mol. Ecol. 24, 2038–2045.

Larzillière A., 2014. Document d'Objectifs Natura 2000 – Rade de Brest-estuaire de l'aulne et Rade de Brest, baie de Daoulas, anse du Poulmic, Tome 3 : Actions et opérations. Parc naturel régional d'Armorique, Brest métropole océane, DREAL Bretagne.

Levitus, S., Antonov, J.I., Boyer, T.P., Stephens, C., 2000. Warming of the world ocean. Science 287, 2225–2229.

Lima, F.P., Ribeiro, P.A., Queiroz, N., Hawkins, S.J., Santos, A.M., 2007. Do distributional shifts of northern and southern species of algae match the warming pattern? Glob. Change Biol. 13, 2592–2604.

Liu, H., Stiling, P., 2006. Testing the enemy release hypothesis: a review and meta-analysis. Biol. Invasions 8, 1535–1545.

Lopes, C.B., Pereira, M.E., Vale, C., Lillebø, A.I., Pardal, M.Â., Duarte, A.C., 2007. Assessment of spatial environmental quality status in Ria de Aveiro (Portugal). Sci. Mar. 293–304.

McKenzie, R.L., Aucamp, P.J., Bais, A.F., Björn, L.O., Ilyas, M., Madronich, S., 2011. Ozone depletion and climate change: impacts on UV radiation. Photochem. Photobiol. Sci. 10, 182–198.

Mooney, H.A., Cleland, E.E., 2001. The evolutionary impact of invasive species. Proc. Natl. Acad. Sci. 98, 5446–5451.

Neira, C., Grosholz, E.D., Levin, L.A., Blake, R., 2006. Mechanisms generating modification of benthos following tidal flat invasion by a *Spartina* Hybrid. Ecol. Appl. 16, 1391–1404.

Norton, T.A., Melkonian, M., Andersen, R.A., 1996. Algal biodiversity. Phycologia 35, 308–326.

Nyberg, C.D., Wallentinus, I., 2005. Can species traits be used to predict marine macroalgal introductions? Biol. Invasions 7, 265–279.

Occhipinti-Ambrogi, A., Savini, D., 2003. Biological invasions as a component of global change in stressed marine ecosystems. Mar. Pollut. Bull. 46, 542–551.

Ojaveer, H., Galil, B.S., Campbell, M.L., Carlton, J.T., Canning-Clode, J., Cook, E.J., Davidson, A.D., Hewitt, C.L., Jelmert, A., Marchini, A., McKenzie, C.H., Minchin, D., Occhipinti-Ambrogi, A., Olenin, S., Ruiz, G., 2015. Classification of non-indigenous species based on their impacts: Considerations for application in marine management. PLOS Biol. 13, e1002130.

Olafsson, E., 2016. Marine Macrophytes as Foundation Species. CRC Press.

Orr, J.C., Fabry, V.J., Aumont, O., Bopp, L., Doney, S.C., Feely, R.A., Gnanadesikan, A., Gruber, N., Ishida, A., Joos, F., Key, R.M., Lindsay, K., Maier-Reimer, E., Matear, R., Monfray, P., Mouchet, A., Najjar, R.G., Plattner, G.-K., Rodgers, K.B., Sabine, C.L., Sarmiento, J.L., Schlitzer, R., Slater, R.D., Totterdell, I.J., Weirig, M.-F., Yamanaka, Y., Yool, A., 2005. Anthropogenic ocean acidification over the twenty-first century and its impact on calcifying organisms. Nature 437, 681–686.

Perrings, C., Dehnen-Schmutz, K., Touza, J., Williamson, M., 2005. How to manage biological invasions under globalization. Trends Ecol. Evol., Special issue: Invasions, guest edited by Michael E. Hochberg and Nicholas J. Gotelli 20, 212–215.

Pessoa, M.F., 2012. Algae and aquatic macrophytes responses to cope to ultraviolet radiation-a Review. Emir. J. Food Agric. 24, 527.

Plouguerné, E., 2006. Etude écologique et chimique de deux algues introduites sur les côtes bretonnes, *Grateloupia turuturu* Yamada et *Sargassum muticum* (Yendo) Fensholt: nouvelles ressources biologiques de composés à activité antifouling. Brest.

Potin, P., Bouarab, K., Salaün, J.-P., Pohnert, G., Kloareg, B., 2002. Biotic interactions of marine algae. Curr. Opin. Plant Biol. 5, 308–317.

Prentis, P.J., Wilson, J.R.U., Dormontt, E.E., Richardson, D.M., Lowe, A.J., 2008. Adaptive evolution in invasive species. Trends Plant Sci. 13, 288–294.

Prince, J.S., Trowbridge, C.D., 2005. Reproduction in the green macroalga *Codium* (Chlorophyta): characterization of gametes. Bot. Mar. 47, 461–470.

Provan, J., Booth, D., Todd, N.P., Beatty, G.E., Maggs, C.A., 2008. Tracking biological invasions in space and time: elucidating the invasive history of the green alga *Codium fragile* using old DNA. Divers. Distrib. 14, 343–354.

Provan, J., Murphy, S., Maggs, C.A., 2005. Tracking the invasive history of the green alga *Codium fragile ssp. tomentosoides*. Mol. Ecol. 14, 189–194.

Pyšek, P., Hulme, P.E., Nentwig, W., 2009. Glossary of the main technical terms used in the handbook, in: Handbook of Alien Species in Europe, Invading Nature - Springer Series in Invasion Ecology. Springer Netherlands, pp. 375–379.

Qiu, J., 2015. A global synthesis of the effects of biological invasions on greenhouse gas emissions. Glob. Ecol. Biogeogr. 24, 1351–1362.

Quéré, E., Magnanon, S., Annézo, N., 2010. Vingt ans de suivi et de conservation du *Limmonium humile* Miller en rade de Brest. ERICA 23, 101–121.

Querné, J., 2011. Invasion de *Spartina alterniflora* dans les marais de la rade de Brest. Comportement invasif et impact sur le cycle biogéochimique du silicium. UBO, Brest.

Querné, J., Ragueneau, O., Poupart, N., 2012. In situ biogenic silica variations in the invasive salt marsh plant, *Spartina alterniflora*: A possible link with environmental stress. Plant Soil 352, 157–171.

Rahel, F.J., Olden, J.D., 2008. Assessing the effects of climate change on aquatic invasive species. Conserv. Biol. 22, 521–533.

Ramade, F., 2002. Dictionnaire encyclopédique de l'écologie et des sciences de l'environnement, seconde édition. Éd Ediscience Dunod–Technique Ind.

Raven, J.A., Geider, R.J., 2003. Adaptation, acclimation and regulation in algal photosynthesis, in: Larkum, A.W.D., Douglas, S.E., Raven, J.A. (Eds.), Photosynthesis in Algae, Advances in Photosynthesis and Respiration. Springer Netherlands, pp. 385–412.

Ricard P. 2015. Le biomimétisme : s'inspirer de la nature pour innover durablement. Les avis du conseil économique social et environnemental (CESE). http://www.lecese.fr/travaux-publies/le-biomim-tisme-sinspirer-de-la-nature-pour-innover-durablement

Richardson, D.M., Pyšek, P., Rejmánek, M., Barbour, M.G., Panetta, F.D., West, C.J., 2000. Naturalization and invasion of alien plants: concepts and definitions. Divers. Distrib. 6, 93–107.

Ross, M. s., Meeder, J. f., Sah, J. p., Ruiz, P. l., Telesnicki, G. j., 2000. The Southeast saline everglades revisited: 50 years of coastal vegetation change. J. Veg. Sci. 11, 101–112.

Rueness, J., 2005. Life history and molecular sequences of *Gracilaria vermiculophylla* (Gracilariales, Rhodophyta), a new introduction to European waters. Phycologia 44, 120–128.

Sabour, B., Reani, A., El-Magouri, H., Haroun, R., 2013. *Sargassum muticum* (Yendo) Fensholt (Fucales, Phaeophyta) in Morocco, an invasive marine species new to the Atlantic coast of Africa. Aquat. Invasions 8, 97.

Sampath-Wiley, P., Neefus, C.D., Jahnke, L.S., 2008. Seasonal effects of sun exposure and emersion on intertidal seaweed physiology: Fluctuations in antioxidant contents, photosynthetic pigments and photosynthetic efficiency in the red alga *Porphyra umbilicalis* Kützing (Rhodophyta, Bangiales). J. Exp. Mar. Biol. Ecol. 361, 83–91. doi:10.1016/j.jembe.2008.05.001

Santelices, B., Bolton, J.J., Meneses, I., 2009. Chapter six marine algal communities. Mar. Macroecology 153.

Schaffelke, B., Hewitt, C.L., 2007. Impacts of introduced seaweeds. Bot. Mar. 50, 397–417.

Schaffelke, B., Smith, J.E., Hewitt, C.L., 2006. Introduced macroalgae — A growing concern, in: Anderson, R., Brodie, J., Onsøyen, E., Critchley, A.T. (Eds.), Eighteenth International Seaweed Symposium, Developments in Applied Phycology. Springer Netherlands, pp. 303–315.

Sorte, C.J.B., Ibáñez, I., Blumenthal, D.M., Molinari, N.A., Miller, L.P., Grosholz, E.D., Diez, J.M., D'Antonio, C.M., Olden, J.D., Jones, S.J., Dukes, J.S., 2013. Poised to prosper? A cross-system comparison of climate change effects on native and non-native species performance. Ecol. Lett. 16, 261–270.

Sorte, C.J.B., Williams, S.L., Carlton, J.T., 2010a. Marine range shifts and species introductions: comparative spread rates and community impacts. Glob. Ecol. Biogeogr. 19, 303–316.

Sorte, C.J.B., Williams, S.L., Zerebecki, R.A., 2010b. Ocean warming increases threat of invasive species in a marine fouling community. Ecology 91, 2198–2204.

Sparfel, L., Fichaut, B., Suanez, S., 2005. Progression de la Spartine (*Spartina alterniflora* Loisel) en rade de Brest (Finistère) entre 1952 et 2004 : de la mesure à la réponse gestionnaire. Norois Environ. Aménage. Société 109–123.

Stengel, D.B., Connan, S., Popper, Z.A., 2011. Algal chemodiversity and bioactivity: Sources of natural variability and implications for commercial application. Biotechnol. Adv., Marine Biotechnology in EuropeEuropean Science Foundation-COST Conference: "Marine Biotechnology: Future Challenges" 29, 483–501.

Stiger-Pouvreau, V., Thouzeau, G., 2015. Marine species introduced on the French Channel-Atlantic Coasts: A review of main biological invasions and impacts. Open J. Ecol. 05, 227–257.

Stiger-Pouvreau, V., Guérard, F., 2017. Bio-Inspired molecules extracted from marine macroalgae: A new generation of active ingredients for cosmetics and human health. In Blue Biotechnology: Production and Use of Marine Molecules, Part 2. La Barre S & Bates SS (Eds).

Sumich, J.L., Morrissey, J.F., 2004. Introduction to the biology of marine life, 8th edition. Jones and Bartlett publishers, USA, pp 98-123.

Tanniou, A., 2014. Etude de la production de biomolécules d'intérêt (phlorotannins, pigments, lipides) par l'algue brune modèle *Sargassum muticum* par des approches combinées de profilage métabolique et d'écophysiologie.

Thévenot, J., 2013. Synthèse et réflexions sur des définitions relatives aux invasions biologiques. Préambule Aux Actions Strat. Natl. Sur EEE Ayant Un Impact Négatif Sur Biodiversité Serv. Patrim. Nat. Muséum Natl. Hist. Nat. Paris 31.

Thomsen, M.S., Gurgel, C.F.D., Fredericq, S., McGlathery, K.J., 2006. *Gracilaria vermiculophylla* (rhodophyta, Gracilariales) in Hog Island Bay, Virginia: A cryptic alien and invasive macroalga and taxonomic correction1. J. Phycol. 42, 139–141.

Thomsen, M.S., McGlathery, K., 2005. Facilitation of macroalgae by the sedimentary tube forming polychaete *Diopatra cuprea*. Estuar. Coast. Shelf Sci. 62, 63–73.

Thomsen, M.S., McGlathery, K.J., Schwarzschild, A., Silliman, B.R., 2009. Distribution and ecological role of the non-native macroalga *Gracilaria vermiculophylla* in Virginia salt marshes. Biol. Invasions 11, 2303–2316.

Thomsen, M.S., Stæhr, P.A., Nyberg, C.D., Schwaerter, S., Krause-Jensen, D., Silliman, B.R., 2007. *Gracilaria vermiculophylla* (Ohmi) Papenfuss, 1967 (Rhodophyta, Gracilariaceae) in northern Europe, with emphasis on Danish conditions, and what to expect in the future. Aquat. Invasions.

Trenberth, K.E., Fasullo, J.T., Kiehl, J., 2009. Earth's global energy budget. Bull. Am. Meteorol. Soc. 90, 311–323.

Trowbridge, C.D., 1998. Ecology of the green macroalga *Codium fragile* (Suringar) Hariot 1889: invasive and non-invasive subspecies. Oceanogr. Mar. Biol. Annu. Rev. 36, 1–64.

Viard, F., Comtet, T., 2009. Déferlantes d'invasions dans les milieux marins. Pour Sci. 65, 20–25.

Walther, G.-R., 2010. Community and ecosystem responses to recent climate change. Philos. Trans. R. Soc. Lond. B Biol. Sci. 365, 2019–2024.

Weinberger, F., Buchholz, B., Karez, R., Wahl, M., 2008. The invasive red alga *Gracilaria vermiculophylla* in the Baltic Sea: adaptation to brackish water may compensate for light limitation. Aquat. Biol. 3, 251–264.

Wiencke, C., Bischof, K., 2012. Seaweed biology. Ecol. Stud. 219.

Wikström, S.A., Pavia, H., 2004. Chemical settlement inhibition versus post-settlement mortality as an explanation for differential fouling of two congeneric seaweeds. Oecologia 138, 223–230.

Williams, S.L., Smith, J.E., 2007. A global review of the distribution, taxonomy, and impacts of introduced seaweeds. Annu Rev Ecol Evol Syst 38, 327–359.

Williamson, M., Fitter, A., 1996. The varying success of invaders. Ecology 77, 1661–1666. doi:10.2307/2265769

Zal, F., Rousselot, M., 2014. Extracellular hemoglobins from annelids, and their potential use in biotechnology, in: Barre, S.L., Kornprobst, J.-M. (Eds.), Outstanding Marine Molecules. Wiley-VCH Verlag GmbH & Co. KGaA, pp. 361–376.

Zepp, R.G., Iii, D.J.E., Paul, N.D., Sulzberger, B., 2007. Interactive effects of solar UV radiation and climate change on biogeochemical cycling. Photochem. Photobiol. Sci. 6, 286–300.

Partie 1 : Quels processus d'acclimatation se déroulent à l'échelle d'une population chez plusieurs espèces de macroalgues invasives?

La variabilité spatiale et temporelle des conditions environnementales induit une acclimatation constante du métabolisme des macrophytes marins, qui leur permet de prévenir des dommages et de favoriser leur survie (Fogg, 2001). Le but de cette partie 1 est d'appréhender cette acclimatation chez trois espèces de macroalgues invasives, appartenant à différentes lignées évolutives : *Gracilaria vermiculophylla*, *Codium fragile* et *Sargassum muticum*. Elle est organisée sous la forme de quatre chapitres qui décrivent plusieurs études portant sur des suivis d'une année mais à une échelle spatiale réduite n'excédant pas la taille d'une population, *i.e.* à l'échelle du site d'étude et à l'échelle de quelques cm et ceci, à différentes échelles biologiques : à l'échelle des populations et du métabolome, ainsi qu'à différentes échelles temporelles en incrémentant l'échelle d'une marée basse à celle des saisons. En effet, selon les processus observés, on se situe à différentes échelles de temps, tous les mécanismes biologiques ne s'effectuant pas à la même échelle (*cf.* Introduction). Ainsi, plusieurs approches ont été utilisées en fonction des échelles spatiale et temporelle considérées et en fonction de la question scientifique sous-jacente. Pour répondre à chaque problématique, différentes macroalgues invasives ont été prises comme modèle :

- Quelles variations des phénotypes écologiques et métabolomiques observe-t-on à l'échelle d'une année ? _ exemple de *C. fragile* et *G. vermiculophylla* (Chapitre 1)
- Quelles sont les caractéristiques particulières de la biologie d'une espèce invasive à une échelle spatiale localisée : mise en évidence de la vie enfouie dans la vase chez une rhodophyte, en prenant l'exemple particulier de *G. vermiculophylla* (Chapitre 2)
- Quelles sont les variations physiologiques observées selon un cycle tidal hivernal ou estival ? _ exemple de *G. vermiculophylla* et *S. muticum* (Chapitre 3)
- Quels sont les impacts de ces espèces invasives sur l'écosystème ? _ exemple de *G. vermiculophylla* dans une vasière (Chapitre 4)

L'ensemble de ces études a pour but d'amener une vision intégrative vis-à-vis de la phénologie, de la biologie et de la physiologie des modèles étudiés au niveau de la Pointe bretonne, réflet d'une latitude intermédiaire entre l'Europe du Nord et l'Europe du Sud.

Chapitre 1. Quelles variations des phénotypes écologiques et métabolomiques observe-t'on à l'échelle d'une année ?

Dans ce chapitre seront présentées les variations phénotypiques à la fois au niveau écologique mais également métabolomique chez deux modèles biologiques invasifs, l'algue verte *Codium fragile* et l'algue rouge *Gracilaria vermiculophylla*. Ce suivi à l'échelle d'une année a eu pour but d'étudier les phénotypes écologiques et biochimiques de *C. fragile* au niveau de trois sites rocheux de la mer d'Iroise et de *G. vermiculophylla* dans trois rias de la Rade de Brest (*cf.* présentation des sites d'étude). La phénologie et la métabolomique de ces deux modèles invasifs des côtes bretonnes ont été suivies durant une année à raison d'un échantillonnage saisonnier (tous les 3 mois) dans le but de comprendre l'acclimatation de ces deux modèles à l'échelle d'un cycle biologique en associant un suivi biochimique et écologique.

Ces travaux illustrent l'intérêt de la RMN classique et de la RMN HR-MAS en particulier dans le domaine de l'écophysiologie et de l'écologie chimique. Cette technique exhaustive apporte une approche de métabolomique non ciblée, consistant en un profilage non prédéfini de l'ensemble des métabolites cellulaires présents majoritairement chez les espèces étudiées.

Les travaux portant sur *C. fragile* consistent en un travail préliminaire avec la mise au point d'une méthodologie de spectrocopie de RMN utilisée dans la suite du manuscrit qui va être soumise à publication. Ce travail est présenté sous la forme d'une note. Une étude analogue et plus approfondie portant sur *G. vermiculophylla* a fait l'objet d'une publication dans le Journal of Applied Phycology, celle-ci est donc présentée sous cette forme.

Manuscrit en préparation

1_ Interest of the HR-MAS NMR technology for the metabolomic and phenological monitoring of the green macroalga *Codium fragile* along the coasts of Iroise Sea (France)

Introduction

Alien seaweeds represent one of the largest groups of marine organisms introduced in Europe and *Codium fragile* (Suringar) Hariot, belongs to one of the most widespread intertidal chlorophyte throughout the world (Campbell, 1999; Trowbridge and Todd, 1999; Provan et al., 2008; Stiger-Pouvreau and Thouzeau, 2015). *Codium fragile* is a green macroalga belonging to Ulvophyceae Class, Bryopsidales Order and Codiaceae family. Native from Japan and North Pacific (Provan et al., 2008; Silva, 1955), this species was extensively studied along the Atlantic West coast and especially in Nova Scotia (Carlton and Scanlon, 1985; Chapman, 1999; Churchill and Moeller, 1972; Garbary et al., 1997; Theriault et al., 2006), as in Australia (Campbell, 1999; Trowbridge, 1995) where it is now considered as a marine pest. *C. fragile* subspecies were also well described in the North of Europe (Chapman, 1999; Trowbridge, 2001; Yang et al., 1997). On another hand, few studies on *Codium fragile* were conducted along French coasts where this invasive seaweed was sighted in 1946 along Atlantic coasts (Silva, 1955).

Face to ecological impacts of invasive species on the ecosystem, numerous studies were carried out to understand the invasiveness in the case of *Codium fragile* (Chapman, 1999; Lyons et al., 2010; Sumi and Scheibling, 2005). Often a trade-off between allocating primary production to growth or production of secondary metabolites for defense is evident in seaweeds (Potin et al., 2002) resulting in an optimal fitness in the considered environment (with its specific biotic and abiotic factors). Thereby, abiotic factors regulating primary production, such as seasonal variations in temperature, luminosity and salinity, can influence the biochemical acclimation in alien seaweeds. Metabolomics allowed to obtained snapshot of the set of metabolites at a precise time, representing the ultimate expression of genotypes as a response to environmental conditions. Thereby, metabolomics constituted a link between genotypes and phenotypes (Fiehn, 2002). Metabolomics aimed at study the metabolotype (*i.e.* the complete biochemical phenotype) in term of quality as quantity.

Initially applied to medicine, potential of metabolomics was extended to ecological approach (Jones et al., 2013). Metabolomics is applicable with a large range of analytical tools like chromatographical methods, high performance liquid chromatography, gaz chromatography, mass spectrometry (MS), Fourier transform infrared spectroscopy (FTIR) and nuclear magnetic resonance (NMR) (Fiehn, 2002). Among various metabolomics tools, NMR provides metabolic fingerprinting allowing both metabolite identification without prior separation of each metabolite and relative quantification of observed metabolites. NMR analyzes require freeze-drying and extraction steps of samples (Heude et al., 2017). Another NMR approach named high resolution magic angle spinning nuclear magnetic resonance or *in vivo* ^{1}H HR-MAS NMR avoids extraction step and allows having an overview of main soluble molecules of intracellular fluids as in D_2O. NMR was indicated to study metabolites like as example osmolytes (Chudek et al., 1987; Kumar et al., 2016) and quantified them using classical ^{1}H NMR or ^{1}H HR-MAS NMR (Jégou et al., 2015; Kamio et al., 2016) In macroalgae, NMR, mass spectrometry and FT-IR analysis have already been carried out for taxonomical studies. It was used to compare populations of *S. muticum* along its geographical range in North Atlantic (Tanniou et al., 2015). HR-MAS NMR and LC-MS were also used as chemotaxonomic tools in the brown macroalgae *Cystoseira* and *Turbinaria* (Jégou et al., 2010; Le Lann et al., 2008). This kind of metabolomic approach using HR-MAS NMR is pertinent almost for low-abundant or small species as for this kind of species where the extraction and purification of molecules are difficult because of limited raw material and also in the case of multiple samples avoiding extraction steps. To our knowledge, no study has been yet carried out on the seasonal ^{1}H HR-MAS profiles or on non-targeted metabolomics approach to assess metabolic regulations occurring within the green macroalga *Codium fragile.*

In this context, this study assessed the use of NMR analysis to study the seasonal variability of some metabolites in relation with ecological variables in *C. fragile*, tracked on three sites along the Iroise Sea during a one year monitoring, by combining phenological and metabolomic (using ^{1}H HR-MAS NMR) approaches.

Material and methods

Samples collection The invasive seaweed*, Codium fragile,* was monitored during low tide in 3 sites situated between the mouth of the bay of Brest and Iroise Sea along West Brittany

coasts: the “Pointe du Diable” (48°21’15,36’’N ; 4°33’31,26’’O), the “Pointe du Minou” (48°20’19,29’’N ; 4°37’6,77’’O) and the “Blancs sablons/Conquet” (48°21’53,24’’N ; 4°46’27,14’’O) rocky shores. The monitoring was performed each three months from December 2013 to December 2014 (i.e five sampling dates).

Ecology Three quadrats were analyzed in three different intertidal rockpools for each site. Due to the discrete presence of this invasive species along this part of Brittany coast, quadrats were placed in intertidal rockpools where *C. fragile* is present and thus randomized monitoring could not be easily performed. The measured ecological variables were the density, *i.e.* number of individuals per m^2, the longest thalli size, and phenological characteristics specific of *C. fragile* as the dichotomy levels and basis width.

^{1}H HR-MAS NMR For the HR-MAS NMR metabolomic analysis, samples of around 100 g of fresh thalli were gathered for each site in rockpools closed to the ones followed during the ecological monitoring. Samples were pooled in order to obtain three replicates for each monitoring point (n = 3; one replicate per site). Collected samples were washed at the laboratory with filtered seawater and removed from epiphytes. Then, the replicates were freeze-dried and ball milled (MM400 Retsch). It resulted a homogeneous powder expected to be representative of the site for each sampling date since the powder provided from several pooled thalli, thus limiting biological variations linked to individuals. The dried powder obtained was stored at −24 °C until analysis. Spectral data were recorded following exactly the same procedure described on the red macroalga *Gracilaria vermiculophylla* by Surget et al. (2017). Around 4mg of powder was introduced in a 4mm Zirconium rotor. Spectra were recorded with 5000Hz spinning rate, at 30°pulse with 64 scans. This methodology results in a high-resoluted ^{1}H NMR spectrum similar to those obtained using liquid samples as described in the brown seaweeds (Simon et al., 2015) and provides a fingerprint of the samples, i.e. a snapshot of metabolites produced by organisms at the time of their collection. Chemical shifts were expressed in parts per million (ppm) using trimethyl silyl proponiate as the chemical shift reference (0 ppm). All recorded spectra were analyzed using the software MestReNov. 6.0.2 (Mestrelab Research S.L., Spain). ^{1}H HR-MAS spectra were phased and afterwards baseline corrected using Bernstein polynomials. They were aligned on the alanine signal (^{1}H, d, 1.47 ppm).

At first, whole spectra were binning into buckets for the chemical shift region of 0.58 ppm to 6.5 ppm and the size of each bin was 0.04 ppm. Once integrated, 146 areas values were thus generated for each spectrum for further analysis. After transformation, a multivariate correspondence analysis (COA) was performed on dataset. Then, the identification of detected metabolites on spectra was performed and signals assigned to an identified metabolite were integrated as illustrated in Figure 1 with the aim to compare relative area of each metabolite throughout sites and monitoring point. All integrated peaks or 0.04 ppm bins were scaled to whole intensity, i.e. intensity resulting from the spectra integration of the chemical shift region from 0.58 ppm to 6.5 ppm. Metabolite identification was checked using 2D NMR spectroscopy (^{1}H-^{1}H correlation spectroscopy: COSY, ^{1}H-^{13}C heteronuclear multiple bond correlation: HMBC and ^{1}H-^{13}C heteronuclear multiple quantum coherence: HMQC). Additionally, spectra of standards or pure molecules available in the laboratory were compared to *in vivo* NMR spectra and to classical liquid ^{1}H NMR spectra (crude sample in D_2O) of *C. fragile*.

Statistics Statistical analyses were performed with RStudio (v.0.95.263) for R (v.3.1.3). All analyses were carried out in triplicate, and results were expressed as means ± standard deviation (SD). If the data met the requirements for parametric tests, they were analyzed using a two-way ANOVA or one-way Anova test at a significance level of 95 %, followed by a Tukey post hoc test. Data were transformed if necessary to respect homoscedasticity. When the data did not meet the requirements for an ANOVA test, they were analyzed using a non-parametric two-way Scheirer-Ray-Hare test (Sokal and Rohlf, 1995) or the one-way Kruskal–Wallis test at a significance level of 95%, followed by the multiple comparisons test after Kruskal–Wallis (kruskalmc function; pirgmess package). All data were compared in relation to sites and sampling dates. Furthermore, multivariate analyses (ade4 package) were conducted on ecological data (principal component analysis: PCA) as on NMR data (correspondance analysis: COA) after a logarithmic transformation of data to reduce the data variance. To go further, Manova was conducted on coordinates of individuals of the selected dimensions generated by multivariate analysis (PCA and COA) since coordinates of individuals on the several dimensions were independent of one another, contrary to morphological parameters as the algal size and the width of the thallus basis for example and relative metabolite concentrations.

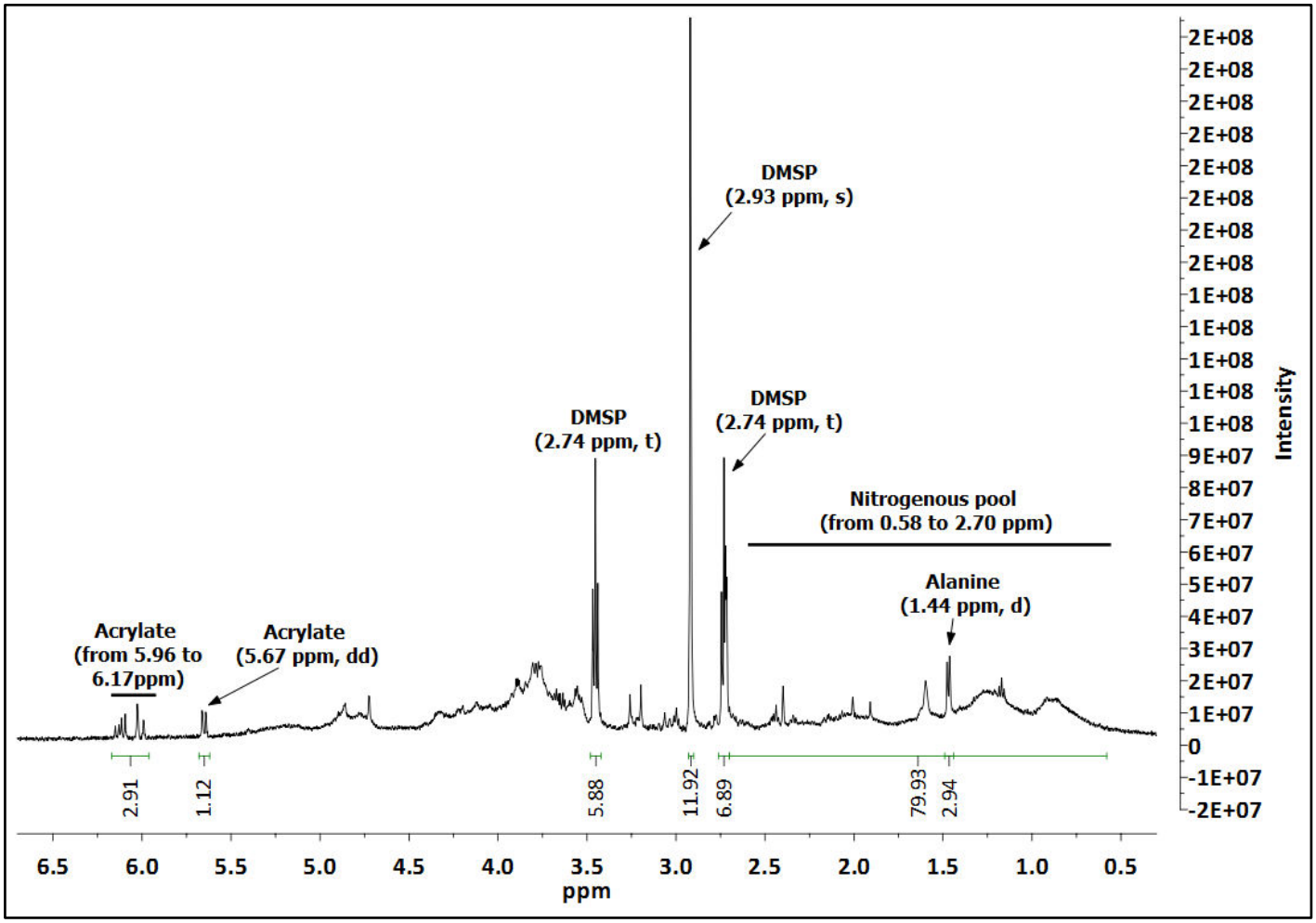

Fig. 1 Example of ^{1}H HR-MAS NMR typical spectrum of freeze-dried powder of the macroalga *Codium fragile* (December 2013, site: "Pointe du Diable"). Major peaks were assigned to a specific metabolite and corresponding chemical shift expressed as ppm was annotated on the spectrum. The alanine signal was used to align spectra at 1.47 ppm. DMSP on certain signals corresponds to dimethylsulfopropionate integrated peaks.

Results

Ecological monitoring Principal analysis component was carried out on ecological data to gain an overview of variations observed among sites and sampling dates as to illustrate possible correlation between morphological parameters (Figure 2). The first two principal components explained 54.96 and 18.02% of the variance respectively. Most of variables, *i.e.* the maximum thallus size, the width of thallus basis and the presence or not of epiphytes, contributed mainly to dimension 1 explaining more than half of the data variability. On

another hand, dimension 2 was mainly explained by the density of *C. fragile* representing 19.39% of the data variability. PCA illustrated correlation between thallus size, thallus basis width and the presence of epiphytes and the lack of correlation for *C. fragile* density (Figure 2 A and B). Thereby, individuals that presented higher size exhibited larger basis, showed generally red seaweed epiphytes as well as a higher number of dichotomic divisions. On the score plot of individuals (Figure 2 C and D), it was illustrated the differentiation of ecological variables of thalli monitored at the site “Pointe du Minou” in September 2014 mainly due to their density (Figure 2 A). Manova analysis confirmed significant difference between the site “Pointe du Minou and the two other sites (p-value=0.0015). Additionally, September 2014 differed of the other sampling dates for the density variable (Kruskal multiple comparison, p-value<0.05) rejoining PCA conclusions.

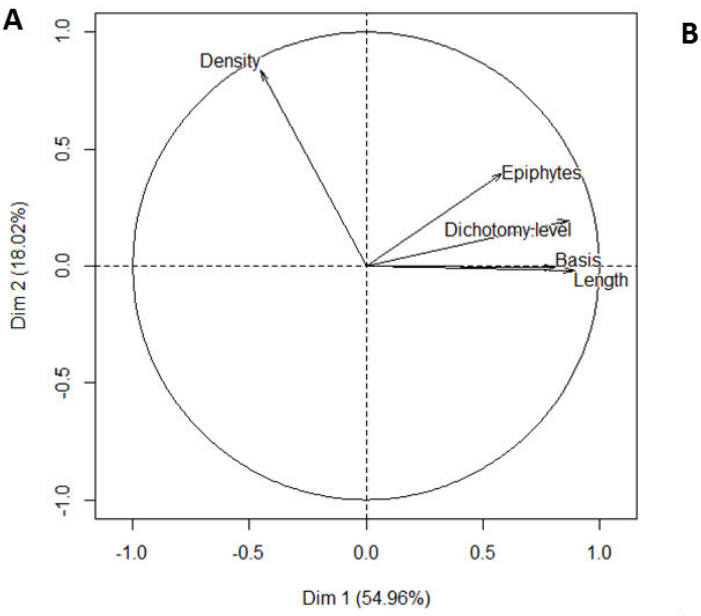

B

	Dim 1	Dim 2
Density	-0.453	0.839
Basis	0.808	-0.00637
Length	0.892	-0.0194
Dichotomy.level	0.867	0.196
Epiphytes	0.584	0.398

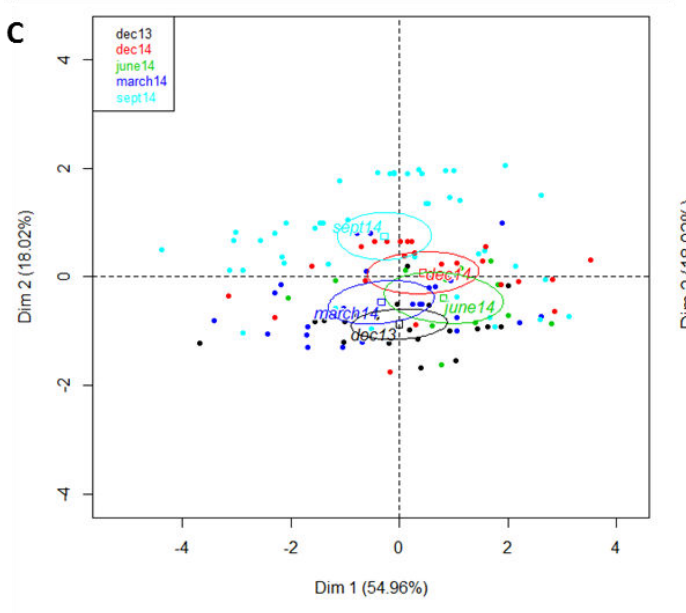

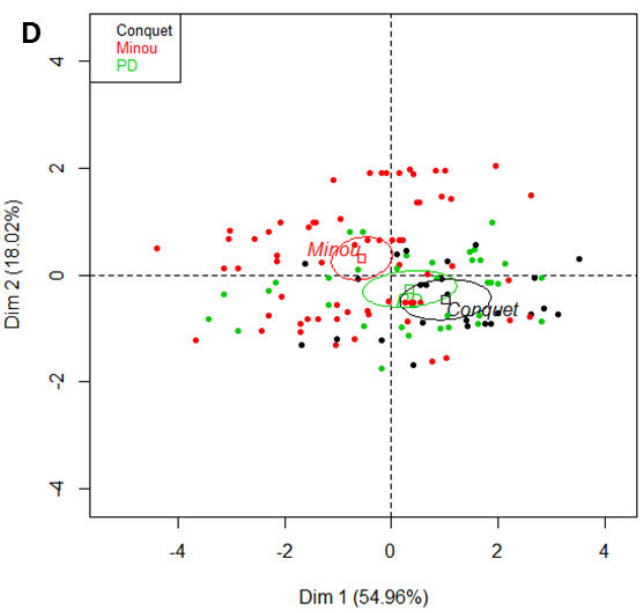

Fig. 2 Principal component analysis (PCA) of ecological variables of *C. fragile* depending on sites and monitored points along the year (from December 2013 to December 2014). **A**: PCA correlation plot of density ("Density"), level of dichotomy ("Dichotomy.level"), basis width ("Basis"), maximum length ("Length") and the presence or absence of epiphytes ("Epiphytes") of thalli. **B**: Correlation table of ecological variables on dimension 1 (Dim 1) and dimension 2 (Dim 2). **C**: PCA score plot of individuals depending of the monitoring date. **D**: PCA score plot of individuals depending of the studied site. Ellipses with a confidence level of 0.99 were drawn around considered factor, ie. site (Conquet for "Blancs sablons/Conquet", Minou for "Pointe du Minou" and PD for "Pointe du Diable") or sampling month (dec13:

December 2013; dec14: December 2014; june14: June 2014; march14: March 2014 and sept14: September 2014).

^{1}H NMR spectra Component ordinate Analysis (COA) was conducted on data generated by the integration of bins on spectra since dataset represented relative area ratios (Figure 3). COA analyses exhibited a clear pattern of differentiation between sites (Figure 3A) and conversely no seasonal differences (data not shown). Manova was conducted on COA coordinates. Manova analyses confirmed significant differences between sites (F = 7.771; p-value = 0.010) with the site “Blancs sablons/Conquet” significantly different from the sites “Pointe du Diable” and “Minou” (pairwise comparisons using permutational Manova, p-value<0.05). Manova analysis also confirmed the lack of significant differences relative to sampling dates (F = 0.579; p-value = 0.782). The spatial differentiation on buckets data was mainly observed along the Axis 1 that explained 51% of dataset variability. The bucket with a range chemical shift from 2.90 to 2.94 ppm contributed for 58.27% to the Axis 1.

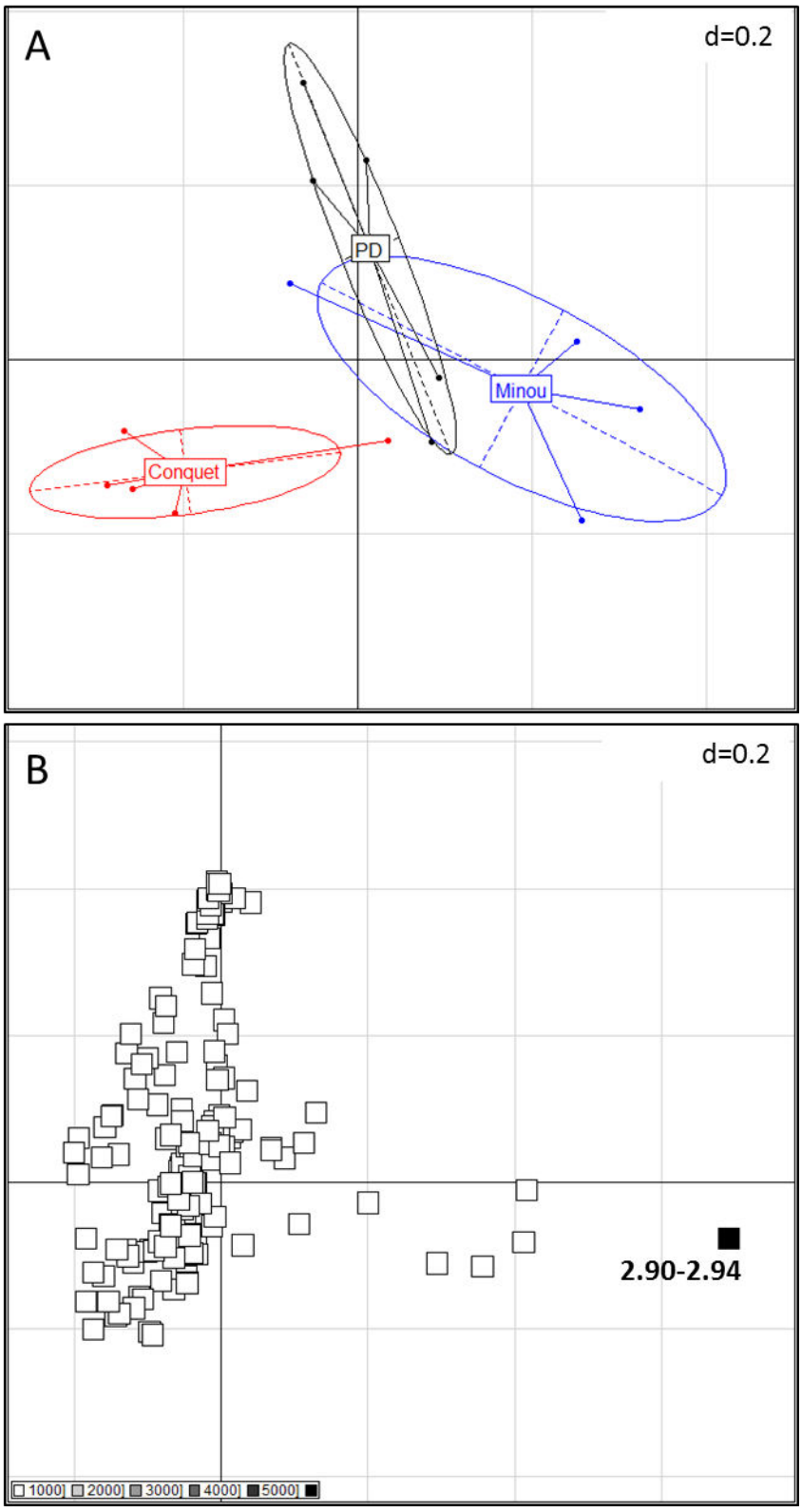

Fig. 3 Component ordinate Analysis (COA) of integrated bins on *C. fragile* spectra. **A**: COA score plot of individuals depending of the sampling site. Ellipses with a confidence level of 99% were drawn around considered factor, ie. site (Conquet for "Blancs sablons/Conquet",

Minou for “Pointe du Minou” and PD for “Pointe du Diable”). **A**: COA correlation plot of 146 integrated bins. Each square represented a bin and the square colour intensity was proportional to the variable contribution on axis 1. The chemical shift range of bins that contributed more than 20% to axis 1 (colored in grey) was precised.

To go further, specific peaks assigned to a precise metabolite were integrated. Several metabolites and class of metabolites were identified on ^{1}H HR-MAS spectra and were quantified relatively to the intensity of the total spectrum: acrylate, dimethylsulfopropionate (DMSP), alanine and nitrogenous pool. Peaks selected and integrated were illustrated in Figure 1. COA was applied on these selected peaks corresponding to identified metabolites. This analysis exhibited spatial differentiation of dataset and conversely no seasonal pattern was identified. This was confirmed by Manova on COA coordinates of the two first axes with a significant difference according to sites (Manova, F=3.403, p-value=0.026).

Results of relative contents of each metabolite as the relative estimation of nitrogenous pool and the ratio of acrylate on acrylate added to DMSP (A/(A+DMSP), were presented in Table 1. The DMSP, the ratio A/(A+DMSP) and the nitrogenous pool relative content varied significantly between sites according to Kruskal-Wallis test (Chi^2=6.94, p-value=0.0311; Chi^2=7.27, p-value=0.0264; F=7.64, p-value=0.0219 respectively). These results joined observations on COA analysis (Figure 3) for which buckets that exhibited the highest contributions to the axis 1 corresponding to DMSP signals (Figure 1), with buckets with a range chemical shift from 2.70 to 2.74 contributing for 9.3% to dimension 1, the ones from 2.74 to 2.78, from 2.90 to 2.94, from 3.42 to 3.46, from 3.46 to 3.50, contributing respectively for 2.37%, 58.27%, 7.20% and 3.82% to dataset variations explained by axis 1. The other metabolites exhibited neither sites differentiation nor seasonal differentiation (Kruskal-Wallis, p-value>0.05). Our monitoring showed that the population of the “Pointe du Minou” (12.88 $\pm$ 5.23 %) produced more DMSP than the population from “Blancs sablons” (4.80 $\pm$ 3.68 %) (Table 1). The reverse tendency is observed for the nitrogenous compounds which is maximal at “Blancs sablons” (40.22 $\pm$ 2.09 %) and minimal at “Pointe du Minou” (34.99 $\pm$ 2.09 %). DMSP high variability between monitoring points was explained by sites differences.

Table 1. Variability of some metabolites present in *Codium fragile* during the monitoring period, presented in relative concentrations (expressed as %) for the alanine, DMSP (dimethylsulfopropionate), acrylate and nitrogenous molecules, together with the ratio of acrylate on DMSP added to acrylate. Data were calculated based on relative signal integrals on ^{1}H HR-MAS spectra for each sampling date (for which data from all sites were pooled) and for each site (for which data from all sampling dates were pooled). Results are expressed as means ± SD. Different letters indicate significant differences between means using the post hoc test after KW (p value<0.05).

		Relative concentrations (%)				
		Alanine	DMSP	Acrylate	Nitrogenous compounds	Acrylate / (DMSP + acrylate) ratio
Sites	Pointe du Diable (n=5)	1.18 ± 0.21	9.44 ± 2.92^{ab}	2.73 ± 0.51	37.65 ± 1.43^{ab}	0.24 ± 0.08^{ab}
	Minou (n=4)	1.23 ± 0.13	12.88 ± 5.23^{a}	1.95 ± 0.67	34.99 ± 2.09^{a}	0.16 ± 0.12^{a}
	Conquet (n=5)	1.23 ± 0.06	4.80 ± 3.68^{b}	2.82 ± 0.75	40.22 ± 2.09^{b}	0.41 ± 0.12^{b}
Monitoring points	December 13 (n=3)	1.25 ± 0.17	7.48 ± 4.48	2.91 ± 0.93	36.91 ± 2.00	0.32 ± 0.18
	March 14 (n=3)	1.15 ± 0.17	10.54 ± 3.90	2.62 ± 0.86	36.73 ± 3.52	0.22 ± 0.12
	June 14 (n=2)	1.28 ± 0.13	7.58 ± 6.88	2.27 ± 0.56	39.78 ± 1.06	0.29 ± 0.16
	September 14 (n=3)	1.20 ± 0.08	9.51 ± 8.24	2.20 ± 0.50	37.18 ± 3.55	0.27 ± 0.19
	December 14 (n=3)	1.20 ± 0.20	8.32 ± 4.80	2.60 ± 0.91	39.10 ± 3.23	0.29 ± 0.19

Discussion

C. fragile appeared in distinctive occasional populations along the three monitored sites and presented low abundance as on each site and for each monitoring date, extensive research of this algae was carried out to find enough thalli (Surget, pers. com.). It was only observed within protected tide pools of low rocky shores, and also sheltered from the direct sunlight. Thalli presented epilithic attachment mainly in the bottom of tide pools, along pool walls or else partially covered by seaweeds canopies (for example canopies of the brown native macroalga *Bifurcaria bifurcata*). These observations were consistent with the bibliography of the seaweed ecology in Southern England (Chapman, 1999). Results showed a divergent phenotype in the site named “Pointe du Minou” compared to the two other sites. These results coincided with metabolomics data discussed below.

The metabolites acrylate, DMSP and alanine were identified as the main soluble metabolites present within this alga (Figure 1) and according to the literature (Kamio et al., 2016). The relative concentrations of the identified metabolites were determined from HR-MAS NMR spectra as published previously on several red seaweed species (Bondu et al., 2007; Surget et al., 2017). NMR was indicated to follow DMSP levels in marine organisms (Kamio et al., 2016; Keller et al., 2012). Indeed, the freeze drying process could induce DMSP enzyme degradation in DMS (dimethylsulfide) and acrylate but acrylate relative concentration was easily determined by NMR. Results indicated a constant degradation of DMSP between samples, link to samples preparation as previously referred (Kamio et al., 2016).

The results exhibited no seasonal effect, thereby illustrating that factors varying between seasons did not involve a seaweed acclimation for these metabolites in populations of *C. fragile* from Brittany coasts. If a seaweed acclimation would occur during the seasons for the studied metabolites, the induced variations were covered by sites differences, *i.e.* increasing standard error for seasons, as for DMSP. Moreover, DMSP was actively studied in marine macroalgae as in phytoplankton and benthic invertebrates for its ecological multiple functions (Alstyne and Puglisi, 2007; Keller et al., 2012). These results did not join the bibliography. Lyons et al. (2007) demonstrated the seasonal variation of DMSP and suggested a correlation between DMSP concentrations and temperature. Thus, they supposed that DMSP would be linked to a physiological response of seaweed (Lyons et al., 2007). Indeed, this molecule was characterized for its cryoprotectant activity (Karsten et al., 1992) and its cleavage derived molecules for their antioxidant properties (Alstyne and Puglisi, 2007; Sunda et al., 2002). This study illustrated that the differential temperature occurring between winter and summer did not inquire an increase of DMSP concentrations. Interestingly, Chapman et al. (1999) carried out a transatlantic comparison of the ecology of *Codium fragile ssp. tomentosoides* between populations of Mahone Bay in Nova Scotia and those of the rocky coast of southern England (Chapman, 1999). They illustrated the difference of *Codium* invasiveness, which is mainly due to its contrasting abundance as well as its thallus size between the Western and Eastern Atlantic coasts. The transatlantic contrasted phenotype of *Codium fragile ssp. tomentosoides* could explain the divergence of observed DMSP patterns between seasons illustrating local adaptation of invasive

populations to their new environment. Additionally, Van Alstyne (2008) compared DMSP geographical distribution in the South hemisphere (Australia, Tasmania and New Zealand) in several green macroalgae. They speculated that DMSP seemed to not protect algae against stressors such as desiccation and extreme temperatures (linked the intertidal location of *Codium* species). Thereby, DMSP would not act as an antioxidant in *Codium* species. Interestingly, they showed that invasive subspecies exhibited higher DMSP amounts than native species and speculated that divergent DMSP observed functions were dependent of the geographical distribution of *C. fragile ssp. tomentosoïdes* and could be the result of specific local adaptations of populations (Van Alstyne, 2008). Genetic diversity studies would be useful to better understand these differential functions of DMSP.

Conversely, spatial differences were observed between both sites named “Pointe du Minou” and “Blancs sablons/Conquet” with lower level of DMSP exhibited for the second, higher relative concentration of nitrogenous compounds as well as higher acrylate on DMSP added to acrylate ratio. Nevertheless, the variation of the ratio of acrylate on DMSP added to acrylate was closed to DMSP variations. These results showed similar patterns between phenotypes and biochemical *in vivo* NMR profiles, with the distinction of the site “Pointe du Minou”. Our results suggested that local stressors induced acclimation of this species for the site “Pointe du Minou” both at a biochemical and morphological phenotype. Furthermore, DMSP physiological functions are still unclear due to the complexity of factors influencing its concentration in the seaweed. Nevertheless, this molecule was also referred for its feeding deterrent properties (Lyons et al., 2010, 2007; Van Alstyne, 2008). Moreover, salinities and temperature did not vary between sites (data not shown), and due to the sites proximity (small spatial scale) and same tidal levels, we supposed that the light intensity exposure was closed between studied sites. Thereby, we hypothesized that the higher levels of DMSP in the site “Pointe du Minou” compared to the named “Blancs sablons/Conquet” could be linked to a differential herbivory pressure. Interestingly, higher DMSP levels in the site “Pointe du Minou” was correlated with lower relative concentration of nitrogenous compounds. Moreover, DMSP was initially described as an osmolyte whereas salinity gradients did not always lead to a regulation of DMSP concentrations in algal species (Van Alstyne and Puglisi, 2007 and references therein). Now, it was considered as a constitutive compatible solute (Stefels, 2000). This last author reviewed the ecological physiological

aspects of DMSP production. Due to regulatory coupling between assimilatory pathways of sulfur and nitrate reductions, osmotic adjustments could occur under N limitation as the production of DMSP allowed to maintain sulfate assimilation even under N-limited conditions. Indeed, DMSP higher concentrations depend of cell's need in compatible solutes including mainly nitrogenous pool, free carbohydrates and amino acids (Stefels, 2000). Thus, N-limitation may results in an increase of sulfur incorporation compared to nitrate assimilation (Stefels, 2000) as illustrated in several studies exhibiting the negative correlation between DMSP and N availability (Colmer et al., 1996; Keller et al., 2012). In this context, we can also hypothesize that a variation of N supplies could occur in the site "Pointe du Minou" relative to the site "Blancs sablons/Conquet".

To conclude, these results exhibited a high phenotypic plasticity as well as a high biochemical plasticity at a small spatial scale than at seasons scale in *Codium fragile* living in Iroise Sea (Brittany, France). Furthermore, this study showed the high interest of coupling several biological scales, *i.e.* individual phenology and biochemical phenotype, to go further in the comprehension/understanding of the link between physiological acclimations and ecological phenotypes. Our methodology to quantify the content of some metabolites is interesting and pertinent, especially in the case of *C. fragile* which is not much abundant in South Brittany. This methodology could be carried out also for any other minor species, and also interesting at individual-scale, without to put in danger the population.

Acknowledgments This study is part of a PhD project carried out by the first author at the Laboratoire des Sciences de l'Environnement Marin (LEMAR UMR6539) in the IUEM (UBO-UBL), under the supervision of the last author. It was supported by the *Ministère de l'Education Nationale, de l'Enseignement Supérieur et de la Recherche* (UBO funding for the first author) and *Région Bretagne* (ARED Labex Mer). This study was co-financed with the support of the European Union ERDF – Atlantic Area Program and French ANR and is related to the research project INVASIVES (Era-net Seas-era. 2012–2016).

References

Alstyne, K.L.V., Puglisi, M.P., 2007. DMSP in marine macroalgae and macroinvertebrates: Distribution, function, and ecological impacts. Aquat. Sci. 69, 394–402.

Bondu, S., Kervarec, N., Deslandes, E., Pichon, R., 2007. The use of HRMAS NMR spectroscopy to study the in vivo intra–cellular carbon/nitrogen ratio of *Solieria chordalis* (Rhodophyta). J. Appl. Phycol. 20, 673–679.

Campbell, S.J., 1999. Occurrence of *Codium fragile subsp. tomentosoides* (Chlorophyta: Bryopsidales) in marine embayments of southeastern Australia. J. Phycol. 35, 938–940.

Carlton, J.T., Scanlon, J.A., 1985. Progression and dispersal of an introduced alga: *Codium fragile ssp. tomentosoid*es (Chlorophyta) on the Atlantic coast of North America. Bot. Mar. 28, 155–166.

Chapman, A.S., 1999. From introduced species to invader: what determines variation in the success of *Codium fragile ssp. tomentosoides* (Chlorophyta) in the North Atlantic Ocean? Helgol. Meeresunters. 52, 277–289.

Chudek, J.A., Foster, R., Moore, D.J., Reed, R.H., 1987. Identification and quantification of methylated osmolytes in algae using proton nuclear magnetic resonance spectroscopy. Br. Phycol. J. 22, 169–173.

Churchill, A.C., Moeller, H.W., 1972. Seasonal patterns of reproduction in New York. Populations of *Codium fragile* (Sur.) Hariot *subsp. tomentosoides* (van Goor) Silva. J. Phycol. 8, 147–152.

Colmer, T.D., Teresa W-M., F., Läuchli, A., Higashi, R.M., 1996. Interactive effects of salinity, nitrogen and sulphur on the organic solutes in *Spartina alterniflora* leaf blades. J. Exp. Bot. 47, 369–375.

Fiehn, O., 2002. Metabolomics – the link between genotypes and phenotypes. Plant Mol. Biol. 48, 155–171.

Garbary, D.J., Vandermeulen, H., Kim, K.Y., 1997. *Codium fragile ssp. tomentosoides* (Chlorophyta) invades the Gulf of St Lawrence, Atlantic Canada. Bot. Mar. 40, 537–540.

Heude, C., Nath, J., Carrigan, J.B., Ludwig, C., 2017. Nuclear Magnetic Resonance Strategies for Metabolic Analysis, in: Sussulini, A. (Ed.), Metabolomics: From Fundamentals to Clinical Applications, Advances in Experimental Medicine and Biology. Springer International Publishing, pp. 45–76.

Jégou, C., Culioli, G., Kervarec, N., Simon, G., Stiger-Pouvreau, V., 2010. LC/ESI-MSn and ^{1}H HR-MAS NMR analytical methods as useful taxonomical tools within the genus *Cystoseira* C. Agardh (Fucales; Phaeophyceae). Talanta 83, 613–622.

Jégou, C., Kervarec, N., Cérantola, S., Bihannic, I., Stiger-Pouvreau, V., 2015. NMR use to quantify phlorotannins: The case of *Cystoseira tamariscifolia*, a phloroglucinol-producing brown macroalga in Brittany (France). Talanta 135, 1–6.

Jones, O.A.H., Maguire, M.L., Griffin, J.L., Dias, D.A., Spurgeon, D.J., Svendsen, C., 2013. Metabolomics and its use in ecology. Austral Ecol. 38, 713–720.

Kamio, M., Koyama, M., Hayashihara, N., Hiei, K., Uchida, H., Watanabe, R., Suzuki, T., Nagai, H., 2016. Sequestration of dimethylsulfoniopropionate (DMSP) and acrylate from the green alga *Ulva spp.* by the Sea Hare *Aplysia juliana*. J. Chem. Ecol. 42, 452–460.

Karsten, U., Kirst, G.O., Wiencke, C., 1992. Dimethylsulphoniopropionate (DMSP) accumulation in green macroalgae from polar to temperate regions: interactive effects of light versus salinity and light versus temperature. Polar Biol. 12, 603–607.

Keller, M.D., Kiene, R.P., Kirst, G.O., Visscher, P.T., 2012. Biological and environmental chemistry of DMSP and related sulfonium compounds. Springer Science & Business Media.

Kumar, M., Kuzhiumparambil, U., Pernice, M., Jiang, Z., Ralph, P.J., 2016. Metabolomics: an emerging frontier of systems biology in marine macrophytes. Algal Res. 16, 76–92.

Le Lann, K., Kervarec, N., Payri, C.E., Deslandes, E., Stiger-Pouvreau, V., 2008. Discrimination of allied species within the genus *Turbinaria* (Fucales, Phaeophyceae) using HRMAS NMR spectroscopy. Talanta 74, 1079–1083.

Lyons, D.A., Alstyne, K.L.V., Scheibling, R.E., 2007. Anti-grazing activity and seasonal variation of dimethylsulfoniopropionate-associated compounds in the invasive alga *Codium fragile ssp. tomentosoides*. Mar. Biol. 153, 179–188.

Lyons, D.A., Scheibling, R.E., Van Alstyne, K.L., 2010. Spatial and temporal variation in DMSP content in the invasive seaweed *Codium fragile ssp. fragile*: effects of temperature, light and grazing. Mar. Ecol. Prog. Ser. 417, 51–61.

Potin, P., Bouarab, K., Salaün, J.-P., Pohnert, G., Kloareg, B., 2002. Biotic interactions of marine algae. Curr. Opin. Plant Biol. 5, 308–317.

Provan, J., Booth, D., Todd, N.P., Beatty, G.E., Maggs, C.A., 2008. Tracking biological invasions in space and time: elucidating the invasive history of the green alga *Codium fragile* using old DNA. Divers. Distrib. 14, 343–354.

Silva, P.C., 1955. The dichotomous species of *Codium* in Britain. J. Mar. Biol. Assoc. U. K. 34, 565–577.

Simon, G., Kervarec, N., Cérantola, S., 2015. HRMAS NMR Analysis of algae and identification of molecules of interest via conventional 1D and 2D NMR: sample preparation and optimization of experimental conditions, in: Stengel, D.B., Connan, S. (Eds.), Natural products from marine algae, methods in molecular biology. Springer New York, pp. 191–205.

Sokal, R.R., Rohlf, F.J., 1995. Biometry: The principles and practice of statistics in biological research.

Stefels, J., 2000. Physiological aspects of the production and conversion of DMSP in marine algae and higher plants. J. Sea Res. 43, 183–197.

Stiger-Pouvreau, V., Thouzeau, G., 2015. Marine species introduced on the French Channel-Atlantic coasts: a review of main biological invasions and impacts. Open J. Ecol. 05, 227–257.

Sumi, C.B.T., Scheibling, R.E., 2005. Role of grazing by sea urchins *Strongylocentrotus droebachiensis* in regulating the invasive alga *Codium fragile ssp tomentosoides* in Nova Scotia.

Sunda, W., Kieber, D.J., Kiene, R.P., Huntsman, S., 2002. An antioxidant function for DMSP and DMS in marine algae. Nature 418, 317–320.

Surget, G., Lann, K.L., Delebecq, G., Kervarec, N., Donval, A., Poullaouec, M.-A., Bihannic, I., Poupart, N., Stiger-Pouvreau, V., 2017. Seasonal phenology and metabolomics of the introduced red macroalga *Gracilaria vermiculophylla*, monitored in the Bay of Brest (France). J. Appl. Phycol. 1–16.

Tanniou, A., Vandanjon, L., Gonçalves, O., Kervarec, N., Stiger-Pouvreau, V., 2015. Rapid geographical differentiation of the European spread brown macroalga *Sargassum muticum* using HRMAS NMR and Fourier-Transform Infrared spectroscopy. Talanta 132, 451–456.

Theriault, C., Scheibling, R., Hatcher, B., Jones, W., 2006. Mapping the distribution of an invasive marine alga (*Codium fragile spp. tomentosoides*) in optically shallow coastal waters using the compact airborne spectrographic imager (CASI). Can. J. Remote Sens. 32, 315–329.

Trowbridge, C.D., 2001. Coexistence of introduced and native congeneric algae: *Codium fragile* and *C. tomentosum* on Irish rocky intertidal shores. J. Mar. Biol. Assoc. U. K. 81, 931–937.

Trowbridge, C.D., 1995. Establishment of the green alga *Codium fragile ssp. tomentosoides* on New Zealand rocky shores: current distribution and invertebrate grazers. J. Ecol. 83, 949–965.

Trowbridge, C.D., Todd, C.D., 1999. The familiar is exotic: II. *Codium fragile ssp. tomentosoides* on Scottish rocky intertidal shores. Bot. J. Scotl. 51, 161–179.

Van Alstyne, K.L.V., 2008. The distribution of DMSP in green macroalgae from northern New Zealand, eastern Australia and southern Tasmania. J. Mar. Biol. Assoc. U. K. 88, 799–805.

Yang, M.-H., Blunden, G., Huang, F.-L., Fletcher, R.L., 1997. Growth of a dissociated, filamentous stage of *Codium* species in laboratory culture. J. Appl. Phycol. 9, 1–3.

Article publié

2_ Variations saisonnières de la phénologie et du métabolome de l'algue rouge introduite *Gracilaria vermiculophylla*, étudiée en rade de Brest (France)

Cet article a été présenté en introduction de ce chapitre.

J Appl Phycol
DOI 10.1007/s10811-017-1060-3

22ND INTERNATIONAL SEAWEED SYMPOSIUM, COPENHAGEN

Seasonal phenology and metabolomics of the introduced red macroalga *Gracilaria vermiculophylla*, monitored in the Bay of Brest (France)

Gwladys Surget[1] · Klervi Le Lann[1] · Gaspard Delebecq[1] · Nelly Kervarec[2] · Anne Donval[1] · Marie-Aude Poullaouec[1] · Isabelle Bihannic[1] · Nathalie Poupart[1] · Valérie Stiger-Pouvreau[1]

Received: 12 August 2016 / Revised and accepted: 10 January 2017

Abstract Seaweeds represent one of the largest groups of marine aliens in Europe and constitute a large percentage of all introduced marine species. In Brittany, the red macroalga *Gracilaria vermiculophylla* has invaded the bare areas of brackish waters in saltmarshes. In the Bay of Brest, the alga forms dense monospecific mats on the mud surface and occupies an empty ecological niche, in association with the invasive halophyte, *Spartina alterniflora*. The phenology of *G. vermiculophylla* was studied through seasonal monitoring of biomass, density and size of fragments, complemented by metabolomic monitoring using ^{1}H HR-MAS NMR chemical footprinting analyses. Moreover, lipids and pigments were quantified, using high-performance thin layer chromatography for the former and high-performance liquid chromatography and spectrophotometry for the latter. This rhodophyte is present throughout the year, never fixed to a substrate on the mud, with a maximum biomass in the summertime. Phenological observations on algal populations demonstrated a high capacity for fragmentation, with a majority of fragments shorter than 3 cm. Metabolomic analyses highlighted a temporal variability of lipids, pigments and osmolytes between seasons. These results, combined with ecological data, improve our understanding of the acclimation of *G. vermiculophylla* in Brittany, where it is mainly present in a vegetative state throughout the year. Our study represents an important contribution to understanding the ecological strategies used by this invasive seaweed to colonize and persist in the Bay of Brest.

Keywords *Gracilaria vermiculophylla* · Invasive seaweed · HR-MAS NMR · Population biology · Lipid class · Osmolyte

Introduction

Among marine organisms, seaweeds represent one of the largest groups of marine aliens in Europe and constitute between 20 and 29 % of all introduced marine species (Schaffelke et al. 2006; Stiger-Pouvreau and Thouzeau 2015). Alien species have been shown to be particularly adaptive through phenotypic changes (Davidson et al. 2011). Moreover, to colonize, survive and reproduce in their new environment, introduced species have to adapt by developing several strategies, including chemical defence, e.g. production of chemical cues (Potin et al. 2002). To date, 21 macroalgal species are listed as introduced species along the French Atlantic coasts (Stiger-Pouvreau and Thouzeau 2015).

In Brittany, the red macroalga *Gracilaria vermiculophylla* (Ohmi) Papenfuss has invaded the bare areas of brackish waters in saltmarshes since 1996 (Rueness 2005). *Gracilaria vermiculophylla* was originally described in Japan, with a native distribution in the East of Asia (Rueness 2005). Today, this invasive species is widespread around the world, in the Eastern Pacific, in the Western and Eastern North

✉ Gwladys Surget
Gwladys.Lediouron@univ-brest.fr

[1] LEMAR UMR 6539 CNRS UBO IRD Ifremer - Institut Universitaire Européen de la Mer (IUEM), Université de Bretagne Occidentale (UBO), Technopôle Brest-Iroise, Rue Dumont d'Urville, 29280 Plouzané, France

[2] Service RMN-RPE, UFR Sciences et Techniques, Université de Bretagne Occidentale (UBO), Avenue Le Gorgeu, 29200 Brest, France

Published online: 08 February 2017

Atlantic and in the North and Baltic seas (Rueness 2005; Thomsen et al. 2006, 2007, 2009; Freshwater et al. 2006; Weinberger et al. 2008), with a distribution range extending from Portugal to Norway in the North-East Atlantic Ocean (Stiger-Pouvreau and Thouzeau 2015).

Previous studies have highlighted the invasiveness of *G. vermiculophylla* in the world (Thomsen et al. 2009; Nettleton et al. 2013) and particularly in Europe, where the expansion rate of its distribution range is similar to other invasive species of concern, such as *Sargassum muticum* (Hu and Juan 2013). Nyberg and Wallentinus (2005) ranked seaweed species according to the risk of dispersal and the possibility of establishment, as well as their potential ecological impact. To do this, they quantified a risk indicator depending on 13 specific species traits. *Gracilaria vermiculophylla* was ranked in the top 5 among 113 introduced macroalgae in Europe, mainly due to its passive transport probabilities, desiccation survival, salinity range as well as its reproductive mode and morphological traits (Nyberg 2007). In Brittany, *G. vermiculophylla* has invaded large areas of soft bottom estuaries and represents a large biomass (Rueness 2005; Surget, personal observation).

Soft bottomed estuaries are harsh habitats, where only a few well-adapted species can survive on the slikken, such as the invasive halophyte *Spartina alterniflora* in the Bay of Brest (Querné 2011). *Gracilaria vermiculophylla* forms dense monospecific mats on mud surfaces and occupies an empty ecological niche, sometimes in association with *S. alterniflora*, as reported in Virginia (Thomsen et al. 2009). Only microphytobenthos was present on the mud surface before its invasion (Davoult et al. 2017, personal communication). The alga has a large impact on the estuarine habitat it invades, as shown in the Faou estuary of the Bay of Brest, by increasing the mud species richness and macrofauna density, increasing ecosystem primary production and integrating food webs (Davoult et al. 2017, personal communication) as in other invaded areas (Thomsen et al. 2009; Gulbransen and McGlathery 2013; Hammann et al. 2013a). *Gracilaria vermiculophylla* is also now considered to be a habitat-forming species due to its multiple effects on estuarine ecosystems (Gulbransen et al. 2013) with a strong invasiveness potential.

In the face of growing concern about *G. vermiculophylla* invasiveness, numerous studies have focused on its invasion mechanisms and ecological impacts, reviewed by Hu and Juan (2013). As a major invasive species, G. *vermiculophylla* shows a high stress acclimation to many environmental factors, like salinity variation, nutrient limitation, turbidity and low light availability or burial (Thomsen et al. 2007; Weinberger et al. 2008; Nylund et al. 2011; Nejrup and Pedersen 2012; Roleda et al. 2012; Gulbransen et al. 2013). To our knowledge, few studies have focused on metabolomics or metabolome profiling, a powerful emerging tool that can be used to understand the metabolic regulations (Kumar et al. 2016) underlying *G. vermiculophylla* capabilities. Two previous studies investigated algal resistance to herbivores using metabolic profiles (Nylund et al. 2011; Rempt et al. 2012). Among the available tools for metabolomics, high-resolution magic angle spinning nuclear magnetic resonance or in vivo ^{1}H HR-MAS NMR can be used to obtain a snapshot of the main soluble organic solutes, such as osmolytes, reflecting the metabolic regulations that occur within the alga, without any extraction step (Bondu et al. 2007; Gupta et al. 2013). For example, this technique has been used to investigate carbohydrate and nitrogenous pools, by measuring the C/N molecular ratio. This ratio provides information concerning the balance between nitrogen and carbon metabolism occurring in the seaweed. It indicates whether the seaweed is under conditions of N storage or N limitation, through the amino acid pool for example (Harrison and Hurd 2001). It was also used to illustrate the adaptive responses of the red macroalga *Solieria chordalis* under salinity stress (Bondu et al. 2007). Furthermore, it was reported that metabolic acclimation to the field conditions (e.g. osmotic adjustments or antioxidant protection) was related to the renewability of invasiveness of macrophytes (Pintó-Marijuan and Munné-Bosch 2013). Additionally, pigment and lipid quantification provide information about algal acclimation capabilities. Pigment and lipid regulations allow the alga to optimize thallus productivity and overcome intertidal stresses. In this way, ecological studies coupled with metabolomics and ecophysiological tools allow an integrative overview of algal metabolism and a more comprehensive understanding of algal biology.

In this context, the aim of the present study was to investigate the phenology of *G. vermiculophylla* through the seasonal monitoring of its biomass, density and size of fragments, in order to follow its biological cycle in the invaded area of the Bay of Brest. To gain an overview of *Gracilaria*'s acclimation in estuaries of the Bay of Brest, ecological data were complemented by metabolomic monitoring using ^{1}H HR-MAS NMR chemical footprinting analyses and quantification of the main pigment and lipid classes of *G. vermiculophylla* (Table 1).

Materials and methods

The ecological monitoring was performed in the Bay of Brest (Brittany, France), on three sites: Moulin (48° 21.490′ N–4° 20.447′ W), Penfoul (48° 21.619′ N–4° 19.186′ W) and Faou (48° 21.497′ N–4° 20.444′ W) rias as illustrated in Fig. 1. Samplings and

Table 1 Overview of measured variables and objectives, with the aim of understanding *Gracilaria vermiculophylla* invasiveness and seasonal regulations in Brittany rias

	Measured variables	Objectives
Ecology (biological cycle)	Biomass	Site and seasonal population dynamic
	Size classes	Population characterization
Metabolomic	Main organic solutes	Identification
		Role in seasonal regulations
	Pigment	Photosynthesis and physiological regulations
	Lipid	Lipid regulations in seasonal acclimation

measurements were carried out during low tides, every 3 months from December 2013 to March 2015.

For the metabolomic analysis (HR-MAS NMR, pigment and lipid analyses), samples of around 100 g of fresh thalli were gathered at three different points in the *G. vermiculophylla* patches for each site. For the HR-MAS NMR and lipid analysis, the samples were pooled in order to obtain three replicates for each monitoring point (n = 3). Due to pigment sensitivity, pigment samples were not pooled and nine replicates were analysed for each monitored point. Collected samples were washed with filtered seawater and epiphytes were removed. Then, the replicates were freeze-dried and ball milled (MM400 Retsch). This produced a homogeneous powder that was representative of each site for each sampling date. The homogeneity of this powder, containing different fragments, limits biological variations linked to individuals; nevertheless, the replicates are independent. The dried powder obtained was stored at −24 °C until analysis.

Population biology (size of fragments and biomass)

For each monitoring point and each site, ecological data was measured on three quadrats of 0.0625 cm^2 size determined during a pre-sampling step. The quadrats were sampled by cutting the algal mat formed by *G. vermiculophylla* thalli on the mud. This gathering technique was employed since the unattached seaweed forms dense mats of small entangled fragments on the mud, making it impossible to distinguish the different fragments along the quadrat limits. Pieces of sampled mat were washed with filtered seawater in the laboratory before measurement of the biomass (fresh and dried weights), and the fragment densities were classified into defined size classes. Due to the huge quantities of fragments, the samples were divided into four equal parts and a quarter of a quadrat was analysed. After sorting, the fragments longer than 3 cm were measured and the fragments shorter than 3 cm were counted. The dry biomass results were represented by means ± standard deviation (SD) and expressed in gram per square meter. The data collected in June 2014 on the Faou site were used to determine the size classes, since the Faou site has the most extensive patch of *G. vermiculophylla* and a maximum of biomass was observed in June. According to Sturges' rule, ten size classes were defined: <3 to >15 cm with a size class amplitude of 1.5 cm. In order to guarantee time-independent data, care was taken to sample different quadrats at each sampling date.

1D ^{1}H HR-MAS NMR spectroscopy

HR-MAS NMR analyses were performed on three independent replicates of homogeneous dried powder for each season. The method has been reported to be efficient in chemotaxonomy (Le Lann et al. 2008, 2014; Jégou et al. 2010) and chemical ecology (Simon-Colin et al. 2004; Bondu et al. 2007; Tanniou et al. 2015) of algae. Spectral data were recorded at 25 °C with a Bruker DRX 500 Spectrometer (Bruker BioSpin, France) equipped with an indirect HR-MAS ^{1}H/^{31}P probe head with gradient Z. About 5 mg of each replicate was put in a zirconium oxide vial and set in a 4-mm MAS rotor. Around 30 μL D_2O was added to the rotor with the sample for 2 H field locking (depending on the quantity of the freeze-dried powder). Good homogenization was obtained at a spinning rate of 5000 Hz. The sample was placed in a rotor spinning around an axis, oriented at the so-called magic angle of 54°7 with respect to the magnetic field B_0. A typical proton ^{1}H HR-MAS spectrum consisted of 32 scans and was performed with presaturation of the water peak. This methodology results in a high-resolution NMR spectrum similar to those obtained using liquid samples (Le Lann et al. 2008) and provides a fingerprint of the samples, i.e. an overview of the metabolites produced by the organism at the time of its collection. Chemical shifts were expressed in parts per million using tetramethylsilane as the chemical shift reference (0 ppm).

Metabolite identification was verified using 2D NMR spectroscopy (^{1}H-^{1}H correlation spectroscopy: COSY, ^{1}H-^{13}C heteronuclear multiple bond correlation: HMBC and ^{1}H-^{13}C heteronuclear multiple quantum coherence: HMQC). Additionally, spectra of standards or pure molecules available in the laboratory were compared to the

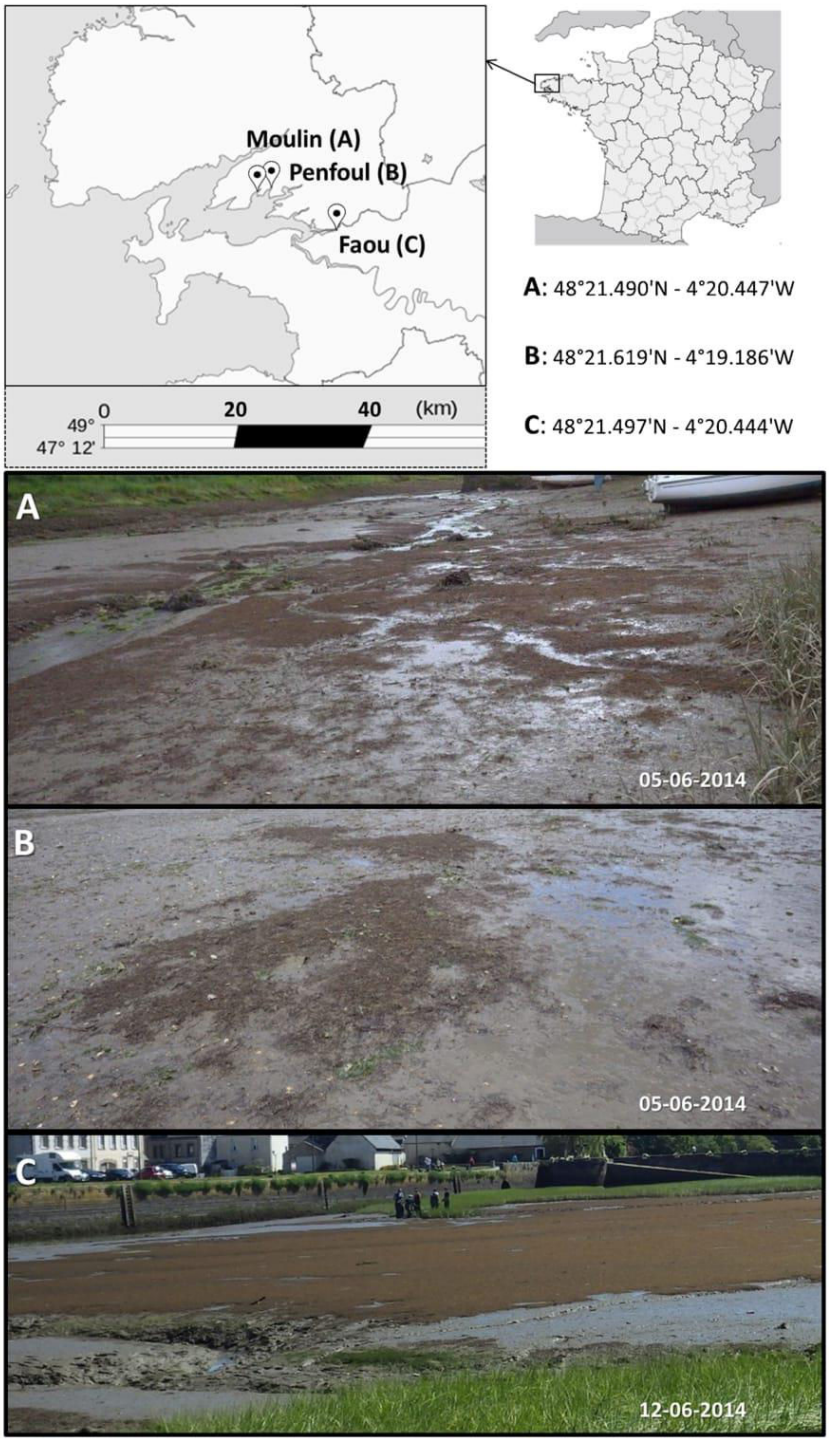

Fig. 1 Locations of the studied sites: Moulin (**a**), Penfoul (**b**) and Faou (**c**) estuaries in Brittany (France); at the *bottom*, photos illustrating the *Gracilaria vermiculophylla* mat in the three Brittany rias (photographs taken in June 2014)

in vivo NMR spectra and to classical liquid ^{1}H NMR spectra (crude sample in D_2O) of *G. vermiculophylla*. In this way, three main metabolites, floridoside, isethionic acid and taurine, were identified in accordance with the literature (Broberg et al. 1998; Simon-Colin et al. 2002; Gupta et al. 2013). All recorded spectra were analysed with MestReNov. 6.0.2 (Mestrelab Research S.L., Spain). ^{1}H HR-MAS spectra were phased and afterwards baseline-corrected using Bernstein polynomials. They were aligned on the alanine signal (^{1}H, d, 1.47 ppm) and standardized on whole spectra (0.5 to 5.5 ppm). Signals assigned to the identified metabolites were integrated as illustrated in

Fig. 2. Metabolite contents were compared between the different sampling dates with the aim of observing seasonal tendencies. As signal integrals represent the relative content of the compound in the dried algal powder (Bondu et al. 2007), the relative proportion of each metabolite, expressed as a percentage, was calculated as follows:

$$\text{Floridoside} = \frac{\sum \text{signal integrals assigned to floridoside}(3.66-3.93,\ 3.98-4.03,\ 4.07-4.13,\ 5.13-5.18\ \text{ppm})}{\text{integral of whole spectrum}(0.5-5.5\ \text{ppm})}$$

$$\text{Isethionic acid} = \frac{\sum \text{signal integrals assigned to isethionic acid}\ (3.13-3.19,\ 3.93-3.98\ \text{ppm})}{\text{integral of whole spectrum}(0.5-5.5\ \text{ppm})}$$

$$\text{Taurine} = \frac{\sum \text{signal integrals assigned to taurine}(3.24-3.30,\ 3.39-3.46\ \text{ppm})}{\text{integral of whole spectrum}(0.5-5.5\ \text{ppm})}$$

Moreover, the ratio of carbohydrate to nitrogenous molecule pool was calculated as described by Bondu et al. (2007).

Pigments

Zeaxanthin, chlorophyll-*a* (chl-*a*) and β-carotene were analysed by high-performance liquid chromatography (HPLC) following the protocol of Ras et al. (2008) and Lasbleiz et al. (2014). Pigments were extracted from dried powder (1:10, *w*/*v*) in a 100 % methanol solution (3 mL) after addition of an internal standard (14:1; vitamin E acetate, Sigma). Pure water was added to the extracts (ratio 1:14) before agitation and incubation for 1 h at −20 °C. After sonication, extracts were incubated a second time, for 1 h at −20 °C. Pigments were analysed using a C8 Zorbax Eclipse XDB column (3 × 150 mm; 3.5-μm particle size), using 250 μL of sample extracts for the injection. Chromatographic separation of pigments was performed within 33 min according to a gradient between a solution (A) of tetrabutylammonium acetate 28 mM (pH = 6.40)/methanol (30:70, *v*/*v*) and a solution (B) of 100 % methanol and using the following program: (*t* (min); %B; %A), (0; 10; 90), (22; 95; 5), (27; 95; 5), (28; 90; 10), and (33; 90; 10). Zeaxanthin and β-carotene were detected at 450 nm and chl-*a* at 667 nm. After an identification based on absorption spectra of each peak, pigment concentrations (expressed as mg g^{-1}) were calculated from the peak areas corrected by the internal standard.

Phycobiliprotein content was determined using a protocol adapted from Sun et al. (2009) and Roleda et al. (2012). Extraction was performed in the dark at 4 °C on 75 mg algal dry matter with 1.5 mL phosphate buffer (0.1 M, pH = 6.8). After sonication for 15 min, extract samples were centrifuged

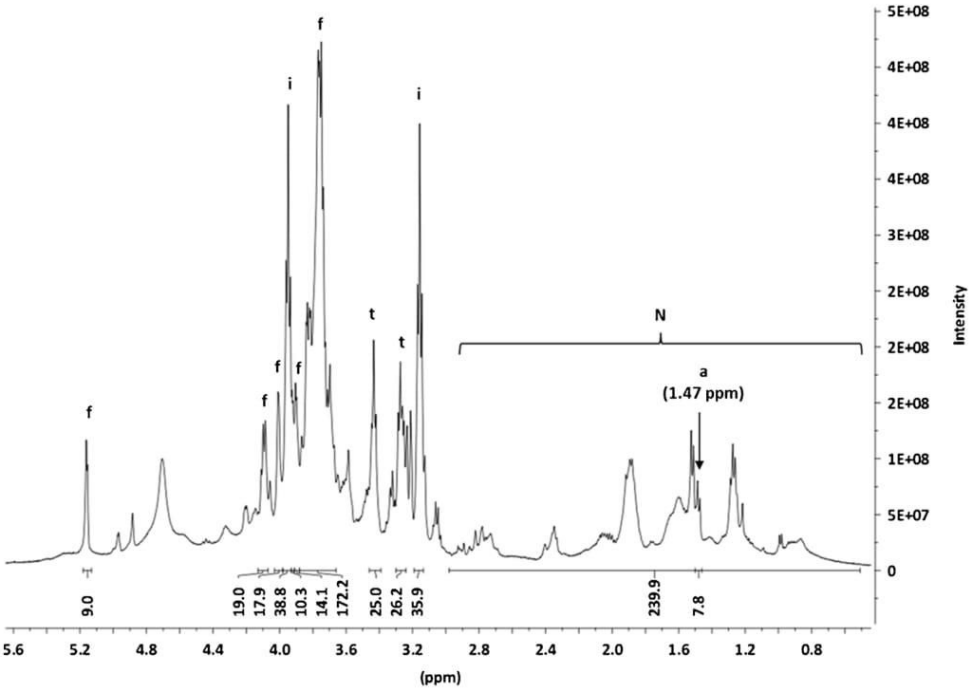

Fig. 2 ^{1}H HR-MAS NMR spectrum of freeze-dried powder of *Gracilaria vermiculophylla* (December 2013, Penfoul). The *f* on certain signals corresponds to floridoside integrated peaks, *i* to isethionic acid, *t* to taurine, *N* to the nitrogenous molecule pool and *a* to the alanine signal used to align spectra at 1.47 ppm

for 20 min at 4 °C. The obtained extracts were stored at 4 °C in the dark until the spectrophotometry was read (POLARstar Omega, BMG LABTECH). The absorbance was measured at 280, 455, 565, 592, 618 and 645 nm. Concentrations of phycobiliproteins, expressed as milligram per gram dry weight (DW), were determined using Beer and Eschel equations (Dumay et al. 2013; Munier et al. 2014; Zubia et al. 2014) as follows:

$$\text{R-PE} = [(A_{565}-A_{592})-(A_{455}-A_{592}) \times 0.20] \times 0.12$$
$$\text{R-PC} = [(A_{618}-A_{645})-(A_{592}-A_{645}) \times 0.50] \times 0.15$$

where A = absorbance, R-PE = R-phycoerythrin and R-PC = R-phycocyanin.

Lipid extraction and lipid class separation by HPTLC

Lipids were extracted by resuspending 25 mg of freeze-dried biomass (previously rehydrated with ultrapure water) in 6 mL of Folch solution (chloroform/methanol, 2:1) and sonicated 10 min at 4 °C. Butylated hydroxytoluene 0.01 % (*w*/*w*) was added as an antioxidant. Vials were centrifuged and supernatant containing lipids were evaporated to dryness under nitrogen and washed three times using a water/chloroform mix (1:1, *v*/*v*). All lipid extracts were stored at −20 °C until analysis.

Lipid classes were analysed by high-performance thin layer chromatography (HPTLC) as described by Haberkorn et al. (2010). A preliminary run was conducted on HPTLC silica glass plates (Darmstadt, Germany) in order to remove any impurities. Three solvent systems were used, depending on the lipid classes that needed to be separated: 9 % KCl polar solvent mixture (methyl acetate/isopropanol/chloroform/methanol/KCl, 10:10:10:4:3.6) for all polar lipid classes, neutral solvent mixture (hexane/diethyl ether/acetic acid, 20:5:0.5) for all neutral lipid classes and 4 % KCl polar solvent mixture (methyl acetate/isopropanol/chloroform/methanol/KCl, 25:25:25:10:4) for glycolipid classes. The plate was then activated for 30 min at 120 °C. Samples were spotted on silica plates by a CAMAG automatic sampler (Muttenz, Switzerland), and plates were developed with appropriate solvent systems. Nine percent KCl polar lipid solvent mixture was used for the separation of all polar lipid classes, 4 % KCl polar lipid solvent mixture was used for the separation of glycolipid classes and two consecutive solvent systems were used for the separation of neutral lipids: the neutral solvent mixture described above and a second solvent mixture composed of hexane/diethyl ether (97:3). Plates were revealed with a cupric sulphate phosphoric acid solution, heated for 20 min at 160 °C and then scanned at 370 nm. Black bands on charred plates were identified and quantified using Wincats software (CAMAG, Switzerland) by comparison with standards. Results were expressed in milligram per gram for the total lipid content and as a percentage of the total lipid (TL) for the classes.

Statistics

Statistical analyses were performed with RStudio (v. 0.95.263) for R (v.3.1.3). All analyses were carried out in triplicate, and results were expressed as means ± standard deviation (SD). If the data met the requirements for parametric tests, they were analysed using a two-way ANOVA test at a significance level of 95 %, followed by a Tukey post hoc test. Data were transformed if necessary to respect homoscedasticity. When the data did not meet the requirements for an ANOVA test, they were analysed using a non-parametric Kruskal–Wallis test at a significance level of 95 %, followed by the multiple comparisons test after Kruskal–Wallis (kruskalmc function; pirgmess package). All data were compared in relation to sites and sampling dates.

Results

Ecological data

A large dominance of vegetative thalli was observed throughout the monitoring period: no carposporophytes and only one tetrasporophyte were sampled (data not shown). A seasonal variability of biomass was observed, with high and low values in June 2014 and March 2015, respectively, across the three sites (ANOVA, $p < 0.001$; Fig. 3). In June 2014, biomass increased significantly with a high biomass of 276.5 ± 64.1 g m^{-2} (mean biomass over all sites). Furthermore, the same seasonal tendency was demonstrated between sites (Fig. 3). As shown in Fig. 1, the three chosen sites showed several stages of *Gracilaria* colonization visually. The Penfoul site was the least impacted, followed by Moulin and Faou, with an attention on Faou which was the most colonized field site. Despite seasonal trends, this inter-site observation is confirmed by biomass data. Indeed, the algal biomass determined in Faou was significantly higher than that in Penfoul (ANOVA, $p < 0.05$). Moulin was similar to the two other sites, with no significant seasonal differences.

Moreover, a large dominance of fragments shorter than 3 cm was observed throughout the year (Fig. 4a). For this size class, the maximum density (64,443 ± 17,293 nb m^{-2}) was observed in March 2014 and the minimum density (22,969 ± 13,894 nb m^{-2}) in December 2014. Fragment densities did not exceed 5419 ± 1153 nb m^{-2} (size class 3–4.5 in June 2014) for the other size classes. The densities of shorter fragments (<3 cm) were high in March and June and progressively decreased until December, despite site differences

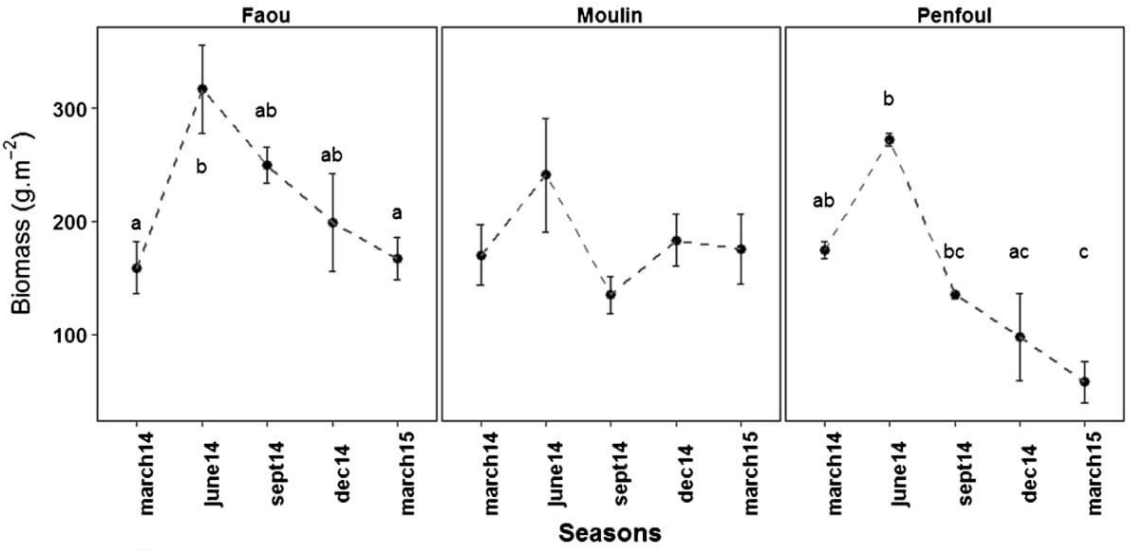

Fig. 3 Dry biomass (g m^{-2}) variations between sites from March 2014 to March 2015. Results represented are means ± SD (error bars; $n = 3$). *Different letters* indicate significant differences between means ($p < 0.05$) according to an ANOVA test, followed by Tukey post hoc tests

(ANOVA on pooled sites, $p < 0.05$). Similarly, the densities of large fragments (>3 and <10.5 cm) were highest in June and declined for the rest of the year (ANOVA on pooled sites, $p < 0.05$). Site differences were observed (Fig. 4b), especially for the Faou site compared to Penfoul and Moulin, where higher densities were only observed in June for the two size classes 7.5 to 9 cm and 9 to 10.5 cm. Moreover, the densities observed for the Moulin site only varied significantly with the seasons for fragments shorter than 7.5 cm. This seasonal tendency was not significant for the highest size classes on the three studied sites (>10.5 cm). These results are similar to those for biomass. Despite site differences, the density results confirmed a seasonal pattern of *G. vermiculophylla* populations, which were more abundant in June 2014.

Temporal variabilities of major metabolites revealed by HR-MAS NMR analysis

A typical in vivo ^{1}H HR-MAS NMR spectrum is presented in Fig. 2. Signals can be seen corresponding to the three dominant metabolites: the floridoside and isethionic acid osmolytes and the taurine amino acid (Fig. 2).

Floridoside represented 24.74–30.89 %, isethionic acid 6.39–8.07 % and taurine 5.14–6.53 % of the main soluble compounds on the ^{1}H HR-MAS spectra (Fig. 5). A seasonal variation of the relative concentration of taurine was observed. Indeed, the relative taurine concentration decreased significantly from March (6.53 ± 0.87 % relatively) to September (5.14 ± 0.19 %; ANOVA, $p < 0.05$). In contrast, no seasonal tendency was observed for floridoside or isethionic acid, despite a minimum reached in March. The C/N ratio was less than 1 for half of the year, in December (2013 and 2014) and in March, with a mean of 0.87 ± 0.23 over the monitoring period. Furthermore, no significant site effect was detected ($p > 0.05$).

Pigments

Carotenoid content changed with the seasons (Fig. 6). The β-carotene content decreased significantly from June to December 2014, but the difference was not significant compared to December 2013 (Kruskal–Wallis, $p < 0.05$). The chl-*a* content followed the same pattern as β-carotene and reached a minimum value in June (0.62 ± 0.05 mg g^{-1} DW) and a maximum in December 2014 (1.39 ± 0.07 mg g^{-1} DW). The high variability observed in September is linked to heterogeneity between the three sites for this specific season, especially between the Faou site and the other two sites (Penfoul and Moulin). Moreover, it was shown that the R-PE/R-PC ratio oscillated with seasons and sites. The phycobilin ratio decreased in March for the three sites and in September for Faou and Moulin. This ratio then rose above 2 in winter (December 2013 and 2014) as well as in June (for pooled sites). Similarly, the chl-*a*-to-carotenoid ratio fluctuated significantly between the years with a maximum observed in December 2013 (9.99 ± 0.33 mg g^{-1} DW) and a minimum in December 2014 (6.33 ± 0.25 mg g^{-1} DW; Kruskal–Wallis, $p < 0.05$), linked to the low carotenoid content in December 2013 compared with 2014 (Kruskal–Wallis, $p < 0.05$).

Lipids

Our biochemical analysis of apolar compounds demonstrated that lipids represented on average 12.75 ± 2.88 mg g^{-1} of the *G. vermiculophylla* dry weight. Among the main lipid classes,

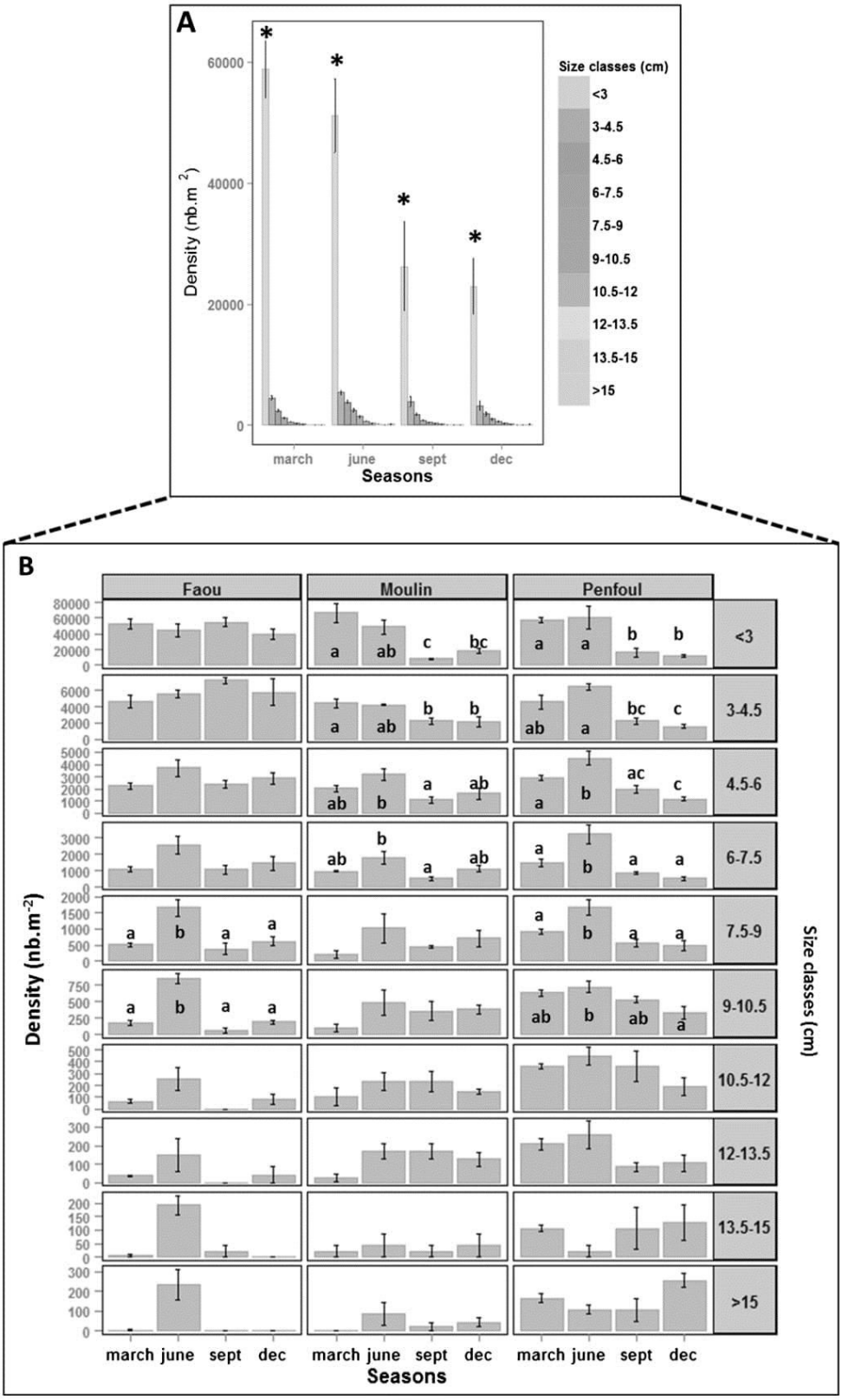

glycolipids were dominant (42.15 ± 11.61 % of TL, mean over the monitoring period), and within the glycolipids, digalactosyldiacylglycerol (DGDG) dominated (22.32 ± 8.59 % of TL, mean on the monitoring period). The relative part of triacylglycerides (TAG) was low, with 2.26 ± 0.96 % of TL.

◀ **Fig. 4** Representations of fragment densities of *Gracilaria vermiculophylla* depending on their size classes (expressed as nb m^{-2}) during the monitoring period, from March 2014 to December 2014. Results are expressed as means ± SD. **a** Density variations of fragment size classes when sites are pooled (n = 9), illustrating significant differences (*asterisk*) in the densities of fragments <3 cm compared with densities of the other size classes (p value <0.05). **b** Density variations for each fragment size class and each site (n = 3). *Different letters* indicate significant differences between means using the Tukey post hoc test or Kruskal multiple comparison test and the *lack of a letter* indicates that no significant difference was observed (p value <0.05)

Algal lipid content fluctuated significantly over the monitored period with a minimum observed in December 2013 and a maximum the next year (Table 2). Conversely, *G. vermiculophylla* lipid composition was homogenous between the sampled sites and no significant site effect was observed, apart from for sterol esters, for which Penfoul was different from Faou and Moulin. The part of neutral lipids increased significantly in December 2013 and June 2014 compared to the rest of the year (ANOVA, $p < 0.05$). The seasonal variability of the percentage of neutral lipids was only due to free fatty acid (FFA) fluctuations. Indeed, FFA constituted the main part of the neutral lipids, while the other neutral lipid classes did not evolve significantly with the seasons. Conversely, the part of glycolipids also decreased in

A

Monitored months	Relative concentration (%)			C/N ratio
	Floridoside	Isethionic acid	Taurine	
December 13	26.83 ± 2.09	8.07 ± 0.67	6.16 ± 0.28 ^{ab}	0.89 ± 0.08
March 14	24.74 ± 2.81	6.39 ± 0.21	6.53 ± 0.87 ^{a}	0.67 ± 0.14
June 14	29.2 ± 4.3	7.85 ± 1.28	5.38 ± 0.30 ^{ab}	1.02 ± 0.29
September 14	30.89 ± 1.07	7.68 ± 0.7	5.14 ± 0.19 ^{b}	1.06 ± 0.18
December 14	24.81 ± 4.91	7.3 ± 0.35	6.02 ± 0.49 ^{ab}	0.72 ± 0.19

B

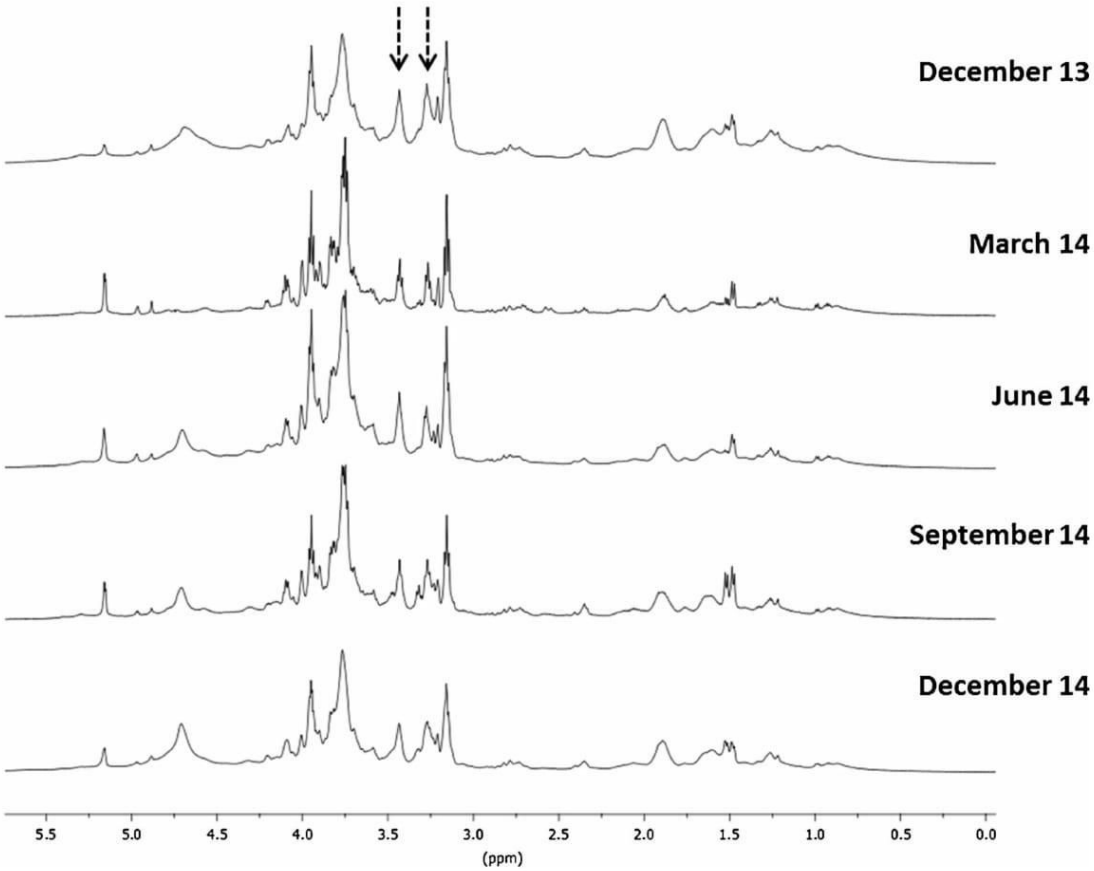

Fig. 5 Variability of some metabolites measured in *Gracilaria vermiculophylla* during the monitoring period. **a** Table of relative concentrations (expressed as %) for the floridoside, isethionic acid and taurine and C/N ratio (ratio of carbonated to nitrogenous molecule pools). Data were calculated based on relative signal integrals on ^{1}H HR-MAS spectra for each season. Data from the different sites were pooled as no site effect was detected (p value >0.05). Results are expressed as means ± SD (n = 3). *Different letters* indicate significant differences between means using the Tukey post hoc test after ANOVA (p value <0.05). **b** An example of superimposed ^{1}H HR-MAS NMR spectra of *G. vermiculophylla* for the Faou site from December 2013 to December 2014. *Arrows* corresponds to taurine integrated peaks

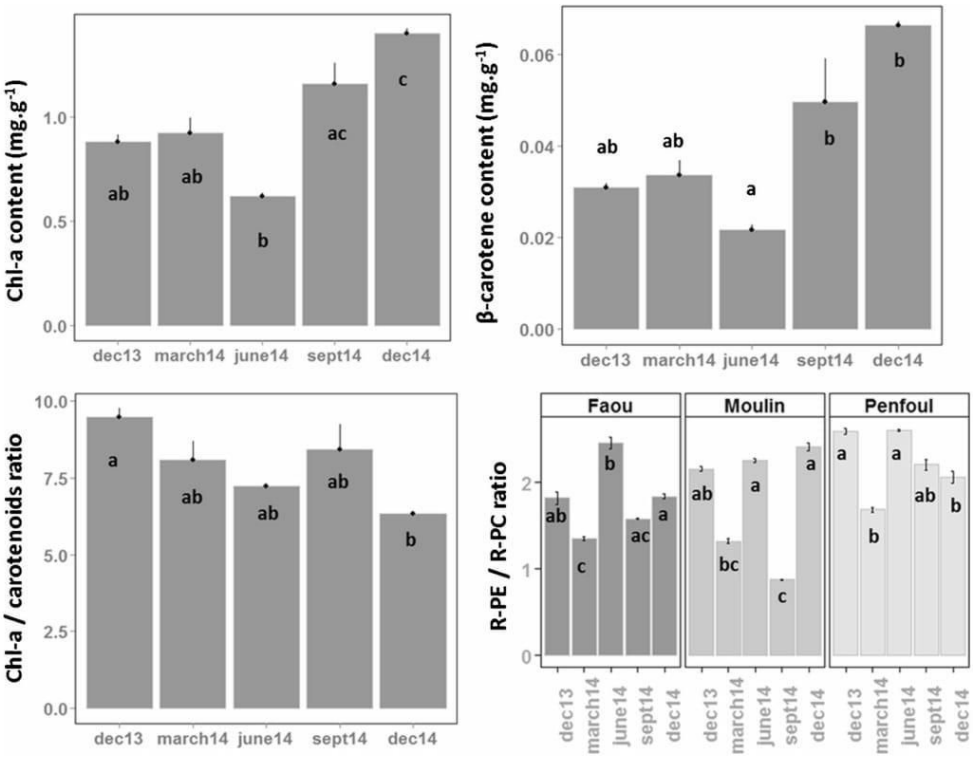

Fig. 6 Pigment contents and ratios of *Gracilaria vermiculophylla* from December 2013 to December 2014: β-carotene and chl-*a* contents (expressed as mg g^{-1}) and chl-*a*/carotenoids (carotenoids are the sum of zeaxanthin and β-carotene contents) and R-PE/R-PC ratios. For β-carotene and chl-*a* contents and the chl-*a*/carotenoid ratio, data from the different sites were pooled as there was no significant site effect ($n = 9$, p value >0.05). For R-PE/R-PC ratios, data were significantly different between sites (p value <0.05, $n = 3$). Results are expressed as means ± SD. *Different letters* indicate significant differences between means with the Kruskal multiple comparison test (p value <0.05). The scale of the ordinate axis is adapted to the data considered. *Chl-a* chlorophyll-*a*, *R-PE*, R-phycoerythrin, *R-PC* R-phycocyanin

December 2013 and June 2014 (ANOVA, $p < 0.05$). Indeed, monogalactosyldiacylglycerol (MGDG) and DGDG reached a minimum in June (ANOVA, p <0.05). Sulfoquinovosyl diacylglycerol (SQDG) followed the opposite tendency with a maximum in December 2013 and June 2014 (Table 2). On the other hand, phospholipids did not vary with the seasons and represented around 25.89 ± 0.42 to 31.62 ± 4.18 % of the algal lipids. Within this lipid class, the two smallest subclasses, cardiolipins (CL) and phosphatidylserine (PS), showed seasonal variations. As these classes represent minor lipids, their variability did not appear in the phospholipid class. CL decreased in June compared to December 2013 but was constant for the rest of the year, and PS decreased continuously over the monitoring period (ANOVA, $p < 0.05$).

Discussion

In Brittany estuaries, *G. vermiculophylla* forms characteristic dense and entangled mats covered by a thin layer of mud. It has previously been reported that *G. vermiculophylla* occurrence on mudflats on the American coasts of Virginia appears to rely on its anchoring capabilities. Indeed, a link was suggested between the distribution of tube-dwelling polychaetes *Diopatra cuprea* and the macroalgal distribution on the mud in Hog Island Bay (Thomsen and McGlathery 2005; Gulbransen et al. 2013). In the studied areas from French Brittany (this present study), the burial of fragments in the sediment was the only way of life observed throughout the monitoring and no attachment seemed necessary for establishment, similar to the observations of Rueness (2005). This fragment burial also seemed to allow the persistence of the perennial mat of *G. vermiculophylla* in Brittany estuaries. Moreover, the Faou ria presented a majority of pelites (<60 μm; Surget, personal observation) indicating that this is a highly sheltered ria. This may explain the characteristic ecology of the seaweed in Brittany compared to the Virginia coasts.

Despite this sustainability of the *G. vermiculophylla* mat on the mud, differing biomass fluctuations were observed among the sites, since thalli were not fixed on the mud. Indeed, biomass loss from September 2014 to March 2015 in the Penfoul site compared to the Faou and Moulin sites explained the site differences. Abreu et al. (2011) highlighted the instability of the mat in relation to environmental factors (wind, currents, etc.). As the Moulin site is situated in an anthropized area, human perturbations might have affected the *Gracilaria* mat. Furthermore, on this site, only fragments shorter than 7.5 cm presented seasonal variations. These small fragments could represent high densities but small biomasses, explaining the absence of significant seasonal variations of biomass all along the study. Despite these local variations, a seasonal pattern emerged, with a maximum of biomass reached in June, coupled with a maximum of most of the described size classes. On Brittany coasts, *G. vermiculophylla* seemed to follow a

Table 2 Total lipid content expressed as milligrams per gram DW and main lipid classes expressed as percent of total lipid (LT) from December 2013 to December 2014 in *Gracilaria vermiculophylla*: neutral lipids correspond to sterol esters, glycerid esters, triacylglycerides, free fatty acids, alcohols and free sterols

Monitored months	Total lipid ($mg.g^{-1}$ DW)	Neutral lipids (% TL)	Glycoplipids (% TL)	Phospholipids (% TL)
December 13	8.38 ± 0.92^{a}	35.22 ± 4.94^{a}	34.94 ± 4.47^{a}	27.79 ± 0.75
March 14	14.51 ± 1.46^{b}	22.87 ± 0.66^{b}	44.40 ± 2.10^{ab}	30.66 ± 2.11
June 14	12.53 ± 1.75^{ab}	45.26 ± 2.66^{c}	25.24 ± 3.27^{c}	27.31 ± 5.04
September 14	13.19 ± 3.07^{b}	18.31 ± 4.90^{a}	54.55 ± 4.36^{d}	25.89 ± 0.42
December 14	15.14 ± 0.42^{b}	15.64 ± 1.70^{a}	51.63 ± 3.00^{bd}	31.62 ± 4.18

	Neutral lipids					
Monitored months	Sterol esters (% TL)	Glycerid esters (% TL)	Triacylglycerids (% TL)	Free fatty acids (% TL)	Alcohols (% TL)	Free sterols (% TL)
December 13	1.35 ± 0.44	0 ± 0	1.28 ± 0.23	23.95 ± 3.97^{a}	$0.16 \pm 3.40\ 10^{-2}$	8.47 ± 1.47
March 14	1.44 ± 0.42	0 ± 0	2.13 ± 0.40	14.68 ± 0.88^{b}	$0.08 \pm 5.35\ 10^{-2}$	4.54 ± 0.30
June 14	1.01 ± 0.15	0 ± 0	1.78 ± 0.45	37.31 ± 1.39^{c}	$0.02 \pm 1.23\ 10^{-2}$	5.14 ± 0.80
September 14	1.44 ± 0.38	0 ± 0	3.01 ± 1.65	8.16 ± 4.03^{bd}	$0.19 \pm 14.30\ 10^{-2}$	5.51 ± 1.12
December 14	1.24 ± 0.14	0 ± 0	2.61 ± 0.78	6.06 ± 1.62^{d}	$0.16 \pm 3.68\ 10^{-3}$	5.58 ± 0.27

	Glycolipids		
Monitored months	MGDG (% TL)	DGDG (% TL)	SQDG (% TL)
December 13	10.29 ± 2.47^{ab}	16.56 ± 3.18^{a}	8.09 ± 0.54^{a}
March 14	14.57 ± 0.62^{bc}	24.22 ± 2.56^{b}	5.61 ± 0.68^{ab}
June 14	7.82 ± 0.99^{a}	9.90 ± 1.80^{c}	7.52 ± 0.83^{ac}
September 14	20.02 ± 3.03^{d}	29.61 ± 1.61^{bd}	4.93 ± 1.68^{bc}
December 14	16.15 ± 0.47^{cd}	31.33 ± 2.39^{d}	4.15 ± 1.08^{b}

	Phospholipids				
Monitored months	PI (% TL)	PC (% TL)	PE+PG (% TL)	CL (% TL)	PS (% TL)
December 13	15.97 ± 0.79	15.97 ± 0.79	5.31 ± 0.23	2.62 ± 0.46^{a}	$0.73 \pm 4.91\ 10^{-2\ a}$
March 14	18.87 ± 1.84	18.87 ± 1.84	4.66 ± 0.29	3.15 ± 0.31^{a}	$0.55 \pm 8.07\ 10^{-2\ ab}$
June 14	16.90 ± 6.27	16.90 ± 6.27	5.81 ± 0.20	1.66 ± 0.39^{b}	$0.33 \pm 9.86\ 10^{-2\ bc}$
September 14	15.77 ± 0.84	15.77 ± 0.84	5.39 ± 0.88	2.37 ± 0.32^{ab}	$0.43 \pm 2.22\ 10^{-2\ ac}$
December 14	18.08 ± 4.98	18.08 ± 4.98	5.76 ± 0.28	2.54 ± 0.20^{ab}	$0.21 \pm 6.35\ 10^{-2\ c}$

Data from the different sites were pooled as no significant site effect was observed, apart from for sterol esters. Results are expressed as means ± SD ($n = 3$). Different superscript letters indicate significant differences between means with the Tukey post hoc test (p value <0.05)

MGDG monogalactosyldiacylglycerol, *DGDG* digalactosyldiacylglycerol, *SQDG* sulfoquinovosyl diacylglycerol, *PI* phosphatidylinositol, *PC* phosphatidylcholine, *PE + PG* phosphatidylethanolamine + phosphatidylglycerol, *CL* cardiolipin, *PS* phosphatidylserine

pattern close to the one described in its native area on Nokonoshima Island in Japan (Muangmai et al. 2014). Moreover, a maximum biomass observed in June is consistent with a higher primary production observed in the same month on the Faou site (Davoult et al. 2017, personal communication).

The abundance of fragments shorter than 3 cm indicates a high level of fragmentation of *Gracilaria* at the surface and also in the mud. This fragmentation might be linked to several factors. On the studied sites, since the fragments are entangled in the mud, the thallus part present at the interface between the

surface and the mud might be weakened due to tide flows (Thomsen and McGlathery 2005) and thallus necrosis linked to anoxic conditions of the mud. Indeed, thalli presented small black areas corresponding to sporadic necrosis along the fragments (Surget, personal observation). Furthermore, in a parallel study, we demonstrated an increase in the density of mud macrofauna as well as species richness in areas colonized by *G. vermiculophylla* compared with bare areas on the Faou site (Davoult et al. 2017, personal communication). Although the palatability of *G. vermiculophylla* to herbivorous grazers decreases in invasive areas (Hammann et al. 2013b) and despite the grazers' preference for native algal species, *G. vermiculophylla* may be grazed in Northern European estuaries that it has invaded (Nejrup et al. 2012). This grazing may facilitate its small-scale dispersal (Thomsen et al. 2007). Bioturbation generated by macrofauna activity might contribute to the fragmentation of the thalli. Moreover, our observations showed a large dominance of vegetative fragments with only one tetrasporophyte observed in the field, as described in the literature. Indeed, *G. vermiculophylla* might proliferate in the field by means of spores and vegetative fragments (Nettleton et al. 2013). Vegetative reproduction (e.g. by fragmentation) might be determinant for the invasiveness of introduced seaweeds (Nyberg and Wallentinus 2005), and *G. vermiculophylla* is known for its reproductive versatility (Hu and Juan 2013). From results obtained in this present study, the high fragmentation of algal thalli might then represent a strong dispersal vector of *G. vermiculophylla* in the Bay of Brest.

The metabolomic analysis showed that floridoside, isethionic acid and taurine were the main organic solutes in *G. vermiculophylla*. This predominance has also been reported in other rhodophytes, such as *S. chordalis* (Bondu et al. 2007) and *Grateloupia turuturu* (previously called *G. doryphora*), another invasive alga on Brittany coasts (Simon et al. 2001), except for taurine in this latter species (Simon-Colin et al. 2004). In the literature, floridoside and isethionic acid are primarily described as osmoprotectants (Holst et al. 1994; Bondu et al. 2009) and taurine as a cytoprotectant, well defined in mammalian cells (Schaffer et al. 2003). This is consistent with the fact that *G. vermiculophylla* is described as euryhaline (Gulbransen et al. 2013), characterized by its high acclimation to the saline variations occurring in estuaries (Lartigue et al. 2003; Nejrup and Pedersen 2012). Interestingly, isethionic acid and floridoside were reported as antifouling molecules in *G. turuturu* (Hellio et al. 2004), as well as quorum sensing inhibitors (Liu et al. 2008). Isethionic acid is also known for its potential qualitative defence against herbivores (Holst et al. 1994). This might partially explain the resistance of *Gracilaria* in mud and to grazers (e.g. low palatability of *G. vermiculophylla*) (Weinberger et al. 2008; Nejrup et al. 2012; Hammann et al. 2013a). In a recent work, Saha et al. (2016) demonstrated in *G. vermiculophylla* studied in both invasive and native areas that populations were found to be equally well defended against co-occurring bacterial epibionts isolated in their respective ranges, which means that the species rapidly adapted its defences against microfoulers in new colonized habitats.

Additionally, taurine is a sulphurated amino acid which is not incorporated in proteins (Wang et al. 2015). The decrease in the relative concentration of taurine in summer might be linked to a low N availability that often occurs in estuaries during summer (Nejrup and Pedersen 2012). Moreover, Lindberg (1955) suggested that taurine might be an intermediate in the metabolic pathway for synthesis of sulphated polysaccharide like the agar present in the *Gracilaria* genus. In parallel, the lack of significant differences in the floridoside relative concentration in summer might be explained by a fast de novo synthesis and the rapid use of the floridoside pool as an intermediate for short-term storage of organic carbon for cell wall synthesis (Bondu et al. 2007, 2009). We suggest then that taurine might be an alternative intermediate to floridoside involved in polysaccharide synthesis, especially in March. Further studies, involving physiological studies coupled with ecological surveys, are needed at a scale representative of the biological cycle of *G. vermiculophylla* in order to obtain a more comprehensive view of its physiology as an invader in the Bay of Brest.

Concerning the seasonal variations of pigments, our study demonstrated a seasonal photoacclimation of *G. vermiculophylla*. During laboratory experiments, Roleda et al. (2012) observed no chl-*a* fluctuation of *G. vermiculophylla* under several radiation treatments (UV-A and UV-A + UV-B) but a significant difference linked to thallus acclimation to laboratory conditions. The laboratory conditions did not reproduce the complexity of interactions between environmental factors that normally occur in the field. Moreover, Roleda et al. (2012) tested the lower limit of irradiance observed in the field (300 μmol photons m^{-2} s^{-1}). High irradiance might be encountered in the field during summertime (up to 2287 μmol photons m^{-2} s^{-1} registered the 2 June 2015 on the Faou site). This might explain the differences observed in our study, as exposure to photosynthetically active radiation (PAR) conditions in the field may require photoacclimation responses from thalli by adjusting the pigment concentration (Bailey and Grossman 2008). Similarly, Beach et al. (2005) observed no photoacclimation of the rhodophyte *Ahnfeltiopsis concinna* during laboratory experiments and, conversely, a range of in situ photoacclimation responses. Moreover, Pereira et al. (2012) showed a link between N availability and light conditions and alterations in pigment content in natural populations of *Gracilaria domingensis*. Consequently, the decrease in chl-*a* contents, like β-carotene, seems to be an acclimation to high PAR and irradiance encountered in June. Additionally, the pigment increase observed in December 2014 seems to be an

acclimation of the species to optimize light harvesting under the light-limiting conditions occurring in winter. An alternative hypothesis might be that this decrease in pigment content for chl-*a* and β-carotene might be due to a dilution of cellular content as a consequence of the fast growth of the thallus. Indeed, maximum biomass was observed in June corresponding to the growth maxima (Muangmai et al. 2014).

Annual fluctuations of environmental factors might explain the differences in pigment content measured between the winters of 2013 and 2014. In particular, turbidity variations might be involved, since turbidity induces a variation of light quality and quantity (Saffo 1987). Indeed, it has been demonstrated that an increase of high suspended solid concentration up to a certain level leads to increases in chl-*a* and phycoerythin contents (Thirb and Benson-Evans 1985). The chl-*a* and carotenoid ratios observed here are consistent with those reported by Roleda et al. (2012), i.e. a *G. vermiculophylla* ratio of 6.77 ± 0.56 on samples collected during autumn in Sweden. Moreover, given that phycobilisomes are sensitive to UV-B and that R-PE is less sensitive than R-PC (Roleda et al. 2012), the increase in the R-PE/R-PC ratio in June compared with March and September might be due to a faster degradation of R-PC than R-PE by UV-B radiation in June.

The composition in lipid classes was also studied in *G. vermiculophylla*, which presented low lipid content. *Gracilaria verrucosa* from Japan presented similar levels of lipids with 15.2 ± 2.7 mg g^{-1} DW (Khotimchenko 2005), but these were higher than the levels encountered in *G. turuturu*, another invasive red alga present on Brittany coasts (Kendel et al. 2012). Khotimchenko (2005) reported a dominance of DGDG in *G. verrucosa*, as demonstrated in our study. This particularity in lipid composition characterizes few Rhodophyta species.

Our study also showed a decrease in MGDG and DGDG percentages in June 2014 and in December 2013, concomitant with an increase in FFA and SQDG in the red alga in the same months. The MGDG and DGDG relative parts followed similar variations to chl-*a* content, but SQDG presented an opposite pattern. The sources of variability affecting the lipid content are numerous, e.g. location, growth conditions, light intensity, temperature or nutrient availability (Pettitt and Harwood 1989; Khotimchenko 2005; Guschina and Harwood 2006; Stengel et al. 2011). Glycolipid variations for the monitored months suggested photosynthesis efficiency adjustments of *G. vermiculophylla* (Kalisch et al. 2016) with the seasons, as glycosylglycerides are confined to chloroplast membranes and are involved in the regulation of chloroplast membrane fluidity and/or light harvesting (Pettitt and Harwood 1989; Dörmann and Hölzl 2009). These results contrast with previous reports in the literature. Indeed, Khotimchenko and Yakovleva (2005) showed an increase of structural lipids, especially SQDG, when the red alga *Tichocarpus crinitus* was exposed to low light conditions, and an increase of TAG, constituting storage lipids, under growth conditions. In our study, we observed low levels of TAG, thus indicating that *G. vermiculophylla* stores little in this lipid form. In contrast to our study, Kendel et al. (2012) observed no seasonal variations of glycolipids but a seasonality of phospholipids in *G. turuturu*. Our study showed an increase of FFA in December 2013 and in June 2014. Illijas et al. (2009) observed a large increase of FFA levels after frozen storage and thawing compared to fresh samples in the Ceramiales *Exophyllum wentii*, linked to the hydrolysis of lipid membranes, but this did not explain the seasonal fluctuations observed in our study. Moreover, it was reported that the increase of FFA was linked to deacylation of polar lipids (Lion et al. 2006; Illijas et al. 2009). In *Gracilaria chilensis*, FFA production was observed following an activation of particular enzymes, i.e. phospholipase and galactosidase, in wounded vegetative fragments. This FFA pool constituted a substrate for oxilipin synthesis (Lion et al. 2006). The results presented in our study also suggest an increase of lipid membrane hydrolysis, linked to a high mechanical stress occurring in December 2013 and especially in June 2014. These results were correlated with fragment densities, as a higher density of fragments <10.5 cm was observed in June. Moreover, the oxilipin production induced by physical wounding played an ecological role in defence against epiphytes in *G. chilensis* (Lion et al. 2006) and against herbivores in *G. vermiculophylla* (Rempt et al. 2012). Indeed, these results suggested a seasonal modulation of these conserved defence mechanisms. In future work, the quantification of specific FFA implicated in oxilipin synthesis will test this hypothesis.

Another hypothesis could be that the decrease observed in MGDG and DGDG might suggest lipid degradation that would explain the FFA increase. This hypothesis is supported by the pigment results showing a decrease in chl-*a*, carotenoids and zeaxanthin at the same sampling dates. These results suggest that *G. vermiculophylla* might have been stressed in December 2013 and, especially, in June 2014. Nevertheless, no impact was observed on the ecology of *G. vermiculophylla*, as the algal biomass (this study) and its primary production were highest in June (Davoult et al. 2017, personal communication). Consequently, the seasonal metabolic acclimations observed do not seem to reach the limit of its physiological capacities. Furthermore, the stratification of the mat of *G. vermiculophylla*, induced by the superposition of fragments entangled in the mud to form a mat of at least 1 cm, may provide a canopy with a protection effect against environmental factors such as light. Partial fragment burial may also insure sustainability of *G. vermiculophylla*, as it was particularly the case in June 2014 in these Brittany estuaries.

In conclusion, the fragmentation potential of *G. vermiculophylla* appears to be an important strategy for species propagation in the Bay of Brest. This study highlighted its seasonal, ecological and metabolic acclimations. Further work

needs to be performed on antioxidant protection and oxidant stress of *G. vermiculophylla*, in order to confirm these results and to determine whether oxidant stress occurs in summertime. We hypothesise that the partial burial of fragments provides a canopy protection against light conditions occurring in summer in Brittany. Moreover, this study underlined the role of organic solutes in the seasonal acclimation of *G. vermiculophylla*. As the metabolic pathway link to osmoregulation and cell wall synthesis is still not clarified, further studies combining ecological monitoring with ecophysiological studies are necessary. These will provide a powerful overview of the metabolic acclimations of *G. vermiculophylla* that occur in its invasive areas.

Acknowledgements This study is part of a PhD project carried out by the first author at the Laboratoire des Sciences de l'Environnement Marin (LEMAR UMR6539) in the IUEM (UBO-UBL), under the supervision of the last author. It was supported by the *Ministère de l'Education Nationale, de l'Enseignement Supérieur et de la Recherche* (UBO funding for the first author) and *Région Bretagne* (ARED Labex Mer). This study was cofinanced with the support of the European Union ERDF—Atlantic Area Program and French ANR and is related to the research project INVASIVES (Era-net Seas-era. 2012–2016). The authors thank Helen McCombie-Boudry of the Bureau de Traduction de l'Université (BTU) of the University of Western Brittany, Brest, France for her fruitful assistance with the improvement and reviewing of the English language of the manuscript.

References

Abreu MH, Pereira R, Sousa-Pinto I, Yarish C (2011) Ecophysiological studies of the non-indigenous species *Gracilaria vermiculophylla* (Rhodophyta) and its abundance patterns in Ria de Aveiro lagoon, Portugal. Eur J Phycol 46:453–464

Bailey S, Grossman A (2008) Photoprotection in cyanobacteria: regulation of light harvesting. Photochem Photobiol 84:1410–1420

Beach KS, Smith CM, Okano R (2005) Experimental analysis of rhodophyte photoacclimation to PAR and UV-radiation using in vivo absorbance spectroscopy. Bot Mar 43:525–536

Bondu S, Kervarec N, Deslandes E, Pichon R (2007) The use of HRMAS NMR spectroscopy to study the in vivo intra-cellular carbon/nitrogen ratio of *Solieria chordalis* (Rhodophyta). J Appl Phycol 20:673–679

Bondu S, Cerantola S, Kervarec N, Deslandes E (2009) Impact of the salt stress on the photosynthetic carbon flux and ^{13}C-label distribution within floridoside and digeneaside in *Solieria chordalis*. Phytochemistry 70:173–184

Broberg A, Kenne L, Pedersén M (1998) In-situ identification of major metabolites in the red alga *Gracilariopsis lemaneiformis* using high-resolution magic angle spinning nuclear magnetic resonance spectroscopy. Planta 206:300–307

Davidson AM, Jennions M, Nicotra AB (2011) Do invasive species show higher phenotypic plasticity than native species and, if so, is it adaptive? A meta-analysis. Ecol Lett 14:419–431

Dörmann P, Hölzl G (2009) The role of glycolipids in photosynthesis. In: Wada H, Murata N (eds) Lipids in photosynthesis. Springer, Netherlands, pp 265–282

Dumay J, Clément N, Morançais M, Fleurence J (2013) Optimization of hydrolysis conditions of *Palmaria palmata* to enhance R-phycoerythrin extraction. Bioresour Technol 131:21–27

Freshwater DW, Montgomery F, Greene JK, Hamner RM, Williams M, Whitfield PE (2006) Distribution and identification of an invasive *Gracilaria* species that is hampering commercial fishing operations in Southeastern North Carolina, USA. Biol Invasions 8:631–637

Gulbransen D, McGlathery K (2013) Nitrogen transfers mediated by a perennial, non-native macroalga: a ^{15}N tracer study. Mar Ecol Prog Ser 482:299–304

Gulbransen DJ, Thomsen MS, McGlathery KJ (2013) A global perspective on the *Gracilaria vermiculophylla invasion*: what is currently known and what is still needed. In: *Gracilaria vermiculophylla* in the Virginia coastal bays: documenting the distribution and effects of a non-native species, PhD Thesis, University of Virginia pp 151–192

Gupta V, Thakur RS, Reddy CRK, Jha B (2013) Central metabolic processes of marine macrophytic algae revealed from NMR based metabolome analysis. RSC Adv 3:7037–7047

Guschina IA, Harwood JL (2006) Lipids and lipid metabolism in eukaryotic algae. Prog Lipid Res 45:160–186

Haberkorn H, Lambert C, Le Goïc N, Moal J, Suquet M, Guégen M, Sunila I, Soudant P (2010) Effects of *Alexandrium minutum* exposure on nutrition-related processes and reproductive output in oysters *Crassostrea gigas*. Harmful Algae 9:427–439

Hammann M, Buchholz B, Karez R, Weinberger F (2013a) Direct and indirect effects of *Gracilaria vermiculophylla* on native *Fucus vesiculosus*. Aquat Invasions 8:121–132

Hammann M, Wang G, Rickert E, Boo SM, Weinberger F (2013b) Invasion success of the seaweed *Gracilaria vermiculophylla* correlates with low palatibility. Mar Ecol Prog Ser 486:93–103

Harrison PJ, Hurd CL (2001) Nutrient physiology of seaweeds: application of concepts to aquaculture. Cah Biol Mar 42:71–82

Hellio C, Simon-Colin C, Clare A, Deslandes E (2004) Isethionic acid and floridoside isolated from the red alga, *Grateloupia turuturu*, inhibit settlement of *Balanus amphitrite* cyprid larvae. Biofouling 20:139–145

Holst PB, Nielsen SE, Anthoni U, Bisht KS, Christophersen C, Gupta S, Parmar VS, Nielsen PH, Sahoo DB, Singh A (1994) Isethionate in certain red algae. J Appl Phycol 6:443–446

Hu ZM, Juan LB (2013) Adaptation mechanisms and ecological consequences of seaweed invasions: a review case of agarophyte *Gracilaria vermiculophylla*. Biol Invasions 16:967–976

Illijas MI, Indy JR, Yasui H, Itabashi Y (2009) Lipid class and fatty acid composition of a little-known and rarely collected alga *Exophyllum wentii* Weber-van Bosse from Bali Island, Indonesia. J Oleo Sci 58:103–110

Jégou C, Culioli G, Kervarec N, Simon G, Stiger-Pouvreau V (2010) LC/ESI-MSn and ^{1}H HR-MAS NMR analytical methods as useful taxonomical tools within the genus *Cystoseira* C. Agardh (Fucales; Phaeophyceae). Talanta 83:613–622

Kalisch B, Dörmann P, Hölzl G (2016) DGDG and glycolipids in plants and algae. In: Nakamura Y, Li-Beisson Y (eds) Lipids in plant and algae development. Springer, Berlin, pp 51–83

Kendel M, Couzinet-Mossion A, Viau M, Fleurence J, Barnathan G, Wielgosz-Collin G (2012) Seasonal composition of lipids, fatty acids, and sterols in the edible red alga *Grateloupia turuturu*. J Appl Phycol 25:425–432

Khotimchenko SV (2005) Lipids from the marine alga *Gracilaria verrucosa*. Chem Nat Compd 41:285–288

Khotimchenko SV, Yakovleva IM (2005) Lipid composition of the red alga *Tichocarpus crinitus* exposed to different levels of photon irradiance. Phytochemistry 66:73–79

Kumar M, Kuzhiumparambil U, Pernice M, Jiang Z, Ralph PJ (2016) Metabolomics: an emerging frontier of systems biology in marine macrophytes. Algal Res 16:76–92

Lartigue J, Neill A, Hayden BL, Puffer J, Cebrian J (2003) The impact of salinity fluctuations on net oxygen production and inorganic nitrogen uptake by *Ulva lactuca* (Chlorophyceae). Aquat Bot 75:339–350

Lasbleiz M, Leblanc K, Blain S, Ras J, Cornet-Barthaux V, Hélias Nunige S, Quéguiner B (2014) Pigments, elemental composition (C, N, P, and Si), and stoichiometry of particulate matter in the naturally iron fertilized region of Kerguelen in the Southern Ocean. Biogeosciences 11:5931–5955

Le Lann K, Kervarec N, Payri CE, Deslandes E, Stiger-Pouvreau V (2008) Discrimination of allied species within the genus *Turbinaria* (Fucales, Phaeophyceae) using HRMAS NMR spectroscopy. Talanta 74:1079–1083

Le Lann K, Kraffe E, Kervarec N, Cerantola S, Payri CE, Stiger-Pouvreau V (2014) Isolation of turbinaric acid as a chemomarker of *Turbinaria conoides* (J. Agardh) Kützing from South Pacific Islands. J Phycol 50:1048–1057

Lindberg B (1955) Methylated taurines and choline sulphate in red algae. Acta Chem Scand 9:1323–1326

Lion U, Wiesemeier T, Weinberger F, Beltrán J, Flores V, Faugeron S, Correa J, Pohnert G (2006) Phospholipases and galactolipases trigger oxylipin-mediated wound-activated defence in the red alga *Gracilaria chilensis* against epiphytes. Chembiochem 7:457–462

Liu HB, Koh KP, Kim JS, Seo Y, Park S (2008) The effects of betonicine, floridoside, and isethionic acid from the red alga *Ahnfeltiopsis flabelliformis* on quorum-sensing activity. Biotechnol Bioprocess Eng 13:458–463

Muangmai N, Vo TD, Kawaguchi S (2014) Seasonal fluctuation in a marine red alga, *Gracilaria vermiculophylla* (Gracilariales, Rhodophyta), from Nokonoshima Island, Southern Japan. J Fac Agric Kyushu Univ 59:243–248

Munier M, Jubeau S, Wijaya A, Morançais M, Dumay J, Marchal L, Jaouen P, Fleurence J (2014) Physicochemical factors affecting the stability of two pigments: R-phycoerythrin of *Grateloupia turuturu* and B-phycoerythrin of *Porphyridium cruentum*. Food Chem 150: 400–407

Nejrup LB, Pedersen MF (2012) The effect of temporal variability in salinity on the invasive red alga *Gracilaria vermiculophylla*. Eur J Phycol 47:254–263

Nejrup LB, Pedersen MF, Vinzent J (2012) Grazer avoidance may explain the invasiveness of the red alga *Gracilaria vermiculophylla* in Scandinavian waters. Mar Biol 159:1703–1712

Nettleton JC, Mathieson AC, Thornber C, Neefus CD, Yarish C (2013) Introduction of *Gracilaria vermiculophylla* (Rhodophyta, Gracilariales) to New England, USA: estimated arrival times and current distribution. Rhodora 115:28–41

Nyberg CD (2007) Introduced marine macroalgae and habitat modifiers: their ecological role and significant attributes. PhD thesis, Göteborg University, Sweden 66 pp

Nyberg CD, Wallentinus I (2005) Can species traits be used to predict marine macroalgal introductions? Biol Invasions 7:265–279

Nylund GM, Weinberger F, Rempt M, Pohnert G (2011) Metabolomic assessment of induced and activated chemical defence in the invasive red alga *Gracilaria vermiculophylla*. PLoS One 6:e29359

Pereira DC, Trigueiro TG, Colepicolo P, Marinho-Soriano E (2012) Seasonal changes in the pigment composition of natural population of *Gracilaria domingensis* (Gracilariales, Rhodophyta). Rev Bras Farmacogn 22:874–880

Pettitt TR, Harwood JL (1989) Alterations in lipid metabolism caused by illumination of the marine red algae *Chondrus crispus* and *Polysiphonia lanosa*. Phytochemistry 28:3295–3300

Pintó-Marijuan M, Munné-Bosch S (2013) Ecophysiology of invasive plants: osmotic adjustment and antioxidants. Trends Plant Sci 18: 660–666

Potin P, Bouarab K, Salaün J-P, Pohnert G, Kloareg B (2002) Biotic interactions of marine algae. Curr Opin Plant Biol 5:308–317

Querné J (2011) Invasion de *Spartina alterniflora* dans les marais de la rade de Brest-Comportement invasif et impact sur le cycle biogéochimique du Silicium. PhD thesis. LEMAR UMR 6539 IUEM, France 217 pp

Ras J, Claustre H, Uitz J (2008) Spatial variability of phytoplankton pigment distributions in the Subtropical South Pacific Ocean: comparison between in situ and predicted data. Biogeosciences 5:353–369

Rempt M, Weinberger F, Grosser K, Pohnert G (2012) Conserved and species-specific oxylipin pathways in the wound-activated chemical defense of the noninvasive red alga *Gracilaria chilensis* and the invasive *Gracilaria vermiculophylla*. Beilstein J Org Chem 8:283–289

Roleda MY, Nyberg CD, Wulff A (2012) UVR defense mechanisms in eurytopic and invasive *Gracilaria vermiculophylla* (Gracilariales, Rhodophyta). Physiol Plant 146:205–216

Rueness J (2005) Life history and molecular sequences of *Gracilaria vermiculophylla* (Gracilariales, Rhodophyta), a new introduction to European waters. Phycologia 44:120–128

Saffo MB (1987) New light on seaweeds. Bioscience 37:654–664

Saha M, Wiese J, Weinberger F, Wahl M (2016) Rapid adaptation to controlling new microbial epibionts in the invaded range promotes invasiveness of an exotic seaweed. J Ecol 104:969–978

Schaffelke B, Smith JE, Hewitt CL (2006) Introduced macroalgae—a growing concern. J Appl Phycol 18:529–541

Schaffer S, Azuma J, Takahashi K, Mozaffari M (2003) Why is taurine cytoprotective? In: Lombardini JB, Schaffer SW, Azuma J (eds) Taurine 5. Springer, US, pp 307–321

Simon C, Gall EA, Deslandes E (2001) Expansion of the red alga *Grateloupia doryphora* along the coasts of Brittany (France). Hydrobiologia 443:23–29

Simon-Colin C, Kervarec N, Pichon R, Deslandes E (2002) Complete ^{1}H and ^{13}C spectral assignment of floridoside. Carbohydr Res 337:279–280

Simon-Colin C, Kervarec N, Pichon R, Deslandes E (2004) NMR ^{13}C-isotopic enrichment experiments to study carbon-partitioning into organic solutes in the red alga *Grateloupia doryphora*. Plant Physiol Biochem 42:21–26

Stengel DB, Connan S, Popper ZA (2011) Algal chemodiversity and bioactivity: sources of natural variability and implications for commercial application. Biotechnol Adv 29:483–501

Stiger-Pouvreau V, Thouzeau G (2015) Marine species introduced on the French channel-Atlantic coasts: a review of main biological invasions and impacts. Open J Ecol 05:227–257

Sun L, Wang S, Gong X, Zhao M, Fu X, Wang L (2009) Isolation, purification and characteristics of R-phycoerythrin from a marine macroalga *Heterosiphonia japonica*. Protein Expr Purif 64:146–154

Tanniou A, Vandanjon L, Gonçalves O, Kervarec N, Stiger-Pouvreau V (2015) Rapid geographical differentiation of the European spread brown macroalga *Sargassum muticum* using HRMAS NMR and Fourier-transform infrared spectroscopy. Talanta 132:451–456

Thirb HH, Benson-Evans K (1985) The effect of suspended solids on the growth of apical tips of gametophyte plants of *Lemanea* and on carpospore germination and subsequent colonisation. Arch Hydrobiol 103:409–417

Thomsen MS, McGlathery K (2005) Facilitation of macroalgae by the sedimentary tube forming polychaete *Diopatra cuprea*. Estuar Coast Shelf Sci 62:63–73

Thomsen MS, Gurgel CFD, Fredericq S, McGlathery KJ (2006) *Gracilaria vermiculophylla* (Rhodophyta, Gracilariales) in Hog Island Bay, Virginia: a cryptic alien and invasive macroalga and taxonomic correction. J Phycol 42:139–141

Thomsen MS, Stæhr PA, Nyberg CD, Schwærter S, Krause-Jensen D, Silliman BR (2007) *Gracilaria vermiculophylla* (Ohmi) Papenfuss, 1967 (Rhodophyta, Gracilariaceae) in northern Europe, with emphasis on Danish conditions, and what to expect in the future. Aquat Invasions 2:83–94

Thomsen MS, McGlathery KJ, Schwarzschild A, Silliman BR (2009) Distribution and ecological role of the non-native macroalga *Gracilaria vermiculophylla* in Virginia salt marshes. Biol Invasions 11:2303–2316

Wang F, Guo XY, Zhang DN, Wu Y, Wu T, Chen ZG (2015) Ultrasound-assisted extraction and purification of taurine from the red algae *Porphyra yezoensis*. Ultrason Sonochem 24:36–42

Weinberger F, Buchholz B, Karez R, Wahl M (2008) The invasive red alga *Gracilaria vermiculophylla* in the Baltic Sea: adaptation to brackish water may compensate for light limitation. Aquat Biol 3: 251–264

Zubia M, Freile-Pelegrín Y, Robledo D (2014) Photosynthesis, pigment composition and antioxidant defences in the red alga *Gracilariopsis tenuifrons* (Gracilariales, Rhodophyta) under environmental stress. J Appl Phycol 26:2001–2010

Chapitre 2. Caractéristiques particulières de la biologie d'une espèce invasive à une échelle spatiale localisée :

La vie enfouie est-elle possible chez un organisme pluricellulaire phototrophe ? Mise en évidence de la vie enfouie dans la vase de *G. vermiculophylla*.

L'étude précédente sur *Gracilaria vermiculophylla* a mis en lumière la particularité du phénotype écologique de cette algue en Rade de Brest en comparaison d'autres régions du Monde où elle est invasive telles que sur les Côtes virginiennes (Thomsen and McGlathery, 2005). En effet, cette espèce forme un tapis dense et homogène à la surface de la vase et présente une forte fragmentation et en particulier un envasement important dans les rias où elle se développe en abondance en Rade de Brest. Le constat de cet envasement observé durant le suivi écologique de cette espèce soulève un certain nombre de questions scientifiques :

1- *G. vermiculophylla* présente-t-elle des caractéristiques de tolérance à l'enfouissement en environnement vaseux ?

2- Cet enfouissement varie-t-il dans le temps et quelle profondeur peut-il atteindre ? Quelle biomasse cela représente-t'il en comparaison des thalles présent en surface, ceci afin de déterminer l'importance écologique de cet enfouissement vis à vis de la biologie de cette espèce invasive ?

3- Cette biomasse a-t'elle les mêmes caractéristiques morphologiques que les fragments en surface ?

4- Les fragments enfouis représentent-t'ils majoritairement de la matière organique détritique ou un pool de fragments vivants, potentiellement vecteur de propagules invasives ?

5- Si ces fragments sont vivants, sont-ils métabolomiquement aussi actifs que ceux en surface ? Le degré de profondeur influe-t'il sur les activités métaboliques et la production de métabolites ? La notion de dormance de tels fragments enfouis peut-elle être avancée ?

Des travaux précédents évoquent l'envasement de *G. vermiculophylla* (Gonzalez et al., 2013; Thomsen and McGlathery, 2007) et apportent quelques éléments de réponses quant à la résistance de cette algue à des conditions extrêmes, d'obscurité notamment (Nyberg and Wallentinus, 2009; Weinberger et al., 2008). Cependant, la résistance à

l'enfouissement est une caractéristique peu commune chez les organismes photosynthétiques et en particulier chez les macrophytes benthiques qui y sont généralement au contraire sensibles. Seuls quelques contre-exemples existent (Glasby et al., 2005; Kamermans et al., 1998). Cette caractéristique peu commune de vie en milieu anaérobie et sans lumière à une telle profondeur, et d'autant plus chez un organisme photosynthétique, consiste donc en une caractéristique majeure de la biologie de l'espèce invasive *G. vermiculophylla* influant sur son potentiel invasif. Ce constast a conduit à présenter dans ce chapitre les caractéristiques phénologiques, physiologiques et biochimiques de cette algue lorsqu'elle est enfouie dans la vase dans l'optique de répondre aux problématiques scientifiques énoncées ci-dessus. Ce travail est présenté sous la forme d'un manuscrit qui va être soumis à publication.

Manuscrit en préparation

The sediment buried life of an invasive red seaweed

Introduction

Gracilaria vermiculophylla (Ohmi) Papenfuss represents one of the most invasive seaweed species with a large distribution range all around the world (Hu and Juan, 2013; Nettleton et al., 2013; Thomsen et al., 2013; Stiger-Pouvreau and Thouzeau, 2015). This agarophyte belongs to the Gracilariales and Gracilariaceae, and is an euryhaline and eurythermal species (Yokoya et al., 1999) that has the ability to colonize mainly unvegetated mudflat such as the low part of saltmarshes of shallow and sheltered estuaries. This engineer macroalga, native from Northwest Pacific and now worldwide introduced, has invaded estuarine mudflats in Brittany (France) since 1996 (Rueness, 2005) and has successfully expanded along the North west Atlantic coasts in few years (Abreu et al., 2011; Guillemin et al., 2008; Rueness, 2005; Weinberger et al., 2008). Its introduction in a new area leads to multiple ecological consequences and modifies in depth invaded ecosystems (Hu and Juan, 2013). Once established, this invader may compete with native macrophytes (Martínez-Lüscher and Holmer, 2010; Nettleton et al., 2013; Thomsen et al., 2013), modify macrofauna richness and abundance (Johnston and Lipcius, 2012; Weinberger et al., 2008; Davoult et al., *in prep.*), transform food web such as biogeochemical flux (Byers et al., 2012; Davoult et al., *in prep.*) and also could impact sessile organism recruitments on hard-bottom assemblage such as oyster reefs in muddy estuaries (Thomsen and McGlathery, 2006).

G. vermiculophylla exhibits multiple phenological variations depending on the characteristics of its introduced area. The alga may form perennial mats of either loose-lying thalli potentially issued of drifting fragments (Thomsen and McGlathery, 2006), or mats of entangled fragments as in Brittany (Surget et al., 2017), or the alga may be attached to worm tube building by *Diopatra cuprea* and/or bivalve shells (Abreu et al., 2011; Thomsen and McGlathery, 2005). Interestingly, this high phenotypic diversity was associated with a low genetic diversity in introduced populations compared to the native one, potentially due to a unique donor region in the native area which seems to be the East of the Japan Sea (Kim et

al., 2010). Hamman et al. (2013) hypothesized a genotype selection with low palatability character during introduction events.

G. vermiculophylla has no native analogue in Brittany rias as reported on mudflats of Georgia and South Carolina (Byers et al., 2012). Only the invasive halophyte *Spartina alterniflora* colonizes the higher level of mudflat in continuity with the lower saltmashes (Surget, pers. obs.). In a previous study, we reported a particular fragmented phenotype of *G. vermiculophylla* in rias of the Bay of Brest (Surget et al., 2017) which went along with a burying. The burial of *G. vermiculophylla* in sediment was reported on previous studies (Thomsen et al., 2007; Thomsen and McGlathery, 2007) in which the authors supposed physiological tolerance of *G. vermiculophylla* to burial. Previous studies gave however insights on physiological tolerances of *G. vermiculophylla* to burial. This invader has been demonstrated to be well adapted to brackish water (Weinberger et al., 2008) and not sensible to prolonged period of darkness longer than five months (Nyberg and Wallentinus, 2009) as well as the potential of unattached small fragments to easily grow (Nyberg, 2007; Rueness, 2005). Nevertheless, thorough studies were not conducted on *in situ* populations of *G. vermiculophylla* concerning this particular behavior.

Few examples of macrophytes resistance to natural burial were described in the literature. In the Veerse Meer lagoon in Netherlands, the burial of *Ulva* spp. during winter allows the species to resist to cold temperatures during the unfavorable season. Events of fragments liberation from sediment, which finally triggers a spring bloom that mainly contributes to a summer explosion of biomasses (Kamermans et al., 1998). Glasby et al. (2005) investigated the resilience such as the recovery rate of buried thalli of another green macroalga, *Caulerpa taxifolia,* and concluded to an underestimation of the species distribution range linked to its burial resistance.

In this context, the tolerance to burial in sediment of this red seaweed was monitored during a year at each season in Britain using sediment core. We hypothesized a perennial occurrence of this invasive macroalga buried into the mud, not only as detrital organic matter but as living fragments under a “dormancy” state. The objective of this study was to investigate the seasonal phenology of buried *G. vermiculophylla* fragments in terms of biomass and size classes and to determine physiological evidence of the living state of this

silted biomass via chlorophyll fluorescence records using imaging pulse amplitude modulated (Imaging-PAM) equipment and respiration measurements. In addition, with the aim to have an overview of *G. vermiculophylla* acclimation to burial, further biochemical analyses were conducted. Metabolite modification in response to burial was explored through metabolomic analyses using quantitative ^{1}H nuclear magnetic resonance (^{1}H qNMR), allowing the identification and also the quantification of the major intracellular metabolites solutes. Pigment quantification by high pressure liquid chromatography (HPLC) or by spectrophotometry according to pigments was also performed to observe the acclimation of this invasive macrophyte to darkness as anaerobic conditions induced by burial. The response to burial by *G. vermiculophylla* will be discussed by integrating these ecological, ecophysiological and metabolomics data derived from our monitoring field studies.

Material and methods

Ecological monitoring

The ecological monitoring was performed in mudflats at the bottom of three different rias located in the Bay of Brest (Brittany, France) named as Moulin (48°21.490'N - 4°20.447'W), Penfoul (48°21.619'N - 4°19.186'W) and Faou (48°21.497'N - 4°20.444'W). Samplings and measurements were carried out during low tides, every three months from December 2013 to December 2014 in parallel of the monitoring performed by Surget et al. (2017).

Algal thalli and sediment core sampling method The burial algae were sampled using a sediment core of length 15 cm and a surface of 0.00679 m^2. For each monitoring point and each site, ecological data was measured on three cores. The cores were first positioned just to gently mark the algal mat. Before driving down the cores in mud, the algal mat was gently cut off all around the edge of the cores, in a way to avoid to pull down potential surface fragments and to avoid mixing them with burial fragments. The surface thalli were then collected manually inside the circle positioned core. It represents the layer named L0 (0 to 0.5 cm depth; Figure 1a). Thus, the core was carefully pressed in sediment to collect the burial algae. Thereafter, cores are closed up and transported to laboratory. Cores were stored at 4°C before their treatment. Cores were manually sliced into four layers of 3 cm thick (Figure 1b and c). The layer L1 corresponds to the three first centimetres of the core (from 0 to 3 cm), the layer L2, from 3 to 6 cm, the layer L3 from 3 to 6cm, and the layer L4, from 9 to 12 cm.

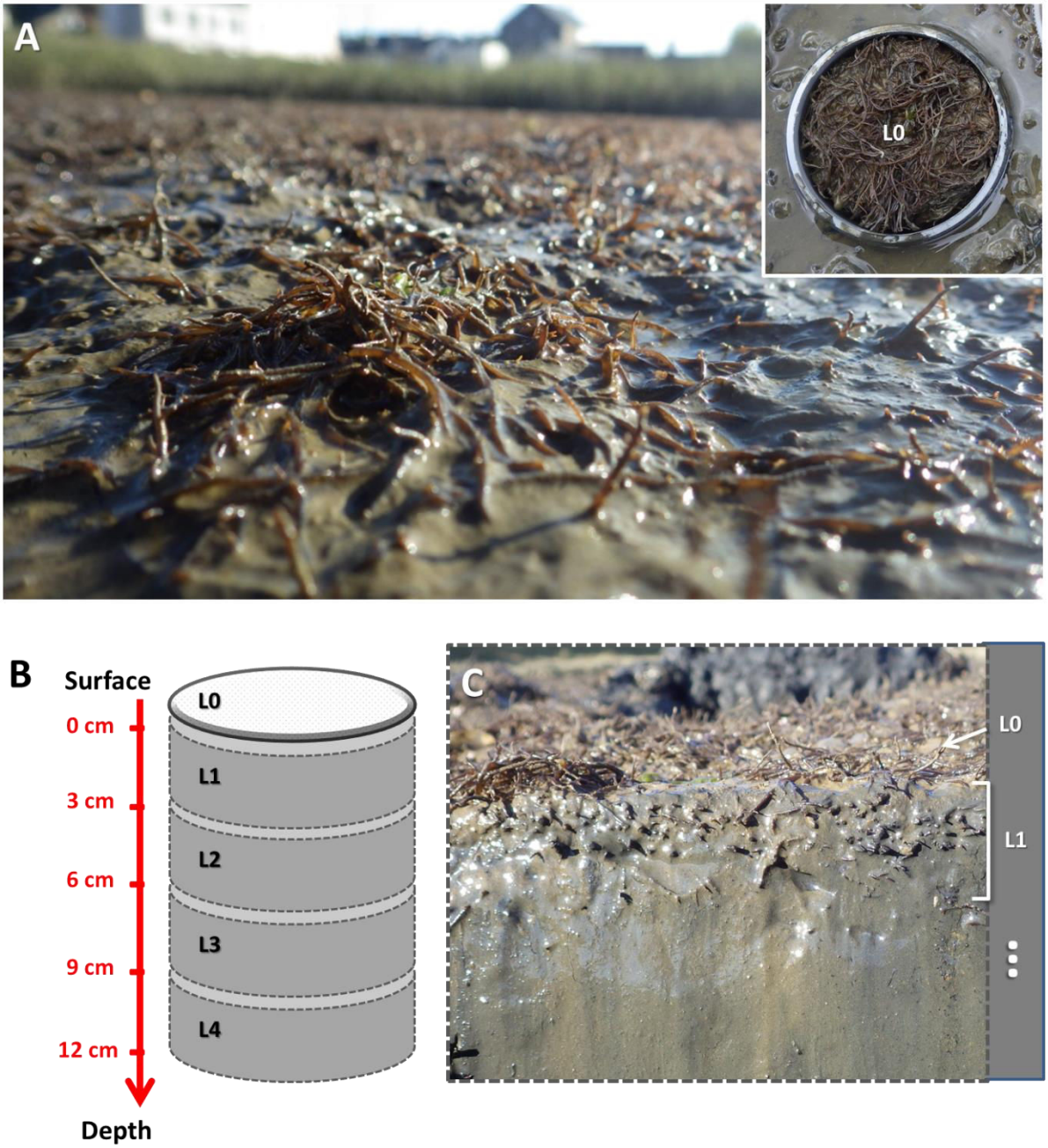

Fig. 1 A: Photo of entangled mat of *Gracilaria vermiculophylla* in the site named Faou with a view of core during sampling (at top right). B: Schematic representation of a mud core with the several mud layers from L1 to L4 (L1: layer from 0 to 3cm depth, L2: layer from 3 to 6 cm, L3: layer from 6 to 9 cm, L4: from 9 to 12 cm) and the surface layer, L0. C: Photograph of a cross section within the mud on the algal mat illustrating the thalli burial. Photographs were taken in February 2016.

Population biology (size of fragments and biomass) Each separate mud core layers was washed with filtered seawater to recover the burial algae fragments before

measurement of the biomass (fresh and dry weights, FW and DW respectively). Same was done for the layer L0 containing the surface algae. During sorting, fragment densities were set. The fragments longer than 3 cm were measured and the fragments shorter than 3 cm were counted. Fragment densities of layer 1 to layer 4 were classified into defined size classes adapted from Surget et al. (2017). Fragment densities of layer 0 were not analysed as this was already done on quadrats at the same time and locations (see Surget et al., 2017). The dry biomass results and densities were represented by means ± standard deviation (SD) and expressed in $g.m^{-2}$ for the former and in $nb.m^{-2}$ for the latter. In order to guarantee time-independent data, care was also taken to sample different cores at each sampling date. Data were compared in relation to sites and sampling dates.

Physiological analyses

Imaging PAM For Imaging PAM analysis, other muddy cores were sampled in the site Faou together with ecological monitoring (as this site presented the most extensive mat of *G. vermiculophylla*). The Imaging PAM analysis was performed 15 h after the field sampling. During layer preparation as fragment washing, care was taken to keep burial fragments in the dark. Before the recording, all thalli (buried and on surface) were acclimated to the darkness for 30 min. Fragments of the same layer from several cores were placed in the air for fluorescence capture by imaging PAM. Chlorophyll fluorescence imaging was carried out with a PAM imaging chlorophyll fluorometer (Open FluorCam FC 800-O, Photon System Instruments, Brno, Czech Republic) as described in Serôdio et al (2013). Images were processed using the FluorCam7 software (Photon System Instruments, Brno, Czech Republic). During picture processing, minimum threshold (allowing distinguishing color of the background from fluorescence of samples) was fixed to 200 (AU). To obtain three replicates with a minimum area of 20 pixels, analyses of layers 2 and 3 were pooled as the deepest fragments were less numerous and smaller than those from upper layers. The maximum quantum yield of PSII (Fv/Fm), corresponding to a proxy of the maximum efficiency of PSII (Genty et al., 1989), was measured on fragments maintained in darkness using a 0.8 s saturating pulse of white light. The ϕPSII, the efficiency of PSII photochemistry, was calculated according to Genty et al. (1989), on thalli at the end of each light-increasing step of 30 s each of the Rapid Light Curves (RLC) (9 light steps, ranging from 30 to 1049 µmol

photons m^{-2} s^{-1}). ϕPSII was used to estimate the relative electron transport rate (rETR) (Gevaert et al., 2003), a proxy of photosynthesis.

ϕPSII = (Fm'-Ft) / Fm'

rETR = ϕPSII * PAR, where PAR corresponds to recorded incident photosynthetically radiation

The light-limited initial slope (α), the light-saturated relative maximum rate of relative electron transfer (rETRmax), and the occurrence of photoinhibition (β) were calculated by plotting rETR against irradiance and by fitting the data using the photosynthetic model of Platt (Platt and Gallegos, 1980), model initially applied to phytoplankton. Corrected model of Walsby including also the occurrence of photoinhibition was tested (Nitschke et al., 2012) but Platt model was favoured as it fitted the best our data.

Respiration rate Respiration was measured at the laboratory on *G. vermiculophylla* fragments from 4 cores sampled in the site Faou, during low tide in January 2017, in order to test the living potential of buried fragments. During layer preparation as fragment washing, care was taken to keep burial fragments of *G. vermiculophylla* in the dark. Fragments of the several layers were kept in seawater, simulating their suspension in the seawater column. An opaque chamber was used to estimate CO_2 fluxes linked to the respiration of *G. vermiculophylla* thalli. Changes in air CO_2 concentration (ppm) in the opaque chamber (0.88 L) were measured with an infrared gas analyser (LiCor Li-820) for 3 min. CO_2 concentrations were recorded using a data logger (LiCor Li-1400) every 1 s. CO_2 flux was calculated as the slope of the linear regression of CO_2 concentration (μmol^{-1}) against time (s) and expressed in $\mu mol.C.m^{-2}.h^{-1}$ assuming a molar volume of 22.4 L at room temperature and ambient pressure.

Biochemical analyses

To complete our monitoring of *Gracilaria vermiculophylla* in Brittany, biochemical analyses were performed on muddy cores sampled during low tide in the Faou site (identical method to biological population) to test algal physiological tolerance to burial. The samples were done on September 2015, for pigment quantification and metabolites. Algal were treated as for biological population studies. Moreover, for these two analyses, layers 1 to 3 were pooled to have sufficient biomass of buried fragment. Thereby, two conditions were

compared “surface vs silted thalli”, ie algae distributed at the surface of the mud (fragments sampled in layer L0) and buried fragments (algae sampled in layers L1-L2-L3).

Pigments Zeaxanthin (zea), violaxanthine (viola), antheraxanthin (anther), chlorophyll-a (chl-a) and β-carotene (β-car) were analysed by High Pressure Liquid Chromatography (HPLC) following the method developed by Schmid and Stengel (2015). Frozen algal samples, kept at -80°C, were ground (Retch® MM400) in liquid nitrogen. Then, pigments were extracted from 100 mg of ground samples in a 90 % acetone solution, for 30 min with stirring, in the dark and at 4°C. After centrifugation, a second extraction was performed during 15 h. Supernatants were pooled before analyses. Pigments were analysed using an Eclipse XDB-C18 column (4.6 x 150 mm; 5 µm; Agilent) with a C18-guard-column. Chromatographic separation of pigments was performed within 40 min according to a gradient according to the method of Schmid and Stengel (2015). Acquisitions were performed using the software Chromeleon 6.60 (Dionex). After an identification based on absorption spectra of each peak and retention time of standards, pigment concentrations (expressed as $mg.g^{-1}$) were calculated using calibration curve (zea, viola, anthera and β-car were ordered from DHI LAB products, Denmark, and chl-a standards from Sigma-Aldrich). When a pigment was not detected in the sample extract, pigment content was fixed to the half of the detection threshold content of the considered pigment to calculate sample pigment concentration, in order to carry out statistical analysis. Viola was detected in 5 replicates on 9 for surface fragments and in 2 replicates on 9 for silted fragments. Chl-c2 and fucoxanthin were detected in some samples linked to the presence of benthic diatoms epiphytes on *G. vermiculophylla* thalli. To go further in the physiological variables measured on *G. vermiculophylla*, deepoxidation level and xanthophylls on chl-a ratio were calculated as follows:

$$\text{Deepoxidation level} = \frac{(\text{anthera} + \text{zea})}{(\text{viola} + \text{anthera} + \text{zea})}$$

$$\text{Xanthophylls / chl-a} = \frac{(\text{viola} + \text{anthera} + \text{zea})}{\text{chl-a}}$$

Phycobiliprotein content was determined using a protocol adapted from Sun et al. (2009) and Roleda et al. (2012). Extraction was performed in the dark at 4°C on 100 mg FW

with phosphate buffer (0.1 M, pH = 6.8). After sonication for 15 min, extract samples were centrifuged for 20 min at 4°C. The obtained extracts were stored at 4°C in the dark until the absorbance was read at 455, 565, 592, 618 and 645 nm (POLARstar Omega, BMG LABTECH). Concentrations of phycobiliproteins, expressed as $mg.g^{-1}$ DW, were determined using Beer and Eschel equations (Dumay et al. 2013; Munier et al. 2014; Zubia et al. 2014) as follows:

$$\text{R-PE} = [(A_{565} - A_{592}) - (A_{455} - A_{592}) \times 0.20] \times 0.12$$

$$\text{R-PC} = [(A_{618} - A_{645}) - (A_{592} - A_{645}) \times 0.50] \times 0.15$$

where A = Absorbance; R-PE = R-phycoerythrin; R-PC = R-phycocyanin.

^{1}H qNMR spectroscopy ^{1}H NMR analyses were performed on eleven replicates (from four cores) gathered in parallel of pigments sampling. Frozen algal samples kept at -80°C, were then and grounded (Retch® MM400) in liquid nitrogen before being freeze-dried. About 15 mg of homogeneous dried powder for each replicate were extracted with 800 µL D_2O (Euristo-Top, D2O 99.96%). Sodium trimethylsilyl-propionate-d4 (TSP) was previously solubilized in D_2O solvent (from 0.55 to 0.83 $mg.mL^{-1}$ depending of the sample series) and used as a standard. After centrifugation (mini centrifuge LMS, MCF2360), the supernatant was placed in NMR tubes (5-mm diameter). Spectral data were recorded at 25°C with a BRUKER Avance III HD Spectrometer (Bruker BioSpin, Wissembourg, France), equipped with a TBI 1H/{BB}/13C probehead. A typical ^{1}H spectrum consisted of 64 scans with a relaxation decay of 10 s. This methodology results in a high-resolution NMR spectrum and provides a fingerprint of the samples, i.e. an overview of the metabolites produced by the organism at the time of its collection (Kamio et al., 2016). Chemical shifts were expressed in ppm using TSP as the chemical shift internal reference (0 ppm) on Topspin software (Bruker Biospin). All recorded spectra were analysed with MestReNova 6.0.2 (Mestrelab Research S.L., Spain). ^{1}H NMR spectra were phased and afterwards baseline-corrected using Bernstein polynomials. They were aligned on TSP peak at 0 ppm.

For multivariate analysis, whole spectra were binned into buckets for the chemical shift region from 0.50 ppm to 6.50 ppm and the size of each bin was 0.04 ppm. Once integrated, 110 area values were thus generated for each spectrum for further analysis. After logarithmic transformation, integration bucket data were scaled on whole spectra, i.e

intensity resulted from the spectra integration of the chemical shift region from 0.50 to 4.54 and from 4.98 to 5.50 ppm, excluding H_2O signal. Multivariate correspondence analysis (COA) was performed on the dataset generated. Furthermore, relative concentrations of nitrogenous molecule pool as the ratio of carbonated on nitrogenous molecule pools were calculated as described by Surget et al. (2017) and Bondu et al. (2007).

The identification of the major metabolites detected on spectra was performed and signals assigned to an identified metabolite were integrated. The identification of floridoside, isethionic acid, taurine and alanine was confirmed according to Surget et al. (2017) and literature (Broberg et al., 1998; Gupta et al., 2013; Simon-Colin et al., 2002). Metabolite contents were compared between fragments from the upper layer of cores and silted fragments standardized on the TSP peak. Signals assigned to the identified metabolites were integrated and concentrations, expressed as $mg.g^{-1}$ DW, were calculated by standardization on integral values of TSP signal (9H, t). Indeed, floridoside concentrations were estimated from the integration of anomeric proton (at 5.17 ppm, d), from the mean of integral value of the two CH_2 groups (at 3.13-3.19 and at 3.93-3.98 ppm, t) for isethionic acid concentrations, from the mean of integral value on 2 protons chemical shift of CH_2 (at 3.39-3.46 ppm, t) for the taurine, and finally from the methyl protons (at 1.47 ppm, d) for alanine.

Statistics Statistical analyses were performed with RStudio (v. 0.95.263) for R (v.3.1.3). All analyses were carried out in triplicate and results were expressed as means ± standard deviation (SD). If the data met the requirements for parametric tests, they were analysed using multiple-way or one-way ANOVA (function of the number of factors) at a significance level of 95%, followed by a Tukey post-hoc test. Data were transformed if necessary to respect homoscedasticity. When the data did not meet the requirements for an ANOVA, they were analysed using the two-way Scheirer Ray Hare test (SRH) (Sokal and Rohlf, 1995), the one-way Kruskal–Wallis test (KW) or the Wilcoxon Mann Whitney test (WMW) depending of the number of factors and conditions, at a significance level of 95%, followed by the multiple comparisons test after Kruskal–Wallis (kruskalmc function; pirgmess package).

Results

Biomass and density Our results illustrated the presence of buried fragments of *G. vermiculophylla* at the three sites and throughout the monitoring period (Figures 2 and 3). Silted fragments represented from 15.57 ± 10.16 to 44.43 ± 13.80% (minimum and maximum percentages means between seasons) of the total biomass of *G. vermiculophylla* mat (surface and buried thalli). They were mainly localized in the three first centimeters of the mud (layer L1) with a maximum of 40.09 ± 11.86% and a minimum of 14.69 ± 10.10% of buried algal biomass (percentages means observed in December 2013 and in June 2014 respectively). As it was expected, differences were observed between layers with a decrease in biomass with depth (SRH, p-value < 0.05). But even if much less biomass is measured in deeper layers, algal thalli were observed all throughout the sediment column until 9 to 12 cm depth with 2.66 to 0.72%, 1.99 to 0.01% and 0.55 to 0.02% of total biomass located in layers L1, L2 and L3 respectively. Furthermore, differences between monitoring dates were observed with a decrease in fragment biomass between December 2013 and December 2014 (with sites and layers pooled, SRH p-value < 0.05).

Fragments smaller than 3 cm were also significantly more abundant within silted fragments compared to other size classes and thus whatever the layer and the sampling date (SRH, p-value < 0.05; Figure 3). Density of fragments from layer 1 presented differences among sites (SRH, p-value < 0.05) unlike deeper layers (layers 2 to 4; SRH p-value > 0.05). On the other hand, few fragments shorter than 3 cm were interestingly sampled from 9 to 12 cm depth (layer 4) during the entire monitoring period (Figure 3).

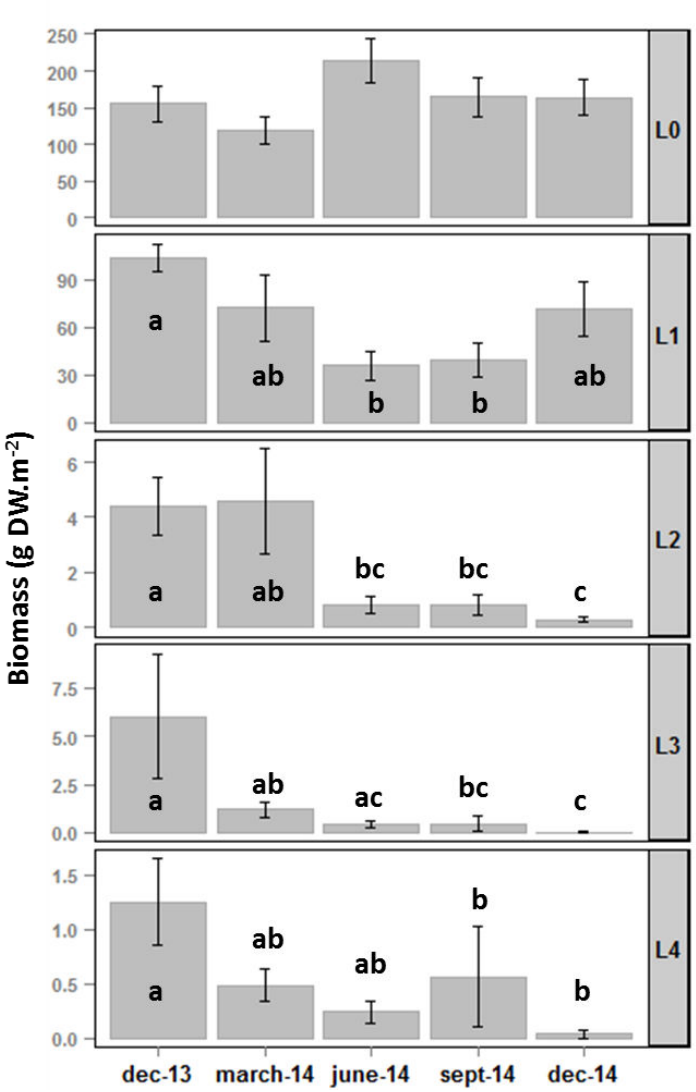

Fig. 2 Biomass (g DW.m^{-2}) variations of *Gracilaria vermiculophylla* fragments according to their depth in sediment (between mud cores layers) from December 2013 to December 2014. Represented results are means ± SD (n = 9). Sites data were pooled as no site effect was detected (SRH, $p > 0.05$). Different letters indicate significant differences between means ($p < 0.05$) according to a Kruskal-Wallis test, followed by non-parametric post-hoc tests. Please note the different scales for the vertical axes. L0: fragments from the surface; L1: fragments from 0 to 3 cm depth; L2: fragments from 3 to 6 cm depth; L3: fragments from 6 to 9 cm depth; L4: fragments from 9 to 12 cm depth.

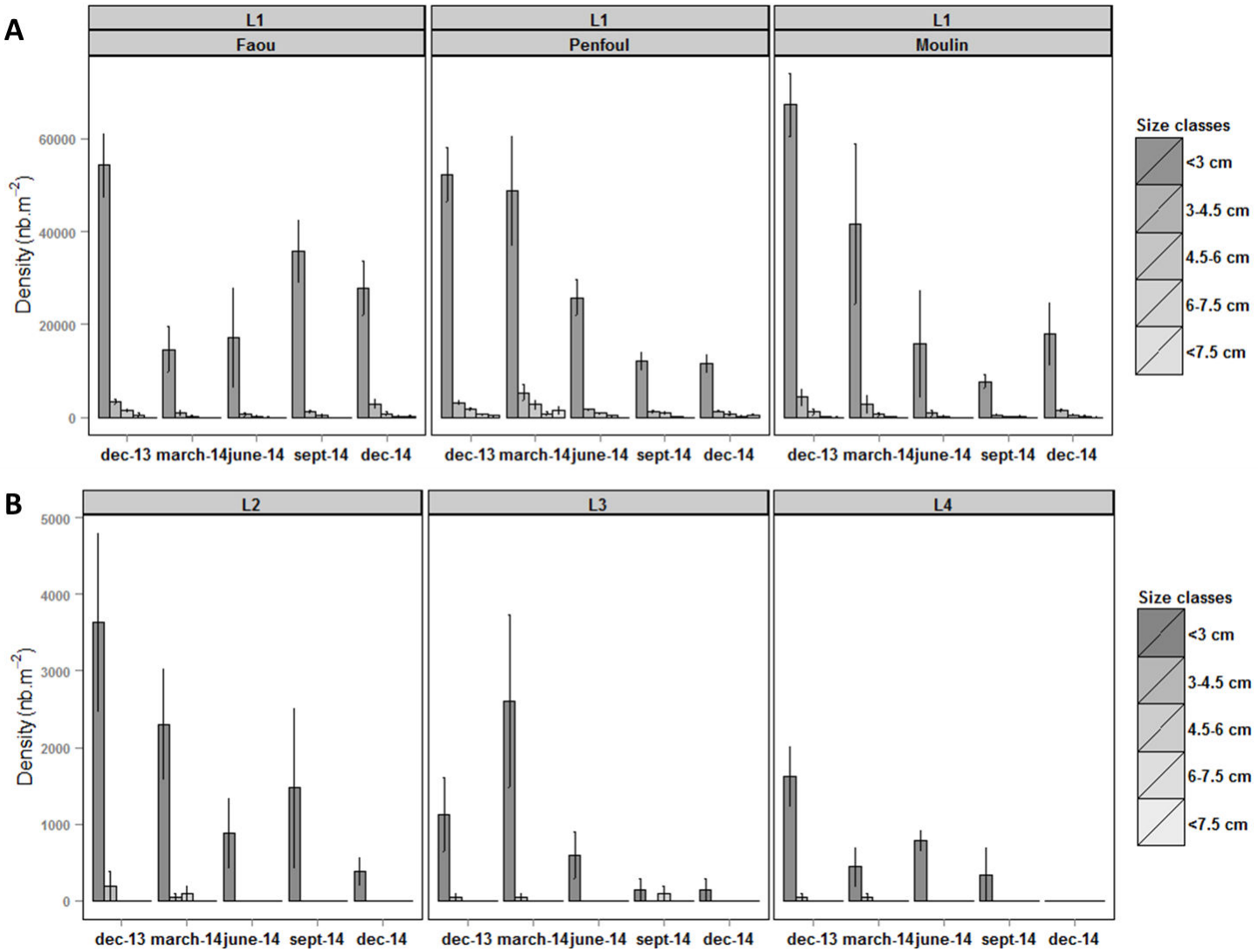

Fig. 3 Fragment density (nb.m^{-2}) variations of the red alga *Gracilaria vermiculophylla* depending on their silting depth (mud layers) and their size classes during the monitoring period, from December 2013 to December 2014. Results are expressed as means ± SD.

A: Density variations of the burial thalli size classes from the layer 1 (from 0 to 3 cm depth) for each site (n = 3) as a significant site effect was detected (SRH, p-value < 0.05).

B: Density variations of fragment size classes from the layers 2 (L1: from 3 to 6 cm depth), 3 (L3: from 6 to 9 cm depth) and 4 (L4: from 9 to 12 cm depth) when sites are pooled (n = 9) as no significant site effect was observed (SRH, p-value > 0.05). Statistics were specified within the text.

Imaging PAM The PAM results referred to Figure 4 and underlined variation of maximum quantum yield (Fv/Fm) measured especially between fragments from different core layers and between seasons of monitoring. Indeed, fragments living at the surface of the mud

(layer 0) exhibited the highest Fv/Fm (0.71 ± 0.05) along the monitoring period and were significantly different from layers 1 and 2-3 with Fv/Fm of 0.62 ± 0.07 and 0.60 ± 0.13, respectively (when seasons were pooled, SRH, p-value < 0.001). Moreover, this global trend was not similar for all sampling dates (when layers were pooled, SRH, p-value = 0.046) as illustrated on Figure 4. Indeed, the ratio Fv/Fm showed even no differences between the layers for two months in March and September 2014 between alga in depth and alga at the surface).

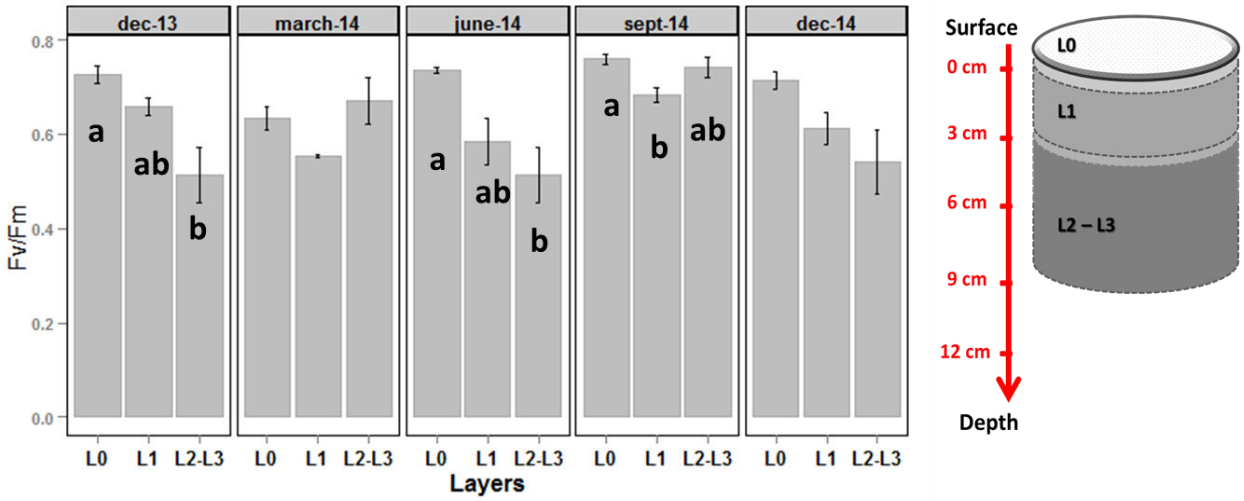

Fig. 4 Fv/Fm or maximum quantum yield of *G. vermiculophylla* fragments function of depth (from layer 0 to layer 3) and seasons (from December 2013 to December 2014). L0: fragments from the surface of the mud; L1: from 0 to 3 cm depth; L2-L3: from 3 to 9 cm depth. Results are expressed as means ± SD (n = 3). Different letters indicate significant differences between means ($p < 0.05$) according to a Kruskal-Wallis test or one-way Anova, followed by the adequate post-hoc tests.

The other photosynthetic parameters were presented in Table 1. Seasonal data were not pooled because a seasonal effect was detected for $rETR_{max}$ parameter (SRH, p-value < 0.05). Indeed, a significantly low $rETR_{max}$ was exhibited in December 2014 for all layers compared to the other sampling dates (KW, p-value < 0.001). On the contrary, the $rETR_{max}$ did not vary between the layers on overall data (KW, p-value = 0.064) indicating similar $rETR_{max}$ between surface algae and buried algae even at 9 cm depth in sediment (see Table 1). On another hand, α and β parameters varied between layers (on the whole data, SRH, p-value=0.038 and KW, p-value = 0.022 respectively). However, a clear pattern was not

exhibited with depth by these photosynthetic parameters since β was significantly different between L1 and L2L3 together to the significant difference detected for α by the two-way non-parametric test (SRH, p-value < 0.05) which was not detected with the multiple non-parametric comparison test after Kruskal-Wallis.

Table 1 Photosynthetic parameters ($rETR_{max}$, α and β) of *Gracilaria vermiculophylla* fragments from different depths (from layer 0 to layer 2-3) and sampled at different dates, from December 2013 to December 2014. Imaging PAM results are means ± SD (n = 3). No significant difference was detected between means of photosynthetic parameters (p < 0.05) according to Kruskal-Wallis test among layers for each season (L0: fragments from surface; L1: from 0 to 3 cm depth; L2L3: from 3 to 9 cm depth).

Sampling date	Layer	α	β	rETRmax
dec-13	L0	0.17 ± 0.02	-	>137.70
	L1	0.16 ± 0.01	3.18 ± 0.28	124.89 ± 12.22
	L2L3	0.20 ± 0.04	4.84 ± 2.22	110.00 ± 25.68
march-14	L0	0.18 ± 0.01	3.87 ± 0.72	113.53 ± 24.54
	L1	0.12 ± 0.02	2.17 ± 0.91	144.75 ± 29.29
	L2L3	0.23 ± 0.10	7.35 ± 2.36	100.76 ± 28.68
june-14	L0	0.20 ± 0.02	4.50 ± 0.83	109.14 ± 10.26
	L1	0.14 ± 0.01	2.52 ± 0.38	141.04 ± 21.38
	L2L3	0.18 ± 0.06	5.53 ± 3.74	95.97 ± 31.28
sept-14	L0	0.20 ± 0.00	3.82 ± 0.19	125.00 ± 8.03
	L1	0.19 ± 0.01	3.62 ± 0.83	130.23 ± 24.87
	L2L3	0.24 ± 0.04	6.73 ± 2.42	90.88 ± 15.44
dec-14	L0	0.22 ± 0.01	13.75 ± 1.81	40.44 ± 4.65
	L1	0.20 ± 0.02	14.56 ± 1.34	33.79 ± 5.50
	L2L3	0.10 ± 0.12	15.80 ± 7.40	8.05 ± 13.95

Respiration rate All analyzed samples showed a respiration activity. However, *G. vermiculophylla* fragments distributed at the surface of the mud presented a significantly higher respiration rate measured as CO_2 flux than buried fragments (48.71 ± 13.85 and 8.55 ± 5.50 µmol $CO_2.h^{-1}.g^{-1}$ FW, respectively; T-test, p-value = 0.037).

Pigment contents (by HPLC) Surface versus buried thalli pigment contents were described in Table 2. A significant variation in pigment content was observed with depth except for violaxanthin and R-phycoerythrin. The other pigments from the xanthophyll cycle increased

in silted fragments with antheraxanthin levels multiplied by 3.3 (WMW, p-value = 0.005) and zeaxanthin increasing by one-third (WMW, p-value = 0.040). With burial, results illustrated an enrichment in chl-a (contents multiplied by around 2, WMW, p-value = 0.003) as in β-carotene (WMW, p-value = 0.024) in *G. vermiculophylla* fragments and a decrease in xanthophylls/chl-a ratio (WMW, p-value < 0.001). A decrease in R-phycocyanin was also observed with depth (WMW, p-value = 0.003).

Table 2 Concentrations of pigment (expressed as $\mu g.mg^{-1}$ FW or $mg.g^{-1}$ FW) depending on the depth of *G. vermiculophylla* fragments (at the surface of the mud or within the mud). Values are means ± SD (n = 9). Different letters indicate significant differences between means (p < 0.05) according to Wilcoxon Mann-Whitney test.

Fragment condition	violaxanthin ($\mu g.g^{-1}$ FW)	antheraxanthin ($\mu g.g^{-1}$ FW)	zeaxanthin ($\mu g.g^{-1}$ FW)	deepoxidation level
surface	0.22 ± 0.17	0.34 ± 0.28[a]	30.45 ± 5.82[a]	0.99 ± 0.01
silted	0.13 ± 0.09	1.12 ± 0.58[b]	40.16 ± 10.23[b]	1.00 ± 0.00

Fragment condition	chla ($\mu g.g^{-1}$ FW)	ratio xanthophylls/chla	β-carotene ($\mu g.g^{-1}$ FW)	R-phycoerythrin ($mg.g^{-1}$ FW)	R-phycocyanin ($mg.g^{-1}$ FW)
surface	164.47 ± 26.10[a]	0.19 ± 0.01[a]	10.99 ± 2.33[a]	0.61 ± 0.06	0.21 ± 0.02[a]
silted	323.76 ± 108.50[b]	0.13 ± 0.02[b]	18.26 ± 5.97[b]	0.58 ± 0.14	0.17 ± 0.03[b]

Algal major metabolites identification and quantification (by ^{1}H qNMR)

A Component Ordinate Analysis (COA) was conducted on data generated by the integration of bins on spectra since dataset represented relative area ratios. COA analyses exhibited a clear pattern of differentiation on axis 1 depending on the burial of *G. vermiculophylla* and allowed to discriminate buckets that contributed to this differentiation (Figure 5). The axis 1 explained 37.5% of data variability and the axis 2 19.1%. The main bins which contribute to the axis 1 were mainly buckets between 0.5 and 3 ppm, corresponding to chemical shift protein as amino acid range in case of D_20 extracts (Figure

5a). MANOVA analyses (conducted on COA coordinates) confirmed the significant difference between conditions, observed visually on COA (Figure 5b). Buckets presented the highest contribution to the axis 1 were reported on superimposed spectra of silted and surface fragments (Figure 6) with the aim to identify peaks discriminating the two conditions. Moreover, examples of spectra were chosen function of COA results with the aim to illustrate the more revealing spectra of silted and surface conditions (Figure 6). These buckets may correspond to a major peak on spectra. They also exhibited biomarkers of silted and surface conditions. In this way, major peaks were assigned to an identified metabolite (i.e alanine, isethionic acid, taurine and floridoside, Figure 6). Estimated concentrations confirmed results obtained by COA with a significant variation of nitrogenous molecule pool between 0.5 and 3 ppm and especially of the amino acid alanine (at 1.47 ppm) that increased 3 times in silted fragments (Table 3). Furthermore, some buckets corresponded partly to the floridoside signal and effectively, estimated concentrations of this metabolite decreased with the burial state of *G. vermiculophylla* fragments (T-test, T = -3.03, p-value = 0.007; Table 3). As a result, the C/N ratio exhibited higher value in fragments from the surface of the mud than buried ones. On another hand, isethionic acid and taurine showed no significant variation with the burial state of fragment (T-test T = -1.58 and T = -0.51 with p-value = 0.13 and p-value = 0.61 respectively) as expected by COA.

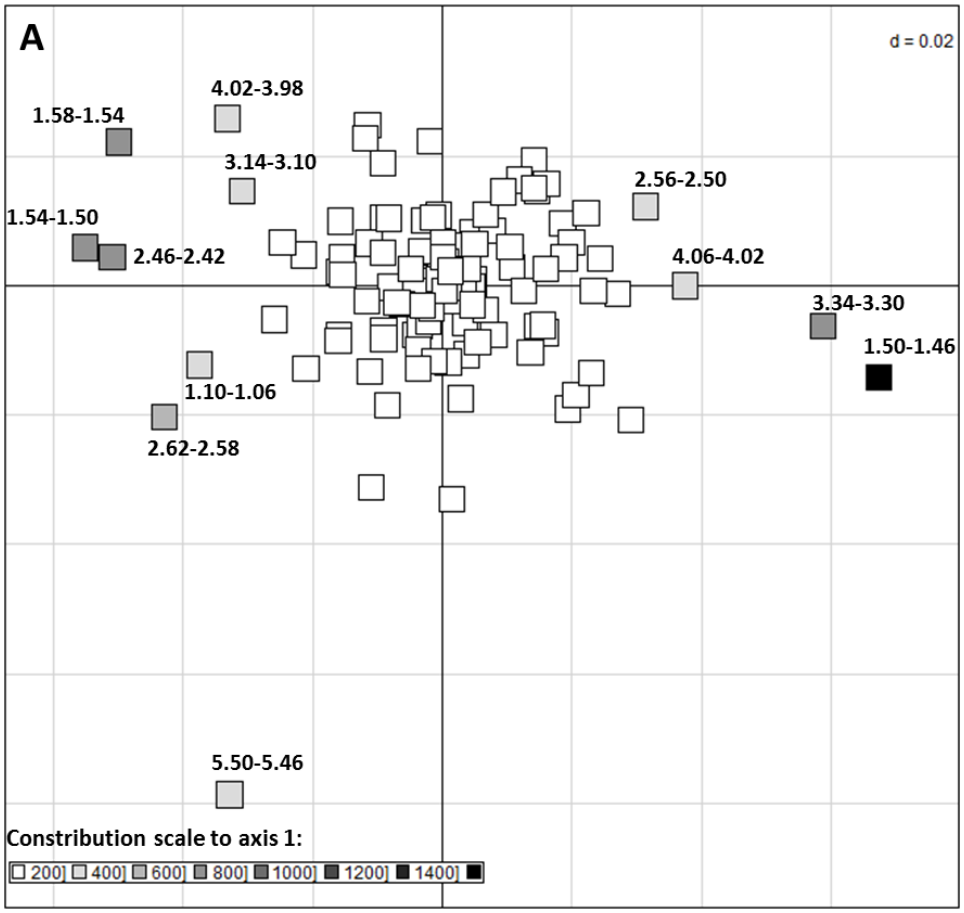
A
d = 0.02
4.02-3.98
1.58-1.54
3.14-3.10
2.56-2.50
1.54-1.50
2.46-2.42
4.06-4.02
3.34-3.30
1.50-1.46
1.10-1.06
2.62-2.58
5.50-5.46
Constribution scale to axis 1:
200] 400] 600] 800] 1000] 1200] 1400]

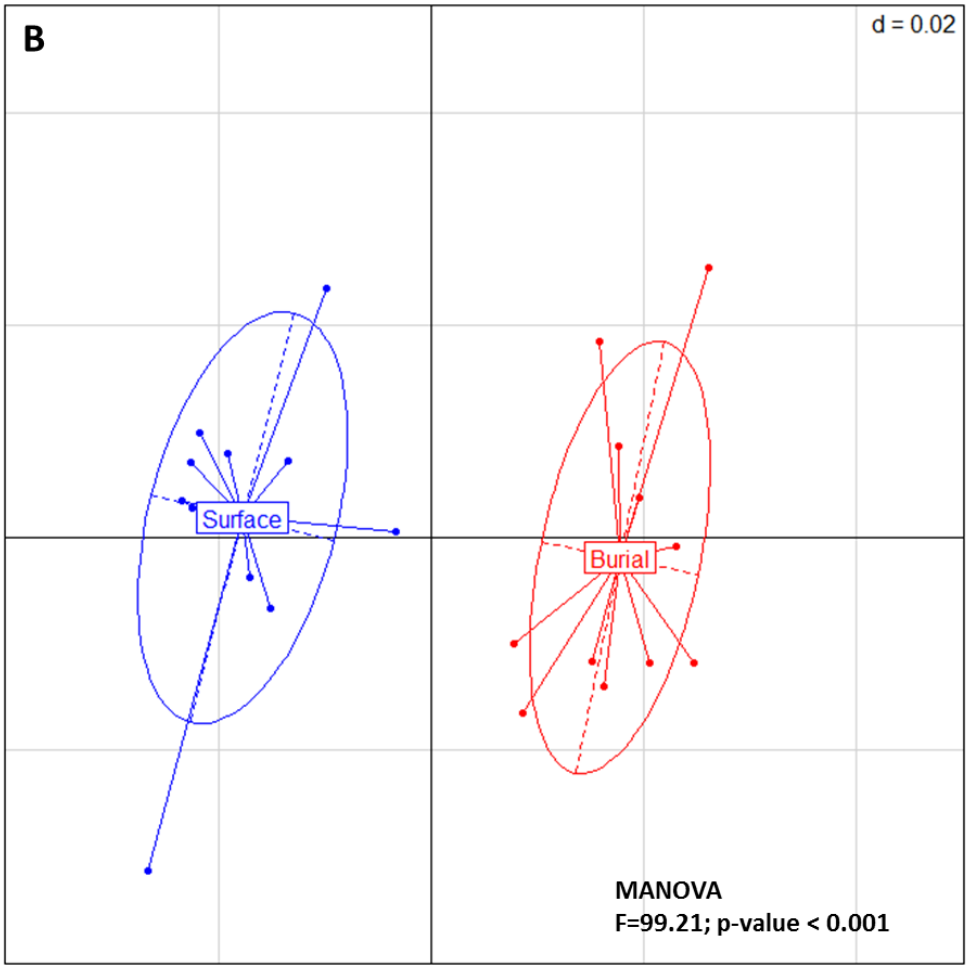
B
d = 0.02
Surface
Burial
MANOVA
F=99.21; p-value < 0.001

Fig. 5 Component ordinate Analyses (COA) of integrated bins on *G. vermiculophylla* spectra depending on the burial of algal fragments. **A**: COA correlation plot of 110 integrated bins. Each square represented a bin and the square color intensity was linked to the variable contribution on axis 1. The chemical shift range of bins that contributed more than 4% to the axis 1 (colored in grey) was noticed. **B**: COA score plot of individuals depending of the burial of algal fragments. Ellipses with a confidence level of 99% were drawn around considered factor, ie. fragment condition (surface versus burial).

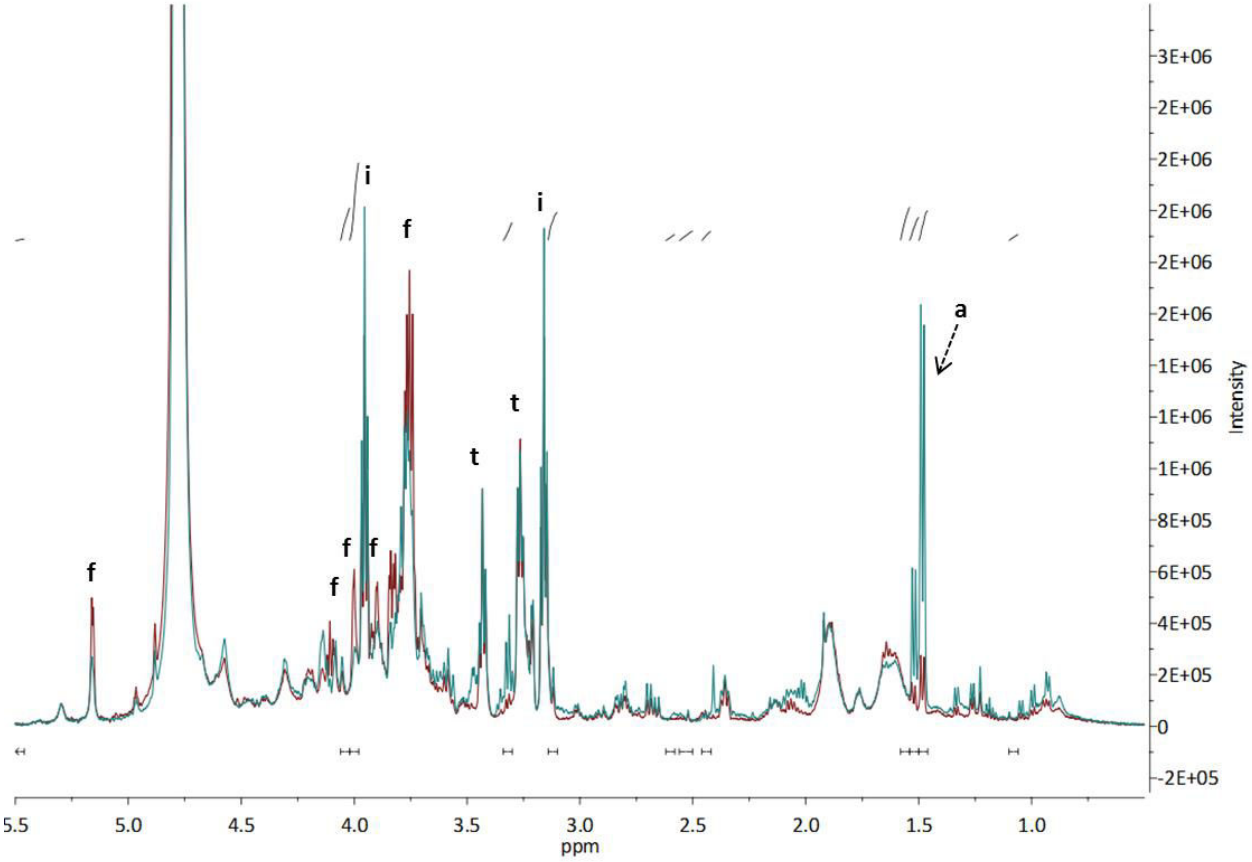

Fig. 6 Superimposed ^{1}H NMR spectra of D_2O extracts of a silted fragment (in blue-green) and a fragment living at the surface of the mud (in dark red) of *Gracilaria vermiculophylla*. Black segments under spectra lines represented bins that mainly contributed to the axis 1 of COA, colored in grey more or less intense on the Fig. 4a. Bold letters indicate the identified metabolite corresponding to the spectral signal(s) with i for isethionic acid, t for taurine, f for floridoside and a for alanine.

Table 3 Metabolite concentrations (expressed as $mg.g^{-1}$ DW) depending on the location of *G. vermiculophylla* fragments (silted or at the surface of the mud), whatever the sampling date. Nitrogenous pool was represented as relative concentration (expressed in %). Values are means ± SD (n = 11). Different letters indicate significant differences between means (p-value < 0.05) according to Wilcoxon Mann-Whitney test or T-test.

	Surface fragments	Silted fragments
Taurine	104.43 ± 16.24	104.28 ± 13.25
Floridoside	217.36 ± 61.86[a]	147.87 ± 47.74[b]
Isethionic acid	142.38 ± 13.34	135.23 ± 18.52
Alanine	14.40 ± 2.72[a]	48.30 ± 11.15[b]
N pool	28.08 ± 4.82[a]	32.38 ± 5.36[b]
C/N ratio	1.23 ± 0.42[a]	0.86 ± 0.30[b]

Discussion

This study highlighted the recurring capacity of *Gracilaria vermiculophylla* fragments to live in sediment at down to 12 cm in depth in the mud in rias from Brittany. The occurrence of *G. vermiculophylla* fragments in depth illustrated the perennial colonization of this macroalga in the studied rias of the Bay of Brest. These rias allowed a relative stability of *G. vermiculophylla* mat (Surget, pers. obs) and thus the establishment of a thick algal mat exhibiting a specific phenology in the Bay of Brest compared to other invasive locations on worldwide (Surget et al., 2017). Indeed, tidal current in Faou as well as in Penfoul and Moulin rias did not exceed 1.2 $m.s^{-1}$ at its maximal intensity during spring tides, estimated for a tidal coefficient of 95 as demonstrated by Guérin (2004). These velocities are the lowest tidal currents exhibiting in the Bay of Brest, characterizing these shallow sheltered estuaries. The partially burial of *G. vermiculophylla* in sediment was also observed in Horsens Fjord (Thomsen et al., 2007). Its burial tolerance was tested *in situ* by artificially burying thalli under 2 to 3 cm of sandy sediment at a mid-lagoon mudflat in the Hog Island Bay, in Virginia (Thomsen and McGlathery, 2007). This invasive macroalga exhibited a slower decomposition rate than two green macroalgae, *Ulva curvata* and *Codium fragile*, with a half-life of 9 days in

this lagoon. It was reported that even after a burial of several weeks, remaining fragments appeared structurally intact and healthy, joining our field observations. Thereby, due to the tolerance of *G. vermiculophylla* to burial, it was expected that important silted biomasses could be observed, as in our study where this buried biomass represented one third of the whole biomass algal mat. This biomass was highly fragmented and mainly composed of small fragments (< 3 cm). This occurrence in depth in the sediment of *G. vermiculophylla* thalli as the significant buried biomasses it represented have to be take into account in the invasive potential of this non-native species.

In rias of the Bay of Brest, the observed algal burial life could not be only explained through mud deposition. This sedimentation phenomenon known to be important in protected rias may contribute to the burial of *G. vermiculophylla* thalli but not explained the occurrence of fragment at down to 9 to 12 cm in depth in sediment. Indeed, sedimentation rates from 0 to 1 $cm.y^{-1}$ were observed on the bare mud of Penfoul ria in 2004 (Fichaut et al., 2004). The specific morphology of this alga may facilitate a self-silting process as known for *Spartina alterniflora* (Querné et al., 2012). Effectively, higher rates could be encountered on areas colonized by the invasive seagrass *Spartina alterniflora* with rates varying between 0.5 and 2 $cm.y^{-1}$ during the same year (Fichaut et al., 2004).

The presence of *G. vermiculophylla* and its high fragmentation in depth could have several origins. Interestingly, it was shown that the colonization of mud by this invasive species leads to an increase in macrofauna densities and especially a higher abundance of the annelid *Nereis diversicolor* (Davoult et al., *in prep.*, Le Guillou, 2012). Thus, these high macrofauna densities may induce bioturbation of the mud and could enhance the fragmentation together with the fragment burial of *G. vermiculophylla*. Thomsen et al. (2007) reported that the grazer *Littorina littorea* induced both a decrease in the algal biomass as well as an increase in the fragmentation rate of *G. vermiculophylla* thalli. The mechanical burial of macroalgae in soft sediment linked to the bioturbation of polychaetes was reported in the literature for shallow coastal environments (Daly, 1973; Hylleberg, 1975; Nordström et al., 2006) such as deep-sea ones (Reichardt, 1987). Rossi et al. (2013) demonstrated that levels of macroalgal detritus in sandy sediments were six times greater in the presence of the lugworm, *Arenicola marina*. These authors supposed that this species

mechanically buried macroalgal fragments in their funnels, inducing an increase in half-time decomposition rate of the algae within the sediment (Rossi et al., 2013). Furthermore, the irrigation of burrow generated by *Nereis diversicolor* bioturbation and the induced sediment oxygenation influenced the decomposition rate of buried macroalgal fragments such as the brown seaweed *Fucus serratus*. As limited irrigated burrow induced a perennial burial, most of macroalgal fragments may thereby remain intact in the sediment (Kristensen and Mikkelsen, 2003). Indeed, bioturbation could explain the presence of some fragments in depth within the mud and could enhance the thallus fragmentation as suggested by Surget et al. (2017). One should also hypothesize the potentiality of *G. vermiculophylla* to resist to bacterial degradation in producing antifouling molecules, and then controlling its epibionts community, as it was demonstrated in North European populations(Denmark, Germany) of this species (Saha et al., 2016; Wang et al., 2017) and which could represent a key feature of the invasive potential of *G. vermiculophylla*.

Additionally, several studies illustrated the low palatability of *G. vermiculophylla* compared to other native macroalgae as it was demonstrated in *Ulva lactuca* (Jensen et al. 2007, in Hu and Juan, 2013). Currently, Ulva species were not developed luxuriantly on muddy bottom of lower rias in the Bay of Brest and *G. vermiculophylla* is the dominant macrophyte of this ria with the invasive halophyte *Spartina alterniflora* (Surget et al., 2017). It was shown that this species could produce defense compounds, i.e oxilipins, acting as chemical feeding deterrents (Nylund et al., 2011; Rempt et al., 2012). This synthesis was induced by mechanical or grazing wounding. Hamman et al. (2013) underlined the capabilities of *G. vermiculophylla* to produce defense compounds by the up-regulation of feeding deterrents explaining the difference of palatability between its native and invasive populations. On another hand, herbivores are known to prefer feeding nitrogen-enriched macrophytes with low C:N ratio since additive N may elicit their fitness (Mattson, 1980) as reported for the snail *Littorina sitkeana* (Van Alstyne et al., 2009) and the amphipod *Gammarus locusta* (Kraufvelin et al., 2006), this latter genus being part of benthic macrofauna in Faou ria (Davoult et al., *in prep.*). In the present study, burial fragments presented lower C:N ratio (based on NMR spectra integration) than thalli present at the surface of the mud. Indeed, it may contribute to a high thalli wounding by macrofauna under burial conditions. However, this hypothesis did not always explain differential feeding

patterns and the production of chemical deterrent could also be determinant (Hammann et al., 2013). Therefore, we hypothesized that the wounding of thalli by grazers accelerated the fragmentation of *G. vermiculophylla* at the surface, facilitating the bioturbation force driving, and then resulting in the fragment burial of few centimeters in the mud.

The buried *G. vermiculophylla* thalli was indeed appeared not degraded as we showed by the different quantitative methods used in our study, *i.e.* Imaging PAM, measurement of respiration rate and pigments contents. Thus, we hypothesize that *G. vermiculophylla* are physiologically active as it maintained its physiology and resist to degradation after burial. Therefore, fragments observed within the mud were potentially still living and not consisted solely of detrital organic matter. After resuspension and exposition to oxygen, buried fragment thalli presented functional photosystems II (exhibited by Imaging PAM results), indicating the physiological ability of *G. vermiculophylla* to tolerate burial in muddy sediments. Positive respiration levels confirmed this hypothesis. However, after burial the exposure to oxygenic conditions may induce a transport of oxygen-dependent electron as it was supposed for cyanobacteria in stromatolites, prior to an induction of photosynthetic electron transport (Perkins et al., 2007). This electron transport could be due to Mehler reactions (water-water cycle), preventing an oxidative stress and limiting photoinhibition under light exposure (Asada, 2000). Therefore, water-water cycle may induce an activation of electron transport within photosystems and may restore modulated fluorescence after prolonged burial as it was demonstrated in stromatolite communities after sandy burial (Perkins et al., 2007). These last authors thus demonstrated the ability of cyanobacteria to activate and inactivate their photosynthetic processes to tolerate burial during several months (Perkins et al., 2007). Our present results thereby demonstrated *a minima* the activation of electron transport in photosystems I and II (linked to Mehler reactions) even if the activation of the photosynthesis cannot be confirmed. Further analysis, after exposition of silted fragment to several low light conditions would be necessary to corroborate this hypothesis. However, our results showed a reduction of only 13% of the photosynthetic efficiency with the burial, which demonstrate that alga was reactive to light after resuspension and exposure to light. Likewise, we showed that the variations of the other photosynthetic parameters ($rETR_{max}$, α and β) seemed not being correlated with the burial and underlined the high physiological resistance of *G. vermiculophylla* to these

conditions. The slower respiration flux of buried fragments after resuspension in seawater illustrated the reduction of metabolic pathways induced by a burial life, suggesting a "dormancy" state of *G. vermiculophylla* within the mud. The physiology of this "dormancy" state was not investigated on previous studies that reported a resistance of macroalgae to burial (Glasby et al., 2005; Kamermans et al., 1998; Kawamata et al., 2012). These studies were mainly focused on the recovery of growth abilities of buried individuals after a return to favorable conditions. Interestingly, these buried fragments could represent a seedling bank, analogous to seed banks of terrestrial plants as it has already been described in a wide range of seaweeds genera: *Codium* (Vidondo and Duarte, 1998), *Fucus* (Creed et al., 1996), *Turbinaria* (Stiger and Payri, 2005) and interestingly *Gelidium* and *Gracilaria* (in Hoffmann and Santelices, 1991).

Furthermore, the results exhibited the metabolite content variations of *G. vermiculophylla* fragments to burial condition. Interestingly, C:N ratio decreased in fragments distributed in depth into the mud, due to the increase in nitrogenous pool relative concentration, illustrating an increase in protein contents such as alanine, together with the decrease in floridoside level. Simon-Colin et al. (2004) demonstrated the high carbon photoassimilation during floridoside biosynthesis under low salinities (*i.e.* hypoosmotic conditions) in another red macroalga *Grateloupia turuturu*. Moreover, Ekman et al. (1991) studied the chemical composition of *Gracilaria sordida* under darkness with nutrient supplementation and observed the decline of C:N ratio as well as of the concentration of floridoside under darkness and this decline was accentuated with nutrient supply. As photosynthesis was not possible for silted fragments, the decrease in floridoside content may be due to the fact that this osmolyte consists in being carbon reserve for the algal cell metabolism (Collén et al., 2004) and this C pool may be recycled within the alga for biosynthesis needs as suggested for *Solieria chordalis* (Bondu et al., 2007). Furthermore, Tyler et al. (2005) reported the ability of *G. vermiculophylla* to uptake both urea and amino acids such as glycine under darkness conditions. In this way, nitrogenous molecules, mainly amino acids as alanine, increased in our red algal species to possibly maintain cell osmotic equilibrium and to compensate the decrease in the organic solute floridoside as it was already demonstrated in the red genera *Gelidium* and *Bangia* (Macler, 1986; Reed, 1985). Finally, pigment concentrations could be explained by the conjunction of two

complementary physiological phenomena: (1) an adaptation to the darkness to optimize the photon capture by antennae as photosystem II and/or (2) the lack of growth of burial fragments compared to those living at the surface of the mud. Indeed, the growth of thalli at the surface could induce a dilution of intracellular metabolites like pigments. However, samples were gathered in September and an increase in biomass mat of *G. vermiculophylla* was observed in June 2014 on this site (Surget et al., 2017) suggesting a growth of this alga in spring in Brittany as observed in its native range (Muangmai et al., 2014). Moreover, our study demonstrated an increase in chl-a with the burial life of *G. vermiculophylla* together with a decrease in R-phycocyanin. Macler et al. (1986) observed also some changes in the pigmentation of red algae and noticed an increase in phycobiliprotein and chlorophyll levels under darkness conditions in nitrogen enriched algae as *Gelidium coulteri*.

In conclusion, the results of the present study provided experimental evidence that *G. vermiculophylla* was perennially present within muddy sediments in the rias of Brest and potentially in other invaded muddy flat. Furthermore, these quantitative data illustrated the living state and the acclimation of *G. vermiculophylla* to burial. Potentially the dissemination of the buried biomass composed of small fragments present in the mud compared to longer fragments developed at the surface, could considerably enhance the propagation potential of *G. vermiculophylla* in the case of resuspension of the algal mat due to anthropic perturbations or climatic events like storms. The algal development by vegetative reproduction was not dependent of the fragment size as it was reported that fragments of 1 mm survived and could developed to generate new thalli (Nyberg and Wallentinus, 2009). Thereby, buried fragments could represent a reserve biomass of small fragments, *i.e*. a seedling bank as terrestrial seed bank, easily disseminated and may contribute significantly to the propagative abilities of *G. vermiculophylla* at a local scale, especially in the Bay of Brest. Moreover, the burial resistance of *G. vermiculophylla* may also contribute to its transoceanic migration and establishment through sediment transports.

Acknowledgments This study is part of a PhD project carried out by the first author at the Laboratoire des Sciences de l'Environnement Marin (LEMAR UMR6539) in the IUEM (UBO-UEB), under the supervision of the last author. It was supported by the *Ministère de l'Education Nationale, de l'Enseignement Supérieur et de la Recherche* (UBO funding for the first author) and *Région Bretagne* (ARED Labex Mer). This study was co-financed with the support of the European Union ERDF – Atlantic Area Program and French ANR and is related to the research project INVASIVES (Era-net Seas-era. 2012–2016). Authors thank Joy Versterren for their fruitful assistance for the sampling and samples analyses.

References

Abreu, M.H., Pereira, R., Sousa-Pinto, I., Yarish, C., 2011. Ecophysiological studies of the non-indigenous species *Gracilaria vermiculophylla* (Rhodophyta) and its abundance patterns in Ria de Aveiro lagoon, Portugal. Eur. J. Phycol. 46, 453–464.

Asada, K., 2000. The water–water cycle as alternative photon and electron sinks. Philos. Trans. R. Soc. B Biol. Sci. 355, 1419–1431.

Bondu, S., Kervarec, N., Deslandes, E., Pichon, R., 2007. The use of HRMAS NMR spectroscopy to study the in vivo intra–cellular carbon/nitrogen ratio of *Solieria chordalis* (Rhodophyta). J. Appl. Phycol. 20, 673–679.

Broberg, A., Kenne, L., Pedersén, M., 1998. In-situ identification of major metabolites in the red alga *Gracilariopsis lemaneiformis* using high-resolution magic angle spinning nuclear magnetic resonance spectroscopy. Planta 206, 300–307.

Byers, J.E., Gribben, P.E., Yeager, C., Sotka, E.E., 2012. Impacts of an abundant introduced ecosystem engineer within mudflats of the southeastern US coast. Biol. Invasions 14, 2587–2600.

Collén, P.N., Camitz, A., Hancock, R.D., Viola, R., Pedersén, M., 2004. Effect of nutrient deprivation and resupply on metabolites and enzymes related to carbon allocation in *Gracilaria tenuistipitata* (rhodophyta)1. J. Phycol. 40, 305–314.

Creed, J.C., Norton, T.A., Harding, S.P., 1996. The development of size structure in a young *Fucus serratus* population. Eur. J. Phycol. 31, 203–209.

Daly, J.M., 1973. Behavioural and Secretory Activity during Tube construction by *Platynereis dumerilii* Aud & M. Edw. [Polychaeta: Nereidae]. J. Mar. Biol. Assoc. U. K. 53, 521–529.

Davoult, D., Surget, G., Stiger-Pouvreau, V., Noisette, F., Riera, P., Stagnol, D., Androuin, T., & Poupart, N., (in prep.) Effects of *Gracilaria vermiculophylla* invasion on estuarine-mudflat functioning and diversity.

Dumay, J., Clément, N., Morançais, M., Fleurence, J., 2013. Optimization of hydrolysis conditions of *Palmaria palmata* to enhance R-phycoerythrin extraction. Bioresour. Technol. 131, 21–27.

Ekman, P., Yu, S., Pedersen, M., 1991. Effects of altered salinity, darkness and algal nutrient status on floridoside and starch content, α-galactosidase activity and agar yield of cultivated *Gracilaria sordida*. Br. Phycol. J. 26, 123–131.

Fichaut, B., Sparfel, L., Suanez, S., 2004. Rapport d'étude sur la progression de la spartine (*Spartina alterniflora*) et dynamique sédimentaire en rade de Brest. Sites de Pont-Callec, du Pédel et de Mengleuz.

Genty, B., Briantais, J.-M., Baker, N.R., 1989. The relationship between the quantum yield of photosynthetic electron transport and quenching of chlorophyll fluorescence. Biochim. Biophys. Acta BBA - Gen. Subj. 990, 87–92.

Gevaert, F., Creach, A., Davoult, D., Migne, A., Levavasseur, G., Arzel, P., Holl, A., Lemoine, Y., 2003. *Laminaria saccharina* photosynthesis measured in situ: photoinhibition and xanthophyll cycle during a tidal cycle. Mar. Ecol. Prog. Ser. 247, 43–50.

Glasby, T.M., Gibson, P.T., Kay, S., 2005. Tolerance of the invasive marine alga *Caulerpa taxifolia* to burial by sediment. Aquat. Bot. 82, 71–81.

Guérin, L., 2004. La crépidule en rade de Brest: un modèle biologique d'espèce introduite proliférante en réponse aux fluctuations de l'environnement. Université de Bretagne occidentale - Brest.

Guillemin, M.-L., Akki, S.A., Givernaud, T., Mouradi, A., Valero, M., Destombe, C., 2008. Molecular characterisation and development of rapid molecular methods to identify species of Gracilariaceae from the Atlantic coast of Morocco. Aquat. Bot. 89, 324–330.

Gupta, V., Thakur, R.S., Reddy, C.R.K., Jha, B., 2013. Central metabolic processes of marine macrophytic algae revealed from NMR based metabolome analysis. RSC Adv. 3, 7037–7047.

Hammann, M., Wang, G., Rickert, E., Boo, S.M., Weinberger, F., 2013. Invasion success of the seaweed *Gracilaria vermiculophylla* correlates with low palatibility. Mar. Ecol. Prog. Ser. 486, 93–103.

Hoffmann, A.J., Santelices, B., 1991. Banks of algal microscopic forms: Hypotheses on their functioning and comparisons with seed banks. Mar. Ecol. Prog. Ser. Oldendorf 79, 185–194.

Hu, Z.-M., Juan, L.-B., 2013. Adaptation mechanisms and ecological consequences of seaweed invasions: a review case of agarophyte *Gracilaria vermiculophylla*. Biol. Invasions 16, 967–976.

Hylleberg, J., 1975. Selective feeding by *Abarenicola pacifica* with notes on *Abarenicola vagabunda* and a concept of gardening in lugworms. Ophelia 14, 113–137.

Jensen AT, Uldahl AG, Sjogren KP, Khan M (2007) The invasive macroalgae *Gracilaria vermiculophylla* - effects of salinity, nitrogen availability, irradiance and grazing on the growth rate. Master thesis, Department of Environmental, Social and Spatial Change, Roskilde University, Denmark.

Johnston, C.A., Lipcius, R.N., 2012. Exotic macroalga *Gracilaria vermiculophylla* provides superior nursery habitat for native blue crab in Chesapeake Bay. Mar. Ecol. Prog. Ser. 467, 137–146.

Kamermans, P., Malta, E., Verschuure, J.M., Lentz, L.F., Schrijvers, L., 1998. Role of cold resistance and burial for winter survival and spring initiation of an *Ulva spp.* (Chlorophyta) bloom in a eutrophic lagoon (Veerse Meer lagoon, The Netherlands). Mar. Biol. 131, 45–51.

Kamio, M., Koyama, M., Hayashihara, N., Hiei, K., Uchida, H., Watanabe, R., Suzuki, T., Nagai, H., 2016. Sequestration of dimethylsulfoniopropionate (DMSP) and acrylate from the green alga *Ulva spp.* by the sea hare *Aplysia juliana*. J. Chem. Ecol. 42, 452–460.

Kawamata, S., Yoshimitsu, S., Tokunaga, S., Kubo, S., Tanaka, T., 2012. Sediment tolerance of *Sargassum* algae inhabiting sediment-covered rocky reefs. Mar. Biol. 159, 723–733.

Kim, S.Y., Weinberger, F., Boo, S.M., 2010. Genetic data hint at a common donor region for invasive atlantic and pacific populations of *Gracilaria vermiculophylla* (gracilariales, Rhodophyta)1. J. Phycol. 46, 1346–1349.

Kraufvelin, P., Salovius, S., Christie, H., Moy, F.E., Karez, R., Pedersen, M.F., 2006. Eutrophication-induced changes in benthic algae affect the behaviour and fitness of the marine amphipod *Gammarus locusta*. Aquat. Bot. 84, 199–209.

Kristensen, E., Mikkelsen, O.L., 2003. Impact of the burrow-dwelling polychaete *Nereis diversicolor* on the degradation of fresh and aged macroalgal detritus in a coastal marine sediment. Mar. Ecol. Prog. Ser. 265, 141–153.

Le Guillou E. (2012) Effets d'espèces invasives sur les peuplements de faune benthiques des milieux estuaires : cas de l'algue rouge *Gracilaria vermiculophylla.* Manuscrit de stage M1 SML SBM, UBO. 20p.

Macler, B.A., 1986. Regulation of carbon flow by nitrogen and light in the red alga, *Gelidium coulteri*. Plant Physiol. 82, 136–141.

Martínez-Lüscher, J., Holmer, M., 2010. Potential effects of the invasive species *Gracilaria vermiculophylla* on *Zostera marina* metabolism and survival. Mar. Environ. Res. 69, 345–349.

Mattson, W.J.J., 1980. Herbivory in relation to plant nitrogen content. Annu. Rev. Ecol. Syst. 11, 119–161.

Muangmai, N., Vo, T.D., Kawaguchi, S., 2014. Seasonal fluctuation in a marine red alga, *Gracilaria vermiculophylla* (Gracilariales, Rhodophyta), from Nokonoshima Island, Southern Japan. J Fac Agric. Kyushu Univ 59, 243–248.

Munier, M., Jubeau, S., Wijaya, A., Morançais, M., Dumay, J., Marchal, L., Jaouen, P., Fleurence, J., 2014. Physicochemical factors affecting the stability of two pigments: R-phycoerythrin of *Grateloupia turuturu* and B-phycoerythrin of *Porphyridium cruentum*. Food Chem. 150, 400–407.

Nettleton, J.C., Mathieson, A.C., Thornber, C., Neefus, C.D., Yarish, C., 2013. Introduction of *Gracilaria vermiculophylla* (Rhodophyta, Gracilariales) to New England, USA: Estimated Arrival Times and Current Distribution. Rhodora 115, 28–41.

Nitschke, U., Connan, S., Stengel, D.B., 2012. Chlorophyll a fluorescence responses of temperate Phaeophyceae under submersion and emersion regimes: a comparison of rapid and steady-state light curves. Photosynth. Res. 114, 29–42.

Nordström, M., Bonsdorff, E., Salovius, S., 2006. The impact of infauna (*Nereis diversicolor* and *Saduria entomon*) on the redistribution and biomass of macroalgae on marine soft bottoms. J. Exp. Mar. Biol. Ecol. 333, 58–70.

Nyberg, C.D., 2007. Introduced marine macroalgae and habitat modifiers : their ecological role and significant attributes.

Nyberg, C.D., Wallentinus, I., 2009. Long-term survival of an introduced red alga in adverse conditions. Mar. Biol. Res. 5, 304–308.

Nylund, G.M., Weinberger, F., Rempt, M., Pohnert, G., 2011. Metabolomic assessment of induced and activated chemical defence in the invasive red alga *Gracilaria vermiculophylla*. PLOS ONE 6, e29359.

Perkins, R.G., Kromkamp, J.C., Reid, R.P., 2007. Importance of light and oxygen for photochemical reactivation in photosynthetic stromatolite communities after natural sand burial. Mar. Ecol. Prog. Ser. 349, 23–32.

Platt, T., Gallegos, C.L., 1980. Modelling Primary Production, in: Falkowski, P.G. (Ed.), Primary Productivity in the Sea, Environmental Science Research. Springer US, pp. 339–362.

Querné, J., Ragueneau, O., Poupart, N., 2012. In situ biogenic silica variations in the invasive salt marsh plant, *Spartina alterniflora*: A possible link with environmental stress. Plant Soil 352, 157–171.

Reed, R.H., 1985. Osmoacclimation in *Bangia atropurpurea* (Rhodophyta, Bangiales): the osmotic role of floridoside. Br. Phycol. J. 20, 211–218.

Reichardt, W.T., 1987. Burial of Antarctic macroalgal debris in bioturbated deep-sea sediments. Deep Sea Res. Part Oceanogr. Res. Pap. 34, 1761–1770.

Rempt, M., Weinberger, F., Grosser, K., Pohnert, G., 2012. Conserved and species-specific oxylipin pathways in the wound-activated chemical defense of the noninvasive red alga *Gracilaria chilensis* and the invasive *Gracilaria vermiculophylla*. Beilstein J. Org. Chem. 8, 283–289.

Roleda, M.Y., Nyberg, C.D., Wulff, A., 2012. UVR defense mechanisms in eurytopic and invasive *Gracilaria vermiculophylla* (Gracilariales, Rhodophyta). Physiol. Plant. 146, 205–216.

Rossi, F., Gribsholt, B., Gazeau, F., Santo, V.D., Middelburg, J.J., 2013. Complex effects of ecosystem engineer loss on benthic ecosystem response to detrital macroalgae. PLOS ONE 8, e66650.

Rueness, J., 2005. Life history and molecular sequences of *Gracilaria vermiculophylla* (Gracilariales, Rhodophyta), a new introduction to European waters. Phycologia 44, 120–128.

Saha, M., Wiese, J., Weinberger, F., Wahl, M., 2016. Rapid adaptation to controlling new microbial epibionts in the invaded range promotes invasiveness of an exotic seaweed. J. Ecol. 104, 969–978.

Schmid, M., Stengel, D.B., 2015. Intra-thallus differentiation of fatty acid and pigment profiles in some temperate Fucales and Laminariales. J. Phycol. 51, 25–36.

Serôdio, J., Ezequiel, J., Frommlet, J., Laviale, M., Lavaud, J., 2013. A method for the rapid generation of nonsequential light-response curves of chlorophyll fluorescence. Plant Physiol. 163, 1089–1102.

Simon-Colin, C., Kervarec, N., Pichon, R., Deslandes, E., 2004. NMR ^{13}C-isotopic enrichment experiments to study carbon-partitioning into organic solutes in the red alga *Grateloupia doryphora*. Plant Physiol. Biochem. 42, 21–26.

Simon-Colin, C., Kervarec, N., Pichon, R., Deslandes, E., 2002. Complete ^{1}H and ^{13}C spectral assignment of floridoside. Carbohydr. Res. 337, 279–280.

Sokal, R.R., Rohlf, F.J., 1995. Biometry: The principles and practice of statistics in biological research.

Stiger, V., Payri, C.E., 2005. Natural settlement dynamics of a young population of *Turbinaria ornata* and phenological comparisons with older populations. Aquat. Bot. 81, 225–243.

Stiger-Pouvreau, V., Thouzeau, G., 2015. Marine species introduced on the French Channel-Atlantic coasts: A review of main biological invasions and impacts. Open J. Ecol. 05, 227–257.

Sun, L., Wang, S., Gong, X., Zhao, M., Fu, X., Wang, L., 2009. Isolation, purification and characteristics of R-phycoerythrin from a marine macroalga *Heterosiphonia japonica*. Protein Expr. Purif. 64, 146–154.

Surget, G., Lann, K.L., Delebecq, G., Kervarec, N., Donval, A., Poullaouec, M.-A., Bihannic, I., Poupart, N., Stiger-Pouvreau, V., 2017. Seasonal phenology and metabolomics of the introduced red macroalga *Gracilaria vermiculophylla*, monitored in the Bay of Brest (France). J. Appl. Phycol. 1–16.

Thomsen, M.S., McGlathery, K., 2006. Effects of accumulations of sediments and drift algae on recruitment of sessile organisms associated with oyster reefs. J. Exp. Mar. Biol. Ecol. 328, 22–34.

Thomsen, M.S., McGlathery, K., 2005. Facilitation of macroalgae by the sedimentary tube forming polychaete *Diopatra cuprea*. Estuar. Coast. Shelf Sci. 62, 63–73.

Thomsen, M.S., McGlathery, K.J., 2007. Stress tolerance of the invasive macroalgae *Codium fragile* and *Gracilaria vermiculophylla* in a soft-bottom turbid lagoon. Biol. Invasions 9, 499–513.

Thomsen, M.S., Stæhr, P.A., Nejrup, L.B., Schiel, D.R., 2013. Effects of the invasive macroalgae *Gracilaria vermiculophylla* on two co-occurring foundation species and associated invertebrates. Aquat. Invasions 8, 133–145.

Thomsen, M.S., Stæhr, P.A., Nyberg, C.D., Schwaerter, S., Krause-Jensen, D., Silliman, B.R., 2007. *Gracilaria vermiculophylla* (Ohmi) Papenfuss, 1967 (Rhodophyta, Gracilariaceae) in northern Europe, with emphasis on Danish conditions, and what to expect in the future. Aquat. Invasions.

Tyler, A.C., McGlathery, K.J., Macko, S.A., 2005. Uptake of urea and amino acids by the macroalgae *Ulva lactuca* (Chlorophyta) and *Gracilaria vermiculophylla* (Rhodophyta). Mar. Ecol. Prog. Ser. 294, 161–172.

Van Alstyne, K.L., Pelletreau, K.N., Kirby, A., 2009. Nutritional preferences override chemical defenses in determining food choice by a generalist herbivore, *Littorina sitkana*. J. Exp. Mar. Biol. Ecol. 379, 85–91.

Vidondo, B., Duarte, C.M., 1998. Population structure, dynamics, and production of the mediterranean macroalga *Codium bursa* (chlorophyceae). J. Phycol. 34, 918–924.

Wang, S., Wang, G., Weinberger, F., Bian, D., Nakaoka, M., Lenz, M., 2017. Anti-epiphyte defences in the red seaweed *Gracilaria vermiculophylla*: non-native algae are better defended than their native conspecifics. J. Ecol. 105, 445–457.

Weinberger, F., Buchholz, B., Karez, R., Wahl, M., 2008. The invasive red alga *Gracilaria vermiculophylla* in the Baltic Sea: adaptation to brackish water may compensate for light limitation. Aquat. Biol. 3, 251–264.

Yokoya, N.S., Kakita, H., Obika, H., Kitamura, T., 1999. Effects of environmental factors and plant growth regulators on growth of the red alga *Gracilaria vermiculophylla* from Shikoku Island, Japan, in: Kain, J.M., Brown, M.T., Lahaye, M. (Eds.), Sixteenth International Seaweed Symposium, Developments in Hydrobiology. Springer Netherlands, pp. 339–347.

Zubia, M., Freile-Pelegrín, Y., Robledo, D., 2014. Photosynthesis, pigment composition and antioxidant defences in the red alga *Gracilariopsis tenuifrons* (Gracilariales, Rhodophyta) under environmental stress. J. Appl. Phycol. 26, 2001–2010.

Chapitre 3. Quelles sont les variations physiologiques observées selon un cycle tidal hivernal ou estival ?

Le cycle tidal influence fortement les macrophytes marins en tout premier lieu en impactant leur répartition (Cabioc'h et al., 2006). Les espèces algales se répartissent le long de l'estran en formant des ceintures selon leur capacité de tolérance à l'émersion. Le cycle tidal entraîne également d'autres variations environnementales comme celles de la quantité et de la qualité de la lumière, de la salinité (désalure lors d'intempéries, augmentation de la salinité lors de fortes chaleurs) et de la température … (Hurd et al., 2014). Cette myriade de microenvironnements changeants lors de chaque marée est particulièrement marquée en Bretagne où l'on observe des marnages importants.

Par ailleurs, cette modification des facteurs abiotiques est amplifiée lors des marées de vives eaux durant lesquelles la durée d'émersion est maximale. Ces fortes marées, durant plusieurs jours, impliquent en particulier une exposition accrue aux radiations solaires, ainsi qu'aux températures atmosphériques. On peut ainsi s'attendre à ce que ces conditions soient particulièrement stressantes (en raison d'une variation accrue des facteurs abiotiques). Ces conditions se répétant durant quelques jours, elles peuvent conduire à un stress chronique.

Le but de cette étude est de comparer des macrophytes vivant dans des environnements côtiers très contrastés : l'une, *Sargassum muticum* vivant en milieu exposé dans les mares d'estrans rocheux et l'autre, *Gracilaria vermiculophylla*, vivant en milieu protégé en substrat vaseux. La période d'étude est volontairement placée lors de marées de vives eaux, l'une en condition hivernale et l'autre estivale. Dans ce contexte, comment ces espèces s'acclimatent-elles ? Subissent-elles des stress chroniques de type photo-oxydatif pouvant induire un stress oxydatif chez ces espèces ? Possèdent-elles une capacité d'acclimatation suffisante en réaction à ces conditions environnementales en régulant par exemple leur cortège pigmentaire ?

Cette étude fait l'objet d'un manuscrit en cours de préparation.

Embedding two time scales (tide course and season) to follow the field acclimation of some invasive macroalgal models

Introduction

In a general context of climate change whose consequences are increasingly visible on the coastal zones, the anthropic activities keep continuing to intensify and the number of invasive species continues to increase, especially along the Brittany coast (Stiger-Pouvreau and Thouzeau, 2015). Not enough data currently exists on the expansion of the introduced marine macroalgae, in particular, on the effects of the climate change (such as increase in the ocean temperature and UV radiations, a dilution of seawater linked to stronger precipitations, an acidification of the ocean) on the production of metabolites by invasive and native seaweeds, key compartment of the coastal ecosystems, and the chemical interactions between marine organisms. Given their broad geographical distribution, especially those occurring along the Northeastern Atlantic Ocean, the invasive species are likely to adapt much more easily and quickly to climatic modifications than native species.

Extensive research has been carried out to understand the invasive potential of some introduced species models (Gulbransen et al., 2013; Nejrup et al., 2012; Roleda et al., 2012). A high plasticity associated to the lack of native enemies leads to a lower pressure of predators in the invasive area and to a less stressful environment compared to the native area. This could also explain in part the invasive potential of these introduced species (Huang et al., 2015; Lande, 2015). Therefore, the high phenotypic or ecophysiological plasticity induced by the new environmental conditions (Eggert, 2012) will favor an adaptive plasticity depending on differences in environmental advantages between the native and invasive areas, including biotic and abiotic factors (Huang et al., 2015; Lande, 2015). This adaptive plasticity confers fitness advantages to the invasive species allowing the optimization of acclimation mechanisms to the new environmental conditions (Davidson et al. 2011). The performance of differential traits were illustrated in common gardens carried out on 20 pairs of higher plants, i.e. invasive and native species, conferring fitness advantage on the former (Godoy et al., 2011).

Fitness depends on growth, morphological and physiological traits (Davidson et al., 2011). Growth rate as ecological traits of major invasive species was well investigated

(Gulbransen et al., 2013; Hu and Juan, 2013) even if scientific efforts are still required. The physiological traits of macroalgae as being photoautotroph organisms were closed to photosynthetic efficiency (Hanelt et al., 2003). Chlorophyll *a* (chl-a) fluorescence approaches allow quantitative, non-invasive and rapid assessment of the physiological status of the photosynthetic apparatus *in vivo* (Häder et al., 1997; Maxwell and Johnson, 2000; Van Kooten and Snel, 1990). PAM (Pulse Amplitude Modulated) fluorescence method revealed to be a powerful tool to elucidate fundamental processes in photosynthesis (Enríquez and Borowitzka, 2010; Van Kooten and Snel, 1990), and to study regulation processes of photosynthetic energy allocation (Häder et al., 1997). Therefore, PAM fluorescence is regarded as a sensitive technique to study photosynthetic performance of macroalgae and their short-term responses to environmental stressors (Enríquez and Borowitzka, 2010; Hanelt et al., 2003). PAM approaches have been applied to laboratory experiments to assess the effect of several abiotic factors on photosynthesis of macroalgae under controlled conditions (Connan and Stengel, 2011; Gevaert et al., 2002; Xiao et al., 2015). To complete laboratory experiments, field measurements are needed to understand the acclimation of macroalgae to withstand to multiple stressors occurring within complex intertidal environments and to assess physiological species fitness. Measuring photosynthesis in the field allows at first to study the real responses of macroalgae to environmental conditions and also to avoid sample transport into the laboratory which could induce artificial changes in temperature, irradiance as well as in salinity, as it was demonstrated for the green macroalga *Caulerpa prolifera* (Häder et al., 1997). Field PAM studies focused essentially on native macroalgae under stressful conditions or threaten by a changing environment (Hanelt et al., 2003), such as in *Laminaria* species in a context of the decline of kelps in western Europe (Delebecq et al., 2013, 2011; Gevaert et al., 2003) or on dominant intertidal macroalgae (Migné et al., 2015). Few studies were conducted on field acclimation of invasive macroalgae (Baer and Stengel, 2010), since most of studies focused on their physiological performances under controlled conditions (Henkel, 2008; Roleda et al., 2012; Zanolla et al., 2015). Moreover, some studies demonstrated the impact of tidal cycles on the photophysiology of macroalgae (Sagert et al., 1997; Sampath-Wiley et al., 2008) and compared species acclimation to this specific environment e.g (Gomez et al., 2004; Migné et al., 2015; Wang et al., 2016). As an example, Sampath-Wiley et al. (2008) worked on *Porphyra umbilicalis*

physiology in regard to emersion and immersion. But no study was carried out on the comparison of invasive species living on contrasted shores: muddy shores with those living on rocky shores, regarding to their photosynthetic performance during tidal cycles.

In this context, two introduced and invasive macroalgae were chosen along Brittany coasts: *Gracilaria vermiculophylla* (Ohmi) Papenfuss, a red macroalga native from East of Asia, introduced in Brittany in 1996 and living in saltmarshes (Rueness, 2005) and *Sargassum muticum* (Yendo) Fensholt, a brown macroalga native from Japan, introduced in Brittany in 1981 and living on rocky shores (Stiger-Pouvreau and Thouzeau, 2015). These two seaweeds were chosen for their dominance along Atlantic European coasts as for their particular invasive potential around the world in two contrasted coastal environments (Stiger-Pouvreau and Thouzeau, 2015). The objective of this study was to investigate the impact of tidal cycles and then changes in light and temperature along the tidal cycle, in relation to the physiology of both macroalgal species. We thus followed the temporal patterns in the natural variation of chl-a fluorescence to determine photosynthetic performance both at a spring tide (in particular at low tide) and season timescales of these two invasive macroalgae when low tide coincides with sun zenith. At the western part of Brittany, spring tide occurs around once's a month alternating with neap tides following moon's cycle and it was expecting that during these spring tides may occur the most stressful conditions for intertidal macroalgae with especially longer emersion. In addition to chl-a fluorescence, pigment quantification allowed to observe biochemical acclimation induced by temperature and irradiance changes occurring at these two time-scales and gave information on the algal acclimation capacities. Moreover, superoxide dismutase activity (SOD activity) and lipid peroxidation were assessed to determine if under spring tides conditions, oxidative stress occurs within both algae.

Material and methods

Sampling Field experiments were performed on two invasive macroalgae on Brittany coasts: *Gracilaria vermiculophylla* on salt marshes and *Sargassum muticum* on rocky shores, on one site for each species: Le Faou (48°21.497'N - 4°20.444'W) for *G. vermiculophylla* and Pointe du Diable (48°21.255'N - 4°33.510'W) for *S. muticum*. Samplings and measurements were carried out during low tides as soon as *G. vermiculophylla* mat on mudflat and

S. muticum rockpool on rockyshores were uncovered by seawater, both in winter (09-02-2015 and 22-01-2015 for *G. vermiculophylla* and *S. muticum* respectively) and summer (02-07-2015 and 03-07-2015 for *G. vermiculophylla* and *S. muticum* respectively) (Figures 1 and 2). Temperature and salinity were followed during field experiments using a multiparameter (Multi 350i, WTW) with Tetracon 325 probe. In parallel, incident photosynthetically available radiation (PAR, 400-700 nm) was also recorded using a Li-COR quantum sensor (LI-192SA) connected to a data logger (Li-COR LI-1400).

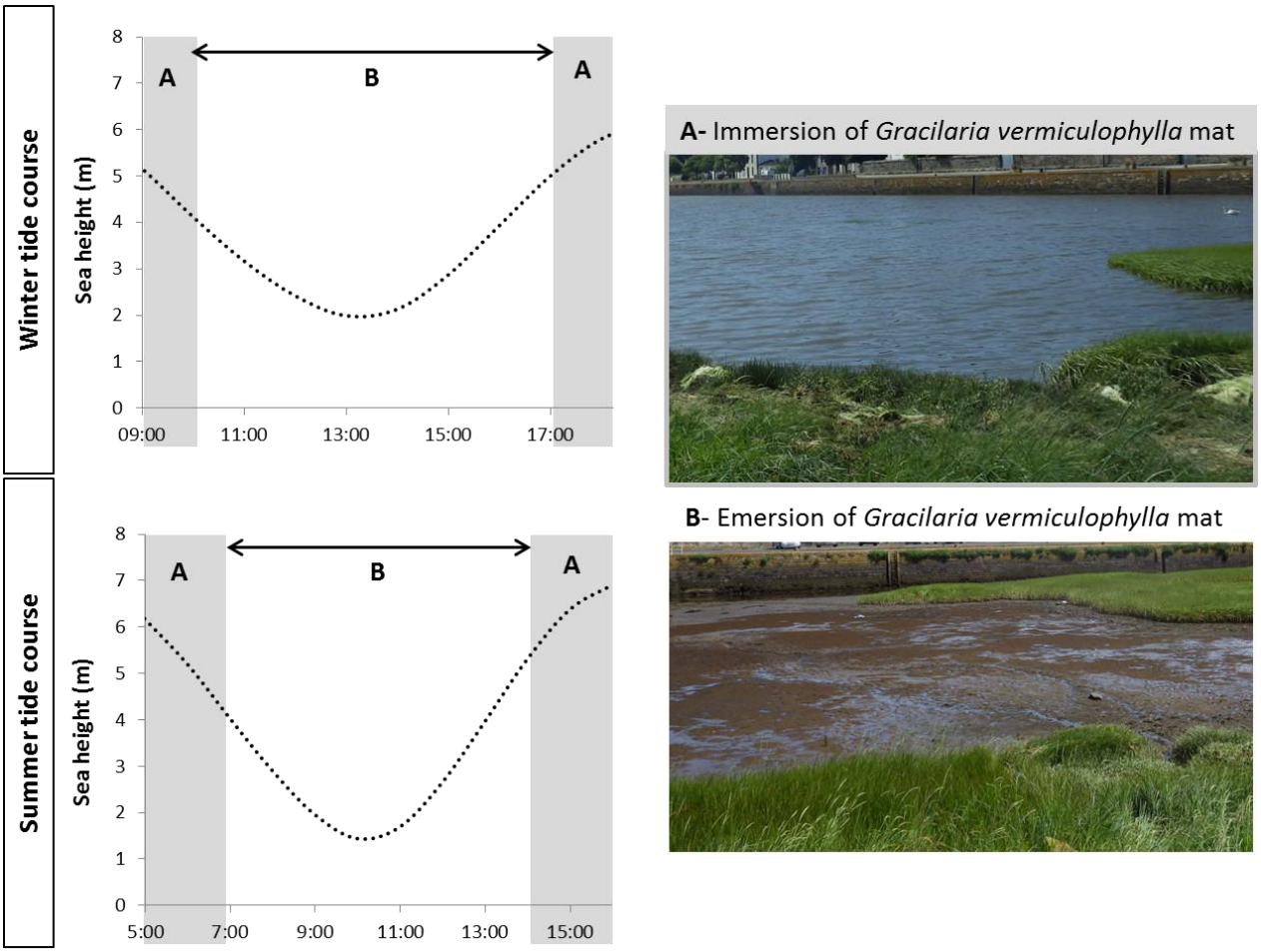

Fig. 1 Tide courses of 09-02-2015 (Winter tide course) and 02-07-2015 (Summer tide course) for Faou salt marshes. Sea heights were issued from SHOM data (on www.maree.info.fr, consulted the 16/04/2017). Photos illustrating the immersion (A) and emersion (B) of *G. vermiculophylla* mat (photographs taken the 02-07-2015 in the Faou estuary). Samplings were performed during B.

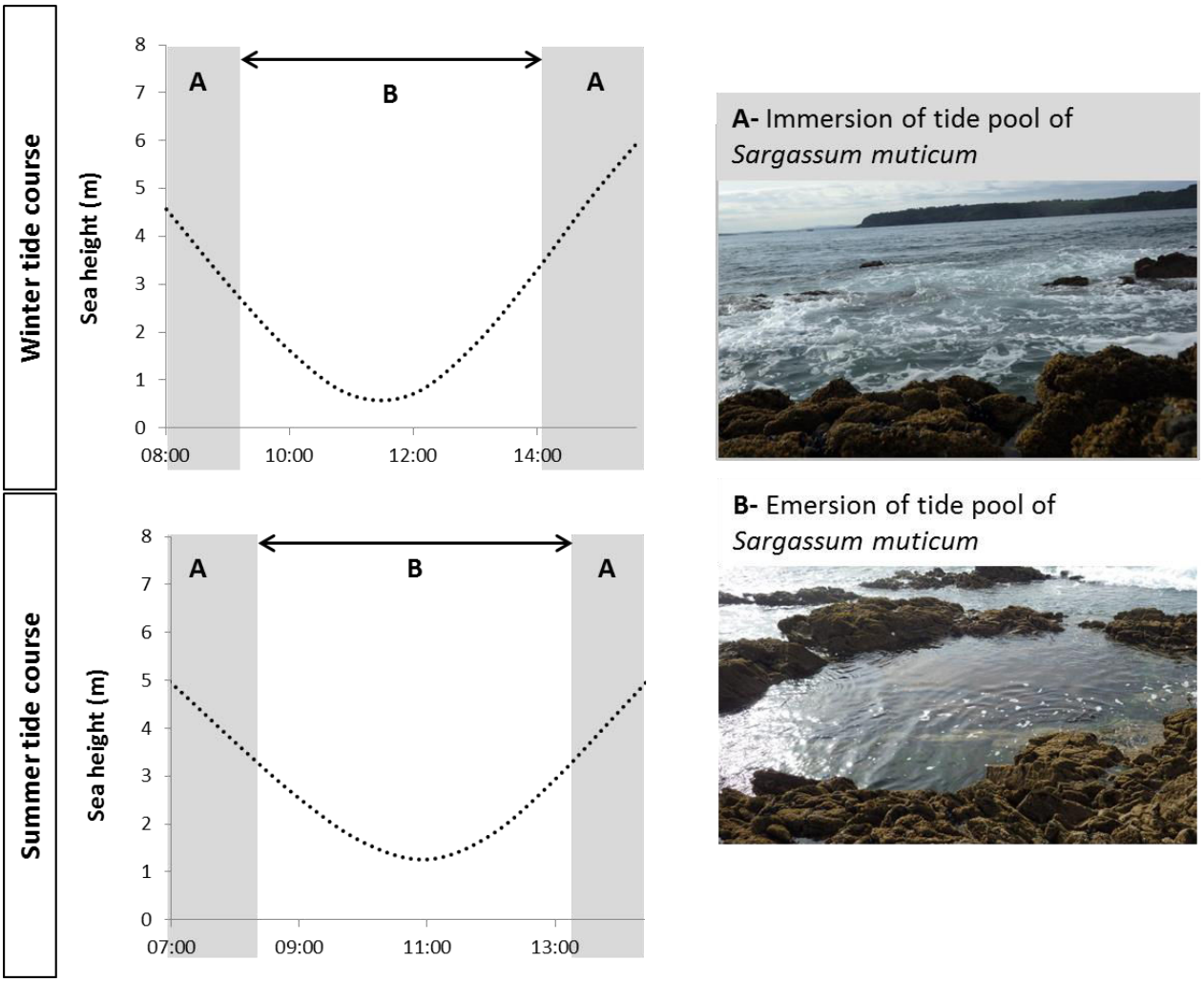

Fig. 2 Tide courses of 22-01-2015 (Winter tide course) and 03-07-2015 (Summer tide course) for "Pointe du Diable" rocky shore. Sea heights were issued from SHOM data (on www.maree.info.fr, consulted the 16/04/2017). Photos illustrating the immersion (A) and emersion of *S. muticum* rockpool (photographs taken the 03-07-2015 at the "Pointe du Diable"). Samplings were performed during B.

Diving PAM In vivo chl-a fluorescence of photosystem II (PSII) of five individual thalli of *S. muticum* and *G. vermiculophylla* was measured using an underwater fluorometer (diving PAM; HeinzWalz, Effeltrich, Germany). The optimal quantum yield (Fv/Fm) of PSII (Genty et al., 1989), a measure of the maximum efficiency of PSII, was measured using a 0.8 s saturating pulse (2500 µmol photons. m^{-2}. s^{-1}) of white light after 10 min of acclimation to darkness.The effective quantum yield of PSII (ϕPSII), the efficiency of PSII photochemistry, was measured under natural ambient light using a custom-made clip to ensure a constant distance of 5 mm and a constant angle of 60° between the probe and the sample. The ϕPSII

was calculated according to Genty et al. (1989) and used to estimate the linear electron transport rate (relative electron transport rate, rETR)(Gevaert et al., 2003), an estimator of photosynthesis.

$\phi PSII = (Fm'-Ft) / Fm'$

$rETR = \phi PSII * PAR$, where PAR corresponds to recorded incident photosynthetically radiation

Sampling For pigment and protein quantifications as for lipid peroxidation and SOD analyses, samples were collected three times on the field during low tide: at the beginning of low tide (B), at low tide maximum (M) and finally during tide rising, just before seawater covered sampling zones (E). Samples were washed with local seawater and immediately stored in liquid nitrogen. Back to the laboratory, algal samples were ground (Retch® MM400) in liquid nitrogen and transferred to -80°C freezer until analyses.

Pigments quantification Zeaxanthin, violaxanthin, antheraxanthin, fucoxanthin, chlorophyll-a (chl a), chlorophyll c2 (chl-c2) and β-carotene were analysed by High Performance Liquid Chromatography (HPLC; Dionex) following the method developed by Schmid and Stengel (2015) (Schmid and Stengel, 2015). Briefly, pigments were extracted from 100 mg of ground samples in a 90% acetone solution for 30 min with stirring, at 4°C in the dark. After centrifugation, a second extraction was performed during 15h in the dark. Supernatants were pooled and 200 µL of obtained extract was filtered and diluted with ammonium acetate buffer (0.5M, pH 7.2) just before analysis. Pigments were separated using a Zorbax Eclipse XDB-C18 column (150 x 4.6 mm; 5 µm; Agilent) with a C18 pre-column over a 40 min run. Acquisitions were performed using the software Chromeleon 6.60 (Dionex). Pigment concentrations (expressed as $\mu g.g^{-1}$ FW) were calculated using pigment standard calibrations (zeaxanthin, violaxanthin, antheraxanthin, chl-c2 and β-carotene supplied by DHI LAB products (Denmark) and fucoxanthine and chl a standards supplied by Sigma-Aldrich France). In order to carry out statistical analysis, when pigment concentration was too low to be detected, pigment content was fixed to the half of the detection threshold content of the considered pigment. Even though not present in red macroalgae, fucoxanthin

was detected in *G. vermiculophylla* extracts due to the presence of benthic diatoms epiphytes living on the macroalgal thalli (these results was not presented).

Phycobiliprotein content was determined using a protocol adapted from Sun et al. (2009) and Roleda et al. (2012). Extraction was performed in the dark at 4°C using 75 mg algal dry matter with 1.5 mL phosphate buffer (0.1 M, pH = 6.8). After sonication for 15 min, extracts were centrifuged for 20 min at 4°C. The obtained extracts were stored at 4°C in the dark until the absorbance was measured at 280, 455, 565, 592, 618 and 645 nm (POLARstar Omega, BMG LABTECH). Concentrations of phycobiliproteins, expressed as $mg.g^{-1}$ DW (dry weight), were determined using Beer and Eschel equations (Dumay et al., 2013; Munier et al., 2014; Zubia et al., 2014) as follows:

$$\text{R-PE} = [(A_{565} - A_{592}) - (A_{455} - A_{592}) * 0.20] * 0.12$$

$$\text{R-PC} = [(A_{618} - A_{645}) - (A_{592} - A_{645}) * 0.50] * 0.15$$

where A= Absorbance; R-PE= R-phycoerythrin concentration; R-PC= R-phycocyanin concentration.

Lipid peroxidation Malondialdehyde (MDA) is one of the most abundant aldehyde generated by lipid peroxidation (Esterbauer and Cheeseman, 1990). The content of lipid peroxidation products was thus determined by the quantification of MDA. The procedure was adapted according to the methods providing by lipid peroxidation (MDA) assay kit (Sigma) and Meudec (2006) (Meudec, 2006). Around 100 mg of sample was extracted with 3 mL of 0.1% trichloroacetic acid solution (TCA, Sigma) and grinded in a mortar at 4°C. BHT (100 $mg.L^{-1}$) was added and samples were centrifuged at 3,220*g* (Eppendorf 5810 R) during 10 min at 4°C to remove cell debris. Resulting extracts were added to 0.5% thiobarbituric acid and 20% TCA solution (Sigma) according to a ratio 1:4 (v:v). Samples were then incubated 60 min at 95°C and cooled on ice to stop the colorimetric reaction. Finally, after the addition of n-butanol (3.75 mL), extracts were centrifuged at 3,220*g* for 20 min at 4°C to separate the n-butanol fraction from the aqueous fraction. After the evaporation of the n-butanol fraction (MinVac Concentrator Range, Genevac) at 40°C, samples were suspended with 700 µL of milliQ water. MDA content was quantified spectrophotometrically by

recording the absorbance at 532 nm corrected by the absorbance at 600 nm and were calculated as follows:

$$\text{MDA content (nmoles.mg}^{-1}\text{ FW)} = \left[\frac{\left(A_{532} - A_{532_{Blank}}\right) - \left(A_{600} - A_{600_{Blank}}\right)}{a} * \text{DF}\right] / \text{W}$$

where A = Absorbance; a = coefficient of MDA standard curve; DF = dilution factor; W = sample fresh weight

Total Superoxide Dismutase (t-SOD) Algal powder was suspended in saline phosphate buffer (PBS) solution (v:w; 5:1) composed of 10 mM PBS, ethylenediaminetetraacetic acid (EDTA, 1 mM) and Triton*100 (0.1%, v:v). After sonication during 10 min at 4°C and incubation on ice during 45 min, samples were centrifuged at 10,000*g* during 45 min at 4°C (miniSpin Ependorf, Rotor F45-12-11) to remove cell debris. On these extracts, total proteins were quantified according to Bradford procedure for *G. vermiculophylla* using BioRad Protein Assay Dye Reagent Concentrate (BioRad France) and Bovine Serum Albumin (BSA) as standard (Bradford, 1976). Due to low protein levels encountered in the extracts of *S. muticum,* total protein content were determined using Lowry assay (Lowry et al., 1951; Tanniou, 2014) despite higher interaction possibilities but higher sensibility (Tanniou, 2014). T-SOD (EC 1.15.1.1) activity was assayed spectrophotometrically by measuring the decrease in absorbance at 440 nm due to the inhibition of the xanthine/xanthine oxidase complex after 20 min-incubation at 25°C. T-SOD activity was determined using the SOD Assay Kit (Sigma-Aldrich, France) and following the protocol developed by Richard et al. (2015) (Richard et al., 2015). The enzyme activity was expressed as Units of enzyme.mg^{-1} of total proteins (U.mg^{-1} total proteins).

Statistics Statistical analyses were performed with RStudio (v. 0.95.263) for R (v.3.1.3). All analyses were carried out in triplicate and results were expressed as mean ± standard deviation (SD). If the data met the requirements for parametric tests, they were analysed using a multi-way ANOVA (function of the number of factors) at a significance level of 95%, followed by a Tukey post-hoc test. Data were transformed if necessary to respect homoscedasticity. When the data did not meet the requirements for an ANOVA, they were analysed using the two-way Scheirer Ray Hare (SRH) test (Sokal and Rohlf, 1995), the one-way Kruskal–Wallis (KW) test or the Wilcoxon Mann Withney (WMW) test depending on the

number of factors and conditions, at a significance level of 95%, followed by a non parametrical multiple comparisons test (kruskalmc function; pirgmess package).

Results

Field parameters Experiments were performed during typical spring tides and sunny days in Brittany (France) in winter and summer for both studied species. At the two seasons, emersions lasted around seven hours thirty minutes for *G. vermiculophylla* mat and five hours for rockpool colonized by *S. muticum*. Recorded temperatures showed an increase more or less stable with the tide course depending of irradiance and cloud cover (Figures 3a-b and 4a-b). Amplitude of temperature enhanced with summer season with a maximum of 1.5°C observed during the winter tide course compared to 6.5°C occurring in summer for *S. muticum* and 3.7°C and 10.5°C for *G. vermiculophylla* living on a muddy shore in winter and summer tide courses, respectively. Overall, irradiance increased from sun zenith and reached a maximum at noon or in early afternoon (between 10:00 and 12:30, UTC) corresponding to the low tide period.

Photosynthetic parameters Fv/Fm and rETR determined in *G. vermiculophylla* during winter and summer tide courses were illustrated in Figures 3c-f. *G. vermiculophylla* exhibited divergent photosynthetically behavior (through Fv/Fm and rETR parameters) between summer and winter tide courses. Indeed, Fv/Fm did not vary significantly during the course of winter tide (KW, p-value=0.281). In parallel of the increase in incident irradiance, rETR reached a high value at 12:30 (UTC) and returned to its initial value at the end of the experiment (KW, p-value<0.0005). Conversely, with summer tide course, *G. vermiculophylla* Fv/Fm declined significantly after the sun zenith (KW, p-value<0.0005). rETR increased significantly (KW, p-value<0.0001) in parallel of the increased irradiance from 10:17 (UTC) with a mean PAR of 1,646 µmol photons m^{-2} s^{-1} until zenith (10:17 to 12:12, UTC). Fluorescence parameters determined in *S. muticum* varied also differentially between a winter and a summer tide course for this species as illustrated in Figures 4c-f. In winter, the maximum quantum yield was stable until low tide and showed a 19.8% decrease linked to the reduction in Fm (data not shown) after the increase in incident irradiance reaching a maximum of 708 µmol photons m^{-2} s^{-1} around 11:00 (UTC). Moreover, rETR was multiplied by 2.8 between 09:55 and 11:03 (UTC) in parallel with the irradiance increase at sun zenith.

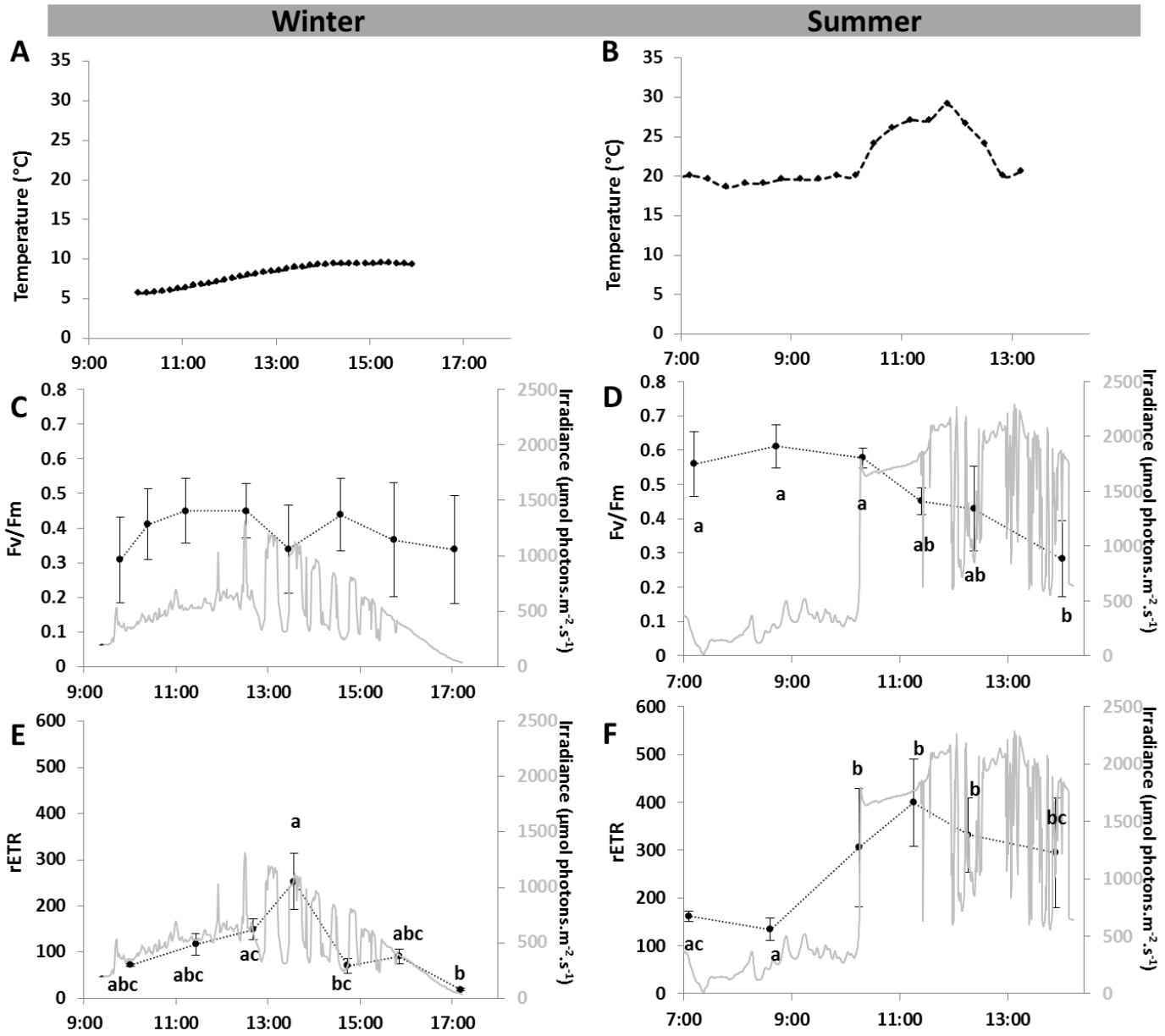

Fig. 3 Variations of field abiotic parameters (air temperature: A and B, and incident irradiance: C, D, E and F) and fluorescence parameters (Fv/Fm: C and D, and rETR: E and F) of *G. vermiculophylla* during a sunny winter and summer tide courses. Represented results for fluorescence parameters are mean ± SD (n=5 in Winter, n≥5 in Summer). Different letters indicate significant differences between means (according to KW tests followed by post-hoc test $p < 0.05$).

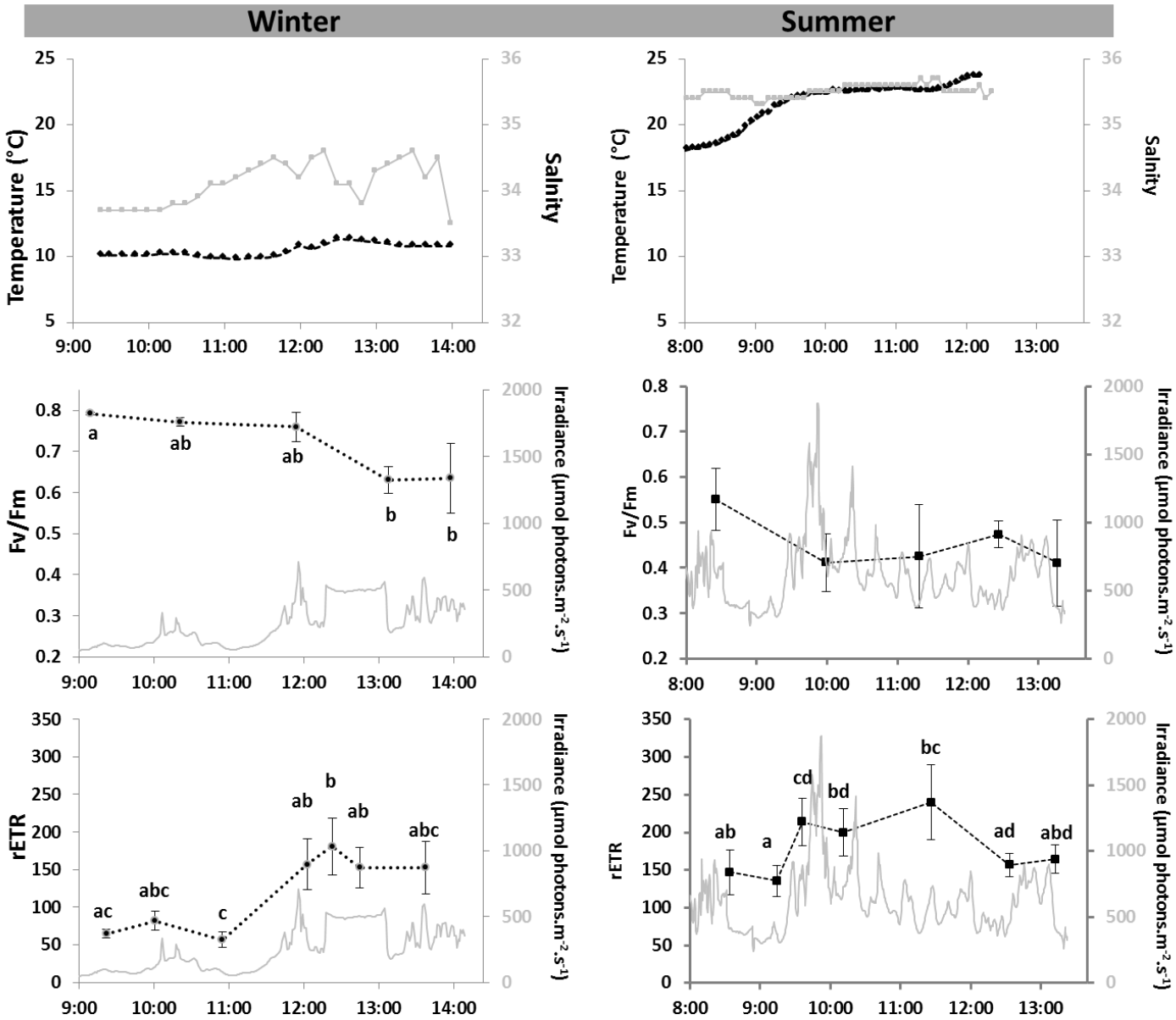

Fig. 4 Variations of field abiotic parameters (temperature of surface rockpool water, rockpool salinity: A and B and incident irradiance: C, D, E and F) and fluorescence parameters (Fv/Fm: C and D, and rETR: E and F) of *S. muticum* during a sunny winter and summer tide courses. Represented results for fluorescence parameters are mean ± SD (n=5 in winter, n≥5 in summer). Different letters indicate significant differences between means ($p < 0.05$) according to KW tests followed by post-hoc tests.

Conversely, Fv/Fm did not vary significantly in summer with tide course (KW, p-value=0.064) whereas a small increase in rETR was observed during sun zenith period (KW, p-value<0.0005) compared to winter variations. Interestingly, these results illustrated opposite photosynthetically behavior between the two studied invasive macroalgae during typical sunny and winter and summer spring tide courses.

Pigments *G. vermiculophylla* exhibited no change in pigment contents during a tide cycle whatever the season (SRH test and two-way ANOVA, p-value > 0.05; Figure 5). However, zeaxanthin (two-way ANOVA, p-value=0.015), chl-a (SRH test, p-value=0.024), β-carotene (SRH test, p-value=0.038) and especially antheraxanthin (SRH test, p-value=0.0047) decreased in summer compared to winter. Phycobilin pigments did not vary both at daily and seasonal scales. For *S. muticum*, all pigments contents varied between winter and summer (Figure 5): on one hand, chlorophylls and carotenoids (fucoxanthin, β-carotene and violaxanthin) were less concentrated in summer than in winter. On the other hand, the two xanthophylls, antheraxanthin and zeaxanthin, presented higher amounts during summer tide course. Like *G. vermiculophylla*, *S. muticum* exhibited no change in pigment contents during a tide cycle whatever the season except for zeaxanthin (SRH test and two-way ANOVA, p-value > 0.05; Figure 5). Furthermore, zeaxanthin levels were enhanced during summer tide course with amounts multiplied by 5.3 between ebb and low tides (with 0.80 ± 0.80 and 4.16 ± 0.75 $\mu g.g^{-1}$ FW respectively).

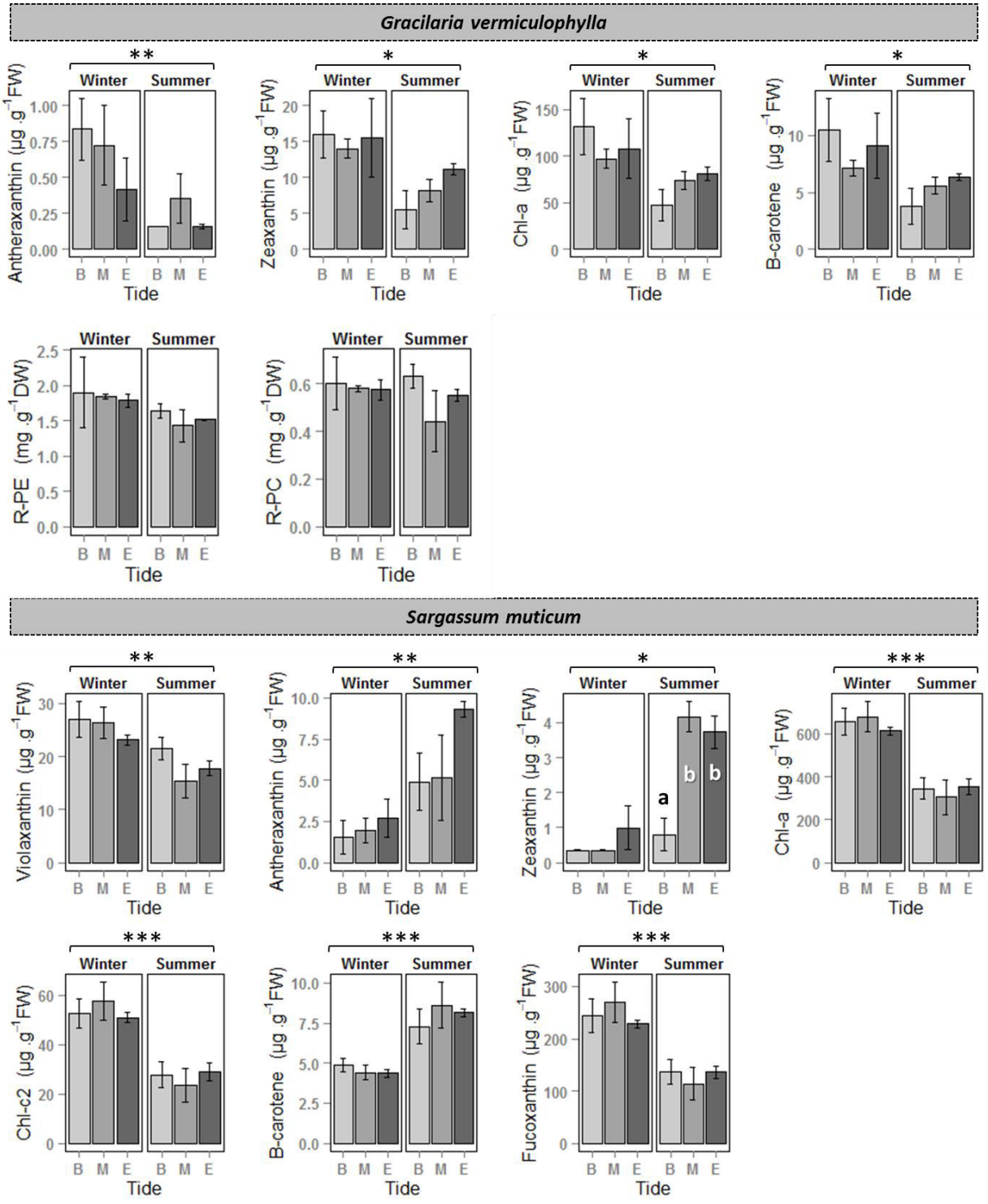

Fig. 5 Concentrations of pigments determined for the red macroalga *Gracilaria vermiculophylla* and the brown macroalga *Sargassum muticum* according to the tide level (B: beginning of low tide when the pool (rocky shore) and the algal mat (muddy shore) were uncovered, M: maximum of low tide, E: end of low tide when seawater begins to recover each shore) and depending on the season (winter vs. summer). Results were expressed as

mean ± SD (n=3) in mg.g^{-1} DW for R-phycoerythrin (R-PE) and R-phycocyanin (R-PC) and in µg.g^{-1} FW for the other pigments. Stars (*) indicate significant differences between seasons (*: p <0.05; **: p<0.01; ***: p<0.001). Different letters indicate significant differences between tide levels (p < 0.05) according to ANOVA followed by Tukey multiple comparisons test.

Lipid peroxydation and SOD Lipid peroxidation through MDA content of *G. vermiculophylla* exhibited no significant difference regardless of tide course and season (SRH test, p-value= 0.51 and 0.089, respectively; Figure 6). On another hand, *S. muticum* showed seasonal variations with MDA levels higher in winter (SRH test, p-value<0.0001) as MDA was not detected in summer. SOD activities of *G. vermiculophylla* and of *S. muticum* varied also with seasons (SRH test, p-value<0.0003 and 0.004 respectively; Figure 7). Level of *G. vermiculophylla* SOD activities declined in summer compared to winter (with 50.8 ± 8.59 and 33.3 ± 13.0 U.mg^{-1} of total proteins, respectively) with no significant variation during tide course (SRH test, p-value=0.73). On the contrary, SOD activities of *S. muticum* increased in winter compared to summer due to a faster increase in SOD activity during tide course (KW, p-value=0.0096), which was multiplied by 16 between the begin of ebb tide and the low tide.

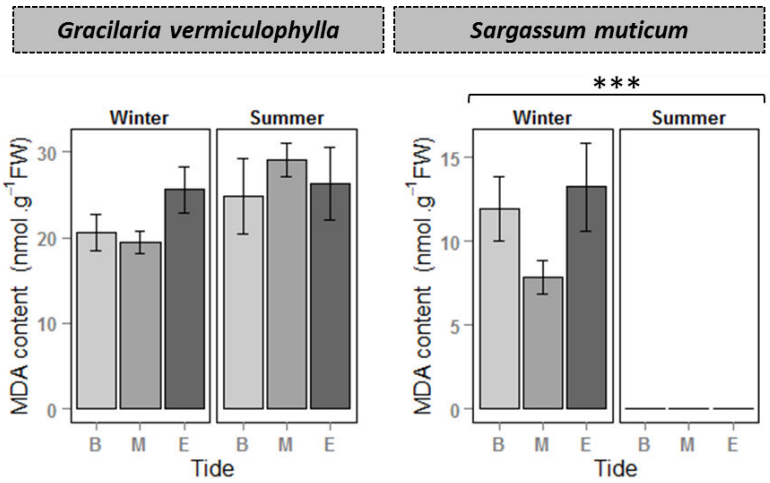

Fig. 6 Variations of MDA content (malondialdehyde; nmol. g^{-1}FW) determined for the red macroalga *Gracilaria vermiculophylla* (n=5) and the brown macroalga *Sargassum muticum* (n=4) during the tide course (B: beginning of low tide when the pool (rocky shore) and the algal mat (muddy shore) were uncovered, M: maximum of low tide, E: end of low

tide when seawater begins to recover each shore) and depending on the season (Winter vs. Summer). Results are expressed as mean ± SD. Stars (*) indicate significant differences between seasons (*: p <0.05; **: p<0.01; ***: p<0.001) according to SRH test.

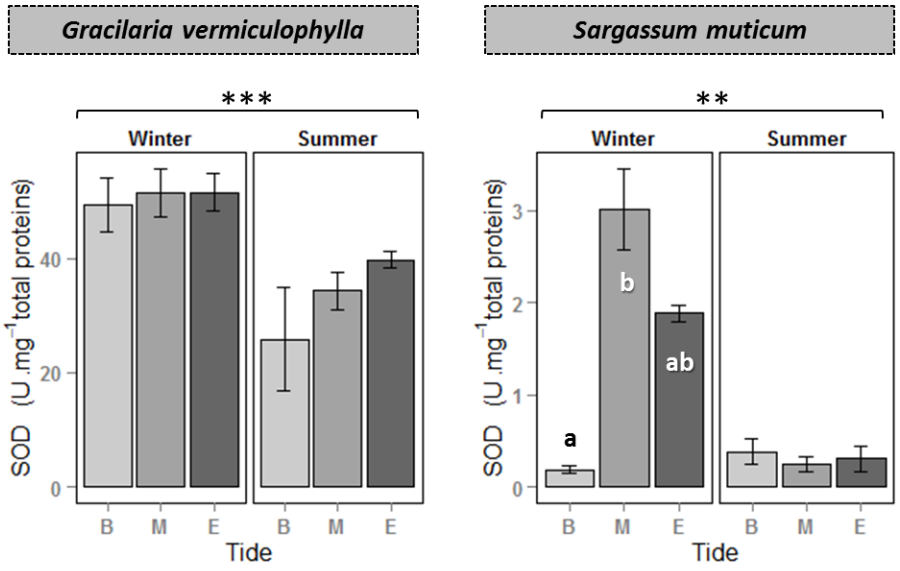

Fig. 7 Variations of SOD (superoxyde dismutase) activity ($U.mg^{-1}$ of total proteins) determined for the red macroalga *Gracilaria vermiculophylla* and the brown macroalga *Sargassum muticum* depending on the tide course (B: beginning of low tide when the pool (rocky shore) and the algal mat (muddy shore) were uncovered, M: maximum of low tide, E: end of low tide when seawater begins to recover each shore) and depending on the season (Winter vs. Summer). Results are expressed as mean ± SD (n=5). Stars (*) indicate significant differences between seasons (*: p <0.05; **: p<0.01; ***: p<0.001). Different letters indicate significant differences between tide levels (p < 0.05) according to KW test followed by a non-parametric multiple comparisons test.

Discussion

Many studies focused on physiological performances of invasive species under laboratory conditions. To understand their acclimation in the field, monitoring their physiological responses *in situ* related to both daily and seasonal environmental changes is important to complete previous studies carried out under controlled conditions in the laboratory. Nevertheless, field studies presented some disadvantages, complex abiotic and biotic multifactorial conditions existed *de facto,* but it allowed working more closely in what

happened in natural environment. In Brittany, during our *in situ* experiment (under sunny weather) when low spring tide coincided with maxima irradiance (as in the present study), *S. muticum* and *G. vermiculophylla* were exposed to the high light stressful conditions and potentially to over-saturating irradiances as observed on *Laminaria* species (Delebecq et al., 2011).

Photosynthetic performance Therefore, this specific field conditions can excess species light harvesting capacities: all harvesting light cannot be used in the photosynthetic electron transfer. Under these conditions, photoinhibition i.e. a reduction in photosynthesis efficiency could occur. This biological process is measured as a decline of the maximum quantum yield, a useful and sensitive parameter of PSII photochemistry efficiency (Maxwell and Johnson, 2000). Additionally, with the aim to follow the overall photosynthetic capacity, rETR was calculated since effective quantum yield did not decline under 0.1 (data not shown) as recommended by Beer and Axelsson (2004) (Beer and Axelsson, 2004). We reported contrasted patterns of *in situ* chl-a fluorescence signals depending on both the invasive macroalga and the season, illustrating the contrasted environmental conditions of shores where they developed. Firstly, the decrease in *S. muticum* Fv/Fm during the winter tide course illustrated the decline of photosynthetic efficiency and the establishment of non-photochemical quenching. In parallel, rETR increased due to high irradiance occurring at sun zenith as during the afternoon. Fv/Fm initial values were not recovered at the end of the experiment suggesting two hypotheses: (1) the establishment of dynamic NPQ with a normal recovery of photosynthetic efficiency during the rising tide and sunset or (2) the damage of the photosystem II of *S. muticum* by chronic photoinhibition occurring during winter spring tides with relative high winter irradiances associated to low temperatures compared to summer field conditions. Dynamic NPQ consists in a photoprotective phenomenon of the photosynthetic apparatus allowing a stronger dissipation of excessive radiation energy and decreasing harmful energy input into the PSII (Hanelt et al., 2003). This photoinhibition phenomenon after exposure to field solar irradiation has already been observed in many macroalgae, such as kelp species (Delebecq et al., 2011; Gevaert et al., 2003) , Fucales and Dictyotales species (Häder et al., 2001) and the green macroalga *Caulerpa prolifera* (Häder et al., 1997). Most of the time, complete recovery in macroalgae can be reached before the sunset (Hanelt et al., 1993) but Delebecq et al. (2011) showed in kelp species, that this

recovery could only occur during the night in case of high light exposure until the end of the experiment. In our study, during the last measurement, relatively high light intensities still occurred with irradiance of 473 ± 136 µmol photons m^{-2} s^{-1} compared to the irradiance at the beginning of the experiment (less than 100 µmol photons m^{-2} s^{-1}). This high irradiance level could be explained by the spring tide occurring together with sunny days, inducing the lengthening of high light exposure window for intertidal macroalgae. Additionnaly, the initial recorded Fv/Fm values of *S. muticum* in the morning suggested the first hypothesis with the establishment of dynamic NPQ with a normal recovery during the previous evening and night.

In contrast, during July tide course, *S. muticum* presented no significant variation of Fv/Fm despite the exposure to higher light intensities than in February. Our results were consistent with Baer and Stengel (2010) who followed the PSII efficiency over different seasons through the *in situ* assessment of the maximal effective quantum yield (Y0) of *S. muticum* along Irish coast. They showed highest values of this Y0 during active growth in February and lowest values during the development of reproductive tissue and senescence in summer but they acclimated samples to the darkness less time than this present study. Opposite pattern was exhibited by *G. vermiculophylla* showing an initiation of NPQ in summer with no recovery of PSII efficiency at the end of the experiment.

These results could suggest several light strategies depending on the invasive macroalga and the season and complementary experiments under controlled conditions would be necessary to confirm it. Furthermore, these results have to be related to other photoprotective mechanisms occurring within the alga for daily and seasonal acclimation. The regulation of light harvesting as the photoprotection of PSII is essential to balance the absorption and utilization of light energy and to avoid photodamage of the photosynthetic apparatus by reactive oxygen species namely photo-oxidative damages under excessive light (Jahns and Holzwarth, 2012; Müller et al., 2001)

Pigment acclimation The irradiance has a pronounced effect on the overall algal pigment composition as previously observed (Lewey and Gorham, 1984; Talarico and Maranzana, 2000; Zubia et al., 2014). The evolution of major photosynthetic pigments (chlorophyll *a* for *G. vermiculophylla* and chlorophyll *a* and *c* and fucoxanthin for *S. muticum*)

showed a similar pattern in both seaweed species with a decrease in their contents in summer compared to winter for most of the tested pigments. Fucoxanthin is known to function efficiently as a primary photosynthetic antenna pigment in marine algae (Katoh et al., 1991). This result could be explained by either a dilution of the pigment due to the growth of the algal thallus during spring and summer periods, or the photobleaching of the pigments due to high lights (quantity of light and longer days) during the summer. However, this is not the case for phycobiliproteins in *G. vermiculophylla*, which contents did not evolve between the two sampling seasons. Under light-limiting conditions, accumulation of chlorophylls leading to higher chlorophyll concentration can improve light absorption and constituted a competitive optimization of photosynthetic efficiency under light limiting conditions in brown and red macroalgae (Delebecq et al., 2013; Miller et al., 2006; Roleda et al., 2012). On the contrary, under excessive irradiance as it can be observed during summer conditions, lower chlorophyll concentrations induce lower level of photon capture preventing photo-oxidative stress (Roleda et al., 2012). This seasonal acclimation in light harvesting can also consist in the photoprotection in *G. vermiculophylla* but also in *S. muticum*.

Additionnally, photo-protective pigments such as some carotenoids which are well known to play a key role in the photoprotection of PSII reaction centres of plants and most of algae (Demmig-Adams and Adams, 1996; Jahns and Holzwarth, 2012) have contrasted evolution in both species: in *S. muticum*, there was an increase in antheraxanthin, zeaxanthin and b-carotene contents but a decrease in violaxanthin level in summer compared to winter. This decrease could be explained through the setup of the violaxanthin cycle (also called xanthophyll cycle): it consists in a reversible and dynamic light-dependent switch with the conversion of violaxanthin into zeaxanthin via antheraxanthin through successive de-epoxidations under excessive light avoiding photodamage and under low light irradiance the conversion of zeaxanthin into antheraxanthin and finally violaxanthin allowing efficient light harvesting (Jahns et al., 2009; Jahns and Holzwarth, 2012; Müller et al., 2001). Under excessive light conditions, antheraxanthin and zeaxanthin are engaged in thermal energy dissipation (Demmig-Adams and Adams, 1996; Verhoeven et al., 1999) and zeaxanthin prevents photo-oxidative damage of thylakoids membrane being thus an effective antioxidant (Havaux et al., 2007). Although this xanthophyll cycle is mainly a short-

term acclimation process (Brunet et al., 2011), *S. muticum* showed an increase in violaxanthin and zeaxanthin in summer linked to the increase in irradiance level.

In *G. vermiculophylla,* antheraxanthin, zeaxanthin and b-carotene were detected in all samples, but no lutein was observed contrary to results obtained by Roleda et al. (2012) on the same species. However, in Gracilariales, different species presented different carotenoid composition mainly due to the presence or not of lutein and its replacement by zeaxanthin (Andersson et al., 2006; Carnicas et al., 1999; Schubert and García-Mendoza, 2008; Ursi et al., 2003; Vershinin and Kamnev, 2009) the accumulation of zeaxanthin being probably an acclimation response to light stress in the Gracilariales (Schubert et al., 2006). The different environmental conditions surrounding the thalli of *G. vermiculophylla* may explain the different carotenoid composition observed in both studies (Roleda et al. 2012 and our study). Contrary to *S. muticum*, no violaxanthin was detected in *G. vermiculophylla* at any sampling time, and a reduction in antheraxanthin, zeaxanthin and b-carotene contents was observed in summer compared to winter. Although the occurrence of an operative xanthophyll cycle in red algae is still under debate (Goss and Jakob, 2010; Marquardt and Hanelt, 2004; Raven, 2011), a shorter version of the xanthophyll cycle has already been observed in two other *Gracilaria* species (*G. gracilis* and *G. multipartita*; (Rmikil et al., 1996). In this cycle, the light stress induced the conversion of antheraxanthin into zeaxanthin and the opposite under low light. Moreover, the three xanthophylls involved into the violaxanthin-cycle have been observed in other red seaweeds and their regulation or not in response to light stress differed between studies (Andersson et al., 2006; Marquardt and Hanelt, 2004; Ursi et al., 2003).

The contrasted seasonal evolution in carotenoid contents between the *S. muticum* and *G. vermiculophylla* could also be explained by the different environmental conditions they both be exposed: *S. muticum* thalli were living in rock pools and were thus still immerged during low tide while *G. vermiculophylla* was lying on the mud exposed to air for more than 7 hours during spring tides. Sampath-Wiley et al. (2008) showed a high impact of emersion on carotenoid contents of the red macroalga *Porphyra umbilicalis*, with a higher content in emerged compared to submersed thalli. Even though carotenoids seem being involved in photoprotection in the red algae the mechanisms of their involvement are still unknown (Schubert and García-Mendoza, 2008).

During a spring tide, no significant evolution of pigments has been observed with the exception of zeaxanthin increase in *S. muticum* along a tide course in summer. The lack of formation of antheraxanthin and zeaxanthin during NPQ occurring in winter tide course indicated no adjustment of light harvesting complex in this brown macroalga. This could suggest a non-efficient thermal dissipation of excessive light energy at a spring tide scale in winter conditions or other thermal dissipation processes would occur within the alga. Moreover, the reconversion of zeaxanthin and antheraxanthin to violaxanthin recovery was considered as the first component of the recovery process, as demonstrated on kelp species (Delebecq et al., 2011). In contrast, during summer spring tide course, *S. muticum* exhibited the formation of zeaxanthin showing the regulation of photoprotective antenna of PSII without the necessity of dynamic NPQ. No tide course acclimation was observed for *G. vermiculophylla* whatever the considered season and even if NPQ conditions occurred during summer tide course. At the opposite, *Porphyra umbilicalis* living on the upper shore showed an increase in carotenoids and antioxidant in summer compared to winter and also a drastic change during emersion over a tide course suggesting the primary role of carotenoids as being an antioxidant (Sampath-Wiley et al. 2008).

Oxidative stress Additionally, the increase in MDA content in *S. muticum* indicated higher level of lipid peroxidation induced mainly by ROS under stressful conditions such as excessive irradiance levels. Also, the increase in SOD activity during winter spring tide illustrated the activation of antioxidant defenses (Lesser, 2006). In the literature, it was shown that oxidative stress generating the increase in ROS production could also induce an increase in lipid peroxidation as well as a decrease in the PSII photosynthetic efficiency (Collén and Davison, 1999) as shown in this study for *S. muticum* during winter spring tide. MDA content as SOD activity may also comfort the hypothesis of chronic deleterious photo-inhibition that could occur in *S. muticum* during winter spring tide. Indeed, higher levels of lipid peroxidation occurring in winter compared to summer as the increase in SOD activity during winter tide course suggested that field conditions generated an oxidative stress for *S. muticum*. On another way, *G. vermiculophylla* exhibited lower SOD activities in summer and no differential MDA content was visible between seasons with no acclimation during tide course. These results suggested that NPQ occurring during summer tide course may be dynamic NPQ with no generation of photo-oxidative stress. Thus, the lack of variation of

pigment with tide and especially of accessory pigment (Betancor et al., 2015) as the lack of apparent oxidative stress during tide courses, illustrated the well adaptation of *G. vermiculophylla* to Brittany saltmarshes relative to *S. muticum* to Brittany rockpools, the former being more resistant to stressful light conditions combined to winter temperatures. Interestingly, these findings completed results obtained by Baer and Stengel (2010). These authors illustrated the heterogeneity of *S. muticum* ecology and physiology between rocky habitats with a slower growth and lower biomass of tide pool thalli compared to open shore thalli, despite similar seasonal reproduction and seasonal pattern of photosynthetic activity (Baer and Stengel, 2010). These results may indicate a possible lower invasive potential of *S. muticum* when macroalgae develop in tide pools on intertidal rocky shores compared to the subtidal zone due to a contrasted acclimation to these two environments.

To conclude, as photosynthesis consists in physiological mechanisms at the basis of plant including algae, photosynthetic efficiency in the field is an important factor determining growth rates and in fine abundance patterns within seaweeds (Saroussi and Beer, 2007) independently of external biotic factors as herbivory or abiotic factors as exceptionally climatic events. Thus, further *in situ* experimental studies have to be ongoing on differential physiological and photosynthetic acclimations of invasive macroalgae through their distribution range and especially at their extremes for a deeper understanding of their abundance patterns as their invasive potential.

Acknowledgments This study is part of the PhD thesis carried out by the first author within the Laboratoire des Sciences de l'Environnement Marin (LEMAR UMR6539) set at the IUEM (UBO-UEB) under the supervision of the last author. It was supported by the Ministère de l'Education Nationale, de l'Enseignement Supérieur et de la Recherche (UBO allocation for the first author) and the Région Bretagne (ARED LabEx Mer). This study was co-financed with the support of the European Union ERDF – Atlantic Area Program and the French ANR and related to the research project INVASIVES (Era-net Seas-era, 2012–2016).

References

Andersson, M., Schubert, H., Pedersén, M., Snoeijs, P., 2006. Different patterns of carotenoid composition and photosynthesis acclimation in two tropical red algae. Mar. Biol. 149, 653–665.

Baer, J., Stengel, D.B., 2010. Variability in growth, development and reproduction of the non-native seaweed *Sargassum muticum* (Phaeophyceae) on the Irish west coast. Estuar. Coast. Shelf Sci. 90, 185–194.

Beer, S., Axelsson, L., 2004. Limitations in the use of PAM fluorometry for measuring photosynthetic rates of macroalgae at high irradiances. Eur. J. Phycol. 39, 1–7.

Betancor, S., Domínguez, B., Tuya, F., Figueroa, F.L., Haroun, R., 2015. Photosynthetic performance and photoprotection of *Cystoseira humilis* (Phaeophyceae) and Digenea simplex (Rhodophyceae) in an intertidal rock pool. Aquat. Bot. 121, 16–25.

Bradford, M.M., 1976. A rapid and sensitive method for the quantitation of microgram quantities of protein utilizing the principle of protein-dye binding. Anal. Biochem. 72, 248–254.

Brunet, C., Johnsen, G., Lavaud, J., Roy, S., 2011. Pigments and photoacclimation processes, in: Phytoplankton Pigments: Characterization, Chemotaxonomy and Applications in Oceanography.

Carnicas, E., Jiménez, C., Niell, F.X., 1999. Effects of changes of irradiance on the pigment composition of *Gracilaria tenuistipitata* var. liui Zhang et Xia. J. Photochem. Photobiol. B 50, 149–158.

Collén, J., Davison, I.R., 1999. Reactive oxygen production and damage in intertidal *Fucus spp.* (Phaeophyceae). J. Phycol. 35, 54–61.

Connan, S., Stengel, D.B., 2011. Impacts of ambient salinity and copper on brown algae: 1. Interactive effects on photosynthesis, growth, and copper accumulation. Aquat. Toxicol. 104, 94–107.

Davidson, A.M., Jennions, M., Nicotra, A.B., 2011. Do invasive species show higher phenotypic plasticity than native species and, if so, is it adaptive? A meta-analysis. Ecol. Lett. 14, 419–431.

Delebecq, G., Davoult, D., Menu, D., Janquin, M.-A., Dauvin, J.-C., Gevaert, F., 2013. Influence of local environmental conditions on the seasonal acclimation process and the daily integrated production rates of *Laminaria digitata* (Phaeophyta) in the English Channel. Mar. Biol. 160, 503–517.

Delebecq, G., Davoult, D., Menu, D., Janquin, M.-A., Migné, A., Dauvin, J.-C., Gevaert, F., 2011. In situ photosynthetic performance of *Laminaria digitata* (Phaeophyceae) during spring tides in Northern Brittany. CBM-Cah. Biol. Mar. 52, 405.

Demmig-Adams, B., Adams, W.W., 1996. The role of xanthophyll cycle carotenoids in the protection of photosynthesis. Trends Plant Sci. 1, 21–26.

Dumay, J., Clément, N., Morançais, M., Fleurence, J., 2013. Optimization of hydrolysis conditions of *Palmaria palmata* to enhance R-phycoerythrin extraction. Bioresour. Technol. 131, 21–27.

Eggert, A., 2012. Seaweed responses to temperature, in: Wiencke, C., Bischof, K. (Eds.), Seaweed Biology, Ecological Studies. Springer Berlin Heidelberg, pp. 47–66.

Enríquez, S., Borowitzka, M.A., 2010. The Use of the fluorescence signal in studies of seagrasses and macroalgae, in: Suggett, D.J., Prášil, O., Borowitzka, M.A. (Eds.), Chlorophyll a fluorescence in aquatic sciences: Methods and Applications, Developments in Applied Phycology. Springer Netherlands, pp. 187–208.

Esterbauer, H., Cheeseman, K.H., 1990. [42] Determination of aldehydic lipid peroxidation products: Malonaldehyde and 4-hydroxynonenal, in: Enzymology, B.-M. in (Ed.), Oxygen Radicals in Biological Systems Part B: Oxygen Radicals and Antioxidants. Academic Press, pp. 407–421.

Genty, B., Briantais, J.-M., Baker, N.R., 1989. The relationship between the quantum yield of photosynthetic electron transport and quenching of chlorophyll fluorescence. Biochim. Biophys. Acta BBA - Gen. Subj. 990, 87–92.

Gevaert, F., Creach, A., Davoult, D., Holl, A.-C., Seuront, L., Lemoine, Y., 2002. Photo-inhibition and seasonal photosynthetic performance of the seaweed *Laminaria saccharina* during a simulated tidal cycle: chlorophyll fluorescence measurements and pigment analysis. Plant Cell Environ. 25, 859–872.

Gevaert, F., Creach, A., Davoult, D., Migne, A., Levavasseur, G., Arzel, P., Holl, A., Lemoine, Y., 2003. *Laminaria saccharina* photosynthesis measured in situ: photoinhibition and xanthophyll cycle during a tidal cycle. Mar. Ecol. Prog. Ser. 247, 43–50.

Godoy, O., Valladares, F., Castro-Díez, P., 2011. Multispecies comparison reveals that invasive and native plants differ in their traits but not in their plasticity. Funct. Ecol. 25, 1248–1259.

Gomez, I., Lopez-Figueroa, F., Ulloa, N., Morales, V., Lovengreen, C., Huovinen, P., Hess, S., 2004. Patterns of photosynthesis in 18 species of intertidal macroalgae from southern Chile. Mar. Ecol. Prog. Ser. 270, 103–116.

Goss, R., Jakob, T., 2010. Regulation and function of xanthophyll cycle-dependent photoprotection in algae. Photosynth. Res. 106, 103–122.

Gulbransen, D.J., Thomsen, M.S., McGlathery, K.J., 2013. A global perspective on the *Gracilaria vermiculophylla* invasion: What is currently known and what is still needed. *Gracilaria vermiculophylla* Va. Coast. Bays Doc. Distrib. Eff. Non-Native Species 151.

Häder, D.-P., Porst, M., Herrmann, H., Schäfer, J., Santas, R., 1997. Photosynthesis of the mediterranean green alga *Caulerpa prolifera* measured in the field under solar irradiation. J. Photochem. Photobiol. B 37, 66–73.

Häder, D.-P., Porst, M., Lebert, M., 2001. Photosynthetic performance of the Atlantic brown macroalgae, *Cystoseira abies-marina*, *Dictyota dichotoma* and *Sargassum vulgare*, measured in Gran Canaria on site. Environ. Exp. Bot. 45, 21–32.

Hanelt, D., Wiencke, C., Bischof, K., 2003. Photosynthesis in marine macroalgae, in: Larkum, A.W.D., Douglas, S.E., Raven, J.A. (Eds.), Photosynthesis in algae, Advances in Photosynthesis and Respiration. Springer Netherlands, pp. 413–435.

Hanelt, D., Huppertz, K., Nultsch, W., 1993. Daily course of photosynthesis and photoinhibition in marine macroalgae investigated in the laboratory and field. Mar. Ecol. Prog. Ser. Oldendorf 97, 31–37.

Havaux, M., Dall'Osto, L., Bassi, R., 2007. Zeaxanthin has enhanced antioxidant capacity with respect to all other xanthophylls in *Arabidopsis* leaves and functions independent of binding to PSII antennae. Plant Physiol. 145, 1506–1520.

Henkel, S.K., 2008. Response to environmental stressors in native and invasive kelp species. ProQuest.

Hu, Z.-M., Juan, L.-B., 2013. Adaptation mechanisms and ecological consequences of seaweed invasions: a review case of agarophyte *Gracilaria vermiculophylla*. Biol. Invasions 16, 967–976.

Huang, Q.Q., Pan, X.Y., Fan, Z.W., Peng, S.L., 2015. Stress relief may promote the evolution of greater phenotypic plasticity in exotic invasive species: a hypothesis. Ecol. Evol. 5, 1169–1177.

Jahns, P., Holzwarth, A.R., 2012. The role of the xanthophyll cycle and of lutein in photoprotection of photosystem II. Biochim. Biophys. Acta BBA - Bioenerg., Photosystem II 1817, 182–193.

Jahns, P., Latowski, D., Strzalka, K., 2009. Mechanism and regulation of the violaxanthin cycle: The role of antenna proteins and membrane lipids. Biochim. Biophys. Acta BBA - Bioenerg. 1787, 3–14.

Katoh, T., Nagashima, U., Mimuro, M., 1991. Fluorescence properties of the allenic carotenoid fucoxanthin: Implication for energy transfer in photosynthetic pigment systems. Photosynth. Res. 27, 221–226.

Lande, R., 2015. Evolution of phenotypic plasticity in colonizing species. Mol. Ecol. 24, 2038–2045.

Lesser, 2006. Oxidative stress in marine environments: Biochemistry and Physiological Ecology. Annu. Rev. Physiol. 68, 253–278.

Lewey, S.A., Gorham, J., 1984. Pigment composition and photosynthesis in *Sargassum muticum*. Mar. Biol. 80, 109–115.

Lowry, O.H., Rosebrough, N.J., Farr, A.L., Randall, R.J., 1951. Protein measurement with the Folin phenol reagent. J Biol Chem 193, 265–275.

Marquardt, J., Hanelt, D., 2004. Carotenoid composition of *Delesseria lancifolia* and other marine red algae from polar and temperate habitats. Eur. J. Phycol. 39, 285–292.

Maxwell, K., Johnson, G.N., 2000. Chlorophyll fluorescence—a practical guide. J. Exp. Bot. 51, 659–668.

Meudec, A., 2006. Exposition au fioul lourd chez *Salicornia fragilis* Ball et Tutin: contamination chimique par les HAPs et réponses biologiques de la plante. Brest.

Migné, A., Delebecq, G., Davoult, D., Spilmont, N., Menu, D., Gévaert, F., 2015. Photosynthetic activity and productivity of intertidal macroalgae: In situ measurements, from thallus to community scale. Aquat. Bot. 123, 6–12.

Miller, S.M., Wing, S.R., Hurd, C.L., 2006. Photoacclimation of *Ecklonia radiata* (Laminariales, Heterokontophyta) in Doubtful Sound, Fjordland, Southern New Zealand. Phycologia 45, 44–52.

Müller, P., Li, X.-P., Niyogi, K.K., 2001. Non-photochemical quenching. A response to excess light energy. Plant Physiol. 125, 1558–1566. doi:10.1104/pp.125.4.1558

Munier, M., Jubeau, S., Wijaya, A., Morançais, M., Dumay, J., Marchal, L., Jaouen, P., Fleurence, J., 2014. Physicochemical factors affecting the stability of two pigments: R-phycoerythrin of *Grateloupia turuturu* and B-phycoerythrin of *Porphyridium cruentum*. Food Chem. 150, 400–407.

Nejrup, L.B., Pedersen, M.F., Vinzent, J., 2012. Grazer avoidance may explain the invasiveness of the red alga *Gracilaria vermiculophylla* in Scandinavian waters. Mar. Biol. 159, 1703–1712.

Raven, J.A., 2011. The cost of photoinhibition. Physiol. Plant. 142, 87–104.

Richard, G., Le Bris, C., Guérard, F., Lambert, C., Paillard, C., 2015. Immune responses of phenoloxidase and superoxide dismutase in the manila clam *Venerupis philippinarum* challenged with *Vibrio tapetis* – Part II: Combined effect of temperature and two *V. tapetis* strains. Fish Shellfish Immunol. 44, 79–87.

Rmikil, N.-E., Brunet, C., Cabioch, J., Lemoine, Y., 1996. Xanthophyll-cycle and photosynthetic adaptation to environment in macro-and microalgae. Hydrobiologia 326, 407–413.

Roleda, M.Y., Nyberg, C.D., Wulff, A., 2012. UVR defense mechanisms in eurytopic and invasive *Gracilaria vermiculophylla* (Gracilariales, Rhodophyta). Physiol. Plant. 146, 205–216.

Rueness, J., 2005. Life history and molecular sequences of *Gracilaria vermiculophylla* (Gracilariales, Rhodophyta), a new introduction to European waters. Phycologia 44, 120–128.

Sagert, S., Forster, R.M., Feuerpfeil, P., Schubert, H., 1997. Daily course of photosynthesis and photoinhibition in *Chondrus crispus* (Rhodophyta) from different shore levels. Eur. J. Phycol. 32, 363–371.

Sampath-Wiley, P., Neefus, C.D., Jahnke, L.S., 2008. Seasonal effects of sun exposure and emersion on intertidal seaweed physiology: Fluctuations in antioxidant contents, photosynthetic pigments and photosynthetic efficiency in the red alga *Porphyra umbilicalis* Kützing (Rhodophyta, Bangiales). J. Exp. Mar. Biol. Ecol. 361, 83–91.

Saroussi, S., Beer, S., 2007. Alpha and quantum yield of aquatic plants derived from PAM fluorometry: Uses and misuses. Aquat. Bot. 86, 89–92.

Schmid, M., Stengel, D.B., 2015. Intra-thallus differentiation of fatty acid and pigment profiles in some temperate Fucales and Laminariales. J. Phycol. 51, 25–36.

Schubert, N., García-Mendoza, E., 2008. Photoinhibition in red algal species with different carotenoid profiles. J. Phycol. 44, 1437–1446.

Schubert, N., García-Mendoza, E., Pacheco-Ruiz, I., 2006. Carotenoid composition of marine red algae. J. Phycol. 42, 1208–1216.

Sokal, R.R., Rohlf, F.J., 1995. Biometry: The principles and practice of statistics in biological research.

Stiger-Pouvreau, V., Thouzeau, G., 2015. Marine species introduced on the French Channel-Atlantic coasts: A review of main bbiological invasions and impacts. Open J. Ecol. 05, 227–257.

Sun, L., Wang, S., Gong, X., Zhao, M., Fu, X., Wang, L., 2009. Isolation, purification and characteristics of R-phycoerythrin from a marine macroalga *Heterosiphonia japonica*. Protein Expr. Purif. 64, 146–154.

Talarico, L., Maranzana, G., 2000. Light and adaptive responses in red macroalgae: an overview. J. Photochem. Photobiol. B 56, 1–11.

Tanniou, A., 2014. Etude de la production de biomolécules d'intérêt (phlorotannins, pigments, lipides) par l'algue brune modèle *Sargassum muticum* par des approches combinées de profilage métabolique et d'écophysiologie.

Ursi, S., Pedersén, M., Plastino, E., Snoeijs, P., 2003. Intraspecific variation of photosynthesis, respiration and photoprotective carotenoids in *Gracilaria birdiae* (Gracilariales: Rhodophyta). Mar. Biol. 142, 997–1007.

Van Kooten, O. van, Snel, J.F.H., 1990. The use of chlorophyll fluorescence nomenclature in plant stress physiology. Photosynth. Res. 25, 147–150.

Verhoeven, A.S., Adams, W.W., Demmig-Adams, B., Croce, R., Bassi, R., 1999. Xanthophyll cycle pigment localization and dynamics during exposure to low temperatures and light stress in: Vinca major. Plant Physiol. 120, 727–738.

Vershinin, A.O., Kamnev, A.N., 2009. Xanthophyll cycle in marine macroalgae. Bot. Mar. 39, 421–426.

Wang, Y., Qu, T., Zhao, X., Tang, Xianghai, Xiao, H., Tang, Xuexi, 2016. A comparative study of the photosynthetic capacity in two green tide macroalgae using chlorophyll fluorescence. SpringerPlus 5, 775.

Xiao, X., Bettignies, T. de, Olsen, Y.S., Agusti, S., Duarte, C.M., Wernberg, T., 2015. Sensitivity and acclimation of three canopy-forming seaweeds to UVB radiation and warming. PLOS ONE 10, e0143031.

Zanolla, M., Altamirano, M., Carmona, R., Rosa, J.D.L., Sherwood, A., Andreakis, N., 2015. Photosynthetic plasticity of the genus *Asparagopsis* (Bonnemaisoniales, Rhodophyta) in response to temperature: implications for invasiveness. Biol. Invasions 17, 1341–1353.

Zubia, M., Freile-Pelegrín, Y., Robledo, D., 2014. Photosynthesis, pigment composition and antioxidant defences in the red alga *Gracilariopsis tenuifrons* (Gracilariales, Rhodophyta) under environmental stress. J. Appl. Phycol. 26, 2001–2010.

Chapitre 4. Quels sont les impacts des espèces invasives sur l'écosystème qu'elles colonisent ?

L'impact des espèces invasives sur les écosystèmes est l'une des préoccupations scientifiques majeures, qu'elles soient animales, végétales ou microbiennes, conduisant à l'étude de la biologie de ces espèces invasives afin de mieux comprendre leur potentiel invasif. Ces impacts peuvent être majeurs et induire des enjeux sociétaux et économiques (Davidson et al., 2015). Ainsi, la problématique des espèces invasives n'est pas restreinte uniquement au domaine scientifique, mais est élargie au domaine sociétal, car de nombreuses questions émanent aussi des citoyens, des élus et acteurs locaux face aux impacts engendrés par la prolifération de certaines espèces invasives.

G. vermiculophylla est une algue plutôt discrète en Rade de Brest du fait de sa couleur foncée et de sa petite taille, qui la rendent peu visible en estran meuble. Elle se confond avec la vase pour un œil non averti et sa présence, quoique notable, est peu remarquée par la société. Cependant, les impacts majeurs sur les écosystèmes, suite à la colonisation des estrans meubles et saumâtres par *G. vermiculophylla* ont été démontrés dans d'autres régions du monde (Hu and Juan, 2013) et ceci à de nombreuses échelles biologiques impliquant même des impacts économiques. En effet en Caroline du Nord (USA), *G. vermiculophylla* est considérée comme une nuisance par son impact sur l'industrie de la pêche (Freshwater et al., 2006).

En Rade de Brest, au sein de la ria du Faou, le tapis de gracilaire est particulièrement étendu, uniforme et épais. Or, avant l'introduction de la gracilaire, les zones de vases molles situées sur la partie la plus basse de la slikke était principalement non végétalisée à l'exception de l'implantation de quelques îlots de la phanérogame *Spartina alterniflora*, et de Fucus… parcemés sur des blocs rocheux. Dans ce contexte, ce travail vise à étudier les impacts de la colonisation de la slikke nue par *G. vermiculophylla* sur le métabolisme de l'écosystème benthique, sur la diversité spécifique et sur l'abondance de la macrofaune et méiofaune benthique, ainsi que sur le réseau trophique au niveau de la Ria du Faou, à l'échelle des saisons et ce durant une année.

Cette partie est rédigée sous forme d'une publication, à laquelle j'ai contribuée en participant à l'ensemble des expérimentations *in situ* de mesure du métabolisme benthique (par l'expérimentation de mesures de flux de CO_2 dans des cloches benthiques) et en réalisant plus particulièrement les prélevements et les dosages de chlorophylle.

Manuscrit en cours de soumission

Effects of *Gracilaria vermiculophylla* invasion on estuarine-mudflat functioning and diversity

D. Davoult*[1], G. Surget[2,3], V. Stiger-Pouvreau[2,3], F. Noisette[1], P. Riera[1], D. Stagnol[1], T. Androuin[1] & N. Poupart[2,3]

[1] Sorbonne Universités, UPMC Univ Paris 6, CNRS, UMR 7144, Station Biologique de Roscoff, 29680 Roscoff, France

[2] Université de Bretagne Occidentale, Institut Universitaire Européen de la Mer, 29280 Plouzané, France

[3] CNRS, UMR 6539 LEMAR-IUEM-UBO, Institut Universitaire Européen de la Mer, 29280 Plouzané, France

*davoult@sb-roscoff.fr

Abstract The invasive Japanese seaweed *Gracilaria vermiculophylla* has established for several years in numerous European estuaries from Portugal to Norway. In several French estuaries, it forms dense populations at the mud surface. The effects of *G. vermiculophylla* on metabolism, diversity and food web have been studied in the Faou estuary (48.295°N-4.179°W, Brittany, France). Community gross primary production (GPP) and respiration (CR) during emersion, chlorophyll-a content, macrofauna and meiofauna diversity and abundance, stable isotopes (δ13C and δ15N) of representative macrofauna and main food sources have been measured at low tide in winter, spring, summer 2014 and winter 2015. Results highlighted significant seasonal variations in GPP and CR. Moreover, GPP was significantly higher where *G. vermiculophylla* was present than on controls (bare mud). However, this high GPP appeared to be linked to the biomass increase of primary producers, their efficiency (primary productivity, i.e. assimilation number) remaining quite stable compared to the control area. Significant variations in abundance of meiofauna and macrofauna were also detected and new epifaunal species were collected, mainly on colonized areas. Isotopic food web Bayesian mixing models strongly suggested the dominant role of *G. vermiculophylla* in the diet of some dominant species. Mechanisms interacting with functioning and diversity of the mud flat are discussed. Finally, the invasive seaweed *G. vermiculophylla* impacted the mudflat ecosystem as a new primary producer (increase of metabolism), a habitat-forming species (changes in diversity and abundance of macrofauna and meiofauna) and a new abundant food source, probably through detrital pathway.

Key-words Invasive – Non-indigenous species – Red alga – Metabolism – Food web – Macrofauna diversity – Meiofauna diversity – Engineer species

Introduction

Among reported marine non-indigenous species (NIS), numerous are macroalgae (Schaffelke et al. 2006). As some of them may act as foundation species (Dayton 1972; Ellison et al. 2005) or ecosystem engineers (Jones et al. 1994, 1997), they are considered to be able to deeply alter structure and functioning of local communities, by changing abiotic conditions (Jones et al. 1997), local diversity (Wallentinus and Nyberg 2007 and references therein) and food webs (Hastings et al. 2007). These changes are generally reported to affect negatively indigenous species (Levine et al. 2003), even if some positive effects may also occur (Crooks 2002). Main macroalgal introductions have been reported on rocky shores and are studied as potential space competitors for native seaweeds (Schaffelke and Hewitt 2007 and references therein). Less frequently, non-indigenous seaweeds may also colonize biotopes originally without or with almost no macroalgae, that is the case for the perennial red seaweed *Gracilaria vermiculophylla* (Ohmi) Papenfuss, now reported on the north Atlantic west and east coasts (Freshwater et al. 2006; Thomsen et al. 2007, 2009) and especially along the French Atlantic coasts (Stiger-Pouvreau and Thouzeau 2015). This species, originated from East Asia, is reported in Europe from Norway to Portugal (Rueness 2005; Hammann et al. 2013 and references therein), probably first in France in the vicinity of oyster farms (Mollet et al. 1998). The presence of *G. vermiculophylla* on mudflats on the northeastern coasts of United States seems to be linked or, at least, facilitated by the presence of the tube-dwelling worm *Diopatra cuprea*, used as substratum for fixation (Wright et al. 2014). However, the settlement of *G. vermiculophylla* seems to occurr on French mudflats without having to attach on a (even small) hard substratum (Surget, pers. comm.).

For more than 10 years, it has been considered as an occasional species, without effect on ecosystems (Martinez-Lüscher and Holmer 2010). Currently, It is now broadly distributed on estuarine ecosystems where it visibly constitutes a habitat-forming species at the surface of mud. *G. vermiculophylla* can be now considered as invasive because it stats to occupy a large part of colonized mudflats (Figure 1). It also represents a new benthic primary producer on the mudflat, microphytobenthos being the only one until this invasion.

The expansion of the species is monitored in 3 estuaries of the Bay of Brest since 2013 (Surget, unpubl. data). A study on the impact of *G. vermiculophylla* was performed from February 2014 to January 2015 on one of them, the Faou estuary. The aim was to understand whether this new primary producer in mud previously colonized only by microphytobenthos, (1) is significantly modifying the mudflat metabolism (primary production and respiration), (2) as a habitat-forming species, is significantly modifying the diversity and abundance of the benthic community (macrofauna and meiofauna), and (3) as a new biomass supplier, is significantly modifying the macrobenthic food web.

Materials and Methods

All samplings and measurements have been performed during low tide at the same dates in February, May, September 2014, and January 2015 in the Faou estuary (48.295°N-4.179°W, Brittany, France) (Figure 1). The part of the mudflat colonized by *Gracilaria vermiculophylla* will be referred in the text and figures as ***Gracilaria*** and the one characterized by bare sediment will be referred as **mud** and used as a control.

Ecosystem metabolism Ecosystem metabolism was measured during low tide by using three 0.071-m^2 benthic chambers to estimate CO2 fluxes at the air-sediment interface using the method described in Migné et al. (2002). Sediment was enclosed down to 10-cm depth. Changes in air CO2 concentration (ppm) in the benthic chamber (10 L) were measured with an infrared gas analyser (LiCor Li-820) for 10-15 min. CO2 concentrations were recorded in a data logger (LiCor Li-1400) with a 5 s frequency. CO2 flux was calculated as the slope of the linear regression of CO2 concentration (µmol mol^{-1}) against time (min) and expressed in mgC m^{-2} h^{-1} assuming a molar volume of 22.4 L at standard temperature and pressure. Transparent chambers were used to estimate the net benthic community production (NCP), balance between community gross primary production (CGP) and the community respiration (CR). Opaque chambers were used to estimate the community respiration (CR). During light incubations, incident photosynthetically available radiation (PAR, 400-700 nm) was monitored with a LiCor SA-190 quantum sensor. At each occasion, 3 replicates were performed on ***Gracilaria*** and on **mud**, considered as a control. Considering the low number of replicates and the absence of homoscedasticity even after metric transformation, we used the non-parametric Scheirer-Ray-Hare test, that is the non-parametric equivalent of a two-

way ANOVA, on dates (n = 4) and substrata (bare mud as control and *G. vermiculophylla*-colonized area, n = 2).

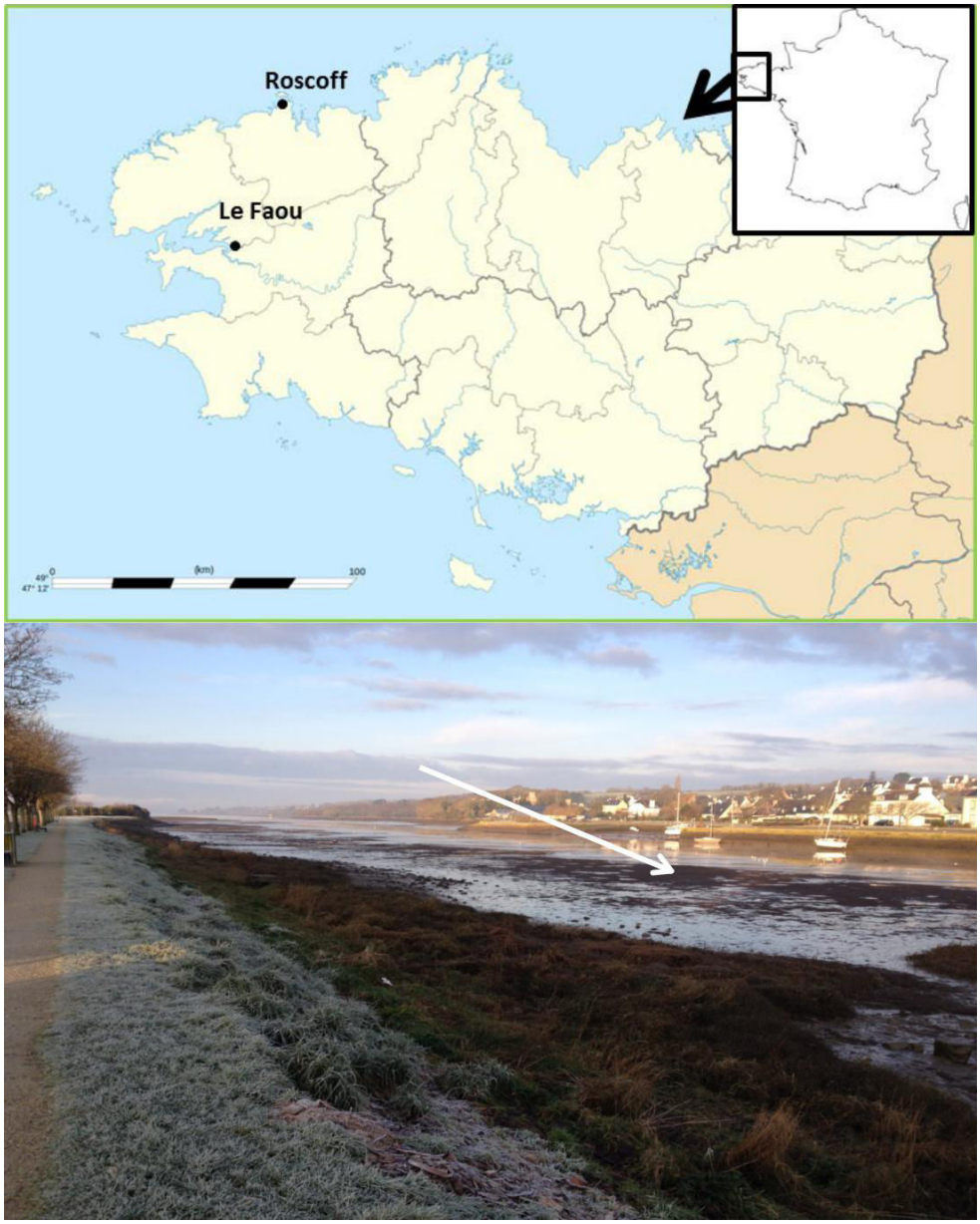

Fig. 1 Location of the studied site in Le Faou estuary. *Gracilaria vermiculophylla* occupying more than 50% of the mudflat

Chlorophyll a Four replicates of 1.96 cm^2 and 1 cm depth were sampled within each benthic chamber at each sampling date during the low tide. Samples were kept cool in darkness until the return to the laboratory where they were stored at -24°C until analysis. Fresh ***Gracilaria*** and **mud** samples were grinded 30 sec in pure acetone (5 mL), placed in the

dark at 4°C during at least 4 hours and centrifuged (4°C, 3500 rpm, Eppendorf Centrifuge 5810R) to extract chlorophyll a. Chlorophyll a contents (Chl a) were determined on homogenized supernatant by spectrophotometry according to the trichromatic method of Jeffrey and Humphrey (1975). In microplates (UVStar F-Bottom, Greiner Bio-one), optical density (DO) of 200 µL samples was read at 630, 647, 664 and 750 nm with a POLARstar Omega spectrophotometer (BMG Labtech). Chlorophyll a contents were calculated using the following equation and expressed in $mg.m^{-2}$:

Chl a ($mg.m^{-2}$) = 50 × [11.85 × (DO664 - DO750) - 1.54 × (DO647 - DO750) - 0.08 × (DO630 -DO750)] / 1.96

Data were also analyzed with the Scheirer-Ray-Hare test

Macro- and meiobenthos At each occasion, three 0.1-m^2 quadrats were sampled on ***Gracilaria*** and three other ones on **mud** for macrofauna identification. Samples were sieved in the field on 1-mm mesh size, stored in 4% salted and buffered formalin in the lab. Individuals were identified at the specific level and counted.

Three replicates (1.77 cm^2, 2-cm deep) were also collected on ***Gracilaria*** and three other ones on **mud**, and sieved on 40-µm mesh size. Individuals of the meiofauna were identified, belonging to the 10 following categories: nematodes, Platyhelminthes, interstitial Polychaetes, Oligochaetes, harpacticoid Copepods, Ostracods, Halacarids, Foraminifers, Gastropods and Bivalves. Considering the low number of replicates and the absence of homoscedasticity even after metric transformation, we used the non-parametric Scheirer-Ray-Hare test.

Food web Sample collection and preparation: Invertebrates and the main potential organic matter sources from the sampling area were collected at the four sampling occasions. POM (suspended particulate organic matter) from the site was sampled by collecting 2 L of seawater. POM was obtained by filtration on precombusted Whatman GF/F glass fiber membranes within 2 h after collection. Subsequently, membranes were acidified (10% HCl) in order to remove carbonates, briefly rinsed with Milli-Q water, dried (60°C) and kept at -32°C until analysis. Sediment samples were taken by scraping the upper 1 cm of the sediment. For the measurements of δ13C of the sedimented organic matter (SOM), the SOM was acidified (10% HCl) rinsed several times with distilled water, dried (60°C) and ground to

powder (Riera 2010). δ13C measurements were conducted on acidified samples, whereas δ15N ones were conducted on non-acidified samples. As samples of terrestrial organic matter, dead leaves of terrestrial plants largely occurring on the muddy sediment were collected by hand and, back to laboratory, were rinsed with filtered seawater (precombusted GF/F) to clean off epibionts, quickly acidified (10% HCl) to remove any possible residual carbonates, and rinsed with distilled water. The macroalga *Gracilaria vermiculophylla* was also collected by hand and washed with distilled water to remove any attached material. In the sampling area, benthic diatoms occurred only as algal mats during May and September, and could then be extracted for stable isotope analyses. The absence of dense mats of benthic microalgae at the sediment surface in January 2014 and February 2015 may be due to local strong hydrodynamic conditions and frequent stormy weather during winter. When present, benthic diatoms mats were collected at low tide by scraping the surface of the sediment and extracting them according to the method of Riera (2007) for intertidal muddy sediment. Diatoms were then collected on previously combusted glass fiber filters, quickly acidified (10% HCl) and rinsed with distilled water. These samples were then dried (60°C) and kept at -32°C until analysis. Individuals of the Bivalve *Scrobicularia plana*, the Gastropod *Hydrobia ulvae* and the Polychaete *Nereis diversicolor* which are among the most representative microbenthic species of the sampling area were collected by hand at low tide. After collection, specimens kept alive overnight at the laboratory in filtered water from the sampling site to allow evacuation of gut contents. Then, they were killed by freezing. After dissection from the shell for mollusks, the flesh was quickly treated with 10% HCl to remove any carbonate debris and rinsed with distilled water. All individuals were then freeze-dried and ground to a powder using mortar and pestle. *N. diversicolor* specimens were treated in a same way as molluscs. As individuals *H. ulvae* collected were too small, composite samples (4-5 individuals) were combined to obtain sufficient tissue for accurate δ15N and δ13C analyses. Finally, all sample were dried (60°C) and kept frozen (-32°C) until analysis. Samples, crushed with a mortar and a pestle, were then put in tin capsules before mass-spectrometry analyses.

Stable isotopes measurements. Carbon and nitrogen isotope ratios were determined using a Flash EA CN analyser coupled with a Finnigan Delta Plus mass spectrometer, via a Finnigan Con-Flo III interface. Data are expressed in the standard δ unit:

$$\delta X\ (‰) = [(Rsample / Rreference) - 1] \times 103$$

with R = 13C/12C for carbon and 15N/14N for nitrogen. These abundances were calculated in relation to the certified reference materials Vienna Pee Dee Belemnite-limestone (V-PDB) and atmospheric dinitrogen (at-air). The VPDB and at-air scaling were achieved using inhouse protein standards that have been calibrated against NBS-19 and IAEA N3 reference materials. The standard deviation of repeated measurements of δ13C and δ15N values of a laboratory standard was 0.10‰ versus V-PDB and 0.05‰ versus at-air, respectively.

Data analysis. As the number of individuals analysed for each species was not sufficient to satisfy the conditions of normality, non-parametric Kruskal-Wallis tests were carried out. For the food web study, the isotopic values of consumers were pooled since (1) the consumers considered showed close isotopic values in sediments with or without apparent macroalgae (see figure 5) and (2) macroalgae can be considered as equally available as detritus to these consumers within the total sampling area through the important physical reworking and the bioturbation of sediments. The trophic links were then considered for the whole area. The Bayesian mixing model SIAR (Stable Isotope Analysis in R; Parnell et al. 2010) was run to infer the feasible contribution of the sources to the consumers' diet at each sampling occasion. Bayesian statistics have proven to be a powerful tool as they allow models to incorporate the variability in the stable isotope ratios of both sources and consumers, as well as in the isotopic fractionation (Parnell et al. 2010). Trophic enrichment factors ranged from 0.30 ± 0.21‰ for $\delta^{13}C$ and 2.5 ± 0.25‰ for $\delta^{15}N$, corresponding to values for invertebrate species (whole body) as reviewed by Caut et al. (2009).

Results

Ecosystem metabolism (Figure 2) Gross primary production showed strong seasonal variations (Scheirer-Ray-Hare test: H = 17.447, df = 3, $p < 0.001$) and significant differences between ***Gracilaria*** and **mud**, (H = 3.853, df = 1, $p < 0.05$), with GPP values for ***Gracilaria*** being more than twice the ones of **mud** in spring (Figure 2A), but without interaction. The same seasonal trend can be seen for community respiration (H = 18.407, df = 3, $p < 0.001$) but no significant difference appeared between ***Gracilaria*** and **mud** at the year scale (H = 3.203, df = 1, $p > 0.05$) despite the higher CR recorded on ***Gracilaria*** than on **mud** in spring and summer (Figure 2B).

As a consequence, NPP also exhibited strong seasonal variations (H = 17.767, df = 3, p <0.001) but no difference was detected between the two conditions (H = 2.430, df = 1, p >0.05) at the year scale (Figure 2C).

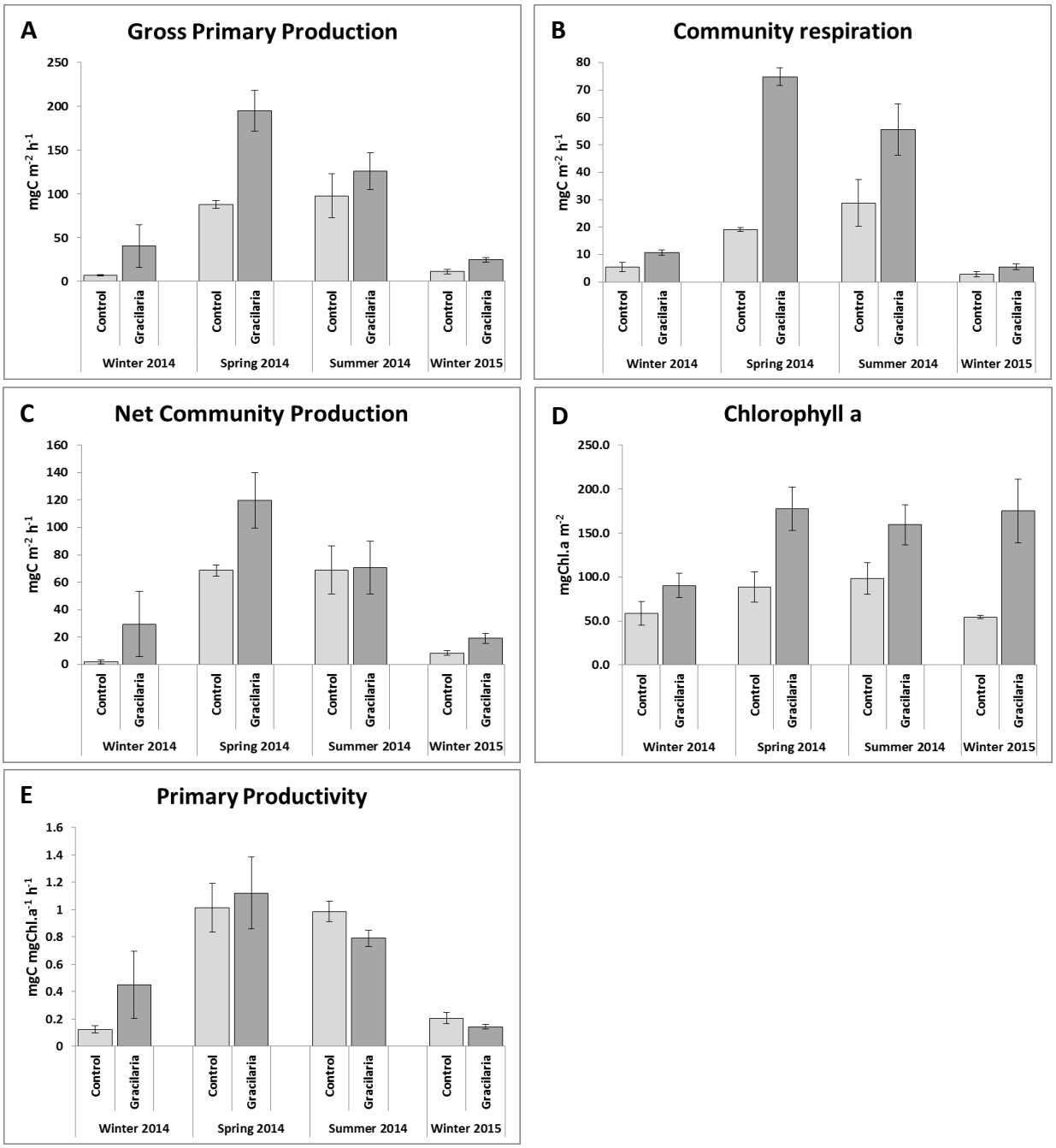

Chlorophyll *a* content was much higher on areas colonized by ***Gracilaria*** (H = 12.813, df = 1, p < 0.001) but no seasonal trend occurred (H = 1.873, df = 3, p > 0.05) and chlorophyll *a* content remained at a high level in winter 2015 on ***Gracilaria*** (Figure 2D). Considering

primary productivity (also called assimilation number) as the ratio between GPP and chlorophyll *a* and expressed in mgC mgChl.a^{-1} h^{-1}, a strong seasonal trend was again highlighted ($H = 17.820$, $df = 3$, $p < 0.001$), with no significant differences ($H = 0.003$, $df = 1$, $p > 0.05$) and very close values between the two conditions at each season (Figure 2E).

Macro- and meiobenthic diversity and abundances (Figures 3 & 4) A total of 5533 macrofaunal individuals belonging to 21 taxa have been collected and identified during the study. The most abundant taxa were the polychaete *Nereis diversicolor* (40.6% of sampled individuals), the gastropod *Hydrobia ulvae* (19.7%), the isopod crustacean *Anthura gracilis* (11.9%), the oligochaetes (9.9%), and the polychaete *Streblospio shrubsolii* (8.2%), this latter only appearing in the last sampling and mainly on the area colonized by ***Gracilaria***.

The number of sampled taxa significantly varied between sampling dates ($H = 11.222$, $df = 3$, $p < 0.05$) but also between the two substratum conditions ($H = 5.026$, $df = 1$, $p < 0.05$), with an important increase in colonized areas (Figure 3A). This increase can be explained by the appearance of species uncommon on mudflats such as epifaunal amphipods (*Jassa marmorata*, *Melita palmata*, *Allomelita pellucida*), decapods (*Pilumnus hirtellus*, *Liocarcinus pusillus*) and polychaetes (tube-dwelling sabellidae and *Streblospio shrubsolii*), mainly found on colonized areas.

Density of macrofauna (Figure 3B) did not exhibit seasonal trend ($H = 5.343$, $df = 3$, $p > 0.05$) but remained higher in colonized areas ($H = 14.313$, $df = 1$, $p < 0.001$). Among abundant taxa, *Nereis diversicolor* (Figure 3C) remained at higher density in colonized areas whatever the season ($H = 14.976$, $df = 1$, $p < 0.001$), as well as *Anthura gracilis* (Figure 3D) ($H = 17.333$, $df = 1$, $p < 0.001$) and oligochaetes (Figure 3E) ($H = 8.316$, $df = 1$, $p < 0.01$).

For meiofauna, a total of 12020 individuals belonging to 10 taxa have been collected during this study. Main taxa were nematodes (83.6% of sampled individuals), harpacticoid copepods (4.9%), Platyhelminthes (3.5%), ostracods (2.5%) and interstitial polychaetes (2.1%). A significant difference occurred for the density (Figure 4A) between dates ($H = 10.800$, $df = 3$, $p < 0.05$) and locations ($H = 7.397$, $df = 1$, $p < 0.01$). Among abundant taxa, the abundance of nematodes (Figure 4B) significantly differed in time ($H = 11.687$, $df = 3$, $p < 0.01$) and space ($H = 6.163$, $df = 1$, $p < 0.05$), as the one of ostracods (Figure 4C; time: $H = 12.718$, $df = 3$, $p < 0.01$; space: $H = 5.572$, $df = 1$, $p < 0.05$). The one of harpacticoid copepods

(Figure 4D) only varied significantly in time (H = 13.058, df = 3, p < 0.01) whereas interstitial polychaetes (Figure 4E) were significantly more abundant in colonized areas (H = 11.519, df = 1, p < 0.001).

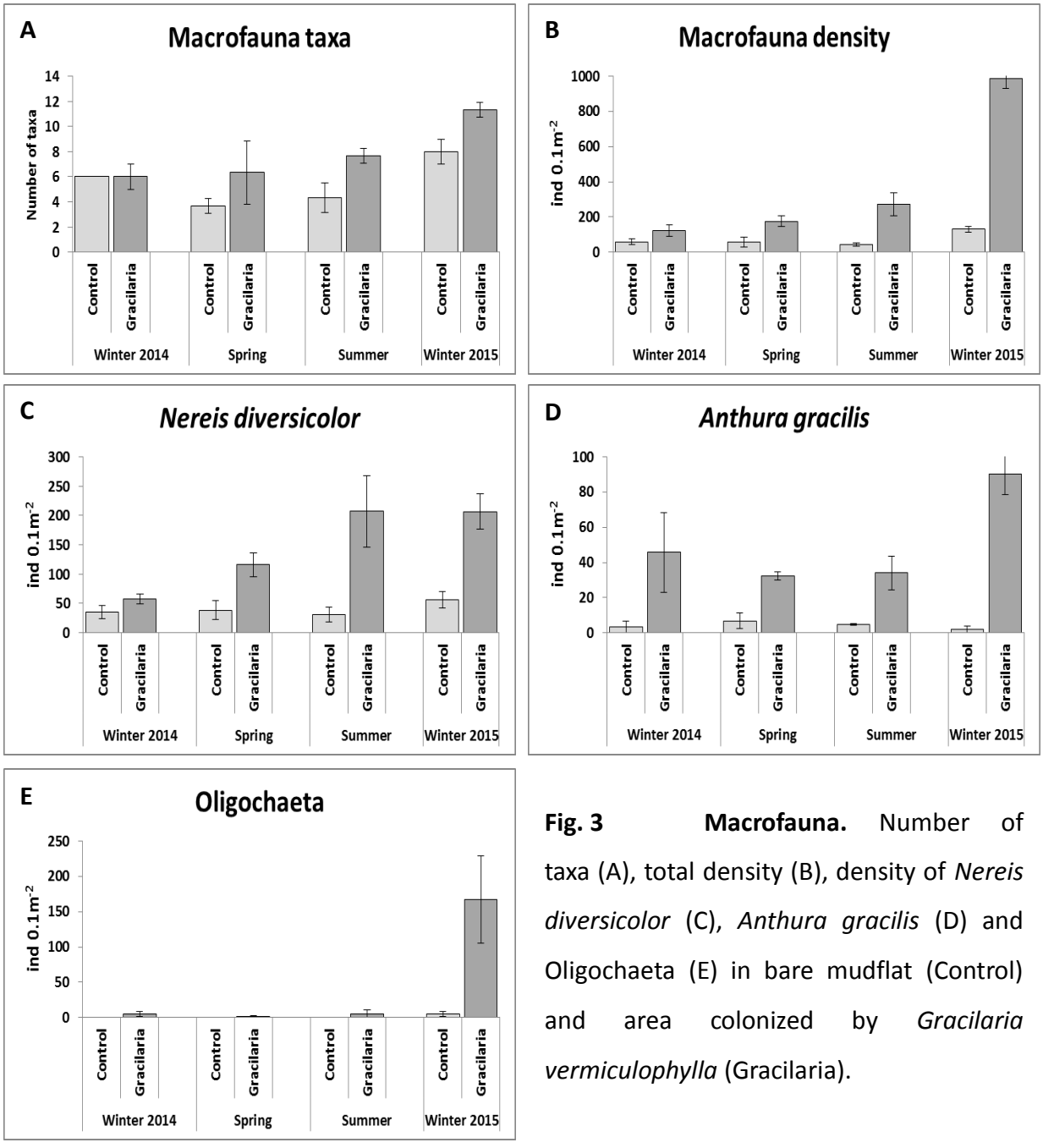

Fig. 3 Macrofauna. Number of taxa (A), total density (B), density of *Nereis diversicolor* (C), *Anthura gracilis* (D) and Oligochaeta (E) in bare mudflat (Control) and area colonized by *Gracilaria vermiculophylla* (Gracilaria).

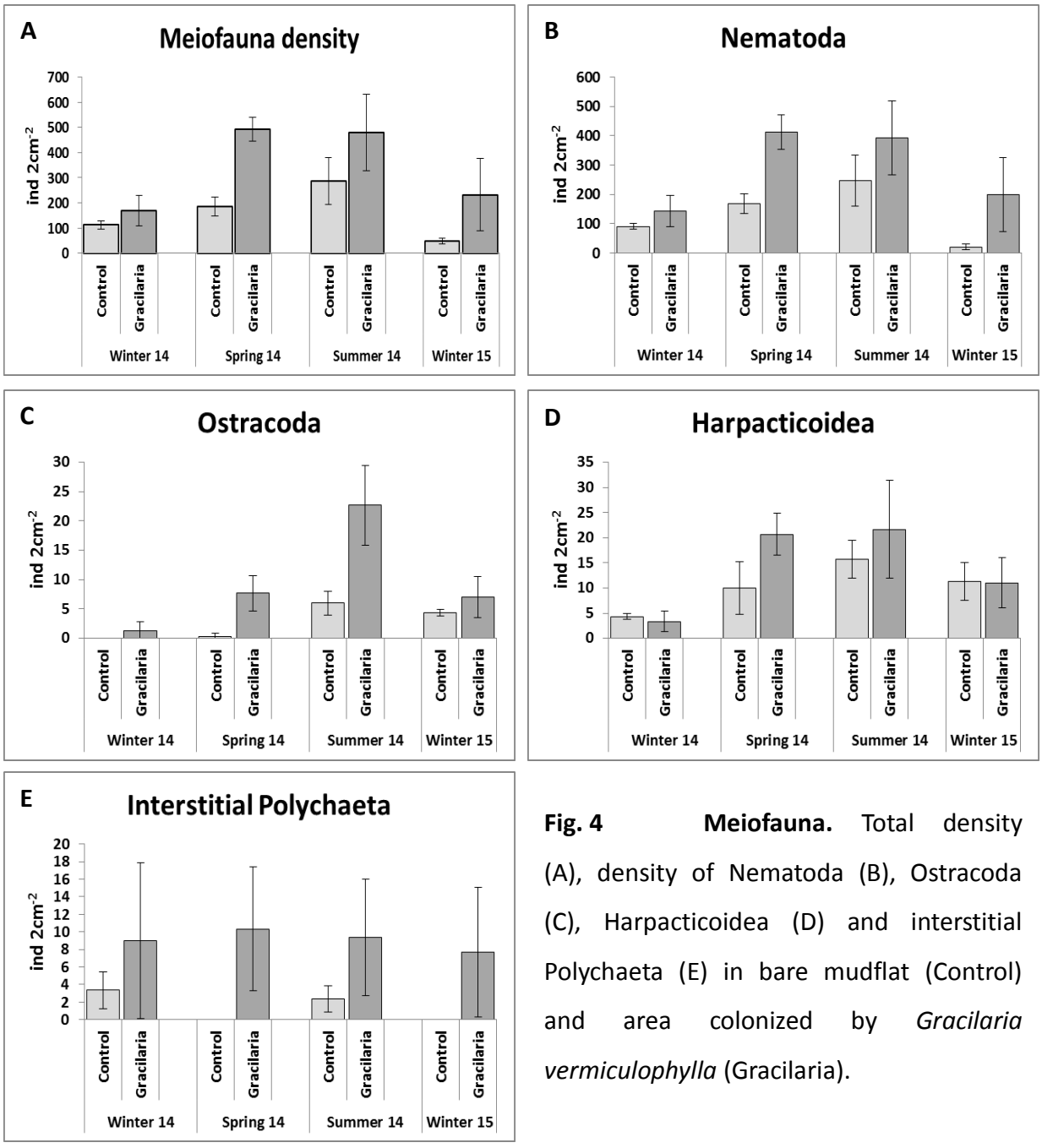

Fig. 4 Meiofauna. Total density (A), density of Nematoda (B), Ostracoda (C), Harpacticoidea (D) and interstitial Polychaeta (E) in bare mudflat (Control) and area colonized by *Gracilaria vermiculophylla* (Gracilaria).

Food web (Figures 5 & 6 and supplementary material) The $\delta^{13}C$ of the potential food sources displayed a wide range (from -30.7‰ for terrestrial organic matter to -17.6‰ for benthic diatoms) due to the presence of ^{13}C-enriched sources (*G. vermiculophylla* and benthic diatoms) as compared to more ^{13}C-depleted SOM, POM and terrestrial inputs. *G. vermiculophylla* was slightly less ^{13}C-depleted and showed similar $\delta^{15}N$ as compared to mean values (-21.7 and 9.6‰ for $\delta^{13}C$ and $\delta^{15}N$, respectively) previously reported in brackish lagoons of Japan (Kanaya et al. 2008). The range of $\delta^{15}N$ displayed by the food sources was slightly less important during the sampling year ranging between 9.6‰ in February and 6‰ in January. Except for $\delta^{13}C$ of benthic diatoms and $\delta^{15}N$ of terrestrial organic matter, there was no isotopic differences among sampling dates for the different food sources whereas consumers' isotopic signatures displayed significant temporal variations for $\delta^{13}C$ and $\delta^{15}N$ (Table 1). At each sampling occasion, significant differences were observed among the consumers species for $\delta^{13}C$ (Kruskal-Wallis, $p = 0.0023$, 0.0025, 0.017 and 0.027 in February, May, September and January, respectively) and for $\delta^{15}N$ (Kruskal-Wallis, $p = 0.043$, < 0.001, < 0.001 and < 0.001 in February, May, September and January, respectively). The $\delta^{15}N$ displayed by both *G. vermiculophylla* (between 9.0 and 10.9‰) and the primary consumers considered in this study (from 10.1 to 14.3‰) were relatively high which may be related to a highly nitrogen polluted environment.

For SIAR calculations, the main potential food sources were considered at each sampling date, namely *G. vermiculophylla*, POM, SOM, and terrestrial organic matter carried by the river within the estuary, and benthic diatoms. In fact, when the number of sources is higher than 5 sources, the solution of Bayesian mixing-models becomes less robust (Parnell et al. 2010). In this study, macroalgae and benthic diatoms in a lesser extent, contributed most of the diet for the three species. During the total sampling period, results of the SIAR models indicated that *G. vermiculophylla* was the major assimilated food source by *Scrobicularia plana* (mean relative contributions from 67.5 to 83.2%), *Hydrobia ulvae* (34.8 to 61.4%) and *Nereis diversicolor* (55.0 to 92.7%). During spring, and in a lesser extent in summer, benthic diatoms also contributed significantly to the diet of the consumers with highest median relative contributions for *Nereis diversicolor* (35% in May) followed by *Scrobicularia plana* (23.9% in May) and *Hydrobia ulvae* (25.3% in May). Local POM and SOM

and terrestrial inputs were much less important in consumer's diet all along the sampling year (Figure 6).

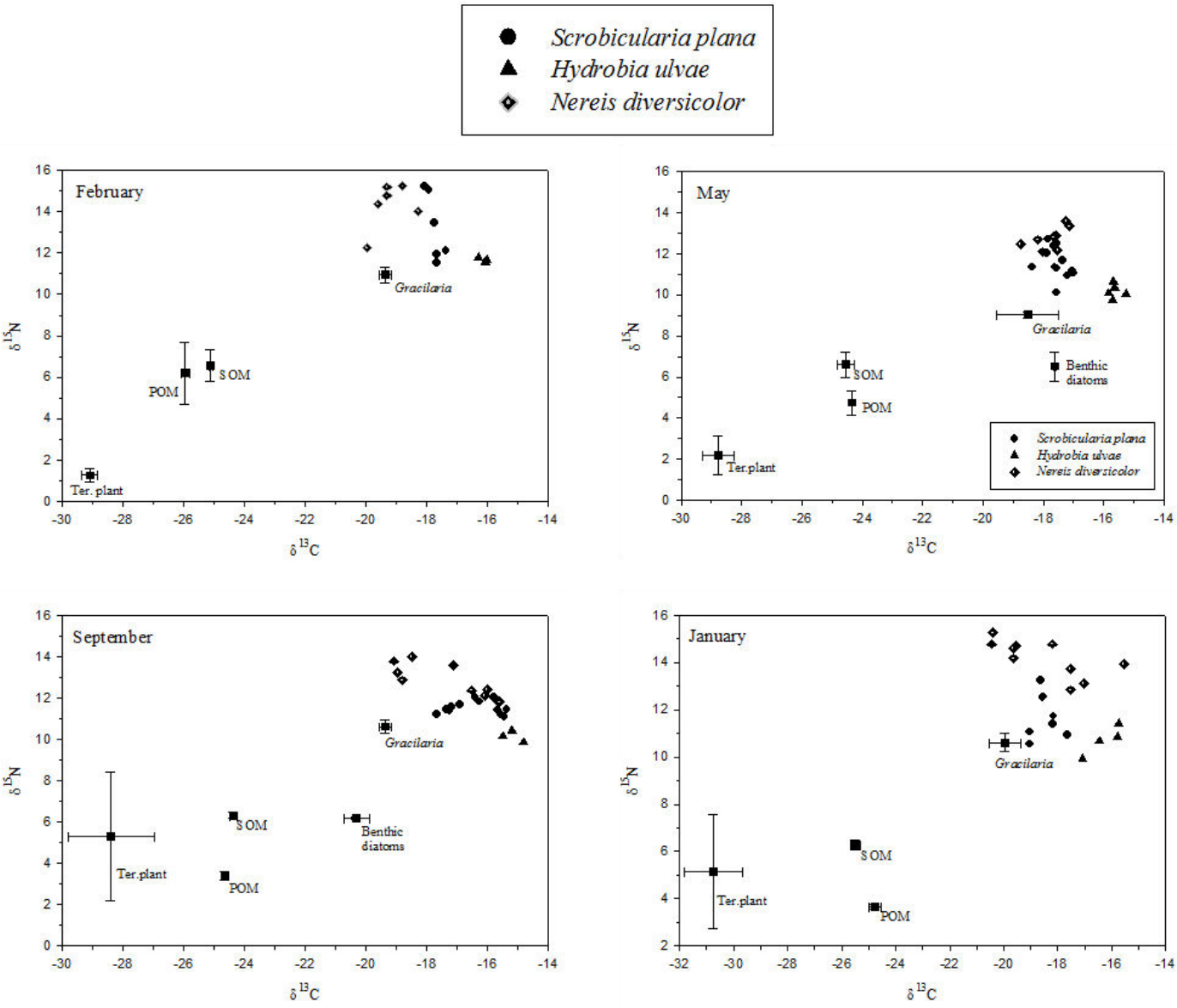

Fig. 5 $\delta^{13}C$ vs $\delta^{15}N$ (mean ± standard deviation) of food sources (*Gracilaria vermiculophylla*, SOM = Sedimented Organic Matter, POM = Particulate Organic Matter, Ter-plant = Terrestrial Plants, and benthic diatoms) and consumers during February, May and September 2014, and January 2015.

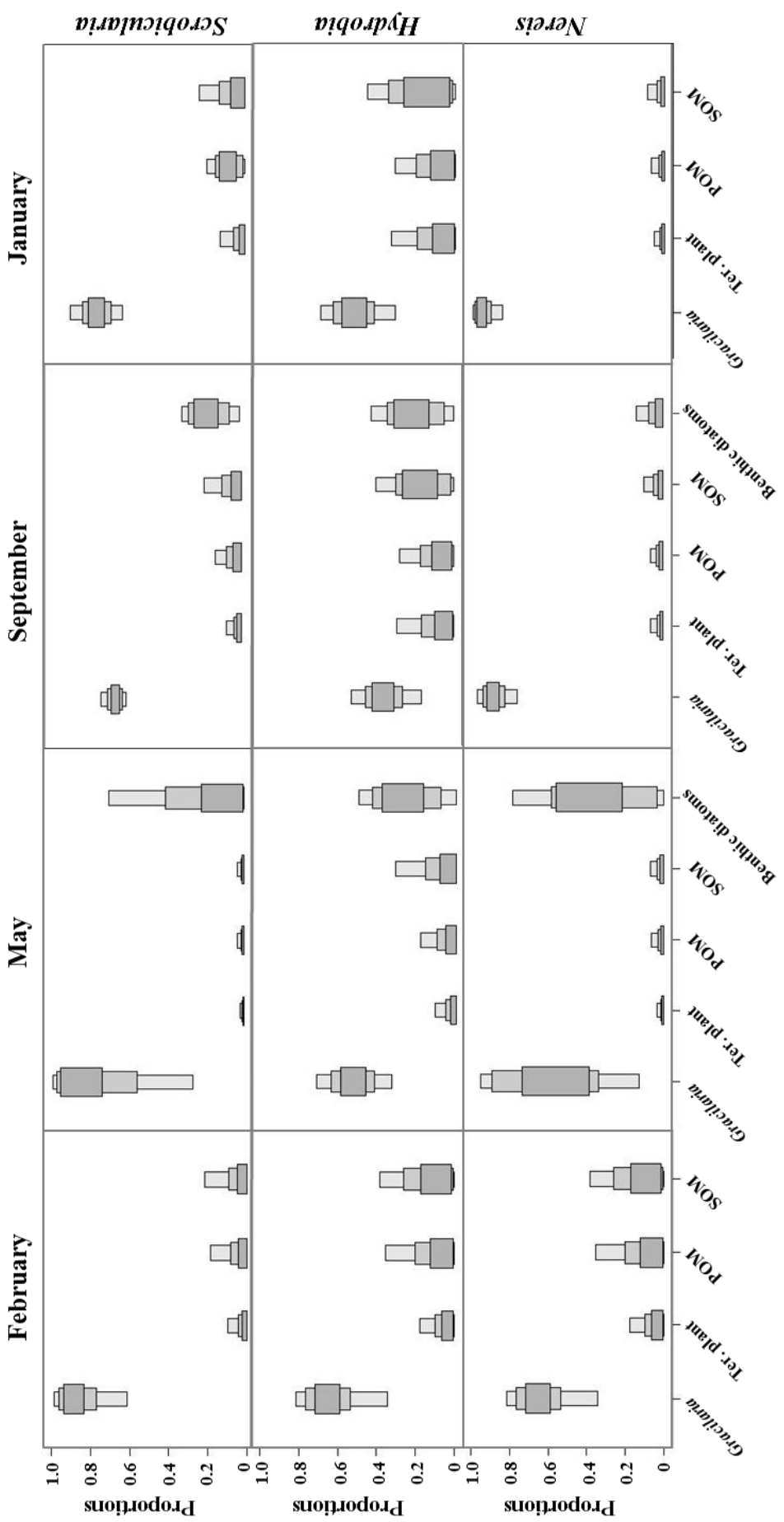
Nereis
Hydrobia
Scrobicularia
January
September
May
February
Gracilaria
Ter. plant
POM
SOM
Benthic diatoms
Proportions
0
0.2
0.4
0.6
0.8
1.0

Fig. 6 Boxplots of the contributions of potential food sources to the diet of the three species *Scrobicularia plana, Hydrobia ulvae* and *Nereis diversicolor*, obtained with Bayesian stable isotope mixing models at four sampling periods. Credibility intervals are 95% (in light grey), 75% (in medium grey) and 50% (in dark grey). POM = Particular Organic Matter, SOM = Sedimented Particular Organic Matter , Ter-plant = Terrestrial Plants.

Supplementary material. δ13C and δ15N (mean values ± sd) of organic matter sources and consumers. 4-dates comparisons and 2-dates comparisons were performed by Kruskal-Wallis test and Mann-Whitney U test, respectively.

	February 2014			May 2014			September 2014			January 2015			*P* value	
Samples	**$\delta^{13}C$**	**$\delta^{15}N$**	**n**	**$\delta^{13}C$**	**$\delta^{15}N$**	**n**	**$\delta^{13}C$**	**d^{15}N**	**n**	**$\delta^{13}C$**	**$\delta^{15}N$**	**n**	**$\delta^{13}C$ - by date**	**$\delta^{15}N$ - by date**
Food sources														
SOM	-25.1 ± 0.06	6.5 ± 0.74	3	-24.5 ± 0.29	6.6 ± 0.61	3	-24.3 ± 0.13	6.3 ± 0.14	3	-25.4 ± 0.16	6.2 ± 0.21	3	0.4	0.94
POM	-25.9 ± 0.14	6.19 ± 1,51	3	-24.3 ± 0.01	4.7 ± 0.59	3	-24.6 ± 0.07	3.4 ± 0.20	3	-24.7 ± 0.22	3.6 ± 0.09	3	0.17	0.07
Gracilaria vermiculophylla	-19.3 ± 0.20	10.9 ± 0.37	3	-18.5 ± 1.03	9.0 ± 0.16	3	-19.3 ± 0.19	10.6 ± 0.34	3	-19.9 ± 0.59	10.6 ± 0.39	3	0.09	0.24
Terrestrial plants	-29.1 ± 0.26	1.3 ± 0.30	3	-28.7 ± 0.53	2.1 ± 0.94	3	-28.4 ± 1.41	5.3 ± 3.11	3	-30.7 ± 1.09	5.1 ± 2.42	3	0.09	**0.04**
Benthic diatoms	—	—		-17.6 ± 0.05	6.52 ± 0.70	3	-20.3 ± 0.41	6.1 ± 0.05	3	—	—		**0.04**	0.5
Consumers														
Scrobicularia plana	-17.7 ± 0.24	13.2 ± 1.61	6	-17.5 ± 0.37	11.5 ± 0.75	12	-16.4 ± 0.83	11.5 ± 0.32	12	-18.3 ± 0.5	11.6 ± 0.92	9	**0.001**	**0.05**
Hydrobia ulvae	-16.1 ± 0.15	11.6 ± 0.12	3	-15.6 ± 0.21	10.1 ± 0.34	5	-15.1 ± 0.34	10.1 ± 0.28	3	-16.2 ± 0.62	10.7 ± 0.60	4	**0.01**	**0.03**
Nereis diversicolor	-19.2 ± 0.59	14.3 ± 1.11	6	-17.7 ± 0.53	12.7 ± 0.52	8	-17.2 ± 1.45	12.7 ± 0.81	10	-18.5 ± 1.62	14.1 ± 0.78	10	**0.02**	**0.001**

Discussion

Seasonal variations in GPP and CR in the bare mudflat seemed to be characteristic of these systems (Spilmont et al. 2006; Davoult et al. 2009; Migné et al. 2016), while rates of the area colonized by *G. vermiculophylla* were intermediate between these ones and values measured on macroalgae-dominated rocky shores (Golléty et al. 2008; Bordeyne et al. 2015). GPP appeared to be strongly increased by the occurrence of the red alga *G. vermiculophylla*. However, this increase tended to follow Chlorophyll *a*-content variations and thus led to the same productivity of the two areas. So, even if *G. vermiculophylla* added biomass in the benthic system, primary productivity remained around 0.8-1 mgC mgChl.a^{-1} h^{-1} in spring and summer, and below in winter, that represent typical values for both mudflats and macroalgae (Davoult et al. 2009). Cacabelos et al. (2012) pointed out that the invasion of a *Zostera noltei* bed by *G. vermiculophylla* tended to decrease photosynthetic efficiency at low light intensity but led to a higher metabolic performance caused by increasing *G. vermiculophylla* biomass. Finally, in spite of the invasion of a new primary producer, productivity of the mudflat remained stable, at least under saturating light and during emersion.

However, these results confirm that this seaweed is well adapted to muddy conditions and remains with good physiological conditions even in this extreme environment. Measurements of primary production were not performed during immersion but one can support the idea that water turbidity remains too important during high tide to allow photosynthesis, as already hypothesized in bays and estuarine mudflats along the English Channel (Spilmont et al. 2006; Migné et al. 2009) and the French Atlantic coast (Migné et al. 2016). Lapointe (1981) showed that growth of another species of *Gracilaria* could be strongly limited by light.

Typical macrofauna was collected both on bare mud and colonized areas. Compared to bare mud, both macrobenthic abundance and diversity were positively impacted in the colonized area. Total density significantly increased in *G. vermiculophylla*-colonized area because of the rise in density of some common species such as *Nereis diversicolor* and high abundances of species which were absent or rare in the bare mud, such as *Streblospio shrubsolii*. Moreover, species newly recorded in the studied area (e.g. the amphipods *Jassa*

marmorata, *Melita palmata* and *Allomelita pellucida*, and the decapods *Pilumnus hirtellus* and *Liocarcinus pusillus*) are generally absent from bare sediments and usually found among seaweeds and hydrozoans on hard substrata or on eelgrass (Hayward and Ryland 1995). These species were found at low density on colonized areas, likely favored by the complexity of the habitat driven by the settlement of this engineer seaweed. These new epifaunal species led to a significant increase in the number of sampled taxa and so in the diversity of the community, as a consequence of a new available habitat (Wallentinus and Nyberg 2007). Heiman and Micheli (2010) also pointed out that non-native ecosystem engineers, such as the reef-building tubeworm *Ficopomatus enigmaticus*, could favor the occurrence of opportunistic species.

Density of some meiofauna taxa was also higher in the colonized area; this was particularly the case of the dominant group of nematodes, but also of ostracods and interstitial polychaetes. As the macrofaunal polychaete *N. diversicolor*, these taxa belong to endofauna and their density is then not supposed to be positively influenced by the occurrence of a new habitat-forming seaweed, even if a part of *G. vermiculophylla* is buried within the mud.

This increase in endofaunal density could be related to a change in food availability, possibly due to the effective use of *G. vermiculophylla* in the diet of these species. The estimation of the proportion of the different food sources in the diet of three common species of the community, the bivalve *Scrobicularia plana*, considered both as a surface deposit-feeder and a suspension-feeder (Hughes 1969), the gastropod *Hydrobia ulvae*, considered as a grazer of benthic diatoms (Hautbois et al. 2005), and the polychaete *Nereis diversicolor*, considered as opportunistic, from suspension-feeding to predator and generalist scavenger (Fidalgo e Costa et al. 2006), supported this hypothesis. At all seasons, stable isotopes showed that *G. vermiculophylla* was the main food source for the three species, even if, in spring and summer, contribution of benthic diatoms was also relatively important, conversely to local POM, SOM and terrestrial inputs.

To our knowledge, there is no previous evidence of such predominance of this invasive macroalga in the diet of suspension- and/or deposit-feeder species. Kanaya et al. (2008) did not report any significant contribution of *G. vermiculophylla* to the local food web inhabiting brackish lagoons of Japan, its native area. Moreover, feeding experiments and

field isotopic data conducted by Wright et al. (2014) showed that the invasive *G. vermiculophylla* could be consumed by the amphipod *Gammarus locusta*, even if this alga was clearly not targeted in its diet as compared to other local food sources. The predominance of *G. vermiculophylla* as food source could appear to be in contrast with the algal chemical defense which protects it from a strong grazing activity (Nylund et al. 2011). However, previous studies have pointed out that macroalgae enter the coastal food web mostly through detrital pathways (Pomeroy 1980; Raffaelli and Hawkins 1996), losing by degradation their repellent properties.

In particular, a fraction of the detrital macroalgal pool degrades *in situ*, becoming available to nearshore pelagic and benthic filter-feeders (Bustamante and Branch 1996). In addition, when abundantly present, macroalgae become also readily available for the organisms inhabiting sediments because of the lack of lignin content in their tissue and their rapid physical fractionation due to the effect of wave action and sediment motion (Rossi 2007).

Besides, our results indicate that benthic diatoms were not preferentially used by the benthic consumers considered even when they were present at the sediment surface as brown mats. Yet, several previous studies highlighted the role of benthic diatoms as major food source for marine invertebrates inhabiting intertidal sediments (De Jonge and Van Beusekom 1992; Decottignies et al. 2007). The significant but not dominant feeding contribution of microphytobenthos observed in our study may be caused by the irregular presence and abundance of this resource in these estuarine sediments, mainly due to hydrodynamic variability. This may also be due to low production at least in winter. In other types of ecosystems, a major feeding contribution of decaying macroalgae for *Hydrobia ulvae* and meiofauna in intertidal muddy/sandy sediments as compared to benthic diatoms was previously pointed out through stable isotopes analyses (Riera and Hubas 2003; Riera 2010).

Finally, these three macrofauna species were likely representative of the dominant macrofauna of this estuarine site and, considering their intermediate trophic position of primary consumer species, the food web of this area would be largely based on the use of this invasive seaweed which probably generate the main source of detritus in this estuarine environment.

Several major points stood out from these results. First of all, there was no difference in consumers' isotopic signatures between bare-mud areas and seaweed-colonized areas. When sampling bare muds, we actually collected some macro detritus of *G. vermiculophylla* which is easily fragmented in the environment, and numerous micro debris certainly also occur, which could explain the homogeneous signatures found in the two sub-systems. It seems that species fed the same way in bare mud and in colonized areas because of this contamination.

The second interesting point was that densities were higher in colonized areas, likely because of a higher food availability. Access to more food would directly favor deposit-feeders and grazers that could ingest both microphytobenthos and micro debris of seaweed. In addition, that would indirectly benefit to suspension-feeders through resuspension of both microphybenthos, when present, and micro debris of seaweed. Finally, this study highlighted that a NIS species deeply influenced and even seemed to change the trophic structure of the macrobenthic community whereas NIS are generally not easily consumed by native species, which could partly explain their success in colonizing new ecosystems (Wright et al. 2014 and references herein).

In a nutshell, the settlement of the NIS *G. vermiculophylla* impacted the mudflat ecosystem of the Faou estuary (1) as a new primary producer by increasing local benthic primary production, (2) as a habitat-forming species by changing vertically the size and shape of the habitat and then favoring the occurrence of epifaunal species, and (3) as a new and abundant food source, confirming its high potential to transform estuaries (Byers et al. 2012). Our study appeared to take place during the expansion of the invasive seaweed in this estuary (Gwladys Surget, pers. obs.). Monitoring should be planned in the aim to follow this expansion and measure consequences on the associated community and potential sedimentation increase.

Acknowledgements The authors thank Klervi Le Lann, Renaud Michel and Gaspard Delebecq for field support and Cédric Leroux for isotopic analyses. The study was part of the project INVASIVES (Invasive seaweeds in rising temperatures: impacts and risk assessments), supported by the EU FP7 ERA-NET Seas-Era (2012-2016) and financed for French partners by ANR (ANR-12-SEAS-0002).

References

Bordeyne F., Migné A., Davoult D. (2015). Metabolic activity of intertidal *Fucus* spp. communities: evidence for high aerial carbon fluxes displaying seasonal variability. Mar Biol 162: 2119-2129.

Bustamante R.H., Branch G.M. (1996). The dependence of intertidal consumers on kelp-derived organic matter on the west coast of South Africa. J Exp Mar Biol Ecol 196: 1-28.

Byers J.E., Gribben P.E., Yeager C., Sotka E.E. (2012). Impacts of an abundant introduced ecosystem engineer within mudflats of the southeastern US coast. Biol Inv 14: 2587-2600.

Cacabelos E., Engelen A.H., Mejia A., Arenas F. (2012). Comparison of the assemblage functioning of estuary systems dominated by the seagrass *Nanozostera noltii* versus the invasive drift seaweed *Gracilaria vermiculophylla*. J Sea Res 72: 99-105.

Caut S., Angulo E., Courchamp F. (2009). Variation in discrimination factors ($\delta^{15}N$ and $\delta^{13}C$): the effect of diet isotopic values and applications for diet reconstruction. J Appl Ecol 46: 443-453.

Crooks J.A. (2002). Characterizing ecosystem-level consequences biological invasions: the role of ecosystem engineers. Oikos 97: 153-166.

Davoult D., Migné A., Créach A., Gévaert F., Hubas C., Spilmont N., Boucher G. (2009). Spatio-temporal variability of intertidal benthic primary production and respiration in the western part of the Mont Saint-Michel Bay (Western English Channel, France). Hydrobiologia 620:163-172.

Dayton P.K. (1972). Toward an understanding of community resilience and the potential effects of enrichments to the benthos at McMurdo Sound, Antarctica. In: Parker BC, editor. Proceedings of the Colloquium on Conservation Problems in Antarctica. Blacksburg 1971. Lawrence: Allen Press. pp 81-96.

De Jonge V.N., Van Beusekom J.E.E. (1992). Contribution of resuspended microphytobenthos to total phytoplankton in the Ems estuary and its possible role for grazers. Neth J Sea Res 30: 91-105.

Decottignies P., Beninger P.G., Rincé Y., Robins R.J., Riera P. (2007). Exploitation of natural food sources by two sympatric, invasive suspension-feeders, *Crassostrea gigas* and *Crepidula fornicata*. Mar Ecol Prog Ser 334: 179-192.

Ellison A.M. et al. (2005). Loss of foundation species: consequences for the structure and dynamics of forested ecosystems. Front Ecol Env 3: 479-486.

Fidalgo E. Costa P., Oliveira R.F., Cancela Da Fonseca L. (2006). Feeding Ecology of *Nereis diversicolor* (O.F. Müller) (Annelida, Polychaeta) on Estuarine and Lagoon Environments in the Southwest Coast of Portugal. Pan-Am J Aqu Sci 1 (2): 114-126.

Freshwater D.W., Montgomery F., Greene J.K., Hamner R.M., Williams M., Whitfield P.E. (2006). Distribution and identification of an invasive *Gracilaria* species that is hampering commercial fishing operations in southeastern North Carolina, USA. Biol Invasions 8: 631-637.

Golléty C., Migné A., Davoult D. (2008). Benthic metabolism on a sheltered rocky shore: role of the canopy in the carbon budget. J Phycol 44: 1146-1153.

Hammann M., Wang G., Rickert E., Boo S.M., Weinberger F. (2013). Invasion success of the seaweed *Gracilaria vermiculophylla* correlates with low palatibility. Mar Ecol Prog Ser 486: 93-103.

Hastings A., Byers J.E., Crooks J.A., Cuddington K., Jones C.G., Lambrinos J.G., Talley T.S., Wilson W.G. (2007). Ecosystem engineering in space and time. Ecol Lett 10: 153-164.

Hautbois A-G., Guarini J-M., Richard P., Fichet D., Radenac G., Blanchard G.F. (2005). Ingestion rate of the deposit-feeder *Hydrobia ulvae* (Gastropoda) on epipelic diatoms: effect of cell size and algal biomass. J Exp Mar Biol Ecol 317: 1-12.

Hayward J., Ryland J.S. (1995). Handbook of the marine fauna of north-west Europe. Oxford University Press, 800 pp.

Heiman K.W., Micheli F. (2012). Non-native ecosystem engineer alters estuarine communities. Integr Comp Biol 50: 226-236.

Hughes R.N. (1969). A study of feeding in *Scrobicularia plana*. J Mar Biol Ass UK 49: 805-823.

Jeffrey S.W., and Humphrey G.F. (1975). New spectrophotometric equations for determining chlorophylls a, b, c1 and c2 in higher plants, algae and natural phytoplankton. Biochem Physiol Pflanz BPP 167: 191-194.

Jones C.G., Lawton J.H., Shachak M. (1994). Organisms as ecosystem engineers. Oikos 69: 373-386.

Jones C.G., Lawton J.H., Shachak M. (1997) Positive and negative effects of organisms as physical ecosystem engineers. Ecology 78: 1946-1957.

Kanaya G., Takagi S., Kikuchi E. (2008). Spatial dietary variations in *Laternula Marilina* (Bivalva) and *Hediste* spp. (Polychaeta) along environmental gradients in two brackish lagoons. Mar Ecol Prog Ser 359: 133-14.

Lapointe B.E. (1981). The effect of light and nitrogen on growth, pigment content, and biochemical composition of *Gracilaria foliifera* V. *angistissima* (Gigartinales, Rhodophyta). J Phycol 17: 90-95.

Levine J.M.,Vila M., Antonio C.M., Dukes J.S., Grigulis K., Lavorel S. (2003). Mechanisms underlying the impacts of exotic plant invasions. Proc Royal Soc London B 270: 775-781.

Martínez-Lüscher J., Holmer M. (2010). Potential effects of the invasive species *Gracilaria vermiculophylla* on *Zostera marina* metabolism and survival. Mar Envir Res 69 (5): 345-349.

Migné A., Davoult D., Spilmont N., Menu D., Boucher G., Gattuso J-P., Rybarczyk H. (2002). A closed-chamber CO_2-flux method for estimating intertidal primary production and respiration under emersed conditions. Mar Biol 140: 865-869.

Migné A., Spilmont N., Boucher G., Denis L., Hubas C., Janquin M.A., Rauch M., Davoult D. (2009). Annual budget of benthic production in Mont Saint-Michel Bay considering cloudiness, microphytobenthos migration, and variability of respiration rates with tidal conditions. Cont Shelf Res 29: 2280-2285.

Migné A., Davoult D., Spilmont N., Ouisse V., Boucher G. (2016). Spatial and temporal variability of CO2 fluxes at the sediment-air interface in a tidal flat of a temperate lagoon (Arcachon Bay, France). J Sea Res 109: 13-19.

Mollet J.C., Rahoui A., Lemoine Y. (1998). Yield, chemical composition and gel strength of agarocolloids of *Gracilaria gracilis*, *Gracilariopsis longissima* and the newly reported *Gracilaria cf. vermiculophylla* from Roscoff (Brittany, France). J Appl Phycol 10: 59–66.

Nylund G.M., Weinberger F., Rempt M., Pohnert G. (2011). Metabolomic assessment of induced and activated chemical defence in the invasive red alga *Gracilaria vermiculophylla*. PLoS ONE 6: e29359.

Parnell A.C., Inger R., Bearhop S., Jackson A.L. (2010) Source partitioning using stable isotopes: coping with too much variation. PloS ONE 5, e9672.

Pomeroy L.R. (1980). Detritus and its role as a food resource. In *Fundamentals of aquatic ecosystems* (Barnes RSK., Mann KH, eds). Blackwell Science, Oxford, pp 84-102.

Raffaelli D., Hawkins S. (1996). Intertidal Ecology. London: Chapman and Hall.

Riera P., Hubas C. (2003). Trophic ecology of nematodes from various microhabitats of the Roscoff Aber Bay (France): importance of stranded macroalgae evidenced through $\delta^{13}C$ and $\delta^{15}N$. Mar Ecol Prog Ser 260: 151-159.

Riera P. (2007). Trophic subsidies of *Crassostrea gigas*, *Mytilus edulis* and *Crepidula fornicata* in the Bay of Mont Saint Michel (France): A $\delta^{13}C$ and $\delta^{15}N$ investigation. Estuar Coast Shelf Sci 72: 33-41.

Riera P. (2010). Trophic plasticity of the gastropod *Hydrobia ulvae* within an intertidal bay (Roscoff, France): a stable isotope evidence. J Sea Res 63: 78-83.

Rossi F. (2007). Recycle of buried macroalgal detritus in sediments: use of dual-labelling experiments in the field. Mar Biol 150: 1073-1081.

Rueness J. (2005). Life history and molecular sequences of *Gracilaria vermiculophylla* (Gracilariales, Rhodophyta), a new introduction to European waters. Phycologia 44: 120–128.

Schaffelke B., Smith J.E., Hewitt C.L. (2006). Introduced macroalgae—a growing concern. J Appl Phycol 18: 529–541.

Schaffelke B., Hewitt C.L. (2007). Impacts of introduced seaweeds. Bot Mar 50: 397–417.

Spilmont N., Davoult D., Migné A. (2006). Benthic primary production during emersion: *in situ* measurements and potential primary production in the Seine Estuary (English Channel, France). Mar Poll Bull 53: 49–55.

Stiger-Pouvreau V., Thouzeau G. (2015). Marine species introduced on the French Channel-Atlantic coasts: a review of main biological invasions and impacts. Open J Ecol 5: 227-257.

Thomsen M.S., Wernberg T., Staehr P., Krause-Jensen D., Risgaard-Petersen N., Silliman B.R. (2007). Alien macroalgae in Denmark: a broad-scale national perspective. Mar Biol Res 3: 61-72.

Thomsen M.S., McGlathery K., Schwarzschild A., Silliman B. (2009). Distribution and ecological role of the nonnative macroalga *Gracilaria vermiculophylla* in Virginia salt marshes. Biol Inv 11: 2303-2316.

Wallentinus I., Nyberg C.D. (2007). Introduced marine organisms as habitat modifiers. Mar Poll Bull 55: 323-332.

Wright J.T., Byers J.E., DeVore J.L., Sotka E.E. (2014). Engineering or food? Mechanisms of facilitation by a habitat-forming invasive seaweed. Ecology 95: 2699-2706.

Conclusion et synthèse de la partie 1

Ces différentes études ont principalement pu montrer le lien entre la plasticité phénotypique et la plasticité métabolique dans différents contextes :

(1) une variation des osmolytes étudiés à petite échelle, en particulier du diméthylsulfoniopropionate (DMSP) ainsi qu'une variation du pool azoté chez *Codium fragile*, variation prédominante sur les régulations saisonnières pour les osmolytes étudiés.

(2) une acclimatation saisonnière du phénotype et du métabolome chez *Gracilaria vermiculophylla* avec notamment la relation probable entre une fragmentation plus élevée au mois de Juin et une augmentation des acides gras libres suggérant l'activation de mécanisme de défense contre le broutage par la synthèse d'oxylipines.

(3) la présence jusqu'à 12 cm de profondeur de fragments de *G. vermiculophylla* illustrant l'envasement important chez cette espèce. Suite à ce processus d'envasement, les fragments en profondeur présentent des caractéristiques photophysiologiques comparables aux thalles se développant en surface ainsi qu'un profil métabolomique divergent (variation des teneurs en floridoside, alanine et du pool de molécules azotées), reliés à un pattern phénotypique différent influencé par l'activité de la macrofaune benthique.

Le profilage métabolomique non ciblé chez *C. fragile* a pu mettre en relief une problématique scientifique complexe, l'acclimatation métabolomique dépendante de l'adaptation locale de l'espèce invasive. Par exemple, il a été démontré que le DMSP présente des rôles biologiques différents en fonction de la position géographique des populations de *Codium fragile* étudiées (Van Alstyne, 2008). Ceci sous-entend que relier des études de diversité génétique à l'analyse fonctionnelle des métabolites cellulaires tels que les osmolytes permettrait d'avoir une compréhension plus fine des régulations métaboliques de ces espèces et *in fine* de mieux comprendre leur potentiel invasif en relation avec les facteurs environnementaux. Ceci est particulièrement le cas pour les espèces invasives pour lesquelles une adaptation locale peut être rapide d'un point de vue évolutif (Phillips et al., 2006; Westley et al., 2013).

D'autre part, ces travaux ont illustré divers impacts, dus à l'introduction d'une espèce invasive dans un milieu présentant peu de compétition avec d'autres macrophytes et

occupant ainsi une nouvelle niche écologique, comme tel est le cas pour *Gracilaria vermiculophylla* en Rade de Brest. Cette arrivée importante de matière organique de nature algale peut avoir d'autres conséquences sur l'écosystème local que celles présentées dans ce manuscrit telles que par exemple la modification de la biogéochimie de l'écosystème en impactant sur les flux azotés (Tyler and McGlathery, 2006) jusqu'à la modification des composantes physiques du milieu. En effet, la gracilaire agit comme un tampon en atténuant les maximum et minimum de température à une profondeur de 4 cm dans la vase en comparaison de la vase nue (données non développées dans ce manuscrit, mais acquises sur le terrain).

L'ensemble de ces études a permis d'avoir une vision intégrée des variations phénotypiques, physiologiques et métabolomiques de ces espèces en Bretagne permettant de mieux comprendre et interpréter les variations observées à l'échelle de l'aire de répartition de ces espèces le long des côtes européennes Nord Atlantique de la Norvège au Portugal, travail qui est développé dans la seconde partie de ce manuscrit.

Références

Cabioc'h, J., Floc'h, J.-Y., Le Toquin, A., Boudouresque, C.F., Meinesz, A., Verlaque, M., 2006. Guide des algues des mers d'Europe. Delachaux et Niestlé.

Davidson, A.D., Campbell, M.L., Hewitt, C.L., Schaffelke, B., 2015. Assessing the impacts of non indigenous marine macroalgae: an update of current knowledge. Bot. Mar. 58, 55–79.

Fogg, G.E., 2001. Algal adaptation to stress — some general remarks, in: Rai, P.D.L.C., Gaur, P.D.J.P. (Eds.), Algal adaptation to environmental stresses. Springer Berlin Heidelberg, pp. 1–19.

Freshwater, D.W., Montgomery, F., Greene, J.K., Hamner, R.M., Williams, M., Whitfield, P.E., 2006. Distribution and identification of an invasive *Gracilaria* species that is hampering commercial fishing operations in Southeastern North Carolina, USA. Biol. Invasions 8, 631–637.

Glasby, T.M., Gibson, P.T., Kay, S., 2005. Tolerance of the invasive marine alga *Caulerpa taxifolia* to burial by sediment. Aquat. Bot. 82, 71–81.

Gonzalez, D.J., Smyth, A.R., Piehler, M.F., McGlathery, K.J., 2013. Mats of the nonnative macroalga, *Gracilaria vermiculophylla*, alter net denitrification rates and nutrient fluxes on intertidal mudflats. Limnol. Oceanogr. 58, 2101–2108.

Hu, Z.-M., Juan, L.-B., 2013. Adaptation mechanisms and ecological consequences of seaweed invasions: a review case of agarophyte *Gracilaria vermiculophylla*. Biol. Invasions 16, 967–976.

Hurd, C.L., Harrison, P.J., Bischof, K., Lobban, C.S., 2014. Seaweed ecology and physiology. Cambridge University Press.

Kamermans, P., Malta, E., Verschuure, J.M., Lentz, L.F., Schrijvers, L., 1998. Role of cold resistance and burial for winter survival and spring initiation of an *Ulva spp*. (Chlorophyta) bloom in a eutrophic lagoon (Veerse Meer lagoon, The Netherlands). Mar. Biol. 131, 45–51.

Nyberg, C.D., Wallentinus, I., 2009. Long-term survival of an introduced red alga in adverse conditions. Mar. Biol. Res. 5, 304–308.

Phillips, B.L., Brown, G.P., Webb, J.K., Shine, R., 2006. Invasion and the evolution of speed in toads. Nature 439, 803–803.

Thomsen, M.S., McGlathery, K., 2005. Facilitation of macroalgae by the sedimentary tube forming polychaete *Diopatra cuprea*. Estuar. Coast. Shelf Sci. 62, 63–73.

Thomsen, M.S., McGlathery, K.J., 2007. Stress tolerance of the invasive macroalgae *Codium fragile* and *Gracilaria vermiculophylla* in a soft-bottom turbid lagoon. Biol. Invasions 9, 499–513.

Tyler, A.C., McGlathery, K.J., 2006. Uptake and release of nitrogen by the macroalgae *Gracilaria vermiculophylla* (rhodophyta)1. J. Phycol. 42, 515–525.

Van Alstyne, K.L.V., 2008. The distribution of DMSP in green macroalgae from northern New Zealand, eastern Australia and southern Tasmania. J. Mar. Biol. Assoc. U. K. 88, 799–805.

Weinberger, F., Buchholz, B., Karez, R., Wahl, M., 2008. The invasive red alga *Gracilaria vermiculophylla* in the Baltic Sea: adaptation to brackish water may compensate for light limitation. Aquat. Biol. 3, 251–264.

Westley, P.A.H., Ward, E.J., Fleming, I.A., 2013. Fine-scale local adaptation in an invasive freshwater fish has evolved in contemporary time. Proc. R. Soc. Lond. B Biol. Sci. 280, 20122327.

Partie 2 : Etude de la plasticité phénotypique de macroalgues invasives et natives à l'échelle d'une aire biogéographique le long de la façade de l'Atlantique Nord-Est

Le réchauffement climatique, induit par le changement climatique (IPCC, 2013), a pour conséquence une modification de l'aire biogéographique des espèces végétales marines (Hellmann et al., 2008). De plus, les macroalgues marines ont la particularité de présenter des aires de répartition très étendues (*e.g.* Engelen et al., 2015). Le travail de recherche présenté dans cette deuxième partie de ce manuscrit est conçu sur la combinaison de ces deux factualités. Il consiste à observer et comparer le comportement de macroalgues invasives se développant à des latitudes Sud et Nord des côtes atlantiques européennes pour permettre de mieux présager du futur comportement de ces espèces invasives lorsqu'elles coloniseront des littoraux situés à des latitudes plus au Nord (ou plus au Sud). Ceci s'applique si l'on raisonne à grande échelle afin d'observer l'évolution globale des espèces de macroalgues invasives en connaissant suffisamment l'effet des principaux facteurs environnementaux influençant l'abondance et le potentiel invasif de ces espèces à une échelle locale (*cf.* objectif de la partie 1 de cette thèse ; la partie 1 a permis d'établir la plasticité phénotypique de ces espèces au niveau de la Pointe bretonne). Le gradient latitudinal le long des côtes atlantiques européennes, s'étendant de la Norvège au Portugal, présente un gradient thermique marquant avec des températures moyennes de l'eau de mer de 7, 11 et 14°C en Janvier et de 14, 16 et 19°C en Norvège, en France et au Portugal respectivement (Gohin et al., 2010). Au centre de ce gradient, la France représente le point d'introduction de certaines espèces invasives étudiées dans cette partie (*Sargassum muticum* et *Gracilaria vermiculophylla*). Le Portugal représente quant à lui la limite Sud de l'aire de répartition de ces trois espèces sur les côtes européennes de l'Atlantique Nord-Est et la Norvège leur limite Nord. Travailler sur les populations du Portugal permettra d'émettre des hypothèses quant à l'évolution des populations en France dans un contexte de changement climatique et de même entre la France et la Norvège. Cependant, il est évident que cette notion de prédiction devra être nuancée étant donné la multiplicité des interactions qu'elles soient antagonistes ou synergiques opérant entre les espèces algales et leur environnement biotique et abiotique. Le choix des trois espèces étudiées : *Sargassum muticum*, *Codium fragile* et *Gracilaria vermiculophylla,* est relié à

l'introduction chronologiquement différente de ces espèces sur les côtes européennes : l'introduction de *C. fragile* est la plus ancienne étant reportée en France dès 1940 (Provan et al., 2008) ; celle de *S. muticum* quant à elle, a été reportée dans les années 80 en France et dans les années 90 au Portugal et en Norvège (Stiger-Pouvreau et Thouzeau, 2015) et l'introduction de *G. vermiculophylla* est la plus récente ayant été observée en 1996 en France et dans les années 2000 au Portugal et en Suède (Rueness, 2005).

Ces espèces, de par leur large distribution, offrent ainsi la possibilité d'effectuer des études de plasticité de leur phénotype écologique, physiologique ou encore biochimique en fonction de la latitude. Par ailleurs, c'est tout l'enjeu de ce présent manuscrit dont le travail s'attèle à relier les données écologiques et les performances physiologiques et biochimiques (afin de mieux comprendre le développement de ces espèces). Dans ce but, les suivis écologiques ont été couplés à des suivis physiologiques et/ou biochimiques à l'échelle du gradient atlantique européen sur le même principe que les études précédemment décrites en partie 1 à l'échelle de la Pointe bretonne.

Cette partie se décompose en deux chapitres. Le premier chapitre se concentre sur des espèces invasives se répartissant en estran rocheux et vise à étudier la plasticité phénologique des deux macroalgues *Codium fragile* et *Sargassum muticum* le long de ce gradient latitudinal puis à comparer au cours d'un cycle tidal la photo-physiologie de *Sargassum muticum* avec celle d'une espèce native de macroalgue brune, *Bifurcaria bifurcata* en France et au Portugal. Le second chapitre comparera l'acclimatation phénologique, physiologique et biochimique de *Gracilaria vermiculophylla* des rias de la Rade de Brest (France) à celles de la Ria de Aveiro (Portugal). Ces données pourront nous permettre de mieux comprendre le devenir de cette algue des vasières et sa progression sur le littoral des pays scandinaves comme la Norvège où elle a été récemment observée (Vivian Husa, communication personnelle dans le cadre du projet INVASIVES).

Chapitre 5. Les macroalgues d'estran rocheux présentent-elles une plasticité phénotypique le long d'un gradient latitudinal sur les côtes européennes de l'Atlantique Nord-Est ?

Etat de l'art

Biologie des populations

Codium fragile a été étudié le long des côtes de l'Atlantique Ouest où cette espèce est particulièrement invasive (*cf.* Partie 1, Chapitre 1. Introduction de la note : « Interest of the HR-MAS NMR for the metabolomic and phenological monitoring of the green macroalga *Codium fragile* along the coasts of Iroise Sea (France) »). En 1999, Chapman a illustré la différence de potentiel invasif de cette même espèce entre les côtes canadiennes et celles du Sud de l'Angleterre (Chapman, 1999) mais peu d'études existent sur la phénologie de *C. fragile,* notamment en France (Silva, 1955).

D'autre part, *Sargassum muticum,* la seconde espèce étudiée le long de ce gradient latitudinal de la Norvège au Portugal, constitue un modèle d'étude au sein du laboratoire et de nombreux travaux ont été réalisés en Bretagne dans le but d'apprécier, localement, la variabilité de la phénologie de cette espèce en fonction des saisons et en fonction des caractéristiques des différents sites étudiés (substrat, hydrodynamisme) (Le Lann et al. 2012 ; Le Lann, 2009; Plouguerné, 2006; Plouguerné et al., 2006). D'autres études ont été réalisées en Europe pour suivre son expansion, *e.g.* Kraan, 2008; Loughnane and Stengel, 2002; Rueness, 1989, et comprendre l'écologie de cette espèce, notamment en Irlande (Baer and Stengel, 2010) mais aussi au Danemark (Pedersen et al., 2005; Wernberg et al., 2005, 2004), en Norvège (Sjøtun et al., 2007), en Espagne (Andrew and Viejo, 1998; Arenas et al., 2002, 1995; Arenas and Fernández, 2009) et au Portugal (Engelen and Santos, 2009; Vaz-Pinto et al., 2014). Cette espèce a été précédemment étudiée le long de gradients latitudinaux pour son écologie chimique en Europe (Tanniou, 2014; Tanniou et al., 2015, 2014) ainsi que son caractère reproductif le long des côtes californiennes (Norton and Deysher, 1989). Donc, peu d'études ont illustré la plasticité phénotypique de *S. muticum* sur de grandes échelles. Dans ce contexte, l'étude de plasticité phénologique de ces deux espèces *Codium fragile* et *Sargassum muticum* s'avère particulièrement pertinente à une grande échelle le long des côtes européennes de la Norvège au Portugal.

Plasticité de la photo-physiologie d'une espèce invasive et native

Seules quelques études reportent la mesure *in situ* de l'acclimatation de l'efficacité photosynthétique d'espèces invasives (*e.g.* Campbell et al., 2005). Zanolla et al. (2015) ont mis en évidence la réponse plastique de la photo-physiologie d'une population de la macroalgue rouge *Asparagopsis armata* affectant sa fitness de manière différentielle entre son aire d'introduction et son aire d'invasion pouvant expliquer son potentiel invasif le long des côtes méditerranéennes (Zanolla et al., 2015). Par ailleurs, Hamel (2012) a comparé la photoacclimatation d'espèces endémiques et invasives du genre *Gracilaria* à Hawaï en réalisant des études comparatives de l'efficacité photosynthétique. De plus, la photo-physiologie de *S. muticum* a été étudiée *in situ* en Irlande en fonction des saisons (Baer and Stengel, 2010) ainsi qu'à la Pointe bretonne en fonction des saisons et du cycle tidal (*cf.* Partie 1- Chapitre 3 de ce manuscrit). L'effet de divers paramètres environnementaux tels que l'effet de l'émersion a également été testé chez cette espèce invasive (Nitschke et al., 2012) mais ces études restent trop éparses. D'un autre côté, l'étude de la photoacclimatation chez d'autres macroalgues brunes et en particulier chez des espèces natives représentatives des grandes ceintures algales, telles que les laminaires et les fucales, ont fait l'objet de nombreuses études, *e.g.* Delebecq et al., 2013, 2011; Gevaert et al., 2003; Migné et al., 2015.

Dans ce contexte, ce chapitre a pour but d'étudier la plasticité phénotypique, en fonction de la latitude (France-Portugal) et en fonction du niveau de la marée, de deux espèces invasives, *Codium fragile* et *Sargassum muticum*.Dans le cas de cette dernière, une comparaison est faite avec *Bifurcaria bifurcata*, une macroalgue brune native prédominante dans les mares rocheuses intertidales des côtes européennes atlantiques.

Matériels et Méthodes

La description des différentes espèces est précisée en introduction.

Sites étudiés et échantillonnage La phénologie de *Codium fragile ssp. fragile* et *Sargassum muticum* ont été suivies au niveau de 3 sites en Norvège, en France ainsi qu'au Portugal (pour une description précise des sites *cf.* introduction) :

- en Norvège (au Sud de Bergen) : site 1, site 2 et site 3 pour *S. muticum* et les sites 2, 3 et 4 pour *C. fragile*
- en France (à la Pointe bretonne) : la « Pointe du Diable », la « Pointe du Minou » et la « Pointe de Kermorvan » (Conquet)
- au Portugal (au Nord de Porto) : les trois sites se situent à « Moledo », à « Âncora », à « Viano do Castelo ».

L'échantillonnage en Norvège a été réalisé en plongée au cours d'une campagne en bateau en raison de l'absence de marnage (en collaboration avec Vivian Husa, de l'IMR à Bergen, en Norvège, partenaire du projet INVASIVES). En France et au Portugal, le suivi a été réalisé au cours de la marée basse.

Suivi écologique Ce suivi a été effectué au moyen de 3 quadrats d'une superficie de 0,0625 m^2 disposés selon un échantillonnage aléatoire raisonné au niveau de 3 mares intertidales pour chaque site (*cf.* Partie 1 - Note sur *Codium fragile*) permettant de suivre la densité, les fréquences d'individus en fonction de classes de taille, ainsi que le pourcentage de recouvrement pour chacune des deux espèces. L'intervalle des classes de taille a été déterminé à partir de la taille maximale des thalles. Le nombre de classes de taille (en appliquant la règle de Sturges) et l'amplitude de classe de taille ont été calculés comme précisé ci-dessous :

Règle de Sturges : Nombre de classe de taille = $1 + 3{,}322 \log_{10}(n)$

Avec n : la densité moyenne d'individus au niveau d'un site

Amplitude de classe de taille = (taille max. – taille min.) / nb de classe

Avec taille max. : moyenne de la taille maximale des individus sur l'ensemble des données ; taille min. : moyenne de la taille minimale des individus sur l'ensemble des données ; nb de classe : le nombre de classe de taille déterminé précédemment.

Ainsi sept classes de taille et une amplitude de 14 cm ont été déterminées pour *S. muticum* et 6 classes de taille ainsi qu'une amplitude de 8 cm l'ont été pour *C. fragile*. Les résultats obtenus pour les fréquences de taille ont été calculés à partir de la somme des données des trois quadrats réalisés pour chaque site, permettant d'obtenir trois répliquats par pays (un répliquat par site équivaut à 3 quadrats) et permettant une définition plus

précise des classes de taille. En plus de ces critères démographiques, des critères morphologiques spécifiques ou non à chaque espèce ont été suivis :

- le nombre de dichotomie et la largeur de la base pour *C. fragile*
- le nombre de latérales, la présence d'aérocystes et de réceptacles pour *S. muticum*

La présence ou l'absence d'autres espèces de macroalgues en épiphytes sur les thalles de *C. fragile* ou de *S. muticum* a également été notée.

Photo-physiologie En parallèle de ce suivi phénologique effectué en Juillet 2014, l'été suivant a été effectué un suivi physiologique de *Sargassum muticum* et d'une espèce native de macroalgue brune, *Bifurcaria bifurcata* se développant également dans les mares rocheuses intertidales sur les sites de la Pointe du Diable (le 03-07-2015) en France et d'Ancôra (le 15-06-2015) au Portugal. Ce suivi a été réalisé dans l'optique d'apprécier la plasticité de la photo-physiologie entre une espèce native et invasive se développant dans un même environnement en fonction de la latitude à laquelle elles se distribuent par la mesure de la modulation de la fluorescence de la chlorophylle a par Diving-PAM (Diving-Pulse Amplitude Modulation). L'espèce *C. fragile* n'a pu être suivie en raison du faible nombre d'individus répertoriés pour ces sites au niveau des mares intertidales suivies. Le protocole utilisé est développé dans la partie précédente (Partie 1, Chapitre 3, article en préparation sur l'enfouissement de *G. vermiculophylla*). Pour compléter cette expérience, un certain nombre de variables environnementales ont été suivies durant l'expérimentation au niveau de ces deux sites : la température, le pH (en utilisant un enregistreur multiparamètre Multi 350i, WTW doté d'une sonde Tetracon 325 et d'une sonde WTW Sentix 41) ainsi que l'éclairement incident (grâce à un capteur Li-COR de type LI-192SA, les données sont enregistrées par un Li-COR LI-1400).

Statistiques Les diverses analyses statistiques ont été effectuées avec le logiciel RStudio (v.0.95.263, avec la version 3.1.3 de R). Tous les résultats sont exprimés sous la forme de moyenne ± écart-type (noté SD pour Standard Deviation). Lorsque les données respectaient les conditions de normalité et d'homoscédasticité requises pour les tests paramétriques, une ANOVA à un ou deux facteurs a été appliquée sur celles-ci avec un degré de signification de 95%. En cas de différence significative, les données ont ensuite été analysées avec le test post-hoc de Tukey. Si nécessaire, les données ont été transformées afin d'être

homoscédastiques. Lorsque les données ne respectaient pas les prérequis aux analyses paramétriques, elles ont été analysées avec le test de Scheirer-Ray-Hare (SRH) (Sokal and Rohlf, 1995), qui consiste en test non paramétrique à 2 facteurs, ou avec le test de Kruskal-Wallis (KW) avec le même degré de signification (95%). De même, en cas de différence significative entre les moyennes, les données ont été analysées par un test de comparaison multiple s'appliquant après un test de KW (la fonction kruskalmc du pack pirgmess de R). D'autre part, des analyses multivariées de type analyse en composante principale (ACP) ont été conduites sur les données de phénologie (avec le pack ade4 de R). Une analyse de type Manova a été effectuée sur les coordonnées des individus générées par les ACP dans le but de discriminer les facteurs étudiés, *i.e.* sites et pays. En effet, les coordonnées des individus sur les différentes dimensions sont des variables indépendantes ce qui n'est pas le cas des paramètres démographiques et morphologiques suivis.

Résultats

- **Effet sur la biologie des populations**

- *Codium fragile ssp. fragile*

Les données écologiques de *C. fragile* pour le Portugal ne sont présentées que pour le site d'Âncora, cette espèce étant absente des deux autres sites malgré une prospection minutieuse au niveau des mares intertidales rocheuses. L'ACP sur les données écologiques de *C. fragile* est illustrée en Figure 1. L'axe 1 permet d'expliquer 37,51% de la variabilité des données, tandis que l'axe 2 permet d'expliquer seulement 25,80%. Le graphique des variables montre une forte corrélation de la largeur de la base, de la taille et du nombre de dichotomie vis-à-vis de l'axe 1 de l'ACP. Ainsi les individus ayant une taille importante, ont tendance à présenter une base plus large et un plus grand nombre de dichotomie. D'un autre côté, l'axe 2 est principalement expliqué par les variables de densité et de recouvrement (Figure 1 a-b). Les graphiques des individus en fonction des sites et des pays sont représentés en Figures 1c et 1d. Ils illustrent la forte variabilité des populations de *C. fragile* en Norvège avec une forte variabilité pour les sites 3 et 4 (N2 et N3) selon l'axe 1 signifiant une forte variation de la taille maximale, du nombre de dichotomie ainsi que de la largeur de la base entre les individus de ces deux sites (Figure 1c). Au contraire, au niveau du site 2 en Norvège (N1), deux groupes d'individus se distinguent selon l'axe 2, principalement par leur densité et par leur taux de recouvrement (par unité de surface). En comparaison des

populations norvégiennes, les populations de *C. fragile* en France et au Portugal sont plus homogènes. On observe aussi une distinction selon l'axe 2 des pays, notamment entre la Norvège et la France (Figure 1d). Cette observation est confirmée par une différence significative sur les coordonnées des individus entre la Norvège, la France et le Portugal (Manova, p-value < 0,05).

Les résultats de densité et de structures en taille des populations (variables contribuant fortement à la variabilité des données selon l'ACP) sont illustrés en Figure 2 et 3. Les populations de *C. fragile* présentent des densités plus élevées pour les sites échantillonnés en Norvège que ceux de la pointe bretonne (SRH, p-value = 5,88 10^{-3}, analyse réalisée uniquement sur les données françaises et norvégiennes) avec 154,67 ± 133,63 et 26,00 ± 16,66 nb.m^{-2} respectivement. Ces résultats moyennés par pays illustrent la forte variabilité en termes de densité entre les quadrats (Figure 2). En effet, les densités moyennes ne sont pas significativement différentes entre les sites que ce soit en Norvège (KW, p-value = 0,30) ou en France (KW, p-value = 0,32). Les profils de fréquence de taille montrent une prédominance de thalles inférieurs à 10 cm et mesurant de 10 à 18 cm (les 2 premières classes de taille) dans les trois pays. Sur l'ensemble des données, les fréquences de la classe de taille de 10 à 18 cm sont significativement plus élevées que celles de la classe de taille > 42 cm (SRH, p-value = 4,04 10^{-3}). Malgré des profils similaires, les pays se distinguent par des densités supérieures en Norvège (SRH, p-value = 0,012).

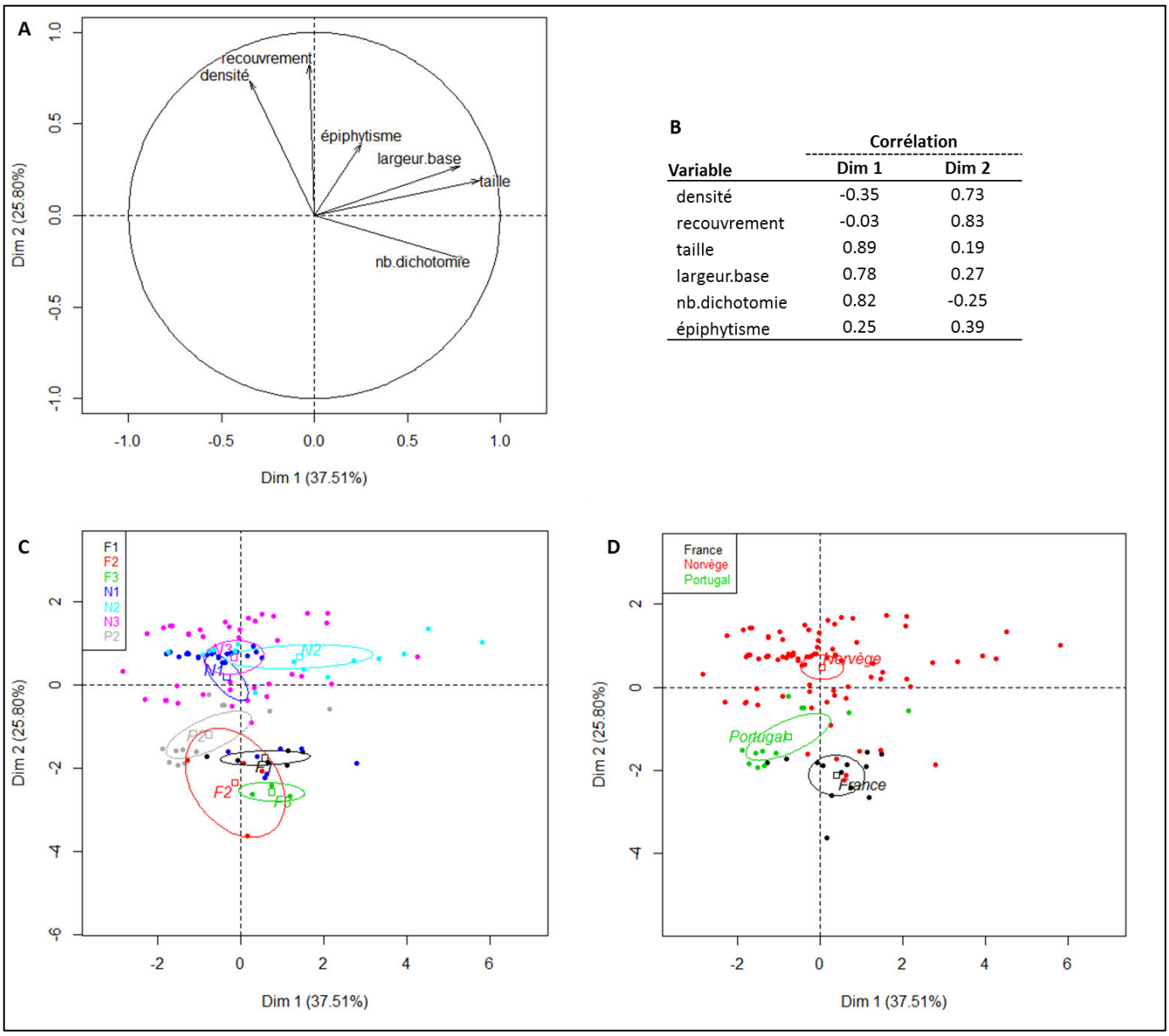

B

Variable	Corrélation Dim 1	Dim 2
densité	-0.35	0.73
recouvrement	-0.03	0.83
taille	0.89	0.19
largeur.base	0.78	0.27
nb.dichotomie	0.82	-0.25
épiphytisme	0.25	0.39

Fig. 1 Analyse en composante principale (ACP) des variables caractérisant la phénologie de *Codium fragile* en fonction des pays et des sites suivis en Juillet 2014. **A** : Graphique des corrélations de la densité, du pourcentage de recouvrement (« recouvrement »), de la longueur maximale (« taille »), de la largeur de la base (« largeur.base »), du nombre de dichotomie (« nb.dichotomie») et de la présence ou l'absence d'épiphytes (« épiphytisme »). **B** : Table des corrélations des variables intégrées à l'ACP selon la dimension 1 (« Dim 1 ») et la dimension 2 (« Dim 2 »). **C** : Graphique des individus de l'ACP en fonction des sites suivis pour chaque pays (F : France, N: Norvège, P: Portugal ; 1, 2, et 3 : numéro de site). D : Graphique des individus de l'ACP en fonction des pays d'échantillonnage (Norvège, France et

Portugal). Des ellipses avec un intervalle de confiance de 99% sont tracées autour du facteur considéré *i.e*, site ou pays.

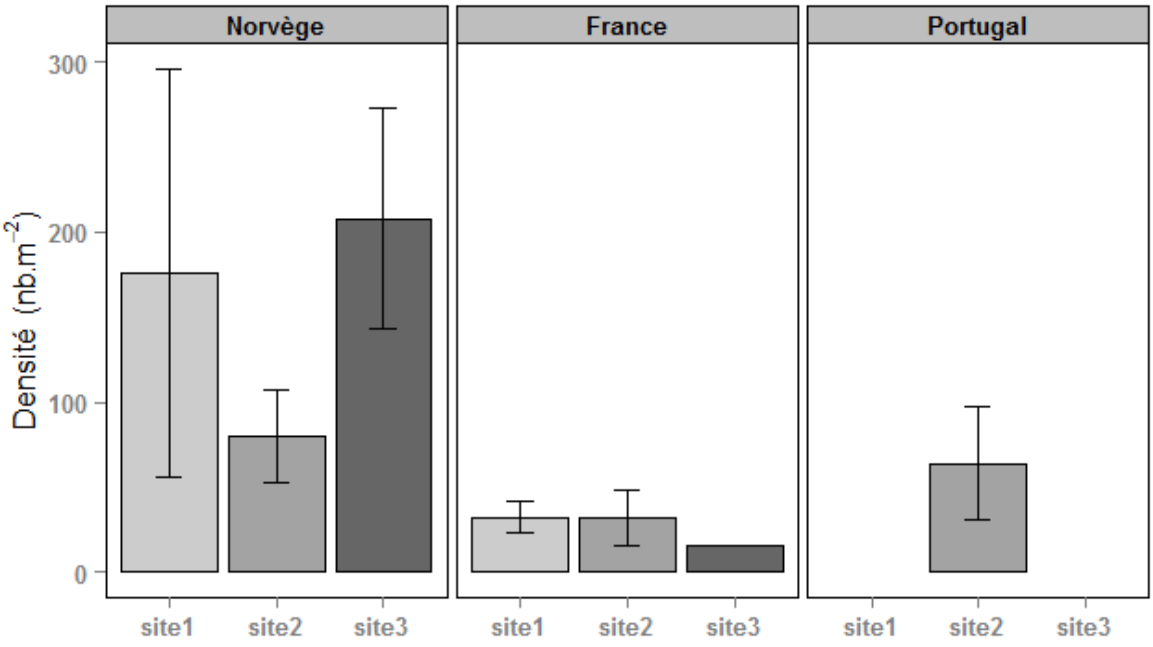

Fig. 2 Variation de la densité de *Codium fragile* exprimée en nombre de thalles par unité de surface (nb.m^{-2}) en fonction du pays d'échantillonnage (Norvège, France et Portugal) et des sites au sein de chaque pays. Pas de différence significative entre les sites de Norvège et de France (KW, p-value < 0.05). Les densités sont représentées sous la forme de moyennes ± SD (n=3) et l'absence de lettre indique l'absence de différence significative entre les sites d'un même pays.

Les résultats obtenus sur la densité, *i.e.* nombre d'individus par unité de surface, montrent clairement des populations norvégiennes plus denses par rapport à celles présentes en France. La population portugaise est comparable au site 2 norvégien Les populations norvégiennes sont bien structurées, et présentent une seule cohorte centrée sur la classe 10-18 cm. Dans la population dominent des individus de tailles restreintes (< 18 cm) mais de plus grands individus sont également présents, jusqu'à une taille supérieure à 42 cm, mais l'effectif des grands individus est moindre. Les populations françaises et portugaises sont structurées différemment, avec une dominance de petits individus, dont la taille est inférieure à 18 cm en France et à 10 cm au Portugal.

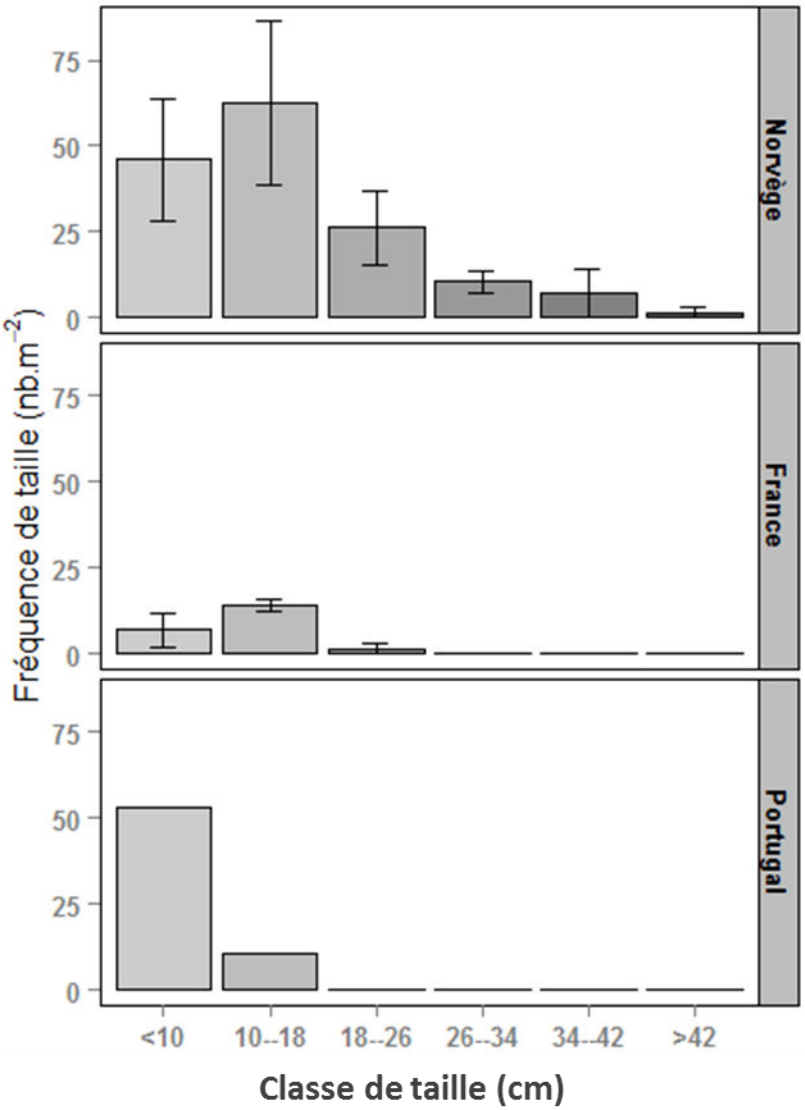

Fig. 3 Variation des fréquences de taille des thalles de *C. fragile* exprimée en nombre de thalle par unité de surface (nb.m^{-2}) en fonction du pays d'échantillonnage (*i.e.* la Norvège, la France et le Portugal). Les fréquences de taille sont représentées sous la forme de moyennes ± SD (n=3 et n=1 pour le Portugal) et l'absence de lettre indique l'absence de différence significative entre les fréquences de taille d'un même pays.

- *Sargassum muticum*

Les graphiques de corrélation des variables (Figure 4a) et des individus (Figure 4c-d) de *S. muticum* issu de l'ACP des données écologiques de cette espèce sont sensiblement proches de ceux obtenus pour *C. fragile*. En effet, pour le graphique de corrélation des variables, les variables démographiques, *i.e.* la densité et le pourcentage de recouvrement sont fortement corrélées à la dimension 2 qui explique 22,18% de la variabilité totale du jeu de donnée (Figures 1a-b). D'autre part, les variables descriptives sont corrélées à la dimension 1 qui représente 32,17% de la variabilité totale des données, en particulier les variables, taille, maturité et nombre de latérales. Il faut également noter que la présente ACP résume 54,35% de la variabilité des données phénologiques de *S. muticum*. De plus, le graphique des individus en fonction des différents sites échantillonnés pour chaque pays montre une variabilité des données principalement selon l'axe 1 pour la France et le Portugal (Figure 4c). En effet, les sites de Moledo et Âncora (P1 et P2 respectivement pour les sites 1 et 2 au Portugal) se distinguent du site de Viano do Castelo (P3). On observe également une répartition des sites français selon cet axe avec les sites de la pointe de Kermorvan, du Minou et de la Pointe du Diable de la gauche vers la droite de l'axe (F3, F2 et F1 respectivement pour les sites 3, 2, 1 de la France). Ainsi, pour ces pays, la variabilité entre les individus est plutôt liée à une variabilité de critères descriptifs comme la taille maximale, le stade de reproduction ainsi que le nombre de latérales au niveau de chaque thalle mais également en moindre proportion, à la présence ou l'absence d'épiphytes et d'aérocystes. Les sites français et norvégiens (en particulier N2 et N3 pour les sites 2 et 3 en Norvège) présentent une variabilité intrasite plus importante que les sites portugais (Figure 4c). Par ailleurs, au sein des populations de *S. muticum* pour les sites échantillonnés en Norvège, on observe plutôt une variation selon l'axe 2 liée à la forte variabilité intrasite indiquant une variabilité prédominante en termes de densité et de pourcentage de recouvrement. Le graphique des individus en fonction des pays (avec les sites non différenciés) illustrent une différenciation des pays selon l'axe 2 et ainsi selon des critères démographiques (*i.e.* densités et pourcentages de recouvrement). Si l'on prend en compte uniquement la densité, celle-ci ne varie pas en fonction des pays (SRH, p-value = 0,088) mais présente une variabilité significative entre les sites pour chaque pays sur l'ensemble des données (SRH, p-value = 0,025).

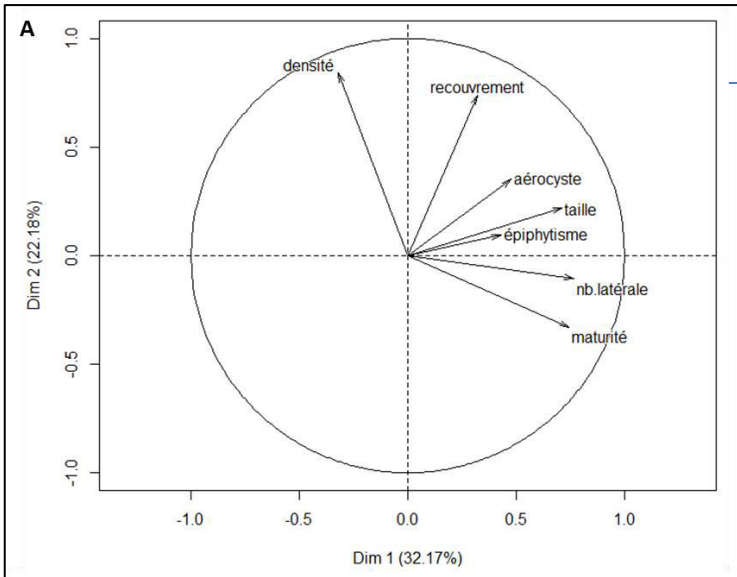

B

Variable	Corrélation Dim 1	Dim 2
densité	-0.32	0.84
nb. latérale	0.76	-0.11
taille	0.71	0.22
maturité	0.74	-0.33
aérocyste	0.47	0.35
épiphytisme	0.43	0.09
recouvrement	0.32	0.74

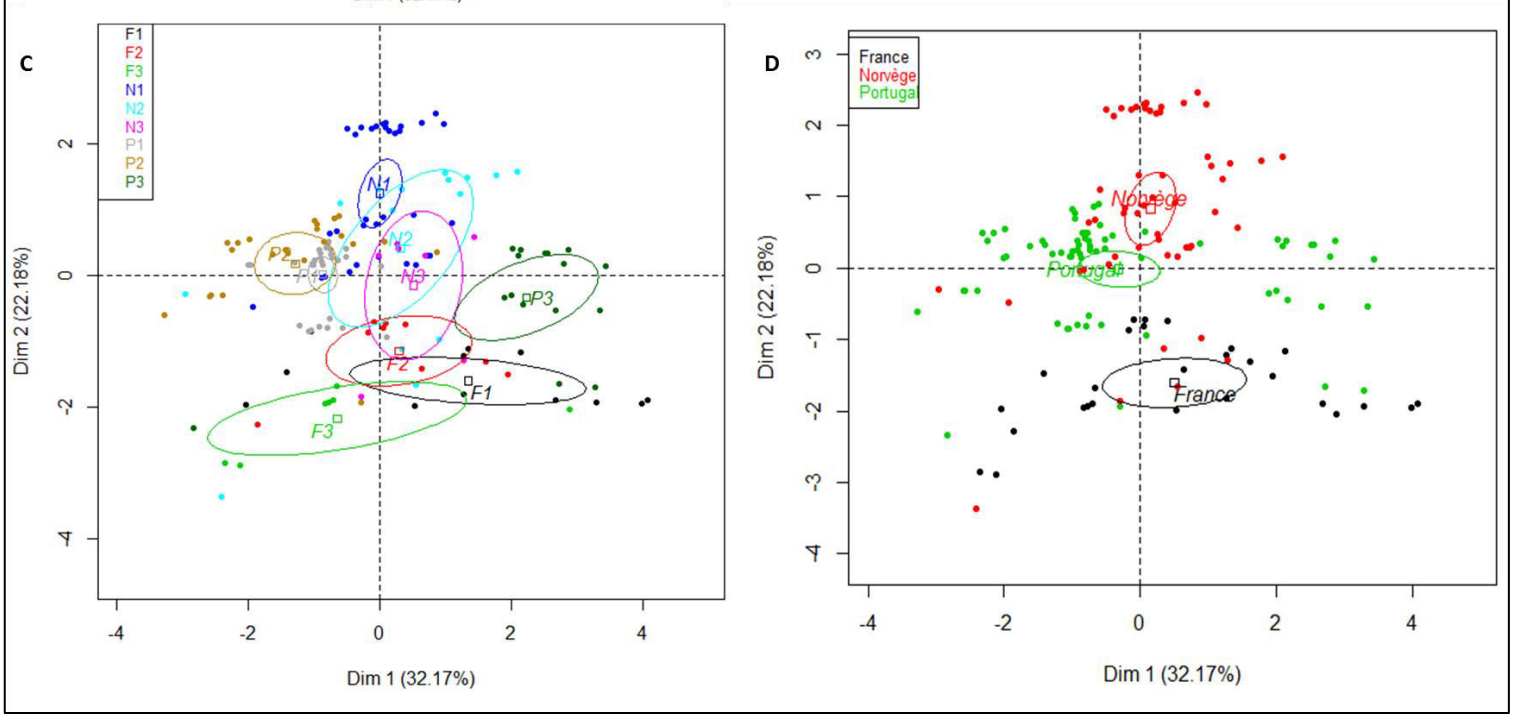

Fig. 4 ACP des variables caractérisant la phénologie de *Sargassum muticum* en fonction des pays et des sites suivis en Juillet 2014. **A** : Graphique des corrélations de la densité, du nombre de latérales (« nb.latérale»), de la longueur maximale (« taille »), de la présence de réceptacle (« matirité »), de la présence d'aérocystes (« aérocystes »), de la présence ou l'absence d'épiphytes (« épiphytisme ») et du pourcentage de recouvrement (« recouvrement »). **B** : Table des corrélations des variables intégrées à l'ACP selon la dimension 1 (« Dim 1 ») et la dimension 2 (« Dim 2 »). **C** : Graphique des individus de l'ACP en fonction des sites suivis pour chaque pays (F : France, N: Norvège, P: Portugal ; 1, 2, et 3 : numéro de site). D : Graphique des individus de l'ACP en fonction des pays d'échantillonnage (Norvège, France et Portugal). Des ellipses avec un intervalle de confiance de 99% sont tracées autour du facteur considéré, *i.e.* site ou pays.

En terme de densité, la variabilité locale des populations de *S. muticum* est supérieure à celle entre les pays du gradient latitudinal. Malgré des profils de fréquence des individus en fonction des classes de taille, qui semblent différer en fonction des pays, aucune différence significative n'est observée entre ceux-ci que ce soit sur l'ensemble des données (SRH, p-value = 0,29) ou pour chaque classe de taille (KW, p-value > 0,05).

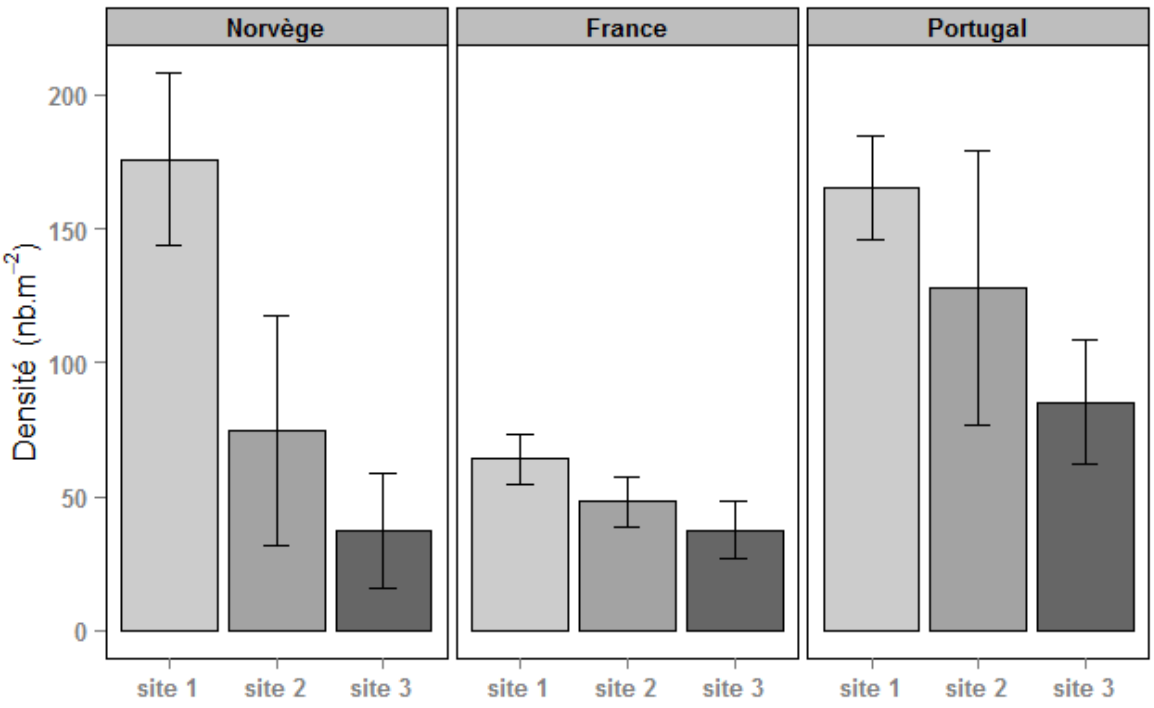

Fig. 5 Variation de la densité de *Sargassum muticum* exprimée en nombre de thalle par unité de surface (nb.m^{-2}) en fonction du pays d'échantillonnage (Norvège, France et Portugal) et des sites au sein de chaque pays. Pas de différence significative entre les sites de Norvège et de France (KW, p-value < 0.05). Les densités sont représentées sous la forme de moyennes ± SD (n=3) et l'absence de lettre indique l'absence de différence significative entre les sites d'un même pays.

Les populations extrêmes du gradient, *i.e.* Norvège et Portugal, montrent des densités qui peuvent être importantes et faibles, alors que les populations françaises, plus anciennes, présentent une densité qui varie peu entre les sites.

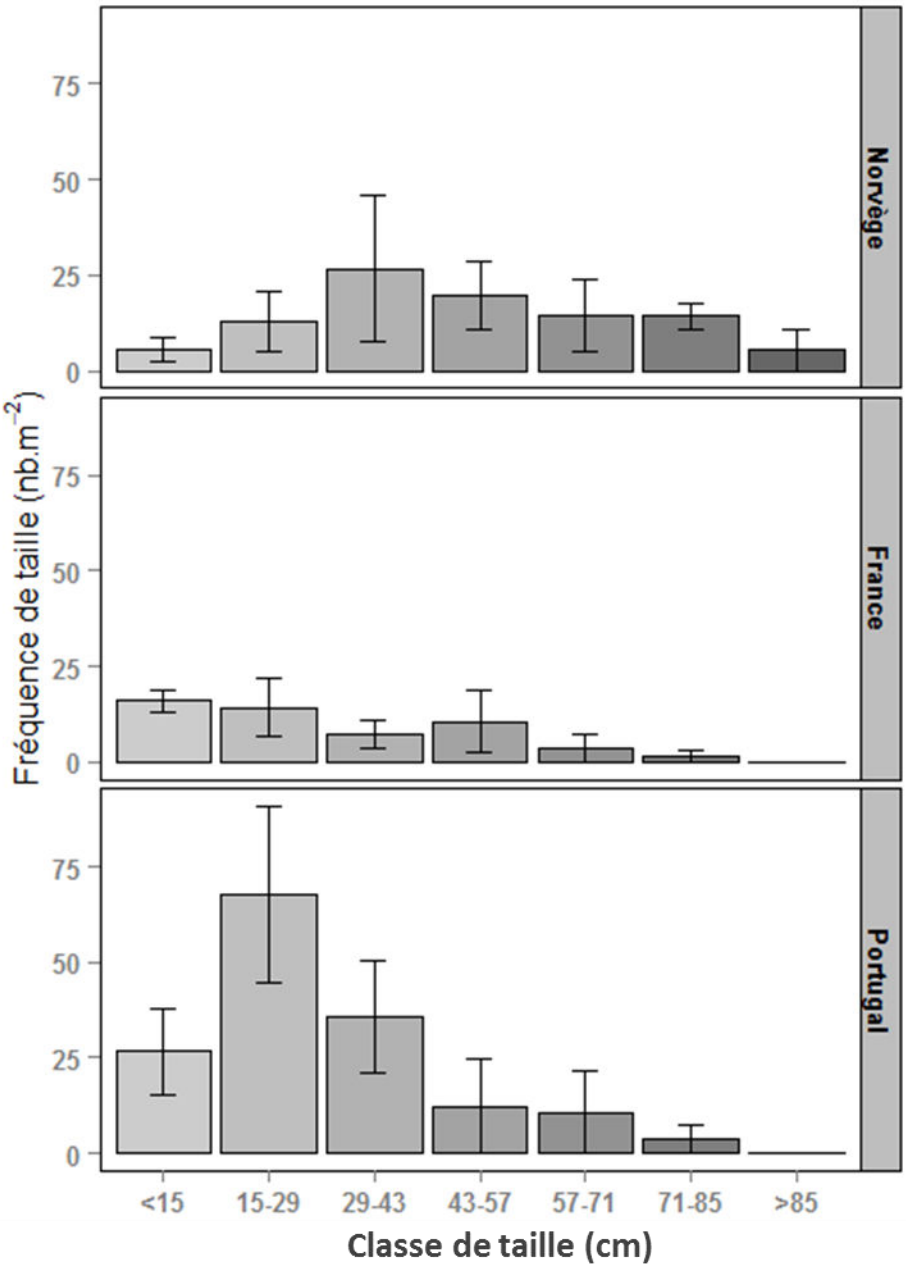

Fig. 3 Variation des fréquences de taille des thalles de *S. muticum* exprimée en nombre de thalle par unité de surface (nb.m^{-2}) en fonction du pays d'échantillonnage (*i.e.* la Norvège, la France et le Portugal). Les fréquences de taille sont représentées sous la forme de moyennes ± SD (n=3) et l'absence de lettre indique l'absence de différence significative entre les fréquences de taille d'un même pays.

Les populations de *Sargassum muticum* présentes à l'extrême du gradient, *i.e.* Portugal et Norvège, sont structurées de façon similaire avec l'existence d'une seule cohorte, centrée au niveau de la fréquence sur la classe 29-43 cm pour la Norvège et sur la classe 15-29 cm pour le Portugal. Les populations françaises, plus anciennes, présentent au moins deux cohortes. De grands individus sont observables pour l'ensemble des populations étudiées, avec des tailles supérieures à 85 cm dans les trois pays. Néanmoins, ils sont plus nombreux en Norvège.

- **L'efficacité photosynthétique**

  - Paramètres environnementaux

Les expérimentations de mesures de l'efficacité photosynthétique de *S. muticum* en comparaison avec *B. bifurcata* ont été menées lors de marées de vives eaux sur un site de la Pointe bretonne, la « Pointe du diable » ainsi qu'un site de la façade Atlantique du Nord du Portugal, « Âncora ». Lors des expérimentations, la marée basse a été marquée par un voile nuageux avec des éclaircies à la « Pointe du Diable » comme l'illustrent les données d'intensité lumineuse (Figures 7 et 8) avec un pic en milieu de marée à près de 2400 µmol photons.m^{-2}.s^{-1} vers 9h50 (h UTC). Sur le site d'Âncora, l'intensité lumineuse a augmenté de manière constante depuis le lever du soleil (Figures 7 et 8) et oscillait en fin de marée en atteignant un maximum d'environ 1700 µmol photons.m^{-2}.s^{-1} vers 9h45 (h UTC). Le temps d'émersion d'environ 3h30 est comparable entre les 2 sites. Le pH des mares à *S. muticum* et *B. bifurcata* présentait des valeurs analogues et augmentait progressivement au cours de la marée basse (Figures 7a et b). Les salinités moyennes mesurées sur les 2 sites étaient aussi très proches avec 35,5 ± 0,1 ppm à la « Pointe du Diable » et 35,3 ± 0,3 ppm à « Âncora ». La température de l'eau de mer des mares intertidales des 2 sites augmentait également de manière continue jusqu'à la fin de l'expérience, avec un réchauffement de 4,8°C à « Âncora » (15,8°C à 6h00 et 20,6°C à 9h40, hUTC) et de 5,5°C à la « Pointe du Diable » (18,2°C à 8h05 et 23,7°C à 12h10, hUTC).

  - Paramètres photosynthétiques

Les paramètres Fv/Fm et rETR de *S. muticum* et *B. bifurcata* sont illustrés par les Figures 7c-f et 8a-d respectivement. *S. muticum* présente des profils d'efficacité photosynthétique contrastés entre les 2 sites. En effet, à la « Pointe du Diable », le

paramètre Fv/Fm ne varie pas de manière significative (KW, p-value = 0,28) au cours de la marée alors que celui-ci décroit significativement de 19,26% au niveau du site d' «Âncora» (KW, p-value = 5,41 10^{-3}). Les données de rETR suivent les tendances des intensités lumineuses avec à une augmentation significative la « Pointe du Diable » (KW, p-value = 4,09 10^{-6}) de 176,9% entre 9h15 et 11h30 (avec 179,00 ± 27,67 et 316,65 ± 65,93 respectivement) suivie d'une baisse jusqu'à la fin de l'expérience. Au contraire, à « Âncora », l'augmentation du rETR est relativement constante et suit ainsi exactement la courbe de l'irradiance. D'autre part, la vitesse relative de transfert des électrons au niveau de PSII (rETR) est multipliée par 10,36 (KW, p-value < 0,0001) entre le début de l'expérience, lorsque la mare vient juste d'être découverte par l'eau de mer, et la fin de l'expérience, juste avant que la mare ne soit à nouveau recouverte avec la marée montante (avec 43,83 ± 1,40 à 5h50 et 454,18 ± 106,31 à 9h20, h UTC).

B. bifurcata présente une baisse peu significative de 13,91% de son rendement quantique du PSII ou Fv/Fm à Âncora (KW, p-value = 0.037 ; pas de différence observée après application des comparaisons multiples). A la « Pointe du Diable », ce paramètre décline de manière significative de 32,07% suite à un pic d'éclairement à 10h00 (h UTC) puis rejoint sa valeur initiale durant le reste de l'expérience (KW, p-value = 0.0034). Les valeurs de rETR augmentent significativement aux plus fortes valeurs d'intensité lumineuse à la Pointe du Diable puis retourne ensuite à sa valeur initiale. Pour le site d' « Âncora », cette vitesse relative de transfert des électrons chez *B. bifurcata* augmente de manière continue suivant une tendance semblable à celle observée pour *S. muticum* mais dans une moindre mesure avec une multiplication de 8,77 entre 5h50 et 8h40 (h UTC) s'abaissant à 6,56 entre le début et la fin de l'expérience (entre 5h50 et 9h30, h UTC).

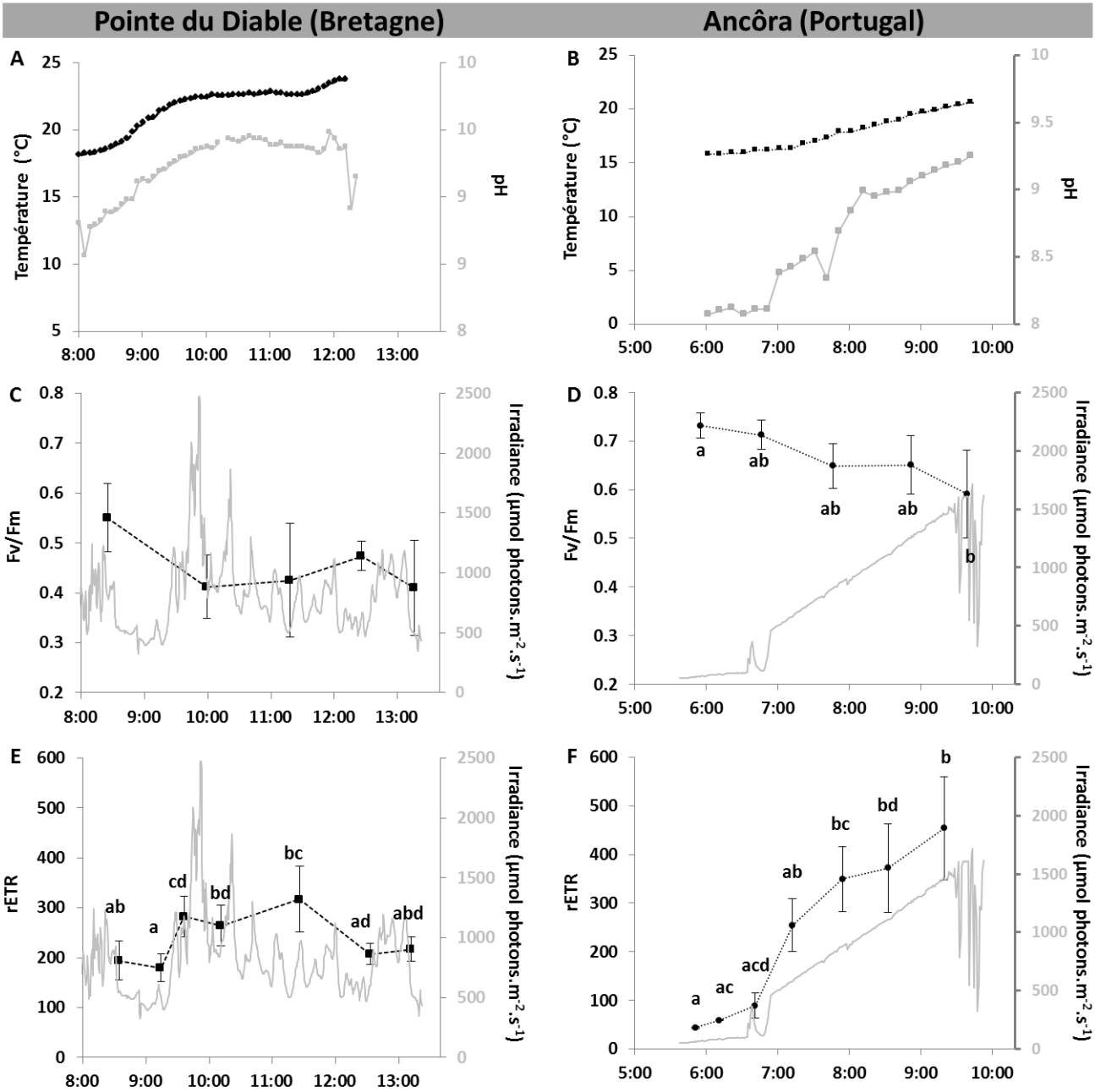

Fig. 7 Variation des paramètres environnementaux (température et pH de surface de l'eau de mer de la mare intertidale : A et B et rayonnement incident : C, D, E et F) et des paramètres photosynthétique (en pointillés : Fv/Fm : C et D, et rETR : E et F) mesurées sur des populations de *Sargassum muticum* au cours d'une marée de vives eaux (heures exprimées en h UTC) au cours de l'été 2015 à la « Pointe du Diable » (France) et à « Ancôra » (Portugal). Les paramètres photosynthétiques sont représentés sous la forme de moyenne ± SD (n ≥ 5). Après le test de KW suivi d'un test post-hoc non paramétrique, une différence significative entre les moyennes est représentée par une lettre différente (p-value < 0,05).

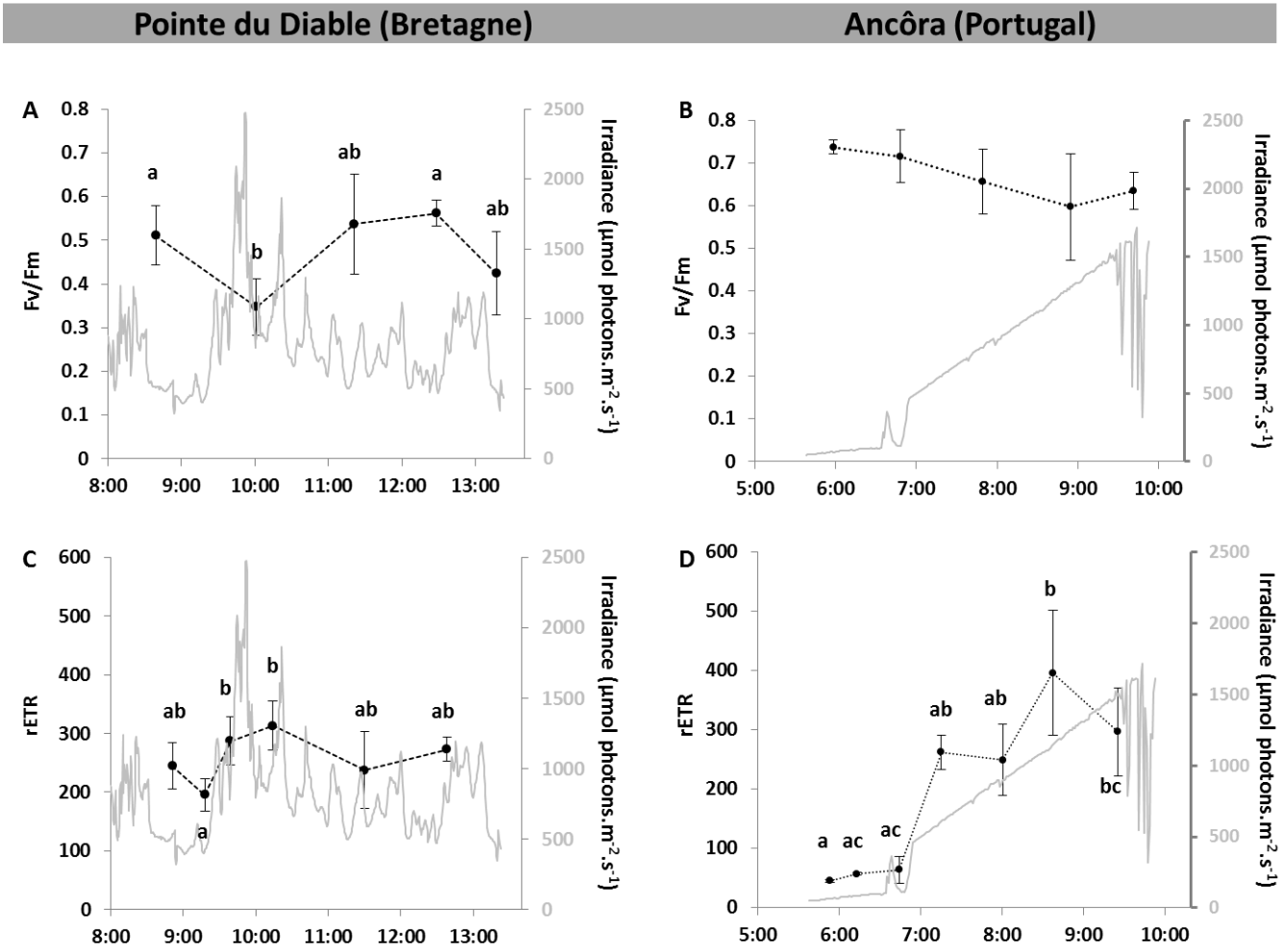

Fig. 8 Variation du rayonnement incident (A, B, C et D) et des paramètres photosynthétiques (en pointillés : Fv/Fm : A et B, et rETR : C et D) de *Bifurcaria bifurcata* au cours d'une marée de vives eaux (heures exprimées en h UTC) au cours de l'été 2015 à la « Pointe du Diable » (France) et à « Ancôra » (Portugal). Les paramètres photosynthétiques sont représentés sous la forme de moyenne ± SD (n ≥ 5). Après le test de KW suivi d'un test post-hoc non paramétrique, une différence significative entre les moyennes est représentée par une lettre différente (p-value < 0,05).

Discussion

Biologie des populations de deux espèces invasives de la Norvège au Portugal

Grâce à l'étude des critères morphologiques, les données obtenues lors de ce travail montrent une forte plasticité de la phénologie de *Codium fragile* et *Sargassum muticum*, en particulier de leurs critères morphologiques, plasticité qui se concentre à une échelle locale, *i.e.* à l'échelle de sites ou d'un ensemble de sites.

La variabilité des traits phénologiques chez *Codium fragile* tels que la taille des individus et la largeur de la base, est en effet prédominante à une échelle locale (*i.e.* à l'échelle de sites comparée à celle du gradient latitudinal). Ces résultats mettent en évidence une différence de densités entre les différents pays. En effet, pour les sites suivis en France et plus particulièrement au Portugal, le suivi a nécessité une recherche intensive de cette espèce alors qu'en Norvège, les populations formaient de véritables forêts sous-marines (observation personnelle). En dehors du gradient thermique qui différencie les différentes latitudes (Gohin et al., 2010), une autre différence environnementale majeure est à prendre en compte en raison de l'absence de marnage en Norvège. Cette absence de marnage induit par voie de conséquence une immersion constante des populations norvégiennes. Les variations de l'intensité lumineuse observées pour ce pays ne sont pas liées à une variation de la hauteur d'eau. Il en va de même pour la taille des individus qui n'est pas restreinte par la marée, d'où leur très grande taille à l'extrême nord du gradient. Ainsi, les populations de *Codium fragile* sont réparties au niveau de l'étage subtidal en Norvège.

De manière intéressante, Chapman (1999) a mis en évidence un potentiel invasif contrasté de *Codium fragile*. Une différence d'abondance importante est observée entre les populations invasives de *C. fragile ssp tomentosoides* sur les côtes Ouest et Est de l'Atlantique avec des populations éparses et des individus n'excédant pas 25 cm dans le Sud de l'Angleterre, contrairement à des populations denses également établies dans la zone subtidale et des individus pouvant mesurer jusqu'à 70 cm en Nouvelle Ecosse (Chapman, 1999). Dans cette présente étude, on observe une taille maximale de 14 cm au Portugal, de 18 cm en France et de 51 cm en Norvège (sur l'ensemble des données). Au cours du suivi saisonnier précédent, réalisé à la Pointe bretonne pour cette espèce (Partie 1 de ce manuscrit, Chapitre 1), la taille maximale rencontrée était de 25 cm ce qui rejoint les

observations de Chapman (1999) dans le Sud de l'Angleterre. Ainsi, les populations suivies en Norvège présenteraient des similitudes, du moins en termes d'abondance et de taille maximale, avec celles de Nouvelle Ecosse. De plus, on peut émettre l'hypothèse d'un potentiel invasif contrasté de cette espèce le long des côtes atlantiques européennes. Il serait pertinent de faire un suivi plus intensif en prospectant le long des côtes norvégiennes dans le but de confirmer l'abondance et le potentiel invasif exacerbé de *Codium fragile* en Norvège.

D'autre part, de même que pour *C. fragile*, cette plasticité locale chez *S. muticum* conduit à une variabilité du phénotype plus importante à l'échelle du site, plutôt qu'à l'échelle du gradient latitudinal étudié. En effet, la phénologie de *S. muticum* est très variable en fonction de divers facteurs environnementaux mais ne semble pas être prédominée par le gradient thermique qui caractérise le gradient latitudinal (Gohin et al., 2010) pour les critères morphologiques suivis. Ce constat est en accord avec la bibliographie. Par exemple, Norton et Deysher (1989) ont illustré une variation de la phénologie de la reproduction de cette espèce liée à des facteurs locaux, plutôt que résultant d'une acclimatation des individus à différentes latitudes le long des côtes californiennes. En effet, des facteurs environnementaux tels que la lumière ou la température (Arenas et al., 1995; Le Lann, 2009) ainsi que les concentrations en nutriments (Le Lann, 2009; Sanchez and Fernandez, 2006) sont connus pour réguler la phénologie de cette espèce invasive et en particulier la longueur des thalles en lien avec les variations saisonnières de ces paramètres environnementaux. La variation en terme de densité entre les sites d'un même pays peut expliquer la plasticité phénotypique rencontrée à cette échelle. En effet, la densité est un facteur déterminant chez *S. muticum* qui influence la taille moyenne ainsi que la morphologie du thalle, et par voie de conséquence, influe sur la reproduction (Arenas et al., 2002). De plus, Le Lann et al. (2012) a montré une variation de la taille des thalles de *S. muticum* à une échelle locale entre différents sites de la Pointe bretonne (dont la Pointe du Diable) laquelle étant principalement dépendante du type de substrat et de l'hydrodynamisme. L'absence de différences significatives entre les profils de classe de taille semble suggérer une homogénéité marquée entre les sites de ce point de vue. Tout comme *C. fragile*, notre étude montre que la taille des individus des populations norvégiennes est plus importante que celles déterminées dans le sud de l'Europe. La position des populations

en zone subtidale ne restreint pas les individus au niveau croissance, contrairement aux populations des mares de l'estran rocheux, dont la taille est dépendante de la hauteur d'eau à marée basse. Un tel constat a été démontré en milieu tropical par Stiger et Payri (1999) qui ont observé chez une Sargassaceae de Polynésie française, *Turbinaria ornata*, une taille des individus en relation avec la hauteur d'eau et un nanisme des individus sur la crête récifale, quand peu d'eau est présente au-dessus des individus.

Plasticité de la photo-physiologie d'une espèce native et invasive entre la France et le Portugal :

Les deux macroalgues brunes étudiées présentent une plasticité différentielle *in situ* de leurs paramètres photosynthétiques en réponse aux conditions environnementales entre la France et le Portugal. D'une part, les résultats suggèrent la mise en place d'une photoinhibition au cours de la marée chez *S. muticum* au Portugal, qui s'exprime par une diminution de l'efficacité photosynthétique du PS II (*i.e.* Fv/Fm) ce qui n'est pas le cas à la « Pointe du Diable » en France. A l'inverse, un déclin du Fv/Fm chez l'algue native *B. bifurcata* en lien avec une augmentation de l'éclairement est observé pour les deux sites. Le retour aux valeurs initiales en fin d'expérience à la « Pointe du Diable » indique que la photoinhibition observée est de type dynamique et permet de prévenir des dommages liés à un éclairement trop intense par une maximisation de la dissipation de l'énergie lumineuse (Hanelt et al., 2003). Cette photoinhibition dynamique n'impliquant pas de photodommage est une régulation réversible de l'efficacité photosynthétique chez les végétaux (Müller et al., 2001). De plus, il est intéressant de noter que les deux espèces présentent en début de marée basse (c'est-à-dire en l'absence de stress lumineux lié au cycle tidal) un Fv/Fm plus bas à la « Pointe du Diable » en comparaison de celui du site d'« Âncôra ». Ceci suggère une plus faible efficacité photosynthétique du PS II lors des expériences au niveau du site de la Pointe bretonne en comparaison du site portugais lors des expérimentations. Ainsi, les conditions environnementales caractéristiques du site d'« Âncôra » ne semblent pas représenter des conditions stressantes pour ces espèces. D'autre part, la photoinhibtion dynamique observée chez *B. bifurcata* à la « Pointe du Diable », contrairement à *S. muticum* qui ne la présente pas, peut indiquer une résilience moins effective de l'espèce native en comparaison de l'espèce invasive vis-à-vis des conditions environnementales propres à ce site.

Conclusion Ces résultats illustrent en particulier une forte variabilité des phénotypes (phénologique et physiologique) qui caractérise de nombreuses espèces invasives végétales (Davidson et al., 2011), même si cette caractéristique ne peut être généralisée et reste controversée (Godoy et al., 2011). Huang et al. (2015) émettent l'hypothèse intéressante que cette plasticité pourrait être favorisée dans un environnement où les stress environnementaux sont mitigés, notamment si l'on tient compte de la théorie de l'ERH (*cf*. Introduction) induisant une diminution des coûts et une augmentation des bénéfices potentiels de la plasticité. Ainsi, en effectuant le raisonnement inverse, on peut émettre l'hypothèse qu'une telle plasticité des phénotypes pourrait constituer un indicateur du niveau de stress que représente un milieu pour une population donnée d'une espèce invasive, caractérisée par cette plasticité. La mise au point d'un tel indicateur couplé à des suivis phénologiques et physiologiques à de grandes échelles permettrait une compréhension pertinente du potentiel invasif d'espèces algales, notamment aux marges, Sud et Nord, de leur aire de distribution.

Dans ce contexte, la différence de densité observée pour *Codium fragile*, peut laisser présager qu'une augmentation des températures pourrait avoir un effet négatif sur les populations. Mais des études complémentaires sont nécessaires afin de comprendre une telle différence dans l'abondance de cette espèce en fonction de la latitude. En effet, cette différence peut être liée à d'autres facteurs environnementaux. Chapman (1999) suggèrent une différence de potentiel invasif entre le Canada et les côtes anglaises liées à une différence de diversité spécifique, ainsi qu'à la présence de nombreuses espèces de *Codium,* présentes sur les côtes européennes (Chapman, 1999). Le genre *Codium* étant également diversifié en Norvège (Armitage and Sjøtun, 2016; Cabioc'h et al., 2006), des études comparatives de la diversité spécifique des macroalgues le long du gradient pourrait apporter un élément de réponse à cet état de fait.

D'autre part, la forte plasticité phénologique observée chez *S. muticum,* ainsi qu'une photoinhibition de type dynamique au Portugal, laisse entrevoir que le réchauffement climatique n'aurait pas d'impact négatif pour ces critères sur cette espèce. La bibliographie confirme cette hypothèse et laisse même soupçonner que le changement climatique serait plutôt favorable à la pérennité de *S. muticum*. En effet, Norton et Deysher (1989) suggèrent que des températures océaniques plus chaudes permettraient un développement plus

rapide ainsi qu'une reproduction avancée de *S. muticum*. D'autre part, Olabarria et al. (2013) ont étudié l'effet simultané d'une augmentation des concentrations en CO_2 et des températures sur des assemblages macroalgaux de mares rocheuses afin d'apprécier la résilience de ces assemblages vis-à-vis du changement climatique. Leurs résultats suggèrent que l'espèce formant une canopée dans de tels assemblages est déterminante et que les assemblages envahis par *S. muticum*, *i.e.* assemblages où la canopée est formée par cette espèce invasive, seraient plus résilients face au changement climatique (Olabarria et al., 2013). De plus, il est intéressant d'ajouter que cette espèce est toujours en phase d'expansion et qu'elle est maintenant introduite au Maroc (Sabour et al., 2013).

Références

Andrew, N.L., Viejo, R.M., 1998. Ecological limits to the invasion of *Sargassum muticum* in northern Spain. Aquat. Bot. 60, 251–263.

Arenas, F., Fernández, C., 2009. Ecology of *Sargassum muticum* (Phaeophyta) on the North Coast of Spain. III. Reproductive Ecology. Bot. Mar. 41, 209–216.

Arenas, F., Fernández, C., Rico, J.M., Fernández, E., Haya, D., 1995. Growth and reproductive strategies of *Sargassum muticum* (Yendo) Fensholt and *Cystoseira nodicaulis* (Whit.) Roberts. Sci. Mar. 59, 1–8.

Arenas, F., Viejo, R.M., Fernández, C., 2002. Density-dependent regulation in an invasive seaweed: responses at plant and modular levels. J. Ecol. 90, 820–829.

Armitage, C.S., Sjøtun, K., 2016. *Codium fragile* in Norway: subspecies identity and morphology. Bot. Mar. 59, 439–450.

Baer, J., Stengel, D.B., 2010. Variability in growth, development and reproduction of the non-native seaweed *Sargassum muticum* (Phaeophyceae) on the Irish west coast. Estuar. Coast. Shelf Sci. 90, 185–194.

Cabioc'h, J., Floc'h, J.-Y., Le Toquin, A., Boudouresque, C.F., Meinesz, A., Verlaque, M., 2006. Guide des algues des mers d'Europe. Delachaux et Niestlé.

Campbell, S.J., Bité, J.S., Burridge, T.R., 2005. Seasonal Patterns in the photosynthetic capacity, tissue pigment and nutrient content of different developmental stages of *Undaria pinnatifida* (Phaeophyta: Laminariales) in Port Phillip Bay, South-Eastern Australia. Bot. Mar. 42, 231–242.

Chapman, A.S., 1999. From introduced species to invader: what determines variation in the success of *Codium fragile ssp. tomentosoides* (Chlorophyta) in the North Atlantic Ocean? Helgol. Meeresunters. 52, 277–289.

Davidson, A.M., Jennions, M., Nicotra, A.B., 2011. Do invasive species show higher phenotypic plasticity than native species and, if so, is it adaptive? A meta-analysis. Ecol. Lett. 14, 419–431.

Delebecq, G., Davoult, D., Menu, D., Janquin, M.-A., Dauvin, J.-C., Gevaert, F., 2013. Influence of local environmental conditions on the seasonal acclimation process and the daily integrated production rates of *Laminaria digitata* (Phaeophyta) in the English Channel. Mar. Biol. 160, 503–517.

Delebecq, G., Davoult, D., Menu, D., Janquin, M.-A., Migné, A., Dauvin, J.-C., Gevaert, F., 2011. In situ photosynthetic performance of *Laminaria digitata* (Phaeophyceae) during spring tides in Northern Brittany. CBM-Cah. Biol. Mar. 52, 405.

Engelen, A., & Santos, R. 2009. Which demographic traits determine population growth in the invasive brown seaweed *Sargassum muticum*?. Journal of Ecology, 97(4), 675-684.

Gevaert, F., Creach, A., Davoult, D., Migne, A., Levavasseur, G., Arzel, P., Holl, A., Lemoine, Y., 2003. *Laminaria saccharina* photosynthesis measured in situ: photoinhibition and xanthophyll cycle during a tidal cycle. Mar. Ecol. Prog. Ser. 247, 43–50.

Godoy, O., Valladares, F., Castro-Díez, P., 2011. Multispecies comparison reveals that invasive and native plants differ in their traits but not in their plasticity. Funct. Ecol. 25, 1248–1259.

Gohin, F., Saulquin, B., Bryere, P., 2010. Atlas de la Température, de la concentration en Chlorophylle et de la Turbidité de surface du plateau continental français et de ses abords de l'Ouest européen.

Hamel, K.M., 2012. Comparative time course of photoacclimation in Hawaiian endemic and invasive species of *Gracilaria* (rhodophyta) (Thesis). Honolulu: University of Hawaii at Manoa.

Hanelt, D., Wiencke, C., Bischof, K., 2003. Photosynthesis in marine macroalgae, in: Larkum, A.W.D., Douglas, S.E., Raven, J.A. (Eds.), Photosynthesis in algae, Advances in photosynthesis and respiration. Springer Netherlands, pp. 413–435.

Hanelt, D., Wiencke, C., Nultsch, W., 1997. Influence of UV radiation on the photosynthesis of arctic macroalgae in the field. J. Photochem. Photobiol. B 38, 40–47.

Huang, Q.Q., Pan, X.Y., Fan, Z.W., Peng, S.L., 2015. Stress relief may promote the evolution of greater phenotypic plasticity in exotic invasive species: a hypothesis. Ecol. Evol. 5, 1169–1177.

Kraan, S., 2008. *Sargassum muticum* (Yendo) Fensholt in Ireland: an invasive species on the move. J. Appl. Phycol. 20, 825–832.

Le Lann K., Connan S., Stiger-Pouvreau V. (2012). Phenology, TPC and size-fractioning phenolics variability in temperate Sargassaceae (Phaeophyceae, Fucales) from Western Brittany: Native versus introduced species. *Marine Environmental Research.* 80: 1-11

Le Lann, K., 2009. Etude de la biodiversité des Sargassaceae (Fucales, Phaeophyceae) en milieux tempéré et tropical : écologie, chimiotaxonomie et source de composés bioactifs (phdthesis). Université de Bretagne occidentale - Brest.

Loughnane, C., Stengel, D.B., 2002. Attached *Sargassum muticum* (Yendo) Fensholt found on the West coast of Ireland. Ir. Nat. J. 27, 70–72.

Migné, A., Delebecq, G., Davoult, D., Spilmont, N., Menu, D., Gévaert, F., 2015. Photosynthetic activity and productivity of intertidal macroalgae: In situ measurements, from thallus to community scale. Aquat. Bot. 123, 6–12.

Müller, P., Li, X.-P., Niyogi, K.K., 2001. Non-photochemical quenching. A response to excess light energy. Plant Physiol. 125, 1558–1566.

Nitschke, U., Connan, S., Stengel, D.B., 2012. Chlorophyll a fluorescence responses of temperate Phaeophyceae under submersion and emersion regimes: a comparison of rapid and steady-state light curves. Photosynth. Res. 114, 29–42.

Norton, T.A., Deysher, L.E., 1989. The reproductive ecology of *Sargassum muticum* at different latitudes. Reprod. Genet. Distrib. Mar. Org. 147–152.

Olabarria, C., Arenas, F., Viejo, R.M., Gestoso, I., Vaz-Pinto, F., Incera, M., Rubal, M., Cacabelos, E., Veiga, P., Sobrino, C., 2013. Response of macroalgal assemblages from

rockpools to climate change: effects of persistent increase in temperature and CO_2. Oikos 122, 1065–1079.

Pedersen, M.F., Stæhr, P.A., Wernberg, T., Thomsen, M.S., 2005. Biomass dynamics of exotic *Sargassum muticum* and native *Halidrys siliquosa* in Limfjorden, Denmark—Implications of species replacements on turnover rates. Aquat. Bot. 83, 31–47.

Plouguerné, E., 2006. Etude écologique et chimique de deux algues introduites sur les côtes bretonnes, *Grateloupia turuturu* Yamada et *Sargassum muticum* (Yendo) Fensholt: nouvelles ressources biologiques de composés à activité antifouling. Brest.

Plouguerné, E., Le Lann, K., Connan, S., Jechoux, G., Deslandes, E., Stiger-Pouvreau, V., 2006. Spatial and seasonal variation in density, reproductive status, length and phenolic content of the invasive brown macroalga *Sargassum muticum* (Yendo) Fensholt along the coast of Western Brittany (France). Aquat. Bot. 85, 337–344.

Provan, J., Booth, D., Todd, N.P., Beatty, G.E., Maggs, C.A., 2008. Tracking biological invasions in space and time: elucidating the invasive history of the green alga *Codium fragile* using old DNA. Divers. Distrib. 14, 343–354.

Rueness, J., 1989. *Sargassum muticum* and other introduced Japanese macroalgae: Biological pollution of European coasts. Mar. Pollut. Bull. 20, 173–176.

Sabour, B., Reani, A., El-Magouri, H., Haroun, R., 2013. *Sargassum muticum* (Yendo) Fensholt (Fucales, Phaeophyta) in Morocco, an invasive marine species new to the Atlantic coast of Africa. Aquat. Invasions 8, 97.

Sanchez, igo, Fernandez, C., 2006. Resource availability and invasibility in an intertidal macroalgal assemblage. Mar. Ecol. Prog. Ser. 313, 85–94.

Silva, P.C., 1955. The dichotomous species of Codium in Britain. J. Mar. Biol. Assoc. U. K. 34, 565–577.

Sjøtun, K., Eggereide, S.F., Høisæter, T., 2007. Grazer-controlled recruitment of the introduced *Sargassum muticum* (Phaeophyceae, Fucales) in northern Europe. Mar. Ecol. Prog. Ser. 342, 127–138.

Sokal, R.R., Rohlf, F.J., 1995. Biometry: The principles and practice of statistics in biological research.

Stiger, V., Payri, C.E. 1999a. Spatial and seasonal variations in the biological characteristics of two invasive brown algae, *Turbinaria ornata* (Turner) J. Agardh and *Sargassum mangarevense* (Grunow) Setchell (Sargassaceae, Fucales) spreading on the reefs of Tahiti (French Polynesia). Botanica Marina 42: 295-306.

Tanniou, A., 2014. Etude de la production de biomolécules d'intérêt (phlorotannins, pigments, lipides) par l'algue brune modèle *Sargassum muticum* par des approches combinées de profilage métabolique et d'écophysiologie.

Tanniou, A., Vandanjon, L., Gonçalves, O., Kervarec, N., Stiger-Pouvreau, V., 2015. Rapid geographical differentiation of the European spread brown macroalga *Sargassum muticum* using HRMAS NMR and Fourier-Transform Infrared spectroscopy. Talanta 132, 451–456.

Tanniou, A., Vandanjon, L., Incera, M., Leon, E.S., Husa, V., Grand, J.L., Nicolas, J.-L., Poupart, N., Kervarec, N., Engelen, A., Walsh, R., Guerard, F., Bourgougnon, N., Stiger-Pouvreau, V., 2014. Assessment of the spatial variability of phenolic contents and associated bioactivities in the invasive alga *Sargassum muticum* sampled along its European range from Norway to Portugal. J. Appl. Phycol. 26, 1215–1230.

Vaz-Pinto, F., Martínez, B., Olabarria, C., Arenas, F., 2014. Neighbourhood competition in coexisting species: The native *Cystoseira humilis* vs the invasive *Sargassum muticum*. J. Exp. Mar. Biol. Ecol. 454, 32–41.

Wernberg, T., Thomsen, M.S., Stæhr, P.A., Pedersen, M.F., 2005. Comparative phenology of *Sargassum muticum* and *Halidrys siliquosa* (Phaeophyceae: Fucales) in Limfjorden, Denmark. Bot. Mar. 44, 31–39.

Wernberg, T., Thomsen, M.S., Staehr, P.A., Pedersen, M.F., 2004. Epibiota communities of the introduced and indigenous macroalgal relatives *Sargassum muticum* and *Halidrys siliquosa* in Limfjorden (Denmark). Helgol. Mar. Res. 58, 154.

Zanolla, M., Altamirano, M., Carmona, R., Rosa, J.D.L., Sherwood, A., Andreakis, N., 2015. Photosynthetic plasticity of the genus *Asparagopsis* (Bonnemaisoniales, Rhodophyta) in response to temperature: implications for invasiveness. Biol. Invasions 17, 1341–1353.

Chapitre 6. *Gracilaria vermiculophylla* présente-t-elle une plasticité phénotypique le long d'un gradient latitudinal sur les côtes européennes de l'Atlantique Nord-Est ?

Les résultats précédents ont illustré des conclusions différentes quant à l'effet potentiel du réchauffement climatique sur deux espèces invasives d'estrans rocheux. Au contraire de ces espèces, *Gracilaria vermiculophylla* se distribue principalement sur la slikke nue non végétalisée. Ainsi, cette espèce ingénieure des estrans meubles et saumâtres (démontré dans la partie 1, Chapitre 4) est peu soumise aux compétitions interspécifiques. On peut donc s'attendre à observer des effets plus facilement transposables entre les latitudes Nord et Sud dans un contexte de réchauffement climatique, du fait de l'absence de ce facteur biotique. En effet, il a été montré au niveau de mares rocheuses intertidales une interaction forte entre la nature de l'espèce formant une canopée et la résilience de l'ensemble de l'assemblage macroalgal face au réchauffement climatique (Olabarria et al., 2013). Ainsi, certaines espèces algales pourtant moins plastiques d'un point de vue physiologique en comparaison d'autres espèces, du fait de leur association avec une espèce précise formant une canopée telle que *Sargassum muticum,* pourront être amenées à mieux résister au changement climatique. Ce type d'interaction n'est pas à prendre en considération pour *G. vermiculophylla*.

Dans ce contexte, ce chapitre présente la variabilité phénologique, photo-physiologique et biochimique de l'espèce invasive *G. vermiculophylla* à deux latitudes, dans la ria du Faou (Rade de Brest, France) et dans la Ria de Aveiro (Portugal) dans le but de présager de l'évolution de la répartition de cette espèce le long des côtes européennes Nord Atlantique dans un contexte de changement climatique.

Cette étude fait l'objet d'un manuscrit en cours de préparation.

Article en préparation

Ecophysiology of *G. vermiculophylla* in function of latitudes along its distribution range on the North European Atlantic coasts

Introduction

Consequences of climate change are numerous and increasingly visible on the coastal areas (Harley et al., 2006). Climate change thorough climate warming will induce the recurrent exposition of species to extreme temperatures, variable in time and leading to a switch of species to northern latitudes but also a succession of scattered local extinctions (Helmuth et al., 2002). Seaweeds resilience face to climate change depends of species. Lima et al. (2007) reported differential behavior between seaweeds from cold water and seaweeds from warm water. The latter may present a more opportunistic life cycle than the former with faster growth, precocious reproduction together with shorter life span.

Additionally, the anthropic activities keep continuing to intensify and the number of invasive species continues to increase (Stiger-Pouvreau and Thouzeau, 2015). The two major anthropogenic forcings on ecosystems, global warming and biological invasions interact at many scales. The climate change has an influence on filters efficacy determining the introduction, naturalization as the invasive potential of non-native species (Rahel and Olden, 2008). In this way, climate warming will alter the distribution range of invasive species already naturalized (Hellmann et al., 2008). Given their broad geographical distribution, especially those occurring along the Northeastern Atlantic Ocean, the invasive species are likely to adapt much more easily and quickly to climatic modifications than native species. A high plasticity associated to the lack of native enemies lead to a lower pressure of predators in the invasive area and to a less stressful environment, compared to the native area. This could also explain the invasive potential of these introduced species (Huang et al., 2015; Lande, 2015). Therefore, the high phenotypic or ecophysiological plasticity induced by the new environmental conditions (Eggert, 2012) will favor an adaptive plasticity depending on differences in environmental advantages between the native and invasive areas, including biotic and abiotic factors (Huang et al., 2015; Lande, 2015). This adaptive plasticity confers fitness advantages to the invasive species allowing the optimization of acclimation mechanisms to the new environmental conditions (Davidson et al., 2011).

The development of a species in a biogeographic area is mainly governed by its physiological tolerance of life cycle. Latitudinal distribution of macroalgae was mainly determined by temperature in interaction with daylength for the synchronization of the life cycle (Bartsch et al. 2012). Most of studies investigated the physiological tolerance of native species along their distribution range to assess their thermal tolerance (*e.g.* Jueterbock et al., 2014; Wernberg et al., 2010). Few data currently exist on the expansion of introduced marine macroalgae, in particular on the plasticity of their photo-physiology as their production of metabolites (Raniello et al., 2006, 2004; Zanolla et al., 2015). On the other hand, analysis of variability suggested that short term variations of temperature associated to inter-annual variations will hide isotherm variations occurring at long term during several decays worldwide (Isaak and Rieman, 2013). In this context, adapted experimental strategies to study climate change effects have to be ongoing.

Studying species which presents a large geographical distribution at several latitudes by comparing southern latitude to northern one, expects to predict the species behavior in a context of climatic change. In particular, it could serve to predict algae behavior invasion in incoming north latitudes by observing the ecophysiological functions in its warmer latitude sites. This experiment strategy was used to determine the vulnerability of native species (*e.g.* Wernberg et al., 2010) and may be applied to invasive species to find out about the plasticity of ecophysiological performance of non-native seaweeds in a context of climatic change. In this context, this work aimed at study the ecophysiology of of *G. vermiculophylla* (Ohmi) Papenfuss, an estuarine red invasive macroalga at two latitudes (at a distance of around 900 km) along its distribution range on North Atlantic European coasts: (1) in the Bay of Brest (in West Brittany, France) and (2) in the ria de Aveiro lagoon (on the North West coast of Portugal). *Gracilaria vermiculophylla* is characterized by a highly invasive potential (Rueness, 2005) with a complex ecophysiology (Surget et al., 2017). This agarophyte, native from the East of Asia and belonging to Gracilariales and Gracilariaceae, is an euryhaline and eurythermal species (Yokoya et al., 1999) colonizing mainly unvegetated mudflat of shallow and sheltered estuaries. The Bay of Brest was chosen as the Brittany represented the first point of introduction of *G. vermiculophylla* along North Atlantic European coasts as this invasive seaweed was described for the first time in the Belon estuary in 1996 (Rueness, 2005). It was described few years later in Portugal in 2004 (Rueness, 2005). So, this study

consists to compare ecophysiology of Portuguese *Gracilaria* population (sites near its most South latitude along North European Atlantic) coasts to French Brittany ones (its primary introduction area) in a way to better predict of the evolution on its distribution range in the European farthest north latitudes. Coupling several aspects of seaweed biology allowed to have a further view of acclimation processes occurring within the alga and to easily connect the several biological scales (Surget et al., 2017) as for example coupling its phenology, its metabolomics as its ecophysiology to understand the invasive potential of *G. vermiculophylla*. In this way, the objective of this study was to investigate the plasticity of the phenology during two consecutive years and the acclimation of the biochemical phenotype through identification and quantification of key metabolites as osmolytes (using high resolution magic angle spinning nuclear magnetic resonance or *in vivo* ^{1}H HR-MAS) and lipids (using High Performance Thin Layer Chromatography or HPTLC) of *G. vermiculophylla* relatively to the latitude during summertime. In addition, the photo-physiology of the invasive was studied in both latitudes/countries in function of the tidal cycles. We determined the algal photosynthetic performance at the emersion during a spring tide thorough the natural variation of chl.a fluorescence. It was expecting that during these spring tides may occur the most stressful conditions for intertidal macroalgae with in particular longer emersion and longer exposition to high irradiance. These analyses were completed by pigment quantification allowing finding out the algal acclimation capacities and by the analysis of superoxide dismutase activity (SOD activity) and lipid peroxidation to determine oxidative stress occurring within the alga under these particular stressful conditions.

Material and methods

Sites and samplings The monitoring was performed in the Bay of Brest (Brittany, France), on three sites: Moulin (48°21.490'N - 4°20.447'W), Penfoul (48°21.619'N - 4°19.186'W) and Faou (48°21.497'N - 4°20.444'W) rias (see Fig. 1 in Surget et al. 2017) and in the Ria de Aveiro at three locations: site 1 (40°36'16.62"N ; 8°44'8.88"O), site 2 (40°33'54.90"N ; 8°45'25.62"O), site 3 (40°35'41.34"N; 8°45'5.88"O; Figure 1). Samplings and measurements were carried out during low tides as soon as *G. vermiculophylla* mat on the mudflat was uncovered by seawater. It was realized in summer 2014 (04-06-2014 and 19-06-2014 for

France and Portugal respectively) and 2015 (02-07-2015 and 12-06-2015 for France and Portugal respectively).

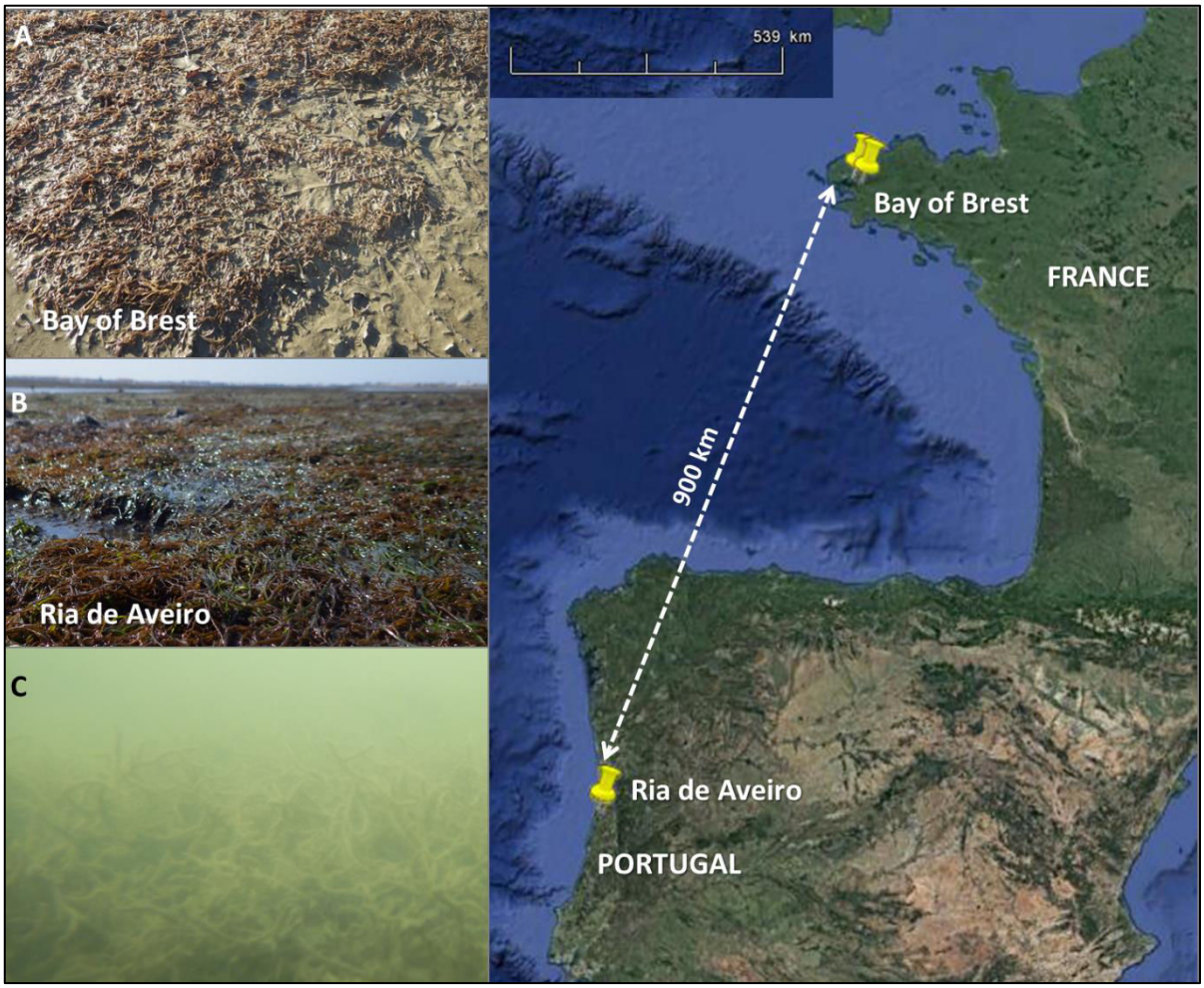

Fig. 1 Locations of studied areas (Bay of Brest and Ria de Aveiro) with respective illustration of *G. vermiculophylla* mat on site Faou(Bay of Brest) and site 1 of Ria de Aveiro (photos taken during *in situ* Diving PAM experiments). C. Illustration *of G.vermiculophylla* mat at high tide (immerged; photo taken on site 2 in Portugal in June 2015)

For ^{1}H HR-MAS NMR and lipid classes quantification, samples of around 100 g of fresh thalli were gathered at three different points on the *Gracilaria vermiculophylla* patches for each sites. These samples were pooled in order to obtain three replicates for each point of the monitoring (n=3). Collected samples were washed with filtered seawater and epiphytes were removed. Then, the replicates were freeze-dried (CHRIST BETA 1-8 LD) and ball milled (MM400 RETSCH). The homogeneity of powder, containing different fragments, allows

limiting biological variations link to individuals; nevertheless replicates are really independent. The dried powder obtained was stored at -24°C until analysis.

Physiological analyses were performed on the field during summertime 2015 in the site Faou for France (02-07-2015) and in site 1 for Portugal (16-06-2015) in parallel of ecological monitoring of this year. These two sites were chosen as they presented the most extensive mat of *G. vermiculophylla*.

For pigment and protein quantifications as lipid peroxidation and SOD analyses, samples were gathered on the field three times during low tide: at the beginning of low tide (B), at low tide maximum (M) and finally during tide rising, just before seawater recovered sampling places (E). Samples were washed with local sea water and immediately stored in liquid nitrogen until back to laboratory. In the lab, algal samples were ground (Retch® MM400) in liquid nitrogen and transferred to -80°C until analyses.

Population biology (size of fragments and biomass) Only results of Ria de Aveiro were presented as population biology. Indeed, results obtained for populations colonizing the Bay of Brest were already presented in a previous study (Surget et al., 2017) and then will be only discussed in regard of Portuguese populations. For each sampling date and each site, ecological data was measured on three quadrats of 0.0625 m^2 and samplings were performed as protocol described by Surget et al. 2017. Algae were washed with seawater on the field before the measurement of the biomass (fresh weights) and the densities of fragments classified in defined size classes. After sorting, the fragments longer than 3 cm were measured and the fragments smaller than 3 cm counted. The dry biomass results were represented as means ± standard deviation (SD) and expressed as $g.m^{-2}$. According to the Sturges' rule, ten size classes were defined: < 3 cm to > 15 cm with a size class amplitude of 1.5 cm. In order to guarantee time-independent data, care was taken to sample different quadrats at each sampling date.

Major metabolites determination (by ^{1}H HR-MAS NMR) For the HR-MAS NMR metabolomic analysis, samples were gathered closely to the ecological monitoring, performed in June 2014 in French and Portuguese sites. Spectral data were recorded following exactly the same procedure described on the red macroalga *Gracilaria vermiculophylla* by Surget et al. (2017). Around 4 mg of powder is introduced in a

4 mm Zirconium rotor. Spectra were recorded with 5000 Hz spinning rate, at 30°pulse with 64 scans. This methodology results in a high-resoluted ^{1}H NMR spectrum similar to those obtained using liquid samples as described in the brown seaweeds (Simon et al., 2015) and provides a fingerprint of the samples, *i.e.* a snapshot of metabolites produced by organisms at the time of their collection. Chemical shifts were expressed in parts per million (ppm) using trimethyl silyl proponiate as the chemical shift reference (0 ppm). All recorded spectra were analyzed using the software MestReNov. 6.0.2 (Mestrelab Research S.L., Spain). ^{1}H HR-MAS spectra were phased and afterwards baseline corrected using Bernstein polynomials. They were aligned on the alanine signal (^{1}H, d, 1.47 ppm).

At first, whole spectra were binning into buckets for the chemical shift region of 0.5 ppm to 5.18 ppm and the size of each bin was 0.04 ppm. Once integrated, 95 areas values were thus generated for each spectrum for further analysis. After logarithmic transformation, integration bucket data were scaled on whole spectra, *i.e.* intensity resulted from the spectra integration of the chemical shift region from 0.5 to 4.22 and from 4.98 to 5.18 ppm, excluding H_2O signal. Multivariate correspondence analysis (COA) was performed on generated dataset. Then, the identification of detected metabolites on spectra was previously performed (Surget et al., 2017) and signals assigned to an identified metabolite were integrated. All integrated peaks or 0.04 ppm bins were scaled to whole intensity, *i.e.* intensity resulted from the spectra integration of the chemical shift region from 0.5 ppm to 5.18 ppm. Indeed, relative concentrations of isethionic acid, taurine, floridoside and nitrogenous molecule pool as the ratio of carbonated on nitrogenous molecule pools were calculated as described by Surget et al. (2017) and Bondu et al. (2007).

Lipid extraction and lipid class separation by HPTLC Lipids were extracted as described by Surget et al. (2017). 25 mg of freeze-dried biomass (previously rehydrated with ultrapure water) were resuspended in 6 mL of Folch solution (chloroform:methanol; 2:1) and sonicated 10 min at 4°C. Butylated hydroxytoluene 0.01% (w:w) was added as an antioxidant. Vials were centrifuged and supernatant containing lipids were evaporated to dryness under nitrogen and washed three times using a water:chloroform mix (1:1, v:v). All lipid extracts were stored at -20°C until analysis.

Lipid classes were analysed by High Performance Thin Layer Chromatography (HPTLC) as described by Haberkorn et al. (2010). A preliminary run was conducted on HPTLC silica glass plates (Darmstadt, Germany) in order to remove any impurities. Three solvent systems were used, depending on the lipid classes that needed to be separated: 9% KCl polar solvent mixture (methyl acetate:isopropanol:chloroform:methanol:KCl, 10:10:10:4:3.6) for all polar lipid classes, neutral solvent mixture (hexane:diethyl ether:acetic acid, 20:5:0.5) for all neutral lipid classes and 4% KCl polar solvent mixture (methyl acetate:isopropanol:chloroform:methanol:KCl, 25:25:25:10:4) for glycolipid classes. The plate was then activated for 30 min at 120°C. Samples were spotted on silica plates by a CAMAG automatic sampler (Muttenz, Arlesheim, Switzerland) and plates were developed with appropriate solvent systems. 9% KCl polar lipid solvent mixture was used for the separation of all polar lipid classes, 4% KCl polar lipid solvent mixture was used for the separation of glycolipid classes and two consecutive solvent systems were used for the separation of neutral lipids: the neutral solvent mixture described above and a second solvent mixture composed of hexane:diethyl ether (97:3). Plates were revealed with a cupric sulfate phosphoric acid solution, heated for 20 min at 160°C and then scanned at 370 nm. Black bands on charred plates were identified and quantified using Wincats software (CAMAG, Darmstadt, Hesse, Switzerland) by comparison with standards. Results were expressed in $mg.g^{-1}$ for the total lipid content and as a percentage of the total lipid (TL) for the classes.

Photo-physiology (by Diving PAM) *In vivo* chl a fluorescence of photosystem II (PSII) of five thalli of *G. vermiculophylla* was measured using an underwater fluorometer (diving PAM; HeinzWalz, Effeltrich, Germany). Temperature and salinity were followed during field experiments using a multiparameter (Multi 350i, WTW) with Tetracon 325 probe. In parallel, incident photosynthetically available radiation (PAR, 400-700 nm) was also recorded using a Li-COR quantum sensor (LI-192SA) connected to a data logger (Li-COR LI-1400). The optimal quantum yield (Fv/Fm) of PSII (Genty et al., 1989), a measure of the maximum efficiency of PSII, was measured with the diving PAM using a 0.8 s saturating pulse (2500 µmol $photons.m^{-2}.s^{-1}$) of white light. The effective quantum yield of PSII (ϕPSII), the efficiency of PSII photochemistry, was measured under natural ambient light using a custom-made clip to ensure a constant distance of 5 mm and a constant angle of 60° between the probe and the

sample. The ϕPSII was calculated according to (Genty et al., 1989) and used to estimate the linear electron transport rate (relative electron transport rate, rETR) (Gevaert et al., 2003), an estimator of photosynthesis.

Pigments quantification (by HPLC) Zeaxanthin, violaxanthin, antheraxanthin, fucoxanthin, chlorophyll-a (chl.a), chlorophyll c2 (chl-c2) and β-carotene were analysed by High Performance Liquid Chromatography (HPLC; Dionex) following the method developed by Schmid and Stengel (2015). Briefly, pigments were extracted from 100 mg of ground samples in a 90% acetone solution for 30 min with stirring, at 4°C in the dark. After centrifugation, a second extraction was performed during 15h in the dark. Supernatants were pooled and 200 µL of obtained extract was filtered and diluted with ammonium acetate buffer (0.5M, pH 7.2) just before analysis. Pigments were separated using a Zorbax Eclipse XDB-C18 column (150 x 4.6 mm; 5 µm; Agilent) with a C18 pre-column over a 40 min run. Acquisitions were performed using the software Chromeleon 6.60 (Dionex). Pigment concentrations (expressed as $\mu g.g^{-1}$ FW) were calculated using pigment standard calibrations (zeaxanthin, violaxanthin, antheraxanthin and β-carotene supplied by DHI LAB products (Denmark) and chl a standards supplied by Sigma-Aldrich France). Even though not present in red macroalgae, fucoxanthin was detected in *G. vermiculophylla* extracts due to the presence of benthic diatoms epiphytes living on the macroalgal thalli (these results was not presented). To go further xanthophylls on chl.a ratio were calculated as follows:

$$\text{Xanthophylls / chl.a} = \frac{(\text{violaxanthin + antheraxanthin + zeaxanthin})}{\text{chl.a}}$$

Phycobiliprotein content was determined using a protocol described by Surget *et al.* (2017) and adapted from Sun *et al.* (2009) and Roleda *et al.* (2012). Extraction was performed in the dark at 4°C using 75 mg algal dry matter with 1.5 mL phosphate buffer (0.1 M, pH = 6.8). After sonication for 15 min, extracts were centrifuged for 20 min at 4°C. The obtained extracts were stored at 4°C in the dark until the absorbance was measured at 280, 455, 565, 592, 618 and 645 nm (POLARstar Omega, BMG LABTECH). Concentrations of phycobiliproteins, expressed as $mg.g^{-1}$ DW (dry weight), were determined using Beer and Eschel equations (Dumay et al., 2013; Munier et al., 2014; Zubia et al., 2014) as follows:

$$\text{R-PE} = [(A_{565} - A_{592}) - (A_{455} - A_{592}) * 0.20] * 0.12$$

$$\text{R-PC} = [(A_{618} - A_{645}) - (A_{592} - A_{645}) * 0.50] * 0.15$$

where A= Absorbance; R-PE= R-phycoerythrin concentration; R-PC= R-phycocyanin concentration.

Lipid peroxidation Malondialdehyde (MDA) is one of the most aldehyde generated by lipid peroxidation (Esterbauer and Cheeseman, 1990). In this way, the content of lipid peroxidation products was determined by the quantification of MDA. The procedure was adapted according to the methods providing by lipid peroxidation (MDA) assay kit (Sigma) and Meudec (2006). Around 100 mg of sample was extracted with 3 mL of 0.1% trichloroacetic acid solution (TCA, Sigma) and then, grinded in a mortar at 4°C. BHT at 100 mg.L-1 (a volume of 10µL) was added and samples were centrifuged at 3220g (Eppendorf 5810 R) during 10 min at 4°C to remove cell debris. Resulting extracts were added to 0.5% thiobarbituric acid and 20% TCA solution (Sigma) according to a ratio 1:4 (v:v). Samples incubated 60min at 95°C and cooled down in ice to stop colorimetric reaction. Finally, after addition of n-butanol (3.75mL), extracts were centrifuged at 3220g for 20 min at 4°C to separate n-butanol fraction to aqueous fraction. After evaporation of 1.5mL of n-butanol fraction (MinVac Concentrator Range, Genevac) at 40°C, samples were resuspended with 700µL of pure water. MDA content was quantified spectrophotometrically by recording absorbance at 532nm and corrected by absorbance at 600nm and were calculated as:

$$\text{MDA content (nmoles.mg}^{-1}\text{ FW)} = \left[\frac{\left(A_{532} - A_{532_{Blank}}\right) - \left(A_{600} - A_{600_{Blank}}\right)}{\text{a}} * \text{DF}\right] / \text{W}$$

where A= Absorbance; a= coefficient of MDA standard curve; DF= dilution factor; c= sample fresh weight.

Total Superoxide Dismutase (t-SOD) Algal powder was resuspended in saline phosphate buffer (PBS) solution (v:w; 5:1) composed of 10mM PBS, ethylenediaminetetraacetic acid (EDTA, 1mM) and Triton*100 (0.1%, v:v). After sonication during 10min at 4°C and incubation on ice during 45 min, samples were centrifuged at 10000g during 45 min at 4°C (miniSpin Eppendorf, Rotor F45-12-11) to remove the cell debris. On obtained extracts, total proteins were quantified according to Bradford procedure using BioRad Protein Assay Dye Reagent Concentrate (BioRad France) and Bovine Serum

Albumin (BSA) as the protein standard (Bradford, 1976). T-SOD activity (EC 1.15.1.1) was assayed spectrophotometrically by measuring the decrease of absorbance at 440 nm due to the inhibition of the xanthine/xanthine oxidase complex after 20 min of incubation at 25°C. T-SOD activity was determined using the SOD Assay Kit (Sigma-Aldrich, France) and following the protocol developed by Richard et al. (2015). The enzyme activity was expressed as Units of enzyme.mg^{-1} of total proteins expressed in equivalent bovine serine albumin (BSA; $U.mg^{-1}$ eq. BSA).

Statistics Statistical analyses were performed with RStudio (v. 0.95.263) for R (v.3.1.3). All analyses were carried out in triplicate and results were expressed as mean ± standard deviation (SD). If the data met the requirements for parametric tests, they were analysed using a multi-way ANOVA (function of the number of factors) at a significance level of 95%, followed by a Tukey post-hoc test. Data were transformed if necessary to respect homoscedasticity. When the data did not meet the requirements for an ANOVA, they were analysed using the two-way Scheirer Ray Hare (SRH) test (Sokal and Rohlf, 1995), the one-way Kruskal–Wallis (KW) test or the Wilcoxon Mann Withney (WMW) test depending on the number of factors and conditions, at a significance level of 95%, followed by a non-parametrical multiple comparisons test (kruskalmc function; pirgmess package). Data were compared in relation to the tide, the year and/or the latitude. Furthermore, multivariate analyses (ade4 package) were conducted on NMR data (*i.e*, correspondance analysis: COA) after logarithmic transformation to reduce data variance. To go further, Manova was conducted on coordinates of individuals of the selected dimensions generated by multivariate analysis (COA) since coordinates of individuals on the several dimensions were independent of one another, contrary to relative metabolite concentrations.

Results

Population biology *Gracilaria vermiculophylla* formed extensive mat of entangled thalli on the mudflats of the two rias. Nevertheless, in ria de Aveiro, *G. vermicculophylla* may develop on *Zoostera marina* areas and *Ulva sp* was found as epiphytes on algal thalli (see Figure 1). A variation of fresh biomass of *Gracilaria vermiculophylla* was observed between years (Figure 2) with an increase in summertime 2015 compared with the previous year (two way Anova, F = 7.60, p-value = 0.017) and with a mean of algal biomass of 476.3 ± 322.5 and 1045.3 ±

565.0 $g.m^{-2}$ in 2014 and 2015 respectively. Moreover, no sites variability was shown (two way Anova, F = 0.37, p-value = 0.41).

Additionally to biomass variation of *G. vermiculophylla*, filamentous thalli densities profiles were strongly different in ria de Aveiro between sampling years (Figure 3). An increase of smallest fragments classes, *i.e.* for classes of fragments smaller than 3 cm, from 3 to 4.5 cm, from 4.5 to 6 cm and from 6 to 7.5 cm, was observed in 2015 compared to 2014 (SRH, p-value < 0.05; Figure 3b). These differential patterns of sizes between years were also illustrated between size classes for each year on Figure 3a (on sites data pooled). In 2014, only the last size classes exhibited significant difference with the first one, all the other size classes were homogenous (KW, Chi^2 = 20.182, p-value = 0.017). On the contrary, during the new sampling in 2015, densities of size classes were decreasing in function of the rise of thalli size with smaller size classes (until 4.5 cm) exhibiting higher densities than larger size classes (from 9 cm) (KW, chi^2 = 66.48, p-value = 7.41 10^{-11}). Furthermore, few sites differences were shown with the two size classes, from 3 to 4.5 cm and from 4.5 to 6 cm (Tukey post-hoc test, p-value < 0.05).

Interestingly, distinctive carposporophytes of *G. vermiculophylla* were observed in ria de Aveiro sites while on the contrary of Brittany sites where only vegetative thalli were observed for the two monitoring years (data not shown).

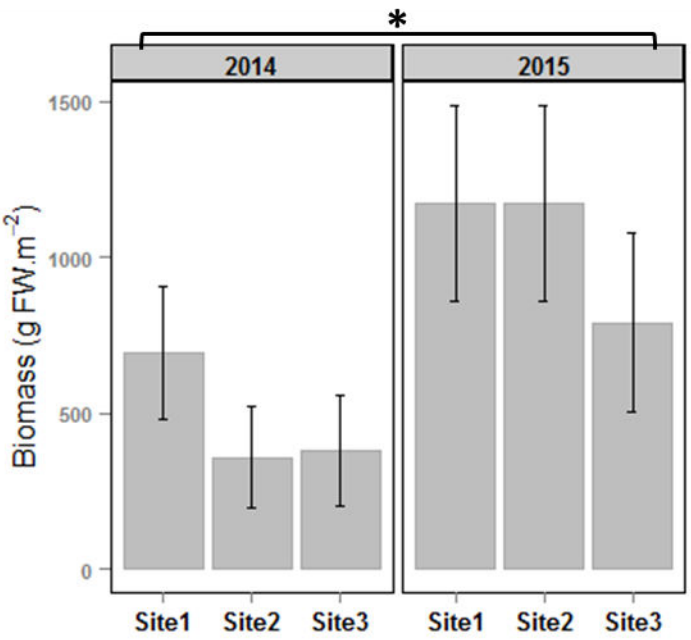

Fig. 2 Fresh biomass (g. m^{-2}) variations between sites during June 2014 and 2015 for three sites located in the ria de Aveiro (Portugal). Results represented are means ± SD (error bars; n = 3). No significant differences was detected between means ($p > 0.05$) according to an ANOVA test and ***** indicates significant differences between years.observed for the two monitoring years (data not shown).

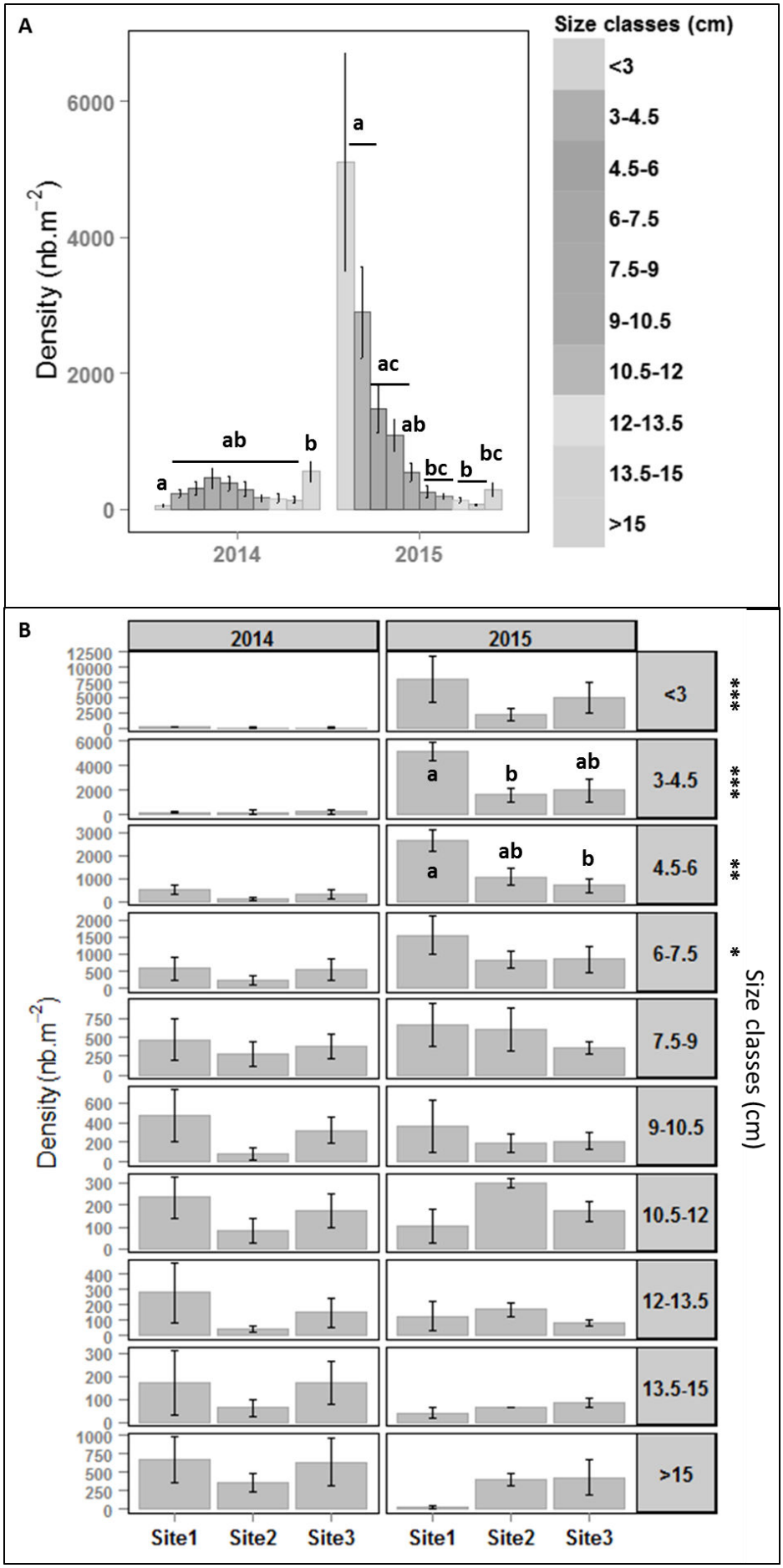
A
Size classes (cm)
<3
3-4.5
4.5-6
6-7.5
7.5-9
9-10.5
10.5-12
12-13.5
13.5-15
>15
Density (nb.m^{-2})
6000
4000
2000
0
a
ab
b
a
ac
ab
bc
b
bc
2014
2015
B
2014
2015
Density (nb.m^{-2})
Size classes (cm)
<3
3-4.5
4.5-6
6-7.5
7.5-9
9-10.5
10.5-12
12-13.5
13.5-15
>15
***
***
**
*
a
b
ab
a
ab
b
Site1
Site2
Site3
Site1
Site2
Site3

Fig. 3 Representations of thalli densities of *Gracilaria vermiculophylla* depending on their size classes (expressed as nb m^{-2}) during summertime 2014 and 2015 in Ria de Aveiro (Portugal). Results are expressed as means ± SD. **A:** Density variations of fragment size classes when sites were pooled (n = 9). **B:** Density variations for each fragment size class and each site (n = 3). Density scale was adapted for each size classes.

Different letters indicate significant differences between means using the Tukey post hoc test or Kruskal multiple comparison test. The lack of a letter indicates that no significant difference was observed (p value <0.05). Stars on the right shows significant differences between years for the corresponding size classes when sites were pooled (*: p-value < 0.05; **: p-value < 0.01; ***: p-value < 0.001)

Metabolomic Component ordinate analysis (Figure 4a) allowed to illustrate differences between spectra of *G. vermiculophylla* issued from ria de Aveiro (Portugal) and Bay of Brest (France) relatively to axis 1 (explaining 56.39% of data variation). This difference was not highly significant (Manova, F = 25.28, p-value = 0.0130) and was mainly explained by buckets ranging from 0.5 to 3 ppm (Figure 4b). These buckets corresponded to minor peaks of this chemical shift area, explaining why no significant differences were exhibited for relative concentration of N pool (Figure 4c). Moreover, three buckets with chemical shift 4.98 to 5.10 ppm, *i.e.* buckets from 4.98 to 5.02, from 5.02 to 5.06 and from 5.06 to 5.10 ppm, contributed to 3.56, 3.19 and 2.07% to the axis 1 respectively. These chemical shifts corresponded to the anomeric proton of floridoside. Contrariwise, no differences on other peaks of floridoside signal were showed. Thus, partial differences exhibited by COA analysis for floridoside signal explained that relative concentrations of floridoside was not significant between French and Portuguese samples of *G. vermiculophylla*. No significant difference of relative concentration of the other identified metabolites, *i.e.* taurine and isethionic acid as for C/N ratio, was observed (t-test, p-value > 0.05).

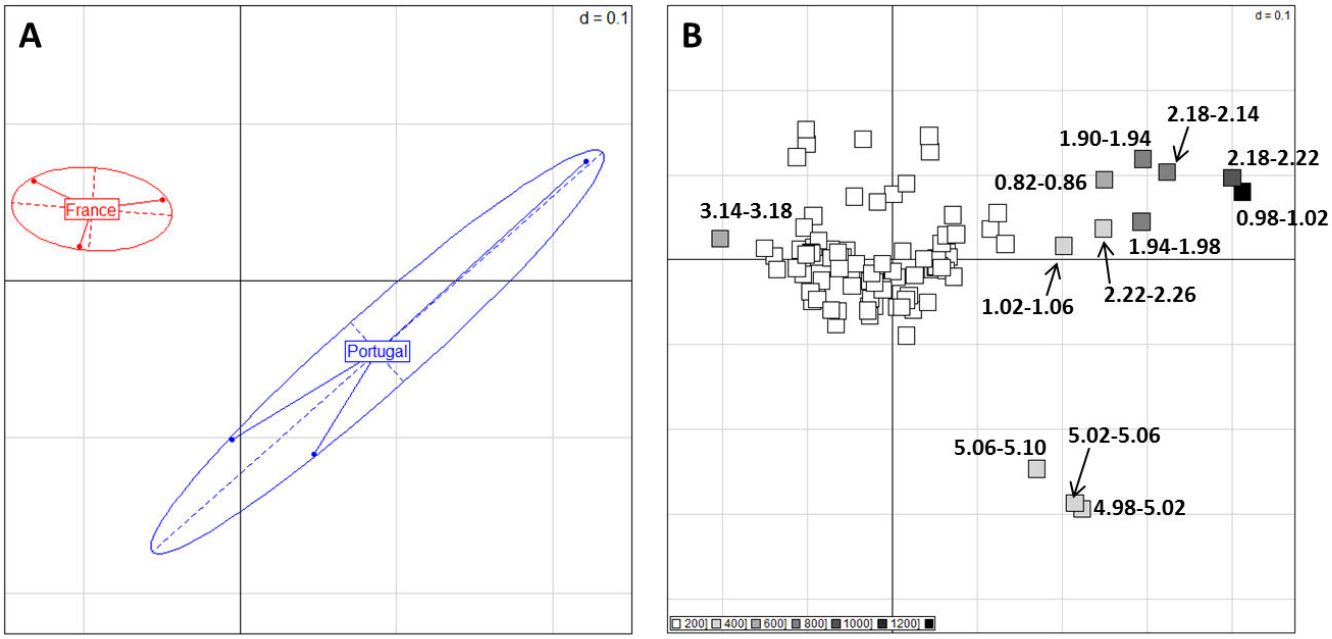

C

	Relative concentration (%)					C/N ratio
	N pool	Alanine	Isethionic acid	Taurine	Floridoside	
France (n=3)	31.96 ± 5.11	0.98 ± 0.15	5.96 ± 1.64	3.99 ± 0.61	33.99 ± 4.78	1.09 ± 0.29
Portugal (n=3)	33.80 ± 9.34	1.09 ± 0.52	6.16 ± 1.95	4.73 ± 1.64	26.58 ± 6.67	0.85 ± 0.37

Fig. 4 Component ordinate Analysis (COA) of integrated bins on HR-MAS ^{1}H spectra (A and B) and variability of some metabolites measured in *Gracilaria vermiculophylla*. **A**- COA score plot of individuals depending of the sampling country. Ellipses with a confidence level of 0.99 were drawn around considered factor, *i.e.* country (France and Portugal). **B**- COA correlation plot of 96 integrated bins. Each square represented a bin and the square colour intensity was proportional to the variable contribution on axis 1. The chemical shift range of bins that contributed more than 4% to axis 1 (colored in grey) was precised. **C**- Table of relative concentrations (expressed as %) for floridoside, isethionic acid, taurine and N pool and C/N ratio (ratio of carbonated to nitrogenous molecule pools). Data were calculated based on relative signal integrals on ^{1}H HR-MAS spectra for each state. Results are expressed as means ± SD (n=3). No significant difference was found using t-test.

Lipid composition Total lipid amount as relative concentrations of main lipid classes, *i.e.* neutral lipids, glycolipids as phospholipids did not vary between between portuguese and

french algal populations (on sites data pooled, n=3). Neutral lipids represented the highest lipid classes with more than 1/3 of total lipids (Table 1). Only the composition of neutral lipids varied significantly between countries with an enrichment of three types of neutral lipids for samples from ria de Aveiro (T-test, p-value < 0.05). Indeed, the algal relative concentration of alcohols was multiplied more than 30 fold between countries, the relative concentration of triacylglycerides by around 2 and sterol esters by around 1.5. Glycolipids as phospholipids compositions did not exhibit significant differences relatively to sites localisation (Wilcoxon or t-test, p-value < 0.05).

Table 1 Total lipid content expressed as mg. g^{-1} DW and main lipid classes expressed as percent of total lipid (TL) between summertime 2014 in the Bay of Brest (France) and Ria de Aveiro (Portugal) for *Gracilaria vermiculophylla*. Results are expressed as means ± SD (n=3). Different superscript letters indicate significant differences between means with T-test (p-value <0.05)

State	Total lipid (mg.g^{-1} DW)	Lipid classes		
		Neutral lipids (% TL)	Glycoplipids (% TL)	Phospholipids (% TL)
France	12.53 ± 1.75	45.26 ± 2.66	25.24 ± 3.27	27.31 ± 5.04
Portugal	11.68 ± 1.16	33.52 ± 16.12	31.84 ± 7.80	18.39 ± 6.04

State	Neutral lipids					
	Sterol esters (% TL)	Glyceride esters (% TL)	Triacylglycerides (% TL)	Free fatty acids (% TL)	Alcohols (% TL)	Free sterols (% TL)
France	**1.01 ± 0.15**^{a}	0.00 ± 0.00	**1.78 ± 0.45**^{a}	37.31 ± 1.39	**0.02 ± 0.01**^{a}	5.14 ± 0.80
Portugal	**1.47 ± 0.17**^{b}	0.00 ± 0.00	**3.69 ± 0.63**^{b}	23.00 ± 15.99	**0.63 ± 0.37**^{b}	4.71 ± 1.19

State	Glycolipids		
	MGDG (% TL)	DGDG (% TL)	SQDG (% TL)
France	7.82 ± 0.99	9.90 ± 1.80	7.52 ± 0.83
Portugal	11.95 ± 5.97	13.50 ± 2.41	6.39 ± 3.24

State	Phospholipids				
	PI (% TL)	PC (% TL)	PE+PG (% TL)	CL (% TL)	PS (% TL)
France	16.90 ± 6.27	16.90 ± 6.27	5.81 ± 0.20	1.66 ± 0.39	0.33 ± 0.10
Portugal	10.65 ± 4.70	10.65 ± 4.70	4.05 ± 1.38	1.38 ± 0.51	0.46 ± 0.68

MGDG: monogalactosyldiacylglycerol, DGDG: digalactosyldiacylglycerol, SQDG: sulfoquinovosyl diacylglycerol, PI: phosphatidylinositol, PC: phosphatidylcholine, PE + PG: phosphatidylethanolamine + phosphatidylglycerol, CL: cardiolipin, PS: phosphatidylserine

Acclimation of the algal photo-physiology During the tide period where the algae were harvested, field parameters, like air temperature (Figure 5a and 5b) and irradiance were measured and they exhibited similar magnitude during the two experiments. On the other hand, temperatures varied differently during the two experiments depending of recorded irradiance. In the Bay of Brest, temperatures increased rapidly from 20.1°C at 10: 10 (h UTC) due to the irradiance increase from 321 to 1776 µmol photons $.m^{-2}.s^{-1}$ in few minutes (from 10:10 to 10:17 h UTC), reached a maximum of 29.1°C at 11:50 (h UTC) and decreased until the end of the experiment. On the contrary, in ria de Aveiro, incident irradiance increased constantly from sunrise to the end of the experiment, reaching 2059 µmol photons $.m^{-2}.s^{-1}$ at sun zenith. The experiments in Portugal began two hours earlier relatively to solar hour (UTC) than experiments performed in France due to the offset of tides between these two states. During experiments, emersions of *G. vermiculophylla* map lasted around 6h in Ria de Aveiro against 7h in Faou ria linked to differential tide amplitude between these two areas (with a tide amplitude of 5.52 and 2.50 m in ria de Aveiro and in Faou ria respectively).

Photosynthetic parameters showed similar patterns between the two experiments with differential intensities during the course of summer spring tides. Indeed, Fv/Fm values decreased with the increase of irradiance, especially from irradiances exceeding 1500 µmol photons $.m^{-2}.s^{-1}$ (Figure 5c and d). In Ria de Aveiro, this decrease reached 82.51% against 49.41% in the Faou ria at the end of low tide just before the recovery of *G. vermiculophylla* map by seawater. For rETR parameter, this parameter firstly increased with incident irradiance intensity (Figure 5e and f). Then, the trend was reversed with the decline of Fv/Fm after around 2h of exposition to high irradiance (from 1500 µmol photons $.m^{-2}.s^{-1}$) for both studied areas. This decrease was not significant in Brittany (KW, $p\text{-value} < 0.05$) in contrast to the Ria de Aveiro with the decline of 53.25% of rETR parameter compared to the maximum at the end of experiment (KW, $p\text{-value} < 0.05$).

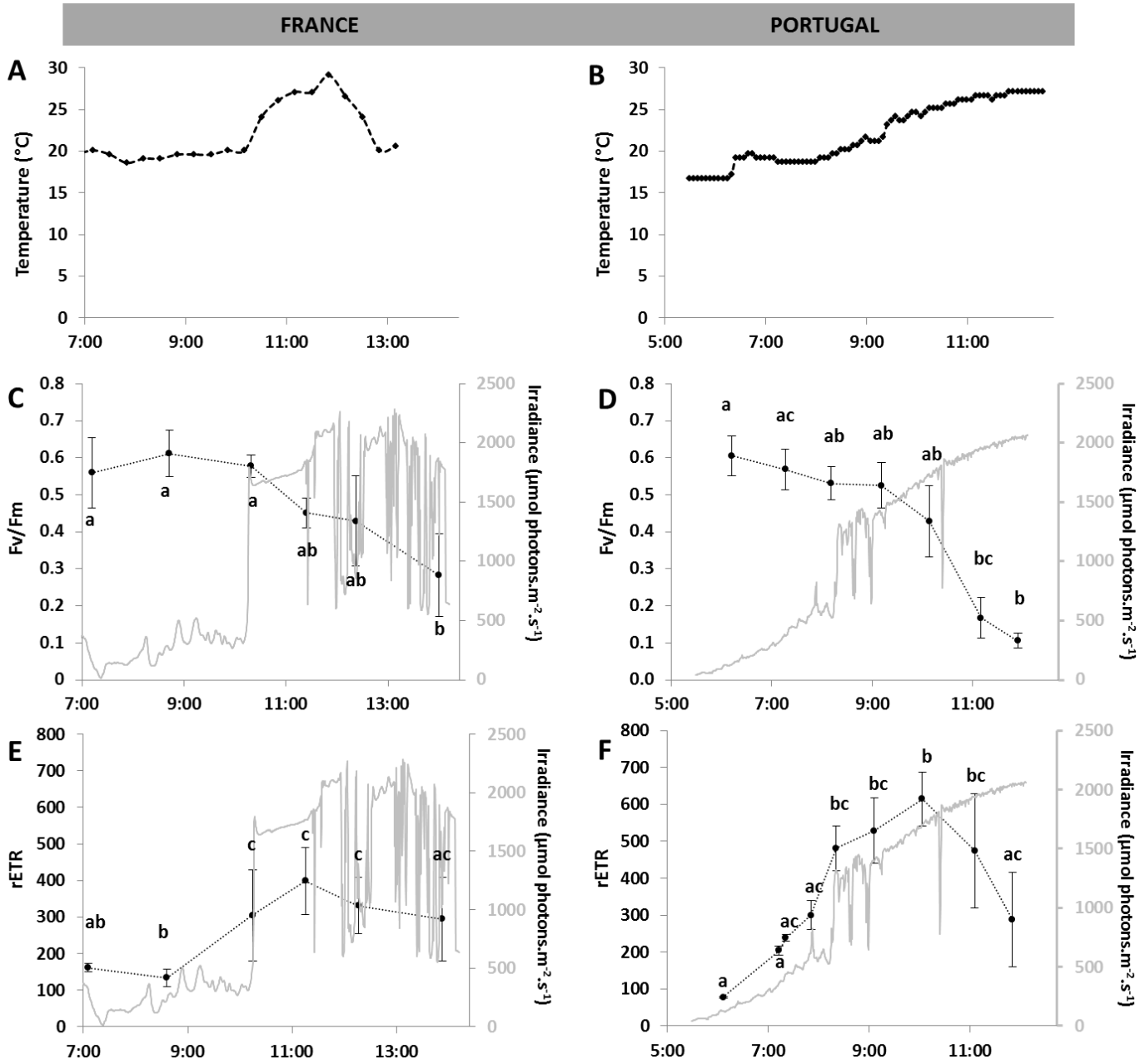

Fig. 5 Variations of field abiotic parameters (air temperature: A and B, and incident irradiance: C, D, E and F) and fluorescence parameters (Fv/Fm: C and D, and rETR: E and F) of *G. vermiculophylla* during a sunny summer tide course in the Bay of Brest (France) and the Ria de Aveiro (Portugal). Represented results for fluorescence parameters are mean ± SD (n ≥ 5). Different letters indicate significant differences between means (according to KW tests followed by post-hoc test, $p < 0.05$).

Pigments Violaxanthin and antheraxanthin data were not illustrated as few samples exhibited detectable contents. Indeed, violaxanthin was detected in two samples from Ria de Aveiro experiment, one sample gathered at the beginning of the ebb tide (B) and one sample gathered just before the *G. vermiculophylla* mat was recovered by the sea water (E). Additionally, antheraxanthin was detected in three samples, in two replicates sampled at the beginning of low tide in Ria de Aveiro site and in one replicate gathered at the maximum of low tide (M) in Faou ria site (in Brittany).

Results (Figure 6) exhibited no pigment variation with the tide in ria de Aveiro site as in the Faou ria for all quantified pigments (SRH and two-way Anova, p-value > 0.05). On the contrary, significant differences were shown between the followed sites, *i.e.* site 1 of ria de Aveiro and Faou ria. *G. vermiculophylla* contents in zeaxanthin, β-caroten as chl a increased in samples from the site located in the ria de Aveiro compared to the one of the Bay of Brest. Phycobiliproteins exhibited similar pigment amounts between French and Portuguese sites (SRH, p-value < 0.05) with 2.30 ± 0.35 and 2.22 ± 1.44 as 0.81 ± 0.22 and 0.95 ± 0.69 mg of phycocyanin.g^{-1} DW in Faou ria and ria de Aveiro respectively. Additionally, pigment ratio was calculated, *i.e.* xanthophylls on chl a concentrations. This ratio did not vary relatively to the two factors tested, *i.e.* the tide level and the latitude with 0.121 ± 0.020 in Faou ria and 0.119 ± 0.011 in ria de Aveiro (two-way Anova, F = 2.03, p-value = 0.17 and F = 0.10, p-value = 0.75 for the factor tide and site respectively without significant interaction between factors: F = 1.87, p-value = 0.20).

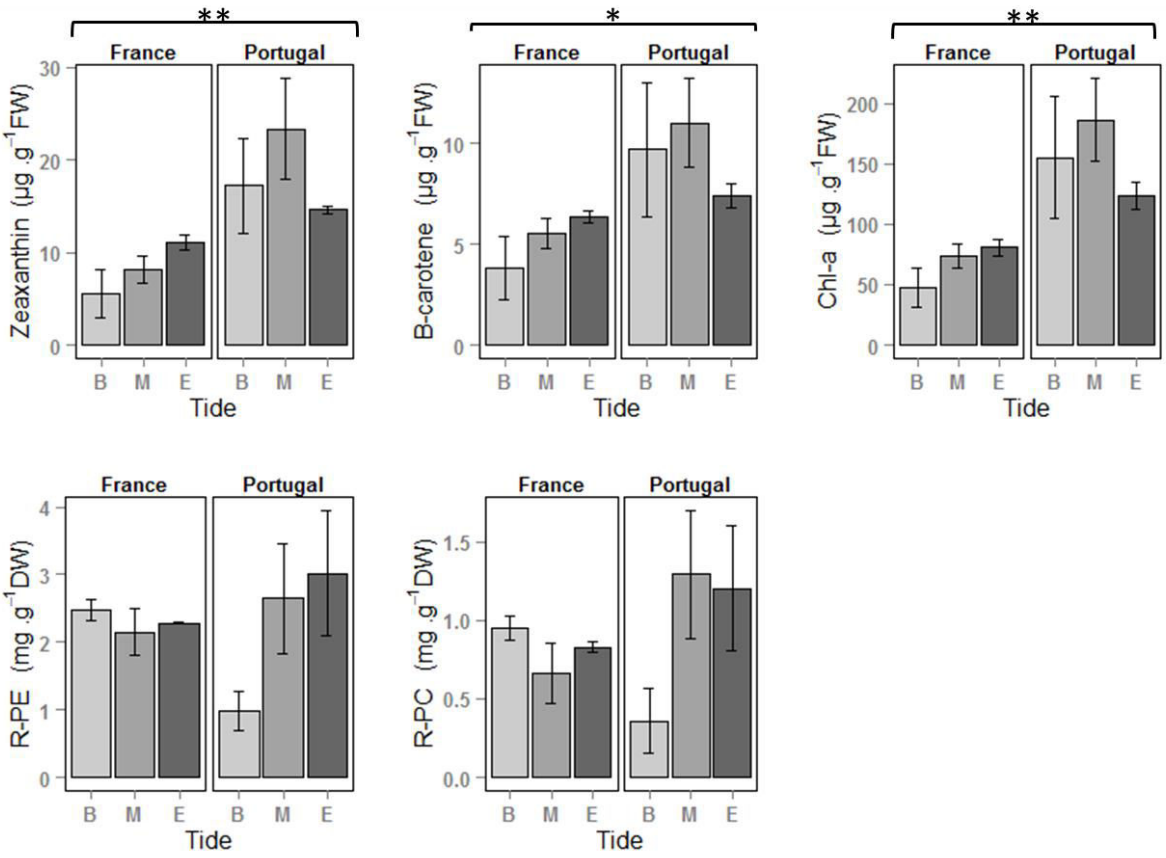

Fig. 6 Concentrations of pigments determined in *Gracilaria vermiculophylla* according to the tide level (B: beginning of low tide when the algal mat were uncovered, M: maximum of low tide, E: end of low tide when seawater begins to recover each shore) and depending on the site's country (France vs. Portugal). Results were expressed as mean ± SD (n=3) in $mg.g^{-1}$ DW for R-phycoerythrin (R-PE) and R-phycocyanin (R-PC) and in $\mu g.g^{-1}$ FW for the other pigments. Stars (*) indicate significant differences between states (*: $p < 0.05$; **: $p < 0.01$; ***: $p < 0.001$) according to SHR or two-way ANOVA.

Oxidative stress Lipid peroxidation through MDA content of *G. vermiculophylla* exhibited significant differences regardless of the location of experiments, *i.e.* Faou ria and ria de Aveiro (SRH test, H = 11.35, p-value= 0.00075; Figure 7a), with higher contents exhibited in ria de Aveiro (with 51.01 ± 15.13 nmol MDA. g^{-1} FW) than in Faou ria (with 26.75 ± 7.92 nmol MDA. g^{-1} FW). Likewise, lipid peroxidation varied depending of the tide only for samples derived from ria de Aveiro. High levels of MDA were exhibited just at the beginning of low tide when *G. vermiculophylla* mat emerged (with 67.96 ± 7.74 nmol MDA. g^{-1} FW). During the remainder of experiment in ria de Aveiro, MDA content declined and was holding

to 42.53 ± 9.16 nmol MDA. g^{-1} FW. On the contrary, SOD activities did not vary between the two countries with 33.28 ± 12.98 U SOD. mg^{-1} eq. BSA and 37.13 ± 8.36 U SOD. mg^{-1} eq. BSA in Faou ria and ria de Aveiro respectively (SRH, H = 0.072, p-value = 0.79). Interestingly, results showed a small significant difference for SOD activities relatively to the tide level on the whole data (SRH, H = 6.02, p-value = 0.049) even if no variation was detected depending of the tide for each states separately (KW, Chi^2 = 1.82, p-value = 0.40 for France and one-way Anova, F = 3.56, p-value = 0.096 for Portugal).

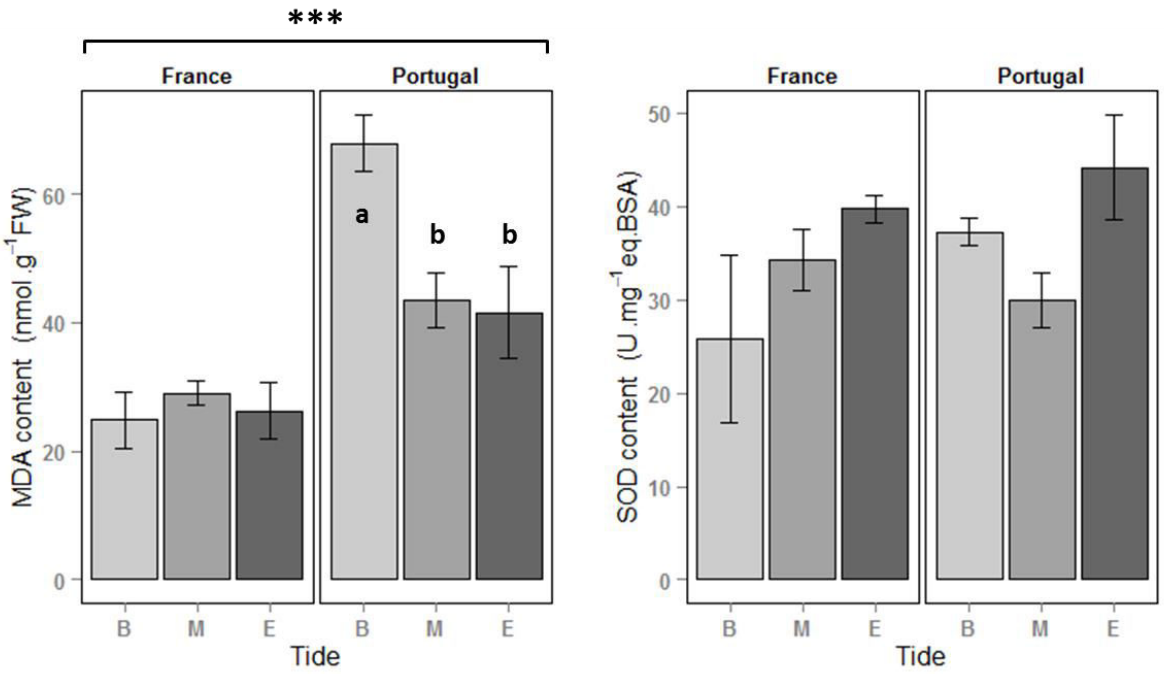

Fig. 7 Variations of MDA content (malondialdehyde; nmol. g^{-1} FW) and variations of SOD (superoxyde dismutase) activity ($U.mg^{-1}$ of total proteins expressed in equivalent bovine serum albumin: BSA) determined for the red macroalga *Gracilaria vermiculophylla* (n=5 for France, n=3 for Portugal) during the tide course (B: beginning of low tide when the algal mat were uncovered, M: maximum of low tide, E: end of low tide when seawater begins to recover the muddy shore) and depending on the state (France vs. Portugal). Results are expressed as mean ± SD. Stars (*) indicate significant differences between states (*: $p < 0.05$; **: $p < 0.01$; ***: $p < 0.001$) according to SRH test. Different letters indicate significant differences depending of the tide level for each state (one-way Anova, p-value < 0.05).

Discussion

Several major points stood out of these results on the phenology, the metabolomic as the ecophysiological characteristics of *G. vermiculophylla* between two countries, France and Portugal, representing contrasted latitudes along on its North european Atlantic coasts distribution range. At first, this invasive seaweed exhibited a high plasticity of its phenology with a fast variation of size classes pattern in only one year in ria de Aveiro. Secondly, the presence of carposporophytes, *i.e.* reproductive thalli, in ria de Aveiro suggested that the biological cycle of the species was completed in field conditions and confirmed previous studies (Abreu et al., 2011). Rarely, reproductive thalli were observed once time in ria of Faou in 2014 but since reproductive thalli did not have been observed in the field for Brittany rel algal populations (Surget et al., 2017) during our monitoring from 2013 to 2015. Nevertheless, the capacities of Brittany populations to complete their biological cycle was checked under laboratory conditions (Rueness, 2005). Moreover, French and Portuguese populations presented no variation of their main osmolytes detected by NMR HR-MAS. The composition of neutral lipids differed between populations with the concentration in sterol esters, triacylglycerides as alcohols in ria de Aveiro. Additionnaly, the present study illustrated the plasticity of ecophysiological responses of *G. vermiculophylla* populations between this two locations with an higher photoinhibition occuring in ria de Aveiro parallel to a concentration in several pigments, *i.e.* zeaxanthin, β-carotene and chl a. High levels of lipid peroxidation fluctuating with the tide without variation of SOD activities was also demonstrated in ria de Aveiro populations.

Phenological plasticity Litterature reported a high plasticity of *G. vermiculophylla* especially of its attachment mechanisms depending of its location as environmental conditions. This invasive macroalgae could form entangled mat of thalli partially buried, a map of loose-lying fragments or could be attached to several biogenic subtrates as tube worms of the polychaete *Diopatra* or snail shells (Abreu et al., 2011; Surget et al., 2017; Thomsen et al., 2009). Abreu et al. (2011) observed a high annual variability of *G. vermiculophylla* mats with the presence of ephemeral patches that reappeared in nearby areas. Interestingly, the fragmentation pattern of *G. vermiculophylla* as the increase biomass illustrated the establishment of a mat partially buried in ria de Aveiro as observed previously in the Bay of Brest (Surget et al., 2017) and contrasting with the seaweed phenology in its

native area (Muangmai et al., 2014). Indeed, fragmentation patterns observed in 2015 was similar to those observed in the Bay of Brest during a seasonal monitoring performed from December 2013 to December 2014 (Surget et al., 2017). Abreu et al. (2011) hypothesized that the instability of *Gracilaria* mat may be due to anthropogenic activities as dredging activities occurring in channels of ria de Aveiro (Silva et al., 2004) together to tidal flushing during spring tides. No known dredging activities occurred in studied rias of the Bay of Brest. Thus, the observation in ria de Aveiro of a highly fragmented thalli pattern during summertime 2015 similar to that of populations of the Bay of Brest suggested that, the presence of loose-lying thalli (little fragmented) as observed in ria de Aveiro during summertime 2014 (possibly linked to anthropogenic perturbations or hydrodynamic events), may quickly formed a more stable mat with a typical highly fragmented phenological pattern. Moreover, biomass sampled during summertime 2015 were consistent with results from July 2007 presented by Abreu et al. (2011) and reinforced the hypothesis that populations sampled during summertime 2014 in Ria de Aveiro exhibited low biomass link potentially to a disturbance of the algal mat. Moreover, Muangmai et al. (2014) desmonstrated the correlation between the thalli size and their biomass in relation to growth period of *G. vermiculophylla*. These results showed on the contrary an increase of algal biomass linked to the higher level of thalli fragmentation.

Metabolomic acclimation Surget et al. (2017) noted the potential link between FFA (Free Fatty Acids) concentrations and the increase of densities of smallest fragments of G. *vermiculophylla*. In the present study, no significative differences was exhibited by FFA concentrations between Portuguese and French populations despite lower concentrations in ria de Aveiro, due to a high variability between sites. It would be interesting to correlate fragmentation level to FFA concentrations. Indeed, FFA may have an important ecophysiological role for *G. vermiculophylla* as they were supposed to be precursors of oxilipins, molecules implies in defense of the algae following a wounding stress (Lion et al., 2006; Rempt et al., 2012). More intensive monitoring coupled with controlled lab experiment may support this hypothesis. Moreover, no glycolipid variations was observed between the two locations. These lipids are involved in the regulation of chloroplast membrane fluidity and/or light harvesting (Dörmann and Hölzl, 2009; Pettit and Harwood, 1989). Our results indicated that differential environmental conditions linked to the latitude

of monitored areas did not imply an acclimation of photosynthesis efficiency in term of glycosylglycerides composition. Interestingly, this type of adjustments was observed linked to seasonal acclimation in *G. vermiculophylla* populations of the Bay of Brest (Surget et al., 2017). Nevertheless, seasonal variations implied the conjunction of several abiotic factors variation. For example, during winter, the macroalgae are commonly exposed to lower incident irradiation and day length as well as lower water temperatures and the opposite in summer. These variations differed to latitudinal environmental conditions since the day length was similar for the two studied areas. Moreover, an acclimation of photosynthesis efficiency may also occur by the change in the fatty acids desaturation level since these adjustments regulated membrane fluidity and thus determining the thermosensitivity of PS II (Allakhverdiev et al., 2008). Variation of lipid desaturation levels was reported on other macrolalgal species in response to differential water temperature (Sanina et al., 2008).

Photosynthetic plasticity and metabolomic involvements We reported contrasted patterns of *in situ* chl a fluorescence signals depending on sites, illustrating the contrasted environmental conditions of shores mainly due to their differential latitude position inducing higher mean temperatures (Gohin et al., 2010) as exposition to higher irradiances. These differential environmental conditions were not observed during the experiments in term of air temperature as irradiance. Fv/Fm declined more important in ria de Aveiro than in Faou ria suggested a more pronounced photoinhibition occuring in Portugal location. Contrariwise, initial Fv/fm values recorded at the beginning of low tide were similar in the two locations indicating a complete recovery of photosynthetic efficiency during the immersion and night. These results suggested the establishment of a dynamic non-photochemical quenching (NPQ) during spring tide in summertime as observed previously on other seaweeds (Delebecq et al., 2011; Gevaert et al., 2003; Häder et al., 2001). The establishment of NPQ allowed to prevent PSII damages by a stronger dissipation of excessive energy and decreasing energy inputs on PSII (Hanelt, 2003). On another hand, the more pronounced photoinhibition in ria de Aveiro may suggest an higher susceptibility to the establishment of chronic photoinhibition.

The major photosynthetic pigment of *G. vermiculophylla*, *i.e.* chl a, was present in higher concentrations in populations from ria de Aveiro. These results may seem surprising since it was commonly assumed that higher light availability was associated to a decrease in

photosynthetic pigments to limit light harvesting capacity and prevent photo-oxidative stress (*e.g*. Delebecq et al., 2013; Miller et al., 2006; Roleda et al., 2012; Schmid, 2016). Several hypotheses could explain these observations. Higher concentrations in chl a may be a consequence of a differential dilution of the pigment due to differential growth of the algal thallus during summer periods between the two populations. Indeed, it was shown previously that populations of the Bay of Brest presented a highest productivity (Davoult et al., *in prep.*) as higher biomass in June (Surget et al. 2017) suggesting that summertime represents the growth period. Moreover, Abreu et al. (2011) showed differential relative growth rate between tetrasporophyte and gametophyte of *G. vermiculophylla* on young sporelings and similar growth was observed on older thalli.

On another hand, as mentioned above, dredging activities in Ria de Aveiro induced the increase of tidal prism and as a consequence the intensification of tidal currents. These factors enhanced the water turbidity (see Figure 1c) and the capacity of sediment transport inducing the decline of seagrass populations replaced by macroalgae (Silva et al., 2004). Thus, concentration in chl a of *Gracilaria* thalli from ria de Aveiro lagoon may be an acclimation to low light availability occurring during immersion due to the turbidity of seawater linked to human activities of this highly entropized area. Effectively, increasing their chlorophyll content significantly, allowing the individuals to reduce their light saturation point and thus allow a higher productivity under low light conditions (Miller et al., 2006; Roleda et al., 2012). On another hand, as illustrated in the present study, by increasing its light harvesting capacity, with a higher overall photosynthetic capacity, *i.e.* higher rETR observed during the the first part of the ebb tide, higher chl a concentrations may induce higher photoinhibition as higher oxidatives stress during emersion.

Linked to an higher overall photosynthetic capacity and face to photoxidative stress enhanced in portugal, several mechanisms of protection may occur within the alga. At first, an increase in carotenoids pigments, *i.e.* zeaxanthin and β-caroten was observed during summertime in ria de Aveiro populations. These photo-protective pigments are well known to play a key role in the photoprotection of PSII reaction centres of plants and most of algae (Demmig-Adams and Adams, 1996; Jahns and Holzwarth, 2012). Furthermore, the accumulation of zeaxanthin is probably an acclimation response to light stress in the Gracilariales (Schubert et al., 2006). Interestingly, xanthophyll cycle not seem to occur

during tide time scale due to the lack of violaxanthin as anteraxanthin (in most of samples for the latter). These results grew the debate concerning an operative violaxanthin cycle occurring in red seaweeds (Goss and Jakob, 2010; Marquardt and Hanelt, 2004; Raven, 2011).

Secondly, the present study illustrated an increase of some neutral lipids such as triacylglycerides (TAG), alcohols and sterol esters in Portuguese populations. Neutral lipids constituted storage compounds of carbon, easily catabolized to provide energy source (Gurr et al., 2002; Guschina and Harwood, 2013; Ohlrogge and Browse, 1995). Interestingly, it was shown that high light conditions can lead to an increase of neutral storage lipids such as TAG, which has been observed in the brown seaweed *Fucus serratus* and the red one, *Tichocarpus crinitus* (Khotimchenko and Yakovleva, 2005). On microalgae, it was reported that the biosynthesis of TAG may serve as electron sink under photo-oxidative stress (Hu et al., 2008).

In this context, lipid peroxydation levels indicated that higher oxidative stress may occur in population of *G. vermiculophylla* from ria de Aveiro lagoon. Moreover, photosynthetic parameters exhibited the establishment of photoinhibition during the spring tide in the two latitudes but this effect was enhanced in Portugal, indicating the exposition to excessive light energy. In this way, high irradiances encountered in the ria de Aveiro, may induce the *de novo* biosynthesis of some storage lipids such as TAG as demonstrated in microalgae (Roessler, 1990 and references therein) with the aim to store excessive energy produce by photosynthetic apparatus. This biosynthesis require large amount of ATP and NAD(P)H and may prevent photochemical damage under excessive irradiance (Roessler, 1990). High rETR exhibited in ria de Aveiro joined this hypothesis as this proxy of electron transport illustrated higher photosynthetic efficiency of *G. vermiculophylla* in ria de Aveiro before establishment of photoinhibition. Nevertheless, this ability to accumulate TAG was not evident in two other red seaweeds, *Palmaria palmata* (Schmid, 2016) and also on another invasive species, *Grateloupia turuturu* (Kendel et al., 2013).

To conclude, even if Portuguese populations may present more susceptible photophysiological patterns associated to a high oxidative stress, this stress seemed to be regulate by the seaweeds, as no photobleaching seems to occur (no degradation in pigments) as no enhancement of SOD activities. *G. vermiculophylla* seemed to be more

sensitive to winter temperature as winter environmental conditions in Faou ria induced an increase of SOD activity compared to summer environmental conditions (Surget et al., 2017) translating an activation of antioxidant defenses (Lesser, 2006). Several limits have to be taken into account between the studied areas: differential biotic factors which could not be controlled (macrofauna, epiphytes, virus…), differential local environmental factors such as nutriments inputs along latitudinal gradient… Despite these limiting factors, such studies like this one, may complete experimentations performed under controlled conditions. Performed these analyses on populations from the South of Sweden will allow to check this hypothesis. Furthermore, the ecological characteristics of the species reinforced these conclusions mainly due to the presence of carposporophytes showing that reproduction may occur throughout the year in ria de Aveiro (Abreu et al., 2011). Furthermore, the ecological capabilities of this species may compensate its stressful environmental conditions. We hypothesized that especially its capacities to be maintained at dormancy state under buried conditions (Surget et al., in preparation) allow *G. vermiculophylla* to thrive in ria de Aveiro (Abreu, 2011 and this present study). In a context of climate change and temperature warming, we can hypothesize that an increase of the seawater temperature in the bay of Brest may facilitate its sustainability by increasing its reproduction window.

References

Abreu, M.H., Pereira, R., Sousa-Pinto, I., Yarish, C., 2011. Ecophysiological studies of the non-indigenous species *Gracilaria vermiculophylla* (Rhodophyta) and its abundance patterns in Ria de Aveiro lagoon, Portugal. Eur. J. Phycol. 46, 453–464.

Allakhverdiev, S.I., Kreslavski, V.D., Klimov, V.V., Los, D.A., Carpentier, R., Mohanty, P., 2008. Heat stress: an overview of molecular responses in photosynthesis. Photosynth. Res. 98, 541.

Bartsch, I., Wiencke, C., Laepple, T., 2012. Global seaweed biogeography under a changing climate: The prospected effects of temperature, in: Wiencke, C., Bischof, K. (Eds.), Seaweed Biology, Ecological Studies. Springer Berlin Heidelberg, pp. 383–406.

Bondu, S., Kervarec, N., Deslandes, E., Pichon, R., 2007. The use of HRMAS NMR spectroscopy to study the in vivo intra–cellular carbon/nitrogen ratio of *Solieria chordalis* (Rhodophyta). J. Appl. Phycol. 20, 673–679.

Bradford, M.M., 1976. A rapid and sensitive method for the quantitation of microgram quantities of protein utilizing the principle of protein-dye binding. Anal. Biochem. 72, 248–254.

Davidson, A.M., Jennions, M., Nicotra, A.B., 2011. Do invasive species show higher phenotypic plasticity than native species and, if so, is it adaptive? A meta-analysis. Ecol. Lett. 14, 419–431.

Davoult, D., Surget, G., Stiger-Pouvreau, V., Noisette, F., Riera, P., Stagnol, D., Androuin, T., & Poupart, N., (in prep.) Effects of *Gracilaria vermiculophylla* invasion on estuarine-mudflat functioning and diversity.

Delebecq, G., Davoult, D., Menu, D., Janquin, M.-A., Dauvin, J.-C., Gevaert, F., 2013. Influence of local environmental conditions on the seasonal acclimation process and the daily integrated production rates of *Laminaria digitata* (Phaeophyta) in the English Channel. Mar. Biol. 160, 503–517.

Delebecq, G., Davoult, D., Menu, D., Janquin, M.-A., Migné, A., Dauvin, J.-C., Gevaert, F., 2011. In situ photosynthetic performance of *Laminaria digitata* (Phaeophyceae) during spring tides in Northern Brittany. CBM-Cah. Biol. Mar. 52, 405.

Demmig-Adams, B., Adams, W.W., 1996. The role of xanthophyll cycle carotenoids in the protection of photosynthesis. Trends Plant Sci. 1, 21–26.

Dörmann, P., Hölzl, G., 2009. The role of glycolipids in photosynthesis, in: Wada, H., Murata, N. (Eds.), Lipids in photosynthesis, advances in photosynthesis and respiration. Springer Netherlands, pp. 265–282.

Dumay, J., Clément, N., Morançais, M., Fleurence, J., 2013. Optimization of hydrolysis conditions of *Palmaria palmata* to enhance R-phycoerythrin extraction. Bioresour. Technol. 131, 21–27.

Eggert, A., 2012. Seaweed responses to temperature, in: Wiencke, C., Bischof, K. (Eds.), Seaweed biology, ecological studies. Springer Berlin Heidelberg, pp. 47–66.

Esterbauer, H., Cheeseman, K.H., 1990. [42] Determination of aldehydic lipid peroxidation products: Malonaldehyde and 4-hydroxynonenal, in: Enzymology, B.-M. in (Ed.), Oxygen Radicals in Biological Systems Part B: Oxygen Radicals and Antioxidants. Academic Press, pp. 407–421.

Genty, B., Briantais, J.-M., Baker, N.R., 1989. The relationship between the quantum yield of photosynthetic electron transport and quenching of chlorophyll fluorescence. Biochim. Biophys. Acta BBA - Gen. Subj. 990, 87–92.

Gevaert, F., Creach, A., Davoult, D., Migne, A., Levavasseur, G., Arzel, P., Holl, A., Lemoine, Y., 2003. *Laminaria saccharina* photosynthesis measured *in situ*: photoinhibition and xanthophyll cycle during a tidal cycle. Mar. Ecol. Prog. Ser. 247, 43–50.

Gohin, F., Saulquin, B., Bryere, P., 2010. Atlas de la Température, de la concentration en Chlorophylle et de la Turbidité de surface du plateau continental français et de ses abords de l'Ouest européen. Ifremer. http://archimer.ifremer.fr/doc/00057/16840/.

Goss, R., Jakob, T., 2010. Regulation and function of xanthophyll cycle-dependent photoprotection in algae. Photosynth. Res. 106, 103–122.

Gurr, M.I., Harwood, J.L., Frayn, K.N., 2002. Lipid biochemistry. Vol. 409. Oxford: Blackwell Science.

Guschina, I.A., Harwood, J.L., 2013. Algal lipids and their metabolism, in: Algae for biofuels and energy. Springer, pp. 17–36.

Haberkorn, H., Lambert, C., Le Goïc, N., Moal, J., Suquet, M., Guégen, M., Sunila, I., Soudant, P.,2010. Effects of *Alexandrium minutum* exposure on nutrition-related processes and reproductive output in oysters *Crassostrea gigas*. Harmful Algae 9:427–439

Häder, D.-P., Porst, M., Lebert, M., 2001. Photosynthetic performance of the Atlanic brown macroalgae, *Cystoseira abies-marina*, *Dictyota dichotoma* and *Sargassum vulgare*, measured in Gran Canaria on site. Environ. Exp. Bot. 45, 21–32.

Hanelt, D., Wiencke, C., Bischof, K., 2003. Photosynthesis in Marine Macroalgae, in: Larkum, A.W.D., Douglas, S.E., Raven, J.A. (Eds.), Photosynthesis in Algae, Advances in Photosynthesis and Respiration. Springer Netherlands, pp. 413–435.

Harley, C.D.G., Randall Hughes, A., Hultgren, K.M., Miner, B.G., Sorte, C.J.B., Thornber, C.S., Rodriguez, L.F., Tomanek, L., Williams, S.L., 2006. The impacts of climate change in coastal marine systems. Ecol. Lett. 9, 228–241.

Hellmann, J.J., Byers, J.E., Bierwagen, B.G., Dukes, J.S., 2008. Five potential consequences of climate change for invasive species. Conserv. Biol. 22, 534–543.

Helmuth, B., Harley, C.D.G., Halpin, P.M., O'Donnell, M., Hofmann, G.E., Blanchette, C.A., 2002. Climate change and latitudinal patterns of intertidal thermal stress. Science 298, 1015–1017.

Hu, Q., Sommerfeld, M., Jarvis, E., Ghirardi, M., Posewitz, M., Seibert, M., Darzins, A., 2008. Microalgal triacylglycerols as feedstocks for biofuel production: perspectives and advances. Plant J. 54, 621–639.

Huang, Q.Q., Pan, X.Y., Fan, Z.W., Peng, S.L., 2015. Stress relief may promote the evolution of greater phenotypic plasticity in exotic invasive species: a hypothesis. Ecol. Evol. 5, 1169–1177.

Isaak, D.J., Rieman, B.E., 2013. Stream isotherm shifts from climate change and implications for distributions of ectothermic organisms. Glob. Change Biol. 19, 742–751.

Jahns, P., Holzwarth, A.R., 2012. The role of the xanthophyll cycle and of lutein in photoprotection of photosystem II. Biochim. Biophys. Acta BBA - Bioenerg., Photosystem II 1817, 182–193.

Jueterbock, A., Kollias, S., Smolina, I., Fernandes, J.M.O., Coyer, J.A., Olsen, J.L., Hoarau, G., 2014. Thermal stress resistance of the brown alga *Fucus serratus* along the North-Atlantic coast: Acclimatization potential to climate change. Mar. Genomics 13, 27–36.

Kendel, M., Couzinet-Mossion, A., Viau, M., Fleurence, J., Barnathan, G., Wielgosz-Collin, G., 2013. Seasonal composition of lipids, fatty acids, and sterols in the edible red alga *Grateloupia turuturu*. J. Appl. Phycol. 25, 425–432.

Khotimchenko, S.V., Yakovleva, I.M., 2005. Lipid composition of the red alga *Tichocarpus crinitus* exposed to different levels of photon irradiance. Phytochemistry 66, 73–79.

Lande, R., 2015. Evolution of phenotypic plasticity in colonizing species. Mol. Ecol. 24, 2038–2045.

Lesser, 2006. Oxidative stress in marine environments: Biochemistry and physiological ecology. Annu. Rev. Physiol. 68, 253–278.

Lima, F.P., Ribeiro, P.A., Queiroz, N., Hawkins, S.J., Santos, A.M., 2007. Do distributional shifts of northern and southern species of algae match the warming pattern? Glob. Change Biol. 13, 2592–2604.

Lion, U., Wiesemeier, T., Weinberger, F., Beltrán, J., Flores, V., Faugeron, S., Correa, J., Pohnert, G., 2006. Phospholipases and galactolipases trigger oxylipin-mediated ound-activated defence in the red alga *Gracilaria chilensis* against epiphytes. ChemBioChem 7, 457–462.

Marquardt, J., Hanelt, D., 2004. Carotenoid composition of *Delesseria lancifolia* and other marine red algae from polar and temperate habitats. Eur. J. Phycol. 39, 285–292.

Meudec, A., 2006. Exposition au fioul lourd chez *Salicornia fragilis* Ball et Tutin: contamination chimique par les HAPs et réponses biologiques de la plante. Brest.

Miller, S.M., Wing, S.R., Hurd, C.L., 2006. Photoacclimation of *Ecklonia radiata* (Laminariales, Heterokontophyta) in Doubtful Sound, Fjordland, Southern New Zealand. Phycologia 45, 44–52.

Muangmai, N., Vo, T.D., Kawaguchi, S., 2014. Seasonal fluctuation in a marine red alga, *Gracilaria vermiculophylla* (Gracilariales, Rhodophyta), from Nokonoshima Island, Southern Japan. J Fac Agric. Kyushu Univ 59, 243–248.

Munier, M., Jubeau, S., Wijaya, A., Morançais, M., Dumay, J., Marchal, L., Jaouen, P., Fleurence, J., 2014. Physicochemical factors affecting the stability of two pigments: R-phycoerythrin of *Grateloupia turuturu* and B-phycoerythrin of *Porphyridium cruentum*. Food Chem. 150, 400–407.

Ohlrogge, J., Browse, J., 1995. Lipid biosynthesis. Plant Cell 7, 957–970.

Pettitt, T.R., Harwood, J.L., 1989. Alterations in lipid metabolism caused by illumination of the marine red algae *Chondrus crispus* and *Polysiphonia lanosa*. Phytochemistry 28, 3295–3300.

Rahel, F.J., Olden, J.D., 2008. Assessing the effects of climate change on aquatic invasive species. Conserv. Biol. 22, 521–533.

Raniello, R., Lorenti, M., Brunet, C., Buia, M.C., 2006. Photoacclimation of the invasive alga *Caulerpa racemosa var. cylindracea* to depth and daylight patterns and a putative new role for siphonaxanthin. Mar. Ecol. 27, 20–30.

Raniello, R., Lorenti, M., Brunet, C., Buia, M.C., 2004. Photosynthetic plasticity of an invasive variety of *Caulerpa racemosa* in a coastal Mediterranean area: light harvesting capacity and seasonal acclimation. Mar. Ecol. Prog. Ser. 271, 113–120.

Raven, J.A., 2011. The cost of photoinhibition. Physiol. Plant. 142, 87–104.

Rempt, M., Weinberger, F., Grosser, K., Pohnert, G., 2012. Conserved and species-specific oxylipin pathways in the wound-activated chemical defense of the noninvasive red alga *Gracilaria chilensis* and the invasive *Gracilaria vermiculophylla*. Beilstein J. Org. Chem. 8, 283–289.

Richard, G., Le Bris, C., Guérard, F., Lambert, C., Paillard, C., 2015. Immune responses of phenoloxidase and superoxide dismutase in the manila clam *Venerupis philippinarum* challenged with *Vibrio tapetis* – Part II: Combined effect of temperature and two *V. tapetis* strains. Fish Shellfish Immunol. 44, 79–87.

Roessler, P.G., 1990. Environmental control of glycerolipid metabolism in microalgae: commercial implications and future research directions. J. Phycol. 26, 393–399.

Roleda, M.Y., Nyberg, C.D., Wulff, A., 2012. UVR defense mechanisms in eurytopic and invasive *Gracilaria vermiculophylla* (Gracilariales, Rhodophyta). Physiol. Plant. 146, 205–216.

Rueness, J., 2005. Life history and molecular sequences of *Gracilaria vermiculophylla* (Gracilariales, Rhodophyta), a new introduction to European waters. Phycologia 44, 120–128.

Sanina, N.M., Goncharova, S.N., Kostetsky, E.Y., 2008. Seasonal changes of fatty acid composition and thermotropic behavior of polar lipids from marine macrophytes. Phytochemistry 69, 1517–1527.

Schmid, M., 2016. Biochemical plasticity in seaweeds: assessment and optimisation of high value compounds.

Schmid, M., Stengel, D.B., 2015. Intra-thallus differentiation of fatty acid and pigment profiles in some temperate Fucales and Laminariales. J. Phycol. 51, 25–36.

Schubert, N., García-Mendoza, E., Pacheco-Ruiz, I., 2006. Carotenoid composition of marine red algae1. J. Phycol. 42, 1208–1216.

Silva, J.F., Duck, R.W., Catarino, J.B., 2004. Seagrasses and sediment response to changing physical forcing in a coastal lagoon.

Simon, G., Kervarec, N., Cérantola, S., 2015. HRMAS NMR analysis of algae and identification of molecules of interest via conventional 1D and 2D NMR: sample preparation and optimization of experimental conditions, in: Stengel, D.B., Connan, S. (Eds.), Natural products from marine algae, Methods in Molecular Biology. Springer New York, pp. 191–205.

Sokal, R.R., Rohlf, F.J., 1995. Biometry: The principles and practice of statistics in biological research.

Stiger-Pouvreau, V., Thouzeau, G., 2015. Marine species introduced on the French Channel-Atlantic Coasts: a review of main biological invasions and impacts. Open J. Ecol. 05, 227–257.

Sun, L., Wang, S., Gong, X., Zhao, M., Fu, X., Wang, L., 2009. Isolation, purification and characteristics of R-phycoerythrin from a marine macroalga *Heterosiphonia japonica*. Protein Expr. Purif. 64, 146–154.

Surget, G., Lann, K.L., Delebecq, G., Kervarec, N., Donval, A., Poullaouec, M.-A., Bihannic, I., Poupart, N., Stiger-Pouvreau, V., 2017. Seasonal phenology and metabolomics of the introduced red macroalga *Gracilaria vermiculophylla*, monitored in the Bay of Brest (France). J. Appl. Phycol. 1–16.

Thomsen, M.S., McGlathery, K.J., Schwarzschild, A., Silliman, B.R., 2009. Distribution and ecological role of the non-native macroalga *Gracilaria vermiculophylla* in Virginia salt marshes. Biol. Invasions 11, 2303–2316.

Wernberg, T., Thomsen, M.S., Tuya, F., Kendrick, G.A., Staehr, P.A., Toohey, B.D., 2010. Decreasing resilience of kelp beds along a latitudinal temperature gradient: potential implications for a warmer future. Ecol. Lett. 13, 685–694.

Yokoya, N.S., Kakita, H., Obika, H., Kitamura, T., 1999. Effects of environmental factors and plant growth regulators on growth of the red alga *Gracilaria vermiculophylla* from Shikoku Island, Japan, in: Kain, J.M., Brown, M.T., Lahaye, M. (Eds.), Sixteenth International Seaweed Symposium, Developments in Hydrobiology. Springer Netherlands, pp. 339–347.

Zanolla, M., Altamirano, M., Carmona, R., Rosa, J.D.L., Sherwood, A., Andreakis, N., 2015. Photosynthetic plasticity of the genus *Asparagopsis* (Bonnemaisoniales, Rhodophyta) in response to temperature: implications for invasiveness. Biol. Invasions 17, 1341–1353.

Zubia, M., Freile-Pelegrín, Y., Robledo, D., 2014. Photosynthesis, pigment composition and antioxidant defences in the red alga *Gracilariopsis tenuifrons* (Gracilariales, Rhodophyta) under environmental stress. J. Appl. Phycol. 26, 2001–2010.

Conclusion et synthèse de la partie 2

La problématique principale de cette partie peut se résumer de la manière suivante :

La plasticité phénotypique des espèces étudiées le long du gradient latitudinal, peut-elle permettre de prédire à grande échelle les effets bénéfiques ou délétères du changement climatique sur la biologie de ces espèces et *in fine* sur leur future répartition ?

Ces études apportent des éléments de réponse et permettent d'établir les constats suivants :

- une abondance différentielle de *C. fragile* associée à une variation des classes de taille le long du gradient qui traduit un potentiel invasif plus important en Norvège. Au vu de ces résultats, il serait particulièrement intéressant d'étudier l'acclimatation de l'efficacité photosynthétique de ces populations sachant qu'elles présentent une diversité génétique faible et correspondent au même haplotype (l'haplotype 1) et seraient issues d'un seul événement d'introduction (Provan et al., 2005). De plus, il serait judicieux de comparer cette acclimatation à celle des populations méditéranéennes d'un autre haplotype (haplotype 2).
- une forte plasticité phénologique de *S. muticum* à une échelle locale sans différences notables le long du gradient ainsi qu'une photo-physiologie acclimatée aux conditions thermiques du gradient lors des expériences menées. Une étude complémentaire portant sur le potentiel du stress oxydant induit par ces conditions environnementales permettrait de compléter ces résultats.
- ces résultats ne permettent pas de conclure quant à une résilience différentielle de la photo-physiologie entre *S. muticum* et *B. bifurcata*. Des analyses du contenu pigmentaire et du niveau de stress oxydant permettraient de compléter ces données.
- une forte plasticité phénologique de *G. vermiculophylla* ainsi qu'une photo-physiologie variable le long du gradient. Des expériences de transplantation entre les populations permettraient de comparer les performances différentielles de ces populations.

Pour *G. vermiculophylla*, les résultats montrent des profils de classe de taille de cette espèce similaires entre la Rade de Brest et la ria de Aveiro en 2015 associés à un envasement

du tapis algal ainsi que la présence de carposporophytes au Portugal. Ces résultats illustrent également une capacité photosynthétique plus élevée associée à l'absence d'activation de la SOD et à l'augmentation de la concentration du β-carotène pour la population étudiée dans la ria de Aveiro. L'ensemble de ces éléments semblent indiquer une persistance de cette espèce dans un contexte de réchauffement climatique aux latitudes plus au Nord comme en Rade de Brest. Cependant, cette question ne peut être complètement tranchée étant donné la multiplicité des interactions qu'elles soient antagonistes ou synergiques opérant entre les espèces algales et leur environnement biotique et abiotique. Par ailleurs, les résultats d'efficacité photosynthétique au niveau du PSII chez *G. vermiculophylla* entre la ria du Faou (Bretagne) et la ria de Aveiro (Portugal) soulignent le compromis existant entre une utilisation optimisée des faibles éclairements (dans ce cas présent potentiellement lié à une turbidité plus importante à l'immersion au Portugal, dans la ria de Aveiro) et la minimisation des dommages causés par l'exposition épisodique aux forts éclairements (une photoinhibition accrue de la population de cette ria) (Hanelt et al., 1997).

Ces résultats ont également illustré une variation différentielle des métabolites à la fois en termes d'osmolytes et de composition lipidique entre les saisons (décrit dans la partie 1) et le long d'un gradient thermique (cette présente partie) et ainsi la richesse des fonctions biologiques que ces métabolites peuvent remplir. La plasticité marquante du phénotype biochimique des macroalgues invasives étudiées (qui a été démontrée tout au long de ce travail) est source de chimiodiversité chez ces macrophytes marins. Cette chimiodiversité pourrait être utilisée pour des applications potentielles dans les domaines de la santé humaine et animale, dans une optique de bio-inspiration. Ainsi, la dernière partie de ce manuscrit présente deux voies de valorisation potentielles de métabolites de végétaux marins et littoraux en étudiant les propriétés biologiques de ces métabolites.

Références

Engelen, A.H., Serebryakova, A., Ang, P., Britton-Simmons, K., Mineur, F., Pedersen, M.F., Arenas, F., Fernandez, C., Steen, H., Svenson, R., 2015. Circumglobal invasion by the brown seaweed *Sargassum muticum*. Oceanogr. Mar. Biol. Annu. Rev. 53, 81–126.

Gohin, F., Saulquin, B., Bryere, P., 2010. Atlas de la température, de la concentration en chlorophylle et de la turbidité de surface du plateau continental français et de ses abords de l'Ouest européen. Ifremer. http://archimer.ifremer.fr/doc/00057/16840/.

Hanelt, D., Wiencke, C., Nultsch, W., 1997. Influence of UV radiation on the photosynthesis of arctic macroalgae in the field. J. Photochem. Photobiol. B 38, 40–47.

Hellmann, J.J., Byers, J.E., Bierwagen, B.G., Dukes, J.S., 2008. Five potential consequences of climate change for invasive species. Conserv. Biol. 22, 534–543.

IPCC, I.P. on C.C., 2013. The physical science basis. Contribution of working group I to the fifth assessment report of the intergovernmental panel on climate change, Climate Change 2013 ed T Stocker et al. ed. USA: Cambridge University Press.

Olabarria, C., Arenas, F., Viejo, R.M., Gestoso, I., Vaz-Pinto, F., Incera, M., Rubal, M., Cacabelos, E., Veiga, P., Sobrino, C., 2013. Response of macroalgal assemblages from rockpools to climate change: effects of persistent increase in temperature and CO_2. Oikos 122, 1065–1079.

Provan, J., Murphy, S., Maggs, C.A., 2005. Tracking the invasive history of the green alga *Codium fragile ssp. tomentosoides*. Mol. Ecol. 14, 189–194.

Provan, J., Booth, D., Todd, N.P., Beatty, G.E., Maggs, C.A., 2008. Tracking biological invasions in space and time: elucidating the invasive history of the green alga *Codium fragile* using old DNA. Divers. Distrib. 14, 343–354.

Rueness, J., 2005. Life history and molecular sequences of *Gracilaria vermiculophylla* (Gracilariales, Rhodophyta), a new introduction to European waters. Phycologia 44, 120–128.

Stiger-Pouvreau, V., Thouzeau, G., 2015. Marine species introduced on the French Channel-Atlantic coasts: a review of main biological invasions and impacts. Open J. Ecol. 05, 227–257.

Partie 3 : Application des modèles de végétaux marins au concept de bio-inspiration

Les algues sont connues pour présenter un grand intérêt pour l'isolement de composés et de principes actifs à usages alimentaire, médical ou cosmétique (Stiger-Pouvreau and Guérard, 2017). Plus particulièrement, les végétaux marins de la zone intertidale (étage médio-littoral) constituent des modèles de choix du fait de leur acclimatation, voire adaptation, aux cycles tidaux, journaliers et saisonniers qui induisent une fluctuation constante des paramètres environnementaux (Hurd et al., 2014; Sampath-Wiley et al., 2008), et comme l'a démontré ce présent travail pour plusieurs espèces algales et pour deux estrans différents. Dans ces habitats, les algues ont développé un panel de stratégies de défense et notamment de défenses chimiques dont les principaux mécanismes sont l'osmorégulation, la résistance à la dessiccation, la photoprotection, le système antioxydant, les défenses liées aux interactions biotiques (défenses contre le broutage, contre l'épiphytisme…) (Amsler, 2012; Bischof and Rautenberger, 2012; Hurd et al., 2014; Iken, 2012; Karsten, 2012). Ces stratégies de défense confèrent aux macrophytes marins une forte chimiodiversité (Stengel et al., 2011).

Par ailleurs, ce potentiel d'acclimatation des espèces de macrophytes et les défenses qu'elles développent sont variables dans l'espace et le temps car intimement liées à leur environnement abiotique et biotique. Par exemple, Saha et al. (2016) ont montré la capacité de *G. vermiculophylla* à s'adapter rapidement à de nouvelles conditions biotiques dans son aire d'introduction, en développant des mécanismes de protection aux nouveaux épibiontes de l'aire d'introduction, tout en perdant la capacité de se défendre face à ceux de son aire d'origine (Saha et al., 2016). Cette acclimatation du mécanisme de défense chez cette algue conduit à une richesse des mécanismes de défense vis-à-vis du biofouling, richesse qui diffère d'une population à l'autre. Dans une optique d'application en anti-fouling, on peut s'attendre à ce que les populations de *G. vermiculopphylla* présentent des activités différentielles en fonction de leur répartition géographique. Comme autre exemple, on peut prendre la molécule soufrée du DMSP (diméthylsulfopropionate). Cette molécule d'importance écologique présente tout un ensemble d'activités biologiques différentes selon la population de *Codium fragile* étudiée (Van Alstyne, 2008), aux applications potentielles

multiples, telle que des activités en tant que cryoprotecteur (Karsten et al., 1992), qu'anti-appétant (Lyons et al., 2007), ou qu'un soluté constitutif (Keller et al., 2012; Stefels, 2000). Ces molécules impliquées dans la défense chimique des macroalgues présentent des activités biologiques indispensables au maintien de la fitness de l'algue, activités qui peuvent se révéler intéressantes pour faire face aux challenges de la société moderne en faisant le lien entre activité biologique et biotechnologie marine.

Ce constat a donné naissance au concept de bio-inspiration, ou « s'inspirer du vivant pour développer de nouveaux produits », tel que le développent d'ingrédients actifs pour le domaine de la cosmétologie et de la santé humaine (Fleurence and Levine, 2016 ; Stiger-Pouvreau and Guérard, 2017). Les fruits de la recherche fondamentale, comme l'isolement de molécules de protection/défense, conduisent ainsi les chercheurs à proposer ces molécules à des industriels qui les formulent ensuite pour diverses applications. Cette stratégie se révèle particulièrement fructueuse dans le développement de nouvelles méthodes pour prévenir le biofouling en milieu marin et l'identification de nouveaux composés pour le développement d'écrans solaires anti-UV (De Nys and Steinberg, 2002).

Parmi les molécules synthétisées par les végétaux marins, les composés phénoliques sont des composés d'intérêts qui possèdent de multiples activités biologiques (Ksouri et al., 2012). Ils constituent une large famille de métabolites secondaires qui sont caractérisés par un noyau aromatique portant un ou plusieurs groupements hydroxyles (Figure 30). Ils peuvent être simples comme les acides phénoliques ou polymérisés formant ainsi des polyphénols comme les flavonoïdes.

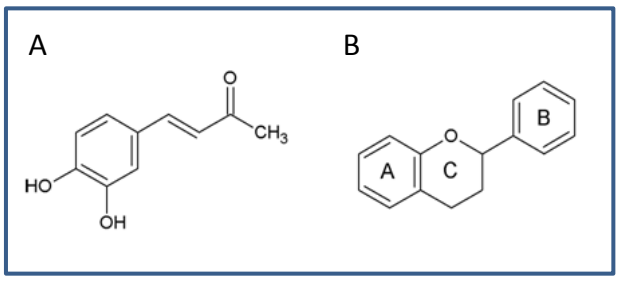

Fig. 30 Représentation d'un exemple d'acide phénolique, l'acide caféique (A) et de la structure de base d'un flavonoïde (B).

Les flavonoïdes constituent le groupe le plus large des composés phénoliques. Ils sont constitués de 15 atomes de carbone formant deux cycles aromatiques séparés par un hétérocycle (Ajila et al., 2011), et comme illustré en Figure 30.

Ils sont particulièrement connus pour leurs activités antioxydantes (Cho et al., 2011; Jallali et al., 2012; Mallick et Mohn, 2000). De nombreuses recherches sont menées afin de trouver de nouvelles sources d'antioxydants pour remplacer les composés synthétiques, utilisés communément dans l'industrie alimentaire (Gupta and Abu-Ghannam, 2011), et dont les caractères toxique et carcinogène ont été démontrés (Chen et al., 1992). Ainsi, il existe un intérêt grandissant pour identifier les espèces de macrophytes présentant un fort potentiel antioxydant en vue d'applications comme ingrédient actif dans l'industrie agro-alimentaire mais également cosmétique et pharmaceutique (Cho et al., 2011; Ksouri et al., 2012).

En marge de cette activité antioxydante bien décrite dans la bibliographie, les composés phénoliques peuvent présenter d'autres activités biologiques encore peu étudiées mais d'un grand intérêt pour les industriels et la société civile. Ces molécules actives peuvent présenter des activités originales ayant un lien direct avec leur rôle biologique, comme des propriétés photoprotectrices (c'est-à-dire lorsqu'ils sont synthétisés *de novo* ou en plus grande quantité par les végétaux marins en cas de stress lumineux ou d'irradiation aux ultraviolets), *e.g.* Cruces et al., 2017, avec une application potentielle en tant qu'écran solaire (Stevanato et al., 2014). Dans ce cas, on pourra parler de démarche de bio-inspiration intuitive.

Elles peuvent également présenter des propriétés sans lien apparent avec leur rôle biologique dans l'organisme dont elles sont extraites, comme par exemple des propriétés ostéogéniques, *i.e.* favorisant la minéralisation osseuse, de molécules présentes dans des organismes non calcaires. En effet, quelques études ont mis en évidence l'effet anabolique des composés phénoliques sur le métabolisme osseux (Zhang et al., 2008) suggérant leur utilisation dans la prévention de l'ostéoporose (Dew et al., 2007 ; Habauzit and Horcajada, 2007). La démarche de bio-inspiration dans ce second cas peut être qualifiée de non intuitive.

Dans ce contexte, deux études sont présentées dans cette partie, une première étude portant sur l'identification de molécules d'un extrait à propriétés photoprotectrices avec des applications potentielles en tant que filtre solaire (Chapitre 7) et une seconde étude sur les propriétés ostéogéniques d'extraits de deux macroalgues vertes, l'une invasive *Codium fragile* et l'autre native, *Cladophora rupestris* avec une application possible dans le domaine biomédical (Chapitre 8). Ces deux études ont fait l'objet au préalable de la mise au point d'un protocole de semi-purification des composés phénoliques initialement mis au point pour les macroalgues brunes au sein du laboratoire (Stiger-Pouvreau et al., 2014). Puis un screening a été réalisé chez trois espèces de phanérogames marines, ainsi que deux macroalgues vertes afin de tester l'efficacité de ce protocole et les activités biologiques des extraits ainsi obtenus (ces travaux ont fait l'objet de mon stage de Master 2). Dans le paragraphe suivant sont présentés les résultats de ce screening qui consiste en une étude préliminaire aux Chapitres 7 et 8.

Criblage de cinq macrophytes marins : étude préliminaire

Ce criblage a pour but de mettre en évidence l'efficacité d'un protocole de semi-purification à concentrer les composés phénoliques extraits de cinq macrophytes marins couramment observés le long des côtes bretonnes. Ainsi ont été sélectionnés deux chlorophytes : *Codium fragile* (Suringar) Hariot, *Cladophora rupestris* (Linnaeus) Kützing et trois plantes halophiles : *Spartina alterniflora* Loisel, *Salicornia fragilis* Ball and Tutin et *Salicornia ramosissima* Woods. Il a également pour objectif de mettre en évidence des activités biologiques intéressantes en analysant le potentiel antioxydant, activités antiradicalaire, photoprotectrices et pro-minéralisantes des extraits obtenus. Ce screening s'est décomposé en deux étapes. Une première étape a eu pour but de caractériser les extraits ainsi obtenus vis-à-vis de leur composition en composés phénoliques. Ainsi, les teneurs en composés phénoliques totaux et en flavonoïdes ont été dosés.

Lors d'une deuxième étape, le screening s'est porté sur les activités antioxydantes et antiradicalaires des différents types d'extraits qui ont été analysées au moyen de trois tests différents : le test antiradicalaire du DPPH (2.2 diphényl-1-picrylhydrasyl), le test du pouvoir réducteur et le test du β-carotène. Ces différents tests antioxydants et antiradicalaire apportent des informations complémentaires sur la nature des antioxydants présents chez les espèces étudiées (Figure 31). Le test DPPH est un test antioxydant non spécifique, c'est-à-dire qu'il permet de déterminer l'activité antioxydante d'extraits ou de molécules sans pouvoir conclure sur la nature de cette activité (Koleva et al., 2002) . Ce test est très sensible mais l'activité antioxydante mesurée est artificielle étant donné que le radical DPPH n'a pas de réalité biologique (Huang et al., 2005). Le test du β-carotène implique un transfert d'atomes d'hydrogène et permet ainsi de simuler la capacité antioxydante face à des mécanismes d'oxydation similaires à la peroxydation lipidique (Huang et al., 2005; Koleva et al., 2002). Le test du pouvoir réducteur implique un transfert d'électrons et comme son nom l'indique permet de déterminer la capacité réductrice des extraits ou des molécules testées (Aparadh et al., 2012; Huang et al., 2005).

Tests *in vitro* : différents tests pour divers mécanismes d'action

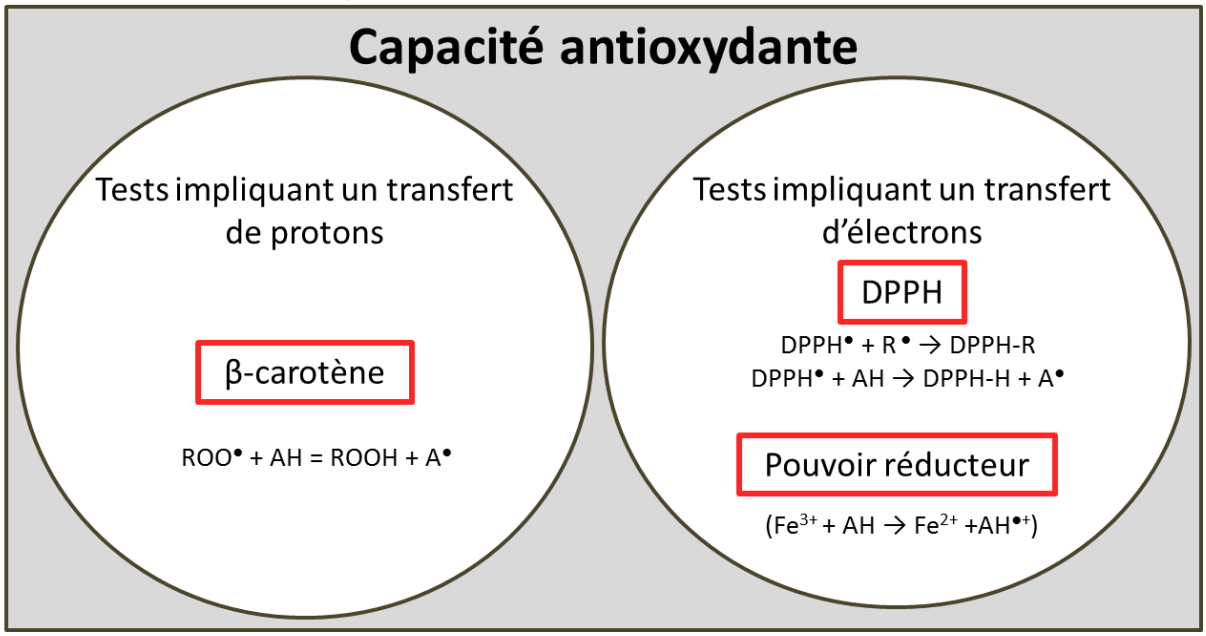

Fig. 31 Mécanismes d'action des différents tests utilisés dans le criblage afin d'analyser la capacité antioxydante des extraits et fractions obtenus à partir de cinq macrophytes marins.

Matériels et méthodes

Les quatre sites de prélèvement des macrophytes sont situés sur la côte Atlantique française. Les chlorophytes ont été prélevés sur l'estran de l'anse de Porsmeur (48°28'55.67"N, 4°46'14.76"O, Lanildult, 29). *Cladophora rupestris* a été échantillonné en haut de l'étage médiolittoral en mode abrité tandis que *Codium fragile* a été échantillonné en mode battu, en bas de l'étage médiolittoral. *Spartina alterniflora*, *Salicornia fragilis* et *Salicornia ramosissima* ont été prélevées respectivement au niveau du marais de la rivière de l'Elorn (48°24'26,10'' N, 4°20'47,82''O ; Le Relecq Kerhuon, 29), du marais de la Ria du Conquet (48°21'47,71'' N, 4°45'21.23'' O ; Le Conquet, 29) et du marais du Port du Collet (47°14140.84'' N, 1°58'57.74''O ; Bouin, 85).

Après récolte, le matériel végétal a été trié avec précaution et identifié. Le matériel a été rincé brièvement à l'eau courante avant d'être congelé (-24°C) et lyophilisé (CHRIST BETA 1-8 LD). Les échantillons ont été réduits en poudre à l'aide d'un broyeur ménager et conservés à l'abri de la lumière à température ambiante.

Méthode d'obtention des extraits bruts et des fractions semi-purifiées Des extraits bruts ont été obtenus pour chaque espèce par extraction solide/liquide à partir de poudres sèches et d'un mélange hydroéthanolique. Le protocole d'extraction puis de semi-purification est illustré par la Figure 32. Ce dernier a été adapté à partir de celui décrit par Stiger-Pouvreau et al. (2014). Il est détaillé dans les parties Matériels et Méthodes des deux chapitres suivants (Chapitre 7 et Chapitre 8).

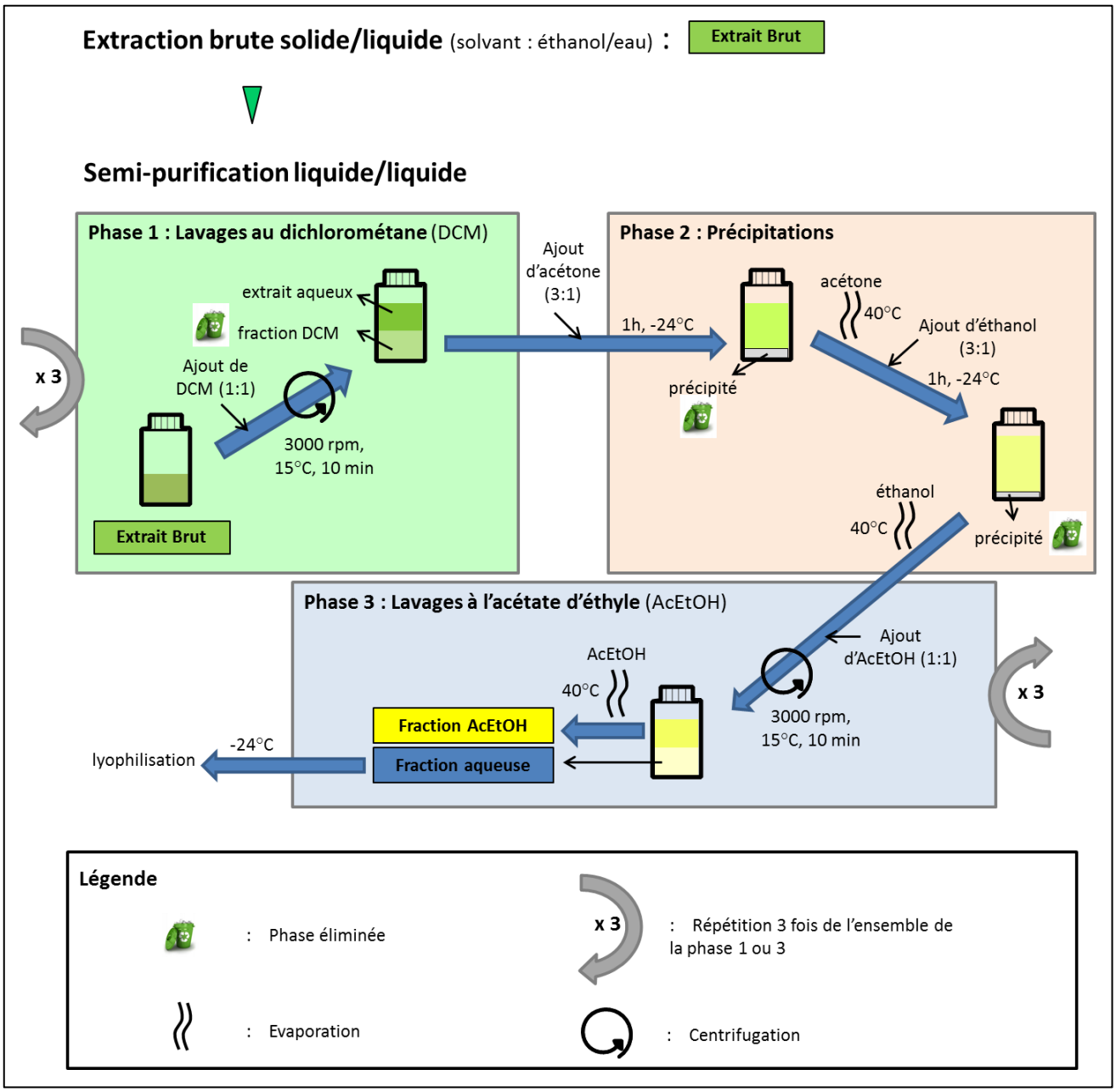

Fig. 32 Synoptique du protocole d'extraction des composés phénoliques et de leur semi-purification.

Ce protocole est composé de deux phases de lavage par des solvants organiques, entrecoupées d'une phase de précipitation. Il permet d'obtenir deux fractions semi-purifiées, une phase acétate d'éthyle et une phase aqueuse. Lors du screening des extraits des cinq espèces étudiées, l'extrait brut initial ainsi que les deux phases finales, *i.e.* fractions semi-purifiées, ont été analysés.

Tests colorimétriques Tous les tests colorimétriques ont été réalisés en microplaques de 96 puits (Greiner bio-one). Un aliquot de chaque extrait sec (brut, phase acétate d'éthyle et phase aqueuse) est pesé et solubilisé dans de l'eau déminéralisée afin d'obtenir une concentration de 10 $g.L^{-1}$. Différentes dilutions de 0,005 à 1 $g.L^{-1}$ sont effectuées et chaque concentration est testée en triplicata. La lecture des différentes absorbances a été réalisée par un spectrophotomètre à microplaque (Multiscan MS, Labsystems). Les produits chimiques utilisés sont de marque SIGMA-ALDRICH®. Les résultats ont été rapportés au poids d'extrait sec, ce qui élimine les variations des valeurs d'activités liées au rendement d'extraction.

Les protocoles du dosage des composés phénoliques totaux (test de Folin Ciocalteu) ainsi que des flavonoïdes sont détaillés dans le paragraphe 2.4 du Chapitre 7. De même, les protocoles de dosage de l'activité anti-radicalaire par le test du DPPH et de dosage de l'activité antioxydante par le test du pouvoir réducteur et par le test du blanchiment du β-carotène sont décrits dans le paragraphe 2.5 du Chapitre 7. Les résultats obtenus pour les dosages d'activités seront comparés à différents témoins positifs, l'acide 6-hydroxy-2,5,7,8-tetramethylchroman-2-carboxylique (trolox), l'α-tocophérol (vitamine E), l'acide ascorbique (vitamine C), l'hydroxyanisole butylé (BHA) et l'hydroxytoluène butylé (BHT).

Statistiques Les analyses statistiques ont été traitées à l'aide du logiciel RStudio (avec la version R 2.13.1). Les critères de faisabilité de l'ANOVA n'étant pas respectés (échantillonnage faible : n=3 à 5), des tests non paramétriques ont été utilisés. Le test de Kruskal-Wallis suivi d'un test *a posteriori* de Behrens Fisher (de la fonction npmc : Non Parametric Multiple Comparisons, de R) ont été appliqués pour effectuer des comparaisons multiples de moyenne. Toutes les analyses sont réalisées au seuil de confiance de 95%.

Résultats

Caractérisation des extraits et fractions semi-purifiées

Teneurs totales en composés phénoliques D'après la Figure 33, on observe que la purification a permis de concentrer de manière efficace les composés phénoliques dans la fraction acétate d'éthyle, les teneurs en composés phénoliques de celles-ci étant significativement plus élevées que celles des extraits bruts et des fractions aqueuses pour les cinq macrophytes étudiés. La purification des composés phénoliques est la plus effective pour *Salicornia ramossissima* avec un facteur 15,7 entre la fraction acétate d'éthyle présentant la teneur la plus élevée avec 431,5 ± 19,9 mg équivalent acide gallique.g^{-1} MS (mg éq. AG.g^{-1} MS) et l'extrait brut initial (27,4 ± 0,7 mg éq. AG.g^{-1} MS). D'un point de vue interspécifique, on observe une forte disparité des teneurs en composés phénoliques notamment pour les fractions acétate d'éthyle des espèces de plantes halophiles avec lesquelles les teneurs en composés phénoliques sont supérieures à 117,7 ± 3,4 mg éq. AG.g^{-1} MS soit 11,7% MS (teneur obtenue pour *Spartina alterniflora*) et celles des espèces algales pour lesquelles ces teneurs n'excèdent pas 22,4 ± 0,2 mg éq. AG.g^{-1} MS soit 2,2% MS (teneur obtenue pour *Codium fragile*).

Teneurs en flavonoïdes Des flavonoïdes ont été mis en évidence chez toutes les espèces, mais leurs teneurs sont très variables (Figure 34). Les fractions acétate d'éthyle des deux espèces de salicorne présentent les teneurs les plus élevées avec 285,1 ± 2,8 mg éq. catéchine.g^{-1} MS pour *Salicornia fragilis* et 309,557 ± 3,7 mg éq. catéchine.g^{-1} MS pour *Salicornia ramossissima*. Les algues chlorophytes contiennent également des flavonoïdes mais à des teneurs faibles en comparaison des teneurs des phases acétate d'éthyle des halophytes. Les résultats obtenus pour la fraction acétate d'éthyle de *Spartina alterniflora* n'ont pas pu être exploités en raison d'une interférence due à la forte coloration de cette fraction.

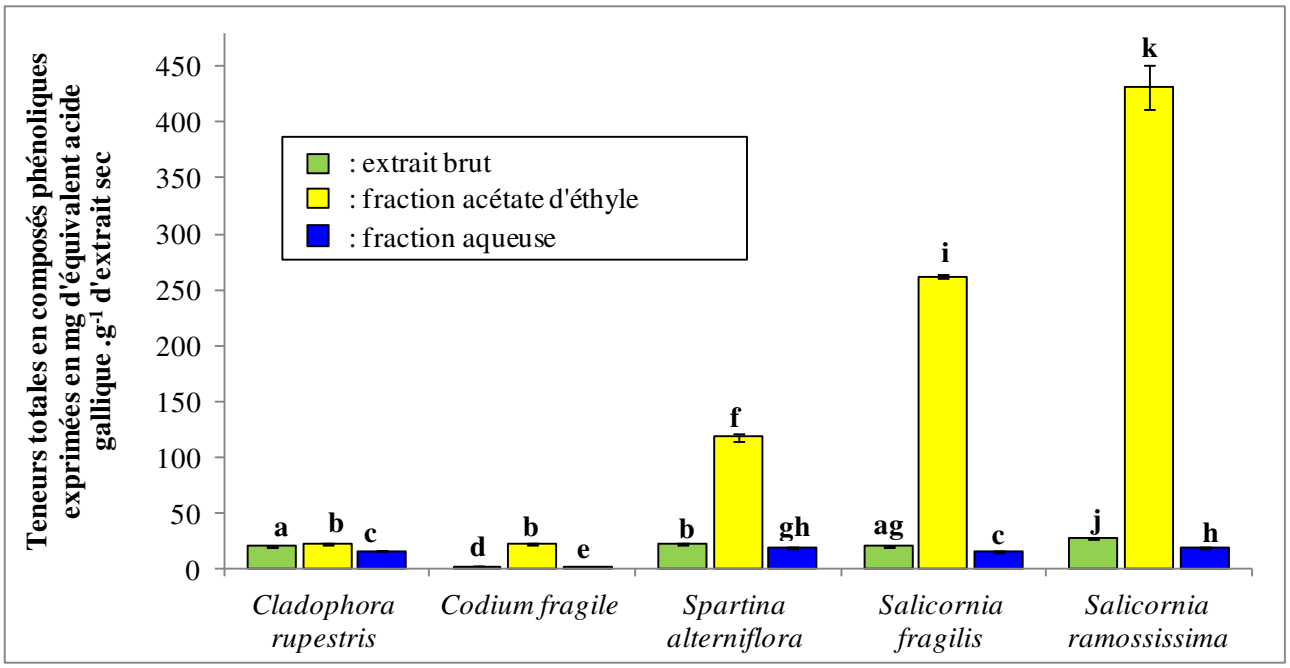

Fig. 33 Teneurs totales en composés phénoliques exprimées en mg éq. AG.g^{-1} d'extrait brut sec des cinq macrophytes marines. Valeurs moyennes avec une barre d'erreur représentant l'écart-type. Analyse statistique donnée par le test de Behrens Fisher (après un test de Kruskal-Wallis, p-value < 0,001). La présence de lettres différentes indique une différence significative (p-value < 0,05, n=3).

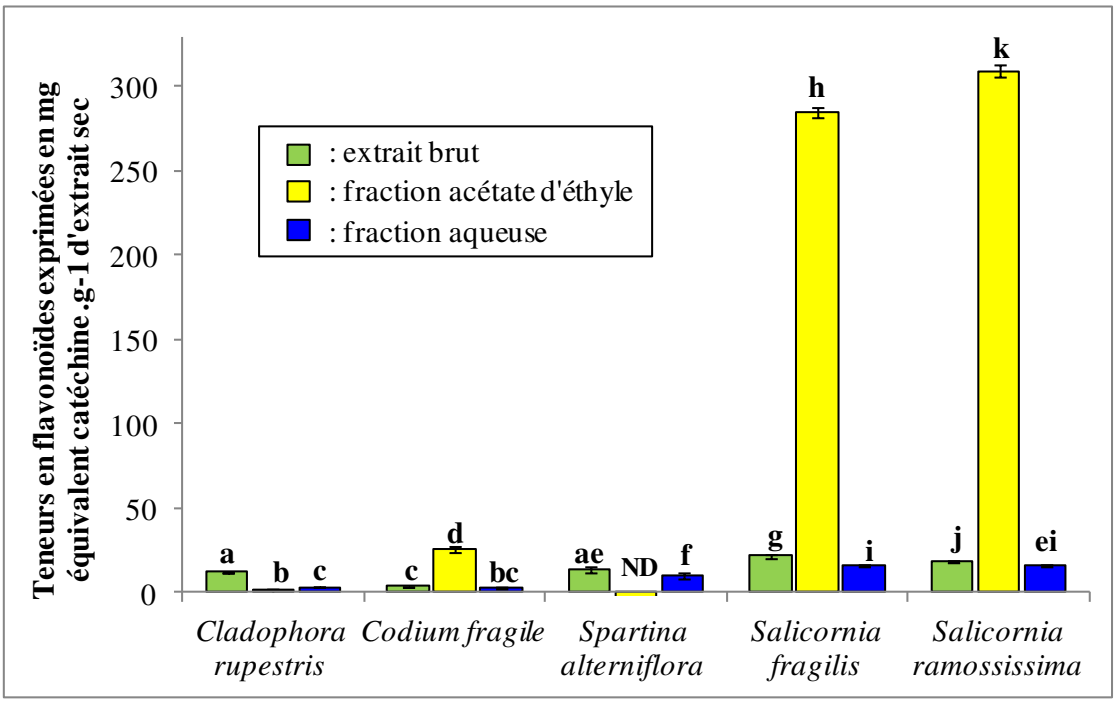

Fig. 34 Activité antiradicalaire au DPPH exprimée sous forme d'IC50 (concentration nécessaire pour que la moitié du DPPH soit oxydé) en g.L^{-1} de cinq macrophytes marins. Valeurs moyennes avec une barre d'erreur représentant l'écart-type. Analyse statistique donnée par le test de Behrens Fisher (après un test de Kruskal-Wallis, p-value < 0.001). La présence de lettres différentes indique une différence significative (p-value < 0,05, n=3).

Potentiel antiradicalaire des extraits bruts et semi-purifiés

Activité antiradicalaire par le test du DPPH Les phases acétate d'éthyle issues de la purification des extraits des différents macrophytes marins présentent des activités nettement supérieures à celles des extraits bruts et des phases aqueuses correspondants, car leurs IC50 sont plus faibles (Figure 35). On observe une variabilité de l'activité des extraits et des fractions semi-purifiées entre les différentes espèces avec par exemple, un facteur 59 entre les phases acétate d'éthyle de *Cladophora rupestris* (avec un IC50 de 0,768 ± 0,021 $g.L^{-1}$) et *Salicornia ramossissima*. On remarque que la phase acétate d'éthyle de *Codium fragile* est aussi peu active que la phase aqueuse de *Spartina alterniflora* en comparaison des témoins positifs. Les phases acétate d'éthyle de *Salicornia fragilis* et *S. ramossissima* (avec un IC50 identique de 0,0131 ± 0,0001$g.L^{-1}$) sont les plus actives.

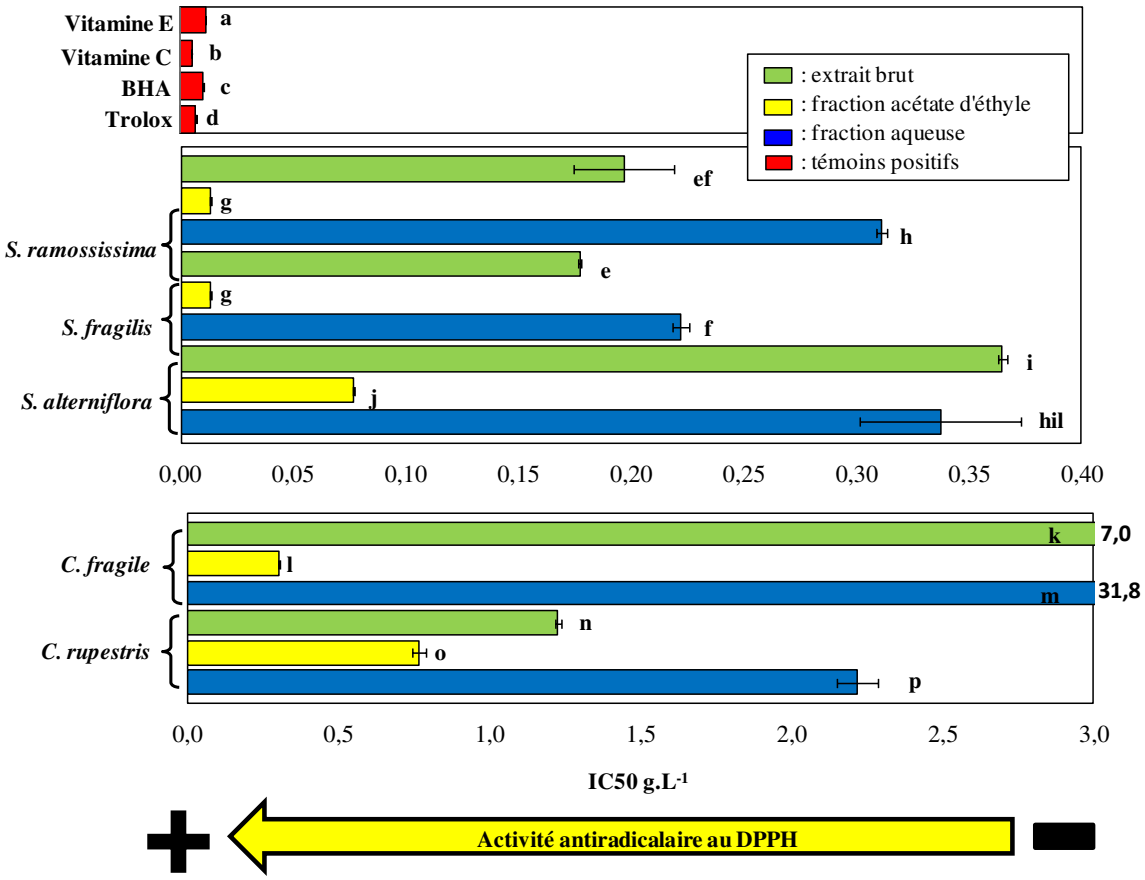

Fig. 35 Activité antiradicalaire au DPPH exprimée sous forme d'IC50 (concentration nécessaire pour que la moitié du DPPH soit oxydé) en $g.L^{-1}$ de cinq macrophytes marins. Valeurs moyennes avec une barre d'erreur représentant l'écart-type. Analyse statistique donnée par le test de Behrens Fisher (après un test de Kruskal-Wallis, p-value < 0,0001). La présence de lettres différentes indique une différence significative (p-value < 0,05, n = 3).

Elles présentent un IC50 proche de ceux des molécules pures utilisées comme témoins positifs, bien que significativement plus élevé (BHA : 0,0100 ± 0,0002 $g.L^{-1}$, vitamine C : 0,0050 ± 0,0001 $g.L^{-1}$, vitamine E : 0,0109 ± 0,0001 $g.L^{-1}$, trolox : 0,0067 ± 0,0001 $g.L^{-1}$).

Activité antioxydante par le test du blanchiment du β-carotène Seuls les extraits ou fractions présentant une activité inférieure à 1$g.L^{-1}$ ont été représentés en Figure 36. Les plantes halophiles sont plus actives que les algues chlorophytes. Si l'on compare par exemple *Spartina alterniflora* et *Codium* fragile, pour l'extrait brut, on obtient respectivement des IC50 de 3,82 ± 0,48$g.L^{-1}$ et 15,82 ± 3,53$g.L^{-1}$, pour les phases acétate d'éthyle, 0,39 ± 0,06 $g.L^{-1}$et 0,72 ± 0,03$g.L^{-1}$ puis pour les phases aqueuses, 7,19 ± 1,50$g.L^{-1}$ et 21,83 ± 0,35$g.L^{-1}$. Ces exemples permettent d'illustrer la forte activité des phases acétate d'éthyle en comparaison de celle des extraits bruts et des phases aqueuses. La phase acétate d'éthyle de *Salicornia ramossissima* présente la plus forte activité avec un IC50 de 0,318 ± 0,004$g.L^{-1}$ mais on remarque qu'elle est environ 46 fois moins active que le standard commercial le moins actif, le BHT (avec un IC50 de 0,0067 ± 0,0004$g.L^{-1}$).

Activité antioxydante par le test du pouvoir réducteur La Figure 37 montre que les activités antioxydantes avec le test du pouvoir réducteur sont les plus élevées pour les phases acétate d'éthyle, quel que soit les espèces testées. En effet, elles ont des IC50 significativement plus faibles que les extraits bruts respectifs. On observe une variabilité importante entre les phanérogames et les algues vertes. Pour ce test, les phases acétate d'éthyle de *Salicornia ramossissima* (avec un EC50 de 0,197 ± 0,003$g.L^{-1}$) et *S. fragilis* (avec un EC50 de 0,250 ± 0,003$g.L^{-1}$) présentent même des activités plus fortes que la vitamine E (avec un IC50 égal à 0,366 ± 0,011 $g.L^{-1}$). La phase acétate d'éthyle de la troisième halophyte, *Spartina alterniflora*, avec un EC50 de 1,10 ± 0,15$g.L^{-1}$, est seulement trois fois moins active que la vitamine E (EC50 de 0,37 ± 0,01$g.L^{-1}$).

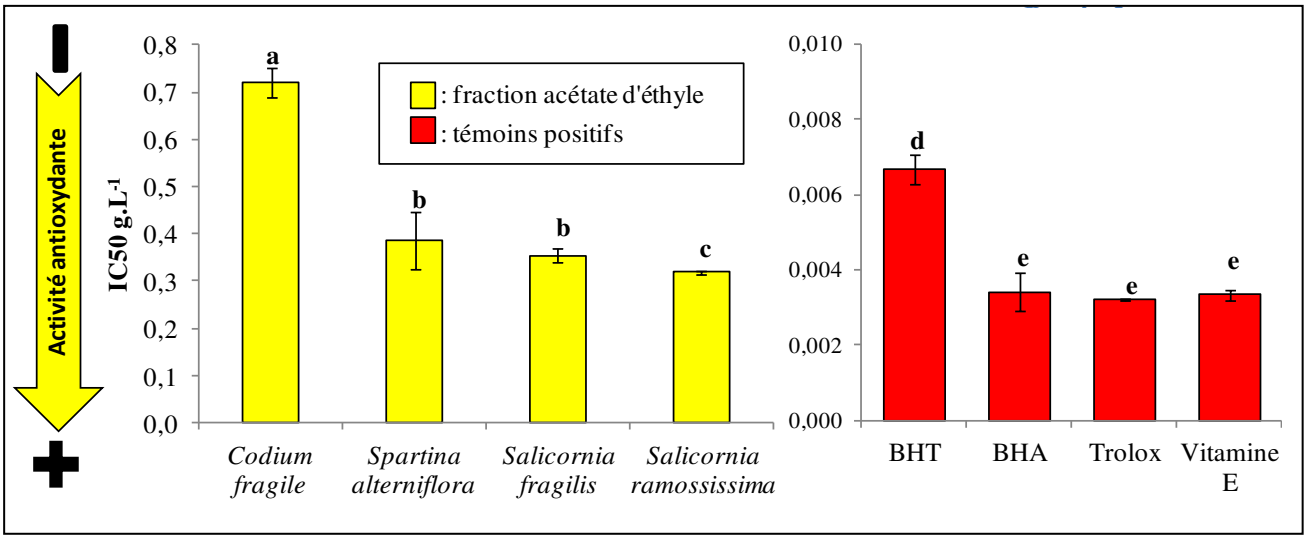

Fig. 36 Activité anti-oxydante des fractions acétate d'éthyle de quatre macrophytes marins par la méthode du blanchiment du β-carotène, exprimée sous forme d'IC50 (concentration nécessaire pour que 50% du β-carotène ne soit pas oxydé) en $g.L^{-1}$. Valeurs moyennes avec une barre d'erreur représentant l'écart-type. Analyse statistique donnée par le test de Behrens Fisher, n = 3 (après un test de Kruskal-Wallis, p-value = 0,0042). La présence de lettres différentes indique une différence significative (p-value < 0,05, n = 3).

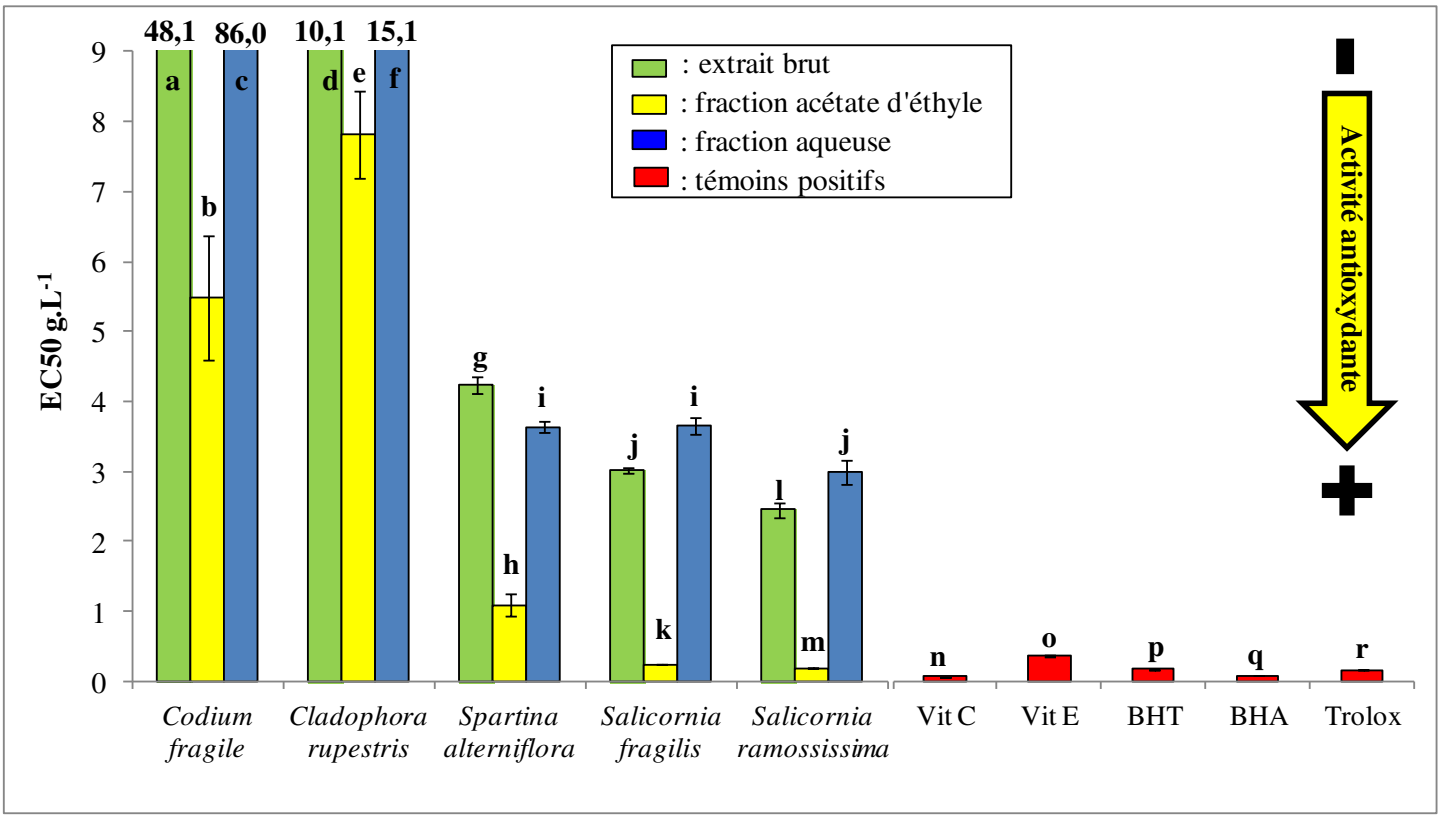

Fig. 37 Activité antioxydante de l'extrait brut et des fractions semi-purifiées de cinq macrophytes marins par la méthode du pouvoir réducteur, exprimée sous forme d'EC50 (concentration nécessaire pour que la DO soit égale à 0,5) en $g.L^{-1}$. Valeurs moyennes avec une barre d'erreur représentant l'écart-type. Analyse statistique donnée par le test de Behrens Fisher, n = 3 (après un test de Kruskal-Wallis, p-value < 0,0001). La présence de lettres différentes indique une différence significative (p-value < 0,05, n = 3).

Discussion

Les macrophytes marins développent des systèmes enzymatiques et non-enzymatiques pour se prémunir de l'effet des EROs. La synthèse de composés phénoliques est une des voies possibles pour contrer le stress oxydant (Grassmann et al., 2002; Mallick and Mohn, 2000; Pessoa, 2012). Dans la littérature, le potentiel antioxydant des composés phénoliques est connu. La relation entre la structure et la fonction antioxydante des composés phénoliques et des flavonoïdes a été expliquée et démontrée depuis longtemps (Heim et al., 2002; Rice-Evans et al., 1996). Les polyphénols tels que les flavonoïdes ont des fonctions antioxydantes multiples. Ce sont entre autre des agents réducteurs, des donneurs de protons et des neutralisateurs de l'oxygène singulet (Grassmann et al., 2002; Rice-Evans et al., 1996).

Hautes teneurs en composés phénoliques et en flavonoïdes Les teneurs en composés phénoliques obtenues et commentées ci-dessous peuvent être considérées comme fiables malgré le fait que le test de Folin-Ciocalteu est un test discuté (Huang et al., 2005). En effet, les protéines présentant des cycles aromatiques hydroxylés interfèrent avec ce dosage mais cette interférence n'excède pas 5% des composés non phénoliques qui s'oxydent dans cette réaction (Alstyne, 1995). De plus, dans les phases purifiées, les résidus protéiques ont été éliminés majoritairement par précipitation dans de l'acétone. Le protocole de semi-purification permet de diminuer ces interférences (Jégou, 2011).

Les résultats montrent que toutes les espèces testées synthétisent des composés phénoliques dont des flavonoïdes. Cette propriété des macrophytes marines est très variable selon les espèces. En effet, les résultats mettent en évidence une forte variabilité des teneurs en composés phénoliques et des teneurs en flavonoïdes en fonction des espèces dans la phase acétate d'éthyle. Deux groupes se distinguent, les algues vertes, *Cladophora rupestris* et *Codium fragile* et les phanérogames halophiles, *Salicornia ramossissima*, *S. fragilis* et *Spartina alterniflora*. Les phanérogames halophiles présentent les plus fortes teneurs en composés phénoliques et en flavonoïdes atteignant respectivement 431,5 ± 19,9 éq. AG.g^{-1} DW et 309,6 ± 3,7 éq. C.g^{-1} DW pour la phase acétate d'éthyle de *Salicornia ramossissima*. Cette tendance est également vérifiée pour les activités antioxydantes et antiradicalaires.

A notre connaissance, peu d'études existent sur le screening simultané d'espèces halophiles et algales. Agoramoorthy et al. (2008) mettent en évidence cette variabilité interspécifique chez des halophytes de milieu tropical. Les teneurs en composés phénoliques obtenues pour trois chénopodiacées, *Arthrocnemum indicum*, *Suaeda monoica* et *S. maritima* illustrent également cette variabilité pour des espèces appartenant à la même famille (avec respectivement 47,3 ± 5,0, 57,1 ± 6,4 et 23,5 ± 4,2 mg d'équivalent acide chlorogénique $.g^{-1}$ MS) (Agoramoorthy et al., 2008). Les teneurs obtenues pour les extraits bruts de *Salicornia ramossissima* et *S. fragilis* sont en adéquation avec ces résultats ayant celles-ci du même ordre de grandeur que *Suaeda maritima* (avec respectivement 27,44 ± 0,68 et 20,18 ± 0,36 mg éq. $AG.g^{-1}$ MS). Cette variabilité est également reportée chez les algues (Sabeena Farvin and Jacobsen, 2013; Wang et al., 2009).

La variabilité interspécifique des activités antioxydantes et des teneurs en composés phénoliques semble illustrer la variabilité des mécanismes antioxydants prépondérants utilisés par chaque espèce macrophyte. En effet, les résultats obtenus semblent indiquer que la synthèse de composés phénoliques serait une voie dominante dans la résistance des plantes halophiles aux stress environnementaux en comparaison des algues vertes pour les espèces étudiées. Ces composés phénoliques seraient en particulier des flavonoïdes chez les espèces de salicornes. Plusieurs études mettent en évidence chez les plantes halophiles des teneurs importantes de composés phénoliques et de flavonoïdes associées à des activités antioxydantes élevées (Agoramoorthy et al., 2008; Maisuthisakul et al., 2007). Trabelsi et al. (2012), pour *Limoniastrum guyonianum,* obtiennent une fraction acétate d'éthyle presque pure en composés phénoliques avec 928,3 ± 1,7 mg d'éq. $AG.g^{-1}$. Cette fraction présente aussi une activité antiradicalaire au DPPH très élevée avec un IC50 de 0,002 $g.L^{-1}$ et une activité réductrice importante avec un EC50 de 0,098 $g.L^{-1}$.

Chez l'espèce *Cladophora glomerata*, Choo et al. (2004) ont montré de fortes activités pour trois enzymes de défense (la superoxyde dismutase, l'ascorbate-péroxydase et la catalase) contre les EROs intracellulaires. Il classifie cette algue comme étant tolérante aux stress induits par les EROs intracellulaires. Cette hypothèse expliquerait les faibles teneurs en composés phénoliques chez *Cladophora rupestris*, celle-ci possédant un système enzymatique de détoxification performant. Wang et al. (2009) montrent que les teneurs en

composés phénoliques sont très faibles chez l'algue verte *Ulva lactuca* (avec environ 2 g d'équivalent phloroglucinol pour 100 g d'extrait) en comparaison des teneurs obtenues pour les algues brunes, la plus élevée ayant été observée pour *Fucus vesiculosus* (avec environ 18 g d'équivalent phloroglucinol pour 100 g d'extrait) (Wang et al., 2009).

D'autres molécules que les composés phénoliques peuvent être produites par les macrophytes marins face à un stress environnemental telles que les MAA (acides aminés de type mycosporine). Ces molécules sont connues pour leur activité écran contre les radiations UV. Leur rôle antioxydant pour prévenir les dommages cellulaires résultant de la formation d'EROs a également été reporté (Singh et al., 2008). La production de telles molécules a été mise en évidence chez les algues vertes et en particulier pour *Codium fragile* (Carreto and Carignan, 2011; Valentão et al., 2010). Singh et al. (2008) suggèrent que si les algues vertes étaient à l'origine des phanérogames, les phanérogames primitives devaient être initialement dépendantes de ces MAA qui ont ensuite été remplacés par les composés phénoliques, tels que les flavonoïdes, pour les protéger en particulier des radiations UV. D'autres composés antioxydants peuvent être également synthétisés par les macrophytes marins tels que des caroténoïdes, des vitamines et des terpénoïdes (Grassmann et al., 2002). Par exemple, Valentão et al. (2010) mettent en évidence des dérivés du β-carotène et des terpénoïdes dans un extrait aqueux de *Codium tomentosum*. Ces différentes hypothèses pourraient expliquer la variabilité observée entre les espèces tant au niveau des teneurs en composés phénoliques et en flavonoïdes qu'au niveau des activités antioxydantes et antiradicalaires entre les phanérogames marines et les algues vertes.

Concentration des molécules actives D'après les résultats, on observe que les teneurs en composés phénoliques des extraits bruts de *Salicornia fragilis* et *Cladophora rupestris* sont statistiquement identiques alors que celles des phases acétate d'éthyle sont très variables avec respectivement 262,0 ± 1,5 mg éq. AG.g^{-1} DW et 21,7 ± 0,9 mg éq. AG.g^{-1} DW. Ces résultats semblent indiquer que les composés phénoliques n'ont pas été concentrés dans la phase acétate d'éthyle de *Cladophora rupestris* ou que ce protocole n'est pas adapté aux molécules produites par cette espèce. Cho et al. (2011) ont partitionné des extraits bruts issus d'une extraction éthanolique à 95%, avec trois solvants, l'hexane, le chloroforme et l'acétate d'éthyle. Chez deux espèces d'algues vertes, la fraction chloroformique présente

les plus fortes teneurs en composés phénoliques et chez deux autres espèces, c'est la fraction acétate d'éthyle. Cette étude met donc en évidence le fait que la polarité des composés phénoliques varie entre les espèces, indiquant que les composés phénoliques extraits sont de nature différente chez ces espèces d'algues vertes. On peut donc suggérer dans le cas de *Cladophora rupestris*, que des composés phénoliques auraient été éliminés lors des lavages au dichlorométhane (un solvant apolaire utilisé pour éliminer les composés lipidiques et les pigments des extraits) ou lors des phases de précipitation à l'éthanol et à l'acétone.

Par ailleurs, pour les autres espèces étudiées, le protocole de purification utilisé semble adapté car les composés phénoliques sont concentrés d'un facteur 10 pour *Codium fragile* jusqu'à un facteur 16 pour *Salicornia ramossissima* dans les phases acétate d'éthyle par rapport aux extraits bruts de départ. L'acétate d'éthyle est un solvant qui a déjà été utilisé pour concentrer les composés phénoliques (Cho et al., 2011; Kim et al., 2011).

Lorsque l'on compare les activités antiradicalaires des extraits bruts des plantes halophiles à la littérature, les activités obtenues sont plus faibles que celles décrites. En effet, les extraits bruts les plus actifs sont obtenus pour les espèces de salicorne avec un IC50 de 0,20 $g.L^{-1}$. Ksouri et al. (2008) obtiennent des IC50 de 0,075 et 0,160 $g.L^{-1}$ pour les extraits méthanoliques de deux halophytes médicinales, respectivement pour *Limoniastrum monopelatum* et *Mesembryanthemum crystallinum*, (Ksouri et al., 2012). Oueslati et al. (2012) trouvent un IC50 encore plus faible de 0,026 $g.L^{-1}$ pour l'extrait brut acétonique (à 80%) de *Suaeda mallis*, espèce appartenant à la famille des *Chenopodiaceae* (Oueslati et al., 2012). Agoramoorthy et al. (2008) trouvent quant à eux un IC50 minimal de 0,084 $g.L^{-1}$ pour *Ipomea pes-caprae* parmi cinq plantes halophiles (à partir d'un extrait hydroalcoolique ; Agoramoorthy et al., 2008). Une autre étude portant sur des plantes médicinales brésiliennes montre une activité antioxydante maximale avec un IC50 de 0,024$g.L^{-1}$ pour *Copernicia cerifera* parmi treize espèces étudiées à partir d'un extrait alcoolique (Silva et al., 2005).

Mais à l'opposé, lorsque l'on considère les activités des phases acétate d'éthyle, non seulement les espèces de salicorne présentent des activités très fortes avec des IC50 deux fois inférieurs aux espèces les plus actives citées ci-dessus mais *Spartina alterniflora* avec un

IC50 de 0,077 $g.L^{-1}$ possède également une forte activité antioxydante. Sans le protocole de purification, dans une démarche de screening, ces espèces halophiles auraient pu être éliminées. Ces résultats montrent ainsi l'efficacité de ce protocole de semi-purification. Ces conclusions se vérifient aussi pour le test du pouvoir réducteur. Nos extraits purifiés présentent des activités réductrices intéressantes si on les compare à d'autres obtenues pour des halophytes telles que *Tamarix gallica* et *Salsola kali* qui ont un EC50 respectivement égal à 0,205 et 0,458 $g.L^{-1}$ (Ksouri et al., 2012).

Ces résultats montrent la forte capacité réductrice et antiradicalaire, par des tests *in vitro*, des espèces halophiles et en particulier des espèces de salicorne offrant des perspectives encourageantes dans l'optique de développement d'ingrédients actifs.

Processus antioxydants potentiels Les meilleurs résultats d'activités ont été obtenus pour le test du pouvoir réducteur où la phase acétate d'éthyle de *Salicornia ramossissima,* avec un EC50 de 0,197 ± 0,004 $g.L^{-1}$, présente une activité antioxydante plus élevée que la vitamine E. Ces résultats semblent indiquer que les phases acétate d'éthyle contiennent principalement des composés antioxydants de type agents réducteurs. En comparaison des deux autres tests, les résultats obtenus pour le test du β-carotène montrent que les activités des extraits pour les cinq espèces étudiées sont très faibles vis-à-vis des témoins positifs. Ces résultats peuvent être expliqués par le fait que ce test est limité par la polarité des extraits. En effet, les antioxydants apolaires montrent des activités plus fortes en émulsion car ils se retrouvent concentrés à l'interface acide linoléique/air protégeant ainsi l'émulsion de l'oxydation. Les composés antioxydants polaires quant à eux montrent des activités plus faibles car ils ne se concentrent pas à cette interface (Huang et al., 2005). C'est le cas des acides phénoliques par exemple (Koleva et al., 2002).

Conclusion A la suite de ce screening, l'espèce *Salicornia ramossisima* a été sélectionnée parmi les cinq macrophytes marins car sa fraction acétate d'éthyle présente les concentrations les plus élevées en composés phénoliques ainsi que la plus forte capacité antioxydante. L'étude des activités biologiques de cette fraction pour ses potentielles propriétés photoprotectrices ainsi que la poursuite de la caractérisation de la fraction acétate d'éthyle a été effectuée suite aux résultats prometteurs de cette étude préliminaire. Les résultats de cette étude ont fait l'objet d'une publication dans le journal Photochemistry and photobiology B : biology et sont présentés dans le chapitre suivant (Chapitre 7).

Chapitre 7. Développement de filtres solaires, bio-inspirés de la photoprotection de macrophytes marines : démarche intuitive

Au cours du cycle tidal, les macrophytes marins peuvent être exposés à un stress lumineux particulièrement important, stress maximisé lorsque la marée basse coïncide avec le zénith comme illustré dans les précédents chapitres de ce manuscrit. Ce stress abiotique comme la plupart des stress environnementaux va entraîner un stress oxydant au niveau cellulaire et stimuler la production d'espèces réactives de l'oxygène (EROs) chez les végétaux marins, les macroalgues mais aussi les phanérogames se développant sur les estrans (Bischof and Rautenberger, 2012; Mallick and Mohn, 2000; Solovchenko and Merzlyak, 2008). Les végétaux marins ont développé de nombreuses stratégies de photoprotection pour limiter la production d'EROs et leurs effets délétères au niveau cellulaire, *e.g.* la péroxydation lipidique, comme illustré dans le chapitre 3. Plusieurs stratégies ont été présentées/développées dans les chapitres précédents tels que le quenching non-photochimique permettant la dissipation thermique de l'énergie lumineuse excessive collectée au niveau des photosystèmes mais aussi la détoxification des EROs par le système antioxydant comme illustré par l'activation d'une enzyme antioxydante telle que la SOD. D'autres stratégies ont été développées par les végétaux marins, en particulier, la production de métabolites ayant la propriété d'absorber les radiations lumineuses afin de limiter la quantité de radiation qui peut atteindre l'appareil photosynthétique (Cockell and Knowland, 1999). Le schéma présenté en Figure 38 présente l'enchaînement des réactions participant à la photoprotection des végétaux, consécutif à de trop forts éclairements et illustre la participation de différentes classes de composés phénoliques à cette protection cellulaire à différents niveaux chez les végétaux supérieurs. En effet, comme évoqué en introduction de cette partie, les composés phénoliques ont des propriétés d'absorption des radiations UV. Cette propriété est dûe à leur noyau aromatique. Leurs propriétés antioxydantes, quant à elles, leur sont conférées par la présence des groupes hydroxyles greffés à ce noyau aromatique (Edreva, 2005; Edreva et al., 2008; Mallick and Mohn, 2000). En fonction de leur structure, les composés phénoliques ont la capacité d'absorber au niveau de deux bandes spectrales dans les UV, à l'exception des anthocyanes qui absorbent dans le visible comme illustré dans la Figure 39 (Anthoni, 2007; Robbins, 2003).

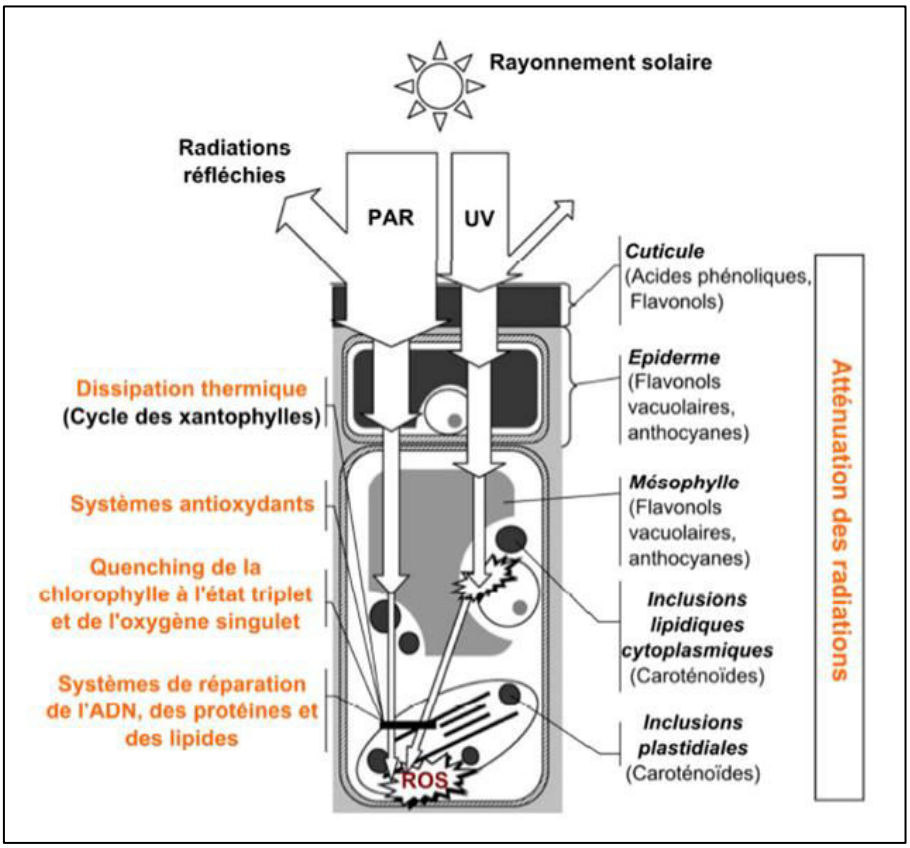

Fig. 38 Localisation au sein de la cellule des divers mécanismes de photoprotection suite à l'exposition à de fortes intensités lumineuses (PAR) et ultraviolettes (UV) chez les végétaux supérieurs (issu de Hupel, 2011, d'après Solovchenko and Merzlyak, 2008).

Ce chapitre présente les activités biologiques antioxydantes et photoprotectrices d'un extrait enrichi en composés phénoliques ainsi que leur analyse structurale chez une halophyte des estrans vaseux, *Salicornia ramosissima*. Ce travail illustre les applications potentielles de ce type d'extrait notamment en tant que filtre solaire.

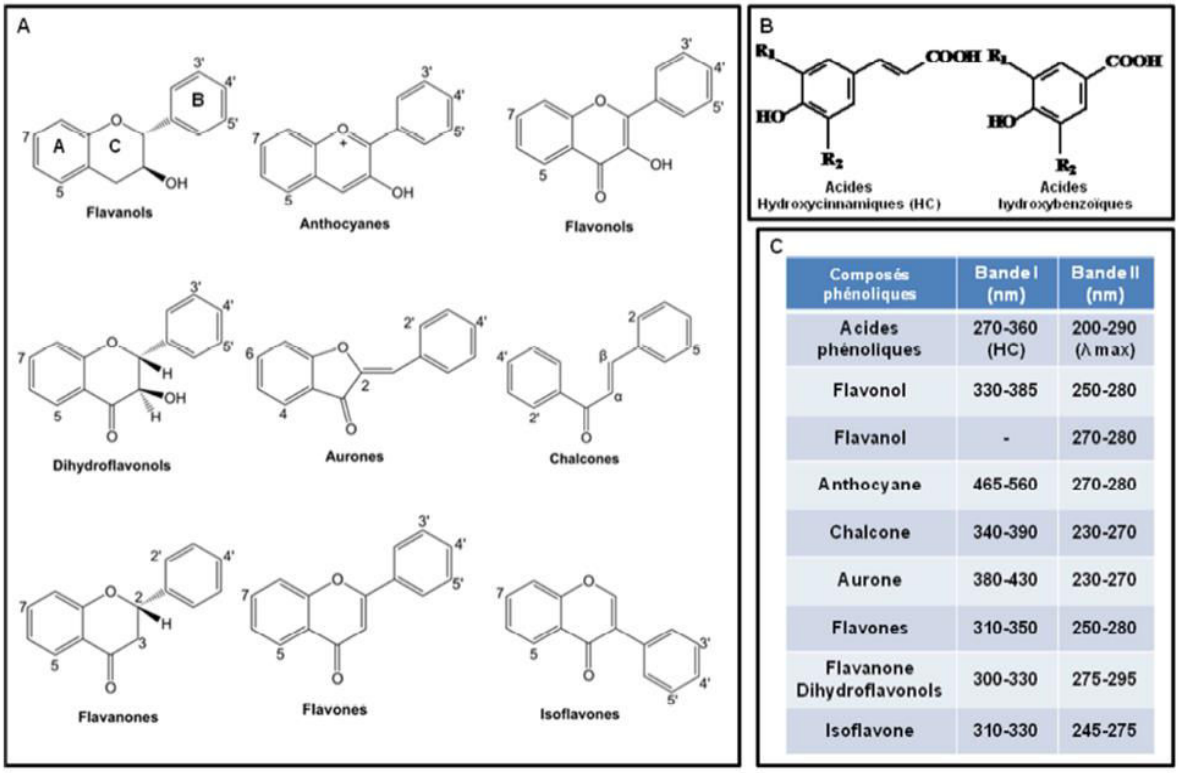

Composés phénoliques	Bande I (nm)	Bande II (nm)
Acides phénoliques	270-360 (HC)	200-290 (λ max)
Flavonol	330-385	250-280
Flavanol	-	270-280
Anthocyane	465-560	270-280
Chalcone	340-390	230-270
Aurone	380-430	230-270
Flavones	310-350	250-280
Flavanone Dihydroflavonols	300-330	275-295
Isoflavone	310-330	245-275

Fig. 39 Diversité chimique des flavonoïdes (A) et des acides phénoliques (B) ainsi que leur caractéristique d'absorption spectrale (C) (issu de Hupel, 2011, d'après Anthoni, 2007; Robbins, 2003).

Journal of Photochemistry and Photobiology B: Biology 143 (2015) 52–60

Contents lists available at ScienceDirect

Journal of Photochemistry and Photobiology B: Biology

journal homepage: www.elsevier.com/locate/jphotobiol

Structural elucidation, *in vitro* antioxidant and photoprotective capacities of a purified polyphenolic-enriched fraction from a saltmarsh plant

Gwladys Surget [a,*], Valérie Stiger-Pouvreau [a], Klervi Le Lann [a], Nelly Kervarec [b], Céline Couteau [c], Laurence J.M. Coiffard [c], Fanny Gaillard [d], Karine Cahier [d], Fabienne Guérard [a], Nathalie Poupart [a]

[a] LEMAR UMR 6539 UBO CNRS Ifremer IRD, European Institute of Marine Studies (IUEM), Université de Bretagne Occidentale (UBO), European University of Brittany (UEB), Technopôle Brest-Iroise, 29280 Plouzané, France
[b] RMN-RPE-MS, Université de Bretagne Occidentale (UBO), European University of Brittany (UEB), 6 avenue, Victor-Le-Gorgeu-CS93837, 29238 Brest Cedex 3, France
[c] Faculty of Pharmacy, Université de Nantes, Nantes Atlantique Universités, LPiC, MMS, EA2160, 1 rue G. Veil BP 53508, 44 000 Nantes, France
[d] Plateforme de spectrométrie de masse FR 2424, CNRS UPMC INSU Station Biologique de Roscoff, Place Georges Teissier, BP 74, F-29682 Roscoff Cedex, France

ARTICLE INFO

Article history:
Received 17 July 2014
Received in revised form 3 December 2014
Accepted 11 December 2014
Available online 27 December 2014

ABSTRACT

In temperate saltmarshes, halophytic plants have to daily protect their internal tissues against sunlight and UV rays. Consequently, they develop adaptive responses such as the synthesis of secondary metabolites, including polyphenols. The present study focused on the biological activities of fractions enriched in polyphenols from *Salicornia ramosissima*. Three different extracts were obtained by purification processes to concentrate polyphenols: a crude hydroalcoholic extract, and two purified fractions: an ethyl acetate fraction (EAF) and an aqueous fraction. Phenolic and flavonoid contents, antioxidant (DPPH radical-scavenging activity, reducing activity, β-carotene linoleic acid system and the ORAC method) and sunscreen properties (Sun Protection Factor and UVA-Protection Factor) were assessed by *in vitro* tests. The purification process was effective in increasing phenolic and flavonoid contents as well as antioxidant and sunscreen capacities of the EAF. The EAF appeared to be a broad spectrum UV absorber. The chemical structure of 10 EAF polyphenols was elucidated using 2D NMR and mass spectrometry spectra. Furthermore, a correlation was observed between phenolic composition and biological activity. These findings are encouraging for the future use of *S. ramosissima* as a potential source of antioxidant and photoprotectant molecules for industrial applications.

1. Introduction

The epidermis of both flora and fauna species have adaptive mechanisms that play a key role in photoprotection, especially the outer cell layer, because this represents the first barrier against the environment. Excessive and chronic, repeated exposure to solar radiation, particularly solar mid-wave ultraviolet radiation (UV-B; 290–320 nm), are the primary cause of immunosuppression, premature aging, melanomas, and benign and malignant tumors, of the skin in human [1]. Skin diseases occur when UV-B radiation overwhelms the cutaneous antioxidant capacity of the skin [2] causing a photodynamic elevation of free radicals and subsequent photo-oxidative stress and damage [3]. As the mortalities from human skin cancers continue to rise [3], it is essential to find preventive measures against photoaging and cancer development of the skin. The use of sunblocks from childhood and oral or topical use of antioxidants, represent possible ways to lower the risk of skin diseases [1]. In addition, as recently reflected by sales of nutraceuticals and in the overall therapeutic use of traditional medicines [4], the development of natural products represents a viable alternative method of preventive skin health care [1], including cosmetic applications [5].

Excessive absorption of photons and UV radiation causes similar destructive disorders in plants as in animals and humans, such as the formation of free radicals and DNA damage including cyclobutane pyrimidine dimers and photoproducts [1,6]. Compared with fauna, plant photoprotection uses specific mechanisms like phytohormones (polyamines) and polyphenol synthesis to mitigate such damage [6]. Polyphenols, which belong to a large family of plant products, are considered as secondary metabolites [7] although they play a crucial role in many interactions between plants and their environment [8]. The nuclear structure of phenolics is based

* Corresponding author at: LEMAR, IUEM, Technopôle Brest-Iroise, Rue Dumont D'Urville, 29280 Plouzané (France). Tel.: +33 2 98 49 86 68.
E-mail address: gwladys.lediouron@univ-brest.fr (G. Surget).

http://dx.doi.org/10.1016/j.jphotobiol.2014.12.018
1011-1344/

on aromatic rings that bear one or more hydroxyl substituents [9], giving polyphenols the capacity to absorb the entire UV-B spectrum of wavelengths and part of the UV-C and UV-A spectra [1].

Phenolic polymer metabolism is thought to have played an important role in the evolution from aquatic to land plants in a terrestrial UV environment [10]. Saltmarsh habitats, at the transition between aquatic and terrestrial ecosystems, are dominated by non woody salt-tolerant vascular plants in the temperate coastal zone [11]. Saltmarsh plants are known to accumulate high levels of phenolic substances [12]. We therefore chose *Salicornia ramosissima* J. Woods, a true saltmarsh halophyte, distributed worldwide [13], for the present study. This succulent and edible glasswort species can be grown in Brittany by soilless cultivation [14,15]. Numerous biological activities beneficial to human health have been reported in extracts of glassworts, such as antioxidant, antihyperlipidemic, antidiabetic, antithrombus, antimicrobial, anti-inflammatory, antiproliferative and anticancer properties; they are also a source of vitamin C and diureticum [16,17]. Within the *Salicornia* genus, these medically-related biological activities have mainly been demonstrated in the species *S. herbaceae L.* and *S. europeae L.*

The aim of this work was to examine a novel natural photoprotective and antioxidant semi-purified fraction from *S. ramosissima*, a species rich in polyphenols. Total phenolic compounds were quantified and *in vitro* assays were used to measure the antioxidant and radical scavenging activities. The photoprotection sunscreen capacity was also tested by measuring the Sun Protection Factor (SPF) and Protection Factor-UV-A (PF-UV-A) *in vitro*. Then, the major phenolic compounds in the active fraction were identified by 2-D nuclear magnetic resonance (NMR) and liquid chromatography coupled with mass spectrometry (LC-MS) analysis.

2. Material and methods

2.1. Reagents

The reagents Tween 40, $FeCl_3$ and acid trichloroacetic were obtained from VWR. Folin–Ciocalteu phenol reagent, gallic acid, 2,2-diphenyl-1-picrylhydrazyl (DPPH) radical and catechin were purchased from Sigma–Aldrich. All other chemicals used were of analytical grade.

2.2. Plant material

S. ramosissima belongs to the family Amaranthaceae and subfamily Salicornioideae. Species identification had been made based on taxonomic criteria on the sampled glasswort population for several years and has since been confirmed by a phylogenetic study within the tribe of the Salicornieae of the Northern Atlantic coast [18]. This succulent halophyte has an articulated, highly branching dark green stem with a height between 20 and 40 cm. *S. ramosissima* has three flowering cymes per bract that form a characteristic triangle with a large central and two similar lateral flowers. It becomes purplish red in summer [19]. Samples were collected, at Bouin, France (47°1′42″N, 1°58′53″O) in an open saltmarsh of Bourgneuf Bay in September 2009. Only the aerial parts of the plants were used. After washing (in deionized water), plant material was frozen, then freeze-dried (CHRIST BETA 1-8 LD), ground and finally stored in darkness at room temperature. This conditioning treatment was chosen with the aim of limiting the degradation of phenolic compounds [20].

2.3. Extraction and liquid–liquid purification processes

Extraction was performed on 15 g plant dry matter using hydroethanolic solvent (v/v, 1:1) at 40 °C for three shaken macerations of 2 h and two of 1 h. Ethanol solvent was removed at 40 °C by vacuum evaporation to obtain a crude extract (CE). After dichloromethane washings, two successive precipitations with acetone and then ethanol and a final washing with ethyl acetate, two semi-purified extracts, an aqueous fraction (AF) and an ethyl acetate fraction (EAF) were obtained using a protocol adapted from Stiger-Pouvreau et al., with the aim of concentrating polyphenols in the final EAF [21].

2.4. Total phenolic and flavonoid contents

The total phenolic content was quantified using the Folin–Ciocalteu procedure adapted to microplates [22]. The wells were filled with 20 μL of extract, 130 μL distilled water and 10 μL Folin–Ciocalteu reagent followed by 40 μL Na_2CO_3 (200 g L^{-1}). The microplate was placed at 70 °C for 10 min and then put on ice to stop the chemical reaction. Absorbance was measured at 620 nm (Multiscan MS, Labsystems). Phenolic content was quantified based on a standard curve of gallic acid and results were expressed in mg gallic acid g^{-1} of dried extract (DW).

Flavonoid content was determined by a method adapted for microplates from Dewanto et al. [23]. Following this procedure, 25 μL of extract were mixed with 100 μL distilled water and 10 μL $NaNO_2$ (5%; w/v). Plates were incubated 5 min at room temperature. Then, 20 μL of $AlCl_3$ (5%; w/v) were added and plates incubated for another 5 min. After addition of 50 μL NaOH (1 M), the absorbance was read at 492 nm. Flavonoid content was determined based on a catechin standard curve and results were expressed as mg catechin g^{-1} DW.

2.5. Antioxidant activities

Coupling several antioxidant assays can provide an overview of the antioxidant capacity of active extracts and thus represent the complexity of antioxidant mechanisms involved in biological systems; this is especially the case for natural antioxidants, which are generally multifunctional [24,25]. In our case, four assays were performed and, for each test, butylated hydroxyanisole (BHA), trolox and α-tocopherol were used as positive controls.

2.5.1. β-Carotene bleaching test (BCBT)

Antioxidant capacity of extracts was quantified with the β-carotene bleaching test [26,27]. The BCBT method implies proton transfer; it simulates the antioxidant capacity of extracts faced with oxidation mechanisms similar to lipidic peroxidation [25,27]. At first, a mixture constituted of 2 mL β-carotene solution in chloroform (0.1 mg mL^{-1}), 20 mg linoleic acid and 200 mg Tween 40 was evaporated under vacuum. The reagent solution (emulsion) was obtained after addition of 50 mL oxygenated distilled water. For the test, 180 μL of reagent was added to 12 μL of extract or control. The absorbance was read at 450 nm immediately and after 2 h at 50 °C. Antioxidant activity was expressed as IC50 (g L^{-1}), the concentration at which 50% of β-carotene mixture bleaching was inhibited. IC50 was obtained from a linear regression analysis of the curve of inhibition percentage as a function of sample concentration, as recommended by Ksouri et al. [28].

2.5.2. DPPH radical scavenging assay

The radical scavenging activity was determined with the DPPH (2,2-diphenyl-1-picrylhydrasyl) assay [29,30]. This non-specific assay tests the capacity of samples to scavenge the synthetic radical, DPPH. It has the advantages of being independent of sample polarity [27] and highly reproducible [31]. For this method, 100 μL of sample were added to 100 μL of DPPH solution (36.9 mg L^{-1}) in a microplate. Absorbance was measured at 540 nm after 60 min of incubation in the darkness at room

temperature. The radical scavenging activity was expressed as IC50 ($g\,L^{-1}$) [20] (the concentration of sample required to reach 50% of inhibition, which was obtained from a linear regression analysis). A low IC50 indicates a high radical scavenging activity.

2.5.3. Reducing power (RP)

Reducing power was determined as described by Oyaizu and was modified for microplates following Kuda et al. and Zubia et al. [32–34]. The RP assay implies an electron transfer and tests the capacity of antioxidants to reduce the Fe^{3+}/ferricyanide complex to the ferrous form [35]. The method consisted of mixing 25 µL of sample with 25 µL sodium phosphate buffer (0.2 M; pH = 6.6) and 25 µL potassium ferricyanide (1%; w/v). The mixture was incubated for 20 min at 50 °C. After cooling down, 25 µL trichloroacetic acid (10%; w/v), 100 µL distilled water and 20 µL $FeCl_3$ (0.1%; w/v) were added. After 10 min, the absorbance was measured at 620 nm. The capacity of plant extracts to reduce Fe^{3+} was expressed as EC50 (in $g\,L^{-1}$), corresponding to the effective concentration at which the absorbance is equal to 0.5. It was obtained by interpolation from a linear regression analysis. A lower EC50 value corresponds to a higher reducing power of the sample.

2.5.4. ORAC test

ORAC value is considered to be a reference in the field of agri-food, as this assay summarizes two results in a single value: the inhibition percentage and inhibition rapidity of peroxyl radicals by antioxidants, in competition with the substrate [36]. The ORAC assay was performed by INVIVO LABS (CS 40234, 56011 Vannes Cedex, France) for the most active fraction (following our screening) using a protocol adapted from Cao et al. [37]. Results were expressed as µmol Trolox equivalent (Te) mg^{-1} DW and were compared to ascorbic acid.

2.6. Protective efficacy: Sun Protection Factor (SPF) and UV-A Protection Factor (PF-UV-A)

The photoprotection efficiency of *S. ramosissima* extracts was determined in UV-A and UV-B ranges, as previously described [38,39]. This *in vitro* method makes it possible to highlight the UV filter role of organic or inorganic substances, which could later be topically applied as part of a sunscreen formulation. Concisely, extracts were incorporated in a basic emulsion O/W (Oil in Water) to finally obtain an emulsion containing 10% (w/w) extracts. Fifty milligrams of prepared emulsion were spread using a cot-coated finger across the entire surface (25 cm^2) of a polymethylmethacrylate (PMMA) plate (Europlast, Aubervilliers). After spreading, only 15 mg of the emulsion remained on the plate. Transmission measurements between 200 and 400 nm were performed using a spectrophotometer equipped with an integrating sphere (UV Transmittance Analyzer UV1000S, Labsphere, North Sutton, US). Three plates were prepared for each extract to be tested and nine measurements were carried out on each plate. Results were given as SPF and PF-UVA, as presented by Pissavini et al. and Villalobos-Hernandez and Müller-Goymann [40,41]. The higher the SPF/PF-UVA value the more protection the sample offers against UV-B/UVA wavelengths by absorbing or reflecting them.

2.7. Structural characterization of active extract

NMR analyses were performed on the crude extract and fractions. Samples were dissolved in 700 µL of MeOD or D_2O according to their polarity. Afterwards, on the most active fraction (EAF), 1D ^1H and 1D ^{13}C NMR, heteronuclear multiple bond correlation (HMBC) and heteronuclear single-quantum correlation spectroscopy (HMQC) spectral data were recorded at 25 °C with a BRUKER AVANCE 400 and BRUKER AVANCE 500. Chemical shifts were expressed in ppm using tetramethylsilane as the chemical shift reference (0 ppm).

Furthermore, LC–MS–MS analyses were carried out on the EAF, following a protocol adapted from Vallverdú-Queralt et al., [42]. The sample was diluted with ethyl acetate (0.1% formic acid) and injected into the UHPLC (Ultimate 3000, Dionex). Chromatographic separation was carried out using a C18 column (Hypersil Gold 100 × 2.1 mm, particle diameter 1.9 µm) kept at 30 °C. A gradient solvent comprising 0.1% formic acid in water (A) and acetonitrile (B) was applied for a total running time of 35 min. The following proportions of solvent B were used for elution: 0–11 min, 0–18%; 11–18 min, 27%; and 18–28 min, 100%; 28–30 min, 0%, with a flow rate of 0.4 mL min^{-1}. Five µL of a sample solution at 10 mg mL^{-1} was injected and detected at three wavelengths (254, 280 and 330 nm). For accurate mass measurements, a LTQ Orbitrap Discovery mass spectrometer (Thermo Fisher Scientific) equipped with an ESI source in negative mode was used to acquire mass spectra in profile mode with a setting of 30,000 resolutions at *m/z* 400. A second data-dependent scan event selected the most intense ion for the acquisition of MSMS spectra after Collision Induced Dissociation.

2.8. Statistics

Statistical analyses were performed with RStudio (v. 0.95.263) integrated R (v.2.12.0). All analyses were carried out in triplicate and results were expressed as means ± standard deviation (SD). As data did not respect the requirements for an ANOVA test (non homogeneity of variances), they were analyzed using the non-parametric Kruskal–Wallis test at a significance level of 95%, followed by the Behrens–Fisher non-parametric multiple comparisons test (npmc package). Correlations between measured biological variables were tested to illustrate correlations between the extract composition and biological activities. This analysis was based on the Spearman method (Hmisc package).

3. Results and discussion

3.1. Phenolic and flavonoid contents and extraction yields

The liquid purification procedure permitted an enrichment of phenolic compounds in the EAF from *S. ramosissima*, as shown by the significantly high phenolic and flavonoid contents (Table 1). Indeed, the semi-purification process effectively concentrated the amount of phenolic compounds by 15.7 to reach 43.2% purity in the EAF compared with the crude extract. Flavonoids represented nearly 86% of this fraction. In contrast, the AF was significantly poorer in phenolic and flavonoid compounds, compared to CE. A similar procedure had previously been carried out on *S. herbacea* [43], where authors obtained the highest phenolic compound and flavonoid concentrations in the EAF (among several fractions including ether, butanol, and water). In another study, a screening of five maritime halophytes from Portugal was carried out and authors tested five extraction solvents: hexane, water, diethyl ether, chloroform and methanol [44]. Maximum phenolic contents were measured in the methanol extract of *Mesembryanthemum edule* (147 mg GAE g^{-1}) and in the ether extract of *Juncus acutus* (94 mg GAE g^{-1}). EAF and AF yields reached $0.3 \pm 8 \cdot 10^{-3}$% DW and 22.1 ± 0.3% DW, respectively. The amount of phenolic compounds in our *S. ramosissima* EAF is high compared with these previous results.

From a general point of view, studies on *Salicornia* species have focused on crude extract activities [45–47], fraction activities for bio-guidance objectives [48,49] and, especially, on pure compound activities [50–58]. To our knowledge, few studies have

Table 1
Phenolic (mg GAE g^{-1} DW: mg of Gallic Acid Equivalent per g^{-1} of Dried Weight extract) and flavonoid (mg C g^{-1} DW: mg of Catechin per g^{-1} of Dried Weight extract) contents of extracts and semi-purified fractions of *Salicornia ramosissima*. Results are expressed as means ± SD ($n = 3$). Different letters indicate significant differences between means according to Berhens–Fisher tests.

	Salicornia ramosissima		
	Crude extract	Ethyl acetate fraction	Aqueous fraction
Phenolic content (mg GAE g^{-1} DW)	27.44 ± 0.68[a]	431.55 ± 19.91[b]	18.63 ± 0.57[c]
Flavonoid content (mg C g^{-1} DW)	9.69 ± 0.28[a]	368.91 ± 13.79[b]	8.43 ± 0.14[c]

concentrated on biological activities of fractions enriched in phenolic compounds [43,59,60]. Yet, study of semi-purified fractions offers numerous advantages, such as enabling the balance between concentrations of active compounds to be obtained, production of wastes, good extraction yield, conservation of potential synergy between active molecules and lower costs for industrial applications (especially cosmetics) than purified molecules [61]. In this context, our study showed the efficiency of the purification process to concentrate phenolic and flavonoid compounds in EAF of *S. ramosissima*. Similar results had been obtained from a hydromethanolic crude extract on the same plant material [62]. Stiger-Pouvreau et al., who developed this protocol for brown algae, demonstrated comparable results on brown macroalgae belonging to the Family Sargassaceae from Brittany (France) [21]. Thus, this protocol could potentially be used to extract and purify polyphenols from a wide diversity of macrophytes, including terrestrial plants.

3.2. Antioxidant activities

In vitro assays make it possible to elucidate the mode of action of antioxidants in extracts and fractions such as those we obtained from *S. ramosissima*, but can diverge significantly from *in vivo* systems [63]. Overall, the EAF exhibited the highest antioxidant activity, whatever assays were performed (Table 2). For BCBT, no activity was detected (high IC50 compared to positive controls), showing that antioxidant properties of extracts, especially the EAF, are less active in emulsion. This effect is mainly due to their polarity, as this test is more specifically for lipophilic molecules [27]. For the DPPH assay, EAF antioxidant activity (with an IC50 equal to $0.013 \pm 1.22 \times 10^{-4}$ g L^{-1}) was equivalent to those of commercial standards like α-tocopherol and BHA, even though a significant difference was shown. Among all assays, the strongest activity for EAF was shown in the reducing power test, with an activity significantly higher than that from α-tocopherol (EC50 equal to 0.197 ± 0.003 and 0.366 ± 0.011, respectively). These results suggest that molecules present in the EAF have a strong capacity to reduce ferric ions, in function of their concentration within the fraction. At 0.1 g L^{-1}, EAF presented the same activity as Trolox (Fig. 1). Additionally, EAF would be suitable for use in an industrial context as it showed an ORAC value of 9.06 ± 1.81 μmol Te mg^{-1}, equivalent to the ORAC value of ascorbic acid (9.35 ± 0.63 μmol Te mg^{-1}) [64] and higher than ORAC values of known antioxidant products, as black, green or white teas (2.64×10^{-3}–1.25×10^{-2} μmol Te mg^{-1}) [65]. To our knowledge, this was only the second time that the antioxidant capacity of *S. ramosissima* has been investigated [66] although other studies have been conducted on other Salicornioideae specimens [43,47,48,60].

3.3. Photoprotective activity

The O/W emulsion made with the enriched fraction of phenolic compounds of the *Salicornia* extracts (*Salicornia* emulsion) showed a high *in vitro* SPF of 13.57, which was much higher than those prepared with the crude or the aqueous extracts: 1.22 ± 0.03 and 1.21 ± 0.02, respectively (Table 3). These results are consistent with a previous study using a methanolic extract [62]. Except for anisotriazine, the SPF obtained for the *Salicornia* emulsion is higher than all those of the eighteen pure synthetic UV filters authorized in the European Union tested in O/W emulsion with the same method [38]. Additionally, this same extract showed sunscreen activity to UV-A. Interestingly, the PF-UV-A value of the EAF emulsion was high and equals to 13.48. UV-B and UV-A protection factors of EAF were balanced, with equivalent SPF and PF-UV-A values (like for the other extracts). Then, EAF obtained from *S. ramosissima* is very interesting because it appears to be a broad-spectrum UV absorber.

Natural substances extracted from organisms have been recently considered as potential sunscreens because of their absorption in the UV region and their antioxidant power [67]. Among terrestrial organisms, Lohézic-Le Dévéhat et al. demonstrated, using the same *in vitro* UV method, that lichens could also act as good UV filters. Among three lichenic species, one acetonic extract of *Lasallia pustulata* had a maximum SPF and PF-UVA equal to 5.52 and 2.45, respectively. Ten lichenic metabolites were also tested and the best result was obtained for a gyrophoric acid (SPF equal to 5.03), the major compound of *L. pustulata* [68]. Furthermore, Rancan et al. showed that isolated aromatic compounds from Chilean lichens, and major alkaloids of the leaves and bark of the boldo tree (*Peumus boldus* M.) could represent interesting UV filters. From their study, usnic acid was described as the best UVB filter tested, with a protection factor (equal to 4.1), similar to the commercial Nivea sun Spray LSF 5, and was tested on five human volunteers [67]. Using a similar protocol, Jarzycka et al. tested *in vitro* three sunscreen emulsions with ethyl acetate plant

Table 2
Antioxidant activities of extracts and semi-purified fractions of *Salicornia ramosissima* and various commercial standards (α-tocopherol, BHA and Trolox). Results were expressed as means ± SD ($n = 3$). Different letters indicate significant differences between means according to Berhens–Fisher tests. Bold characters represent the most active fraction.

		β-carotene (IC50 g L^{-1})	DPPH scavenging activity (IC50 g L^{-1})	Reducing power (EC50 g L^{-1})	ORAC value (μmol Te mg^{-1})
Salicornia ramosissima	CE	$1.629 \pm 4.21\ 10^{-02}$ [a]	$0.197 \pm 2.23\ 10^{-02}$ [a]	$2.455 \pm 1.03\ 10^{-01}$ [a]	–
	EAF	**$0.318 \pm 4.29\ 10^{-03}$** [b]	**$0.013 \pm 1.22\ 10^{-04}$** [b]	**$0.197 \pm 2.88\ 10^{-03}$** [b]	**9.06 ± 1.81**
	AF	$2.028 \pm 1.41\ 10^{-01}$ [c]	$0.311 \pm 2.52\ 10^{-03}$ [c]	$2.991 \pm 1.69\ 10^{-01}$ [c]	–
Positive controls	α-tocopherol	$0.003 \pm 1.50\ 10^{-04}$ [d]	$0.011 \pm 7.91\ 10^{-05}$ [d]	$0.366 \pm 1.12\ 10^{-02}$ [d]	–
	BHA	$0.003 \pm 5.08\ 10^{-04}$ [d]	$0.010 \pm 2.17\ 10^{-04}$ [e]	$0.091 \pm 1.24\ 10^{-03}$ [e]	–
	Trolox	$0.003 \pm 2.44\ 10^{-05}$ [d]	$0.007 \pm 1.25\ 10^{-04}$ [f]	$0.169 \pm 3.08\ 10^{-03}$ [f]	–
	Ascorbic acid	–	–	–	9.35 ± 0.63 [64]

Te: Trolox equivalent; CE: Crude Extract; EAF: Ethyl Acetate Fraction; AF: Aqueous Fraction; – : not tested.

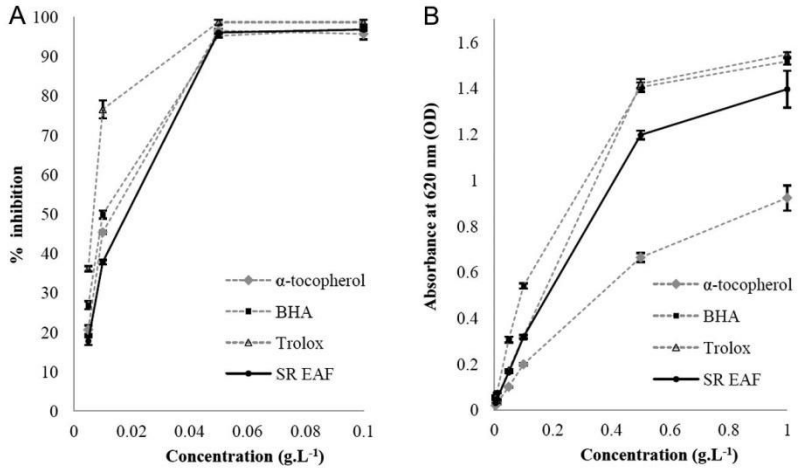

Fig. 1. Free radical DPPH scavenging activity (A) and reducing power (B) of the ethyl acetate fraction of *Salicornia ramosissima* (SR EAF) compared with commercial standards (α-tocopherol, BHA and Trolox) under different concentrations. Results represented are means ($n = 3$).

Table 3
Sunscreen activity of extract and semi-purified fractions of *Salicornia ramosissima* in emulsion. Results are expressed as means ± SD ($n = 3$). Different letters indicate significant differences between means according to Berhens–Fisher tests.

		SPF	PF-UVA	*R*
Salicornia ramosissima	CE	1.22 ± 0.03^{a}	1.21 ± 0.02^{a}	1.01
	EAF	13.57 ± 1.15^{b}	13.48 ± 1.08^{b}	1.01
	AF	1.21 ± 0.02^{a}	1.21 ± 0.02^{a}	1.00

CE: Crude Extract; EAF: Ethyl Acetate Fraction; AF: Aqueous Fraction; SPF: Sun Protective Factor; PF-UVA: Protection Factor against UVA; *R* = SPF/PF-UVA.

Table 4
Spearman correlation matrix between phenolic contents (TPC), flavonoid contents (FC) and biological activities (BCBT: β-carotene bleaching test, DPPH: DPPH assay, RP: Reducing Power, PF.UVA: protection factor against UVA, SPF: Sun Protection Factor). Bold values are significant (with ∗: p-value < 0.05; ∗∗: p-value < 0.01; ∗∗∗: p-value < 0.001).

	BCBT	DPPH	RP	FC	TPC	PF.UVA	SPF
BCBT		**0.88****	**0.86****	**−0.97*****	**−0.86****	**−0.68***	**−0.71***
DPPH			**0.93*****	**−0.86****	**−0.93*****	−0.56	−0.65
RP				**−0.9*****	**−0.9*****	**−0.7***	**−0.79***
FC					**0.9*****	**0.74***	**0.77***
TPC						0.63	**0.7***
PF.UVA							**0.97*****
SPF							

extract (10 wt.%) and obtained SPF and PF-UVA values ranging from 6.00 ± 0.42 to 9.88 ± 1.66 and from 3.64 ± 0.07 to 6.96 ± 0.21, respectively [69]. Compared with this literature, it appears then that the pool of molecules present in EAF from *S. ramosissima* represents an interesting and original candidate to provide effective protective screen action across the whole UVA-UVB range. Indeed, cosmetic regulations require that one should formulate a mix of compounds and simultaneously characterize all molecules present in the active fraction (as we did in this present study). The effect of the pool created in the EAF of the present work is similar to UV pure synthetic filters currently used in the cosmetic industry.

3.4. Correlations between biological activities and phenolic content

Table 4 presents the correlation matrix between seven biological variables measured in this study. Antioxidant activity, regardless of which of the three assessment methods was used, was correlated with phenolic and flavonoid contents. BCBT showed the lowest correlation for phenolic content and the highest for flavonoid content (respectively $r = -0.86$ and $r = -0.97$). The opposite trend was obtained for DPPH and the same levels of correlation were observed for the RP tests. Considering results of antioxidant activity, these results suggested that the phenolic compounds contained in the extracts were hydrophilic in nature. Moreover, phenolic compounds of extracts contributed their antioxidant activity and this would explain the high activity displayed by EAF. The role of phenolic compounds, especially flavonoids, as good antioxidants is well described in the literature [70–72].

Furthermore, SPF was significantly correlated with phenolic content ($r = 0.70$) and with flavonoid content ($r = 0.77$). The same trend was observed for PF-UVA, which was significantly correlated with flavonoid content ($r = 0.74$) and non-significantly with phenolic content ($r = 0.63$), implying that the sunscreen activity of extracts was explained mainly by phenolic and, especially, flavonoid composition. This finding was in agreement with the literature. Indeed, the functional role of phenolic compounds in photoprotection has often been suggested but little research has demonstrated their function as sunscreens [69,73,74]. Moreover, biological activities were correlated with one another. An especially strong link was seen between sunscreen capacity and antioxidant activity, i.e., between SPF and RP, $r = -0.79$ and SPF and BCBT $r = -0.71$. Similar results for PF-UVA confirmed the interest of *S. ramosissima* EAF and illustrate that it is a pool of molecules that gives the multiple biological activities of this fraction. In the aim of characterize this pool, we elucidate the chemical structure of main compounds present in the EAF (see following paragraph).

3.5. Structure elucidation of compounds from the active EAF

Major mixed phenolic compounds (Fig. 2) present in admixture in the active EAF isolated from *S. ramosissima* were identified by NMR analysis. Additionally, ESI-MS-MS coupled to HPLC made it possible to test hypotheses formulated with NMR analysis and to identify major phenolic compounds of EAF (Fig. 3 and Table 5).

– Compounds 1 and 2

The first two compounds were identified as isorhamnetin (compound 1) and isorhamnetin 3-glucoside (compound 2). On the ^{1}H NMR spectrum of the EAF, four proton signals were

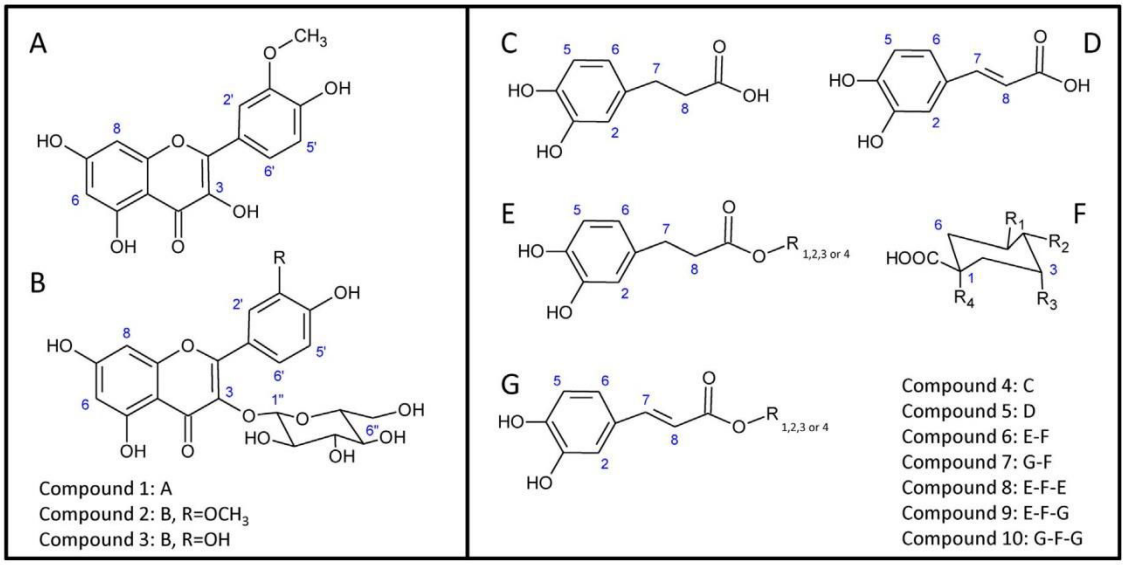

Fig. 2. Structures of molecules identified in the EAF of *Salicornia ramosissima*. Left: isorhamnetin, isorhamnetin 3-glucoside and quercetin 3-glucoside (compounds 1, 2 and 3, respectively). Right: caffeic acid derivatives: C = hydrocaffeic acid, D = caffeic acid, E = hydrocaffeoyl chain, G = caffeoyl chain, F = quinic acid moiety (if R_1, R_2, R_3 or $R_4 \neq$ E or F; R_1, R_2, R_3 or R_4 = OH).

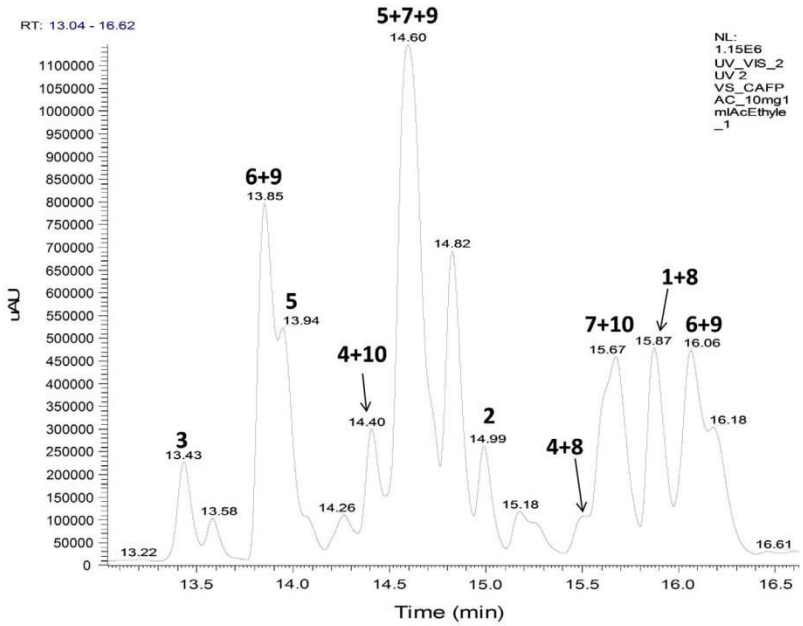

Fig. 3. HPLC–ESI–MS–MS chromatogram (negative ionization mode) of *Salicornia ramosissima* EAF at 280 nm.

Table 5
Retention time (RT), theoretical mass and *m/z* value of ion parent (corresponding to $[M-H]^-$) and ion fragments of the compounds identified in *Salicornia ramosissima* EAF.

	RT (min)	Theorical mass	Ion parent (*m/z*)	Ion fragments (*m/z*)
(1) Isorhamnetin	15.9	316	314.99	271.1, 255.1, 243.1
(2) Isorhamnetin glucoside	15	478	477.10	357.1, 314.1, 285.1, 271.1
(3) Quercetin glucoside	13.4	464	463.09	301.1
(4) Hydrocaffeic acid	14.4, 15.5	182	181.05	137.1, 119.1, 109.1
(5) Caffeic acid	13.9, 14.6	180	179.03	135.0, 107.0, 91.2
(6) Hydrocaffeoylquinic acid	13.9, 16.1	356	355.10	191.1, 181.1, 173.1, 155.1, 137.1
(7) Caffeoylquinic acid	14.6, 15.7	354	353.08	191.1, 179.1, 173.1, 135.1
(8) Dihydrocaffeoyl quinic acid	15.5, 15.9	520	519.11	355.1, 337.1, 181.1
(9) Caffeoyl-hydrocaffeoylquinic acid	13.8, 14.6, 16.1	518	517.13	355.1, 337.1, 335.1, 181.1, 179.1, 173.0
(10) Dicaffeoyl quinic acid	14.4, 15.7	516	515.12	353.1, 335.1, 299.2, 203.1, 191.2, 179.1, 173.1

distinguishable; at 7.92 (H-2′, d, J = 2.0 Hz), 6.90 (H-5′, d, J = 8.0 Hz), 6.21 (H-6, d, 2 Hz) and 6.42 (H-8, d, 2 Hz). The fifth proton, corresponding to H-6″, was not identified clearly on ^{1}H NMR although it could be seen by HMQC (^{1}H: 7.61 ppm and ^{13}C: 123.96). Moreover, the ^{1}H spectrum revealed the presence of a methoxyl group at 3.94 ppm (3H, s). These data suggest that the aglycone of compounds 1 and 2 is isorhamnetin. The isorhamnetin moiety was substituted with a glucoside. Three protons of the sugar moiety were identified, H1″ at 5.39 ppm (^{1}H, d, J = 7.5 Hz), H6″ (a) at 3.55 ppm (^{1}H, dd, J = 2.5, J = 14 Hz) and H-6″(b) at 3.72 ppm (^{1}H, dd, J = 5.5, J = 17.5 Hz). The links between these protons were checked by HMBC. The $^{2,3}J$-CH correlation between H1″ of glucose and C-3 of the flavonoid demonstrated the substitution of the isorhamnetin with a glucoside in C-3 (^{1}H: 5.40 and ^{13}C: 135.24). These hypotheses were confirmed with LC-MS-MS spectrum (Fig. 3), which revealed a UV–Vis peak at 15.9 min with an m/z value of 315 $[M–H]^{-}$, corresponding to isorhamnetin, and a UV–Vis peak at 15 min with an m/z value of 477 $[M–H]^{-}$ with a fragment ion of 314; corresponding to isorhamnetin 3-glucoside (Table 5).

– Compound 3

This third compound, identified as quercetin 3-glucoside, has a ^{1}H RMN spectrum closely related to that of compound 2. On ^{1}H NMR, the difference between these two molecules was the chemical shift of proton H-2′ at 7.70 ppm (^{1}H, d, J = 2.0 Hz) for quercetin glucoside and at 7.92 ppm (^{1}H, d, J = 2.0 Hz) for compound 1. This variation can be explained by the absence of the methoxyl group in C-3′ for the quercetin derivative. For the UV–Vis peak at 13.4 min, LC–MS–MS analysis showed an m/z value of 463 $[M–H]^{-}$ with a fragment at m/z 301 corresponding to a quercetin residue.

– Compounds 4–10

Caffeic acid derivatives were identified mainly with HMBC and LC–MS–MS analysis. The HMBC spectrum revealed the presence of five protons characteristic of a caffeoyl moiety at 7.05 (H-2), 6.76 (H-5), 6.97, 6.94, 6.92 (H-6), 7.61, 7.59, 7.55, 7.51 and 7.47 (H-7), 6.36, 6.26 and 6.20 (H-8). In the same way, the HMBC spectrum also included five other proton signals at 6.64 (H-2), 6.59 (H-5), 6.41 (H-6), 2.68 and 2.77 (H-7) and 2.48, 2.55 (H-8), which were characteristic of a hydrocaffeoyl moiety. Additionally, different protons of the quinic acid moiety were correlated with C9 of caffeoyl or hydrocaffeoyl chains (^{1}H/^{13}C: 5.57/174.4, 5.44/168.26, 5.37/174.07, 5.32/174.05). Thus, the EAF of *S. ramosissima* was composed of hydrocaffeoyl and caffeoyl quinic acid derivatives.

As presented above, several signals corresponding to the same proton were recorded in the HMBC analysis, suggesting that several caffeic and hydrocaffeic derivatives were present in the EAF from *S. ramosissima*. LC-MS–MS analysis confirmed this hypothesis and made it possible to identify seven molecules, caffeic and hydrocaffeic acids and five derivatives (Table 5).

- Compound 4: With an m/z value of 181.05 $[M–H]^{-}$, compound 4 was identified as hydrocaffeic acid with a fragment ion on the MS–MS spectrum at 137 $[M–CO_2–H]^{-}$.
- Compound 5: With an m/z value of 179.03 $[M–H]^{-}$, compound 5 was identified as caffeic acid with a fragment ion on the MS–MS spectrum at 135 $[M–CO_2–H]^{-}$.
- Compound 6: This compound had an m/z value of 355.1, $[M–H]^{-}$, and was detected at 13.9 and 16.1 min on the UV chromatogram (Fig. 3). On the MS–MS spectrum, it presented four main fragments, at 137, 173, 181 and 191, characteristic of hydrocaffeic acid (Table 5). The ions at m/z, 191 and 173 (adding a loss of H_2O) corresponded to fragments of a quinic acid moiety, and the ions at m/z 181 and 137 (adding a loss of CO_2) indicated a hydrocaffeoyl group.
- Compound 7: The mass spectrum showed an m/z value of 353.08 corresponding to caffeoyl quinic acid. Compound 7 exhibited an MS–MS spectrum closely related to that of compound 6, except for fragment ions at m/z 179 and 135 (adding a loss of CO_2) indicating a caffeoyl group (Table 5). This compound was identified at two retention times (14.6 and 15.7 min) on the UV chromatogram (Fig. 3).
- Compound 8: Compound 8, with an m/z value of 519.11 $[M–H]^{-}$, was identified as a dihydrocaffeoyl quinic acid: a quinic acid substituted with two hydrocaffeoyl chains. The molecule structure is illustrated in Fig. 2. The fragmentation patterns obtained demonstrated the identification of this compound. The ion fragment at m/z 355 corresponds to the loss of a hydrocaffeoyl moiety, [M-164-H], followed by the loss of H_2O at m/z 337, [M-164-H_2O-H]. This compound was identified at two retention times (15.5 and 15.9 min) on the UV chromatogram (Fig. 3).
- Compound 9: The mass spectrum revealed the presence of a ninth compound at m/z 517.13, composed of quinic acid substituted with one caffeoyl and one hydrocaffeoyl moiety. Several fragmentation patterns were observed depending on the retention time (13.9, 14.6 and 16.1 min). As this compound is constituted at the same time of hydrocaffeoyl and caffeoyl moieties, the two types of fragmentation patterns, separate or admixed, were observed on the mass spectrum. For example at 13.9 min, the fragment ions produced were similar to those of compound 8, which is characteristic of a hydrocaffeoyl derivative except for the fragment ion at 179, corresponding to a caffeoyl residue.
- Compound 10: It presented an m/z value of 515.12 ($[M–H]^{-}$) and was identified as a quinic acid substituted with two caffeoyl chains. The parent ion was fragmented to give several ions. The first one, at m/z 353, indicated a chlorogenic acid residue, due to the loss of a caffeoyl chain. The ions at m/z 191 and 173 (adding a loss of H_2O) corresponded to fragments of quinic acid moiety and the ion at m/z 179 indicated a caffeoyl group. This compound was identified at two retention times (14.4 and 15.7 min) on the UV chromatogram (Fig. 3).

Phenolic compounds in *S. ramosissima* were identified in compliance with the bibliography [48,75–77] and the elucidation of their structure was supported by detailed literature on the *Salicornia* genus, especially on the species *S. herbacea* [16,17]. To our knowledge, it is the first time that these molecules have been described for this glasswort species. Furthermore, identification of phenolics strengthens the hypothesis of a correlation between biological activities, i.e., the link between antioxidant and sunscreen capacities exhibited by EAF is supported by its polyphenol composition because identified derivatives of phenolic compounds and flavonoids have already been reported for their antioxidant activity [48,54]. Indeed, Capitani et al. explained that phenolic compounds like caffeic acid showed the highest ability to react with the peroxyl radicals in the ORAC method, compared with other compounds such as α-tocopherol, BHT or Trolox, due to their phenolic structure [78]. Moreover, Huang et al. demonstrated the high antioxidant activity of quercetin (39.4 ± 2.45 μmol Te mg^{-1}) and caffeic acid (57.5 ± 2.39 μmol Te mg^{-1}) in the ORAC test [64]. Interestingly, many synthetic UV-filters, such as benzophenone and cinnamic acid derivatives (like caffeic acid) and homosalate, have an aromatic structure [79]. Choquenet et al., using the same protocol as the present study, reported that two flavonoids, quercetin and rutin, are efficient sunscreens (SPF = 4.52 ± 0.38 and 4.72 ± 0.20; PF-UVA = 5.77 ± 0.55 and 4.92 ± 0.20, respectively)

and authors demonstrated their photostability [73]. So, while it is interesting to test pure flavonoids and caffeic derivatives, our results show that this EAF, a purified fraction composed of a complex of polyphenols (structurally elucidated), exhibits complementary biological activities: an effective broad spectrum *in vitro* sunscreen activity coupled with antioxidant activities.

4. Conclusion

To conclude, the current study demonstrated both the high antioxidant and sunscreen potential of polyphenols extracted and purified from the halophyte *S. ramosissima*. In particular, the mixture of compounds present in the ethyl acetate fraction was found to be more efficient than commercial antioxidant (α-tocopherol) and synthetic UV-filters. Moreover, it was shown that this salt-marsh plant produces a large diversity of phenolic compounds, several flavonols and caffeic acid derivatives, which present an EtOAc solvent affinity. These findings highlight the potential interest of this halophyte as a natural source of sunscreen phytochemicals. Further studies on cultivated samples are now needed, as are tests on EAF photostability with time and for the absence of cytotoxicity. Additionally, it would be worth conducting experiments to isolate and to test bioactive polyphenols present in EAF separately and in combination for a better understanding of their action mechanisms. Finally, this sunscreen activity marks a novel and original application of the glasswort *Salicornia* in cosmetic and pharmaceutical domains and therefore adds one more application to the long list of biological activities already known for this taxon.

Acknowledgements

This study is part of the PhD thesis work carried out by the first author at the Laboratoire des Sciences de l'Environnement Marin (LEMAR UMR 6539), which is part of the IUEM (UBO-UEB). It was supported by the Université de Bretagne Occidentale (France), the Région Bretagne and the Labex Mer initiative, a State Grant from the French Agence Nationale de la Recherche (ANR) in the Program «Investissements d'avenir» with the reference ANR-10-LABX-19-01, Labex Mer. We would like to thank Helen McCombie-Boudry from the Bureau de Traduction de l'Université (BTU) of the University of Western Brittany, Brest, France for her fruitful assistance with the improvement of the English in this article. This work was co-financed with the support of the European Union ERDF - Atlantic Area Programme, MARMED Project No. 2011-1/164 and the project RIV-ALG (n° 13006760), financed by CBB Development and the Région Bretagne (France).

References

[1] M. Ichihashi, M. Ueda, A. Budiyanto, T. Bito, M. Oka, M. Fukunaga, et al., UV-induced skin damage, Toxicology 189 (2003) 21–39.
[2] J.A. Nichols, S.K. Katiyar, Skin photoprotection by natural polyphenols: anti-inflammatory, anti-oxidant and DNA repair mechanisms, Arch. Dermatol. Res. 302 (2010) 71–83.
[3] D. Bennet, S.C. Kang, J. Gang, S. Kim, Photoprotective effects of apple peel nanoparticles, Int. J. Nanomedicine 9 (2013) 93–108.
[4] J.A. Yáñez, C.M. Remsberg, J.K. Takemoto, K.R. Vega-Villa, P.K. Andrews, C.L. Sayre, et al., Polyphenols and flavonoids: an overview, Flavonoid Pharmacokinet. Methods Anal. Preclin. Clin. Pharmacokinet. Saf. Toxicol. (2012) 1–69
[5] M. Andreassi, L. Andreassi, Antioxidants in dermocosmetology: from the laboratory to clinical application, J. Cosmet. Dermatol. 2 (2003) 153–160.
[6] J. Rozema, J. van de Staaij, L.O. Björn, M. Caldwell, UV-B as an environmental factor in plant life: stress and regulation, Trends Ecol. Evol. 12 (1997) 22–28.
[7] D. Ryan, K. Robards, S. Lavee, Determination of phenolic compounds in olives by reversed-phase chromatography and mass spectrometry, J. Chromatogr. A 832 (1999) 87–96.
[8] A.-M. Boudet, Evolution and current status of research in phenolic compounds, Phytochemistry 68 (2007) 2722–2735.
[9] L. Bravo, Polyphenols: chemistry, dietary sources, metabolism, and nutritional significance, Nutr. Rev. 56 (1998) 317–333.
[10] J. Rozema, L.O. Björn, J.F. Bornman, A. Gaberščik, D.-P. Häder, T. Trošt, et al., The role of UV-B radiation in aquatic and terrestrial ecosystems—an experimental and functional analysis of the evolution of UV-absorbing compounds, J. Photochem. Photobiol. B 66 (2002) 2–12.
[11] C. Little, The Terrestrial Invasion: An Ecophysiological Approach to the Origins of Land Animals, CUP Archive, 1990.
[12] T.M. Arnold, N.M. Targett, Marine tannins: the importance of a mechanistic framework for predicting ecological roles, J. Chem. Ecol. 28 (2002) 1919–1934.
[13] A.J. Davy, G.F. Bishop, C.S.B. Costa, *Salicornia L.* (*Salicornia pusilla* J. Woods, *S. ramosissima* J. Woods, *S. europaea* L., *S. obscura* PW Ball & Tutin, *S. nitens* PW Ball & Tutin, *S. fragilis* PW Ball & Tutin and *S. dolichostachya* Moss), J. Ecol. 89 (2001) 681–707.
[14] A. Meudec, Exposition au fioul lourd chez *Salicornia fragilis* Ball et Tutin: contamination chimique par les HAPs et réponses biologiques de la plante, PhD of marine biology, Brest, 2006. <http://www.theses.fr/2006BRES2008> (accessed 15.07.14).
[15] A. Meudec, N. Poupart, Méthode de culture hors-sol pour la production d'halophytes, WO2010066857 A1, 2010.
[16] M.H. Rhee, H.-J. Park, J.Y. Cho, *Salicornia herbacea*: botanical, chemical and pharmacological review of halophyte marsh plant, J. Med. Plants Res. 3 (2009) 548–555.
[17] V. Isca, A.M. Seca, D.C. Pinto, A. Silva, An overview of *Salicornia* genus: the phytochemical and pharmacological profile, in: V.K. Gupta (Ed.), Natural Products: Research Review, vol. 2, Daya Publishing House, New Delhi, 2014, pp. 145–164.
[18] E.P. Murakeözy, A. Aïnouche, A. Meudec, E. Deslandes, N. Poupart, Phylogenetic relationships and genetic diversity of the *Salicornieae* (*Chenopodiaceae*) native to the Atlantic coasts of France, Plant Syst. Evol. 264 (2007) 217–237.
[19] C. Lahondère, Les salicornes s.l. (*Salicornia* L., *Sarcocornia* A. J. Scott et *Arthrocnemum* Moq.): sur les côtes françaises, Société Botanique du Centre-Ouest, 2004.
[20] K. Le Lann, C. Jégou, V. Stiger-Pouvreau, Effect of different conditioning treatments on total phenolic content and antioxidant activities in two Sargassacean species: comparison of the frondose *Sargassum muticum* (Yendo) Fensholt and the cylindrical *Bifurcaria bifurcata* R. Ross, Phycol. Res. 56 (2008) 238–245.
[21] V. Stiger-Pouvreau, C. Jégou, S. Cérantola, F. Guérard, K. Le Lann, Phlorotannins in Sargassaceae species from Brittany (France): interesting molecules for ecophysiological and valorisation purposes, Sea Plants (2014) 379–412.
[22] K.L. van Alstyne, Comparison of three methods for quantifying brown algal polyphenolic compounds, J. Chem. Ecol. 21 (1995) 45–58.
[23] V. Dewanto, X. Wu, K.K. Adom, R.H. Liu, Thermal processing enhances the nutritional value of tomatoes by increasing total antioxidant activity, J. Agric. Food Chem. 50 (2002) 3010–3014.
[24] E.N. Frankel, A.S. Meyer, The problems of using one-dimensional methods to evaluate multifunctional food and biological antioxidants, J. Sci. Food Agric. 80 (2000) 1925–1941.
[25] D. Huang, B. Ou, R.L. Prior, The chemistry behind antioxidant capacity assays, J. Agric. Food Chem. 53 (2005) 1841–1856.
[26] C. Kaur, H.C. Kapoor, Anti-oxidant activity and total phenolic content of some Asian vegetables, Int. J. Food Sci. Technol. 37 (2002) 153–161.
[27] I.I. Koleva, T.A. van Beek, J.P.H. Linssen, A. de Groot, L.N. Evstatieva, Screening of plant extracts for antioxidant activity: a comparative study on three testing methods, Phytochem. Anal. 13 (2002) 8–17.
[28] R. Ksouri, H. Falleh, W. Megdiche, N. Trabelsi, B. Mhamdi, K. Chaieb, et al., Antioxidant and antimicrobial activities of the edible medicinal halophyte *Tamarix gallica* L. and related polyphenolic constituents, Food Chem. Toxicol. 47 (2009) 2083–2091.
[29] S. Connan, E. Deslandes, E.A. Gall, Influence of day–night and tidal cycles on phenol content and antioxidant capacity in three temperate intertidal brown seaweeds, J. Exp. Mar. Biol. Ecol. 349 (2007) 359–369.
[30] R.G. Marwah, M.O. Fatope, R.A. Mahrooqi, G.B. Varma, H.A. Abadi, S.K.S. Al-Burtamani, Antioxidant capacity of some edible and wound healing plants in Oman, Food Chem. 101 (2007) 465–470.
[31] J. Buenger, H. Ackermann, A. Jentzsch, A. Mehling, I. Pfitzner, K.-A. Reiffen, et al., An interlaboratory comparison of methods used to assess antioxidant potentials1, Int. J. Cosmet. Sci. 28 (2006) 135–146.
[32] M. Oyaizu, Studies on products of browning reaction: antioxidative activity of products of browning reaction, Jpn. J. Nutr. 44 (1986) 307–315.
[33] T. Kuda, M. Tsunekawa, H. Goto, Y. Araki, Antioxidant properties of four edible algae harvested in the Noto Peninsula, Japan, J. Food Compos. Anal. 18 (2005) 625–633.
[34] M. Zubia, M.S. Fabre, V. Kerjean, K.L. Lann, V. Stiger-Pouvreau, M. Fauchon, et al., Antioxidant and antitumoural activities of some Phaeophyta from Brittany coasts, Food Chem. 116 (2009) 693–701.
[35] I.C.F.R. Ferreira, P. Baptista, M. Vilas-Boas, L. Barros, Free-radical scavenging capacity and reducing power of wild edible mushrooms from northeast Portugal: individual cap and stipe activity, Food Chem. 100 (2007) 1511–1516.
[36] S. Dudonné, X. Vitrac, P. Coutière, M. Woillez, J.-M. Mérillon, Comparative study of antioxidant properties and total phenolic content of 30 plant extracts of industrial interest using DPPH, ABTS, FRAP, SOD, and ORAC Assays, J. Agric. Food Chem. 57 (2009) 1768–1774.
[37] G. Cao, H.M. Alessio, R.G. Cutler, Oxygen-radical absorbance capacity assay for antioxidants, Free Radical Biol. Med. 14 (1993) 303–311.

[38] C. Couteau, M. Pommier, E. Paparis, L.J.M. Coiffard, Study of the efficacy of 18 sun filters authorized in European Union tested *in vitro*, Pharm. - Int. J. Pharm. Sci. 62 (2007) 449–452.
[39] S. Elboury, C. Couteau, L. Boulande, E. Paparis, L. Coiffard, Effect of the combination of organic and inorganic filters on the Sun Protection Factor (SPF) determined by *in vitro* method, Int. J. Pharm. 340 (2007) 1–5.
[40] M. Pissavini, L. Ferrero, V. Alard, U. Heinrich, H. Tronnier, D. Kockott, et al., Determination of the *in vitro* SPF, Cosmet. Toiletries 118 (2003) 63–72.
[41] J.R. Villalobos-Hernández, C.C. Müller-Goymann, *In vitro* erythemal UV-A protection factors of inorganic sunscreens distributed in aqueous media using carnauba wax–decyl oleate nanopartices, Eur. J. Pharm. Biopharm. 65 (2007) 122–125.
[42] A. Vallverdú-Queralt, O. Jáuregui, A. Medina-Remón, C. Andrés-Lacueva, R.M. Lamuela-Raventós, Improved characterization of tomato polyphenols using liquid chromatography/electrospray ionization linear ion trap quadrupole Orbitrap mass spectrometry and liquid chromatography/electrospray ionization tandem mass spectrometry, Rapid Commun. Mass Spectrom. 24 (2010) 2986–2992.
[43] S. Kang, D. Kim, B.H. Lee, M.-R. Kim, M. Chiang, J. Hong, Antioxidant properties and cytotoxic effects of fractions from glasswort (*Salicornia herbacea*) seed extracts on human intestinal cells, Food Sci. Biotechnol. 20 (2011) 115–122.
[44] M.J. Rodrigues, K.N. Gangadhar, C. Vizetto-Duarte, S.G. Wubshet, N.T. Nyberg, L. Barreira, et al., Maritime halophyte species from southern Portugal as sources of bioactive molecules, Mar. Drugs 12 (2014) 2228–2244.
[45] I. Essaidi, Z. Brahmi, A. Snoussi, H. Ben Haj Koubaier, H. Casabianca, N. Abe, et al., Phytochemical investigation of Tunisian *Salicornia herbacea* L., antioxidant, antimicrobial and cytochrome P450 (CYPs) inhibitory activities of its methanol extract, Food Control 32 (2013) 125–133.
[46] H.-S. Jang, K.-R. Kim, S.-W. Choi, M.-H. Woo, J.-H. Choi, Antioxidant and antithrombus activities of enzyme-treated *Salicornia herbacea* extracts, Ann. Nutr. Metab. 51 (2007) 119–125.
[47] J.-H. Sung, S.-H. Park, D.-H. Seo, J.-H. Lee, S.-W. Hong, S.-S. Hong, Antioxidative and skin-whitening effect of an aqueous extract of *Salicornia herbacea*, Biosci. Biotechnol. Biochem. 73 (2009) 552–556.
[48] J.Y. Kim, J.-Y. Cho, Y.-K. Ma, K.Y. Park, S.-H. Lee, K.-S. Ham, et al., Dicaffeoylquinic acid derivatives and flavonoid glucosides from glasswort (*Salicornia herbacea* L.) and their antioxidative activity, Food Chem. 125 (2011) 55–62.
[49] C.-S. Kong, J.I. Lee, Y.A. Kim, J.-A. Kim, S.S. Bak, J.W. Hong, et al., Evaluation on anti-adipogenic activity of flavonoid glucopyranosides from *Salicornia herbacea*, Process Biochem. 47 (2012) 1073–1078.
[50] E.H. Han, J.Y. Kim, H.G. Kim, H.K. Chun, Y.C. Chung, H.G. Jeong, Inhibitory effect of 3-caffeoyl-4-dicaffeoylquinic acid from *Salicornia herbacea* against phorbol ester-induced cyclooxygenase-2 expression in macrophages, Chem. Biol. Interact. 183 (2010) 397–404.
[51] Y.P. Hwang, H.J. Yun, J.H. Choi, H.K. Chun, Y.C. Chung, S.K. Kim, et al., 3-Caffeoyl, 4-dihydrocaffeoylquinic acid from *Salicornia herbacea* inhibits tumor cell invasion by regulating protein kinase C-δ-dependent matrix metalloproteinase-9 expression, Toxicol. Lett. 198 (2010) 200–209.
[52] Y.P. Hwang, H.J. Yun, H.K. Chun, Y.C. Chung, H.K. Kim, M.H. Jeong, et al., Protective mechanisms of 3-caffeoyl, 4-dihydrocaffeoyl quinic acid from *Salicornia herbacea* against tert-butyl hydroperoxide-induced oxidative damage, Chem. Biol. Interact. 181 (2009) 366–376.
[53] S.-A. Im, K. Kim, C.-K. Lee, Immunomodulatory activity of polysaccharides isolated from *Salicornia herbacea*, Int. Immunopharmacol. 6 (2006) 1451–1458.
[54] C.-S. Kong, Y.A. Kim, M.-M. Kim, J.-S. Park, J.-A. Kim, S.-K. Kim, et al., Flavonoid glycosides isolated from *Salicornia herbacea* inhibit matrix metalloproteinase in HT1080 cells, Toxicol. In Vitro 22 (2008) 1742–1748.
[55] C.-S. Kong, J.-A. Kim, Z.-J. Qian, Y.A. Kim, J.I. Lee, S.-K. Kim, et al., Protective effect of isorhamnetin 3-O-β-d-glucopyranoside from *Salicornia herbacea* against oxidation-induced cell damage, Food Chem. Toxicol. 47 (2009) 1914–1920.
[56] Q. Wang, X. Liu, Y. Shan, F. Guan, Y. Chen, X. Wang, et al., Two new nortriterpenoid saponins from *Salicornia bigelovii* Torr. and their cytotoxic activity, Fitoterapia 83 (2012) 742–749.
[57] X. Wang, M. Zhang, Y. Zhao, H. Wang, T. Liu, Z. Xin, Pentadecyl ferulate, a potent antioxidant and antiproliferative agent from the halophyte *Salicornia herbacea*, Food Chem. 141 (2013) 2066–2074.
[58] Y. Zhao, X. Wang, H. Wang, T. Liu, Z. Xin, Two new noroleanane-type triterpene saponins from the methanol extract of *Salicornia herbacea*, Food Chem. 151 (2014) 101–109.
[59] W. Bi, M. Tian, K.H. Row, Separation of phenolic acids from natural plant extracts using molecularly imprinted anion-exchange polymer confined ionic liquids, J. Chromatogr. A 1232 (2012) 37–42.
[60] J.H. Oh, E.O. Kim, S.K. Lee, M.H. Woo, S.W. Choi, Antioxidant activities of the ethanol extract of Hamcho (*Salicornia herbacea* L.) cake prepared by enzymatic treatment, Food Sci. Biotechnol. 16 (2007) 90–98.
[61] G. Bedoux, K. Hardouin, A.S. Burlot, N. Bourgougnon, Bioactive components from Seaweeds: cosmetic applications and future development, in: Advances in Botanical Research Sea Plant, Elsevier, 2014, pp. 345–378.
[62] M. Hupel, Radiations UV et composés photoprotecteurs: étude comparée chez deux végétaux marins, l'algue brune *Pelvetia canaliculata* et l'angiosperme *Salicornia ramosissima*, Brest, 2011. <http://www.theses.fr/2011BRES2010> (accessed 15.07.2014).
[63] G.R.M.M. Haenen, M.J.T.J. Arts, A. Bast, M.D. Coleman, Structure and activity in assessing antioxidant activity in vitro and in vivo: a critical appraisal illustrated with the flavonoids, Environ. Toxicol. Pharmacol. 21 (2006) 191–198.
[64] W.-Y. Huang, K. Majumder, J. Wu, Oxygen radical absorbance capacity of peptides from egg white protein ovotransferrin and their interaction with phytochemicals, Food Chem. 123 (2010) 635–641.
[65] D.J. Charles, Antioxidant Properties of Spices, Herbs and Other Sources, Springer Science & Business Media, 2012.
[66] M. Hupel, C. Lecointre, A. Meudec, N. Poupart, E.A. Gall, Comparison of photoprotective responses to UV radiation in the brown seaweed *Pelvetia canaliculata* and the marine angiosperm *Salicornia ramosissima*, J. Exp. Mar. Biol. Ecol. 401 (2011) 36–47.
[67] F. Rancan, S. Rosan, K. Boehm, E. Fernández, M.E. Hidalgo, W. Quihot, et al., Protection against UVB irradiation by natural filters extracted from lichens, J. Photochem. Photobiol. B 68 (2002) 133–139.
[68] F. Lohézic-Le Dévéhat, B. Legouin, C. Couteau, J. Boustie, L. Coiffard, Lichenic extracts and metabolites as UV filters, J. Photochem. Photobiol. B 120 (2013) 17–28.
[69] A. Jarzycka, A. Lewińska, R. Gancarz, K.A. Wilk, Assessment of extracts of *Helichrysum arenarium*, *Crataegus monogyna*, *Sambucus nigra* in photoprotective UVA and UVB; photostability in cosmetic emulsions, J. Photochem. Photobiol. B 128 (2013) 50–57.
[70] C.A. Rice-Evans, N.J. Miller, G. Paganga, Structure–antioxidant activity relationships of flavonoids and phenolic acids, Free Radical Biol. Med. 20 (1996) 933–956.
[71] G. Agoramoorthy, F.-A. Chen, V. Venkatesalu, D.-H. Kuo, P.-C. Shea, Evaluation of antioxidant polyphenols from selected mangrove plants of India, Asian J. Chem. 20 (2008) 1311–1322.
[72] N. Trabelsi, S. Oueslati, H. Falleh, P. Waffo-Téguo, Y. Papastamoulis, J.-M. Mérillon, et al., Isolation of powerful antioxidants from the medicinal halophyte *Limoniastrum guyonianum*, Food Chem. 135 (2012) 1419–1424.
[73] B. Choquenet, C. Couteau, E. Paparis, L.J.M. Coiffard, Quercetin and rutin as potential sunscreen agents: determination of efficacy by an in vitro method, J. Nat. Prod. 71 (2008) 1117–1118.
[74] G. Agati, M. Tattini, Multiple functional roles of flavonoids in photoprotection, New Phytol. 186 (2010) 786–793.
[75] H. Gao, Y.-N. Huang, B. Gao, P.-Y. Xu, C. Inagaki, J. Kawabata, A-Glucosidase inhibitory effect by the flower buds of *Tussilago farfara* L, Food Chem. 106 (2008) 1195–1201.
[76] D. Gutzeit, V. Wray, P. Winterhalter, G. Jerz, Preparative isolation and purification of flavonoids and protocatechuic acid from sea buckthorn juice concentrate (*Hippophaë rhamnoides L. ssp. rhamnoides*) by high-speed counter-current chromatography, Chromatographia 65 (2006) 1–7.
[77] Y. Tamura, M. Hattori, K. Konno, Y. Kono, H. Honda, H. Ono, et al., Triterpenoid and caffeic acid derivatives in the leaves of ragweed, *Ambrosia artemisiifolia* L. (Asterales: Asteraceae), as feeding stimulants of *Ophraella communa* LeSage (Coleoptera: Chrysomelidae), Chemoecology 14 (2004) 113–118.
[78] C.D. Capitani, A.C.L. Carvalho, D.P. Rivelli, S.B.M. Barros, I.A. Castro, Evaluation of natural and synthetic compounds according to their antioxidant activity using a multivariate approach, Eur. J. Lipid Sci. Technol. 111 (2009) 1090–1099.
[79] C. Couteau, C. Chauvet, E. Paparis, L. Coiffard, UV filters, ingredients with a recognized anti-inflammatory effect, PLoS ONE 7 (2012) e46187.

Chapitre 8. Molécules antioxydantes, prominéralogéniques et ostéogéniques isolées de deux macroalgues (native et invasive) pour le domaine de la santé humaine : une bio-inspiration non intuitive

Le rôle du stress oxydant comme expliqué précédemment joue un rôle important chez les végétaux marins mais également chez l'homme et en particulier dans les maladies osseuses (Wauquier et al., 2009). En effet, la formation et le renouvellement du tissu osseux sont régulés par les ostéoblastes qui forment du tissu osseux et par les ostéoclastes qui le résorbent. Une dérégulation entraîne l'apparition de maladies métaboliques comme l'ostéoporose (Habauzit and Horcajada, 2008). Arai et al. (2007) ont reporté que les EROs pouvaient être responsables du développement de la perte osseuse et que l'activité des enzymes antioxydantes, comme la SOD, représente un marqueur du stress oxydant chez la femme ménopausée (Arai et al., 2007). Les auteurs ont montré que l'ajout de H_2O_2 (molécules induites par le stress oxydant) pouvait inhiber *in vitro* de 50 % le taux de calcification des cellules ostéoblastiques. Ainsi, des molécules antioxydantes qui ne présentent pas de cytotoxicité pourraient jouer le rôle de détoxifiant cellulaire et favoriser la minéralisation. Cette hypothèse selon laquelle des composés antioxydants et en particulier les polyphénols pourraient être des candidats efficaces à la prévention de maladies osseuses telles que l'ostéoporose en prévenant la perte osseuse par inhibition du stress oxydant est reportée dans la littérature (Đudarić et al., 2015; Rao and Rao, 2015; Sun et al., 2011). Mais, la limite de cette utilisation est la nécessité que ces molécules ne présentent pas de cytotoxicité pour les tissus/cellules/organes.

Dans ce contexte, l'identification de molécules permettant de prévenir l'ostéoporose représente un intérêt médical important sachant que cette pathologie est reconnue comme un problème majeur de santé publique (Eddy et al., 1998). Ainsi, ce chapitre a pour but d'analyser les propriétés antioxydantes et ostéogéniques (*in vitro* et *in vivo*) de différents extraits de macrophytes marins. Pour y parvenir, cette présente étude a bénéficié d'une collaboration avec le CCMAR (Center of Marine Sciences, Université de Faro, Portugal) qui s'inscrit dans le projet européen MARMED. Ce laboratoire a développé un ensemble de techniques *in vitro* (par cultures cellulaires) et *in vivo* afin d'évaluer le potentiel minéralisant d'extraits. Cette collaboration m'a permis de réaliser au CCMAR les expérimentations *in vitro*, au cours d'un stage de 4 mois, en utilisant une lignée cellulaire, nommée VSa13,

obtenue à partir de vertèbres de la dorade royale, *Sparus aurata*. Cette lignée est capable de minéraliser sa matrice extracellulaire et présente un phénotype chondrocytaire (Rafael et al., 2010). Elle a été développée par le laboratoire du Pr Leonor Cancela, au CCMAR selon un protocole simple et performant (Marques et al., 2007). De précédentes études ont montré que cette lignée cellulaire était un modèle pertinent pour évaluer le potentiel minéralisant de molécules (Viegas et al., 2012). Avant de pouvoir tester ce potentiel sur les extraits générés lors du screening, leur effet prolifératif, ainsi que leur cytotoxicité potentielle, sur cette lignée cellulaire ont été évalués *in vitro*. Ces deux tests ont permis de vérifier la compatibilité des extraits avec la lignée cellulaire. Les tests effectués sur *Salicornia ramossisima* et *S. fragilis* ont montré une mauvaise répétabilité avec des possibles phénomènes d'interaction avec la lignée cellulaire. Par ailleurs, les extraits de *Spartina alterniflora*, *Codium fragile* et *Cladophora rupestris* n'ont pas présenté ce type d'interaction. En conséquence, l'activité pro-minéralisante des extraits de ces trois espèces a pu être poursuivi. La démarche de l'ensemble des tests effectués sur des cultures cellulaires de type VSa13 est illustrée par la Figure 40.

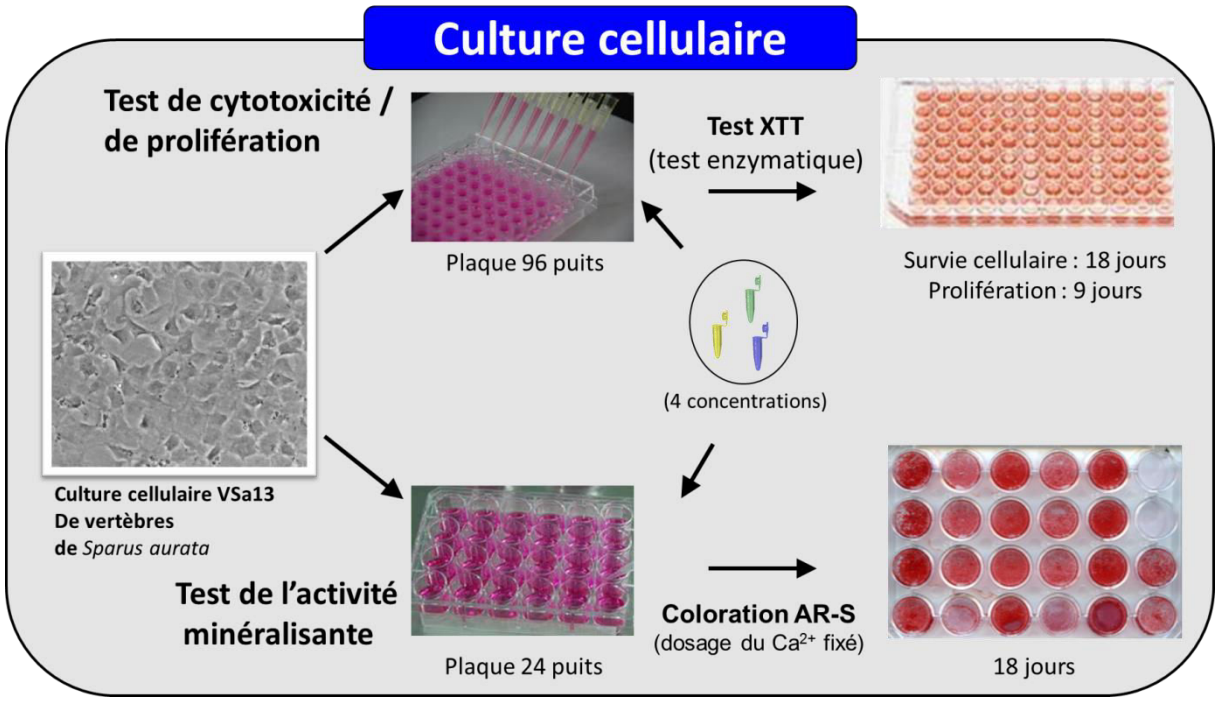

Fig. 40 Description de la démarche suivie pour l'analyse de l'effet prolifératif et cytotoxique d'extraits algaux sur une culture cellulaire de type VSa 13 ainsi que de la détermination du potentiel antioxydant par coloration à l'alizarine rouge (AR-S), colorant qui se fixe spécifiquement sur le calcium présent dans les cristaux d'hydroxyapatite de la phase minérale de la matrice extracellulaire de la culture cellulaire.

Les deux chlorophytes ont présenté des résultats particulièrement intéressants et le CCMAR a complété ces analyses *in vitro* en expérimentant *in vivo*, le potentiel minéralisant des extraits actifs des deux macroalgues vertes sur l'espèce de poisson *Danio rerio* communément appelé zebrafish. Ces résultats ouvrent des perspectives innovantes car peu d'études ont montré l'effet anabolique de fractions enrichies en composés phénoliques de macroalgues marines, natives et invasives, sur la minéralisation des vertèbres du zebrafish.

J Appl Phycol (2017) 29:575–584
DOI 10.1007/s10811-016-0968-3

ORIGINAL PAPER

Marine green macroalgae: a source of natural compounds with mineralogenic and antioxidant activities

Gwladys Surget[1] · Vânia P. Roberto[2] · Klervi Le Lann[1] · Sara Mira[2] · Fabienne Guérard[1] · Vincent Laizé[2] · Nathalie Poupart[1] · M. Leonor Cancela[2,3] · Valérie Stiger-Pouvreau[1]

Received: 11 March 2016 / Revised and accepted: 18 September 2016 / Published online: 21 October 2016

Abstract Marine macroalgae represent a valuable natural resource for bioactive phytochemicals with promising applications in therapeutics, although they remain largely under-exploited. In this work, the potential of two marine green macroalgae (*Cladophora rupestris* and *Codium fragile*) as a source of bioactive phenolic compounds was explored, and antioxidant, mineralogenic, and osteogenic activities were evaluated. For each species, a crude hydroalcoholic extract (CE) was prepared by solid/liquid extraction and fractionated by liquid/liquid purification into an ethyl acetate fraction (EAF) enriched in phenolic compounds and an aqueous fraction (AF). Antioxidant activity, assessed through radical scavenging activity and reducing power assay, was increased in EAF fraction of both species and closely related to the phenolic content in each fraction. Mineralogenic activity, assessed through extracellular matrix mineralization of a fish bone-derived cell line, was induced by EAF fractions (up to 600 % for *C. rupestris* EAF). Quantitative analysis of operculum formation in zebrafish larvae stained with alizarin red S further confirmed the osteogenic potential of EAF fractions in vivo, with an increase of more than 1.5-fold for both *C. fragile* and *C. rupestris* fractions, similar to vitamin D (control). Our results demonstrated a positive correlation between phenolic fractions and biological activity, suggesting that phenolic compounds extracted from marine green macroalgae may represent promising molecules toward therapeutic applications in the field of bone biology.

Keywords Ulvophyceae · Phenolic compounds · Antioxidant activity · Mineralogenic activity · Proliferative activity

Gwladys Surget, Vânia P. Roberto, Sara Mira contributed equally to this work.

✉ M. Leonor Cancela
leocancela@gmail.com; lcancela@ualg.pt

Valérie Stiger-Pouvreau
valerie.stiger@univ-brest.fr

[1] CNRS, IRD, Ifremer, LEMAR UMR 6539, IUEM, University of Brest, 29280 Plouzané, France

[2] Centre of Marine Sciences (CCMAR), University of Algarve, Faro, Portugal

[3] Department of Biomedical Sciences and Medicine (DCBM), University of Algarve, Faro, Portugal

Introduction

A priority in biotechnological innovation in the last decade has been the exploration of natural resources toward the discovery of new and promising bioactivities, e.g., with therapeutic potential or industrial applications (reviewed in Donia and Hamann 2003; Imhoff et al. 2011; Bonifácio et al. 2014). Surfactants for biomaterials are of particular interest to improve biocompatibility and efficacy, and in this regard, phytochemicals were found to have antioxidant capacities and also to promote osteoblast proliferation and differentiation (Habauzit and Horcajada 2007; Woo et al. 2010; Karadeniz et al. 2014, 2015), which make them suitable for applications related to bone regeneration or increased bone density (Córdoba et al. 2015a,b; Watson and Schönlau 2015). Marine macroalgae, beside their role in the provision of alginates, carrageenans, fibers, and minerals for agrifood (Marsham et al. 2007; Mouritsen 2013; Stiger-Pouvreau et al. 2016), also represent a valuable source for bioactive phytochemicals (reviewed in Imhoff et al. 2011; Stengel and Connan 2015). While macroalgae are largely under-exploited in Europe, they are commonly harvested in Brittany for industrial applications such as cosmetic, food, thalassotherapy, and medicinal products (Bourgougnon and Stiger-Pouvreau 2011). Brown algae are by far the most harvested species (97.2 %), followed by red (2.7 %) and green (0.06 %) algae. Among the green algae, species of the

genus *Ulva* and *Enteromorpha* are mainly valorized in Brittany (Chambre Syndicale des Algues et Végétaux Marins (CSAVM), personal communications). Phenolic compounds from marine and terrestrial plants exhibit a wide range of chemical structures (Singh and Bharate 2006; Ajila et al. 2011) and a large spectrum of biological activities (Li et al. 2011; Ksouri et al. 2012). For example, they showed antidiabetic (Lee and Jeon 2013), antimicrobial (Eom et al. 2012), antioxidative (Le Lann et al. 2008, 2012; Andrade et al. 2013; Tanniou et al. 2013, 2014; Stiger-Pouvreau et al. 2014; Surget et al. 2015), photoprotective (Surget et al. 2015), antitumoral (Deslandes et al. 2000; Zubia et al. 2009; Montero et al. 2016), anti-inflammatory (Kim et al. 2009; Kang et al. 2013), and radioprotective effects (Liu et al. 2011). Properties of bioceramic-based medical scaffolds have been successfully improved upon supplementation with phenolic compounds from marine origin, in particular toward increased bone tissue regeneration (Yeo et al. 2012; Córdoba et al. 2015a,b). Phlorotannins, i.e., phenolic compounds from brown seaweeds, extracted from *Ecklonia* brown algal species have also been shown to increase alkaline phosphatase (ALP) activity, mineralization, total protein, and collagen synthesis in human osteosarcoma cells (MG-63 cells) (Ryu et al. 2009; Ali and Hasan 2012; Yeo et al. 2012; Karadeniz et al. 2015), suggesting that they may act as regulators of osteoblast differentiation and bone formation. In the context of the biotechnological valorization of marine algae in Europe and the discovery of new bioactive molecules as potential biomaterials for regenerative medicine, this work intended to get insights into the osteogenic and antioxidant capacities of the phenolic compounds extracted from two green seaweeds, the native *Cladophora rupestris* and the introduced *Codium fragile*. In that sense, crude extracts and semi-purified fractions were evaluated for total phenolic content, antioxidative activity, and mineralogenic and proliferative effects, in this case using a bone-derived cell line from gilthead seabream (*Sparus aurata*) capable of extracellular matrix mineralization (Pombinho et al. 2004). The most active fractions were then tested in vivo, using the zebrafish as a model system to assess mineralization (Laizé et al. 2014).

Material and methods

Regular reagents and materials

Solvents and chemicals (analytical grade) were from Carlo Erba Reagent and Sigma-Aldrich, respectively, unless otherwise stated. Cell culture reagents and plastic consumables were from Invitrogen and Sarstedt, respectively.

Biological material

Samples of the green seaweeds *Codium fragile* (Suringar) Hariot (Ulvophyceae, Bryopsidales, Codiaceae) and *Cladophora rupestris* (Linnaeus) Kützing (Ulvophyceae, Cladophorales, Cladophoraceae) were collected in rock pools of Porsmeur Bay (Lanildut, France; 48° 28′ 55.67″ N, 4° 46′ 14.76″ E). *Codium fragile* is an introduced species in Europe, with a worldwide spread. *Cladophora rupestris* is a native species in Brittany, widely distributed in temperate and cold temperate Atlantic Ocean. After collection and removal of epiphytes, seaweeds were washed with deionized water, frozen, freeze-dried, ground into powder, and stored in the darkness at room temperature to limit the phenolic compound degradation, as described in Le Lann et al. (2008).

Extraction and liquid-liquid semi-purification process

Fifteen gram of dry powder was macerated for 2 h at 40 °C in 150 mL of hydroethanolic solvent (1:1 distilled water/100 % ethanol mixture) under agitation (200 rpm) in the dark. After centrifugation (3000 rpm, 15 °C, 10 min), supernatant was collected and pellet was resuspended in 150 mL of hydroethanolic solvent and macerated for an additional 1 h. This last step was repeated once more, and the three supernatants were pooled and passed through glass fiber filters. Ethanol was removed at 40 °C by vacuum evaporation, and distilled water was added to obtain a 100-mL crude extract (CE). Crude extract was separated into two semi-purified extracts, an aqueous fraction (AF) and an ethyl acetate fraction (EAF), using a protocol adapted from Stiger-Pouvreau et al. (2014) to concentrate polyphenols in EAF. Briefly, lipidic compounds and chlorophyllic pigments were removed through several washes with dichloromethane; then, proteins and carbohydrates were precipitated using pure acetone and 100 % ethanol. Purified extract was then divided into ethyl acetate and aqueous fractions.

Total phenolic content

Total phenolic content (TPC) was determined by spectrophotometry using Folin-Ciocalteu assay (Sanoner et al. 1999) modified according to Le Lann et al. (2008). Wells of a 96-well plate were successfully filled with 20 μL of extracts (dilution ranging from 1 to 0.01 g L^{-1}), 130 μL of distilled water, 10 μL of Folin-Ciocalteu reagent, and 40 μL of sodium carbonate solution (200 g L^{-1}). After agitation, plate was incubated at 70 °C for 10 min, then placed on ice to stop the chemical reaction. Absorbance was measured at 620 nm using a Multiskan MS plate reader (LabSystems), and phenolic content was determined using a standard curve of gallic acid ranging from 0 to 200 μg mL^{-1}. Results are expressed as milligram of gallic acid per gram of dried weight (DW). All measurements were performed in triplicate.

Antioxidant assays

2,2-Diphenyl-1-picrylhydrasyl radical scavenging activity

Radical scavenging activity of extracts/fractions and positive

controls was determined using the 2,2-diphenyl-1-picrylhydrasyl (DPPH) assay adapted from Le Lann et al. (2008) and Zubia et al. (2009). This assay tests the capacity of samples to scavenge the synthetic radical DPPH but is independent of sample polarity and highly reproducible (Huang et al. 2005). Briefly, 100 μL of extract/fraction, positive control (ascorbic acid, butylated hydroxyanisole or BHA, 6-hydroxy-2,5,7,8-tetramethylchroman-2-carboxylic acid or Trolox), or negative controls (distilled water and 100 % ethanol) were added to 100 μL of DPPH solution (36.9 mg L^{-1}) in a 96-well plate. Several dilutions of extracts/fractions and positive controls (ranging from 0.005 to 1 g L^{-1}) were tested. Plate was incubated for 1 h in the dark, and absorbance was measured at 540 nm. Radical scavenging activity of algal extracts was calculated as previously described in Le Lann et al. (2008) and Surget et al. (2015). For each sample, a curve of extract concentration against percent of DPPH inhibition was generated to determine the concentration of extract needed to cause a 50 % reduction of the initial DPPH concentration (IC_{50} in g L^{-1}). A high IC_{50} is indicative of a weak radical scavenging activity and vice versa. All measurements were performed in triplicate.

Reducing power Reducing power (RP) of seaweed extracts was determined following the method in Zubia et al. (2009). RP assay implies an electron transfer and tests the capacity of antioxidants to reduce Fe^{3+}/ferricyanide complex to the ferrous form (Huang et al. 2005). A volume of 25 μL of extracts/fractions, negative controls (water and ethanol), or positive controls (ascorbic acid, BHA, Trolox) was mixed with 25 μL of sodium phosphate buffer (0.2 M; pH 6.6) and 25 μL of potassium ferricyanide (1 %; *w*/*v*). Mixture was incubated for 20 min at 50 °C. After cooling on ice, 25 μL of 10 % (*w*/*v*) trichloroacetic acid, 100 μL of distilled water, and 20 μL of 0.1 % (*w*/*v*) $FeCl_3$ were added, and mixture was incubated at room temperature for 10 min. Absorbance was measured at 620 nm. Capacity of extracts/fractions to reduce Fe^{3+} was determined from EC_{50} in g L^{-1} (calculated by interpolation of a regression linear curve) and corresponds to the effective concentration of the sample to obtain an optical density equal to 0.5. All measurements were performed in triplicates.

Cultures of bone-derived cell line VSa13

Cell culture maintenance Gilthead Seabream bone-derived cell line VSa13 (Pombinho et al. 2004) was used to evaluate mineralogenic and proliferative capacities of seaweed extracts. Cells were cultured in Dulbecco's modified Eagle medium (DMEM) supplemented with 10 % fetal bovine serum (FBS), 1 % penicillin–streptomycin, 1 % L-glutamine, and 0.2 % fungizone and incubated at 33 °C in a 10 % CO_2-humidified atmosphere (Marques et al. 2007). Cells were subcultured 1:4 twice a week using trypsin-EDTA solution (0.2 % trypsine, 1.1 mM EDTA, pH 7.4).

Cell exposure to seaweed molecules Dry extracts/fractions from green macroalgae were dissolved in distilled water, 50 % ethanol (in distilled water), or 100 % ethanol according to their polarity to prepare ×1000 stock solutions. CE, EAF, and AF stock solutions were added to the culture medium to achieve concentrations of 0.05, 0.5, 5, 50, 100, or 250 μg mL^{-1} for EAF and 0.5, 5, 50, or 100 μg mL^{-1} for CE and AF. Medium supplemented with extracts/fractions was 0.2 μm filtered before applied to the cell culture.

Cytotoxicity assay Cells were seeded in 96-well plates at a density of 10^4 cells $well^{-1}$ and further cultured until confluence. Culture medium was replaced with fresh medium containing either the vehicle (control) or algal extracts and renewed every 3–4 days. Cell viability was assessed after 9- and 18-day exposure using the Cell Proliferation Kit XTT (AppliChem). Viability of the cells exposed to seaweed extracts was calculated as percentage of survival in comparison with cells cultured in respective controls.

Proliferation assay Cells were seeded in 96-well plates at a density of 1.5×10^3 cells $well^{-1}$. After 24 h, culture medium was replaced with fresh medium containing either the vehicle (control) or seaweed extracts and renewed every 3–4 days. Cell proliferation was determined after 9 days of exposure using the Cell Proliferation Kit XTT (AppliChem). Results are presented as percentage of cell proliferation, in comparison with respective controls.

Extracellular matrix mineralization Cells were seeded in 24-well plates at a density of 5×10^4 cells $well^{-1}$. Extracellular matrix (ECM) mineralization was induced in confluent cultures by supplementing culture medium with 50 μg mL^{-1} L-ascorbic acid, 10 mM β-glycerophosphate, and 4 mM calcium chloride (differentiation medium). Seaweed extracts or vehicles were added to differentiation medium and renewed twice a week. After 17 days of culture, mineral deposition was revealed through alizarin red S (AR-S; Sigma-Aldrich) staining and quantified by spectrophotometry (Stanford et al. 1995). Results are expressed as percentage of ECM mineralization, relative to the respective controls.

Quantification of in vivo mineralization

Zebrafish larvae were exposed to increasing concentrations of EAF fractions of green macroalgae, *C. fragile* (1, 5, and 10 μg mL^{-1}) and *C. rupestris* (5, 50, and 100 μg mL^{-1}), and control (ethanol), from 9 to 11 days post-fertilization (dpf). Briefly, from 9 to 11 dpf, larvae were reared in a 24-well dish (2 larvae $well^{-1}$) placed in the dark, to avoid photodegradation of the compounds, at 28.5 °C. Each well was filled with 1 mL of embryo medium (Westerfield 2007) supplemented with

EAF, the most active fraction. Medium was renewed once a day, and larvae were fed with *Artemia nauplii* (EG strain, INVE) twice a day. After 48-h exposure, larvae were euthanatized with 168 μg mL^{-1} of tricaine (MS-222; Sigma-Aldrich) and fixed in 4 % paraformaldehyde in phosphate-buffered saline (PBS) for 16 h at 4 °C. After two washes with PBS, larvae were stained with 0.01 % alizarin red S solution for 30 min, washed twice with distilled water, and maintained in 25 % glycerol until analysis. AR-S fluorescence in zebrafish larvae was imaged under a MZ75 stereomicroscope (Leica) equipped with a green filter (excitation filter 546/10 nm, barrier filter 590 nm) and a F-view camera (Olympus). Mineralized area of the operculum was determined from the morphometric analysis of the fluorescence images using ImageJ software (National Institutes of Health) and normalized with the area of the head. Zebrafish larvae were also exposed to 1 fg mL^{-1} of vitamin D (calcitriol; Sigma-Aldrich) as a positive control.

Statistical analysis

Results are presented as the mean of at least three replicates with standard deviation (SD). Homogeneity of variance was tested with the Bartlett's test at the 0.05 significance level. As the sample panel was small for the in vitro tests, a Kruskal-Wallis test was performed to highlight potential significant difference. In the case of significant difference between the data, non-parametric multiple comparisons (Behrens-Fisher test) were tested using the nmpc package. Statistical analysis of ECM mineralization assay and in vivo assay was performed with GraphPad Prism 4 (GraphPad, USA) using one-way ANOVA followed by Dunnett's or Tukey's multiple comparisons tests, respectively, to determine statistical differences among groups. Differences were considered statistically significant for $p < 0.05$.

Results

Total phenolic contents and antioxidant activities

TPC was determined in the CE and semi-purified fractions (EAF and AF) of *C. fragile* and *C. rupestris* (Table 1). While all the three fractions prepared from *C. rupestris* presented high phenolic contents (ranging from 15.833 ± 0.103 to 21.726 ± 0.899 mg GAE g^{-1} DW; Table 1) with EAF showing the highest TPC, only EAF prepared from *C. fragile* exhibited a high TPC value, 10-fold higher than CE content (22.381 ± 0.206 and 2.202 ± 0.103 mg GAE g^{-1} DW, respectively; Table 1). AF prepared from *C. fragile* exhibited the lowest TPC (0.298 ± 0.103 mg GAE g^{-1} DW; Table 1), indicating an absence of aromatic compounds in this fraction. Antioxidant activities of each extract and those from the three positive controls (Trolox, BHA, and ascorbic acid) were determined through the measurement of DPPH radical scavenging activity and reducing power and expressed as IC_{50} and EC_{50}, respectively. In both assays, antioxidant activity was significantly higher in the ethyl acetate fractions of both species when compared to crude extracts and aqueous fractions (Table 1). Even though, EAF antioxidant activities were lower than the positive controls tested. The lowest antioxidant activity (i.e., high IC_{50} and EC_{50}) was always found in AF. Our data indicates that highest antioxidant activities were associated with EAF, which have the highest phenolic content, whereas lowest antioxidant activities were associated with aqueous fractions, exhibiting the lowest phenolic content.

Proliferative and mineralogenic activities of seaweed extracts

Seaweed extracts were further characterized for their capacity to alter cell proliferation and ECM mineralization (Figs. 1 and 2).

Table 1 Phenolic content and antioxidant activities of *Cladophora rupestris* and *Codium fragile* extracts. Phenolic content, DPPH scavenging activity, and reducing power were determined for crude extracts and semi-purified fractions and commercial standards (ascorbic acid, BHA, and Trolox). Values are expressed as mean ± SD ($n = 3$)

		Phenolic content (mg GAE g^{-1} DW)	DPPH scavenging activity IC50 (g L^{-1})	Reducing power EC50 (g L^{-1})
C. rupestris	CE	20.179 ± 0.179 a	1.228 ± 0.010 a	10.129 ± 0.250 a
	EAF	21.726 ± 0.899 b	*0.768 ± 0.021* b	*7.825 ± 0.618* b
	AF	15.833 ± 0.103 c	2.220 ± 0.069 c	15.125 ± 0.953 c
C. fragile	CE	2.202 ± 0.103 d	7.026 ± 0.090 d	48.082 ± 7.130 d
	EAF	22.381 ± 0.206 b	*0.303 ± 0.002* e	*5.478 ± 0.891* e
	AF	0.298 ± 0.103 e	31.815 ± 7.800 f	85.959 ± 52.100 f
Positive controls	Ascorbic acid	n.d.	$0.005 \pm 8.91 \times 10^{-05}$ g	$0.072 \pm 1.58 \times 10^{-03}$ g
	BHA	n.d.	$0.010 \pm 2.17 \times 10^{-04}$ h	$0.091 \pm 1.24 \times 10^{-03}$ h
	Trolox	n.d.	$0.007 \pm 1.25 \times 10^{-04}$ i	$0.169 \pm 3.08 \times 10^{-03}$ i

The different letters indicate the significant difference between means according to Berhens Fisher's test ($p < 0.05$). The values in italic indicate the most active fraction. *GAE* gallic acid equivalent, *DW* dry weight, *CE* Crude extract, *EAF* Ethyl acetate fraction, *AF* Aqueous extract, *BHA* Butylated hydroxyanisole, *IC50* half maximal inhibitory concentration, *EC50* Half maximal effective concentration.

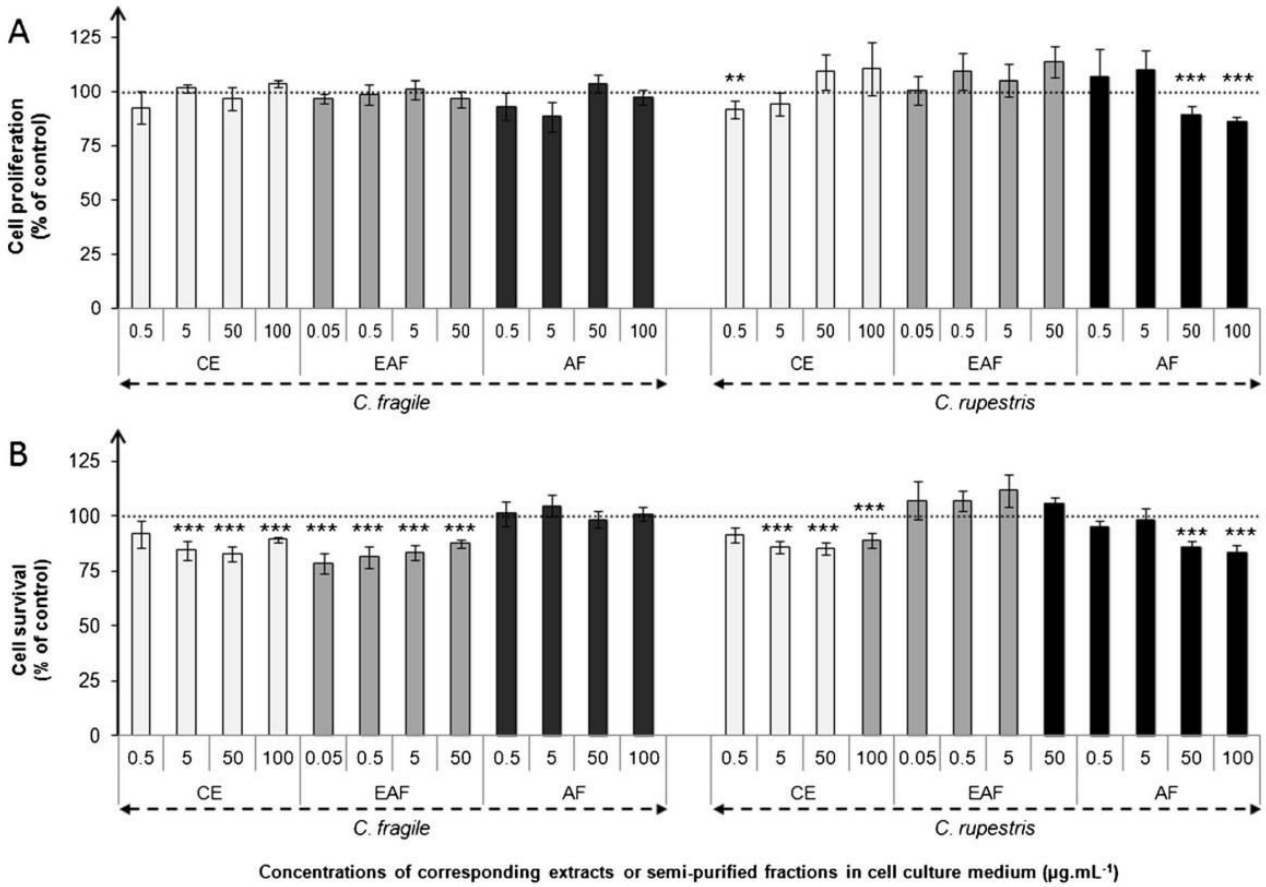

Fig. 1 Effect of crude extract and semi-purified fractions of *Codium fragile* and *Cladophora rupestris* on VSa13 cell proliferation (**a**) and survival (**b**) at 9 days. Control values were determined in vehicle-treated cells and set to 100 % (*dotted line*). Proliferation and survival data are presented as mean values ± standard deviation, $n > 5$. The *asterisks* indicate the values significantly different from the control value according to Berhens Fisher's test (**$p < 0.01$, ***$p < 0.001$). *CE* crude extract, *EAF* ethyl acetate fraction, *AF* aqueous fraction

Cytotoxicity of the extracts/fractions was first evaluated to determine non-toxic concentrations to be tested in subsequent assays. In that sense, cell viability was evaluated at 9 days (endpoint to assess cell proliferation) and 18 days (endpoint to assess extracellular matrix mineralization) using a wide range of extract/fraction concentrations and presented as cell survival rates. Survival rates were not concentration dependent and always above 80 % for all samples/concentrations at 9 days (Fig. 1b) and above 75 % at 18 days (Fig. 2b). All concentrations were further used to evaluate proliferative and mineralogenic activities of the extracts.

Effect of seaweed molecules on cell proliferation

For both *C. fragile* and *C. rupestris*, none of the extracts/fractions had a pro-proliferative effect at the concentrations tested (Fig. 1a). At the highest concentrations (50 and 100 µg mL^{-1}), the AF of *C. rupestris* presented a statistically significant negative effect of 10.7 and 13.6 %, respectively, compared to the control (Fig. 1a), likely indicating a toxic effect of the highest doses tested, also supported by the fact that cell survival was also negatively affected with the same doses (Fig. 1b).

Effect of the EAF fractions on ECM mineralization

Alizarin red S staining revealed that mineralization of VSa13 extracellular matrix was strongly increased (80 % over control cultures) upon chronic exposure to the highest concentration (50 µg mL^{-1}) of both ethyl acetate fractions (Fig. 2a). In the case of *C. rupestris* EAF, pro-mineralogenic effect increased with concentration indicating a dose dependency. Aqueous fraction of *C. fragile* (50 µg mL^{-1}) significantly increased mineral deposition (30 % over control cultures), but no increase was observed at higher concentration, indicating that this result might not be of biological significance. To further validate the pro-mineralogenic effect of ethyl acetate fractions, new EAFs prepared from the same algal powder were prepared and evaluated for their capacity to increase ECM mineralization using an increased range of concentrations 5, 50, 100, and 250 µg mL^{-1}. Highest concentrations of *C. fragile* EAF (100 and 250 µg mL^{-1}) were toxic to the cells (data not

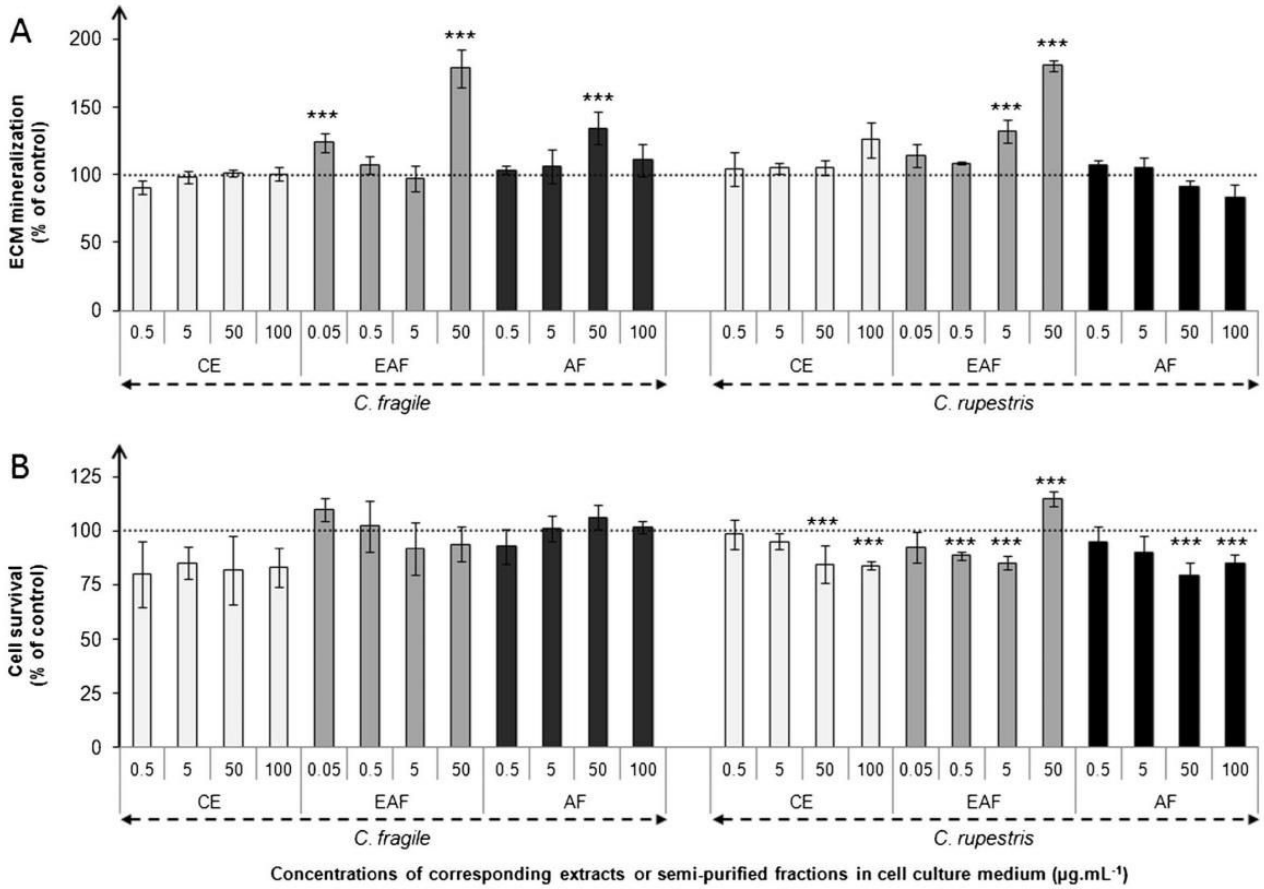

Fig. 2 Effect of crude extract and semi-purified fractions of *Codium fragile* and *Cladophora rupestris* on VSa13 extracellular matrix (ECM) mineralization (**a**) and survival (**b**) at 18 days. Control values were determined from vehicle-treated cells and set to 100 % (*dotted line*). Mineralization and survival data are presented as mean values ± standard deviation, $n = 4$ (**a**) and $n = 5$ (**b**). The *asterisks* indicate the values significantly different from the control value according to Berhens Fisher's test (**$p < 0.01$, ***$p < 0.001$). *CE* crude extract, *EAF* ethyl acetate fraction, *AF* aqueous fraction

shown) and therefore were not tested for mineralogenic activity. At 5 and 50 µg mL^{-1}, new EAF of *C. fragile* induced mineral deposition by 50 and 370 %, respectively, when compared to the control, indicating a dose-dependent effect (Fig. 3a). Similarly, new EAF of *C. rupestris* stimulated ECM mineralization in a dose-dependent manner, reaching a 630 % increase over the control at the highest concentration (250 µg mL^{-1}) (Fig. 3b). These data further confirmed the mineralogenic potential of ethyl acetate fractions prepared from both green macroalgae. For the same concentrations, the effect was higher in the second assay (recent extracts).

In vivo effect of the ethyl acetate fractions on bone-mineralized area

To further study the osteogenic action of both phenolic-enriched seaweed extracts, zebrafish larvae were exposed to ethyl acetate fractions, and in vivo bone formation and mineralization were assessed through the histomorphometric analysis of the operculum of exposed versus control larvae. After 48 h of exposure, larvae were immersed in alizarin red S, a calcium-specific dye, to stain mineralized bone structures (Gavaia et al. 2000; Bensimon-Brito et al. 2016), which at this age (11 dpf) are mainly localized in the head. The operculum is among the first structures to develop and also straightforward to identify (Laizé et al. 2014), and its area was measured to assess EAF osteogenic activity. As expected from previous studies (Fleming et al. 2005), vitamin D (used here as a positive control) increased the mineralized area of zebrafish operculum approximately 1.5-fold over vehicle, therefore validating our experiment (Fig. 4). Ethyl acetate fractions of both *C. fragile* and *C. rupestris* also increased the mineralized area of zebrafish operculum (Fig. 4). At 1, 5, and 10 µg mL^{-1}, *C. fragile* EAF significantly increased the mineralized area up to approximately 1.8-fold change over the vehicle (Fig. 4a). Higher concentrations were tested but were lethal to the larvae (data not shown). At 50 and 100 µg mL^{-1}, *C. rupestris* EAF significantly increased the mineralized area of zebrafish operculum, up to approximately 1.6-fold change over the vehicle (Fig. 4b). Our data shows that both ethyl

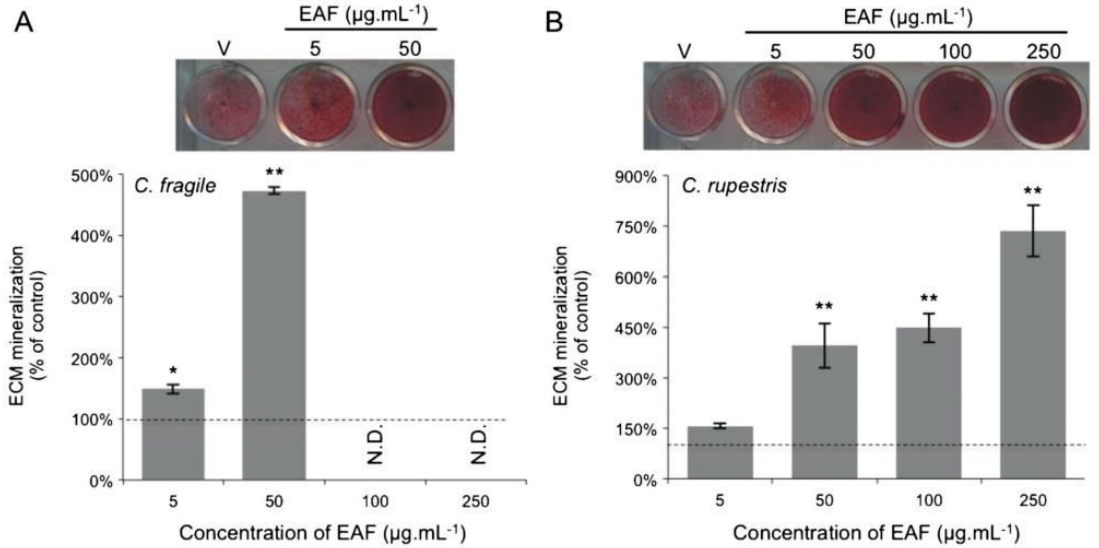

Fig. 3 Effect of ethyl acetate fraction (EAF) of *Codium fragile* (**a**) and *Cladophora rupestris* (**b**) on VSa13 extracellular matrix (ECM) mineralization. *Pictures* of cell cultures treated with either the vehicle (*V*) or different EAF concentrations and stained with alizarin red S are shown *above each graph*. Level of ECM mineralization in vehicle-treated cell cultures was set to 100 % (*dotted line*). Mineralization data are presented as mean values ± standard deviation, $n = 4$. The *asterisks* indicate the values significantly different from the vehicle value (one-way ANOVA followed by Dunnett's post hoc test; $*p < 0.05$, $**p < 0.01$). *N.D.* not determined

acetate fractions enriched in phenolic compounds increased the mineralized area of zebrafish operculum at similar or higher levels than the positive control vitamin D.

Discussion

Marine macroalgae represent an under-exploited source of phenolic compounds with high potential for therapeutic or industrial applications. In this work, we explored the bioactive potential of extracts prepared from two marine Ulvophyceae, *C. fragile* and *C. rupestris*, focusing on antioxidant and osteogenic activities. The fractionation process proved to be efficient, since the phenolic content was higher in EAF from both species, although this process seems to depend on the species studied, since the aqueous fraction from *C. rupestris*, but not from *C. fragile*, presented residual levels of phenolic compounds. The difference in the polarity of phenolic compounds produced by each species could explain the differences that occurred on each fraction. To further characterize the extracts/fractions prepared from green macroalgae, their antioxidant capacity was evaluated through two simple, fast, reliable, and classical biochemical methods—the DPPH and reducing power tests—both measuring electron transfers (Huang et al. 2005). As antioxidant molecules can act through several and complex mechanisms (Frankel and Meyer 2000), the combination of two antioxidant tests allowed us to better highlight the in vivo complexity of interactions among antioxidants in foods and biological systems (Frankel and Meyer 2000). Our results revealed that independently of the assay or the species considered, EAF fraction exhibited the highest in vitro antioxidant activities, which was also the fraction with highest content in phenolic compounds (Table 1), in agreement with previous studies indicating the antioxidative properties of phenolic compounds (Fujii et al. 2013; Tanniou et al. 2013; Stiger-Pouvreau et al. 2014; Surget et al. 2015). Since antioxidants counteract oxidative stress promoted by the increase of reactive oxygen species (ROS) and reducing power assay depends on the redox (reduction-oxidation) potential of the compounds present in a sample, we propose that phenolic compounds present in the marine macrophyte EAF are probably highly efficient antioxidants against ROS (e.g., peroxyl or hydroxyl radicals) because of their low redox potential as proposed by Zhu et al. (2002). Moreover, oxidative stress plays a key role in bone cell function (reviewed in Wauqier et al. 2009), and recent studies have evidenced bone mineralization/remodeling as one of the many biological processes influenced by natural compounds with antioxidant activity (Karadeniz et al. 2015; Córdoba et al. 2015a,b; Watson and Schönlau 2015). In agreement, our in vitro data clearly demonstrated the mineralogenic properties of *C. fragile* and *C. rupestris* EAF, the fractions with higher phenolic content and higher antioxidant activity. In vitro assays on VSa13 cells exposed to all the extracts and purified fractions evidenced that only EAF from both species increased ECM mineralization, probably by promoting cell differentiation since no proliferative effect was observed. A pro-mineralogenic effect of phenolic compounds from higher plants was previously shown in mouse osteoblastic MC3T3-E1 cells by promoting calcium deposition alone (Hagiwara et al. 2011) or in

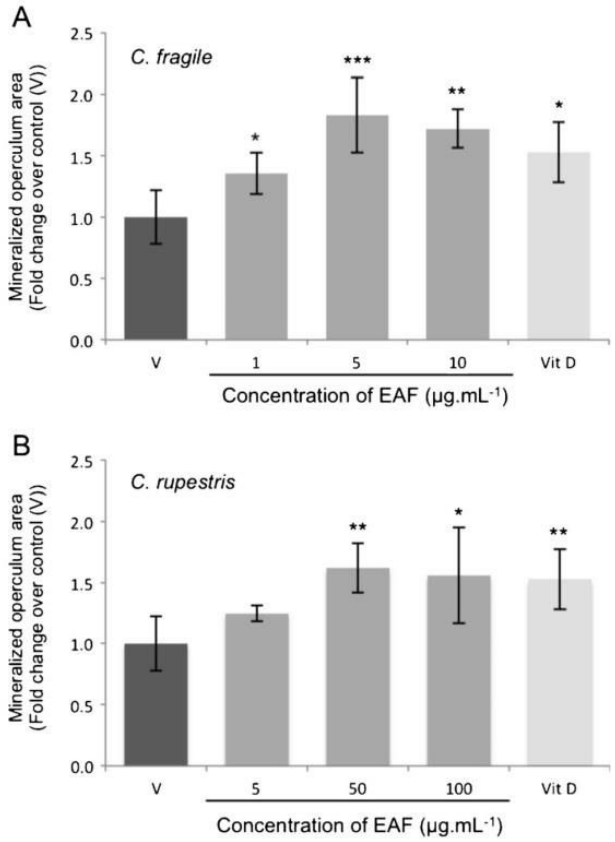

Fig. 4 Effect of ethyl acetate fraction (EAF) of *Codium fragile* (**a**) and *Cladophora rupestris* (**b**) on the mineralization of zebrafish operculum area. Larvae at 9 days post-fertilization were exposed for 48 h to increasing EAF concentrations, to vehicle (*V*), or to 1 fg mL^{-1} of vitamin D (positive control). Mineralization data are presented as mean values ± standard deviation, $n \geq 3$. The *asterisks* indicate the values significantly different from the vehicle value (one-way ANOVA followed by Tukey's post hoc test; $*p < 0.05$, $**p < 0.01$, $***p < 0.001$)

combination with increased cell viability, alkaline phosphatase activity, and collagen synthesis (Ding et al. 2010). Similar pro-mineralogenic effects were obtained with phlorotannins on the human fetal lung fibroblast MRC-5 cells (Ryu et al. 2009) or human osteosarcoma MG-63 cells (Ryu et al. 2009; Yeo et al. 2012). Several in vitro studies also evidenced the role of antioxidant molecules in restoring bone formation affected by oxidative stress through the inhibition of osteoblast differentiation (reviewed in Wauquier et al. 2009). In this regard, ROS were found to inhibit osteoblast ECM mineralization by inducing an alteration of osteogenic gene expression and an up-regulation of antioxidant systems (Mody et al. 2001; Arai et al. 2007). Also, Rao et al. (2008) discussed the stimulatory effect of polyphenol complex on osteoblast activity concomitant with a decrease of hydrogen peroxide. This suggests that compounds exhibiting antioxidant capacities could be effective by reducing tissues and intracellular ROS levels in prevention of bone diseases like osteoporosis (Wauqier et al. 2009; Rao and Rao 2015).

To get more insights on the high potential of *C. fragile* and *C. rupestris* phenolic compounds as pro-mineralogenic/osteogenic phytochemicals for biomedical applications, we confirmed our in vitro data through an in vivo assay based on developing zebrafish larvae. Indeed, the mineralized area of the operculum (a dermal bone derived from neural crest cells; Eames et al. 2012) was increased in fish exposed to EAF fractions, at similar levels promoted by vitamin D (positive control), indicating a pro-osteogenic activity of the compounds present in both *C. fragile* and *C. rupestris* phenolic-enriched fractions, validating our in vitro data, and reinforcing the pro-mineralogenic and osteogenic activities of these fractions. Importantly, these data also evidences the effect of the antioxidant phenolic-enriched fractions here studied in an in vivo system and their ability to impact on bone formation, an important feature for future biomedical applications. In fact, osteoporotic patients exhibit lower bone mineral density associated with higher oxidative stress (Almeida et al. 2007), whereas the activity of the main antioxidant enzymes is diminished (Ozgocmen et al. 2007). Mice models also showed that treatment with antioxidant enzymes inhibits bone loss (Lean et al. 2005). Recently, several studies have highlighted the therapeutic use of natural antioxidants, e.g., as dietary supplements in bone diseases such as osteoporosis or as nanocoatings to functionalize biomaterials and improve for instance current bone implants (Córdoba et al. 2015a,b; Karadeniz et al. 2015; Watson and Schönlau 2015). Thus, alternative approaches in the treatment of bone-related diseases are still needed and the potential of combined polyphenols, minerals, and vitamins which act in increasing the antioxidant capacity of the complex and thus reducing the oxidative stress correlated to bone loss as been suggested as a viable option (Rao and Rao 2015).

As a conclusion, the ethyl acetate fraction, which is rich in phenolic compounds, evidenced high antioxidant activity and high mineralogenic effect, promoting ECM mineralization of osteoblast-like cells in vitro and increasing the mineralized area of the zebrafish operculum in vivo. Thus, this study emphasized the biological potential of marine macroalgae and especially the use of invasive species, such as *C. fragile*, for future biomedical applications related to the improvement of bone status. To our knowledge, this is the first report of pro-mineralogenic activity in extracts/fraction prepared from two green macroalgae *C. fragile* and *C. rupestris*. Moreover, we demonstrated also the suitability of using zebrafish as a model for the screening of osteogenic and mineralogenic natural products. Purified extracts generated in our study and exhibiting multiple biological activities present interesting potential for industrial applications, especially in nutraceutics to prevent bone loss but also in medicine, as for example, to complement existing treatments of post-menopausal osteoporosis (Wauquier et al. 2009; Rao and Rao 2015).

Even though the identification of the active phenolic compound(s) responsible for EAF fraction activities was not the

objective of this study, compounds such as bromophenols, coumarin, or derivative from vanillic acids are known to be produced by green algae (Stengel et al. 2011) and could be the pro-mineralogenic compounds in these extracts. In that regard, future studies should be conducted to isolate, identify, and test separately the bioactive compounds present in EAF of both Ulvophyceae, *C. fragile* and *C. rupestris*, in order to better understand their mechanisms of action.

Acknowledgments This work was financed by the European Regional Development Fund (ERDF)-Atlantic Area Programme through MARMED project (grant no. 2011-1/164), the European Era-Net, Seas-Era program through the project INVASIVES (grant no. ANR-12-SEAS-0002-01), and by the Portuguese Foundation for Science and Technology (FCT) through project UID/Multi/04326/2013. The authors thank Paulo Gavaia for his help with the in vivo zebrafish system.

References

Ajila CM, Brar SK, Verma M, Tyagi RD, Godbout S, Valéro JR (2011) Extraction and analysis of polyphenols: recent trends. Crit Rev Biotechnol 31:227–249

Ali TF, Hasan T (2012) Phlorotannin-incorporated mesenchymal stem cells and their promising role in osteogenesis imperfecta. J Med Hypotheses Ideas 6:85–89

Almeida M, Han L, Martin-Millan M, Plotkin LI, Stewart SA, Roberson PK, Kousteni S, O'Brien CA, Bellido T, Parfitt AM, Weinstein RS, Jilka RL, Manolagas SC (2007) Skeletal involution by age-associated oxidative stress and its acceleration by loss of sex steroids. J Biol Chem 282:27285–27297

Andrade PB, Barbosa M, Matos RP, Lopes G, Vinholes J, Mouga T, Valentão P (2013) Valuable compounds in macroalgae extracts. Food Chem 138:1819–1828

Arai M, Shibata Y, Pugdee K, Abiko Y, Ogata Y (2007) Effects of reactive oxygen species (ROS) on antioxidant system and osteoblastic differentiation in MC3T3-E1 cells. IUBMB Life 59:27–33

Bensimon-Brito A, Cardeira J, Dionísio G, Huysseune A, Cancela ML, Witten PE (2016) Revisiting in vivo staining with alizarin red S—a valuable approach to analyse zebrafish skeletal mineralization during development and regeneration. BMC develop. Biol 16:2–9

Bonifácio BV, da Silva PB, Aparecido dos Santos Ramos M, Silveira Negri KM, Bauab TM, Chorilli M (2014) Nanotechnology-based drug delivery systems and herbal medicines: a review. Int J Nanomedicine 9:1–15

Bourgougnon N, Stiger-Pouvreau V (2011) Chemodiversity and bioactivity within red and brown macroalgae along the French coasts, metropole and overseas departments and territories. In: Kim, S-K (ed) Handbook of Marine Macroalgae: Biotechnology and Applied Phycology. Wiley, NY, pp. 58–105

Córdoba A, Satué M, Gómez-Florit M, Hierro-Oliva M, Petzold C, Lyngstadaas SP, González-Martín ML, Monjo M, Ramis JM (2015a) Flavonoid-modified surfaces: multifunctional bioactive biomaterials with osteopromotive, anti-inflammatory, and anti-fibrotic potential. Adv Healthc Mater 4:540–549

Córdoba A, Monjo M, Hierro-Oliva M, González-Martín ML, Ramis JM (2015b) Bioinspired quercitrin nanocoatings: a fluorescence-based method for their surface quantification, and their effect on stem cell adhesion and differentiation to the osteoblastic lineage. ACS Appl Mater Interfaces 7(30):16857–16864

Deslandes E, Pondaven P, Auperin T, Roussakis C, Guezennec J, Stiger V, Payri C (2000) Preliminary study of the in vitro antiproliferative effect of a hydroethanolic extract from the subtropical seaweed *Turbinaria ornata* (Turner) J. Agardh on a human non-small-cell bronchopulmonary carcimona line (NSCLC-N6). J Appl Phycol 12:257–262

Ding Y, Liang C, Yang SY, Ra JC, Choi EM, Kim J-A, Kim YH (2010) Phenolic compounds from *Artemisia iwayomogi* and their effects on osteoblastic MC3T3-E1 cells. Biol Pharm Bull 33:1448–1453

Donia M, Hamann MT (2003) Marine natural products and their potential applications as anti-infective agents. Lancet Infect Dis 3:338–348

Eames BF, Amores A, Yan Y-L, Postlethwait JH (2012) Evolution of the osteoblast: skeletogenesis in gar and zebrafish. BMC Evol Biol 12: 27–40

Eom S-H, Kim Y-M, Kim S-K (2012) Antimicrobial effect of phlorotannins from marine brown algae. Food Chem Toxicol 50: 3251–3255

Fleming A, Sato M, Goldsmith P (2005) High-throughput *in vivo* screening for bone anabolic compounds with zebrafish. J Biomolec. Screen 10:823–831

Frankel EN, Meyer AS (2000) The problems of using one-dimensional methods to evaluate multifunctional food and biological antioxidants. J Sci Food Agric 80:1925–1941

Fujii Y, Tanaka R, Miyake H, Tamaru Y, Ueda M, Shibata T (2013) Evaluation for antioxidative properties of phlorotannins isolated from the brown alga *Eisenia bicyclis*, by the H-ORAC method. Food Nutr Sci 04:78–82

Gavaia PJ, Sarasquete C, Cancela ML (2000) Detection of mineralized structures in early stages of development of marine Teleostei using a modified Alcian blue-alizarin red double staining technique for bone and cartilage. Biotech Histochem 75:79–84

Habauzit V, Horcajada M-N (2007) Phenolic phytochemicals and bone. Phytochem Rev 7:313–344

Hagiwara K, Goto T, Araki M, Miyazaki H, Hagiwara H (2011) Olive polyphenol hydroxytyrosol prevents bone loss. Eur J Pharmacol 662:78–84

Huang D, Ou B, Prior RL (2005) The chemistry behind antioxidant capacity assays. J Agric Food Chem 53:1841–1856

Imhoff JF, Labes A, Wiese J (2011) Bio-mining the microbial treasures of the ocean: new natural products. Biotech Adv 29:468–482

Kang Y-M, Eom S-H, Kim Y-M (2013) Protective effect of phlorotannins from *Eisenia bicyclis* against lipopolysaccharide-stimulated inflammation in HepG2 cells. Environ Toxicol Pharmacol 35:395–401

Karadeniz F, Kim J-A, Ahn B-N, Kwon MS, Kong C-S (2014) Effect of *Salicornia herbacea* on osteoblastogenesis and adipogenesis in vitro. Mar Drugs 12:5132–5147

Karadeniz F, Ahn B-N, Kim J-A, Seo Y, Jang MS, Nam K-H, Kim M, Lee S-H, Kong C-S (2015) Phlorotannins suppress adipogenesis in pre-adipocytes while enhancing osteoblastogenesis in pre-osteoblasts. Arch Pharmacol Res 38:2172–2182

Kim A-R, Shin T-S, Lee M-S, Park J-Y, Park K-E, Yoon N-Y, Kim J-S, Choi J-S, Jang B-C, Byun D-S, Park N-K, Kim H-R (2009) Isolation and identification of phlorotannins from *Ecklonia stolonifera* with antioxidant and anti-inflammatory properties. J Agric Food Chem 57:3483–3489

Ksouri R, Ksouri WM, Jallali I, Debez A, Magné C, Hiroko I, Abdelly C (2012) Medicinal halophytes: potent source of health promoting biomolecules with medical, nutraceutical and food applications. Crit Rev Biotechnol 32:289–326

Laizé V, Gavaia PJ, Cancela ML (2014) Fish: a suitable system to model human bone disorders and discover drugs with osteogenic or osteotoxic activities. Drug Discov Today: Disease Mod 13:29–37

Le Lann K, Jégou C, Stiger-Pouvreau V (2008) Effect of different conditioning treatments on total phenolic content and antioxidant activities in two Sargassacean species: comparison of the frondose *Sargassum muticum* (Yendo) Fensholt and the cylindrical *Bifurcaria bifurcata* R. Ross. Phycol Res 56:238–245

Le Lann K, Ferret C, VanMee E, Spagnol C, Lhuillery M, Stiger-Pouvreau V (2012) Total phenolic, size-fractionated phenolics and fucoxanthin content of tropical Sargassaceae (Fucales, Phaeophyceae) from the South Pacific Ocean: spatial and specific variability. Phycol Res 60:37–50

Lean JM, Jagger CJ, Kirstein B, Fuller K, Chambers TJ (2005) Hydrogen peroxide is essential for oestrogen deficiency bone loss and osteoclast formation. Endocrinology 146:728–735

Lee S-H, Jeon Y-J (2013) Anti-diabetic effects of brown algae derived phlorotannins, marine polyphenols through diverse mechanisms. Fitoterapia 86:129–136

Li Y-X, Wijesekara I, Li Y, Kim S-K (2011) Phlorotannins as bioactive agents from brown algae. Process Biochem 46:2219–2224

Liu M, Hansen PE, Lin X (2011) Bromophenols in marine algae and their bioactivities. Mar Drugs 9:1273–1292

Marques CL, Rafael MS, Cancela ML, Laizé V (2007) Establishment of primary cell cultures from fish calcified tissues. Cytotechnology 55:9–13

Marsham S, Scott GW, Tombin ML (2007) Comparison of nutritive chemistry of a range of temperate seaweeds. Food Chem 100: 1331–1336

Mody N, Parhami F, Sarafian TA, Demer LL (2001) Oxidative stress modulates osteoblastic differentiation of vascular and bone cells. Free Radic Biol Med 31:509–519

Montero L, Sánchez-Camargo AP, García-Canas V, Tanniou A, Stiger-Pouvreau V, Russo MT, Rastrelli L, Cifuentes A, Herrero M, Ibánez E (2016) Anti-proliferative activity and chemical characterization by comprehensive two-dimensional liquid chromatography coupled to mass spectrometry of phlorotannins from the brown macroalga *Sargassum muticum* collected on North-Atlantic coasts. J Chromatogr A 1428:115–125

Mouritsen OG (2013) Seaweeds: edible, available, and sustainable. University of Chicago Press

Ozgocmen S, Kaya H, Fadillioglu E, Aydogan R, Yilmaz Z (2007) Role of antioxidant systems, lipid peroxidation and nitric oxide in postmenopausal osteoporosis. Mol Cell Biochem 295:45–52

Pombinho AR, Laizé V, Molha DM, Marques SMP, Cancela ML (2004) Development of two bone-derived cell lines from the marine teleost *Sparus aurata*; evidence for extracellular matrix mineralization and cell-type-specific expression of matrix Gla protein and osteocalcin. Cell Tissue Res 315:393–406

Rao LG, Rao AV (2015) Oxidative stress and antioxidants in the risk of osteoporosis—role of phytochemical antioxidants lycopene and polyphenol-containing nutritional supplements. In: Rao AV, Rao LG (eds) Phytochemicals—isolation, characterisation and role in human health. InTech, Rijeka, pp. 247–260

Rao LG, Balachandran B, Rao AV (2008) Polyphenol extract of Greens + TM nutritional supplement stimulates bone formation in cultures of human osteoblast-like SaOS-2 cells. J Diet Suppl 5:264–282

Ryu B, Li Y, Qian Z-J, Kim M-M, Kim S-K (2009) Differentiation of human osteosarcoma cells by isolated phlorotannins is subtly linked to COX-2, iNOS, MMPs, and MAPK signaling: implication for chronic articular disease. Chem Biol Interact 179:192–201

Sanoner P, Guyot S, Marnet N, Molle D, Drilleau J-F (1999) Polyphenol profiles of French cider apple varieties (*Malus domestica sp.*). J Agric Food Chem 47:4847–4853

Singh IP, Bharate SB (2006) Phloroglucinol compounds of natural origin. Nat Prod Rep 23:558–591

Stanford CM, Jacobson PA, Eanes ED, Lembke LA, Midura RJ (1995) Rapidly forming apatitic mineral in an osteoblastic cell line (UMR 106_01 B.P. J Biol Chem 270:9420–9428

Stengel DB, Connan S (2015) Marine algae: a source of biomass for biotechnological applications. In: Stengel DB, Connan S (eds) Natural products from marine algae. Springer, Cham, pp. 1–37

Stengel DB, Connan S, Popper ZA (2011) Algal chemodiversity and bioactivity: sources of natural variability and implications for commercial application. Biotechnol Adv 29:483–501

Stiger-Pouvreau V, Jégou C, Cérantola S, Guérard F, Le Lann K (2014) Phlorotannins from *Sargassaceae* species: interesting molecules for ecophysiological and valorisation purposes. Adv Bot Res 71:379–412

Stiger-Pouvreau V, Bourgougnon N, Deslandes E (2016) Carbohydrates from seaweeds. In: Fleurence J, Levine I (eds) Seaweed in health and disease prevention. Elesevier, Amsterdam, pp. 223–274

Surget G, Stiger-Pouvreau V, Le Lann K, Kervarec N, Couteau C, Coiffard L, Gaillard F, Cahier K, Guérard F, Poupart N (2015) Structural elucidation, in vitro antioxidant and photoprotective capacities of a purified polyphenolic-enriched fraction from a saltmarsh plant. J Photochem Photobiol B 143:52–60

Tanniou A, Serrano Léon E, Vandanjon L, Ibánez E, Mendiola JA, Cérantola S, Kervarec N, La Barre S, Maréchal L, Stiger-Pouvreau V (2013) Green improved processes to extract bioactive phenolic compounds from brown macroalgae using *Sargassum muticum* as model. Talanta 104:44–52

Tanniou A, Vandanjon L, Incera M, Serrano Léon E, Husa V, Le Grand J, Nicolas J-L, Poupart N, Kervarec N, Engelen A, Walsh R, Guérard F, Bourgougnon N, Stiger-Pouvreau V (2014) Assessment of the spatial variability of phenolic contents and associated bioactivities in the invasive alga *Sargassum muticum* sampled along its European range from Norway to Portugal. J Appl Phycol 26:1215–1230

Watson RR, Schönlau F (2015) Nutraceutical and antioxidant effects of a delphinidin-rich maqui berry extract Delphinol®: a review. Minerva Cardioangiol 63(2 Suppl):1–12

Wauquier F, Leotoing L, Coxam V, Guicheux J, Wittrant Y (2009) Oxidative stress in bone remodelling and disease. Trends Mol Med 15:468–477

Westerfield M (2007) The zebrafish book, 5th Edition; A guide for the laboratory use of zebrafish (*Danio rerio*). Eugene, University of Oregon Press.

Woo J-T, Yonezawa T, Nagai K (2010) Phytochemicals that stimulate osteoblastic differentiation and bone formation. J Oral Biosci 52:15–21

Yeo M, Jung W-K, Kim G (2012) Fabrication, characterisation and biological activity of phlorotannin-conjugated PCL/beta-TCP composite scaffolds for bone tissue regeneration. J Mater Chem 22:3568–3577

Zhu QY, Hackman RM, Ensunsa JL, Holt RR, Keen CL (2002) Antioxidative activities of oolong tea. J Agric Food Chem 50: 6929–6934

Zubia M, Fabre MS, Kerjean V, Le Lann K, Stiger-Pouvreau V, Fauchon M, Deslandes E (2009) Antioxidant and antitumoural activities of some Phaeophyta from Brittany coasts. Food Chem 116:693–701

Conclusion et synthèse de la partie 3

Ce travail met en évidence la diversité des applications possibles des macrophytes dans un contexte de bio-inspiration et montre :

- l'efficacité du protocole de semi-purification utilisé qui permet de concentrer les composés phénoliques dans une phase acétate d'éthyle. Cette semi-purification a permis de révéler des activités biologiques importantes et nouvelles qui ne sont pas visibles dans les extraits de départ.
- la capacité antioxydante élevée, parfois comparable aux standards commerciaux, des extraits de ces macrophytes marins
- la corrélation entre une phase d'acétate d'éthyle riche en composés phénoliques et une forte activité photoprotectrice supérieure à un SPF de 13 (dans une émulsion concentrée à 10 %). Cette corrélation a également été démontrée chez une macroalgue brune native en Bretagne, *Halydris siliquosa*. La fraction acétate d'éthyle de cette espèce a été obtenue par le même protocole de semi-purification que celui décrit dans cette partie. Cette fraction est enrichie en divers phlorotannins identifiés (composés phénoliques spécifiques des macroalgues brunes). Cette fraction présente de manière intéressante un SPF d'environ 3,5. Cette étude a fait l'objet d'une publication illustrée en Annexe 1.
- La richesse en composés phénoliques chez *S. ramossisima* avec l'identification de 10 composés majoritaires dans la fraction acétate d'éthyle. Ces composés phénoliques sont des isorhamnétines, des quercétines, des acides caféiques et caféoyl (Surget et al., 2015).
- les activités photoprotectrices et ostéogéniques de ce type d'extrait. Cette dernière étude a en particulier pu montrer l'effet pro-minéralisant important des fractions acétate d'éthyle d'algues vertes (Surget et al., 2017).
- les propriétés multifonctionnelles des extraits obtenus (antioxydantes et photoprotectrices ou ostéogéniques). Une activité anti-microbienne additionnée à une activité photoprotectrice et antioxydante de la fraction acétate d'éthyle d'*Halydris siliquosa* a été démontrée (*cf.* Annexe 1).
- la corrélation entre activité antioxydante et photoprotectrice du fait de la structure propre aux composés phénoliques (structure présentée en introduction

de cette partie) mais aussi la corrélation entre activité antioxydante et pro-minéralisante.

Ainsi, de tels extraits pourraient être valorisés dans l'industrie cosmétique, pharmaceutique ou encore dans l'industrie agroalimentaire en tant qu'ingrédient actif. Bien que ce travail demeure un travail préliminaire dans l'optique d'une application industrielle de ces extraits actifs, les applications potentielles d'extraits de *Salicornia ramossisima* et *Codium fragile* seraient facilitées sachant que *Salicornia* fait partie de la liste des végétaux comestibles en France (source : CEVA) et que *Codium fragile* est largement consommé en Corée, au Japon et en Chine (Andreakis and Schaffelke, 2012; Hwang et al., 2008). De manière intéressante, cette dernière espèce présente un contenu protéique et un profil d'acides aminés similaires aux céréales, telles que le blé ou le maïs, associés à d'importantes teneurs en éléments minéraux, ainsi que de faibles teneurs en lipides (Andreakis and Schaffelke, 2012). De plus, *C. fragile* est particulièrement abondante selon les régions du monde du fait de son potentiel invasif. Cette espèce constituerait ainsi une bonne candidate en complément alimentaire non seulement pour ses propriétés nutritives (Ortiz et al., 2009) mais aussi pour ses propriétés antioxydantes et ostéogéniques démontrées par les résultats de ce travail.

Par ailleurs, des applications dans les biomatériaux seraient intéressantes à explorer. L'idée serait de complexer les composés phénoliques d'origine naturelle à une architecture temporaire en ingénierie tissulaire. De ce point de vue, ces travaux ont démontré une multifonctionnalité des extraits avec des propriétés antioxydantes, pro-minéralisantes mais également anti-microbiennes, comme illustré pour la fraction acétate d'éthyle *d'Halydris siliquosa* (*cf.* Annexe 1). D'autre part, combiner des composés phénoliques naturels à l'ingénierie des polymères permettrait de développer des composés bio-inspirés capables d'améliorer la fonctionnalité des matériaux et/ou de leur en apporter de nouvelles (Chow et al., 2013; Madhan et al., 2005).

Enfin, appliquer cette démarche de bio-inspiration à l'espèce *G. vermiculophylla* reste à être développé. En effet, *S. ramossisima* et *G. vermiculophylla* se développent dans le même type de milieu, en estran vaseux. Ces travaux ont montré également la présence de composés phénoliques chez les macroalgues et pas uniquement chez les phanérogames

marines. Même s'ils sont synthétisés dans de moindres proportions, ils peuvent présenter des activités biologiques importantes. Par ailleurs, les parties précédentes de ce manuscrit ont illustré l'efficacité des mécanismes de photoprotection impliqués dans la photoacclimatation de *G. vermiculophylla* à une variabilité des facteurs environnementaux. Il reste donc à mener la démarche chez cette macroalgue rouge invasive.

Références

Agoramoorthy, G., Chen, F.-A., Venkatesalu, V., Kuo, D.-H., Shea, P.-C., 2008. Evaluation of antioxidant polyphenols from selected mangrove plants of India. Asian J. Chem. 20, 1311.

Ajila, C.M., Brar, S.K., Verma, M., Tyagi, R.D., Godbout, S., Valéro, J.R., 2011. Extraction and analysis of polyphenols: Recent trends. Crit. Rev. Biotechnol. 31, 227–249.

Alstyne, K.L. van, 1995. Comparison of three methods for quantifying brown algal polyphenolic compounds. J. Chem. Ecol. 21, 45–58.

Amsler, C.D., 2012. Chemical ecology of seaweeds, in: Seaweed Biology. Springer, pp. 177–188.

Andreakis, N., Schaffelke, B., 2012. Invasive Marine Seaweeds: Pest or Prize?, in: Wiencke, C., Bischof, K. (Eds.), Seaweed Biology, Ecological Studies. Springer Berlin Heidelberg, pp. 235–262.

Anthoni, J., 2007. Synthèse enzymatique, modélisation moléculaire et caractérisation d'oligomères de flavonoïdes. Vandoeuvre-les-Nancy, INPL. 230.

Aparadh, V.T., Naik, V.V., Karadge, B.A., 2012. Antioxidative properties (TPC, DPPH, FRAP, Metal chelating ability, reducing power and TAC) within some cleome species. Ann. Bot. 2, 49–56.

Arai, M., Shibata, Y., Pugdee, K., Abiko, Y., Ogata, Y., 2007. Effects of reactive oxygen species (ROS) on antioxidant system and osteoblastic differentiation in MC3T3-E1 cells. IUBMB Life 59, 27–33.

Bischof, K., Rautenberger, R., 2012. Seaweed responses to environmental stress: reactive oxygen and antioxidative strategies, in: Wiencke, C., Bischof, K. (Eds.), Seaweed biology, Ecological Studies. Springer Berlin Heidelberg, pp. 109–132.

Carreto, J.I., Carignan, M.O., 2011. Mycosporine-like amino acids: relevant secondary metabolites. Chemical and ecological aspects. Mar. Drugs 9, 387–446.

Chen, C., Pearson, A.M., Gray, J.I., 1992. Effects of synthetic antioxidants (BHA, BHT and PG) on the mutagenicity of IQ-like compounds. Food Chem. 43, 177–183.

Cho, M., Lee, H.-S., Kang, I.-J., Won, M.-H., You, S., 2011. Antioxidant properties of extract and fractions from *Enteromorpha prolifera*, a type of green seaweed. Food Chem. 127, 999–1006.

Choo, K., Snoeijs, P., Pedersén, M., 2004. Oxidative stress tolerance in the filamentous green algae *Cladophora glomerata* and *Enteromorpha ahlneriana*. J. Exp. Mar. Biol. Ecol. 298, 111–123.

Chow, J.P., Simionescu, D.T., Warner, H., Wang, B., Patnaik, S.S., Liao, J., Simionescu, A., 2013. Mitigation of diabetes-related complications in implanted collagen and elastin scaffolds using matrix-binding polyphenol. Biomaterials 34, 685–695.

Cockell, C.S., Knowland, J., 1999. Ultraviolet radiation screening compounds. Biol. Rev. 74, 311–345.

Cruces, E., Rautenberger, R., Rojas-Lillo, Y., Cubillos, V.M., Arancibia-Miranda, N., Ramírez-Kushel, E., Gómez, I., 2017. Physiological acclimation of *Lessonia spicata* to diurnal changing PAR and UV radiation: differential regulation among down-regulation of photochemistry, ROS scavenging activity and phlorotannins as major photoprotective mechanisms. Photosynth. Res. 131, 145–157.

De Nys, R., Steinberg, P.D., 2002. Linking marine biology and biotechnology. Curr. Opin. Biotechnol. 13, 244–248.

Đudarić, L., Fužinac-Smojver, A., Muhvić, D., Giacometti, J., 2015. The role of polyphenols on bone metabolism in osteoporosis. Food Res. Int., Food bioactive compounds: quality control and bioactivity. 77, Part 2, 290–298.

Eddy, D.M., C.c, J.J., Cummings, S.R., Dawson-Hughes, B., Lindsay, R., Melton, L.J., Slemenda, C.W., 1998. Osteoporosis: Review of the evidence for prevention, diagnosis, and treatment and cost-effectiveness analysis. Status report. Osteoporos. Int. 8.

Edreva, A., 2005. The importance of non-photosynthetic pigments and cinnamic acid derivatives in photoprotection. Agric. Ecosyst. Environ., Photosynthesis and abiotic stresses 106, 135–146.

Edreva, A., Velikova, V., Tsonev, T., Dagnon, S., Gürel, A., Aktaş, L., Gesheva, E., 2008. Stress-protective role of secondary metabolites: diversity of functions and mechanisms. Gen Appl Plant Physiol 34, 67–78.

Fleurence, J., Levine, I., 2016. Seaweed in health and disease prevention. Academic Press. 459p.

Grassmann, J., Hippeli, S., Elstner, E.F., 2002. Plant's defence and its benefits for animals and medicine: role of phenolics and terpenoids in avoiding oxygen stress. Plant Physiol. Biochem., Free radicals and oxidative stress in plants: A new insight 40, 471–478.

Gupta, S., Abu-Ghannam, N., 2011. Recent developments in the application of seaweeds or seaweed extracts as a means for enhancing the safety and quality attributes of foods. Innov. Food Sci. Emerg. Technol. 12, 600–609.

Habauzit, V., Horcajada, M.-N., 2008. Phenolic phytochemicals and bone. Phytochem. Rev. 7, 313–344.

Heim, K.E., Tagliaferro, A.R., Bobilya, D.J., 2002. Flavonoid antioxidants: chemistry, metabolism and structure-activity relationships. J. Nutr. Biochem. 13, 572–584.

Huang, D., Ou, B., Prior, R.L., 2005. The chemistry behind antioxidant capacity assays. J. Agric. Food Chem. 53, 1841–1856.

Hupel, M., 2011. Radiations UV et composés photoprotecteurs : étude comparée chez deux végétaux marins, l'algue brune *Pelvetia canaliculata* et l'angiosperme *Salicornia ramosissima*. Brest. 234.

Hurd, C.L., Harrison, P.J., Bischof, K., Lobban, C.S., 2014. Seaweed ecology and physiology. Cambridge University Press. 551.

Hwang, E.K., Baek, J.M., Park, C.S., 2008. Cultivation of the green alga, *Codium fragile* (Suringar) Hariot, by artificial seed production in Korea. J. Appl. Phycol. 20, 469–475.

Iken, K., 2012. Grazers on benthic seaweeds, in: Wiencke, C., Bischof, K. (Eds.), Seaweed biology, ecological studies. Springer Berlin Heidelberg, pp. 157–175.

Jallali, I., Megdiche, W., M'Hamdi, B., Oueslati, S., Smaoui, A., Abdelly, C., Ksouri, R., 2012. Changes in phenolic composition and antioxidant activities of the edible halophyte *Crithmum maritimum* L. with physiological stage and extraction method. Acta Physiol. Plant. 34, 1451–1459.

Jégou, C., 2011. Étude du genre *Cystoseira* des côtes bretonnes : taxinomie, écologie et caractérisation de substances naturelles. Brest, UBO. 311.

Karsten, U., 2012. Seaweed acclimation to salinity and desiccation stress, in: Seaweed biology. Springer, pp. 87–107.

Karsten, U., Kirst, G.O., Wiencke, C., 1992. Dimethylsulphoniopropionate (DMSP) accumulation in green macroalgae from polar to temperate regions: interactive effects of light versus salinity and light versus temperature. Polar Biol. 12, 603–607.

Keller, M.D., Kiene, R.P., Kirst, G.O., Visscher, P.T., 2012. Biological and environmental chemistry of DMSP and related sulfonium compounds. Springer Science & Business Media.

Kim, J.Y., Cho, J.-Y., Ma, Y.-K., Park, K.Y., Lee, S.-H., Ham, K.-S., Lee, H.J., Park, K.-H., Moon, J.-H., 2011. Dicaffeoylquinic acid derivatives and flavonoid glucosides from glasswort (*Salicornia herbacea* L.) and their antioxidative activity. Food Chem. 125, 55–62.

Koleva, I.I., van Beek, T.A., Linssen, J.P.H., Groot, A. de, Evstatieva, L.N., 2002. Screening of plant extracts for antioxidant activity: a comparative study on three testing methods. Phytochem. Anal. 13, 8–17.

Ksouri, R., Ksouri, W.M., Jallali, I., Debez, A., Magné, C., Hiroko, I., Abdelly, C., 2012. Medicinal halophytes: potent source of health promoting biomolecules with medical, nutraceutical and food applications. Crit. Rev. Biotechnol. 32, 289–326.

Lyons, D.A., Alstyne, K.L.V., Scheibling, R.E., 2007. Anti-grazing activity and seasonal variation of dimethylsulfoniopropionate-associated compounds in the invasive alga *Codium fragile ssp. tomentosoides*. Mar. Biol. 153, 179–188.

Madhan, B., Subramanian, V., Rao, J.R., Nair, B.U., Ramasami, T., 2005. Stabilization of collagen using plant polyphenol: Role of catechin. Int. J. Biol. Macromol. 37, 47–53.

Maisuthisakul, P., Suttajit, M., Pongsawatmanit, R., 2007. Assessment of phenolic content and free radical-scavenging capacity of some Thai indigenous plants. Food Chem. 100, 1409–1418.

Mallick, N., Mohn, F.H., 2000. Reactive oxygen species: response of algal cells. J. Plant Physiol. 157, 183–193.

Marques, C.L., Rafael, M.S., Cancela, M.L., Laizé, V., 2007. Establishment of primary cell cultures from fish calcified tissues. Cytotechnology 55, 9–13.

Ortiz, J., Uquiche, E., Robert, P., Romero, N., Quitral, V., Llantén, C., 2009. Functional and nutritional value of the Chilean seaweeds *Codium fragile*, *Gracilaria chilensis* and *Macrocystis pyrifera*. Eur. J. Lipid Sci. Technol. 111, 320–327.

Oueslati, S., Trabelsi, N., Boulaaba, M., Legault, J., Abdelly, C., Ksouri, R., 2012. Evaluation of antioxidant activities of the edible and medicinal *Suaeda* species and related phenolic compounds. Ind. Crops Prod. 36, 513–518.

Pessoa, M.F., 2012. Algae and aquatic macrophytes responses to cope to ultraviolet radiation-a Review. Emir. J. Food Agric. 24, 527.

Rafael, M.S., Marques, C.L., Parameswaran, V., Cancela, M.L., Laizé, V., 2010. Fish bone-derived cell lines: an alternative in vitro cell system to study bone biology. J. Appl. Ichthyol. 26, 230–234.

Rao, L.G., Rao, A.V., 2015. Oxidative stress and antioxidants in the risk of osteoporosis — Role of phytochemical antioxidants lycopene and polyphenol-containing nutritional supplements, in: Rao, A.V., Rao, L.G. (Eds.), Phytochemicals - Isolation, characterisation and role in human health. InTech.

Rice-Evans, C.A., Miller, N.J., Paganga, G., 1996. Structure-antioxidant activity relationships of flavonoids and phenolic acids. Free Radic. Biol. Med. 20, 933–956.

Robbins, R.J., 2003. Phenolic Acids in Foods: An overview of analytical methodology. J. Agric. Food Chem. 51, 2866–2887.

Sabeena Farvin, K.H., Jacobsen, C., 2013. Phenolic compounds and antioxidant activities of selected species of seaweeds from Danish coast. Food Chem. 138, 1670–1681.

Saha, M., Wiese, J., Weinberger, F., Wahl, M., 2016. Rapid adaptation to controlling new microbial epibionts in the invaded range promotes invasiveness of an exotic seaweed. J. Ecol. 104, 969–978.

Sampath-Wiley, P., Neefus, C.D., Jahnke, L.S., 2008. Seasonal effects of sun exposure and emersion on intertidal seaweed physiology: Fluctuations in antioxidant contents, photosynthetic pigments and photosynthetic efficiency in the red alga *Porphyra umbilicalis* Kützing (Rhodophyta, Bangiales). J. Exp. Mar. Biol. Ecol. 361, 83–91.

Silva, C.G., Herdeiro, R.S., Mathias, C.J., Panek, A.D., Silveira, C.S., Rodrigues, V.P., Rennó, M.N., Falcão, D.Q., Cerqueira, D.M., Minto, A.B.M., Nogueira, F.L.P., Quaresma, C.H., Silva, J.F.M., Menezes, F.S., Eleutherio, E.C.A., 2005. Evaluation of antioxidant activity of Brazilian plants. Pharmacol. Res. 52, 229–233.

Singh, S.P., Kumari, S., Rastogi, R.P., Singh, K.L., Sinha, R.P., 2008. Mycosporine-like amino acids (MAAs): chemical structure, biosynthesis and significance as UV-absorbing/screening compounds.

Solovchenko, A.E., Merzlyak, M.N., 2008. Screening of visible and UV radiation as a photoprotective mechanism in plants. Russ. J. Plant Physiol. 55, 719.

Stefels, J., 2000. Physiological aspects of the production and conversion of DMSP in marine algae and higher plants. J. Sea Res. 43, 183–197.

Stengel, D.B., Connan, S., Popper, Z.A., 2011. Algal chemodiversity and bioactivity: Sources of natural variability and implications for commercial application. Biotechnol. Adv., Marine Biotechnology in Europe European Science Foundation-COST Conference: “Marine Biotechnology: Future Challenges” 29, 483–501.

Stevanato, R., Bertelle, M., Fabris, S., 2014. Photoprotective characteristics of natural antioxidant polyphenols. Regul. Toxicol. Pharmacol. 69, 71–77.

Stiger-Pouvreau, V., Jégou, C., Cérantola, S., Guérard, F., & Le Lann, K., 2014. Phlorotannins in Sargassaceae species from Brittany (France): interesting molecules for ecophysiological and valorisation purposes. *Advances in Botanical Research*, *71*, 379-412.

Stiger-Pouvreau, V., Guérard, F., 2017. Bio-inspired molecules extracted from marine macroalgae: a new generation of active ingredients for cosmetics and human health. In blue biotechnology: Production and use of marine molecules, Part 2. La Barre S & Bates SS (Eds). 878.

Sun, L., Zhang, J., Lu, X., Zhang, L., Zhang, Y., 2011. Evaluation to the antioxidant activity of total flavonoids extract from persimmon (*Diospyros kaki* L.) leaves. Food Chem. Toxicol. 49, 2689–2696.

Surget, G., Stiger-Pouvreau, V., Le Lann, K., Couteau, C., Coiffard, L., Guérard, F., Poupart, N., 2015. Sunscreen and antioxidant photoprotective capacities of polyphenolic compounds originated from a salt-marsh plant extract from Brittany (France). Journal of Photochemistry and Photobiology B: Biology 143, 52–60.

Surget, G., Roberto, V., Le Lann, K., Mira, S., Laizé, V., Guérard, F., Poupart, N., Cancela, M.L., Stiger-Pouvreau, V., 2017. Green algae: a source of natural compounds with proliferative, mineralogenic and antioxidant activities. J Appl Phycol 29:575–584.

Trabelsi, N., Oueslati, S., Falleh, H., Waffo-Téguo, P., Papastamoulis, Y., Mérillon, J.-M., Abdelly, C., Ksouri, R., 2012. Isolation of powerful antioxidants from the medicinal halophyte *Limoniastrum guyonianum*. Food Chem. 135, 1419–1424.

Valentão, P., Trindade, P., Gomes, D., de Pinho, P.G., Mouga, T., Andrade, P.B., 2010. *Codium tomentosum* and *Plocamium cartilagineum*: chemistry and antioxidant potential. Food Chem. 119, 1359–1368.

Van Alstyne, K.L.V., 2008. The distribution of DMSP in green macroalgae from northern New Zealand, eastern Australia and southern Tasmania. J. Mar. Biol. Assoc. U. K. 88, 799–805.

Viegas, M.N., Dias, J., Cancela, M.L., Laizé, V., 2012. Polyunsaturated fatty acids regulate cell proliferation, extracellular matrix mineralization and gene expression in a gilthead seabream skeletal cell line. J. Appl. Ichthyol. 28, 427–432.

Wang, T., Jonsdottir, R., Ólafsdóttir, G., 2009. Total phenolic compounds, radical scavenging and metal chelation of extracts from Icelandic seaweeds. Food Chem. 116, 240–248.

Wauquier, F., Leotoing, L., Coxam, V., Guicheux, J., Wittrant, Y., 2009. Oxidative stress in bone remodelling and disease. Trends Mol. Med. 15, 468–477.

Zhang, D., Cheng, Y., Zhang, J., Wang, X., Wang, N., Chen, Y., Yang, M., Yao, X., 2008. Synergistic effect of trace elements and flavonoids from *Epimedium koreanum* Nakai on primary osteoblasts. Chin. Sci. Bull. 53, 347–356.

Conclusion générale et perspectives

Ce travail pluridisciplinaire, concernant plusieurs espèces invasives et natives appartenant aux trois grandes classes de macroalgues, ainsi que plusieurs espèces de phanérogames marines également natives et invasives, dans deux milieux constratés, *i.e.* en estran rocheux et vaseux, a porté sur les 3 problématiques suivantes :

- Quel est l'état des populations de ces espèces invasives à une échelle locale, *i.e.* en Bretagne ? Impactent-elles les écosystèmes marins qu'elles colonisent ? (Partie 1)

- Quelle est la variabilité écophysiologique de ces espèces à grande échelle ? Existe-il une acclimatation du métabolome de ces espèces invasives en limite Sud et/ou limite Nord de leur répartition ? (Partie 2)

- En s'inspirant des mécanismes d'adaptation des végétaux marins qu'ils soient natifs ou invasifs (bio-inspiration), quelles sont les voies de valorisations possibles de ces macrophytes? (Partie 3)

Pour répondre à ces trois problématiques, la première partie de ce travail (Chapitre 1 à 4) a eu pour but d'établir un socle de connaissances sur la variabilité temporelle (à l'échelle d'un cycle tidal et/ou de la saison) de la phénologie, de l'écophysiologie et de l'écologie chimique des espèces invasives étudiées au niveau de la Pointe bretonne. La seconde partie de ce manuscrit (Chapitre 5 et 6) à chercher à approfondir les connaissances sur la plasticité de la phénologie, du métabolome et de la photo-physiologie de ces espèces en fonction d'un gradient latitudinal Portugal-France-Norvège dans le but de les interpréter dans un contexte de réchauffement climatique. Et la troisième partie (Chapitre 7 et 8) a illustré comment les acquis scientifiques sur l'étude du métabolome des macrophytes marins peuvent être appliqués aux biotechnologies marines à travers deux exemples de bio-inspiration : la photoprotection et la minéralisation *in vivo*. L'ensemble de ces travaux a permis de faire progresser la réflexion et les connaissances scientifiques sur les points suivants :

- ***Gracilaria vermiculophylla,* une espèce invasive aux caractéristiques biologiques singulières**

- **Variations phénologiques de macroalgues invasives reliées aux variations environnementales**
- **Acclimatation de l'écophysiologie des macroalgues invasives étudiées**
- **La bio-inspiration : deux voies de valorisation émergentes à concrétiser**

- ***Gracilaria vermiculophylla* une espèce invasive aux caractéristiques biologiques singulières**

Ces travaux se sont concentrés notamment sur l'algue rouge *Gracilaria vermiculophylla*, bien connue à travers le monde mais encore peu étudiée en Rade de Brest. A notre connaissance, hormis la localisation géographique et l'étude du cycle de vie de *G. vermiculophylla* menée par Rueness (2005), l'étude de cette espèce dans les vasières de la Rade de Brest n'avait fait l'objet d'aucune publication au commencement de ce travail. En Rade de Brest, contrairement aux autres littoraux qu'elle colonise, les thalles forment de grands tapis denses et très envasés avec une phénologie atypique (Chapitre 1). Nous avons ainsi décrits que des fragments de thalles de *G. vermiculophylla* sont présents dans les sédiments à plus de 10 cm de profondeur, que ces fragments enfouis représentent une forte biomasse (environ un tiers de celle du tapis) et qu'ils se fragmentent proportionnellement à la profondeur. Ces thalles sont vivants puisque nous avons montré qu'ils maintenaient leurs fonctions physiologiques élémentaires telles que la respiration et la photosynthèse, et ce tout au long de l'année (Chapitre 2). II a été démontré par imaging Pam la fonctionnalité de son photosystème II, laquelle méthode nous a permis de travailler sur des thalles isolés et de voir que les thalles étaient physiologiquement actifs bien que présents dans des sédiments enfouis à plusieurs cm. Cette tolérance à de telles conditions de vie, montre que *Gracilaria vermiculophylla* est fortement résistante à l'anaérobie et à l'absence de lumière. Ces résultats sous-entendent également un état de dormance en mode enfoui. Ces caractéristiques sont en effet, très singulières pour un organisme photosynthétique marin et elles amènent de nombreuses questions notamment au sujet de la compréhension des capacités physiologiques de cette espèce face à son enfouissement dans la vase, ainsi qu'au sujet du processus même d'enfouissement de cette algue dans le sédiment. Aussi, pour compléter ces résultats, le suivi de la physiologie de cette algue suite à un enfouissement artificiel permettrait de quantifier le temps de résidence minimal et maximal dans le substrat

de fragments ayant la capacité de croître après une remise en suspension dans la collonne d'eau.

D'autre part, *G. vermiculophylla* est une espèce invasive ingénieure qui modifie profondément les habitats qu'elle envahit, en impactant notamment le compartiment biotique des environnements colonisés comme dans la ria du Faou (Chapitre 4). Cette espèce invasive n'affecte pas les espèces locales en modifiant l'habitat puisque une diminution de l'abondance et de la richesse spécifique de la macrofaune benthique n'a pas été observée durant le suivi. Au contraire, l'introduction de *G. vermiculophylla* induit une augmentation de la diversité de cette macrofaune en raison de la présence d'espèces épibenthiques liée à une complexification de l'habitat. Elle induit également une augmentation de la production primaire et de la respiration de l'écosystème sans influer sur sa productivité. Enfin, cette espèce est intégrée au réseau trophique et représente une source supplémentaire de matière organique comme démontré chez trois espèces communes de la macrofaune benthique des estrans vaseux. Poursuivre un tel suivi permettrait d'observer l'évolution dans le temps de l'impact de cette espèce sur l'écosystème vaseux. D'autre part, il serait intéressant d'élargir ce suivi à l'étude d'un autre site moins colonisé que celui du Faou afin de mesurer le degré de l'impact de cette espèce en fonction de l'étendue de sa colonisation.

- **Variations phénologiques de macroalgues invasives reliées aux variations environnementales**

Ces travaux ont mis en évidence une forte variation des critères morphologiques chez les deux espèces invasives d'estrans rocheux, *i.e*. *Codium fragile* et *Sargassum muticum*, à une échelle locale (Chapitres 1 et 5) ainsi qu'une variation rapide de la structure en tailles de la population de *G. vermiculophylla* dans la ria de Aveiro (Portugal) entre l'été 2014 et 2015.

Chez *C. fragile*, il a pu être démontré l'existence d'une forte hétérogénéité de la densité et du taux de recouvrement entre la Norvège d'une part, et la France et le Portugal d'autre part. La poursuite d'un suivi du *C. fragile* entre la France et la Norvège pourrait permettre de confirmer cette première observation. Le même type d'hétérogénéité a été observé précédemment entre les côtes anglaises et canadiennes, en l'imputant à une plus forte diversité de la flore en Europe (Chapman, 1999). Ainsi, coupler un suivi écologique

associant suivi de la densité des populations de *C. fragile* et suivi de la diversité spécifique de la flore benthique à des mesures physiologiques (mesures de photosynthèse et du stress oxydant), telles qu'effectuées sur *G. vermiculophylla* en France et au Portugal permettrait de mieux comprendre l'origine de cette variabilité.

Cette forte plasticité chez *C. fragile* et *S. muticum* soulève de nombreux questionnements quant au rôle de celle-ci dans le succès de la colonisation de ces espèces invasives. Lande (2015) émet l'hypothèse selon laquelle la plasticité phénotypique d'une espèce atteindrait un maximum au cours de l'ensemble de sa période de colonisation. Une plasticité accrue dans les zones d'introduction des espèces invasives est dépendante de différents facteurs : de la différence de phénotype optimal entre les environnements (d'origine et d'introduction), de la différence de prévisibilité des deux environnements, du coût de la plasticité et du temps écoulé depuis l'introduction des populations non-natives. De plus, l'importance relative de ces facteurs dépend du fait qu'un caractère phénotypique se développe par une plasticité, labile ou non, induisant un développement continu et réversible tout au long de la vie adulte (Lande, 2015). La mise en place d'indicateur(s) quantifiable(s) de cette plasticité permettrait une comparaison basée sur des critères homogènes d'un suivi à l'autre et permettrait ainsi de suivre la temporalité de la plasticité des espèces invasives afin de vérifier les hypothèses émises par Lande (2015).

- **Acclimatation de l'écophysiologie des macroalgues invasives étudiées**

Les mesures des paramètres photosynthétiques sont des indicateurs pertinents de la physiologie générale. La capacité d'acclimatation de la photo-physiologie des organismes photosynthétiques leur fournit un avantage compétitif dans un environnement hétérogène ou sujet à des changements environnementaux, comme c'est le cas dans un contexte de changement climatique (Delebecq, 2011; Walters, 2005). L'étude de la photo-physiologie de *Sargassum muticum* et *Gracilaria vermiculophylla* a montré une photoinhibition du photosystème II de type dynamique accrue (au cours de la marée basse d'une marée de vives eaux) en été au Portugal, en comparaison de la Pointe bretonne illustrant le potentiel d'acclimatation de ces espèces (Chapitres 5 et 6).

D'autre part, le niveau de stress oxydant est un autre bon indicateur de la fitness d'un organisme et le système antioxydant joue un rôle clé dans la protection de l'appareil

photosynthétique chez les végétaux. Les résultats mettent en évidence l'activation de la SOD chez *S. muticum* en hiver couplée à un niveau élevé de la péroxydation lipidique en comparaison de l'été (Chapitre 3). Aucune variation de l'activité de cette enzyme n'a pu être mise en évidence pour *G. vermiculophylla,* que ce soit en fonction des saisons ou du gradient entre la France et le Portugal (Chapitres 3 et 6). Le test SOD est un test pertinent pour détecter des traits adaptatifs (à travers la profondeur ou le gradient latitudinal par exemple) alors que des réponses à court terme à un stress important sont moins reflétés par des variations de l'activité de la SOD (Hurd et al., 2014). Ces résultats semblent ainsi indiquer une faible adaptation physiologique chez *G. vermiculophylla* entre la France et le Portugal en s'appuyant sur ces résultats de l'activité de la SOD. Cette hypothèse reste à être confirmée en conditions contrôlées. Cependant, l'activité de la SOD mesurée dans ce manuscrit, soit celle de la SOD totale, reflète l'activité de cette enzyme pour l'ensemble de la cellule. Mais cette enzyme présente plusieurs formes selon sa localisation cellulaire : dans les mitochondries et peroxysomes, le cytosol ou dans les chloroplastes. Il serait intéressant d'affiner la connaissance du stress oxydant notamment en discriminant l'activité des différentes formes de la SOD (Alscher et al., 2002).

Comme suggéré dans le paragraphe précédent, des expériences de « common garden » (en effectuant des expériences sur les différentes populations dans les mêmes conditions abiotiques) permettraient de compléter ces diverses données *in situ* et d'apprécier la variation de la résilience des différentes populations le long du gradient latitudinal vis-à-vis du stress thermique notamment. En effet, la capacité d'acclimatation, voire d'adaptation des espèces aux changements de température, va déterminer leur résilience face au réchauffement climatique et ainsi leur vulnérabilité (Harley et al., 2006). De telles données permettraient de confirmer ou d'infirmer les hypothèses émises à partir de ces différentes observations *in situ*. Cependant, ce type d'étude implique une maîtrise du cycle de vie ou au minimum le maintien en culture des thalles des différentes espèces.

D'autre part, ces travaux ont mis en évidence la variabilité du métabolome de ces espèces invasives, en particulier chez *C. fragile* et *G. vermiculophylla* en fonction des saisons et/ou du gradient latitudinal et de l'enfouissement. Ainsi, les analyses du métabolome effectuées sur l'ensemble des chapitres (Chapitres 1, 2 et 6) mettent en évidence la

pertinence des analyses RMN dans la compréhension de la variabilité des osmolytes en fonction des conditions environnementales, ainsi que l'intérêt de l'analyse des classes de lipides dans la compréhension de l'écologie et de la physiologie de ces espèces (Chapitres 1 et 6). Les analyses RMN permettent non seulement l'identification mais aussi la quantification de plusieurs métabolites simultanément (Chapitre 1, 2 et 6). Ces analyses pourraient être élargies à d'autres types d'extraits dans le but de cibler d'autres familles de molécules que les osmolytes. Ces études très informatives nécessitent cependant au préalable l'identification des métabolites observés. Ce travail d'identification peut constituer un frein à l'utilisation de ce type d'analyse. Cependant, ce travail d'identification peut être limité par l'utilisation d'analyses multivariées permettant de cibler les métabolites à identifier.

- **La bio-inspiration : deux voies de valorisation émergentes à concrétiser**

La dernière partie de ce manuscrit a illustré deux exemples de bio-inspiration. Tout d'abord, il a été démontré quelles étaient les molécules responsables de l'activité photoprotectrice et antioxydante d'un extrait enrichis en composés phénoliques (identifiés) chez une halophyte et une algue brune, puis la mise en évidence de l'activité ostéogénique et antioxydante de ce même type d'extrait de deux macroalgues vertes, une invasive et l'autre native. Les propriétés multifonctionnelles des extraits reflètent les multiples fonctions des métabolites au sein des végétaux marins (comme les multiples activités biologiques du DMSP citées dans la partie 2 de ce manuscrit). Ainsi, faire le lien entre une compréhension fine de la biologie marine et ses applications biotechnologiques est primordial dans une optique de bio-inspiration efficace (Le Lann, 2009 ; Stengel et al., 2011 ; Bourgougnon et Stiger-Pouvreau 2011 ; Stiger-Pouvreau and Guérard, 2017).

Dans un premier temps, il serait prioritaire de rechercher à obtenir ce même type d'extrait en utilisant des procédés d'extraction écoresponsables tout en conservant leurs propriétés intéressantes. En effet, Tanniou et al. (2013) a montré que certains procédés écoresponsables tels que l'extraction accélérée par solvant ou la chromatographie de partage centrifuge représentaient d'intéressants procédés pour extraire des composés phénoliques actifs de *S. muticum*. C'est également tout l'enjeu du projet FUI20 RIV-AGE2.0 qui a démarré en décembre 2015 au LEMAR, en partenariat avec le laboratoire MMS de l'université de Nantes et trois sociétés, CHIMEX, C-Weed Aquaculture et TechNature (pilote

du projet). Les objectifs de ce projet sont de valoriser les champs d'algues bretons ainsi que les algues cultivées par un algoculteur, dans le but d'en extraire des polyphénols actifs, par des procédés écoresponsables à partir d'algues stables (biomasse, activités) dans l'année. D'autre part, l'obtention de fractions purifiées de composés phénoliques actifs et « propres » permettrait de les proposer comme ingrédients pour divers secteurs industriels, comme la cosmétologie par exemple.

Dans la prolongation de l'étude des propriétés pro-minéralisantes des extraits semi-purifiés obtenus dans ce travail, il serait intéressant de tester cette activité sur un autre modèle cellulaire de type mammifère (par exemple, MC3T3-E1). Par ailleurs, dans l'optique d'une application potentielle en parapharmaceutique et plus spécifiquement en tant que complément alimentaire contre l'ostéoporose par exemple, une étude de digestibilité des extraits serait nécessaire afin de savoir si les composés actifs sont assimilés par le système digestif humain et dans quelles proportions.

Enfin, l'utilisation de ressources naturelles impose une connaissance de la variabilité de la biomasse, mais également de la variabilité des activités des molécules d'intérêt, ceci en lien avec l'acclimatation spatiale et temporelle de la physiologie et du métabolome des algues, comme illustré dans les deux premières parties de ce manuscrit. C'est tout l'enjeu des études pluridisciplinaires fédérant les chercheurs de divers domaines, *i.e.* biologistes, biochimistes, écologues, économistes, généticiens, géographes, physiologistes.

En conclusion, les études réalisées sur les macroalgues des estrans rocheux démontrent la grande capacité d'adaptation de ces végétaux, en particulier des espèces invasives venues du l'autre côté du globe. Ces présents travaux démontrent que ces macroalgues risquent de bien s'acclimater voire de s'adapter au réchauffement climatique (pouvant impliquer une remontée des espèces vers les latitudes Nord). Mais la mise en évidence de telles algues est comparativement beaucoup moins étudiée dans les milieux protégés de type estuarien. Ce travail en grande partie mené sur *G. vermiculophylla* a permis de découvrir des modes de vie originaux et permet de supposer de la grande envergure potentielle de colonisation de cette algue sur l'ensemble du globe.

Références

Alscher, R.G., Erturk, N., Heath, L.S., 2002. Role of superoxide dismutases (SODs) in controlling oxidative stress in plants. J. Exp. Bot. 53, 1331–1341.

Bourgougnon, N., Stiger-Pouvreau, V., 2011. Chapter 4: Chemodiversity and bioactivity within red and brown macroalgae along the French coasts, Metropole and overseas departements and territories. In handbook of marine macroalgae: Biotechnology and Applied Phycology (ed S.-K. Kim) (2011), pp. 58-105.

Chapman, A.S., 1999. From introduced species to invader: what determines variation in the success of *Codium fragile ssp. tomentosoides* (Chlorophyta) in the North Atlantic Ocean? Helgol. Meeresunters. 52, 277–289.

Delebecq, G., 2011. Impact des facteurs hydroclimatiques sur la production primaire des macroalgues (thèse de doctorat). Lille 1.

Harley, C.D.G., Randall Hughes, A., Hultgren, K.M., Miner, B.G., Sorte, C.J.B., Thornber, C.S., Rodriguez, L.F., Tomanek, L., Williams, S.L., 2006. The impacts of climate change in coastal marine systems. Ecol. Lett. 9, 228–241.

Hurd, C.L., Harrison, P.J., Bischof, K., Lobban, C.S., 2014. Seaweed ecology and physiology. Cambridge University Press.

Lande, R., 2015. Evolution of phenotypic plasticity in colonizing species. Mol. Ecol. 24, 2038–2045.

Le Lann, K., 2009. Etude de la biodiversité des Sargassaceae (Fucales, Phaeophyceae) en milieux tempéré et tropical : écologie, chimiotaxonomie et source de composés bioactifs (thèse de doctorat). Université de Bretagne occidentale - Brest.

Rueness, J., 2005. Life history and molecular sequences of *Gracilaria vermiculophylla* (Gracilariales, Rhodophyta), a new introduction to European waters. Phycologia 44, 120–128.

Stengel, D.B., Connan, S., Popper, Z.A., 2011. Algal chemodiversity and bioactivity: Sources of natural variability and implications for commercial application. Biotechnol. Adv., Marine Biotechnology in EuropeEuropean Science Foundation-COST Conference: “Marine Biotechnology: Future Challenges” 29, 483–501.

Stiger-Pouvreau, V., Guérard, F., 2017. Bio-inspired molecules extracted from marine macroalgae: a new generation of active ingredients for cosmetics and human health. In blue biotechnology: Production and use of marine molecules, Part 2. La Barre S & Bates SS (Eds). 878.

Tanniou, A., Serrano Léon, E., Vandanjon, L., Ibanez, E., Mendiola, J.A., Cérantola, S., Kervarec, N., La Barre, S., Marchal, L., Stiger-Pouvreau, V., 2013. Green improved processes to extract bioactive phenolic compounds from brown macroalgae using as model. Talanta 104: 44-52.

Walters, R.G., 2005. Towards an understanding of photosynthetic acclimation. J. Exp. Bot. 56, 435–447.

ANNEXE

J Appl Phycol
DOI 10.1007/s10811-016-0853-0

Sunscreen, antioxidant, and bactericide capacities of phlorotannins from the brown macroalga *Halidrys siliquosa*

Klervi Le Lann[1] · Gwladys Surget[1] · Céline Couteau[2] · Laurence Coiffard[2] · Stéphane Cérantola[3] · Fanny Gaillard[4] · Maud Larnicol[5] · Mayalen Zubia[6] · Fabienne Guérard[1] · Nathalie Poupart[1] · Valérie Stiger-Pouvreau[1]

Received: 8 January 2016 / Revised and accepted: 5 April 2016

Abstract The present study focused on a brown macroalga (*Halidrys siliquosa*), with a particular emphasis on polyphenols and their associated biological activities. Two fractions were obtained by liquid/liquid purification from a crude hydroethanolic extract: (i) an ethyl acetate fraction and (ii) an aqueous fraction. Total phenolic contents and antioxidant activities of extract and both fractions were assessed by in vitro tests (Folin–Ciocalteu test, 2,2-diphenyl-1-picrylhydrazyl (DPPH) radical scavenging activity, reducing power assay, superoxide anion scavenging assay, and β-carotene–linoleic acid system). For the most active fraction, i.e., the ethyl acetate fraction, the oxygen radical absorbance capacity (ORAC) value, antibacterial activities, and sunscreen potential (Sun Protection Factor and UV-A-Protection Factor) were tested in vitro. A high correlation found between antioxidant activities and total phenolic content was interpreted as the involvement of polyphenolic compounds in antioxidant mechanisms. Interestingly, the ethyl acetate fraction appeared to be a broad-spectrum UV absorber and showed a strong bactericidal activity against *Pseudomonas aeruginosa*, *Staphylococcus aureus*, and *Escherichia coli*. In this fraction, four phenolic compounds (trifuhalols and tetrafuhalols and, for the first time, diphlorethols and triphlorethols) were identified using 1D and 2D nuclear magnetic resonance (NMR) and MS analysis. These findings are promising for the use of *H. siliquosa*, abundant in Brittany, as a valuable source of photoprotectant molecules for sunscreen and cosmetic applications.

Keywords Antioxidant · Bactericidal · Phenolic compounds · Phaeophyceae · Seaweed · ORAC value · Sunscreen potential

✉ Klervi Le Lann
klervi.lelann@gmail.com

[1] European Institute of Marine Studies (IUEM), LEMAR UMR 6539 UBO CNRS Ifremer IRD, Université de Bretagne Occidentale (UBO), Technopôle Brest-Iroise, 29280 Plouzané, France

[2] Faculty of Pharmacy, Université de Nantes, Nantes Atlantique Universités, LPiC, MMS, EA2160, 9 rue Bias, BP 53508, 44 000 Nantes, France

[3] RMN - RPE - MS, Université de Bretagne Occidentale (UBO), 6 avenue, Victor-Le-Gorgeu-CS93837, 29238 Brest Cedex 3, France

[4] Plateforme de spectrométrie de masse MétaboMER, CNRS, FR2424, Station Biologique, Place Georges Teissier, BP 74, 29682 Roscoff Cedex, France

[5] Laboratoires Science et Mer, Venelle du Carros, CS 70002, 29480 Le Relecq-Kerhuon, France

[6] EIO UMR 244, Université de la Polynésie française, LabEx CORAIL, B.P. 6570, 98702 Faa'a, Tahiti, Polynésie française

Introduction

One of the consequences of global change is an increase in the ambient level of ultraviolet (UV) radiation, particularly in southern areas (resulting from ozone depletion) (Thomas et al. 2012). This phenomenon, in addition to chronic sun exposure behavior, induces various skin-related disorders in humans, such as premature aging and skin cancer development (Lautenschlager et al. 2007; Thomas et al. 2012; Saewan and Jimtaisong 2015). UV radiation mostly consists of UV-A radiation, which penetrates deep into the dermis and epidermis and is known to be responsible for the production of reactive oxygen species (ROS), which can cause DNA damage. UV-A is also known to cause premature skin aging by damaging the underlying structures of the dermis (Ichihashi et al. 2003; Lautenschlager et al. 2007). UV-B radiation, which represents a lesser proportion of the total UV radiation

Published online: 22 April 2016

than UV-A, is known to be the solar light component the most inductive of skin cancer and can also cause DNA damage. It penetrates into the epidermis layer and causes some acute biological effects such as skin sunburn (Ichihashi et al. 2003; Lautenschlager et al. 2007). In order to lower the risk of skin diseases, topical sunscreen applications have been developed (Ichihashi et al. 2003; Lautenschlager et al. 2007; Sambandan and Ratner 2011). An optimal sunscreen combines UV-A and UV-B filters in order to provide broad-spectrum protection (Lautenschlager et al. 2007; Sambandan and Ratner 2011). Present UV filters are, however, based on chemical compounds and cause many side effects, such as irritant or allergic reactions, dermatitis, and, in a few cases, severe anaphylactic reactions (reviewed in Lautenschlager et al. 2007). Thus, biotechnological research is now focusing on natural compounds, such as phytochemicals, that show promising bioactivities for sunscreen applications (Saewan and Jimtaisong 2015), such as absorption and scattering properties and conservative actions, respectively, in sunscreen and other cosmetic products, and are suitable to replace some synthetic compounds. Among the organisms recognized as valuable sources of diverse bioactive chemicals, seaweeds remain an underexploited resource, especially in Brittany (Bourgougnon and Stiger-Pouvreau 2011). Indeed, marine brown algae synthesize polyphenols, known as phlorotannins, that present various chemical structures (Singh and Bharate 2006) and have a large spectrum of biological activities (Li et al. 2011) of interest for skin protection. For example, phenolic compounds could have some antimicrobial (Eom et al. 2012), antioxidative (Liu et al. 2011), anticancer, radioprotective, and anti-inflammatory properties (Kim et al. 2009; Kang et al. 2013). Moreover, in brown seaweeds, phlorotannins are of special interest regarding to the UV-radiation protective effect (Pavia and Brock 2000; Swanson and Druehl 2002; Schoenwaelder 2002; Huovinen and Gómez 2015).

Previous studies on development of innovative natural products for preventive skin health care have been done by our laboratory (Surget et al. 2015). Among brown macroalgae which grow along the coasts of Brittany (France) and can form dense forests in the subtidal zone, *Halidrys siliquosa* has been reported to have a high phenolic content (Stiger-Pouvreau et al. 2014) and potentially useful biological properties, such as strong antioxidant and interesting antitumor activities (Zubia et al. 2009). Moreover, this species belongs to the Sargassaceae, a family which is known to present a natural diversity in bioactive compounds and is usually used as a model system for chemotaxonomic studies (Kornprobst 2010; Stiger-Pouvreau et al. 2014).

The goal of this study was to show the sunscreen potential of phlorotannins from this marine brown alga, in particular to identify active compounds (phytochemicals) with several biological activities. It focused on antioxidative activities associated with antibacterial and photoprotection capabilities of the phenolic-enriched fraction. Moreover, the total phenolic content of this active fraction was quantified with the Folin–Ciocalteu assay and qualified by nuclear magnetic resonance (NMR) and MS analysis.

Materials and methods

Halidrys siliquosa (Linnaeus) Lyngbye (Ochrophyta, Phaeophyceae, Fucales, Sargassaceae) was collected on January 30, 2013, from the sheltered side of the Porsmeur site (N48° 28′ 51″; W4° 46′ 8″) near Lanildut (France). Apical and median parts of thalli were collected, while the holdfasts were left on place to minimize collection impact on the seaweed population. Immediately after collection, epiphytes were removed and parts of thalli were thoroughly washed with distilled water. The cleaned algae were cut into small fragments and homogenized to remove effects of intra- and inter-individual variability. Samples were freeze-dried for 72 h and ground into powder for extraction.

Crude extraction and liquid–liquid purification processes

As described below and in Fig. 1, two fractions (an ethyl acetate fraction (EAF) and an aqueous fraction (AqF)) were obtained from the purification of the hydroethanolic crude extract (CE).

Crude extraction To obtain the CE, 30 g of powder of thalli was extracted with 300 mL of ethanol/water (50/50, *v*/*v*) mixture (EtOH 50) in the dark at 40 °C for 2 h under rotary agitation (200 rpm). Sample was centrifuged at 3000×*g* at 10 °C for 10 min, and supernatant was collected. Next, the pellet was again extracted twice with 300 mL EtOH 50 in the dark at 40 °C for 1 h under rotary agitation (200 rpm), and centrifugation was repeated. Finally, 900 mL of the supernatant was obtained, pooled, and evaporated at 40 °C under vacuum to reach 100 mL of CE.

Liquid–liquid purification process CE was semi-purified in order to concentrate the phenolic compounds using a process already described (Stiger-Pouvreau et al. 2014). Briefly, the process consisted of three steps. The first step was three dichloromethane washings. The second step consisted in rinsing the aqueous phase (containing phlorotannins) with acetone and then with ethanol. Finally, the third step was three ethyl acetate rinses that permitted to obtain the aqueous (AqF) and the ethyl acetate (EAF) fractions. All further analyses were carried out on the CE and these two purified fractions.

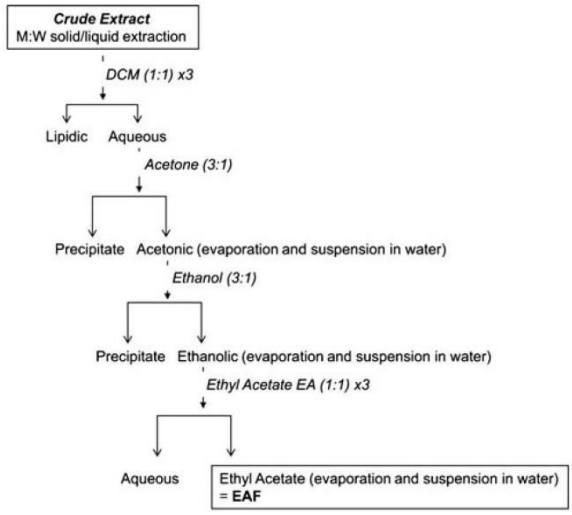

Adapted from Stiger-Pouvreau et al. 2014

Fig. 1 Procedure of liquid/liquid purification carried out on the hydroethanolic crude extract of *Halidrys siliquosa*

Total phenolic content

Total phenolic content (TPC) was determined by spectrophotometry using an adapted Folin–Ciocalteu assay as described by Le Lann et al. (2008) and Zubia et al. (2009). The samples (100 μL) were mixed with 50 μL Folin–Ciocalteu reagent, 200 μL of 20 % sodium carbonate solution, and 650 μL distilled water. Then, the mixture was allowed to stand at 70 °C in the dark for 10 min. After a blue color was produced, the absorbance was read at 650 nm. The TPC was expressed in milligram per gram of dry weight (mg g^{-1} DW) from a standard curve of phloroglucinol (1,3,5-trihydroxybenzene). This analysis was carried out in triplicate for each extract.

Antioxidant assays

2,2-Diphenyl-1-picrylhydrazyl radical scavenging activity The 2,2-diphenyl-1-picrylhydrazyl (DPPH) radical scavenging activity was determined by the method described by Zubia et al. (2009), modified from Fukumoto and Mazza (2000) and Turkmen et al. (2007). Briefly, 22 μL of CE and both fractions at various concentrations were mixed with 200 μL of a DPPH solution (25 mg L^{-1}) prepared fresh daily. The reaction was allowed to develop for 60 min in the dark at room temperature, before absorbance was read at 540 nm with a multi-well spectrophotometer. Water was used as a negative control and ascorbic acid (vitamin C), 6-hydroxy-2,5,7,8-tetramethylchroman-2-carboxylic acid (Trolox), and 2(3)-*t*-butyl-4-hydroxyanisole (butylated hydroxyl-anisole (BHA)) as positive controls. This assay was done in triplicate for each sample. The percentage of DPPH inhibition was calculated using the equation published in Surget et al. (2015). For each sample, a curve of extract concentration against % of DPPH inhibition was generated to estimate the concentration of extract needed to cause a 50 % reduction of the initial DPPH concentration. IC_{50} was expressed in milligram per milliliter. A high IC_{50} is considered as indicative of a weak radical scavenging activity and vice versa.

Reducing power assay Total antioxidant capacity of the seaweed extract was determined using the ferric reducing–antioxidant power assay, as described by Zubia et al. (2009) and slightly modified by Surget et al. (2015). Briefly, 25 μL of sample at different concentrations was mixed with 25 μL sodium phosphate buffer (0.2 M, pH 6.6) and 25 μL 1 % potassium ferricyanide [$K_3Fe(CN)_6$]. After homogenization and incubation at 50 °C for 20 min, the mixture was cooled down in an ice bath prior to the addition of 25 μL 10 % trichloroacetic acid, 100 μL deionised water, and 20 μL 0.1 % $FeCl_3 \cdot 6H_2O$. After homogenization, the reaction was allowed to develop for 10 min at room temperature and the absorbance was then read at 620 nm on a multi-well spectrophotometer. An increase of the absorbance at 650 nm of the reaction mixture indicated that the molecules had some reducing power. Results are expressed as EC_{50} in milligram per milliliter. This value was obtained by interpolation of a regression linear curve. This assay was carried out in triplicate for each sample and for the positive controls (ascorbic acid, Trolox, and BHA, as described above).

Superoxide anion scavenging activity (nitroblue tetrazolium) The superoxide anion scavenging assay was carried out according to Chua et al. (2008), as slightly modified by Tanniou et al. (2014). The reaction mixture consisted of 203 μL of 5×10^{-3} M Tris–HCl buffer (pH 7.5), 57 μL 5 mM hypoxanthine, 30 μL 0.33 mM nitroblue tetrazolium (NBT), and 13 μL of the extracts, positive controls (ascorbic acid, Trolox, and BHA) or negative controls (distilled water and ethanol). After incubation at 25 °C for 10 min, the reaction was started by adding 30 μL xanthine oxidase. The absorbance was measured every 3 min for 21 min at 560 nm. The inhibition ratio (%) was calculated from the equation published in Chua et al. (2008). Results were then expressed as IC_{50} in milligram per milliliter (the concentration of substrate that causes a 50 % inhibition).

β-Carotene–linoleic acid system test The antioxidant activity of samples was measured by the β-carotene bleaching method in accordance with Kaur and Kapoor (2002) and Koleva et al. (2002) after slight modifications, as described in Le Lann et al. (2008) and Zubia et al. (2009). Briefly, 2 mL of a solution of β-carotene in chloroform (0.1 mg mL^{-1}) was added to round-bottom flasks containing 20 mg linoleic acid and 200 mg Tween 40. After evaporation with a rotavapor, oxygenated distilled water (50 mL) was added and the mixture

was shaken to form a liposome solution. This mixture was added to 12 μL of extracts, positive controls (α-tocopherol, Trolox, and BHA) or negative controls (distilled water and ethanol). The absorbance of the solution at 450 nm was measured immediately ($t = 0$ min) and after 2 h at 50 °C ($t = 120$ min). All samples were assayed in triplicate. Antioxidant activity was expressed through the antioxidant activity coefficient (AAC700 in mg per mL) described by Le Lann et al. (2008). Furthermore, the lower the AAC700 was, the stronger the antioxidant activity became.

Oxygen radical absorbance capacity Oxygen radical absorbance capacity (ORAC) assay summarizes two results in a single value: the inhibition percentage and inhibition rapidity of peroxyl radicals by antioxidants, in competition with the substrate (Dudonné et al. 2009). The ORAC assay was performed by INVIVO LABS company (www.invivo-labs.com) on the most antioxidant fraction. The protocol was adapted from Cao et al. (1993). Results were expressed as micromole Trolox equivalent (Te) per milligram.

Antibacterial activity

Antibacterial assays were performed by IDEA LAB company (www.groupeideatests.com), Plouzané, France. The most antioxidant fraction was tested against bacteria at 5 mg mL^{-1} in 1 % EtOH. The three tested bacterial strains, referenced in the European Pharmacopoeia 7.0 - (2011), were as follows: *Pseudomonas aeruginosa* (ATCC 9027), *Staphylococcus aureus* (ATCC 6538), and *Escherichia coli* (ATCC 8739). According to the benchmarks used, a product is bactericidal if a reduction of 4 or 5 log (AFNOR and European standards) of the bacterial concentration is obtained.

Protective efficacy: sun protection factor and UV-A protection factor

The photoprotective efficiency of *H. siliquosa* extracts was determined in UV-A and UV-B ranges (respectively, 320–400 and 290–320 nm) using a previously described in vitro method (Couteau et al. 2007; El-Boury et al. 2007). Sun protection factor (SPF) is used as a universal indicator to give information about the capacity of a product to reduce UV-induced solar erythema. An in vitro method makes it possible to highlight the UV filter role of organic or inorganic substances, which could later be incorporated into a sunscreen formulation for topical application.

Concisely, extracts were incorporated in a basic oil in water (O/W) emulsion to finally obtain an emulsion at 10 % (*w*/*w*) of extracts. Fifty milligrams of prepared emulsion was spread using a cot-coated finger across the entire surface (25 cm^2) of a polymethylmethacrylate (PMMA) plate (Europlast, France). After spreading, only 15 mg of the emulsion remained on the plate. Transmission measurements between 200 and 400 nm were measured using a spectrophotometer equipped with an integrating sphere (UV Transmittance Analyzer UV1000S, Labsphere, USA). Three plates were prepared for each extract to be tested, and nine measurements were carried out on each plate. SPF and UV-A protection factor (PF-UV-A) were calculated using the following equations:

$$\mathrm{SPF} = \frac{\sum_{290}^{400} E\lambda S\lambda d\lambda}{\sum_{290}^{400} E\lambda S\lambda T\lambda d\lambda}$$

$$\mathrm{PF{-}UV{-}A} = \frac{\sum_{320}^{400} E\lambda S\lambda d\lambda}{\sum_{320}^{400} E\lambda S\lambda T\lambda d\lambda}$$

where E_λ is the erythemal spectral effectiveness at λ, S_λ is the solar spectral irradiance at λ, and T_λ is the spectral transmittance of the sample at λ (Diffey and Robson 1989).

Results are given as SPF and PF-UV-A. A higher SPF/PF-UV-A value indicates that a sample offers more protection against UV-B/UV-A by absorbance or reflection.

Structural elucidation of active molecules by nuclear magnetic resonance and matrix-assisted laser desorption/ionization time-of-flight mass spectrometry analysis

The most antioxidant fraction was analyzed by ^{1}H and ^{13}C NMR. The 1D ^{1}H- and ^{13}C-NMR heteronuclear multiple bond correlation (HMBC) and heteronuclear single-quantum correlation spectroscopy (HSQC) experiments were carried out on a Bruker Avance 500. Samples were dissolved in 750 μL MeOD. Homonuclear and heteronuclear NMR spectra were recorded at 25 °C. Chemical shifts were measured in parts per million using tetramethylsilane (TMS) as a chemical shift reference at 0 ppm.

Analysis by matrix-assisted laser desorption/ionization time-of-flight (MALDI-TOF MS) was performed using a Voyager DE-STR MALDI-TOF mass spectrometer (Applied Biosystems). The most active fraction (EAF) of *H. siliquosa* was first diluted to 1 mg mL^{-1} in water. Then, 1 μL of this solution was diluted with matrix at 1/1, 1/10, 1/100, and 1/1000 and spotted onto the MALDI target. The matrix solution consisted of 2,5 dihydroxybenzoic acid (Sigma) 10 mg mL^{-1} in 50 % ACN and 0.1 % TFA. Spectra were acquired in positive ion reflector mode under 20-kV accelerating voltage, a delay time of 80 s, and a mass range of 100–5000 Da. Each spectrum was the sum of 10,000 single laser shots randomized over ten positions within the same spot (1000 shots/position) at a laser frequency of 20 Hz. External calibration was performed using the Peptide mix 4 calibration mixture (Laser Bio Labs).

Statistical analysis

The software R (v. 2.12.0) for Windows was used, with the RStudio (v. 0.95.263) integrated development environment. All laboratory analyses were performed in triplicate, and results were expressed as mean values ± standard deviation (SD). As data did not respect the requirements for ANOVA (homogeneity of variances, tested with the Bartlett's test at the 0.05 significance level), Kruskal–Wallis tests were performed, at a significance level of 95 %, to reveal potential significant differences. In the case of significant differences between the data, non-parametric multiple comparisons (Behrens–Fisher test) were applied using the nmpc package. Moreover, to test the correlation between phenolic content and antioxidant activity, principal component analysis (PCA) was performed with the FactoMineR package and cluster analysis with the fpc and pvclust packages. Pvclust is designed to assess the uncertainty in hierarchical cluster analysis. For each cluster in the hierarchical clustering, quantities called p values are calculated via multi-scale bootstrap resampling. The p value of a cluster indicates how strongly the cluster is supported by the data. Clusters with p values larger than 95 % are strongly supported by data.

Results

Total phenolic content

The purification of the CE of *H. siliquosa* was efficient in generating a phenolic-enriched EAF, as shown in Table 1, which compares the total phenolic contents (TPCs) of the CE and semi-purified fractions. Phenolic compounds were strongly concentrated in EAF. Indeed, almost 98 % of this fraction (975.73 ± 19.26 mg g^{-1} DW) consisted of phenolic compounds. The last 2 % is probably constituted of traces of fatty acids and carbohydrates, as it is shown by the ^{1}H NMR analysis (Fig. 2). Conversely, AqF showed lower TPC (164.19 ± 7.58 mg g^{-1} DW) than CE (182.47 ± 3.33 mg g^{-1} DW; Kruskal–Wallis test: $p < 0.05$; Behrens–Fisher test).

Antioxidant activities

Table 1 shows results of the antioxidant activities of the CE and both semi-purified fractions compared with positive controls, assessed by DPPH radical scavenging activity, reducing power assay, superoxide anion scavenging activity, and the β-carotene bleaching method.

The CE and both fractions showed high DPPH radical scavenging activities. EAF exhibited the lowest IC_{50} (0.020 ± 3.54 × 10^{-4} mg mL^{-1}), close to that obtained for the positive controls (e.g., 0.010 ± 4.82 × 10^{-5} mg mL^{-1} for BHA). The other antioxidant assays confirmed the results obtained by the DPPH test. Indeed, in the reducing power assay, EAF showed a low EC_{50} compared with those of the positive controls ($p < 0.05$, Behrens–Fisher test; 0.058 ± 0.001 mg mL^{-1} and 0.074 ± 0.002 mg mL^{-1} for EAF and BHA, respectively). In the superoxide anion scavenging test, the IC_{50} displayed by EAF (0.664 ± 0.019 mg mL^{-1}) was equal to the IC_{50} obtained for BHA (0.664 ± 0.022 mg mL^{-1}). In the β-carotene bleaching method, EAF showed the lowest AAC700 (0.206 ± 0.001 mg mL^{-1}, $p < 0.05$, Behrens–Fisher test). It should be noted, however, that this AAC700 value is significantly higher than those of the positive controls (e.g., 0.015 ± 0.001 mg mL^{-1} for BHA) (Table 1). Despite this last result, EAF showed strong antioxidant activities. Furthermore, whatever the antioxidant assay considered, AqF always showed the lowest activity by exhibiting a high IC_{50} (DPPH and superoxide anion scavenging tests), a high EC_{50} (reducing power assay), and a strong AAC700 (β-carotene bleaching method). These results meant that AqF showed a weak antioxidant activity.

The EAF of *H. siliquosa* showed an interesting ORAC value of 5.39 ± 1.08 μmol TE mg^{-1} (Table 1), which is comparable to the ORAC value measured for ascorbic acid (9.35 ± 0.63) mentioned by Huang et al. (2010).

Correlations between antioxidant activities and phenolic content

It is worth noting that the EAF, with marked antioxidant activities, had the highest phenolic content (975.73 ± 19.26 mg mL^{-1} DW) whereas the AqF, which showed low antioxidant activities, had the lowest phenolic content (164.19 ± 7.58 mg mL^{-1} DW). These observations were confirmed by statistical analysis. Cluster analysis revealed a significant association between TPC and antioxidant activities (100 %). Moreover, non-significant associations were found between the two scavenging tests (DPPH radical scavenging and superoxide anion scavenging assays, 70 %) and between the reducing power test and β-carotene bleaching method (61 %). The principal component analysis (PCA, Fig. 3) confirmed that antioxidant activities were correlated with the TPC of the samples. Moreover, PCA showed that TPC values were strongly negatively correlated with EC_{50} obtained with reducing power. This means that the higher the measured TPC of a sample, the lower its EC_{50} and the stronger its antioxidant activity. Other antioxidant assays were less correlated with TPC. PCA also confirmed that DPPH radical scavenging and superoxide anion scavenging assays were positively associated.

Bactericidal activities

Results of the antibacterial assays are reported in Table 2. The negative control (1 % EtOH) had no effect on bacterial growth, whatever the pathogen. In contrast, at a concentration of 5 mg mL^{-1}, EAF showed a strong bactericidal

Table 1 Results of total phenolic content (TPC) and screening of several antioxidant activities measured on crude extract and fractions from *Halidrys siliquosa*, using radical scavenging activity (DPPH; IC_{50}), reducing power assay (RP; EC_{50}), superoxide anion scavenging test (NBT; IC_{50}), β-carotene bleaching method (BCBM, AAC_{700}), and ORAC value

Samples		TPC (mg g^{-1} DW)	DPPH; IC_{50} (mg mL^{-1}) Mean ± SD	RP; EC_{50} (mg mL^{-1}) Mean ± SD	NBT; IC_{50} (mg mL^{-1}) Mean ± SD	BCBM; AAC_{700} (mg mL^{-1}) Mean ± SD	ORAC value (μmol TE mg^{-1}) Mean ± SD
Halidrys siliquosa	CE	182.47 ± 3.33 b	0.226 ± 0.032 f	0.618 ± 0.039 e	1.345 ± 0.273 c	1.007 ± 0.01 f	nd
	AqF	164.19 ± 7.58 a	1.002 ± 0.055 e	0.59 ± 0.014 e	2.441 ± 0.401 d	1.502 ± 0.077 e	nd
	EAF	975.73 ± 19.26 c	0.02 ± 3.54E10-4 d	0.058 ± 0.001 a	0.664 ± 0.019 b	0.206 ± 0.001 d	5.39 ± 1.08
Positive controls	BHA	nd	0.01 ± 4.82E10-5 c	0.074 ± 0.002 b	0.664 ± 0.022 b	0.015 ± 0.001 c	nd
	Trolox	nd	0.007 ± 3.40E10-4 b	0.404 ± 0.037 d	0.368 ± 0.042 a	0.007 ± 0 b	nd
	Ascorbic acid	nd	0.005 ± 8.06E10-4 a	0.088 ± 0.001 c	0.367 ± 0.045 a	nd	9.35 ± 0.63[a]
	α-Tocopherol	nd	nd	nd	nd	0.005 ± 0 a	nd
	BHT	nd	nd	nd	nd	nd	24.1 ± 1.18[a]

Each value corresponds to the mean ± SD ($n = 3$). Significant differences determined by the Behrens–Fisher test ($p < 0.05$) are indicated by different letters

nd not determined, *CE* crude extract, *AqF* aqueous fraction, *EAF* ethyl acetate fraction, *TE* Trolox equivalent

[a] According to Huang et al. (2010)

activity. Indeed, this fraction showed a reduction higher than 5 log of the initial bacterial concentration with *Pseudomonas aeruginosa* and *Escherichia coli* (<1 UFC mL^{-1}). Concerning *Staphylococcus aureus*, EAF showed a bactericidal activity with a reduction of 4.5 log of the initial bacterial concentration (75 UFC mL^{-1}).

Photoprotective sunscreen activity

The absorption spectrum of the *H. siliquosa* EAF shows a band with a maximum at 376 nm. Moreover, the O/W emulsion manufactured with this phlorotannin-enriched fraction (*Halidrys* emulsion) had a SPF of 3.55 ± 0.29 and a PF-UVA value of 2.20 ± 0.13.

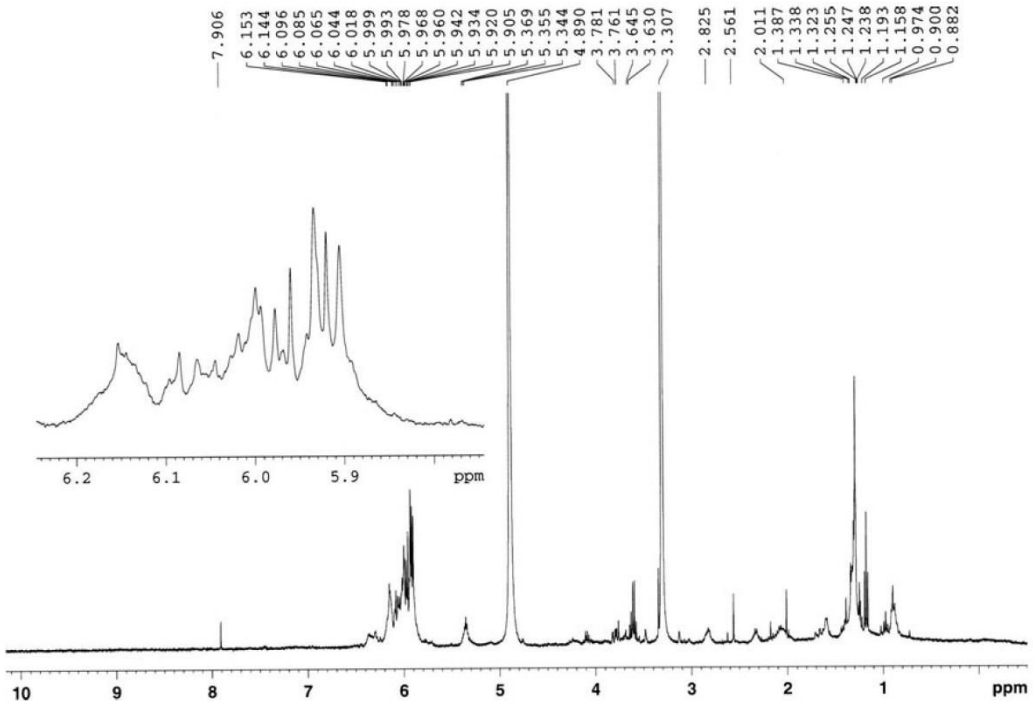

Fig. 2 ^{1}H NMR spectrum of the ethyl acetate fraction of the brown macroalga *Halidrys siliquosa* (in MeOD), focusing on the aromatic region

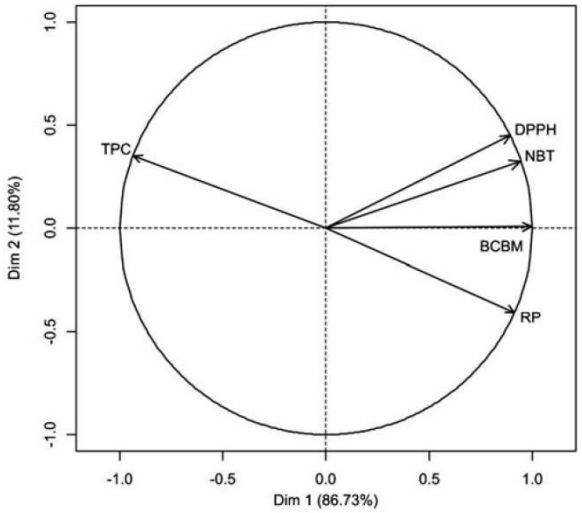

Fig. 3 Principal component analysis (PCA), applied to the active variables of radical scavenging activity (DPPH), reducing power assay (RP), superoxide anion scavenging test (NBT), and the β-carotene bleaching method (BCBM)

Structural elucidation of active molecules

Nuclear magnetic resonance analysis The ^{1}H NMR spectrum of the EAF of *H. siliquosa* showed a broader distribution of the ^{1}H signals between 5.8 and 6.3 ppm, characteristic of phlorotannins (Fig. 2). Observations from the HMBC experiments (Fig. 4 and Table 3) confirmed the presence of polyphenolic structures. Indeed, the HMBC spectrum showed characteristic carbon atom resonances at (1) 96.10 ppm, corresponding to quaternary methine groups; (2) between 124 and 132 ppm, corresponding to diaryl-ether bonds (ether-linked phloroglucinol units); (3) between 142 and 148 ppm for additional OH functions other than the 1,3,5 OH groups originally present in each phloroglucinol unit; and finally, (4) between 152 and 159 ppm, signals for phenolic carbons (Fig. 4 and Table 3). We can, therefore, hypothesize that fuhalol-type units, and also phlorethol-type units, are present. Moreover, it is worth noting the absence of signals between 100 and 105 ppm indicative of the absence of aryl-aryl carbons and, thus, the absence of fucol-type units in this purified phenolic sample.

Matrix-assisted laser desorption/ionization time-of-flight mass spectrometry

The MALDI-TOF analysis of the EAF of *H. siliquosa* revealed a molecular weight ranging from 222 to 763 Da (Table 4). It could be resumed that the EAF contained small polyphenolic compounds with no more than six phloroglucinol units (oligomers). The peak-to-peak mass increments observed at 273.06, 413.29, 523.36, and 537.38 Da could correspond to the formation of M+ Na adducts of (**1**) (250 Da), (**3**) (390 Da), and (**4**) (514 Da) (Table 4 and Fig. 5). Moreover, the peak-to-peak mass increment observed at 375.03 Da could correspond to the formation of M+ H adducts of (**2**) (374 Da). The peak-to-peak mass increments observed at 343.31 and 365.30 Da could correspond to the formation of M+ H and M+ Na adducts of a compound with a native mass of about 342 Da that seems not to be a phloroglucinol oligomer. Table 4 gives the experimental and calculated masses of the polyphenolic oligomers identified for the EAF sample (Fig. 5), together with their putative chemical structures. Masses of phlorethols and fuhalols were calculated using the respective chemical formula of a typical phlorethol and fuhalol (respectively, $C_{6n}H_{4n+2}O_{3n}$ and $C_{6n}H_{4n+2}O_{3n+i}$, where n is the number of phloroglucinol units and i was the number of additional hydroxyl groups).

Discussion

The purification process used in the present study to purify phenolic compounds from *H. siliquosa* was highly efficient to isolating oligophlorotannins. This procedure was also

Table 2 Antibacterial activity of *Halidrys siliquosa* ethyl acetate fraction (EAF, 5 mg mL^{-1} in 1 % EtOH against three selected bacterial pathogens (*Pseudomonas aeruginosa*; *Staphylococcus aureus*, and *Escherichia coli*)

Bacterial strains		T0	T24 h	Remark
Pseudomonas aeruginosa (ATCC 9027)	Growth control	1.1×10^{6}	1.3×10^{9}	
	1 % EtOH	1.1×10^{6}	1.5×10^{9}	No effect
	EAF	1.1×10^{6}	<1	Bactericide activity
Staphylococcus aureus (ATCC 6538)	Growth control	1.9×10^{6}	2.2×10^{9}	
	1 % EtOH	1.9×10^{6}	2.1×10^{9}	No effect
	EAF	1.9×10^{6}	7.5×10^{1}	Bactericide activity
Escherichia coli (ATCC 8739)	Growth control	1.6×10^{6}	1.5×10^{9}	
	1 % EtOH	1.6×10^{6}	2.5×10^{9}	No effect
	EAF	1.6×10^{6}	<1	Bactericide activity

Data are expressed in colony-forming units per milliliter

EtOH ethanol

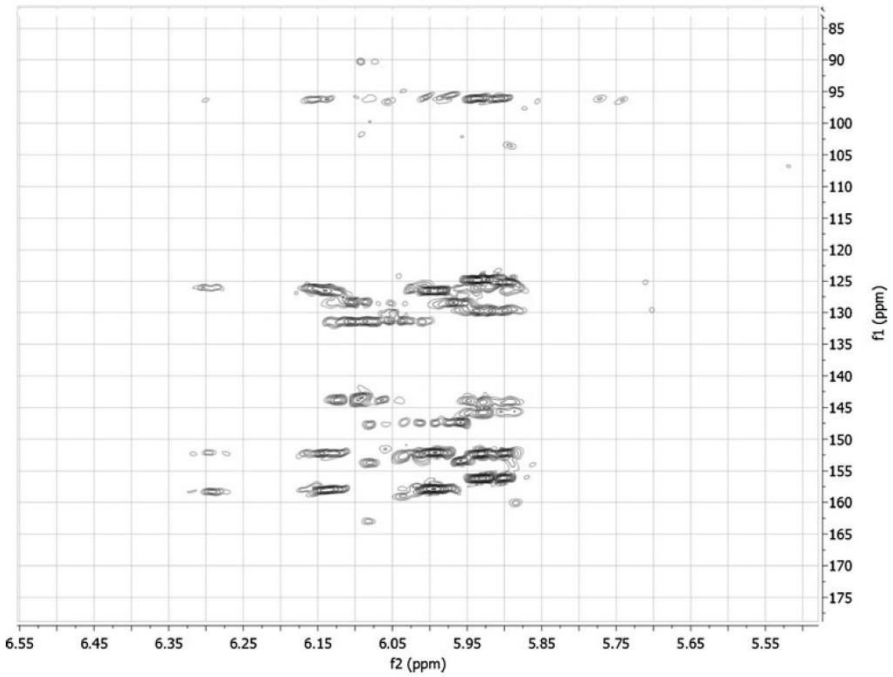

Fig. 4 HMBC contour plots of the ethyl acetate fraction of *Halidrys siliquosa* (in MeOD)

Table 3 HMBC assignments of the ethyl acetate fraction of *Halidrys siliquosa* (in MeOD)

	^{13}C (δ in ppm)	^{1}H (δ in ppm, *J* in Hz)
Quaternary methine groups	96.10	5.95, *s*
Diaryl-ether bond (ether linkage)	124.82	5.95, *s*
	125.07	5.92, *s*
	126.22	6.15, *s*
	126.52	6.14, *s*
	128.40	5.97, *s*
	129.74	5.92, *s*
	129.76	5.95, *s*
	131.21	6.05, *s*
	131.31	6.04, *s*
	131.41	6.10, *s*
Additional OH function (characteristic of fuhalol-type units)	143.80	6.12, *s*
	144.19	5.93, *s*
	145.77	5.93, *s*
	147.36	5.96, *d*, 2.5
Aromatic methine carbons (phenolic carbons)	152.26	6.14, *s*
	152.31	5.93, *s*
	152.66	6.03, *s*
	156.12	5.93, *s*
	156.21	5.2, *s*
	157.86	5.99, *s*
	158.04	6.14, *s*

described as efficient for other Sargassaceae species belonging to the genera *Bifurcaria*, *Cystoseira*, and *Sargassum* (Stiger-Pouvreau et al. 2014), for Fucaceae species such as *Pelvetia canaliculata* and *Ascophyllum nodosum* (Ar Gall et al. 2015), and also for halophytes (Surget et al. 2015). The preliminary structural analyses of the EAF, combined with data from the literature (McInnes et al. 1984; Cérantola et al. 2006), allowed the identification of four phenolic compounds: diphlorethols and triphlorethols and trifuhalols and tetrafuhalols. Until now, little information has existed on the chemical nature of phenolic compounds produced by *H. siliquosa*. Fuhalols had already been described in this species (Glombitza and Sattler 1973; Sattler et al. 1977), but as these studies were done on non-native compounds (peracetylated compounds), the true nature of the phlorotannins present in *H. siliquosa* was not fully explored. Moreover, the present study is the first time which identified phlorethol-type compounds in this species. Phlorethols are known to be present in other Sargassaceae species, such as in *Sargassum muticum* and some *Cystoseira* species from Brittany (see Stiger-Pouvreau et al. 2014 for a review). Moreover, the co-occurrence of fuhalols and phlorethols was already known in other Sargassaceae species, like *Cystoseira tamariscifolia* (Glombitza et al. 1975) and *Sargassum spinuligerum* (Keusgen and Glombitza 1995), but not in *H. siliquosa*. Additionally, the phenolic compounds identified in *H. siliquosa* in the present study were oligomers of phloroglucinol. These results are in line with previous data on Sargassaceae species, which produces low-molecular-weight phenolic compounds (Le Lann et al. 2012a; Le Lann

Table 4 Experimental and calculated masses and putative chemical structures of polyphenolic oligomers identified by MALDI-TOF assisted by $^{13}C/^{1}H$ NMR, for the ethyl acetate fraction of *Halidrys siliquosa*

Experimental measure (*m/z*)	Calculated *m/z*		Identified phloroglucinol oligomers	Calculated native masses (Da)
	M+ Na (+22.99 Da)	M+ H (+1 Da)		
273.06	273.19		(1) Diphlorethol	250.20
375.03		375.30	(2) Triphlorethol	374.30
413.29	413.29		(3) Trifuhalol	390.30
537.38	537.39		(4) Tetrafuhalol	514.40

et al. 2012b; Harnita et al. 2013; Jégou et al. 2015; Montero et al. 2016) rather than high-molecular-weight phlorotannins as observed in the Fucaceae and Laminariales (Wang et al. 2012; Shibata et al. 2015; Heffernan et al. 2015).

In order to characterize the antioxidant capacity of extracts and fractions of *H. siliquosa*, four fast, reliable, and classical biochemical methods were used. Three of them (DPPH, NBT, and reducing power tests) represent a single-electron transfer (SET) reaction, whereas the β-carotene bleaching method (BCBM) represents a hydrogen atom transfer (HAT) reaction (Huang et al. 2005). The antioxidant molecules can act as inhibitors of lipid oxidation through various different mechanisms in addition to free radical trapping, e.g., prevention of chain initiation, binding of transition metal ion catalysts, or peroxide decomposition (Frankel and Meyer 2000). Thus, simple in vitro tests are an approach to evaluate the antioxidant capacity of samples, and the combination of four of them made it possible to bypass the inability of a one-dimensional test of antioxidant capacity to accurately mirror the in vivo complexity of interactions between antioxidants in foods and biological systems (Frankel and Meyer 2000).

Among the tested samples, the EAF exhibited the highest antioxidant activity independent of what assay was used. Moreover, its antioxidant activity was equivalent to those displayed by the commercial antioxidants used as positive controls in this study (ascorbic acid, α-tocopherol, BHA, and Trolox) for the SET assays (DPPH, NBT, and reducing power). These results were reinforced by the ORAC value obtained for the EAF. Indeed, the ORAC value of the EAF (5.39 ± 1.08 μmol TE mg^{-1}) was close to the ORAC values obtained for ascorbic acid in the literature (Huang et al. 2010; Ishimoto et al. 2012; Fujii et al. 2013). For the BCBM, the activity of the EAF is higher than those of commercial antioxidants. This test measures the activity of lipophilic molecules (Koleva et al. 2002; Le Lann et al. 2008), so the active compounds would therefore tend to be polar or faintly apolar compounds. Moreover, in the BCBM, the system is complex, and the emulsified lipid in use introduces additional variables liable to affect the oxidation process (Zubia et al. 2009).

To our knowledge, this study is the second to provide evidence for the existence of high antioxidant activity in this seaweed species, following a screening of antioxidant and antitumor activities of non-identified phlorotannins (Zubia et al. 2009). However, our paper is the first to identify active purified native phlorotannins from *H. siliquosa*. Moreover, the antioxidant activities exhibited by the extract and fractions of *H. siliquosa* were positively correlated with their phenolic contents. Additionally, Fujii et al. (2013) evaluated the antioxidative properties of phlorotannins isolated from the brown alga *Eisenia bicyclis* (Laminariales, Lessoniaceae). These

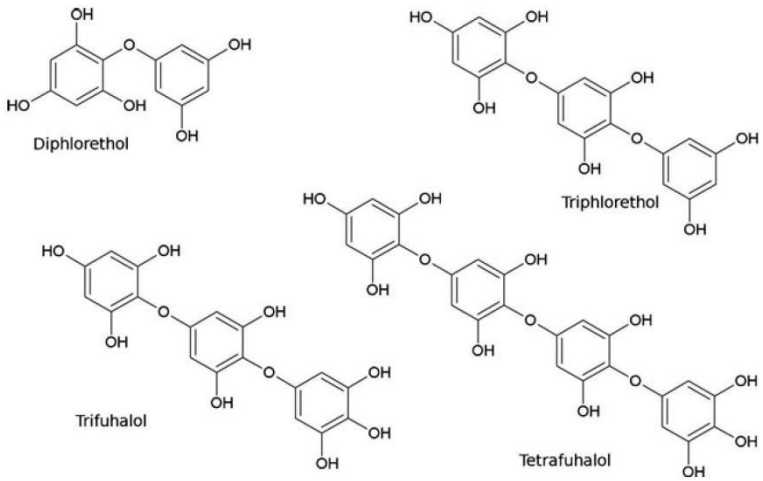

Fig. 5 Chemical structures of phlorotannins identified in the ethyl acetate fraction of the brown alga *Halidrys siliquosa*

authors found H-ORAC values of phloroglucinol (20.38 ± 1.11 μmol TE mg^{-1}) and various eckols (H-ORAC values between 11.6 ± 1.2 and 20.62 ± 1.46 μmol TE mg^{-1}). In the same way, in 2010, Parys et al. (2010) published ORAC values for phloroglucinol and fucophlorethols isolated from *Fucus vesiculosus*. Despite the unusual units used by these authors, their results showed that phloroglucinol was a little more active than fucophlorethols, meaning that oligomers of phloroglucinol could be more active than polymers for this test. Thus, our present study highlights, for the first time, the antioxidative potential of small phenolic compounds (oligofuhalols and oligophlorethols) from *H. siliquosa*. This enhances previous results on the high antioxidant potential of phenolic compounds from brown seaweeds. Further studies should now be carried out to isolate each phenolic compound and test them separately, to study potential synergy between phytochemicals. Furthermore, the marked correlation between the reducing power and the TPC could provide information on the antioxidant mechanism of phenolic compounds from *H. siliquosa*. Indeed, the reducing power determined in this work depends on the redox potentials of the compounds present in the sample. Therefore, it can be predicted that the phlorotannins present in the *H. siliquosa* EAF show low redox potential and, thus, a high antioxidant efficiency against free radicals (peroxyl or hydroxyl radicals) (Zhu et al. 2002).

The EAF of *H. siliquosa* also showed bactericidal activities against three bacterial strains: *Pseudomonas aeruginosa*, *Escherichia coli*, and *Staphylococcus aureus*. The antimicrobial activities of phenolic compounds from seaweeds are very well known (see Eom et al. 2012 for a review), including phenolic compounds from *H. siliquosa* (Sattler et al. 1977). The antibacterial activities of phlorotannins were reviewed by Li et al. (2011), but this is the first time that bactericidal activities have been reported for a phenolic-rich fraction from *H. siliquosa*. More specifically, phlorotannins from *Ascophyllum nodosum* showed bactericidal activities against *Escherichia coli* (Wang et al. 2009). The bactericidal activities of phenolic compounds seemed to be related to the number of hydroxyl groups (Smith et al. 2003; Wang et al. 2009) and to the degree of polymerization of phloroglucinol within phlorotannins (Nagayama et al. 2002). Moreover, Wang et al. (2009) suggested that condensed phlorotannins with high hydroxylation may inhibit bacterial growth by altering the cell membrane (Wang et al. 2009). The fuhalol compounds identified in the EAF of *H. siliquosa* have high hydroxyl functions. The oxidation potential of hydroxyl groups, well known in phlorotannins (Ragan and Glombitza 1986), could explain their bactericidal activity, by alteration of bacterial cell membranes. Because this work is a preliminary study, there is now a need to test the dose effect to identify the minimum inhibitory concentration (MIC) and the minimum bactericidal concentration (MBC) of the EAF. Nevertheless, such fraction is interesting and could be used in cosmetic formula itself as natural conservators.

The SPF obtained for the *Halidrys* emulsion is similar to eight UV pure synthetic filters authorized in the European Union, like homosalate for example, tested in O/W emulsion with the same method (Couteau et al. 2007). While UV-B protection is imperative, UV-A protection is now recognized as being equally essential. Indeed, if UV-B is considered as "burning rays," then UV-A can be considered as "aging rays" (Lautenschlager et al. 2007; Saewan and Jimtaisong 2015). With a maximal absorbance (376 nm) in the UV-A range (400–320 nm) and a PF-UV-A about 2.20 ± 0.13, the EAF of *H. siliquosa* exhibited an absorbance and a sunscreen activity similar to the synthetic filter Avobenzone (358 nm and 2.76 ± 0.31 for maximal absorbance and PF-UV-A, respectively) (Lohézic-Le Dévéhat et al. 2013). So, the EAF obtained from *H. siliquosa* is interesting because it appears to be a broad-spectrum UV absorber, useful to be included as a natural filter in solar cream for example.

The photoprotective capacities of plant extracts have been demonstrated in previous studies. Indeed, using a similar in vitro UV method, three sunscreen emulsions with ethyl acetate plant extract (10 wt%) were tested in vitro and authors obtained SPF and PF-UV-A values ranging from 6.00 ± 0.42 to 9.88 ± 1.66 and from 3.64 ± 0.07 to 6.96 ± 0.21, respectively (Jarzycka et al. 2013). Likewise, using the same protocol as the present study, one acetonic extract of the lichen *Lasallia pustulata* was found to have SPF and PF-UV-A maxima of 5.52 and 2.45, respectively (Lohézic-Le Dévéhat et al. 2013). Furthermore, usnic acid, extracted from the lichen *Xanthoparmelia farinosa*, was described as the best UV-B filter tested, with a protection factor similar to a commercial product called LSF 5 (4.1; Rancan et al. 2002). Among marine macrophytes, the EAF from a *Salicornia ramosissima* extract is an interesting candidate to provide an effective protective action over the whole UV-A–UV-B range, with large SPF and PF-UV-A values (Surget et al. 2015). Moreover, the photoprotection efficiency of seaweed extracts has been demonstrated for several species, as recently reviewed by Saewan and Jimtaisong (2015). For example, the photoprotective potential of extracts obtained from 11 commercial brown algae and 10 commercial red algae was evaluated against UV-B radiation (Guinea et al. 2012). In the same way, phlorotannins isolated and purified from *Ecklonia cava* were demonstrated as effective at protecting against UV-B radiation (Cha et al. 2012). Both of these studies used an in vivo test with a zebrafish (*Danio rerio*) embryo assay. In a more generalistic point of view, the common feature of UV-absorbing secondary metabolites is the presence of aromatic or conjugated bond structures as it is found in phlorotannins. Such molecules present a π-electron system, which is one of the most effective UV radiation absorbers (Cockell and Knowland 1999).

One other point that would be taken into consideration is the spatio-temporal variability of phenolic contents. Indeed, the phlorotannin pool strongly depends on sites, seasons, and phenology of algae (i.e., Parys et al. 2009; Le Lann et al. 2012a; Celis-Plá et al. 2016). So, knowledge of the chemical ecology of potentially exploitable species is essential to identify the best sites and seasons for the highest bioactivities.

In conclusion, this study emphasized, for the first time, the sunscreen potential and strong antioxidant and antibacterial capacities of a mix of four small phlorotannins, i.e., diphlorethols and triphlorethols and trifuhalols and tetrafuhalols, from the brown macroalga *H. siliquosa*. The antioxidant and sunscreen activities were found to be equivalent to several commercial antioxidant molecules and to some synthetic UV filters. Moreover, the correlation found between antioxidant activities and TPC supports the involvement of phenolic compounds in the antioxidant mechanisms. Furthermore, the EAF showed bactericidal activities against *Pseudomonas aeruginosa*, *Staphylococcus aureus*, and *Escherichia coli*, which represents interesting properties for proposing these compounds as natural preservatives in cosmetics for example. These findings therefore highlight the potential of this brown seaweed as a natural source of phytochemicals with several biological activities of interest to both the cosmetics and pharmaceutical industries. Nevertheless, it would be worth carrying out additional experiments in order to evaluate the photostability of compounds over time and to check for the absence of cytotoxicity so they can be used in formulations. Moreover, because our results suggest that bioactivities of the EAF are derived from the synergy between the active phlorotannins, other further studies need to be carried out to isolate and to separately test the bioactive compounds present in the active fraction in order to gain a better understanding of their mechanisms of action.

Acknowledgments This work was co-financed with the support of the European Union ERDF-Atlantic Area Programme, MARMED project no. 2011-1/164 and the project RIV-ALG (n° 13006760), financed by CBB Development, and the region Bretagne (France). Authors from LEMAR would like to thank the Labex Mer initiative, a State Grant from the French Agence Nationale de la Recherche (ANR) in the "Investissements d'avenir" Program (reference ANR-10-LABX-19-01, Labex Mer). The first author thanks Alexandre Canton for his assistance during the extraction and purification process and Helen McCombie for reviewing English.

Compliance with ethical standards

Conflict of interest The authors declare that they have no conflict of interest. All authors contributed significantly to this work and are in agreement with the content of the manuscript.

Authors' contributions Klervi Le Lann, Valérie Stiger-Pouvreau and Laurence Coiffard conceived and designed the experiments. Klervi Le Lann, Gwladys Surget, Céline Couteau, Stéphane Cérantola, and Fanny Gaillard performed the experiments. Klervi Le Lann analyzed the data. Mayalen Zubia, Fabienne Guérard, Nathalie Poupart, and Valérie Stiger-Pouvreau contributed materials and analysis tools. Klervi Le Lann, Valérie Stiger-Pouvreau, Fabienne Guérard, Gwladys Surget, Stéphane Cérantola, Mayalen Zubia, and Laurence Coiffard wrote the paper.

References

Ar Gall E, Lelchat F, Hupel M, Jegou C, Stiger-Pouvreau V (2015) Extraction and purification of phenols (phlorotannins) from brown algae. In: Stengel D, Connan S (eds) Natural products from marine algae: methods and protocols. Springer, New York, pp 131–143

Bourgougnon N, Stiger-Pouvreau V (2011) Chemodiversity and bioactivity within red and brown macroalgae along the French coasts, metropole and overseas departments and territories. In: Kim S-K (ed) Handbook of marine macroalgae. Wiley, Ltd, London, pp 58–105

Cao G, Alessio HM, Cutler RG (1993) Oxygen-radical absorbance capacity assay for antioxidants. Free Radic Biol Med 14:303–311

Celis-Plá PSM, Bouzon ZL, Hall-Spencer JM et al (2016) Seasonal biochemical and photophysiological responses in the intertidal macroalga *Cystoseira tamariscifolia* (Ochrophyta). Mar Environ Res 115:89–97

Cérantola S, Breton F, Gall EA, Deslandes E (2006) Co-occurrence and antioxidant activities of fucol and fucophlorethol classes of polymeric phenols in *Fucus spiralis*. Bot Mar 49:347–351

Cha S-H, Ko C-I, Kim D, Jeon Y-J (2012) Protective effects of phlorotannins against ultraviolet B radiation in zebrafish (*Danio rerio*). Vet Dermatol 23:51–e12

Chua M-T, Tung Y-T, Chang S-T (2008) Antioxidant activities of ethanolic extracts from the twigs of *Cinnamomum osmophloeum*. Bioresour Technol 99:1918–1925

Cockell CS, Knowland J (1999) Ultraviolet radiation screening compounds. Biol Rev Camb Philos Soc 74:311–345

Couteau C, Pommier M, Paparis E, Coiffard LJM (2007) Study of the efficacy of 18 sun filters authorized in European Union tested *in vitro*. Pharm - Pharmazie 62:449–452

Diffey BL, Robson J (1989) A new substrate to measure sunscreen protection factors throughout the ultraviolet spectrum. J Soc Cosmet Chem 40:127–133

Dudonné S, Vitrac X, Coutière P, Woillez M, Mérillon JM (2009) Comparative study of antioxidant properties and total phenolic content of 30 plant extracts of industrial interest using DPPH, ABTS, FRAP, SOD, and ORAC assays. J Agric Food Chem 57:1768–1774

El-Boury S, Couteau C, Boulande L, Paparis E, Coiffard LJM (2007) Effect of the combination of organic and inorganic filters on the sun protection factor (SPF) determined by in vitro method. Int J Pharm 340:1–5

Eom S-H, Kim Y-M, Kim S-K (2012) Antimicrobial effect of phlorotannins from marine brown algae. Food Chem Toxicol 50: 3251–3255

European Pharmacopoeia 7.0 - 2011. https://www.edqm.eu. Accessed 27 Oct 2015

Frankel EN, Meyer AS (2000) The problems of using one-dimensional methods to evaluate multifunctional food and biological antioxidants. J Sci Food Agric 80:1925–1941

Fujii Y, Tanaka R, Miyake H et al (2013) Evaluation for antioxidative properties of phlorotannins isolated from the brown alga *Eisenia bicyclis*, by the H-ORAC method. Food Nutr Sci 4:78–82

Fukumoto LR, Mazza G (2000) Assessing antioxidant and prooxidant activities of phenolic compounds. J Agric Food Chem 48:3597–3604

Glombitza K-W, Sattler E (1973) Trifuhalol, ein neuer triphenyldiäther aus *Halidrys siliquosa* (1). Tet Lett 14:4277–4280

Glombitza K-W, Rosener H-U, Müller D (1975) Bifuhalol und diphlorethol aus *Cystoseira tamariscifolia*. Phytochemistry 14: 1115–1116

Guinea M, Franco V, Araujo-Bazán L, Rodríguez-Martín I, González S (2012) In vivo UVB-photoprotective activity of extracts from commercial marine macroalgae. Food Chem Toxicol 50:1109–1117

Harnita ANI, Santosa IE, Martono S, Sudarsono S, Widyarini S, Harren FJ (2013) Inhibition of lipid peroxidation induced by ultraviolet radiation by crude phlorotannis isolated from brown algae *Sargassum hystrix* v. *buxifolium* C. Agardh. Indones J Chem 13: 14–20

Heffernan N, Brunton NP, FitzGerald RJ, Smyth TJ (2015) Profiling of the molecular weight and structural isomer abundance of macroalgae-derived phlorotannins. Mar Drugs 13:509–528

Huang D, Ou B, Prior RL (2005) The chemistry behind antioxidant capacity assays. J Agric Food Chem 53:1841–1856

Huang W-Y, Majumder K, Wu J (2010) Oxygen radical absorbance capacity of peptides from egg white protein ovotransferrin and their interaction with phytochemicals. Food Chem 123:635–641

Huovinen P, Gómez I (2015) UV sensitivity of vegetative and reproductive tissues of two antarctic brown algae is related to differential allocation of phenolic substances. Photochem Photobiol 91: 1382–1388

Ichihashi M, Ueda M, Budiyanto A, Bito T, Oka M, Fukunaga M, Horikawa T (2003) UV-induced skin damage. Toxicology 189: 21–39

Ishimoto H, Tai A, Yoshimura M, Amakura Y, Yoshida T, Hatano T, Ito H (2012) Antioxidative properties of functional polyphenols and their metabolites assessed by an ORAC assay. Biosci Biotech Biochem 76:395–399

Jarzycka A, Lewińska A, Gancarz R, Wilk KA (2013) Assessment of extracts of *Helichrysum arenarium*, *Crataegus monogyna*, *Sambucus nigra* in photoprotective UVA and UVB; photostability in cosmetic emulsions. J Photochem Photobiol B 128:50–57

Jégou C, Kervarec N, Cérantola S, Bihannic I, Stiger-Pouvreau V (2015) NMR use to quantify phlorotannins. The case of *Cystoseira tamariscifolia*, a phloroglucinol-producing brown macroalga in Brittany (France). Talanta 135:1–6

Kang Y-M, Eom S-H, Kim Y-M (2013) Protective effect of phlorotannins from *Eisenia bicyclis* against lipopolysaccharide-stimulated inflammation in HepG2 cells. Environ Toxicol Pharmacol 35:395–401

Kaur C, Kapoor HC (2002) Anti-oxidant activity and total phenolic content of some Asian vegetables. Int J Food Sci Technol 37:153–161

Keusgen M, Glombitza K-W (1995) Phlorethols, fuhalols and their derivatives from the brown alga *Sargassum spinuligerum*. Phytochemistry 38:975–985

Kim AR, Shin TS, Lee MS, Park JY, Park KE, Yoon NY, Kim JS, Choi JS, Jang BC, Byun DS, Park NK, Kim HR (2009) Isolation and identification of phlorotannins from *Ecklonia stolonifera* with antioxidant and anti-inflammatory properties. J Agric Food Chem 57: 3483–3489

Koleva II, Van Beek TA, Linssen JPH, Groot AD, Evstatieva LN (2002) Screening of plant extracts for antioxidant activity: a comparative study on three testing methods. Phytochem Anal 13:8–17

Kornprobst JM (2010) Encyclopedia of marine natural products. Wiley-Blackwell, Weinheim

Lautenschlager S, Wulf HC, Pittelkow MR (2007) Photoprotection. Lancet 370:528–537

Le Lann K, Jégou C, Stiger-Pouvreau V (2008) Effect of different conditioning treatments on total phenolic content and antioxidant activities in two Sargassacean species: comparison of the frondose *Sargassum muticum* (Yendo) Fensholt and the cylindrical *Bifurcaria bifurcata* R. Ross. Phycol Res 56:238–245

Le Lann K, Connan S, Stiger-Pouvreau V (2012a) Phenology, TPC and size-fractioning phenolics variability in temperate Sargassaceae (Phaeophyceae, Fucales) from Western Brittany: native vs. introduced species. Mar Environ Res 80:1–11

Le Lann K, Ferret C, VanMee E, Spagnol C, Lhuillery M, Payri C, Stiger-Pouvreau V (2012b) Total phenolic, size-fractionated phenolics and fucoxanthin content of tropical Sargassaceae (Fucales, Phaeophyceae) from the South Pacific Ocean: spatial and specific variability. Phycol Res 60:37–50

Li Y-X, Wijesekara I, Li Y, Kim S-K (2011) Phlorotannins as bioactive agents from brown algae. Process Biochem 46:2219–2224

Liu H, Zhao L, Guo S, Xia Y, Zhou P (2011) Modification of fish skin collagen film and absorption property of tannic acid. J Food Sci Technol 51(6):1102–1109

Lohézic-Le Dévéhat F, Legouin B, Couteau C, Boustie J, Coiffard L (2013) Lichenic extracts and metabolites as UV filters. J Photochem Photobiol B 120:17–28

McInnes AG, Ragan MA, Smith DG, Walter JA (1984) High-molecular-weight phloroglucinol-based tannins from brown algae: structural variants. Hydrobiologia 116-117:597–602

Montero L, Sánchez-Camargo AP, García-Cañas V, Tanniou A, Stiger-Pouvreau V, Russo M, Rastrelli L, Cifuentes A, Herrero M, Ibáñez E (2016) Anti-proliferative activity and chemical characterization by comprehensive two-dimensional liquid chromatography coupled to mass spectrometry of phlorotannins from the brown macroalga *Sargassum muticum* collected on North-Atlantic coasts. J Chromatogr A 1428:115–125

Nagayama K, Iwamura Y, Shibata T, Hirayama I, Nakamura T (2002) Bactericidal activity of phlorotannins from the brown alga *Ecklonia kurome*. J Antimicrob Chemother 50:889–893

Parys S, Kehraus S, Pete R, Küpper FC, Glombitza KW, König GM (2009) Seasonal variation of polyphenolics in *Ascophyllum nodosum* (Phaeophyceae). Eur J Phycol 44:331–338

Parys S, Kehraus S, Krick A, Glombitza KW, Carmeli S, Klimo K, Gerhäuser C, König GM (2010) In vitro chemopreventive potential of fucophlorethols from the brown alga *Fucus vesiculosus* L. by anti-oxidant activity and inhibition of selected cytochrome P450 enzymes. Phytochemistry 71:221–229

Pavia H, Brock E (2000) Extrinsic factors influencing phlorotannin production in the brown alga *Ascophyllum nodosum*. Mar Ecol Process Ser 193:285–294

Ragan MA, Glombitza K-W (1986) Phlorotannins, brown algal polyphenols. Prog Phycol Res 4:129–241

Rancan F, Rosan S, Boehm K, Fernández E, Hidalgo ME, Quihot W, Rubio C, Boehm F, Piazena H, Oltmanns U (2002) Protection against UVB irradiation by natural filters extracted from lichens. J Photochem Photobiol B 68:133–139

Saewan N, Jimtaisong A (2015) Natural products as photoprotection. J Cosmet Dermatol 14:47–63

Sambandan DR, Ratner D (2011) Sunscreens: an overview and update. J Am Acad Dermatol 64:748–758

Sattler E, Glombitza K-W, Wehrli FW, Eckhardt G (1977) Antibiotica aus algen—XVI: Polyhydroxyphenyläther aus der Phaeophycee *Halidrys siliquosa*. Tetrahedron 33:1239–1244

Schoenwaelder MEA (2002) The occurrence and cellular significance of physodes in brown algae. Phycologia 41:125–139

Shibata T, Nagayama K, Sugiura S, Makino S, Ueda M, Tamaru Y (2015) Analysis on composition and antioxidative properties of phlorotannins isolated from Japanese *Eisenia* and *Ecklonia* species. Am J Plant Sci 06:2510–2521

Singh IP, Bharate SB (2006) Phloroglucinol compounds of natural origin. Nat Prod Rep 23:558–591

Smith AH, Imlay JA, Mackie RI (2003) Increasing the oxidative stress response allows *Escherichia coli* to overcome inhibitory effects of condensed tannins. Appl Environ Microbiol 69:3406–3411

Stiger-Pouvreau V, Jégou C, Cérantola S, Guérard F, Le Lann K (2014) Phlorotannins in Sargassaceae species from Brittany (France): Interesting molecules for ecophysiological and valorisation purposes. In: Nathalie Bourgougnon, Editor(s), Advances in Botanical Research, Academic Press. 71: 379–411

Surget G, Stiger-Pouvreau V, Le Lann K, Kervarec N, Couteau C, Coiffard LJM, Gaillard F, Cahier K, Guérard F, Poupart N (2015) Structural elucidation, in vitro antioxidant and photoprotective capacities of a purified polyphenolic-enriched fraction from a saltmarsh plant. J Photochem Photobiol B 143:52–60

Swanson AK, Druehl LD (2002) Induction, exudation and the UV protective role of kelp phlorotannins. Aquat Bot 73:241–253

Tanniou A, Vandanjon L, Incera M, Serrano Leon E, Husa V, Le Grand J, Nicolas JL, Poupart N, Kervarec N, Engelen A, Walsh R, Guerard F, Bourgougnon N, Stiger-Pouvreau V (2014) Assessment of the spatial variability of phenolic contents and associated bioactivities in the invasive alga *Sargassum muticum* sampled along its European range from Norway to Portugal. J Appl Phycol 26:1215–1230

Thomas P, Swaminathan A, Lucas RM (2012) Climate change and health with an emphasis on interactions with ultraviolet radiation: a review. Glob Change Biol 18:2392–2405

Turkmen N, Velioglu YS, Sari F, Polat G (2007) Effect of extraction conditions on measured total polyphenol contents and antioxidant and antibacterial activities of black tea. Molecules 12:484–496

Wang T, Jónsdóttir R, Olafsdóttir G (2009) Total phenolic compounds, radical scavenging and metal chelation of extracts from Icelandic seaweeds. Food Chem 116:240–248

Wang T, Jónsdóttir R, Liu H, Gu L, Kristinsson HG, Raghavan S, Ólafsdóttir G (2012) Antioxidant capacities of phlorotannins extracted from the brown algae *Fucus vesiculosus*. J Agric Food Chem 60:5874–5883

Zhu QY, Hackman RM, Ensunsa JL, Holt RR, Keen CL (2002) Antioxidative activities of oolong tea. J Agric Food Chem 50: 6929–6934

Zubia M, Fabre MS, Kerjean V, Le Lann K, Stiger-Pouvreau V, Fauchon M, Deslandes E (2009) Antioxidant and antitumoural activities of some Phaeophyta from Brittany coasts. Food Chem 116:693–701

Gwladys SURGET, 2017. Processus adaptatifs des végétaux marins face au changement climatique à différentes échelles de temps et d'espace : dynamique de populations, métabolomique, écophysiologie et potentiels de valorisation

Résumé : Trois modèles invasifs à large répartition en Europe, le long d'un gradient latitudinal Norvège-Portugal, ont été choisis : *Sargassum muticum*, *Codium fragile* et *Gracilaria vermiculophylla*. Cette thèse a pour objectif l'étude de la phénologie, de l'écophysiologie et du métabolome de ces macrophytes invasifs face à une variation de facteurs environnementaux 1) à une échelle locale, 2) à l'échelle du gradient latitudinal (en lien avec le changement climatique global) ainsi que l'étude 3) des voies de valorisation possibles des métabolites de stress par bio-inspiration. Le gradient latitudinal, se traduisant par un gradient thermique, permet de mimer le réchauffement climatique car les conséquences de ce changement climatique sur les espèces en milieu naturel ne sont généralement appréciables qu'à l'échelle de dizaines d'années. Les suivis de l'écologie, du métabolome ainsi que des impacts potentiels de ces espèces à une échelle locale en France, a permis d'étudier le développement et le cycle de vie des espèces. En particulier, *G. vermiculophylla* se caractérise par une phénologie spécifique (avec la prépondérance de petits fragments végétatifs, <3cm) en Rade de Brest et par une tolérance accrue à l'envasement jusqu'à 12 cm de profondeur en acclimatant son métabolome tout en maintenant une physiologie dormante. Cette espèce ingénieur impacte en profondeur l'écosystème vaseux de la Rade. Le suivi le long du gradient latitudinal a permis d'illustrer la plasticité phénologique des espèces et notamment un potentiel invasif contrasté de *C. fragile* entre les différentes latitudes. Lors de marée basse de vives eaux, les espèces présentent une acclimatation de leur photo-physiologie en fonction de la latitude avec la mise en évidence d'une photoinhibition du PSII, lié au stress engendré par les conditions environnementales. Enfin, ce travail a illustré les propriétés multifonctionnelles d'extraits enrichis en composés phénoliques, présentant des activités antioxydantes mais également photoprotectrices ou ostéogéniques, soulignant l'émergence de voies de valorisation originales par bio-inspiration pour divers secteurs tels que la cosmétologie et les biomatériaux en santé humaine.

Mots clés : *Gracilaria vermiculophylla, Sargassum muticum, Codium fragile,* Invasions biologiques, Gradient latitudinal, Phénologie, Métabolome, Photo-physiologie, Impacts, Envasement, Activités biologiques

Gwladys SURGET, 2017. Adaptative process of marine macrophytes in a context of climatic change at several time and spatial scales: phenology, metabolomic, ecophysiology and bio-inspired applications

Abstract: Three model species with a large distribution along European coasts, along a latitudinal gradient from Norway to Portugal was chosen: *Sargassum muticum*, *Codium fragile* and *Gracilaria vermiculophylla*. The aims of this PhD thesis were to study the phenology, ecophysiology and the metabolom of these non-native marine macrophytes and their ability to cope with a variation of environmental factors 1) at a population scale, 2) along the latitudinal gradient (in relation with the global climatic change) and to propose 3) bio-inspired molecules for industrial purposes. The latitudinal gradient corresponding to a thermic gradient, allows to imitate the global warming as climatic change impacts are most of the time only visible at decennial scale. Monitorings of ecology, metabolome and potential impacts of these macroalgae, at a population scale, allowed to study the development and life cycle of these models. In particular, *G. vermiculophylla* exhibited a specific phenology (with a majority of small vegetative fragments, <3cm) in the Bay of Brest and a highly tolerance to burial until 12 cm depth in the sediment by acclimatizing its metabolome together with the ability to maintain a dormancy physiology. This engineer species modifies deeply muddy shores of this Bay. Latitunal gradients's monitoring highlighted the phenological plasticity and a contrasted invasive potential of *C. fragile* between latitudes. During low spring tides, species exhibited an acclimation of their photophysiology between latitudes with photoinhibition process related to induced environmental stress. Furthermore, this work showed the multifunctional properties of polyphenols enriched extracts with antioxidant, photoprotective or osteogenic activities, highlighting the emergence of original bio-inspired pathways for cosmetic or biomaterial applications.

Key words: *Gracilaria vermiculophylla, Sargassum muticum, Codium fragile,* biological invasions, latitudinal gradient, Phenology, Metabolome, Photo-physiology, Impacts, Burial, Biological activities